

NASA Computational Fluid Dynamics Conference

Volume 1: Sessions I - VI

(NASA-CP-10038-Vol-1) NASA COMPUTATIONAL
FLUID DYNAMICS CONFERENCE. VOLUME 1:
SESSIONS 1-6 (NASA) 475 p

CSCL 01A

N91-10839

--THRU--

N91-10867

Uncclas

H1/02 0270283

*Proceedings of a
conference held at
Ames Research Center
Moffett Field, California
March 7-9, 1989*

NASA

NASA Conference Publication 10038

NASA Computational Fluid Dynamics Conference

Volume 1 : Sessions I - VI

ORIGINAL CONTAINS
COLOR ILLUSTRATIONS

*Proceedings of a conference
sponsored by the Aerodynamics Division,
Office of Aeronautics
and Space Technology, NASA,
held at Ames Research Center
Moffett Field, California
March 7-9, 1989*

NASA

National Aeronautics and
Space Administration

Ames Research Center
Moffett Field, California

1989

TABLE OF CONTENTS — VOLUME 1

PREFACE	ix
PANEL SESSION SUMMARY	xiii
CONFERENCE COMMITTEE	xv
CONFERENCE PROGRAM	xvii
PAPERS	
Session I (Center Overviews)	1
Computational Fluid Dynamics Program at NASA Ames Research Center	
T. Holst	3
Computational Fluid Dynamics Research and Applications at NASA Langley Research Center	
J. South, Jr.	35
Computational Fluid Dynamics at the Lewis Research Center: An Overview	
R. Stubbs	49
Session II (Center Overviews Continued)	63
Marshall Space Flight Center CFD Overview	
L. Schutzenhofer	65
Johnson Space Center CFD Overview	
C. Li	95
NASA's CFD Validation Program	
D. Satran	123
Session III (Transition and Turbulence)	135
Understanding Transition and Turbulence Through Direct Simulations	
P. Spalart and J. Kim	137
Direct Simulation of Compressible Turbulence	
T. Zang, G. Erlebacher, and M. Hussaini	151
Non Linear Evolution of a Second Mode Wave in Supersonic Boundary Layers	
G. Erlebacher and M. Hussaini	167
Numerical Simulation of Nonlinear Development of Instability Waves	
R. Mankbadi	183
More Accurate Predictions with Transonic Navier-Stokes Methods Through Improved Turbulence Modeling	
D. Johnson	193
Session IV (CFD Codes)	205
Recent Advances in Runge-Kutta Schemes for Solving 3-D Navier-Stokes Equations	
V. Vatsa, B. Wedan, and R. Abid	207

Computations of Three-Dimensional Steady and Unsteady Viscous Incompressible Flows	
D. Kwak, S. Rogers, S. Yoon, M. Rosenfeld, and L. Chang	223
SAGE: A 2-D Self-Adaptive Grid Evolution Code and Its Application in Computational Fluid Dynamics	
C. Davies, E. Venkatapathy, and G. Deiwert	239
Time Dependent Viscous Incompressible Navier-Stokes Equations	
J. Goodrich	255
CFD for Applications to Aircraft Aeroelasticity	
G. Guruswamy	271
Application of Unstructured Grid Methods to Steady and Unsteady Aerodynamic Problems	
J. Batina	287
Session V (Fighter Aircraft)	309
Grid Generation and Inviscid Flow Computation about Aircraft Geometries	
R. Smith	311
A Zonal Navier-Stokes Methodology for Flow Simulation about a Complete Aircraft	
J. Flores	327
Numerical Simulation of F-18 Fuselage Forebody Flows at High Angles of Attack	
L. Schiff, R. Cummings, R. Sorenson, and Y. Rizk	345
Navier-Stokes Solutions about the F/A-18 Forebody-LEX Configuration	
F. Ghaffari, J. Luckring, J. Thomas, and B. Bates	361
Navier-Stokes Solutions for Flows Related to Store Separation	
O. Baysal, R. Stallings, Jr., and E. Plentovich	385
TranAir: Recent Advances and Applications	
M. Madson	411
Session VI (Rotorcraft)	429
Numerical Simulation of Rotorcraft	
W. McCroskey, J. Baeder, R. Border, E. Duque, G. Srinivasan and S. Stanaway	431
Calculation of the Rotor Induced Download on Airfoils	
C. Lee	447
Three-Dimensional Viscous Drag Prediction for Rotor Blades	
C. Chen	459
Progress Toward the Development of an Airfoil Icing Analysis Capability	
M. Potapczuk, C. Bidwell, B. Berkowitz	473
The Breakup of Trailing-Line Vortices	
D. Jacqmin	489
APPENDIX: LIST OF ATTENDEES	495

TABLE OF CONTENTS — VOLUME 2

PREFACE	vii
PANEL SESSION SUMMARY	ix
CONFERENCE COMMITTEE.....	xiii
CONFERENCE PROGRAM.....	xv
PAPERS	
Session VII (Hypersonics/NASP)	1
A Comparative Study of Navier-Stokes Codes for High-Speed Flows	
D. Rudy, J. Thomas, A. Kumar, P. Gnoffo, and S. Chakravarthy	3
Modeling of High Speed Chemically Reacting Flow Fields	
J. Drummond, M. Carpenter, and H. Kamath	19
Three-Dimensional Calculation of Supersonic Reacting Flows Using an LU Scheme	
S. Yu, P. Tsai, and J. Shuen	43
Progress in Computing Nozzle/Plume Flowfields	
S. Ruffin, E. Venkatapathy, W. Feiereisen, and S. Lee	59
Application of CFD Codes for the Simulation of Scramjet Combustor Flowfields	
T. Chitsomboon and G. Northam	75
Hypersonic CFD Applications at NASA Langley Using CFL3D and CFL3DE	
P. Richardson	91
Session VIII (Space Shuttle)	115
Numerical Aerodynamic Simulation of the Space Shuttle Ascent Environment	
J. Slotnick and F. Martin, Jr.	117
Computational Fluid Dynamics Analysis of Space Shuttle Main Propulsion Feed	
Line 17-Inch Disconnect Valves	
M. Kandula and D. Pearce	133
Analysis of SSME HPOTP Bearing Inlet Cavity	
P. McConnaughey	149
A Combined Eulerian-Lagrangian Two-Phase Analysis of the SSME HPOTP	
Nozzle Plug Trajectories	
R. Garcia, P. McConnaughey, F. de Jong, J. Sabnis, and D. Pribik	161
Conjugate (Solid/Fluid) Computational Fluid Dynamics Analysis of the Space Shuttle	
Solid Rocket Motor Nozzle/Case and Case Field Joints	
D. Doran, L. Keeton, P. Dionne, and A. Singhal	179
Session IX (Turbomachinery)	193
Simulation of Turbomachinery Flows	
J. Adamczyk	195
Prediction of Turbine Rotor-Stator Interaction Using Navier-Stokes Methods	
N. Madavan, M. Rai, and S. Gavali	205

VOLUME 2 (Continued)

Turbine Stage Aerodynamics and Heat Transfer Prediction	217
L. Griffin and H. McConaughey	217
Automated Design of Controlled Diffusion Blades	231
J. Sanz	231
Numerical Analysis of Flow Through Oscillating Cascade Sections	245
D. Huff	245
Analysis of Three-Dimensional Viscous Flow in a Supersonic Throughflow Fan	259
R. Chima	259
Session X (STOVL)	273
Simulation of Powered-Lift Flows	
W. Van Dalsem, K. Chawla, K. Roth, M. Smith, K. Rao, and T. Blum	275
A Numerical Study of the Hot Gas Environment Around a STOVL Aircraft in	
Ground Proximity	
T. Van Overbeke and J. Holdeman	291
CFD Analysis for High Speed Inlets	311
T. Benson	311
The Use of a Navier-Stokes Code in the Wing Design Process	
S. McMillin	321
Applications of a Transonic Wing Design Method	
R. Campbell and L. Smith	343
Session XI (Algorithms and Tools)	359
An Embedded Grid Formulation Applied to Delta Wings	
J. Thomas and S. Krist	361
Unstructured Mesh Solution of the Euler and Navier-Stokes Equations	
T. Barth	379
3-D Unstructured Grids for the Solution of the Euler Equations	
C. Gumbert, P. Parikh, S. Pirzadeh, and R. Löhner	395
Flux Splitting Algorithms for Two-Dimensional Viscous Flows with Finite-	
Rate Chemistry	
J. Shuen and M. Liou	437
Visualization of Fluid Dynamics at NASA Ames	
V. Watson	451
Computational Fluid Dynamics on a Massively Parallel Computer	
D. Jespersen and C. Levit	467
Session XII (Hypersonics/AFE)	483
Conservation Equations and Physical Models for Hypersonic Air Flows Over the	
Aeroassist Flight Experiment Vehicle	
P. Gnoffo	485
The Computation of Thermo-Chemical Nonequilibrium Hypersonic Flows	
G. Candler	501

VOLUME 2 (Concluded)

Aerodynamic Stability and Heating Analyses for the Aeroassist Flight Experiment Vehicle

J. McGary and C. Li 515

Aeroassist Flight Experiment Aerodynamics and Aerothermodynamics

E. Brewer 529

Direct Simulation of Rarefied Hypersonic Flows

J. Moss 545

APPENDIX: LIST OF ATTENDEES 559

PREFACE

This publication is a collection of the presentations given at the NASA Computational Fluid Dynamics (CFD) Conference held at NASA Ames Research Center, Moffett Field, California, March 7-9, 1989. The objectives of the conference were to disseminate CFD research results to industry and university CFD researchers, to promote synergy among NASA CFD researchers, and to permit feedback from researchers outside NASA on issues pacing the discipline of CFD. The focus of the conference was on the application of CFD technology but also included fundamental activities. The conference was sponsored by the Aerodynamics Division, Office of Aeronautics and Space Technology (OAST), NASA Headquarters, Washington, DC 20546.

The conference consisted of twelve sessions of papers representative of CFD research conducted within NASA and three non-NASA panel sessions. For each panel session, the panel membership consisted of industry and university CFD researchers. A summary of the comments made during the panel sessions have been included in this publication.

The conference proceedings are published in two volumes. Volume 1 contains the papers presented in Sessions I-VI; Volume 2 contains those given in Sessions VII-XII. Each volume contains the same front matter, and each contains a list of attendees as an appendix.

PANEL SESSION SUMMARY

**NASA CFD Conference
NASA Ames Research Center
March 7-9, 1989**

Panel Sessions Summary

The NASA CFD Conference was held at Ames Research Center on March 7-9, 1989. To conclude each day's presentations, a panel session with participation from the audience furnished a great deal of excellent feedback from the industry and academic communities. During the conference it was evident that the panel members proffered comments only after having spent considerable time in preparing them.

The members of the panel sessions are listed below:

March 7	P. Rubbert - Boeing Commercial Airplanes R. Melnik - Grumman Aerospace Corporation D. Whitfield - Mississippi State University
March 8	I. Bhateley - General Dynamics - Fort Worth Division R. Agarwal - McDonnell Douglas Research Laboratories R. MacCormack - Stanford University
March 9	V. Shankar - Rockwell International Science Center J. Carter - United Technologies Research Center A. Jameson - Princeton University

The crucial comments from the three panel sessions have been combined and are summarized as follows:

- NASA's CFD program is now too heavily focused on applications: program balance has swung from fundamentals (1970's) to applications (1980's)
- Three critical "needs" emerged:
 - (1) More algorithm research is needed; especially for Navier-Stokes solvers with unstructured grids
 - (2) More research is required on geometric modelling; need rapid, accurate, and effective surface definition techniques
 - (3) More research is needed on grid generation methods with the focus on speed, efficiency, and grid quality to reduce set up time and complexity
- Developers of CFD need to understand the needs of the users; designers of aerospace vehicles have requirements that are different than the CFD researchers perceptions
- Industry needs more reliable and cost effective CFD tools

Additional detail comments from the three panel sessions are listed below:

- CFD has matured during the last decade and is being used to solve real problems; however, industry lacks confidence in Navier-Stokes solutions
- Industry needs codes that have been validated to increase confidence in CFD technology
- Improved communality between codes would increase usability; standards are needed
- Improved data storage, networking, data transfer, and graphics required to assimilate information provided by CFD
- Improved turbulence modeling for separated flows
- Accurate prediction of drag for complete powered aerospace vehicles
- Develop multidisciplinary CFD technology with optimization capability
- NASA must maintain focus on technology development and high risk research
- Technology transfer is not complete until design engineers are using CFD codes successfully
- Industry needs NASA to improve CFD technology for codes simpler than Navier-Stokes solvers
- NAS program has been extremely helpful to industry in transferring CFD technology
- Industry needs to be more aggressive in their use of CFD
- Improved understanding of CFD by design engineers required; cooperative programs or workshops were suggested to bring CFD researchers and designers together
- Design cycle time needs to be reduced with CFD; codes must be cost effective, reliable, and useable, and robust to work at flight Reynolds Numbers
- Improved coordination/reduced overlap of CFD applications between NASA centers

Organizing Committee

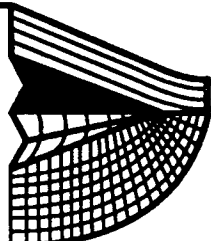
General Chairman	Dale Satran
Administrative Chairman	Paul Kutler
Deputy Administrative Chairman	Anthony R. Gross
Conference Coordinator	Lyz Dunham
Administrative Associate	Linda Callison
Publications	Betty Rogers
Budget	Karl Talarico
Secretary & Consultant	Aggie Ernst

Center Focal Points

Ames Research Center	Terry Holst
Langley Research Center	Jerry South
Lewis Research Center.....	Robert Stubbs
Marshall Space Flight Center.....	Luke Schutzenhofer
Johnson Space Center.....	C. P. Li

NASA CFD CONFERENCE

March 7-9, 1989



Ames Research Center

PROGRAM

**NASA CFD Conference
NASA Ames Research Center
March 7-9, 1989**

Tuesday, March 7

7:30 am Registration

8:00 am Welcome
D. Satran - Conference Chairman
K. Szalai - Ames Acting Associate Director
R. Graves - OAST Aerodynamics Division Director

Session I (Center Overviews) Chairman: R. Graves

8:30 am Ames Research Center CFD Overview
by T. Holst

9:10 am Langley Research Center CFD Overview
by J. South, Jr.

9:50 am Lewis Research Center CFD Overview
by R. Stubbs

10:30 am Break

Session II (Center Overviews Continued) Chairman: P. Kutler

10:50 am Marshall Space Flight Center CFD Overview
by L. Schutzenhofer

11:20 am Johnson Space Center CFD Overview
by C. Li

11:50 am CFD Validation Program Overview
by D. Satran

12:10 pm Lunch

NASA CFD CONFERENCE PROGRAM

Session III (Transition and Turbulence) Chairman: T. Pulliam

1:10 pm Understanding Transition and Turbulence Through Direct Simulations
by P. Spalart and J. Kim

1:30 pm Direct Simulation of Compressible Turbulence
by T. Zang, G. Erlebacher, and M. Hussaini

1:50 pm Nonlinear Evolution of a Second Mode Wave in Supersonic Boundary Layers
by G. Erlebacher and M. Hussaini

2:10 pm Numerical Simulation of Nonlinear Development of Instability Waves
by R. Mankbadi

2:30 pm More Accurate Predictions with Transonic Navier-Stokes Methods Through
Improved Turbulence Modeling
by D. Johnson

2:50 pm Break

Session IV (CFD Codes) Chairman: J. South

3:10 pm Recent Advances in Runge-Kutta Schemes for Solving 3-D Navier-Stokes Equations
by V. Vatsa, B. Wedan, and R. Abid

3:30 pm Computations of Three-Dimensional Steady and Unsteady Viscous Incompressible
Flows
by D. Kwak, S. Rogers, S. Yoon, M. Rosenfeld, and L. Chang

3:50 pm SAGE - A Self-Adaptive Grid Evolution Code and Its Application in Computational
Fluid Dynamics
by C. Davies, E. Venkatapathy, and G. Deiwert

4:10 pm Time Dependent Viscous Incompressible Navier-Stokes Equations
by J. Goodrich

4:30 pm CFD for Applications to Aircraft Aeroelasticity
by G. Guruswamy

4:50 pm Application of Unstructured Grid Methods to Steady and Unsteady Aerodynamic
Problems
by J. Batina

5:10 pm Break

5:20 pm Panel Session Chairman: P. Rubbert - Boeing Commercial
R. Melnick - Grumman Aerospace
D. Whitfield - Mississippi State

6:20 pm Adjourn to Officer's Club

6:30 pm Cocktail Party at Moffet Field Officer's Club

NASA CFD CONFERENCE PROGRAM

Wednesday, March 8

7:50 am Administrative Announcements

Session V (Fighter Aircraft) Chairman: T. Holst

8:00 am Grid Generation and Inviscid Flow Computation about Fighter Airplanes
by R. Smith

8:20 am A Zonal Navier-Stokes Methodology for Flow Simulation about a Complete Aircraft
by J. Flores

8:40 am Numerical Simulation of F-18 Fuselage Forebody Flows at High Angles of Attack
by L. Schiff, R. Cummings, R. Sorenson, and Y. Rizk

9:00 am Navier-Stokes Solutions about the F-18 Forebody-Strake Configuration
by F. Ghaffari, J. Luckring, and J. Thomas

9:20 am Navier-Stokes Solutions for Store Separation and Related Problems
by O. Baysal, R. Stallings, Jr., and E. Plentovich

9:40 am TRANAIR: Recent Advances and Applications
by M. Madison

10:00 am Break

Session VI (Rotorcraft) Chairman: W. McCroskey

10:20 am Computations of Airloads and Acoustics of Rotorcraft
by W. McCroskey, J. Baeder, C. Chen, E. Duque, and G. Srinivasan

10:40 am Calculation of Rotor Induced Download on Airfoils
by C. Lee

11:00 am Three-Dimensional Viscous Drag Prediction for Rotor Blades
by C. Chen

11:20 am Progress Toward the Development of an Airfoil Icing Analysis Capability
by M. Potapczuk, C. Bidwell, B. Berkowitz

11:40 am The Breakup of Trailing-Line Vortices
by D. Jacqmin

12:00 pm Lunch

NASA CFD CONFERENCE PROGRAM

Session VII (Hypersonics/NASP) Chairman: D. Dwoyer

1:00 pm A Comparative Study of Navier-Stokes Codes for High-Speed Flows
by D. Rudy, J. Thomas, A. Kumar, P. Gnoffo, and S. Chakravarthy

1:20 pm Modeling of High Speed Chemically Reacting Flow Fields
by J. Drummond, M. Carpenter, and H. Kamath

1:40 pm Three-Dimensional Simulation of Supersonic Reacting Flows with Finite Rate Chemistry
by S. Yu, J. Shuen, and P. Tsai

2:00 pm Progress in Computing Nozzle/Plume Flowfields
by S. Ruffin, E. Venkatapathy, W. Feiereisen, and S. Lee

2:20 pm Application of CFD Codes for the Simulation of Scramjet Combustor Flow Fields
by T. Chitsomboon and G. Northam

2:40 pm Hypersonic CFD Applications at NASA Langley Using CFL3D and CFL3DE
by P. Richardson

3:00 pm Break

Session VIII (Space Shuttle) Chairman: L. Schutzenhofer

3:20 pm Comparison of the ARC Shuttle Ascent Simulations with Wind Tunnel and Flight Data
by J. Slotnick and F. Martin, Jr.

3:40 pm Computational Fluid Dynamics Analysis of Space Shuttle Main Propulsion Feed Line 17-Inch Disconnect Valves
by M. Kandula and D. Pearce

4:00 pm Analysis of SSME HPOTP Bearing Inlet Cavity
by P. McConnaughey

4:20 pm A Combined Eulerian-Lagrangian Two-Phase Analysis of the SSME HPOTP Nozzle Plug Trajectories
by R. Garcia, P. McConnaughey, F. de Jong, J. Sabnis, and D. Pribik

4:40 pm Conjugate (Solid/Fluid) Computational Fluid Dynamics Analysis of the Space Shuttle Solid Rocket Motor Nozzle-to-Case and Case-to-Field Joints
by D. Doran, L. Keeton, P. Dionne, and A. Singhal

5:00 pm Break

5:10 pm **Panel Session Chairman: I. Bhateley - General Dynamics**
R. Agarwal - McDonnell Douglas
R. MacCormack - Stanford University

6:10 pm Adjourn to Banquet at Santa Clara Marriott Hotel

7:00 pm Banquet at Marriott Hotel

NASA CFD CONFERENCE PROGRAM

Thursday, March 9

7:50 am Administrative Announcements

Session IX (Turbomachinery) Chairman: R. Stubbs

8:00 am Simulation of Turbomachinery Flows
by J. Adamczyk

8:20 am Prediction of Turbine Rotor-Stator Interaction Using Navier-Stokes Methods
by N. Madavan, M. Rai, and S. Gavali

8:40 am Turbine Stage Aerodynamics and Heat Transfer Prediction
by L. Griffin and H. McConnaughey

9:00 am Automated Design of Controlled Diffusion Blades
by J. Sanz

9:20 am Numerical Analysis of Flow Through Oscillating Cascade Sections
by D. Huff

9:40 am Numerical Analysis of Three-Dimensional Viscous Internal Flows
by R. Chima and J. Yokota

10:00 am Break

Session X (STOVL) Chairman: M. Liou

10:20 am Simulators of PoweredLift Flows
by W. Van Dalsem, K. Chawla, M. Smith, K. Rao, and T. Blum

10:40 am A Numerical Study of the Hot Gas Environment Around a STOVL Aircraft in
Ground Proximity
by T. Van Overbeke and J. Holdeman

11:00 am CFD Analysis for High Speed Inlets
by T. Benson

11:20 am The Use of a Navier-Stokes Code in the Wing Design Process
by S. McMillin

11:40 am Application of a Transonic Wing Design Method
by R. Campbell and L. Smith

12:00 pm Lunch

NASA CFD CONFERENCE PROGRAM

Session XI (Algorithms and Tools) Chairman: J. Steger

1:00 pm An Embedded Grid Formulation Applied to Delta Wings
by J. Thomas and S. Taylor

1:20 pm Unstructured Mesh Solution of the Euler and Navier-Stokes Equations
by T. Barth

1:40 pm 3-D Unstructured Grids for the Solution of the Euler Equations
by C. Gumbert, P. Parikh, S. Pirzadeh, and R. Lohner

2:00 pm Flux Splitting Algorithms for Two-Dimensional Real Gas Flows
by J. Shuen and M. Liou

2:20 pm Visualization of Fluid Dynamics at NASA Ames
by V. Watson

2:40 pm Computational Fluid Dynamics on a Massively Parallel Computer
by D. Jespersen and C. Levit

3:00 pm Break

Session XII (Hypersonics/AFE) Chairman: C. Li

3:20 pm Conservation Equations and Physical Models for Hypersonic Air Flows Over the Aeroassist Flight Experiment Vehicle
by P. Gnoffo

3:40 pm The Computation of Thermo-Chemical Nonequilibrium Hypersonic Flows
by G. Candler

4:00 pm Aerodynamic Heating and Stability Analyses for Aeroassist Flight Experiment Vehicle
by J. McGary and C. Li

4:20 pm Aeroassist Flight Experiment Aerodynamics and Aerothermodynamics
by E. Brewer

4:40 pm Direct Simulation of Rarefied Hypersonic Flows
by J. Moss

5:00 pm Break

5:10 pm Panel Session Chairman: V. Shankar - Rockwell
J. Carter - United Technology
A. Jameson - Princeton University

6:10 pm Conference Adjourned

SESSION I

CENTER OVERVIEWS

Chairman:
Randolph A. Graves, Jr.
Director, Aerodynamics Division
NASA Headquarters

N91-10840

COMPUTATIONAL FLUID DYNAMICS PROGRAM AT NASA AMES RESEARCH CENTER

Terry L. Holst

Chief, Applied Computational Fluids Branch
NASA Ames Research Center, Moffett Field, California

ABSTRACT

The Computational Fluid Dynamics (CFD) Program at NASA Ames Research Center is reviewed and discussed. The presentation is broken into several sections as follows: First, the technical elements of the CFD Program are generally listed and briefly discussed. These elements include algorithm research, research and pilot code development, scientific visualization, advanced surface representation, volume grid generation, and numerical optimization. Next, the discipline of CFD is briefly discussed and related to other areas of research at NASA Ames including Experimental Fluid Dynamics, Computer Science Research, Computational Chemistry, and Numerical Aerodynamic Simulation. These areas combine with CFD to form a larger area of research, which might collectively be called computational technology. The ultimate goal of computational technology research at NASA Ames is to increase the physical understanding of the world in which we live, solve problems of national importance, and increase the technical capabilities of the aerospace community.

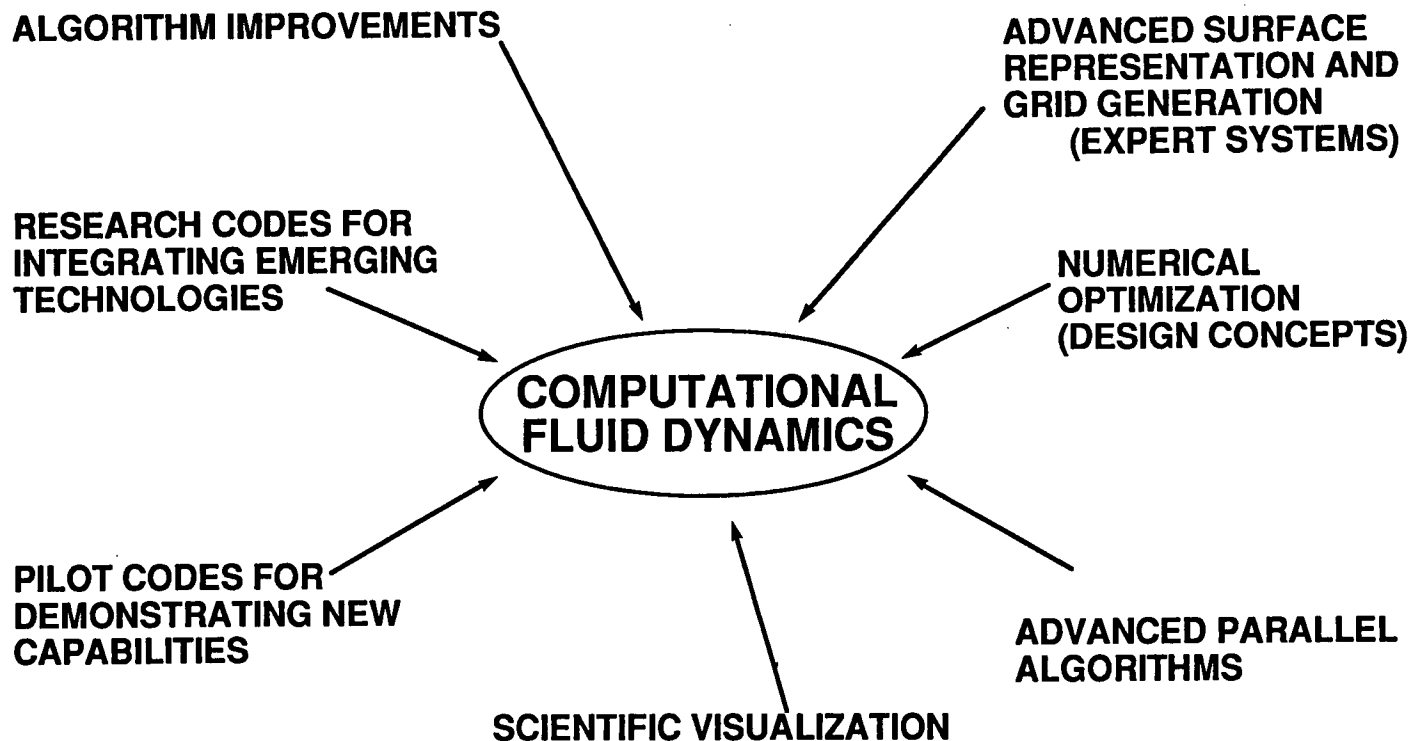
Next, the major programs at NASA Ames that either use CFD technology or perform research in CFD are listed and discussed. Briefly, this list includes turbulent/transition physics and modeling, high-speed real gas flows, interdisciplinary research, turbomachinery demonstration computations, complete aircraft aerodynamics, rotorcraft applications, powered lift flows, high alpha flows, multiple body aerodynamics, and incompressible flow applications. Some of the individual problems actively being worked in each of these areas is listed to help define the breadth or extent of CFD involvement in each of these major programs.

State-of-the-art examples of various CFD applications are presented to highlight most of these areas. The main emphasis of this portion of the presentation is on examples which will not otherwise be treated at this conference by the individual presentations. Thus, a good survey of CFD applications research at NASA Ames can be obtained by looking at this presentation in conjunction with the individual NASA Ames presentations made at this conference.

Finally, this overview is concluded with a list of principal current limitations and expected future directions. Some of the future directions include algorithm research, turbulence/transition research, multidisciplinary research, graphics and workstation research and applications which will address more realistic simulations in the engineering world.

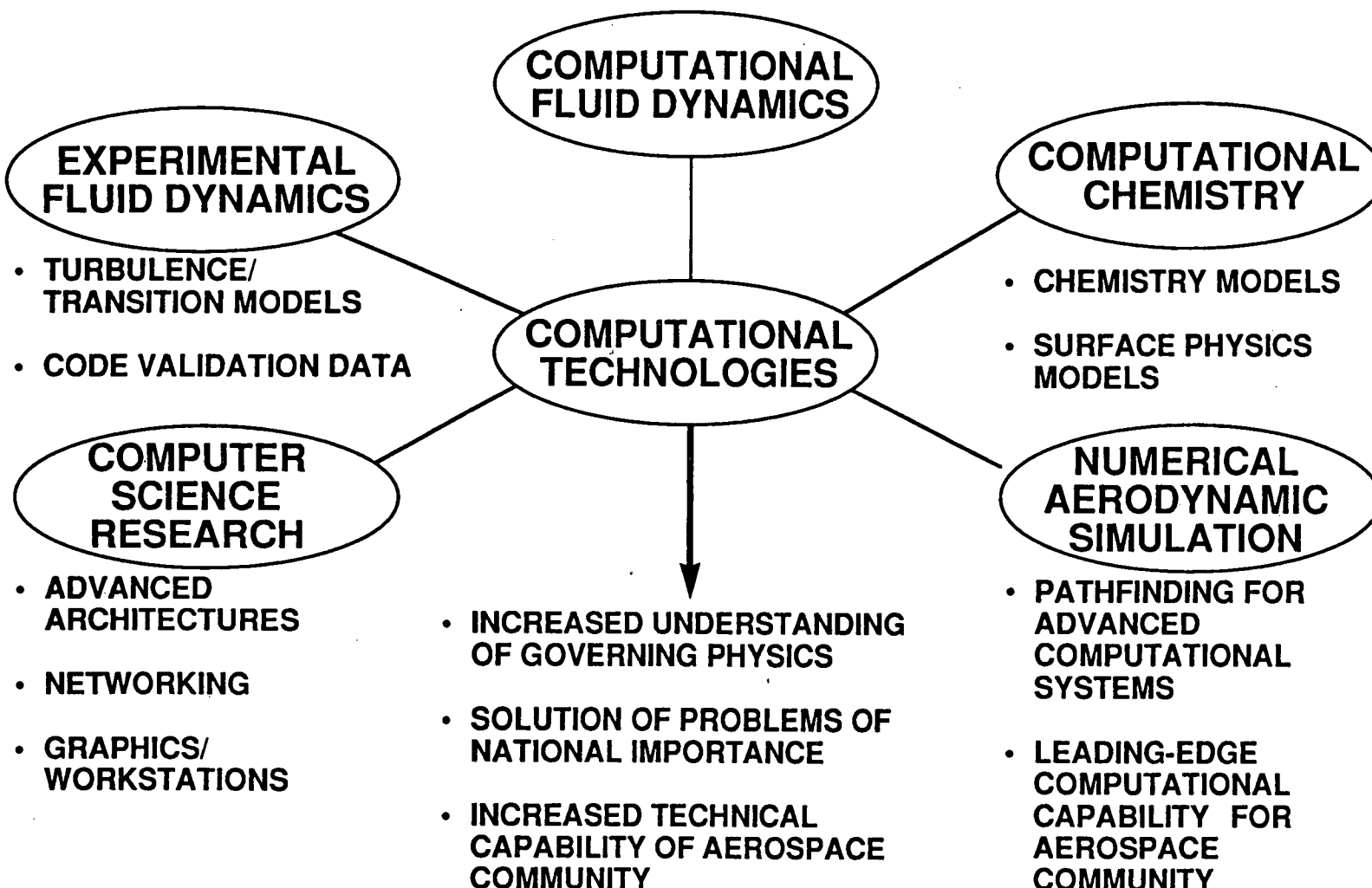
COMPUTATIONAL FLUID DYNAMICS

TECHNICAL ELEMENTS



COMPUTATIONAL TECHNOLOGIES

THRUSTS



MAJOR PROGRAMS USING CFD

NASA Ames Research Center

TURBULENT/TRANSITION PHYSICS AND PHYSICAL MODELING

HIGH-SPEED REAL GAS FLOWS

- THERMO- AND CHEMICAL-NONEQUILIBRIUM
- RADIATION
- COMBUSTION
- RAREFIED FLOW EFFECTS

INTERDISCIPLINARY RESEARCH

- CFD + COMPUTATIONAL ELECTROMAGNETICS
- CFD + COMPUTATIONAL STRUCTURAL MECHANICS
- CFD + ACTIVE CONTROLS
- CFD + HEAT CONDUCTION

TURBOMACHINERY DEMONSTRATION COMPUTATIONS

- 3D TURBINE ROTOR-STATOR
- MULTI-STAGE COMPRESSOR ROTOR-STATOR

COMPLETE AIRCRAFT AERODYNAMICS

- NASP
- F-16 (TNS, TRANAIR)

MAJOR PROGRAMS USING CFD (CONTINUED)

NASA Ames Research Center

ROTORCRAFT APPLICATIONS

- AEROACOUSTICS
- ROTOR/FUSELAGE INTERACTION
- HELICOPTER/TILTROTOR PERFORMANCE PREDICTIONS
- DYNAMIC STALL COMPUTATIONS

POWERED LIFT

- STOVL AIRCRAFT (HARRIER, E-7)
- UPPER SURFACE BLOWING APPLICATIONS
- JET FREESTREAM MIXING
- THRUST AUGMENTOR EJECTORS
- STOVL DELTA WING IN GROUND EFFECT

HIGH ALPHA

- HARV APPLICATIONS (F-18)
- OGIVE CYLINDER COMPUTATIONS
- UNSTEADY FLOWS

MAJOR PROGRAMS USING CFD (CONCLUDED)

NASA Ames Research Center

MULTIPLE BODY AERODYNAMICS

- SPACE SHUTTLE (LAUNCH CONFIGURATION)
- SRB/ET-ORBITER SEPARATION
- AIRCRAFT STORE SEPARATION
- SPACE SHUTTLE C/ SPACE SHUTTLE II

INCOMPRESSIBLE NAVIER-STOKES

- SSME APPLICATIONS
- HYDRODYNAMICS
- HIGH LIFT CONFIGURATIONS
- ARTIFICIAL HEART BLOOD FLOW SIMULATION

ADVANCED SIMULATION AND ANALYSIS PROJECT (ASAP)

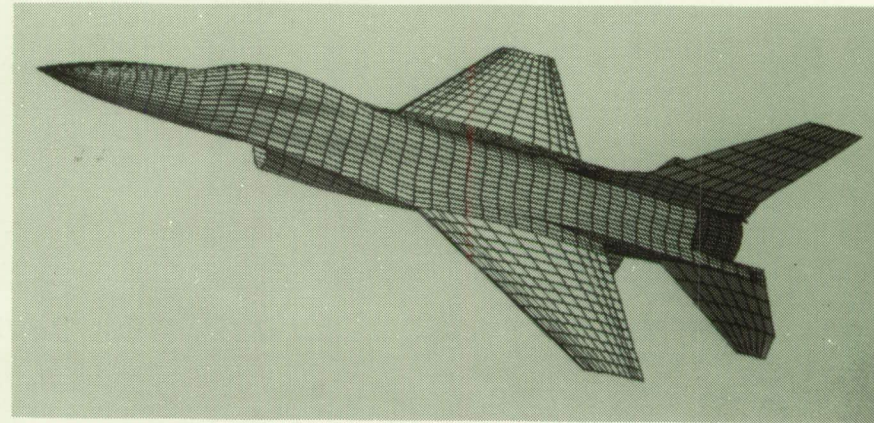
VAN DALSEM, VOGEL, LUH, SORENSEN, ATWOOD

OBJECTIVE

- REDUCE THE “CLOCK TIME” REQUIRED TO OBTAIN THE SURFACE DEFINITION AND GRID ABOUT A COMPLEX CONFIGURATION BY AT LEAST AN ORDER OF MAGNITUDE

APPROACH

- DEVELOP AN INTEGRATED, INTERACTIVE SURFACE DEFINITION AND GRID GENERATION CAPABILITY TAILORED TO THE CFD ENVIRONMENT



FUTURE DIRECTIONS

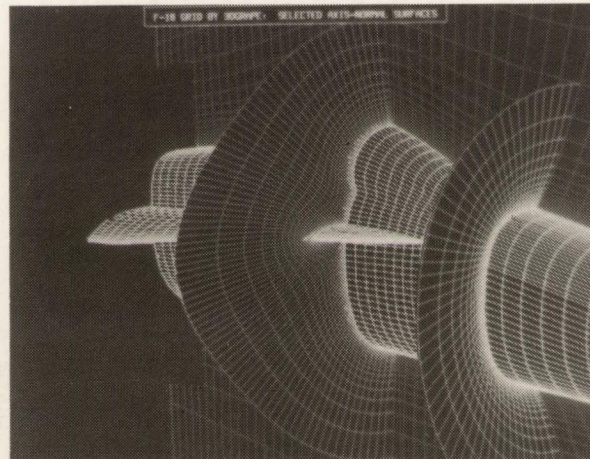
- EXPLORE APPLICATION OF AI TO ENHANCE NONEXPERT USER PERFORMANCE
- INVESTIGATE:
 - GRID QUALITY MEASURES
 - SOLUTION-ADAPTIVE TECHNIQUES
 - NEW GRID GENERATION APPROACHES (STRUCTURED AND UNSTRUCTURED)

PAYOUT

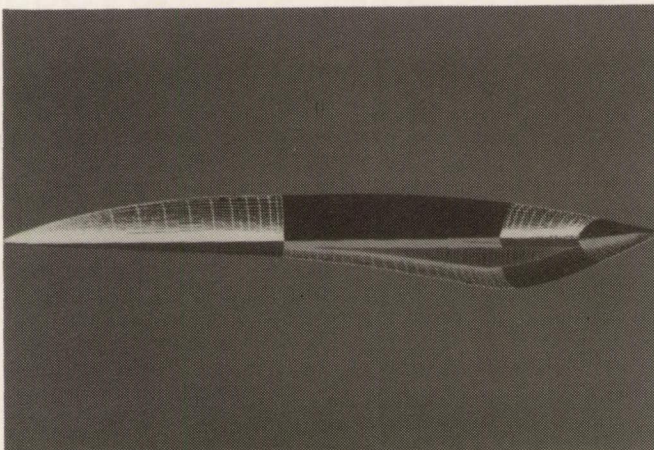
- A POWERFUL, EASY-TO-USE TOOL THAT SIGNIFICANTLY REDUCES THE TURNAROUND TIME FOR CURRENT AND FUTURE CFD ANALYSES

ADVANCED SIMULATION AND ANALYSIS PROJECT (ASAP)

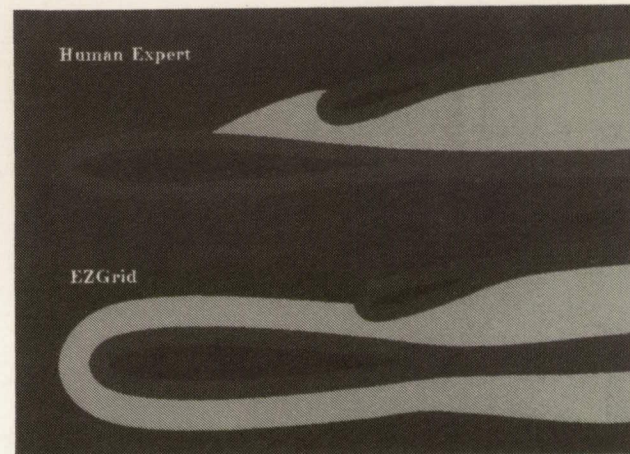
VOGEL, LUH, SORENSEN, ATWOOD



F-18 FOREBODY GRID BY 3DGRAPE: SELECTED AXIS-NORMAL SURFACES



SURFACE GRID FOR GENERIC
HYPERSONIC AIRPLANE



2D ZONING COMPARISON: HUMAN
EXPERT vs EXPERT SYSTEM (EZGRID)

PANEL METHOD APPLICATIONS

ASHBY, IGUCHI, BROWN

OBJECTIVES

- DEVELOP CAPABILITY TO ANALYZE COMPLEX GEOMETRIES VERY QUICKLY
 - INCLUDES LEADING-EDGE SEPARATION, JET PLUMES, AND UNSTEADY EFFECTS (TIME STEPPING)

APPROACH

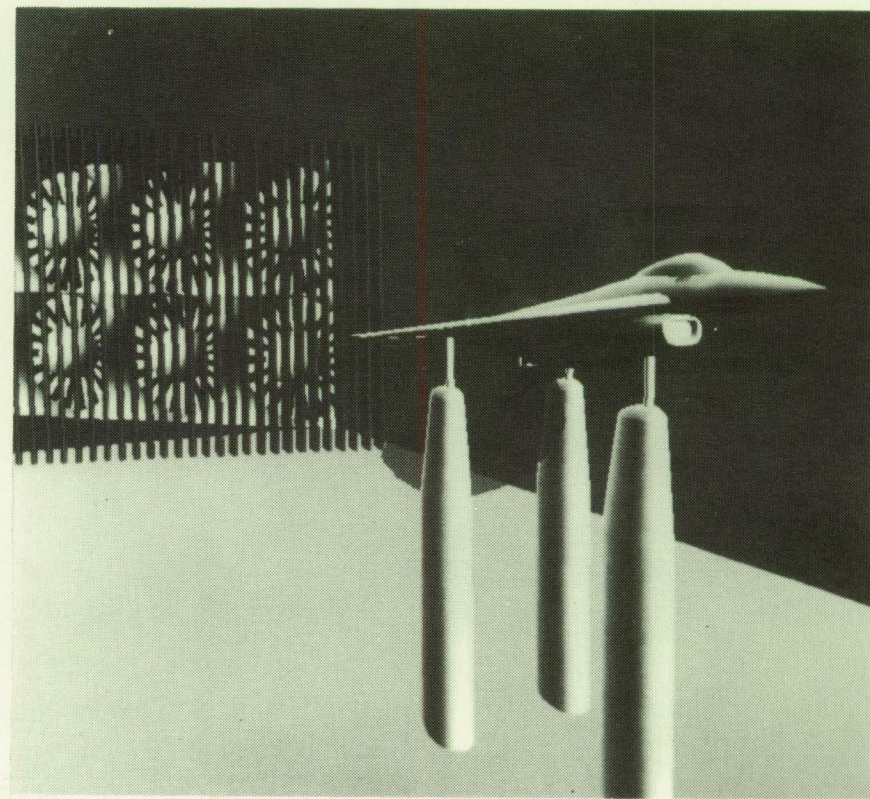
- LOW-ORDER PANEL METHOD WITH TIME-STEPPED WAKES

FUTURE DIRECTIONS

- COUPLE WITH BOUNDARY LAYER CODE TO INCLUDE VISCOUS EFFECTS
- USE FOR DESIGN AND ANALYSIS OF WIND TUNNEL MODELS AND TO DETERMINE WIND TUNNEL WALL INTERFERENCE

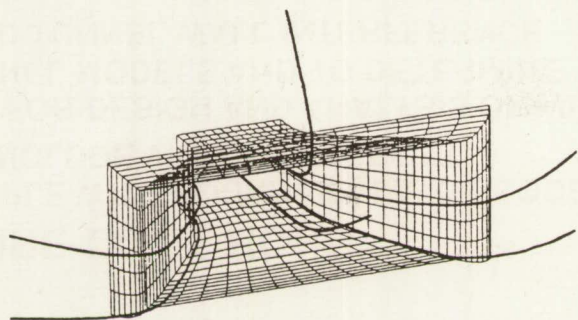
PAYOUT

- EFFICIENT, RELIABLE TOOL FOR USE IN LOW SPEED APPLICATIONS

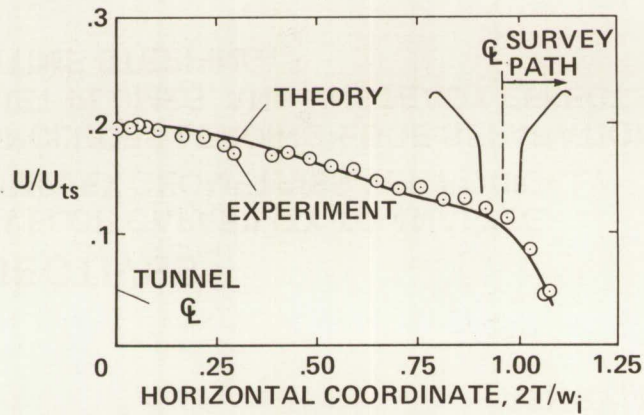


PANEL METHOD APPLICATIONS

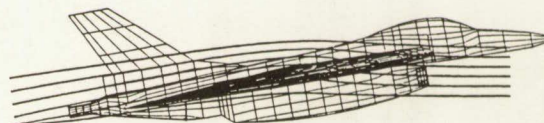
ASHBY, IGUCHI, BROWN



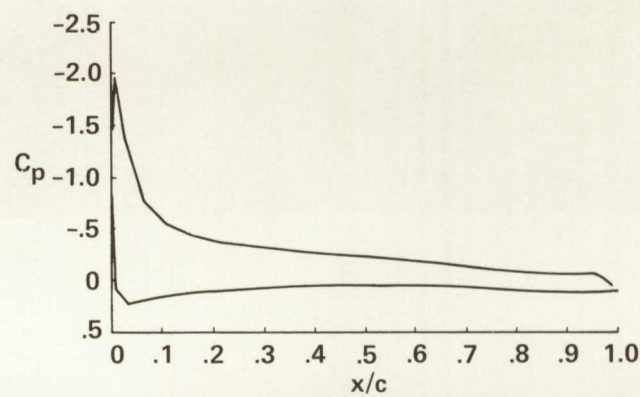
80- BY 120-FOOT WIND TUNNEL INLET



VELOCITY VARIATION ACROSS INLET



E-7 STOVL MODEL



CHORDWISE PRESSURE DISTRIBUTION
ON E-7 WING PMARC COMPUTATION;
 $2y/b = 0.6$, $\alpha = 8^\circ$

TWO-DIMENSIONAL COMPUTATIONS OF MULTI-STAGE COMPRESSOR FLOWS

GUNDY-BURLET, RAI

OBJECTIVE

- DEVELOP CAPABILITY TO CALCULATE UNSTEADY VISCOUS FLOWS WITHIN MULTI-STAGE TURBOMACHINES

CURRENT APPROACH

- SOLVE THE TWO-DIMENSIONAL NAVIER-STOKES EQUATIONS USING A ZONAL METHOD TO SIMULATE ROTOR-STATOR INTERACTION

FUTURE DIRECTIONS

- EXTEND TO THREE-DIMENSIONS

PAYOUT

- BETTER UNDERSTANDING OF UNSTEADY FLUID DYNAMICS IN TURBOMACHINES
- INCREASED RELIABILITY AND EFFICIENCY OF TURBOMACHINES

INSTANTANEOUS TEMPERATURE CONTOURS

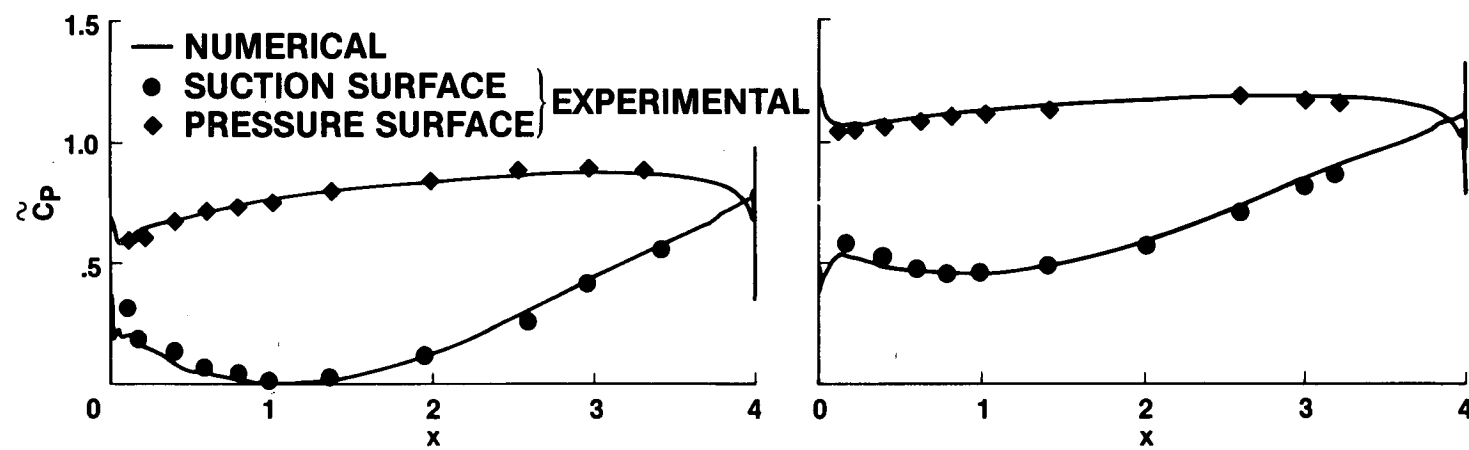
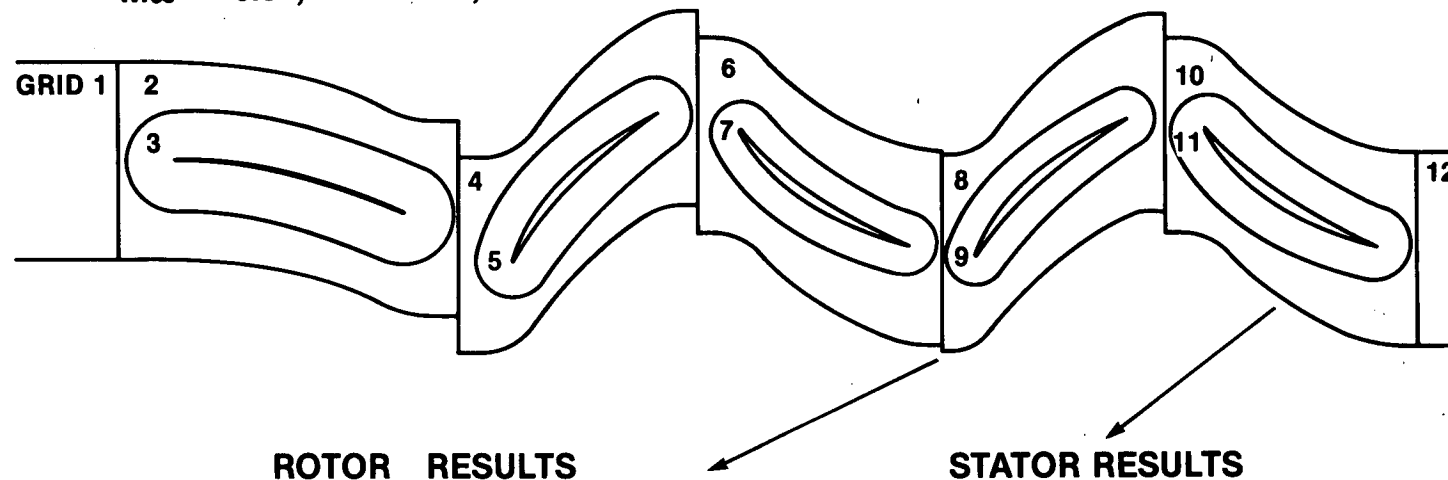
$M_\infty = 0.07$, $Re = 100,000/\text{in.}$



TIME-AVERAGED PRESSURES IN THE SECOND STAGE OF A 2.5 STAGE COMPRESSOR

GUNDY-BURLET, RAI

$M_\infty = 0.07$, $Re = 100,000/\text{in.}$



EFFECT OF TANGENTIAL LEADING EDGE BLOWING ON VORTICAL FLOW

YEH, TAVELLA, ROBERTS

OBJECTIVE

- TO INVESTIGATE THE ABILITY OF TANGENTIAL LEADING EDGE BLOWING TO CONTROL VORTICAL FLOW AT HIGH ALPHA

APPROACH

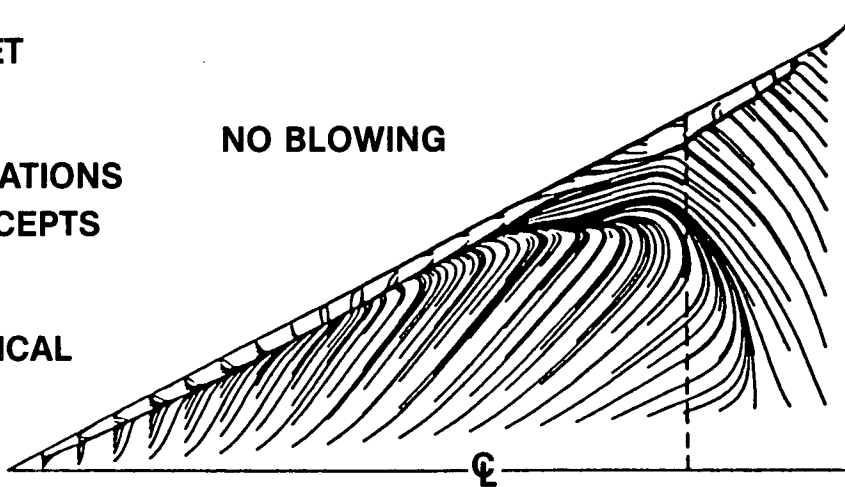
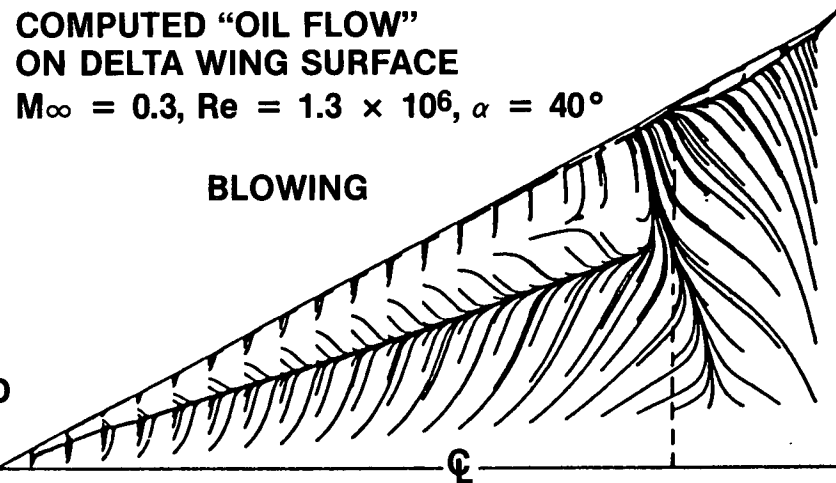
- UTILIZE DELTA WING GEOMETRY
- SOLVE THIN-LAYER NAVIER-STOKES EQUATIONS USING MULTIPLE-ZONE GRID APPROACH TO ACCOMODATE JET-SLOT GEOMETRY
- UTILIZE ALGEBRAIC TURBULENCE MODEL FOR SURFACE BL AND WALL JET

FUTURE DIRECTIONS

- EXTEND TO FULL AIRCRAFT CONFIGURATIONS
- INVESTIGATE BLOWING CONTROL CONCEPTS

PAYOUT

- INCREASED UNDERSTANDING OF VORTICAL FLOW PHYSICS
- NEW TOOL FOR STUDYING BLOWING CONTROL CONCEPTS



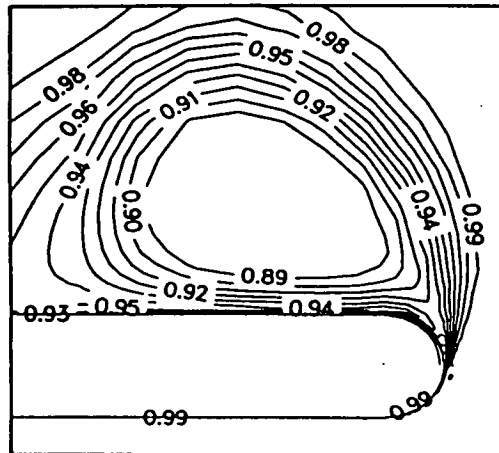
EFFECT OF TANGENTIAL LEADING EDGE BLOWING ON VORTICAL FLOW

YEH, TAVELLA, ROBERTS

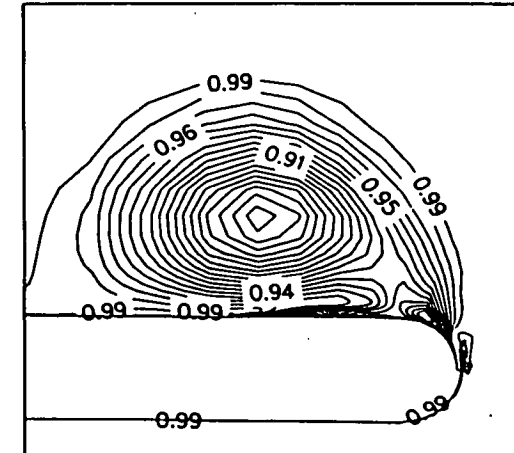
($M_\infty = 0.3$, $\alpha = 40^\circ$, $Re = 1.3 \times 10^6$, $X/C = 0.36$)

16
NORMALIZED
TOTAL
PRESSURE
CONTOURS

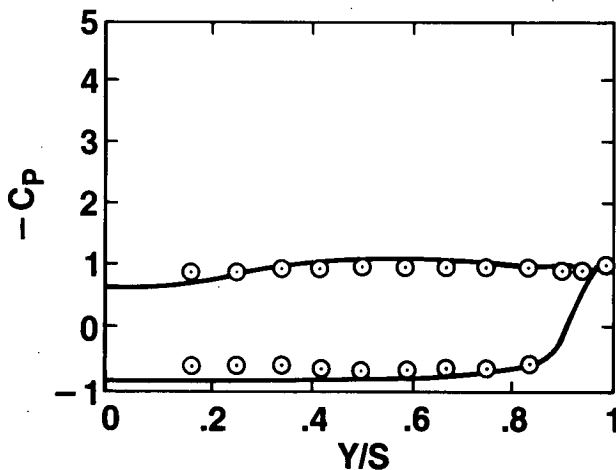
NO BLOWING



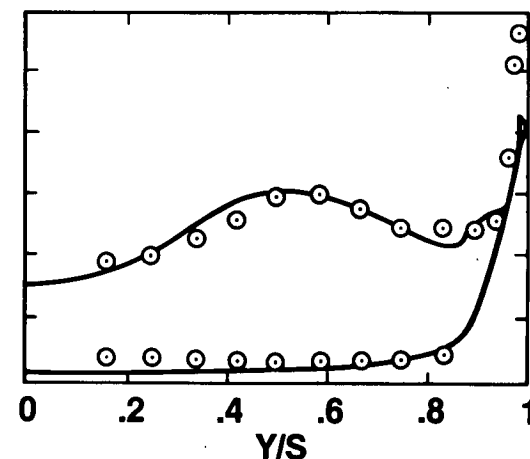
BLOWING



SURFACE
PRESSURE
DISTRIBUTION



○ EXPERIMENT
— CALCULATED



EULER VALIDATION/PRESSURE INTEGRATION

MELTON, ROBERTSON, MOYER

OBJECTIVES

- CFD VALIDATION FOR FLO57 EULER CODE
- ENHANCE WIND TUNNEL PRESSURE INTEGRATION FOR PREDICTING FORCES AND MOMENTS

APPROACH

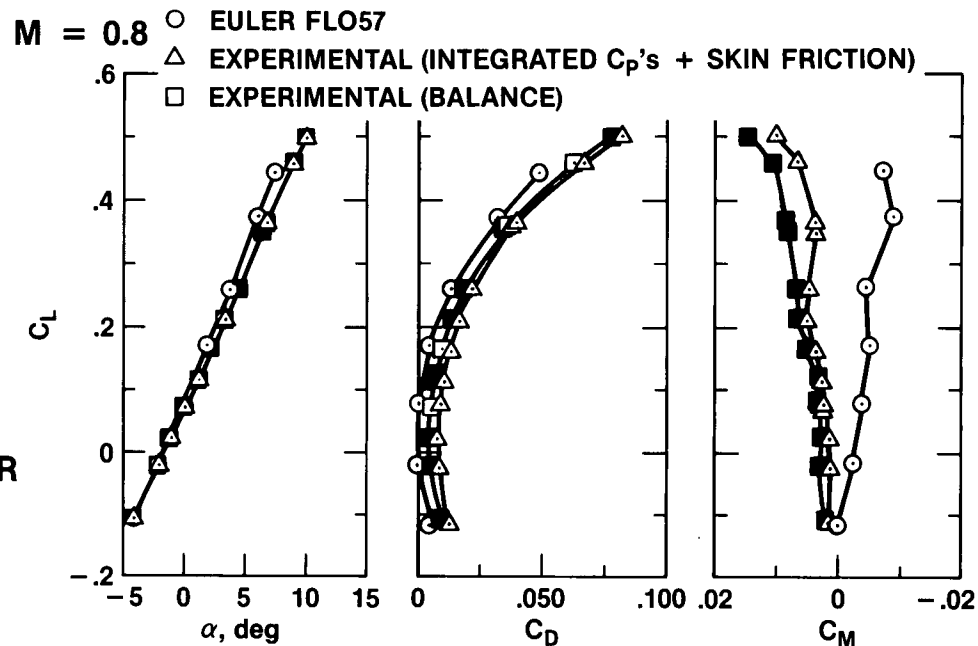
- FLO57 FINITE VOLUME 3D EULER CODE
- COMPUTE DISCRETIZATION ERROR BY COMPARING CFD FORCE AND MOMENT INTEGRATION WITH CFD PRESSURES INTERPOLATED AND INTEGRATED AT MODEL TAP LOCATIONS

FUTURE DIRECTIONS

- INVESTIGATE NEW METHODS FOR INTEGRATING CFD AND EXPERIMENTAL RESULTS

PAYOUT

- VALIDATION OF FLO 57 FOR DELTA CONFIGURATIONS
- REDUCE INSTRUMENTATION CONSTRAINTS ON COMPLEX WIND TUNNEL MODELS
- INCREASE ACCURACY OF FORCE AND MOMENT PREDICTIONS FROM WIND TUNNEL PRESSURE INTEGRATIONS



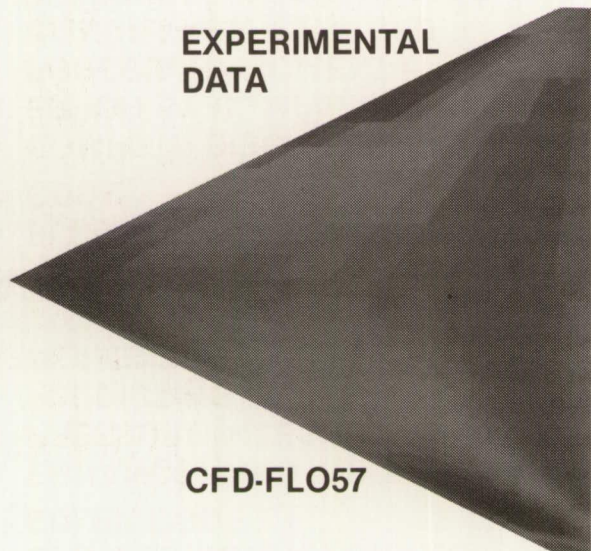
EULER VALIDATION/PRESSURE INTEGRATION

MELTON, ROBERTSON, MOYER

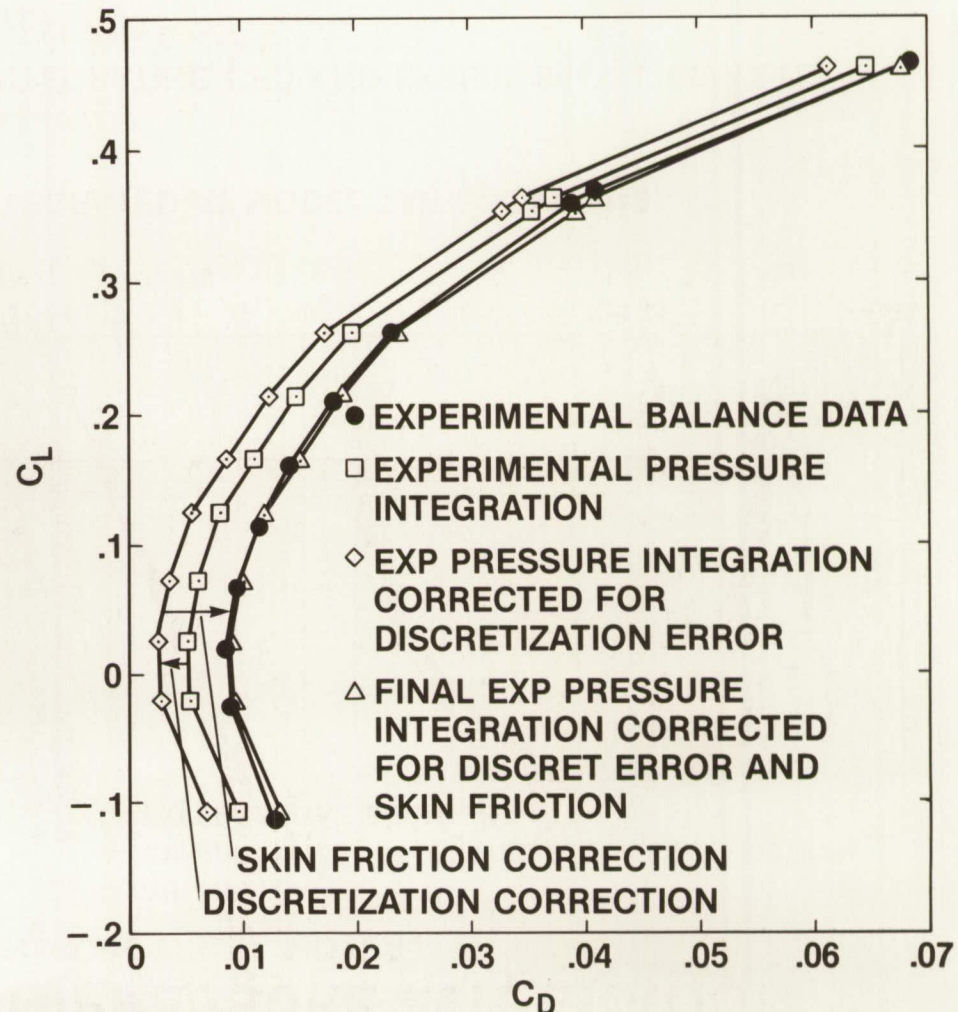
M = 0.8 DRAG POLAR

UPPER SURFACE Cp's

M = 0.8 $\alpha = 9.0^\circ$ $C_L = 0.45$



18



SPACE SHUTTLE LAUNCH CONFIGURATION

STEGER, RIZK, OBAYASHI, MARTIN, CHIU, BUNING

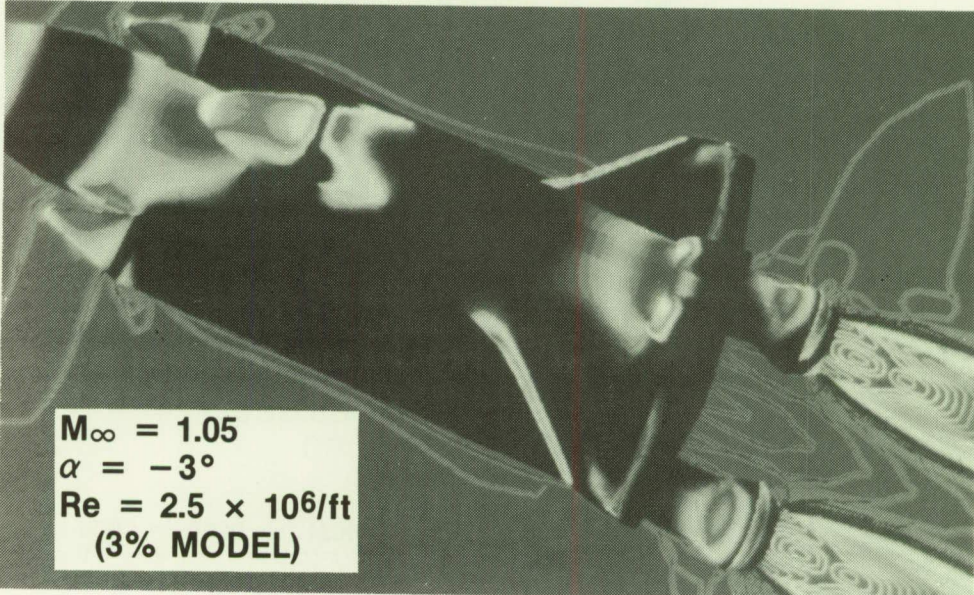
OBJECTIVE

- DEVELOP CAPABILITY TO COMPUTE FLOW OVER INTEGRATED SPACE SHUTTLE IN ASCENT

19

APPROACH

- SOLVE 3D REYNOLDS-AVERAGED NAVIER-STOKES EQUATIONS
- USE CHIMERA GRID APPROACH



FUTURE DIRECTIONS

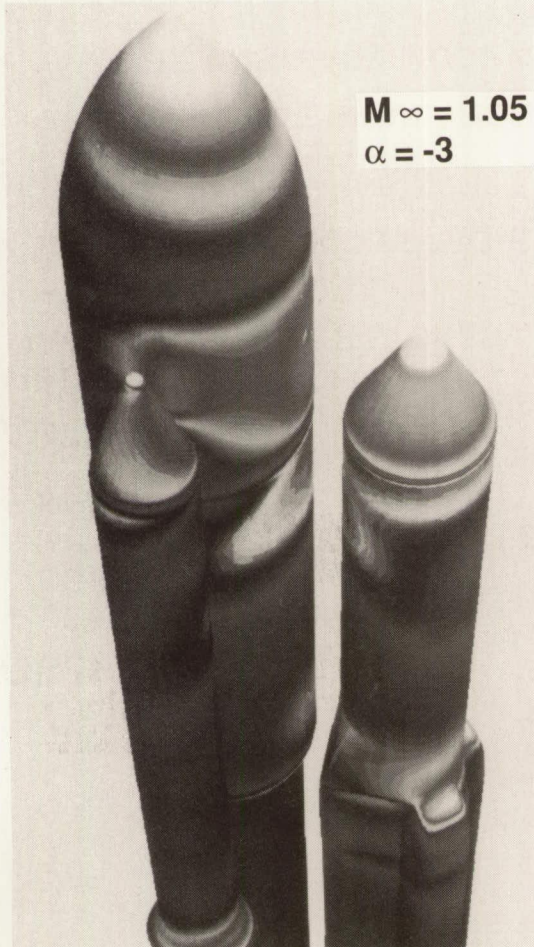
- IMPROVE PLUME SIMULATION CAPABILITY AND CODE EFFICIENCY
- VALIDATE UNSTEADY MODE AND STUDY FAST SEPARATION SIMULATIONS

PAYOUT

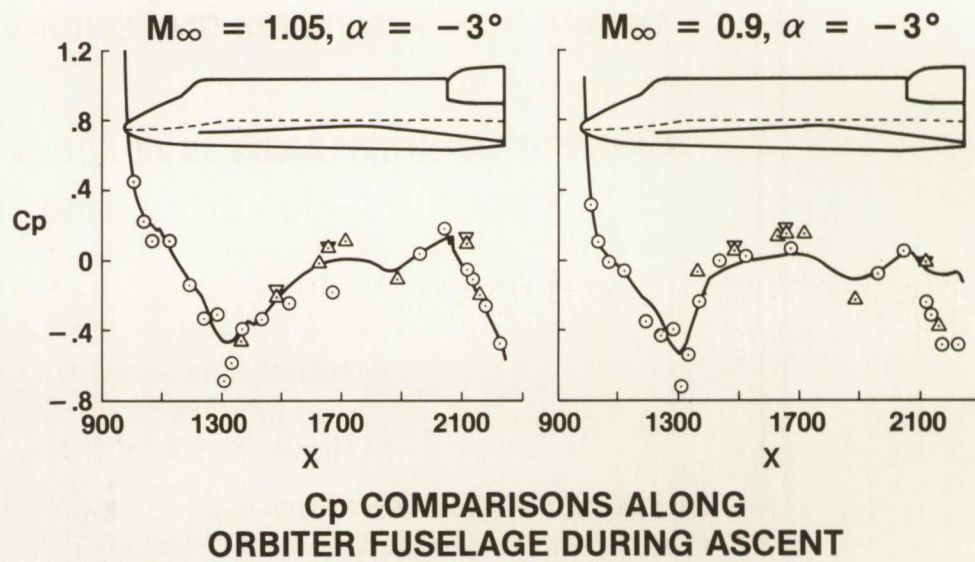
- PREDICTIVE TOOL FOR UNDERSTANDING AND REFINING AERODYNAMIC PERFORMANCE OF MULTIPLE BODY VEHICLES

SPACE SHUTTLE ASCENT-MODE RESULTS

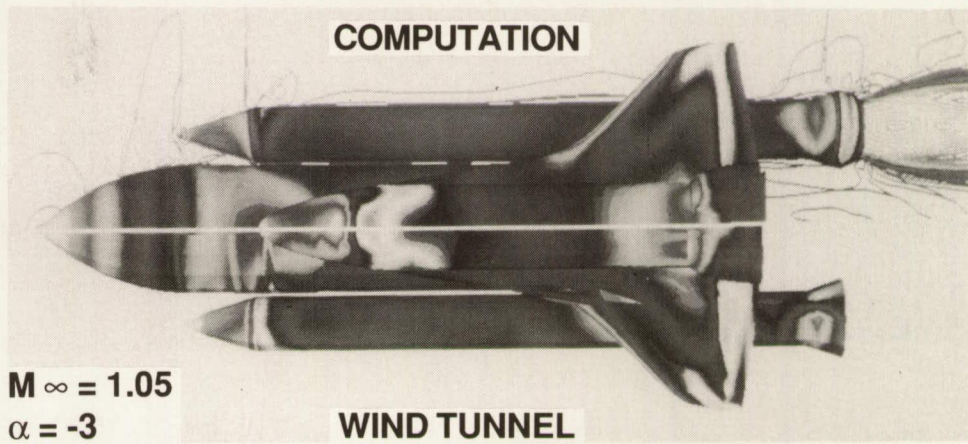
20



SURFACE PRESSURES
ON SHUTTLE C



C_p COMPARISONS ALONG
ORBITER FUSELAGE DURING ASCENT



WIND TUNNEL

COMPARISON OF SURFACE PRESSURES

UNSTEADY MULTIPLE BODY AERODYNAMICS

OBJECTIVE

- TO DEVELOP A GENERAL CAPABILITY FOR TIME-ACCURATE SIMULATION OF 3-D MULTIPLE BODY VISCOUS FLOWS GIVEN ARBITRARY GRID COMBINATIONS, BODY SHAPES, AND RELATIVE MOTION BETWEEN GRID SYSTEMS

CURRENT APPROACH

- UNSTEADY CHIMERA COMPOSITE GRID TECHNIQUES
- IMPLICIT TIME-ACCURATE SOLVER FOR THE THIN-LAYER NAVIER-STOKES EQUATIONS

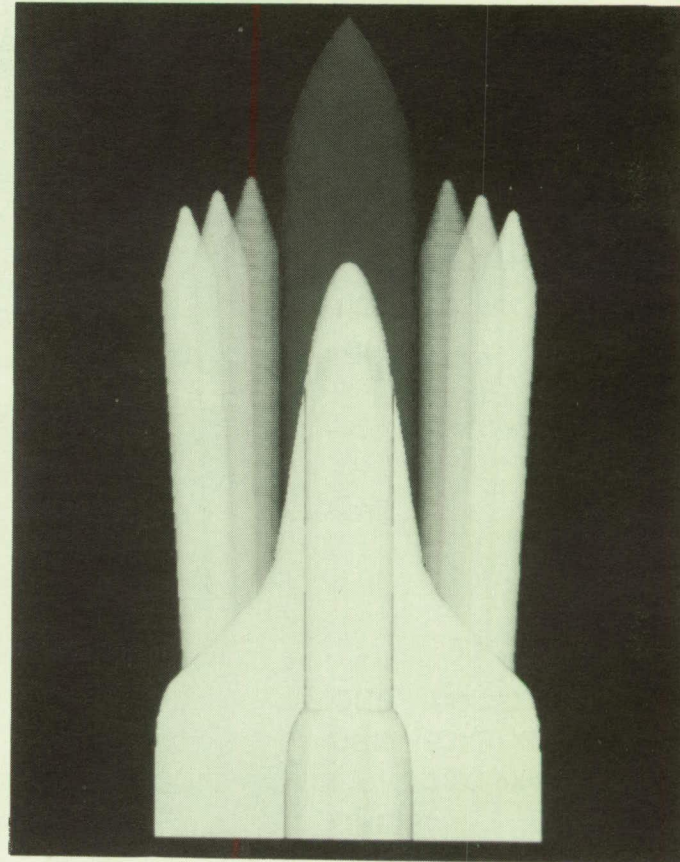
21

FUTURE DIRECTIONS

- DEVELOP TRAJECTORY PREDICTION ROUTINES
- IMPROVE EFFICIENCY AND ACCURACY OF BASIC ALGORITHMS
- CODE VALIDATION STUDIES

PAYOUT

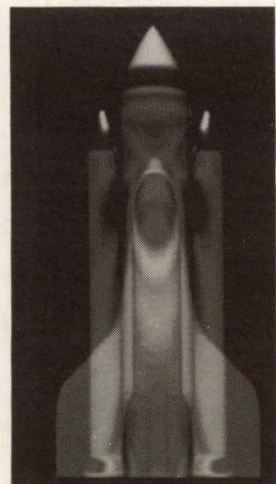
- A VALIDATED COMPUTATIONAL TOOL FOR ANALYZING COMPLEX AERODYNAMIC PROBLEMS INVOLVING MULTIPLE BODIES IN RELATIVE MOTION



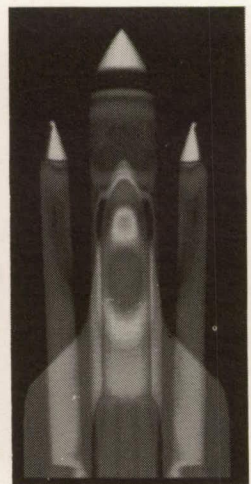
TIME-ACCURATE SIMULATION OF THE SPACE SHUTTLE SRB SEPARATION SEQUENCE

PRESSURE CONTOURS

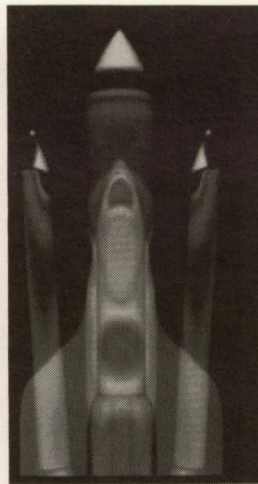
$$\begin{aligned}M_{\infty} &= 4.5 \\ \alpha &= +2^\circ \\ R_e &= 6.95 \times 10^6\end{aligned}$$



$t = 0.00 \text{ sec}$



$t = 0.34 \text{ sec}$



$t = 0.68 \text{ sec}$

DISCRETIZATION

GRIDS:

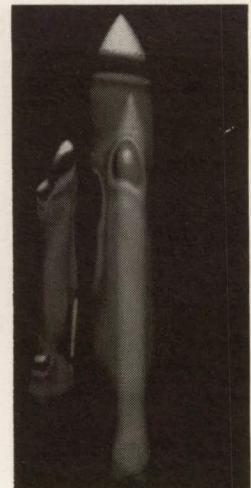
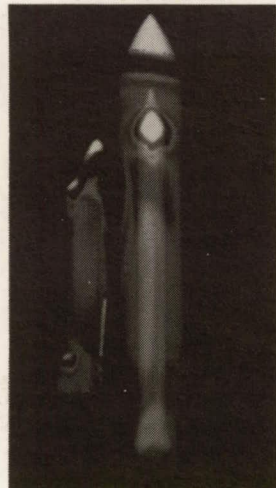
ET 73X39X45
SRB 53X37X21
ORB 74X77X33

22

ASSUMPTIONS:

- SIMPLIFIED GEOMETRY
- NO PLUMES
- PRESCRIBED SRB TRAJECTORY

(MEAKIN, SUHS)



TIME-STEP =

$1.36 \times 10^{-3} \text{ sec}$

500 STEPS THROUGH BSM
BURN

BOOSTER
SEPARATION
MOTOR
(BSM)

BURN-TIME = 0.68 sec

AIRCRAFT STORE SEPARATION

MEAKIN, SUHS

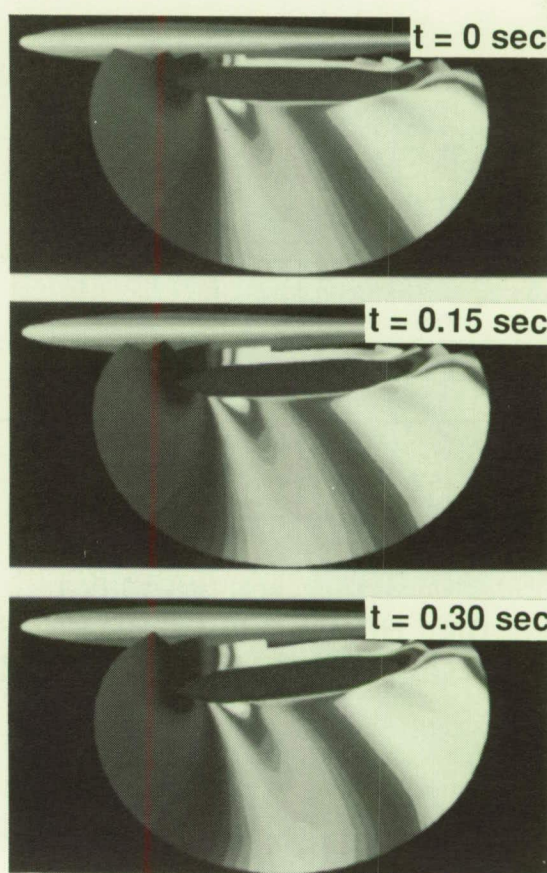
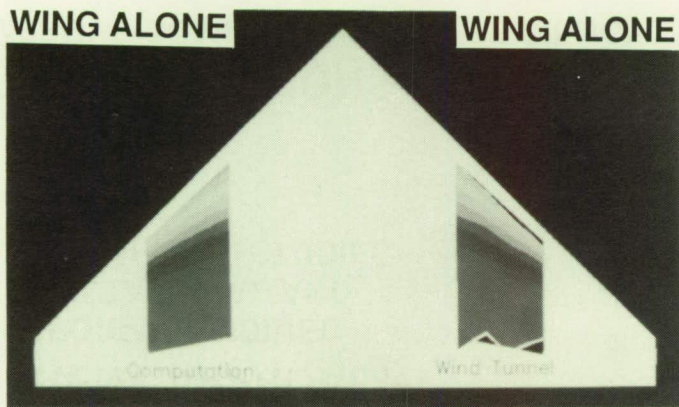
FREESTREAM CONDITIONS: $M_\infty = 1.05$, $\alpha = +2^\circ$, $Re = 2.4 \times 10^6$

WING LOWER SURFACE C_p DISTRIBUTION

MACH CONTOURS ABOUT STORE

STEADY-STATE

TIME-ACCURATE STORE-SEPARATION SIMULATION



TURBULENCE MODELING FOR HYPERSONIC FLOWS

COAKLEY, HORSTMAN, KUSSOY, MARVIN

OBJECTIVE

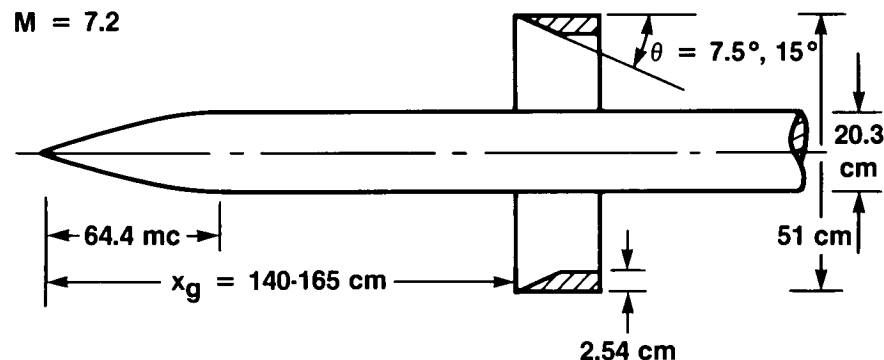
- IMPROVE AND DEVELOP MODELS FOR HYPERSONIC FLOWS

TEST MODEL GEOMETRIES USED FOR COMPARISONS OF COMPUTATION AND EXPERIMENT

CURRENT APPROACH

- PERFORM COMBINED COMPUTATIONAL AND EXPERIMENTAL STUDIES

24



FUTURE DIRECTIONS

- IMPROVE COMPUTATIONAL EFFICIENCY
- DEVELOP SECOND ORDER CLOSURE MODELS
- PERFORM EXPERIMENTS USING NEWLY DEVELOPED NON INTRUSIVE INSTRUMENTATION

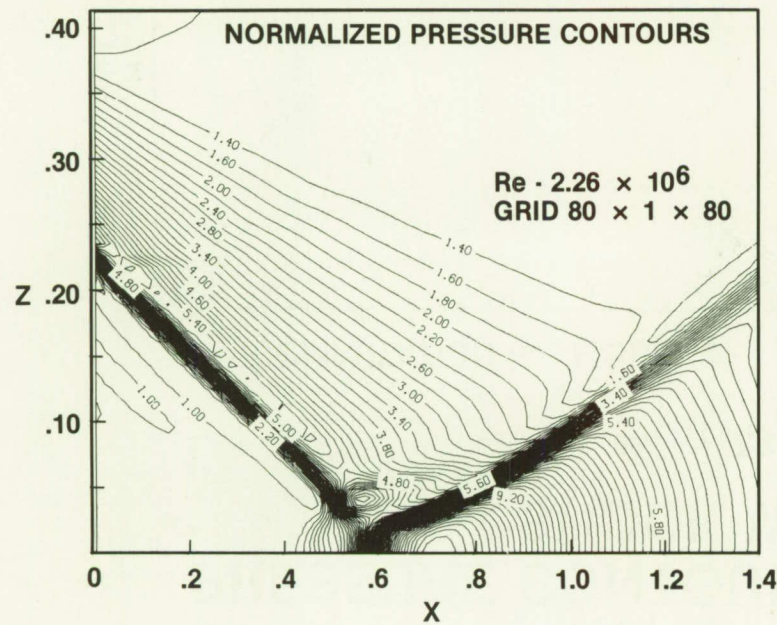
PAYOUT

- ACCURATE COMPUTATIONS OF HEAT TRANSFER, SKIN FRICTION, AND COMPLEX FLOW STRUCTURES

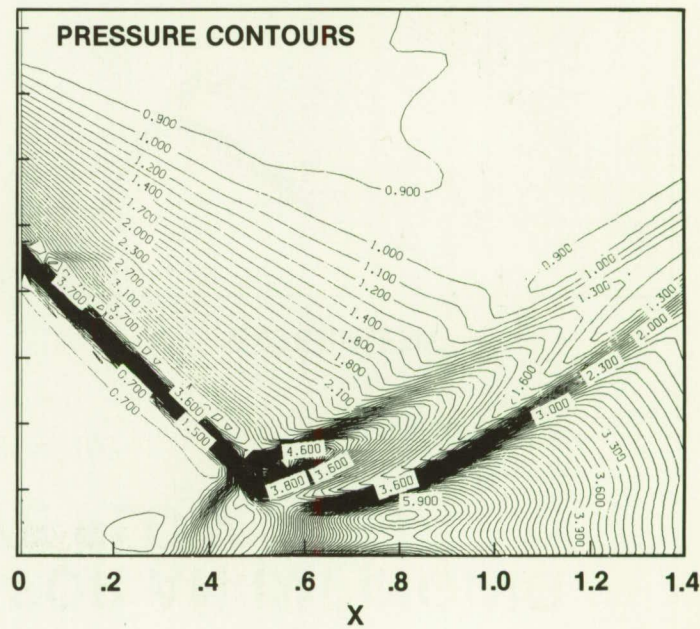
PRESSURE CONTOURS FOR AN IMPINGING SHOCK WAVE FLOW

$M_\infty = 7.2$ $\theta = 15^\circ$

BALDWIN-LOMAX MODEL



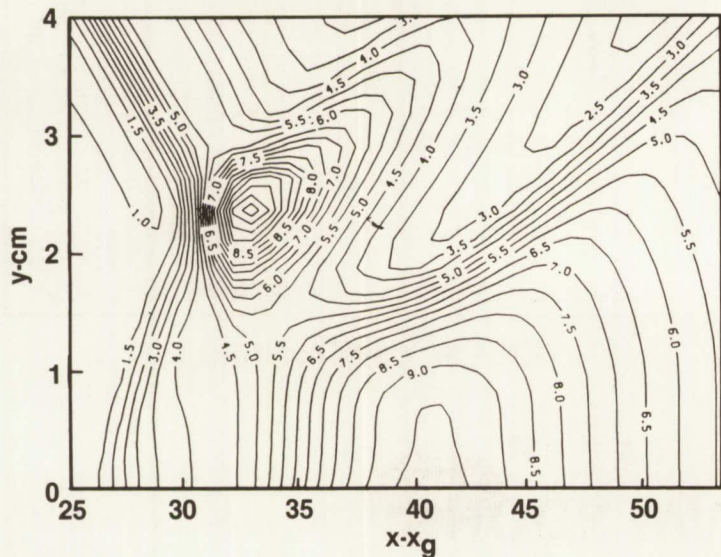
$q \cdot \omega$ MODEL c



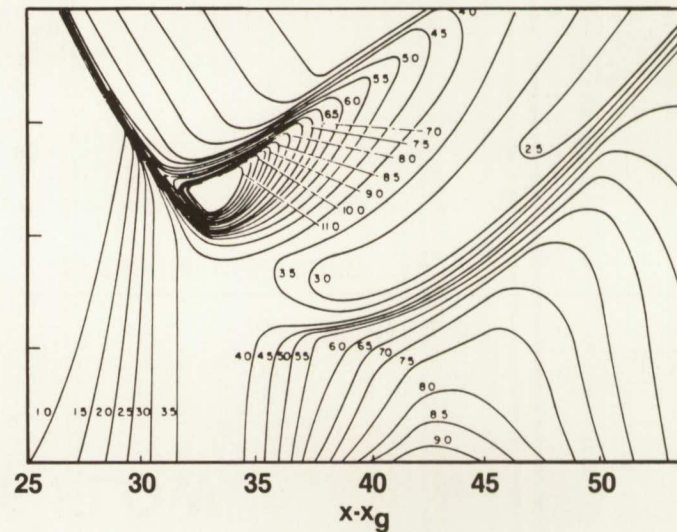
PRESSURE CONTOURS FOR AN IMPINGING SHOCK WAVE FLOW

$M_\infty = 7.2$ $\theta = 15^\circ$

COMPUTATION $q\text{-}\omega$ MODEL C



EXPERIMENT



HYPersonic APPLICATIONS

OBJECTIVE

- DEVELOP CAPABILITY TO COMPUTE REAL-GAS AEROTHERMODYNAMIC CHARACTERISTICS OF HYPERSONIC VEHICLES
- USE CAPABILITY TO GUIDE VEHICLE DESIGNS

APPROACH

- SOLVE 3D REYNOLDS-AVERAGED NAVIER-STOKES AND PARABOLIZED NAVIER-STOKES EQUATIONS USING VARIOUS TRANSITION/TURBULENCE MODELS WITH PERFECT GAS, EQUILIBRIUM REAL GAS AND NONEQUILIBRIUM REAL GAS MODELS

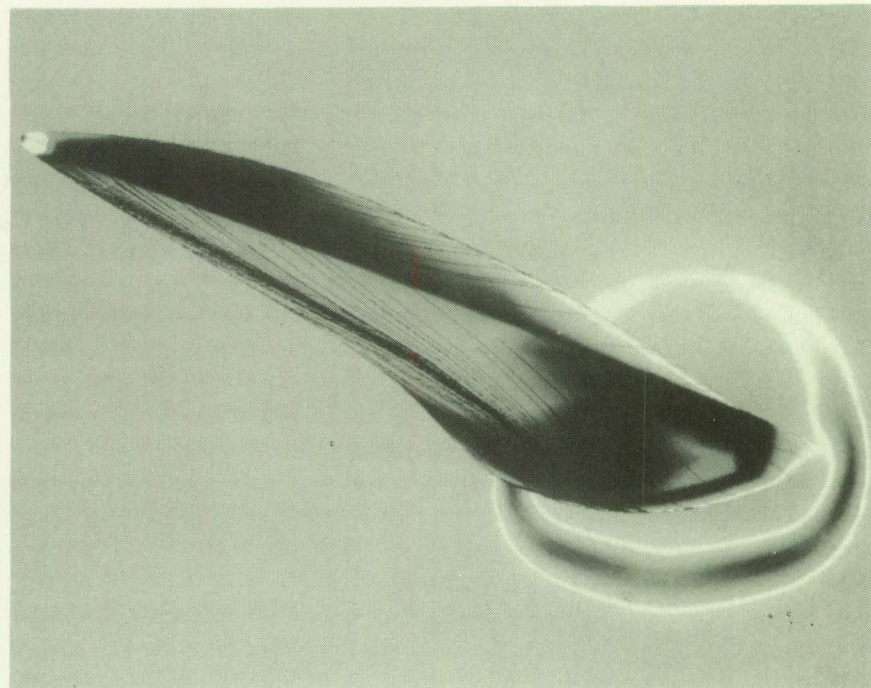
27

FUTURE DIRECTIONS

- IMPROVE TRANSITION/TURBULENCE MODELS, REAL GAS MODELS, AND COMPUTATIONAL EFFICIENCY
- EXTEND APPLICATIONS TO MORE COMPLEX GEOMETRIES

PAYOUT

- PROVIDE DESIGN INFORMATION NOT POSSIBLE TO MEASURE IN GROUND-BASED TEST FACILITIES
- ENABLE DEVELOPMENT OF AEROASSISTED VEHICLES AND AIRBREATHING HYPERSONIC AIRCRAFT

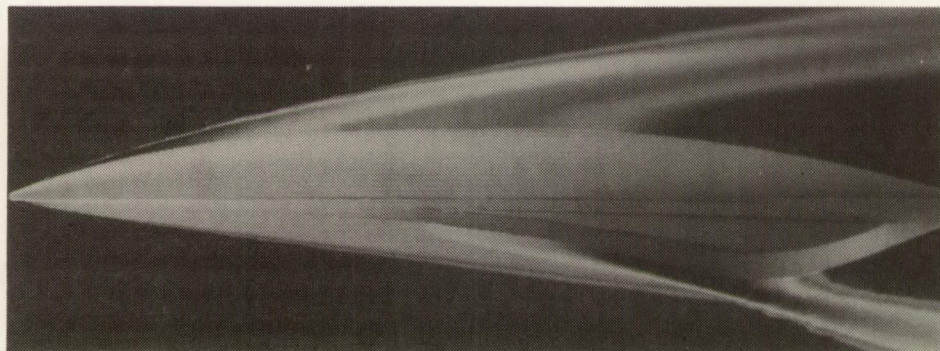


GENERIC HYPERSONIC AEROTHERMODYNAMIC RESULTS

LAWRENCE

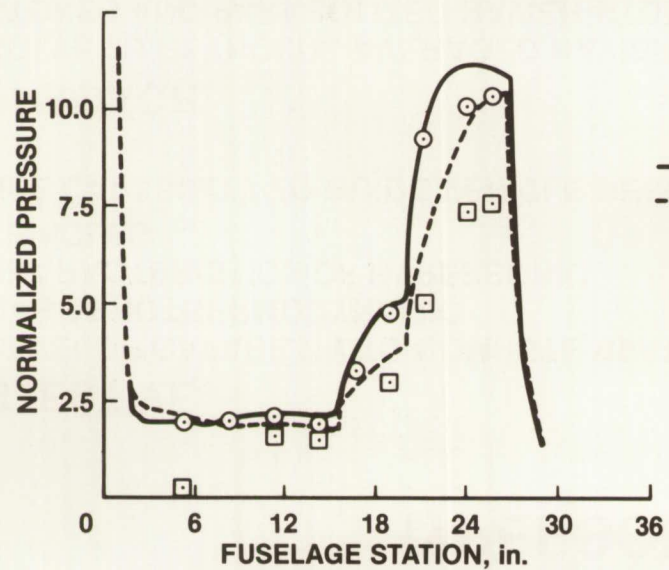
$M_\infty = 11.4, \alpha = 0^\circ, Re_L = 29 \times 10^6$

SYMMETRY PLANE
PRESSURE CONTOURS

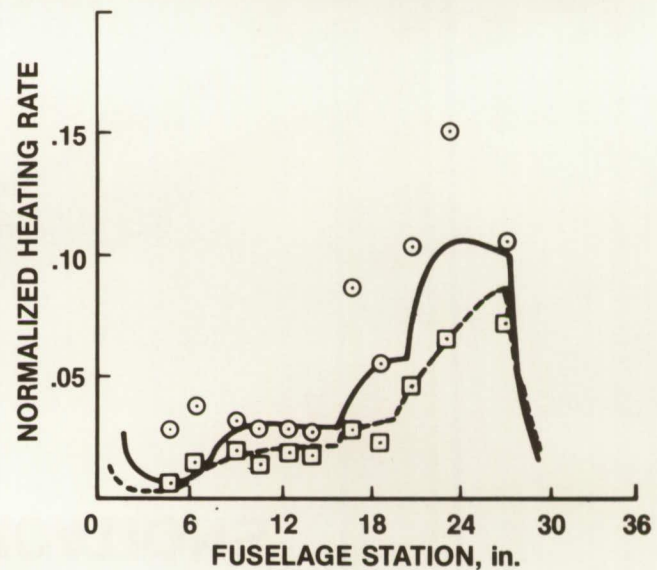


28

WINDWARD SYMMETRY PLANE PRESSURES



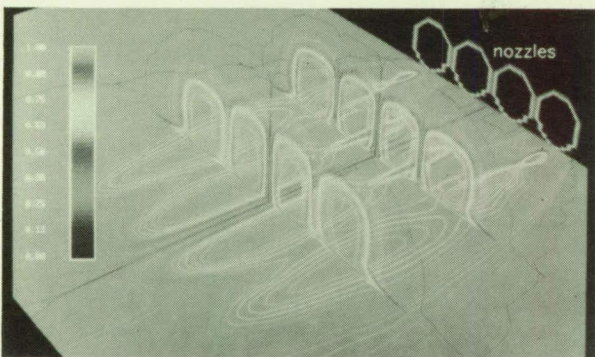
WINDWARD SYMMETRY PLANE HEAT TRANSFER



HYPersonic EXHAUST PLUME/AFTERBODY INTERACTION

EDWARDS

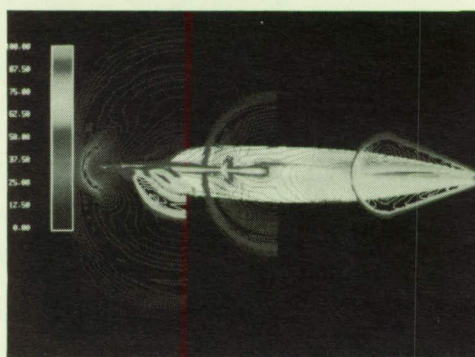
NOZZLE/AFTERSHOCK MODEL



EXHAUST GAS CONCENTRATION
CONTOURS

$M_\infty = 6, \text{NPR} = 4, \alpha = 0^\circ$

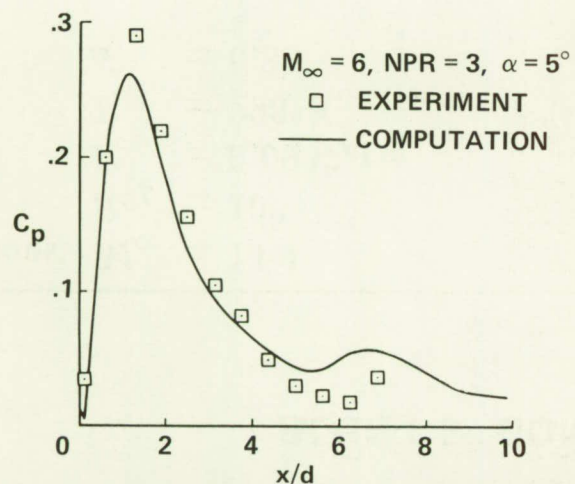
GENERIC HYPERSONIC VEHICLE



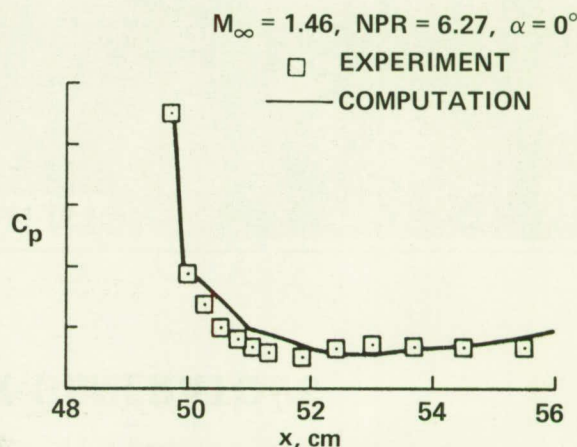
PRESSURE CONTOURS

$M_\infty = 6, \text{NPR} = 100, \alpha = 0^\circ$

29



AFTERBODY PRESSURE COMPARISON
BETWEEN 2ND AND 3RD NOZZLES



PRESSURE COMPARISON
WINDWARD PLANE OF SYMMETRY
DOWNSTREAM OF NOZZLE

BLUNT 5° CONE WITH SHOCK GENERATORS

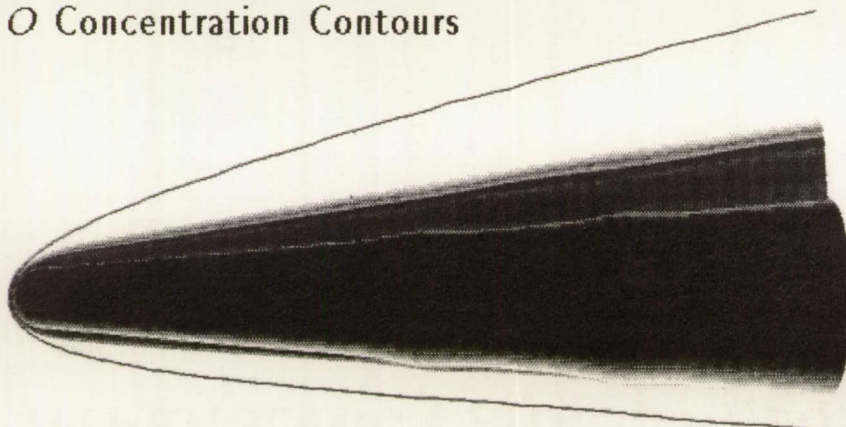
Molvik, Straw

Conditions: $M_\infty = 14.4$
 $Re_L = 10^6$
 $P_\infty = 0.0932 \text{ atm}$
 $T_\infty = 298^\circ \text{K}$
 $\alpha = 6.35^\circ$

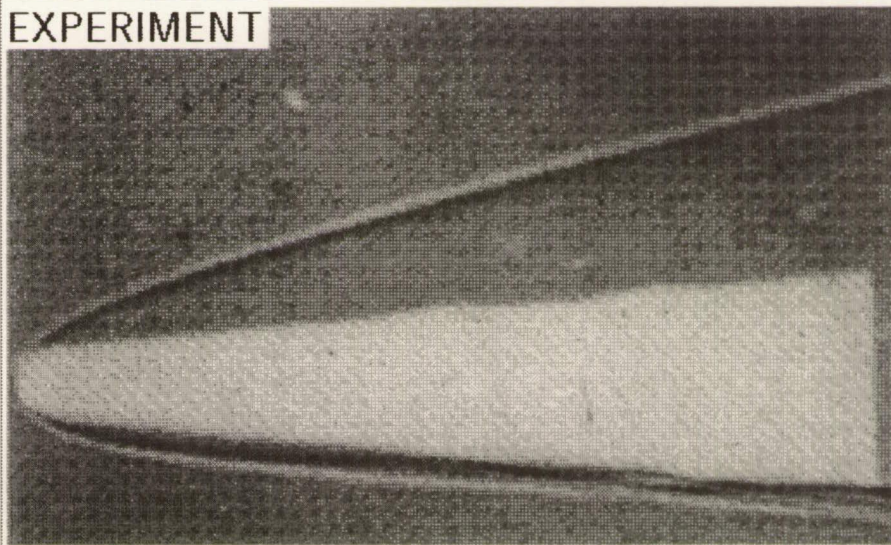
30 Experimental Facility: Ames Ballistic Range

Flow Solvers: Three-Dimensional Navier-Stokes
with Finite Rate Chemistry
(TUFF and STUFF)

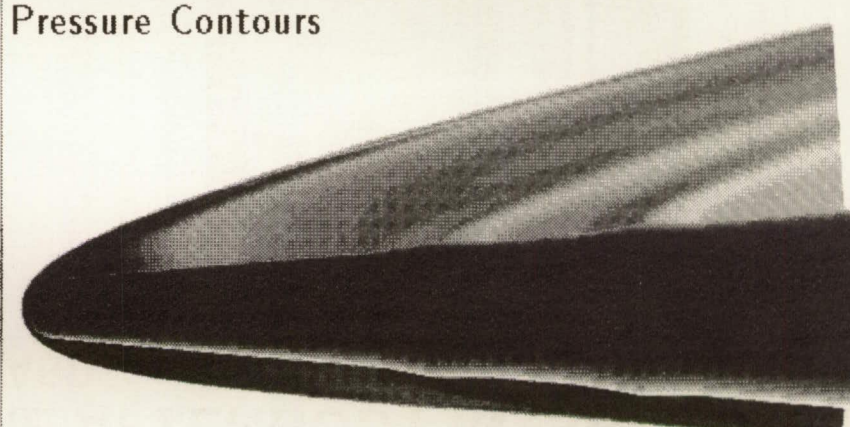
REAL GAS COMPUTATION
 O Concentration Contours



EXPERIMENT



REAL GAS COMPUTATION
Pressure Contours



DIRECT PARTICLE SIMULATION OF HYPERSONIC FLOWS

OBJECTIVE:

- DEVELOP THE CAPABILITIES OF A NEW DISCRETE PARTICLE SIMULATION METHOD FOR RAREFIED HYPERSONIC FLOWS IN 3D WITH NON-EQUILIBRIUM CHEMISTRY.

APPROACH:

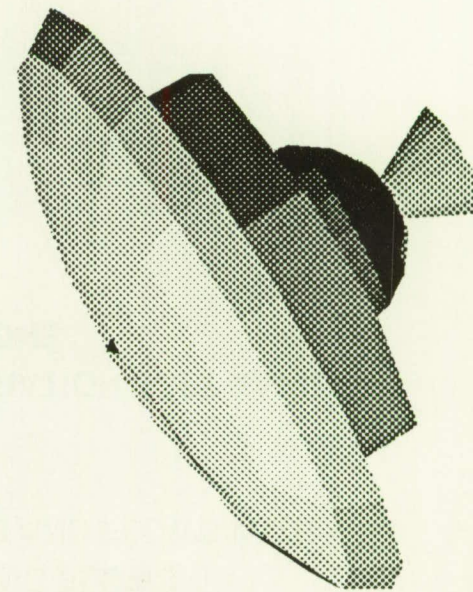
- FLUID IS MODELED AS A LARGE COLLECTION OF DISCRETE PARTICLES THAT INTERACT WITH EACH OTHER THROUGH COLLISIONS.
- SIMPLIFIED PHYSICAL MODELS ARE USED ALLOWING ORDERS OF MAGNITUDE INCREASE IN COMPUTATIONAL EFFICIENCY WHILE ENHANCING STATISTICAL ACCURACY.

FUTURE DIRECTIONS:

- REALISTIC 3D GEOMETRIES WITH MORE GENERAL BOUNDARY CONDITIONS.
- EXTENDED MOLECULAR MODELS TO ACCOUNT FOR ADDITIONAL INTERNAL DEGREES OF FREEDOM, CHEMISTRY AND WALL-PARTICLE INTERACTIONS.

PAYOUT:

- DIRECT PARTICLE SIMULATION IS APPLICABLE AT LOW DENSITIES AND HIGH MACH NUMBERS BEYOND THE REACH OF CONTINUUM METHODS.
- ENABLES PARTICLE SIMULATIONS ON A MUCH LARGER SCALE THAN PREVIOUSLY POSSIBLE.
- PROVIDES NEEDED INSIGHT IN THE DESIGN OF PROPOSED HYPERSONIC VEHICLES.



PRINCIPAL CURRENT LIMITATIONS

PHYSICAL MODELS/ALGORITHMS

- BOUNDARY LAYER TRANSITION MODELS
- TURBULENCE MODELS FOR SEPARATING AND REATTACHING FLOWS
- TRANSITION/TURBULENCE MODELS FOR REAL GAS FLOWS AND FLOWS WITH COMBUSTION
- REAL GAS FLOW VALIDATION DATA
- FAST, USER FRIENDLY GEOMETRY DEFINITION/GRID GENERATION SOFTWARE
- FAST, ACCURATE ALGORITHMS FOR COMPLETE SIMULATIONS
- SCIENTIFIC VISUALIZATION SOFTWARE

COMPUTER SYSTEMS

- COMPUTATIONAL SPEED
- NETWORK BANDWIDTHS
- HIGH-SPEED LARGE-VOLUME MASS STORAGE
- TOOLS FOR ANALYZING MASSIVE RESULT FILES

FUTURE DIRECTIONS

ALGORITHM RESEARCH

- IMPROVED ALGORITHMS FOR COMPUTING REAL-GAS TURBULENT FLOWS
- NEW ALGORITHMS TO EXPLOIT ADVANCED MULTIPLE PROCESSOR COMPUTER ARCHITECTURES
- NEW GRID-GENERATION CONCEPTS FOR COMPLEX CONFIGURATIONS, MULTIPLE MOVING BODIES AND UNSTEADY FLOWS

TURBULENCE RESEARCH

- IMPROVED TURBULENCE MODELS FOR PERFECT-GAS SEPARATING AND REATTACHING FLOWS
- NEW TURBULENCE MODELS FOR REAL-GAS FLOWS
- METHODS FOR MANAGING TURBULENCE TO REDUCE DRAG, IMPROVE COMPONENT PERFORMANCE, MINIMIZE HEAT TRANSFER, AND CONTROL COMBUSTION PROCESSES

MULTIDISCIPLINARY RESEARCH

- NUMERICAL METHODS FOR SOLVING FULLY COUPLED COMBINATIONS OF EQUATIONS FOR AERODYNAMICS, GAS CHEMISTRY, STRUCTURES, CONTROLS, PROPULSION AND ELECTROMAGNETICS

FUTURE DIRECTIONS (CONCLUDED)

GRAPHICS AND WORKSTATION RESEARCH

- IMPROVED USER EFFICIENCY THROUGH ADVANCES IN GRAPHICS AND WORKSTATION TECHNOLOGY**

34

APPLICATIONS CODES

- AIRCRAFT MANEUVERING NEAR PERFORMANCE BOUNDARIES**
- POWERED LIFT AIRCRAFT OPERATING IN AND OUT OF GROUND EFFECT**
- HYPERSONIC VEHICLES INCLUDING INLET, ENGINE AND EXHAUST FLOWS**
- ROTORCRAFT IN HOVER, TRANSITION AND FORWARD FLIGHT**
- TURBOMACHINERY INCLUDING PUMPS, COMPRESSORS AND TURBINES**
- METHODS FOR NUMERICALLY OPTIMIZING DESIGNS**
- DESIGNER-FRIENDLY CODES WITH 'EXPERT SYSTEMS' ELEMENTS**

COMPUTATIONAL FLUID DYNAMICS RESEARCH AND APPLICATIONS AT NASA Langley Research Center

**Jerry C. South, Jr.
Head, Analytical Methods Branch
Fluid Mechanics Division**

Research at Langley includes all aeronautics disciplines and selected space disciplines. Nearly all the aeronautics disciplines have a significant component of CFD research which complements wind-tunnel and flight experimental research; in space research, aerothermodynamics of planetary entry vehicles is heavily dependent on CFD as a research tool. Langley's CFD strategy contains four major thrusts: Focus efforts on critical CFD barriers; focus efforts on critical aerodynamics barriers; validate CFD codes; and transfer technology to United States users. The Langley presentations in this conference are representative of our strategy. They are grouped in six broad areas:

1. Direct Simulation of Transition and Turbulence
2. Hypervelocity Aerothermodynamics and Rarified Flows
3. Hypersonic External and Internal (scramjet) Flows
4. Unsteady Aerodynamics and Aeroelasticity Applications
5. Grid Generation and Applications for Complex Configurations
6. Supersonic and Transonic Wing Design Applications

35

Three examples of important work not shown in this conference are described in the conclusion of the presentation.

NOV-10841

LANGLEY CFD STRATEGY

- FOCUS EFFORT ON CRITICAL CFD BARRIERS
 - GRIDS & ALGORITHMS FOR COMPLEX CONFIGURATIONS
 - TRANSITION & TURBULENCE MODELS FOR RANS CODES
 - NEW ALGORITHMS FOR MASSIVELY-PARALLEL PROCESSORS
 - ENABLE ROUTINE APPLICATIONS
- FOCUS EFFORT ON CRITICAL AERODYNAMICS BARRIERS
 - DIRECT SIMULATION OF TRANSITION AND TURBULENCE
 - SIMULATION/PREDICTION OF HIGH-ALPHA FLOWS
 - SIMULATION/PREDICTION OF HYPersonic PROPULSION

LANGLEY CFD STRATEGY (Concluded)

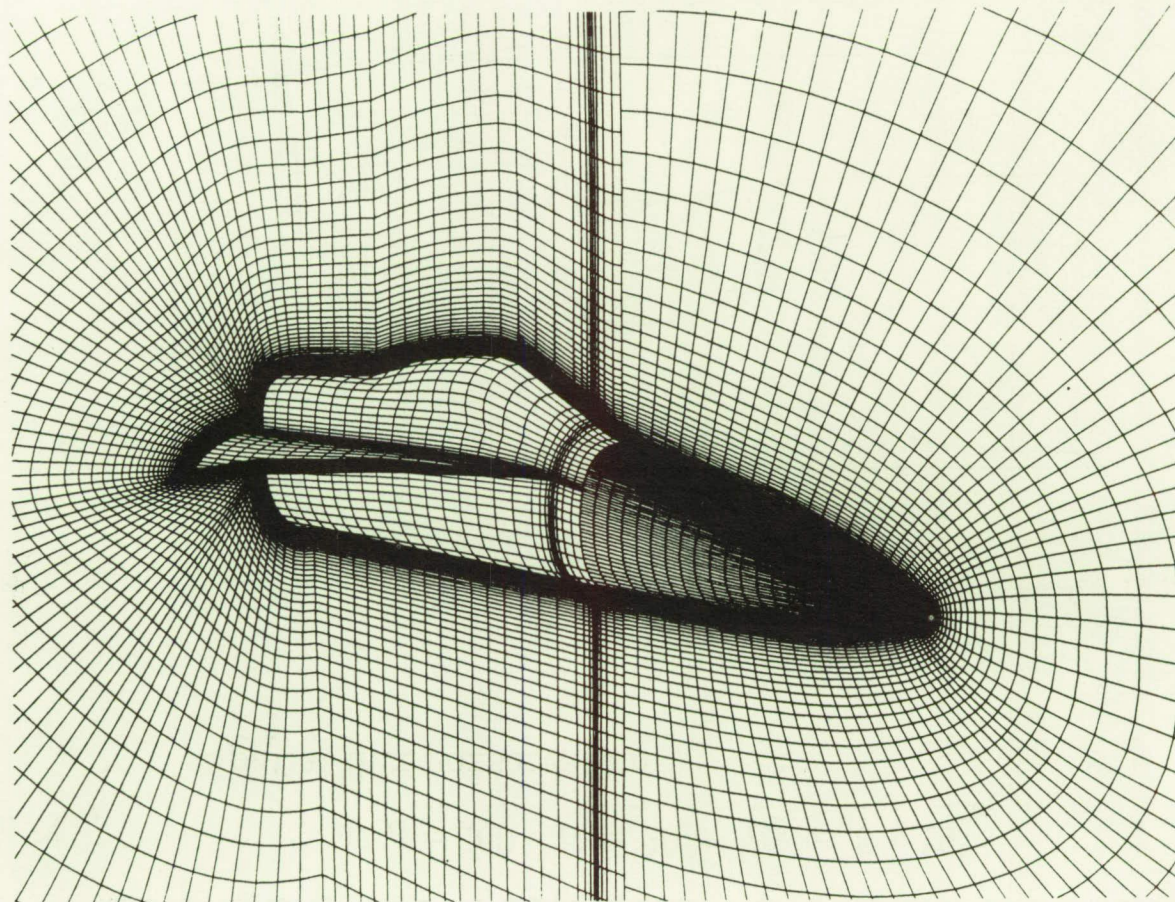
- **VALIDATE CFD CODES**
 - CODE-ON-CODE
 - CODE-ON-EXPERIMENT (GROUND & FLIGHT)
- **TRANSFER TECHNOLOGY**
 - RESEARCHER EXCHANGES (ARC ↔ LaRC ↔ LeRC)
 - NAS NETWORK DATA/CODE EXCHANGES
 - TRAINING APPLICATIONS RESEARCHERS

CFD FIVE-YEAR PLAN

THRUST	YEAR					GOAL
	89	90	91	92	93	
CFD DEVELOPMENT						PREDICTIVE CAPABILITY FOR COMPLEX 3D VISCOUS FLOWS FOR ADVANCED A/C MISSILES, & PROP. SYS.
	IMPROVE SPEED/ACCURACY N-S STOKES					
	COMPLEX GEOMETRY/GRIDS					
	PARALLEL PROCESSOR ALGORITHMS					
	TRANSITION & TURBULENCE MODELS					
	HIGH-SPEED REACTING FLOWS					
FLOW PHYSICS						HIGHLY DETAILED DATA BASE TO EXTRACT UNDER- STANDING OF PHYSICS OF 2D & 3D FLOWS
	LOW SPEED-TRANSITION, TURB., & SEPARATION					
	HIGH SPEED TRANSITION & TURB.					
	TURBULENCE/CHEM. KINETICS INTERACTION					

3-BLOCK GRID TOPOLOGY

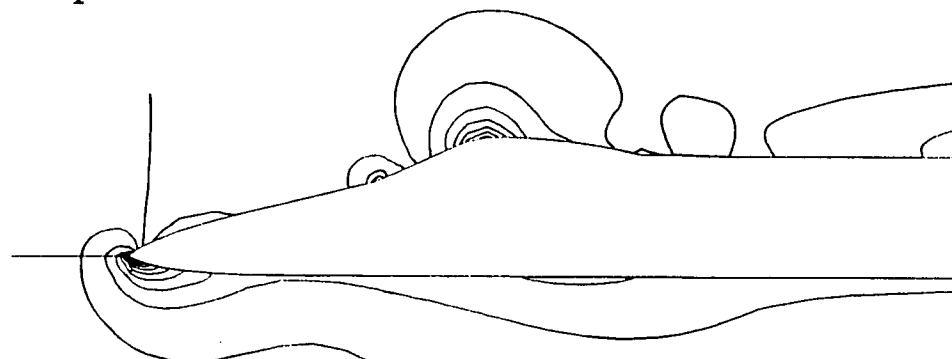
Nearfield view F-18 ; 300,000 points total



EFFECT OF PATCHING ALGORITHM

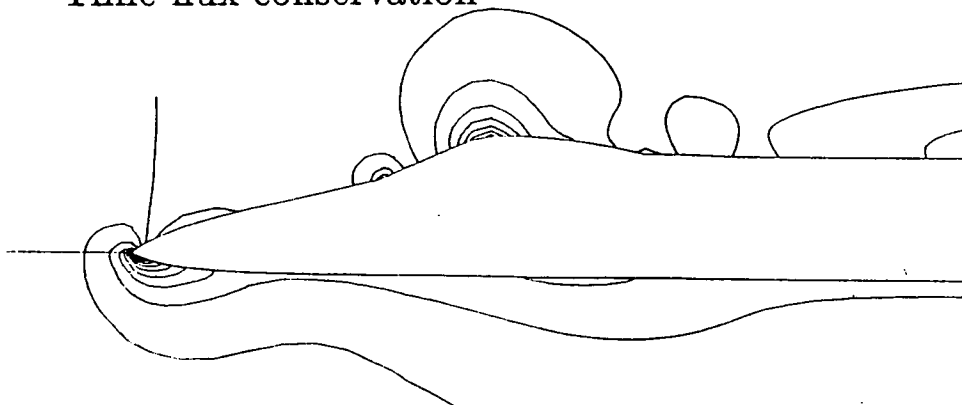
$$M_\infty = .60 \quad \alpha = 20^\circ \quad R_c = .8 \times 10^6$$

Spatial-flux conservation



04

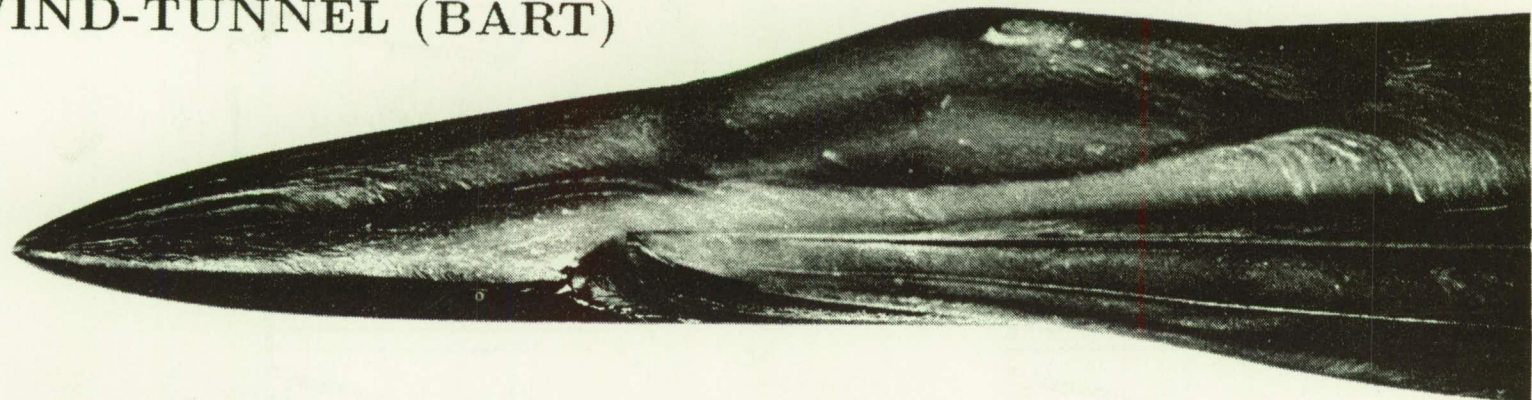
Time-flux conservation



F-18 SURFACE FLOW

$$\alpha = 30^\circ \quad R_c = 2.7 \times 10^6$$

WIND-TUNNEL (BART)



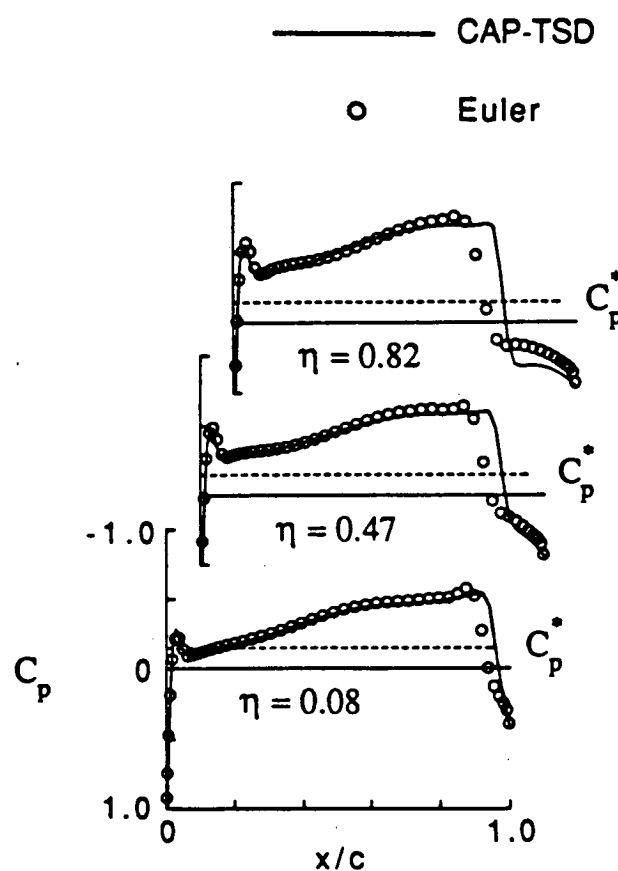
14

NAVIER-STOKES (CFL3D)

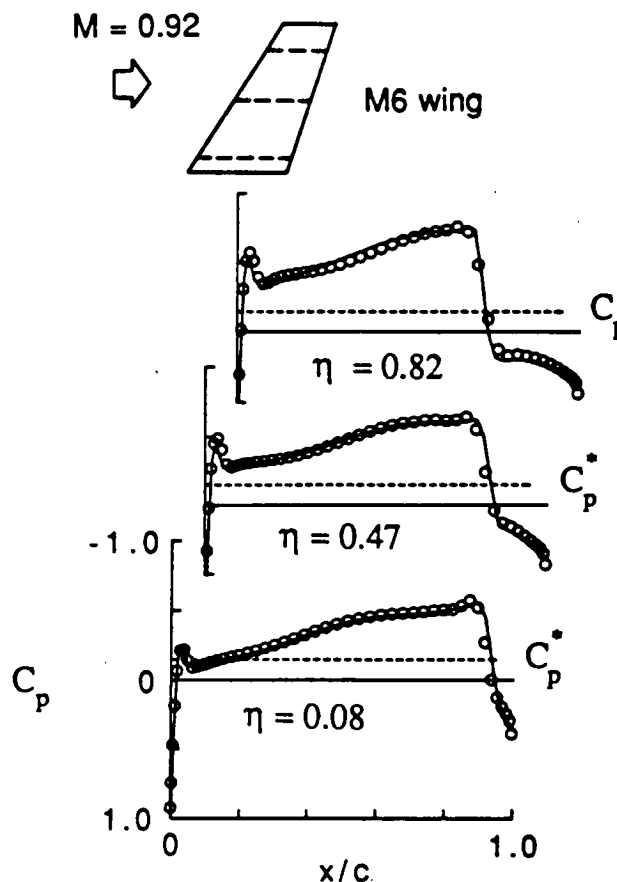


ENTROPY AND VORTICITY EFFECTS IMPROVE ACCURACY OF UNSTEADY TRANSONIC SMALL-DISTURBANCE (TSD) THEORY

- UNMODIFIED THEORY GIVES INACCURATE SHOCK PREDICTION

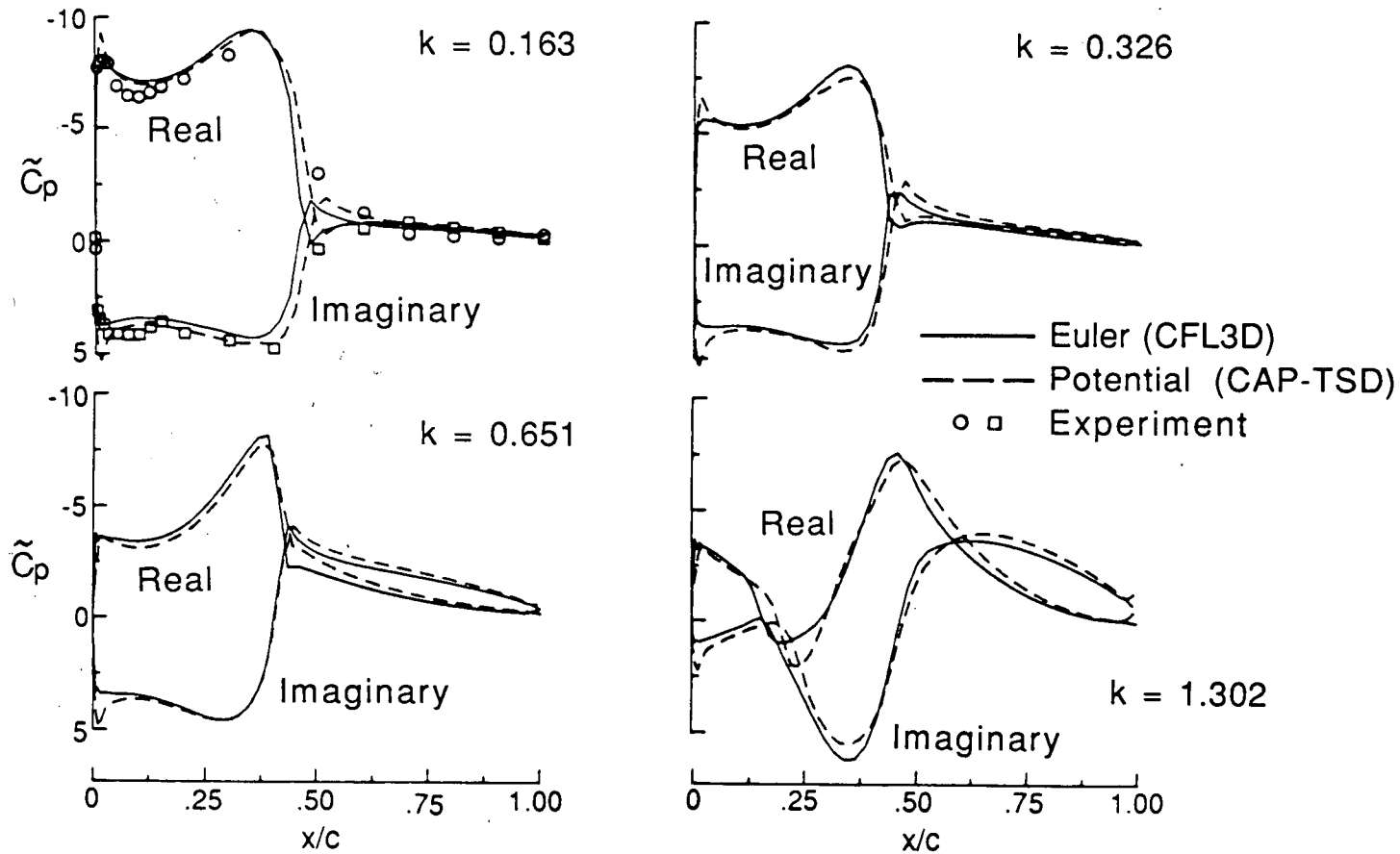


- ENTROPY AND VORTICITY CORRECTIONS YIELD EULER-LIKE RESULTS



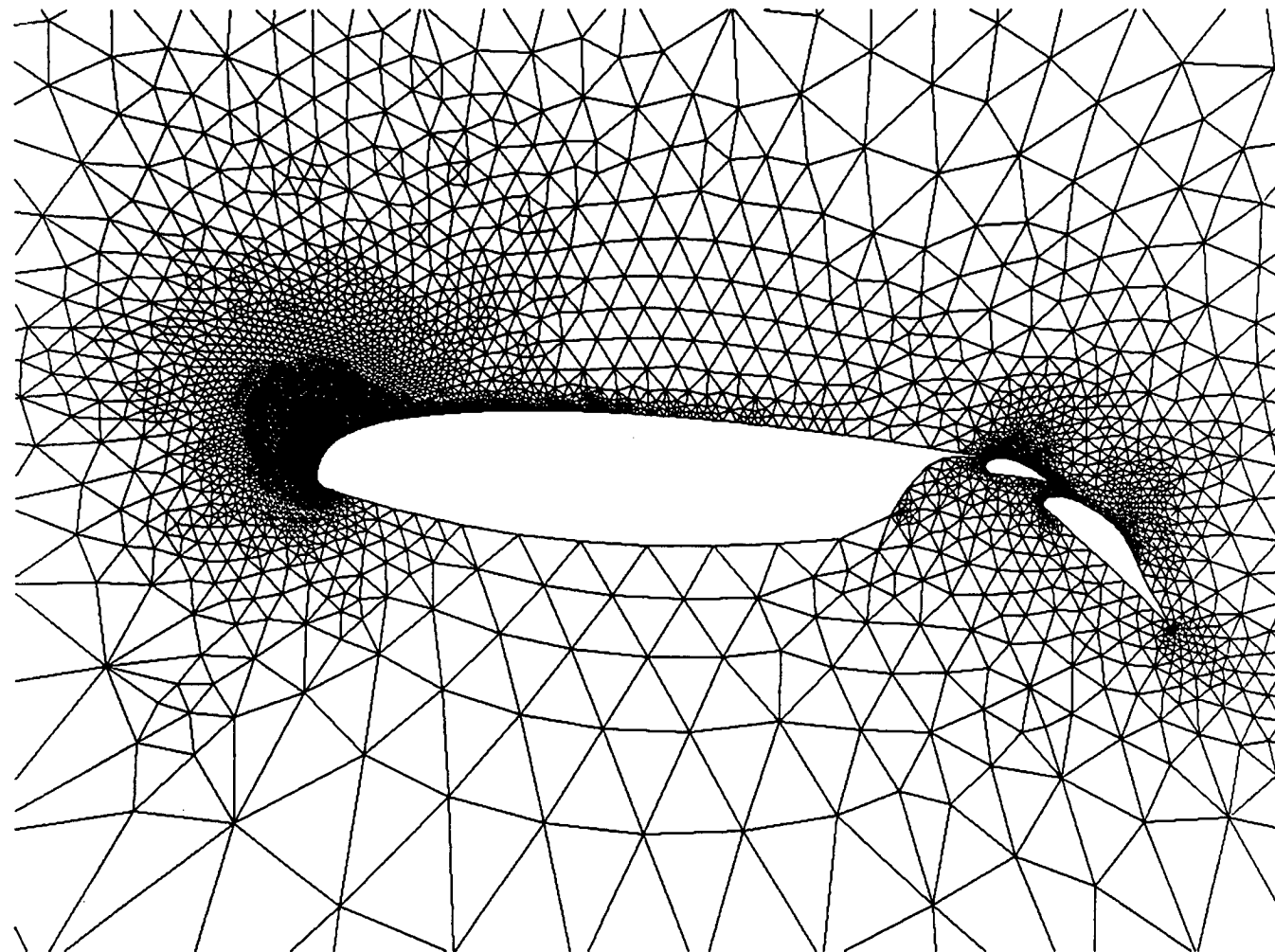
EFFECTS OF REDUCED FREQUENCY ON FIRST HARMONIC COMPONENTS OF UNSTEADY PRESSURES DUE TO AIRFOIL PITCHING

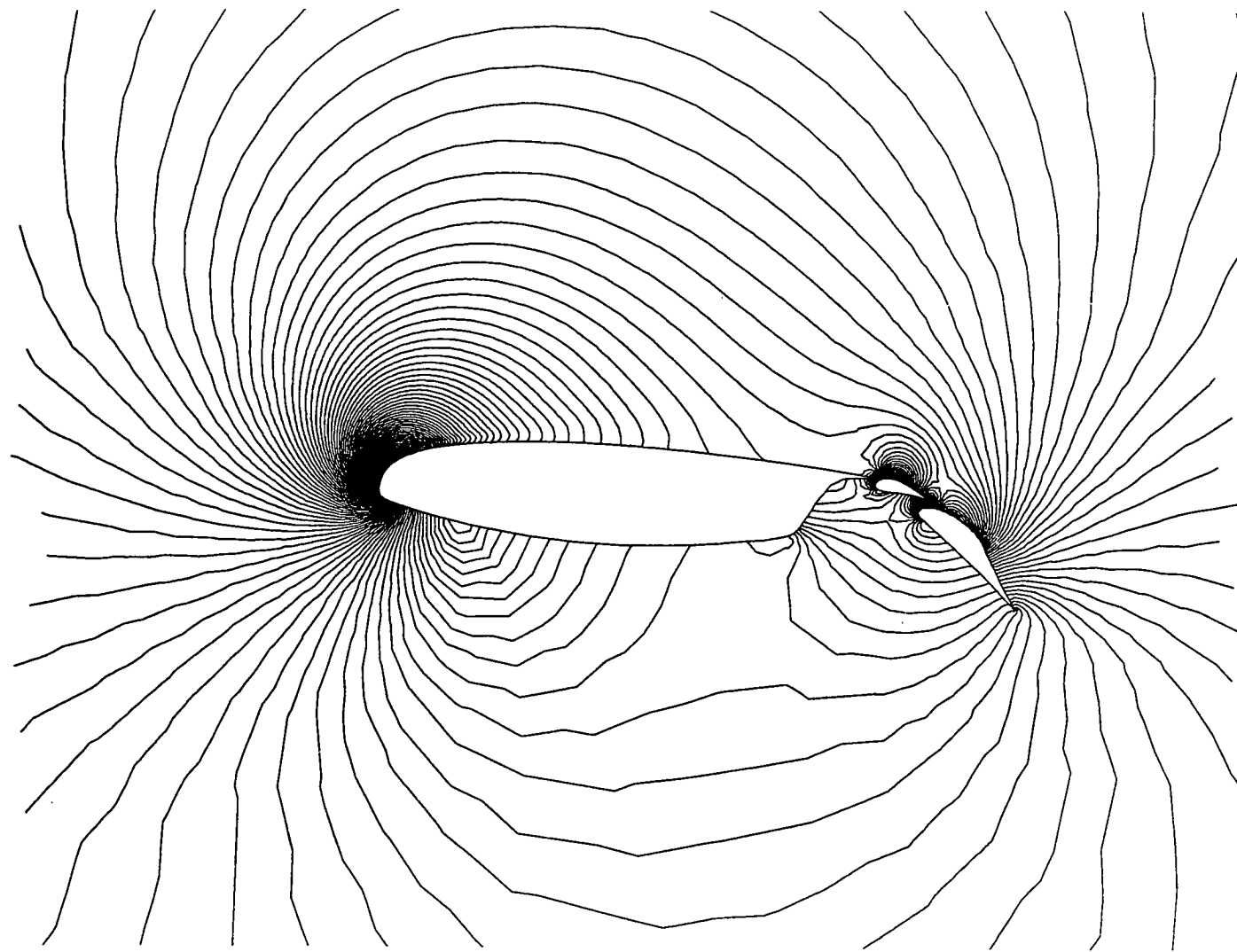
- NACA 0012 airfoil at $M_\infty = 0.755$, $\alpha_0 = 0.016^\circ$, $\alpha_1 = 2.51^\circ$



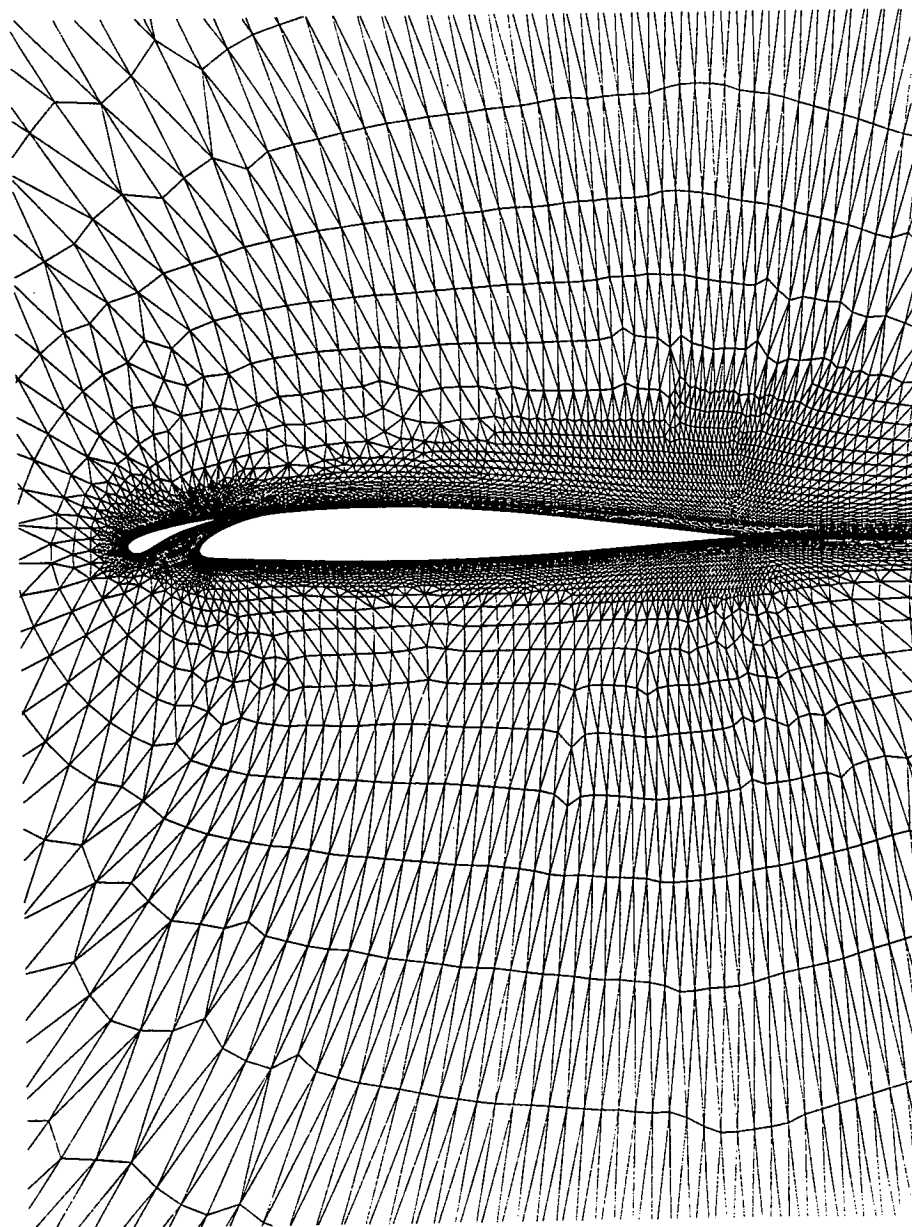
UNSTRUCTURED ADAPTIVE GRID FOR INVISCID SOLUTION
FOR 3-ELEMENT AIRFOIL (MAVRIPPLIS, ICASE)

44

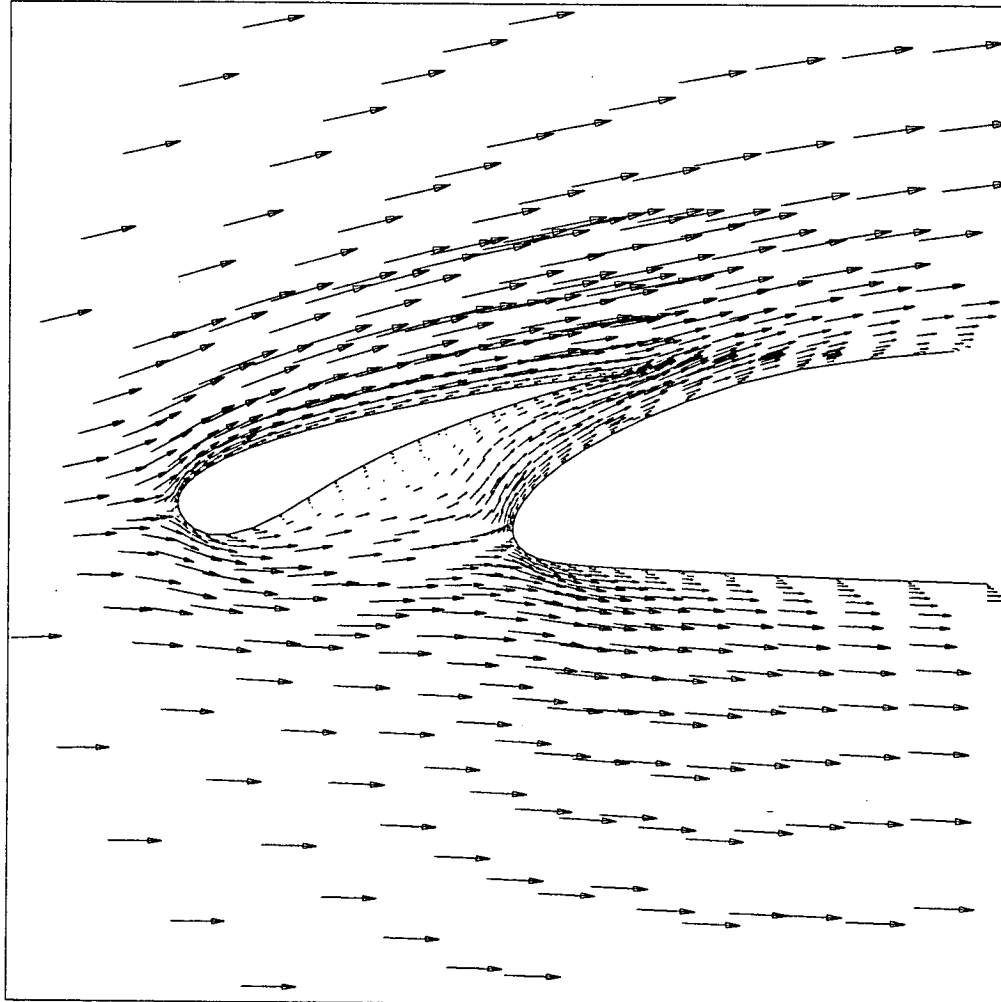




FINITE-VOLUME EULER SOLUTION FOR 3-ELEMENT AIRFOIL (MAVRIPPLIS, ICASE)



UNSTRUCTURED GRID FOR AIRFOIL WITH SLAT. HIGHLY-STRETCHED TRIANGLES TO RESOLVE LAMINAR BOUNDARY LAYER.
(MAVRIPPLIS, ICASE)



LAMINAR NAVIER-STOKES CALCULATIONS ON UNSTRUCTURED MESH IN SLAT REGION (MAVRIPPLIS, ICASE)

N91-10842

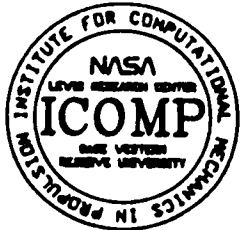
Computational Fluid Dynamics at the Lewis Research Center
An Overview

By
Robert M. Stubbs
NASA-Lewis Research Center
Cleveland, Ohio 44135

Lewis is a multidisciplinary Center with strong research and development programs in aeronautical and space propulsion, power, space communications, space experiments and materials. Computational fluid dynamics (CFD) is playing an important and growing role in most of these areas. This presentation describes how CFD is integrated into these programs and highlights elements of the CFD activities. Examples are presented of codes developed to predict flow fields in advanced propulsion systems and several of the code validation experiments are described. As will be evident in the several Lewis authored papers to be presented at this conference, the CFD effort at Lewis ranges from basic research on new and improved algorithms through code development to the application of these codes to specific engineering problems. Because of the substantial improvement in CFD's predictive capability its use at Lewis is on a steep growth path, spreading rapidly into new areas which had not traditionally taken advantage of the techniques of numerical simulation. The presentation concludes with a discussion of multidisciplinary codes and the future direction of CFD at Lewis.

LEWIS COMPUTER RESOURCES

- **CRAY X-MP/24**
- **SCIENTIFIC VAX CLUSTER**
- **2 AMDAHLs (VM/CMS AND MVS/XA)**
- **ALLIANT FX/8 PARALLEL PROCESSOR**
- **ADVANCED WORK STATIONS (SILICON GRAPHICS, SUN, APOLLO)**
- **T1 LINK TO NAS**



INSTITUTE FOR COMPUTATIONAL MECHANICS IN PROPULSION

OBJECTIVE

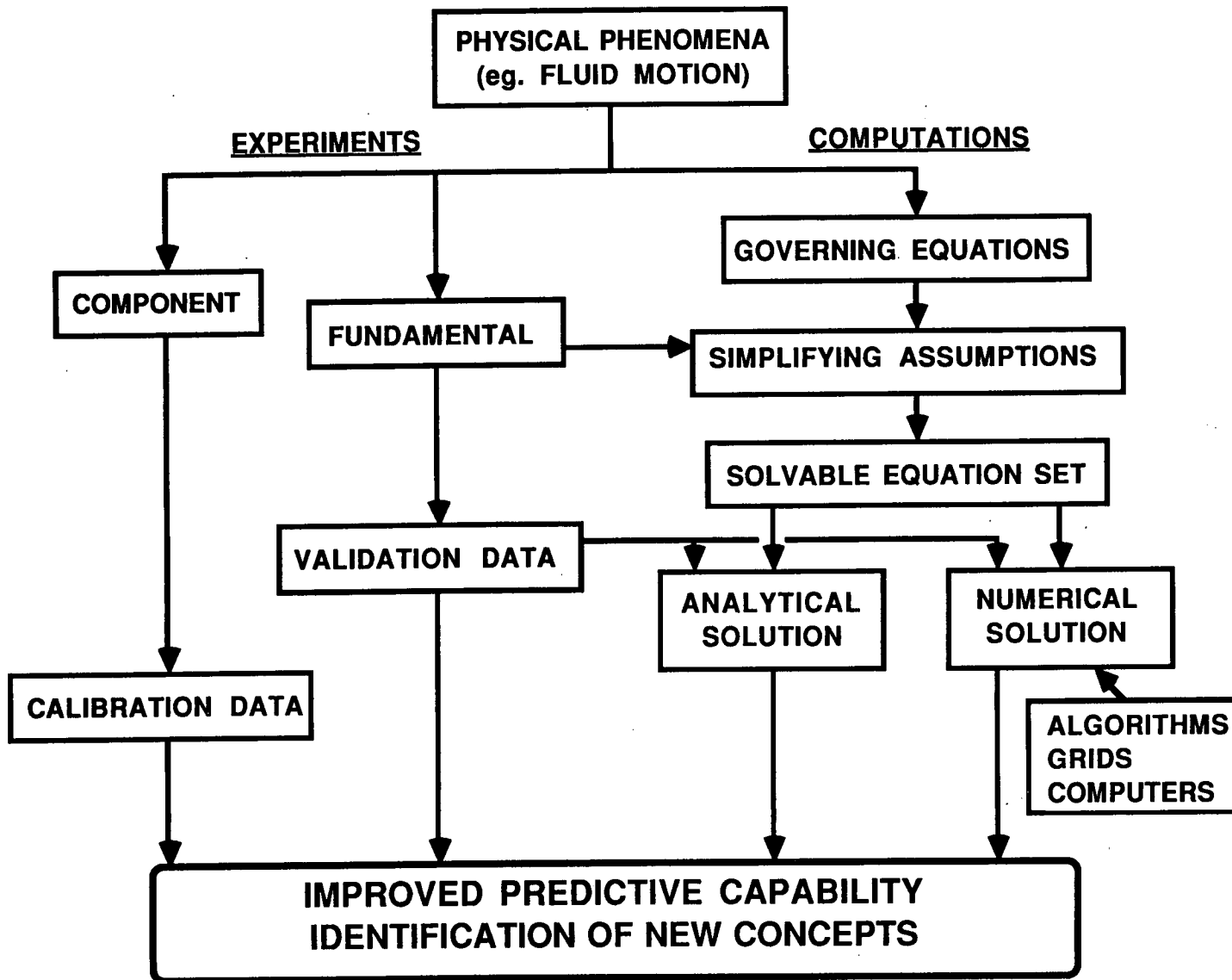
- o TO DEVELOP ADVANCED COMPUTATIONAL METHODS REQUIRED FOR THE SOLUTION OF INTERNAL FLUID MECHANICS AND STRUCTURAL PROBLEMS

51

ROLE

- o GENERATE NEW IDEAS/APPROACHES TO PROPULSION RESEARCH THROUGH INTERACTION WITH LeRC STAFF
- o PROVIDE OPPORTUNITY TO ICOMP PERSONNEL TO DO ORIGINAL RESEARCH UTILIZING WORLD-CLASS COMPUTERS

CFD'S ROLE IN THE PROBLEM SOLVING PROCESS

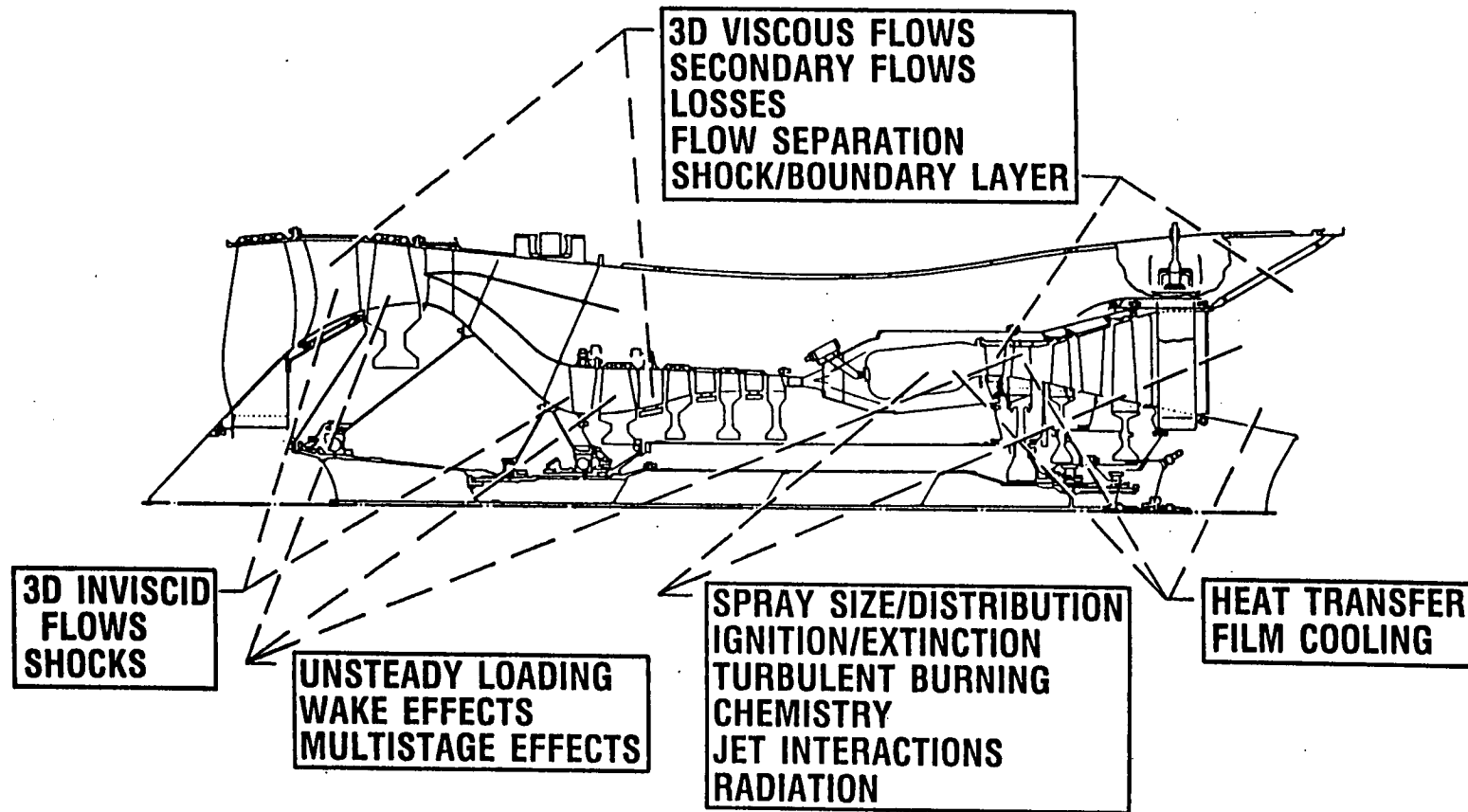


COMPUTATIONAL FLUID DYNAMICS AT LEWIS

WHERE DOES CFD PLAY A ROLE?

- AERO PROPULSION
- SPACE PROPULSION
- OTHER
 - SPACE POWER
 - MATERIALS PROCESSING
 - FLUIDS IN MICROGRAVITY

CONCEPTUAL ADVANCED TURBOFAN ENGINE PHYSICAL PHENOMENA REQUIRING ANALYSES



RVC3D (ROTOR VISCOUS CODE 3-D)

BY DR. R. V. CHIMA

- NAVIER-STOKES ANALYSIS FOR 3D FLOWS IN TURBOMACHINERY**
- STACKED C-TYPE GRIDS FOR AXIAL OR CENTRIFUGAL MACHINES**
- THIN-LAYER NAVIER-STOKES FORMULATION RETAINS HUB-TO-TIP AND BLADE-TO-BLADE VISCOUS TERMS**
- BALDWIN-LOMAX TURBULENCE MODEL**
- EXPLICIT 4-STAGE RUNGE-KUTTA TIME-MARCHING SCHEME WITH VARIABLE TIME STEP AND IMPLICIT RESIDUAL SMOOTHING**
- HIGHLY VECTORIZED FOR CRAY X-MP**

RPLUS 3D

BY DRS. S.T. YU, J. S. SHUEN & P. TSAI

- **3D NAVIER-STOKES CODE FOR CHEMICALLY REACTING FLOWS**
- **FINITE RATE CHEMISTRY MODEL**
 - o 9 SPECIES INVOLVING O, H, AND N
 - o 18 REACTION STEPS
- **TIME-MARCHING LU SCHEME**
- **FAST AND ROBUST**

PROTEUS

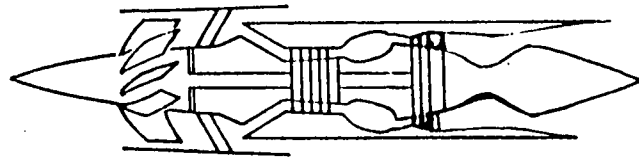
- **IMPLICIT 2D AND 3D NAVIER-STOKES CODE**
- **READILY MODIFIED, WELL DOCUMENTED GENERAL SOLVER**
- **FULL, COMPRESSIBLE NAVIER-STOKES WITH ENERGY EQUATION**
- **EULER AND THIN-LAYER OPTIONS**
- **LINEARIZED BLOCK IMPLICIT (LBI) SOLVER**
- **IMPLICIT BOUNDARY CONDITIONS**
- **FIRST OR SECOND ORDER IN TIME**
- **ALGEBRAIC (BALDWIN-LOMAX) AND 2-EQUATION TURBULENCE MODELS CURRENTLY BEING IMPLEMENTED**

MULTISTAGE AVERAGE PASSAGE CODE

BY DR. JOHN ADAMCZYK

- MULTISTAGE SIMULATIONS FOR ARBITRARY GEOMETRIES**
- 3D VISCOUS**
- EXPLOITS MACROTASKING**
- FIRST SIMULATION OF A 3D MULTISTAGE TURBINE**
- COMPATIBLE WITH THE DESIGN ENVIRONMENT**
- CODE/METHODOLOGY CURRENTLY BEING USED IN DESIGN OF TURBOMACHINERY**

PUTTING IT ALL TOGETHER



65

INLETS, DUCTS,
AND NOZZLES

TURBOMACHINERY

CHEMICAL
REACTING
FLOWS

COMPUTATIONAL
AND EXPERIMENTAL
TECHNOLOGY

INTEGRATED MULTIDISCIPLINARY ANALYSIS AND TEST

NUMERICAL PROPULSION SYSTEM SIMULATION

LEWIS RESEARCH CENTER

NUMERICAL SIMULATION OF NONLINEAR DEVELOPMENT OF INSTABILITY WAVES	R. MANKBADI
TIME DEPENDENT VISCOUS INCOMPRESSIBLE NAVIER-STOKES EQUATIONS	J. GOODRICH
PROGRESS TOWARD THE DEVELOPMENT OF AN AIRFOIL ICING ANALYSIS CAPABILITY	M. POTAPCZUK C. BIDWELL B. BERKOWITZ
THE BREAKUP OF TRAILING-LINE VORTICES	D. JACQMIN
THREE DIMENSIONAL SIMULATION OF SUPERSONIC REACTING FLOWS WITH FINITE RATE CHEMISTRY	S. YU J. SHUEN P. TSAI
SIMULATION OF TURBOMACHINERY FLOWS	J. ADAMCZYK
AUTOMATED DESIGN OF CONTROLLED DIFFUSION BLADES	J. SANZ
NUMERICAL ANALYSIS OF FLOW THROUGH OSCILLATING CASCADE SECTIONS	D. HUFF
NUMERICAL ANALYSIS OF THREE-DIMENSIONAL VISCOUS INTERNAL FLOWS	R. CHIMA J. YOKOTA
A NUMERICAL STUDY OF THE HOT GAS ENVIRONMENT AROUND A STOVL AIRCRAFT IN GROUND PROXIMITY	T. VAN OVERBEKE J. HOLDEMAN
CFD ANALYSIS FOR HIGH SPEED INLETS	T. BENSON
FLUX SPLITTING ALGORITHMS FOR TWO-DIMENSIONAL REAL GAS FLOWS	J. SHUEN M. LIOU

FUTURE DIRECTIONS

- **SEVERAL FACTORS CONTRIBUTING TO A CFD EXPLOSION AT LEWIS**
 - IMPROVED PREDICTIVE CAPABILITY
 - INCREASE IN MACHINE CAPACITY AND AVAILABILITY
- **CFD NO LONGER LOCALIZED, NOW IN WIDE USE IN SEVERAL DISCIPLINE AREAS**
- **GROWING EMPHASIS ON MULTIDISCIPLINARY SYSTEM SIMULATIONS**

SESSION II

CENTER OVERVIEWS

(Continued)

Chairman:
Paul Kutler
Chief, Fluid Dynamics Division
NASA Ames Research Center

N91-10843

Marshall Space Flight Center CFD Overview

L. A. Schutzenhofer, NASA/MSFC

Computational Fluid Dynamics (CFD) activities at Marshall Space Flight Center (MSFC) have been focused on hardware specific and research applications with strong emphasis upon benchmark validation. The purpose of this overview is to provide insight into the MSFC CFD related goals, objectives, current hardware related CFD activities, propulsion CFD research efforts and validation program, future near-term CFD hardware related programs, and CFD expectations. The current hardware programs where CFD has been successfully applied are the Space Shuttle Main Engines (SSME), Alternate Turbopump Development (ATD), and Aeroassist Flight Experiment (AFE). For the future near-term CFD hardware related activities, plans are being developed that address the implementation of CFD into the early design stages of the Space Transportation Main Engine (STME), Space Transportation Booster Engine (STBE), and the Environmental Control And Life Support System (ECLSS) for the Space Station. Finally, CFD expectations in the design environment will be delineated.

MARSHALL SPACE FLIGHT CENTER CFD OVERVIEW

- COMPUTATIONAL FLUID DYNAMICS BRANCH ACTIVITIES
 - OBJECTIVES
 - INTERACTION
 - APPROACH TOWARD SOLUTIONS OF COMPLEX FLOWS
- MSFC HARDWARE RELATED ACTIVITIES
 - INHOUSE
 - ROCKETDYNE - SSME
 - PRATT AND WHITNEY - ATD
- NASA EARTH-TO-ORBIT PROPULSION R&T PROGRAM
 - PROGRAM DEFINITION
 - WORK ELEMENT SUMMARY; CFD EMPHASIS
 - EXPERIMENTAL APPARATUS
 - CONSORTIUM
- NEW NEAR TERM CFD ACTIVITIES
 - ADVANCED LAUNCH SYSTEM, ALS
 - ENVIRONMENTAL CONTROL AND LIFE SUPPORT SYSTEM, ECLSS
- CFD EXPECTATIONS

COMPUTATIONAL FLUID DYNAMICS BRANCH ACTIVITIES

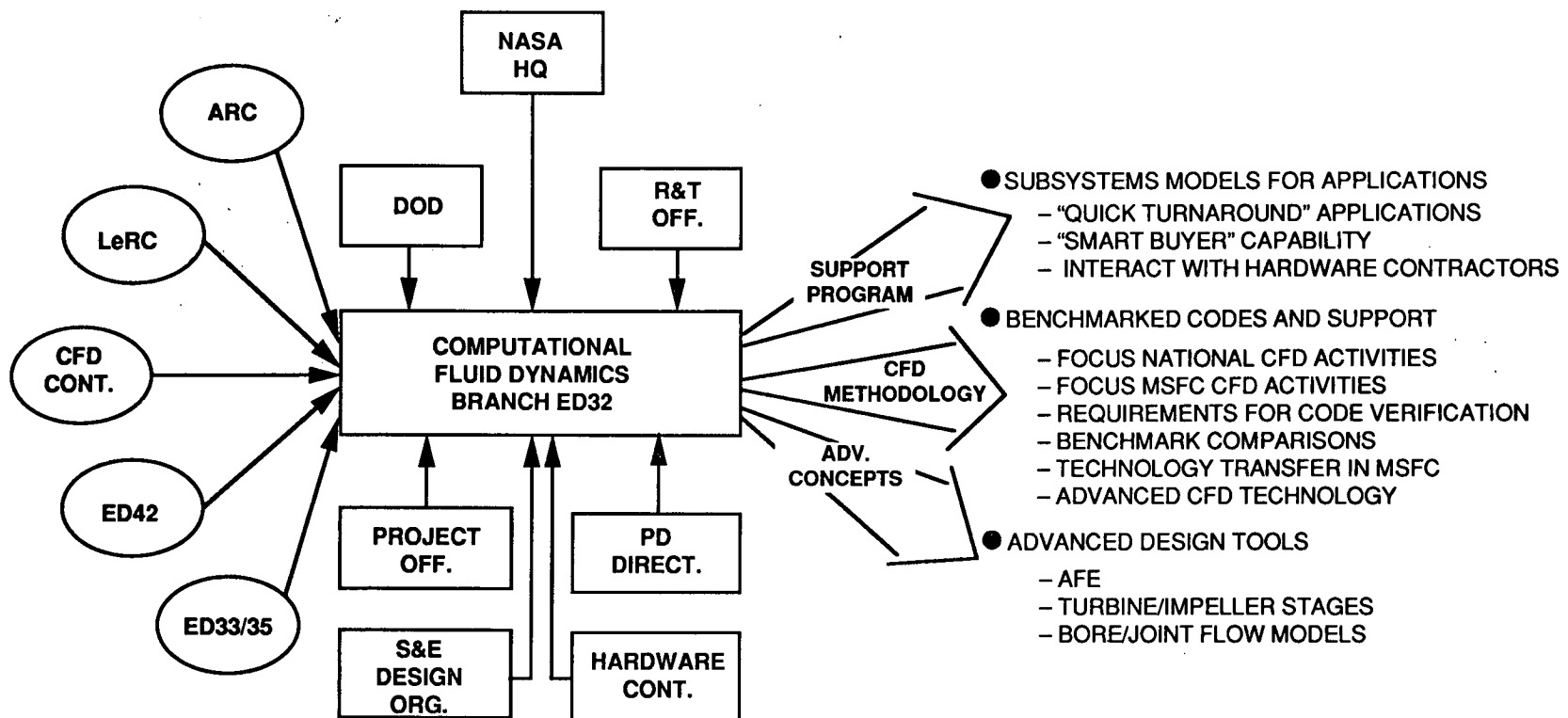
OBJECTIVES

- SUPPORT PROGRAM OFFICES
 - "QUICK TURNAROUND" APPLICATIONS
 - INTERACT WITH HARDWARE CONTRACTORS IN DEVELOPMENT OF DESIGN ENVIRONMENTS
 - PROVIDE "SMART BUYER" CAPABILITY FOR LONG-TERM APPLICATIONS
 - DEVELOP SUBSYSTEMS CFD MODELS
 - FOCUS MSFC CFD ACTIVITIES/PROVIDE CENTERWIDE CFD SUPPORT
- FOCUS DEVELOPMENT OF CFD METHODOLOGY
 - INTERACT WITH ARC, LeRC, LaRC, AND OTHER RESEARCH ORGANIZATIONS TO FOCUS TECHNOLOGY DEVELOPMENT TOWARDS MSFC HARDWARE RELATED PROBLEMS
 - DEVELOP REQUIREMENTS FOR CFD CODE VERIFICATION
 - VERIFY CODES THROUGH BENCHMARK COMPARISONS
 - ADVANCE CFD TECHNOLOGY FOR APPLICATIONS
- DEVELOP ADVANCED HARDWARE TECHNOLOGY CONCEPTS
 - TURBINE STAGE
 - IMPELLER STAGE
 - NOZZLES, PREBURNERS, ETC.

COMPUTATIONAL FLUID DYNAMICS BRANCH ACTIVITIES

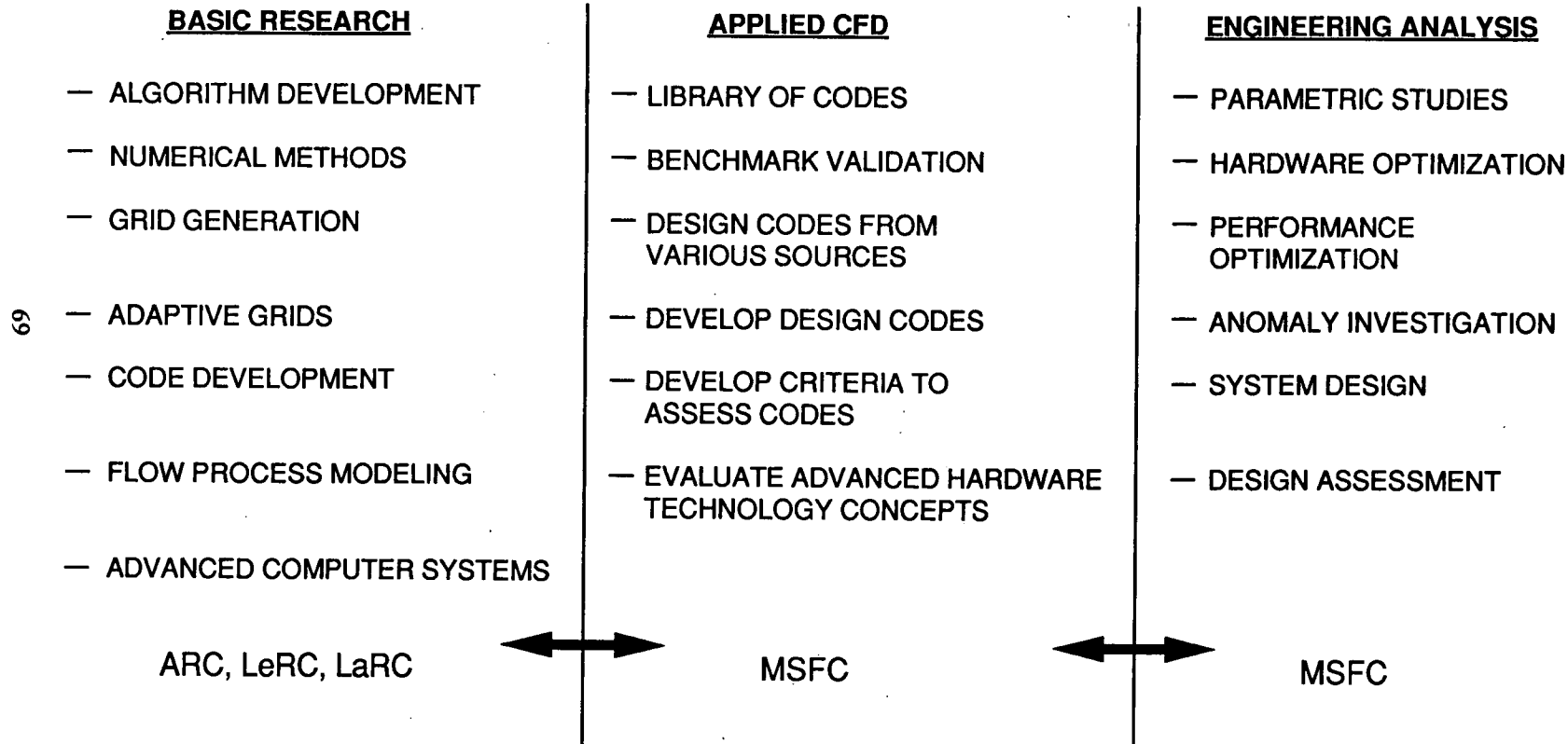
ORGANIZATIONAL INTERACTIONS AND UNIQUE CFD RESOURCES CAPABILITY

88



COMPUTATIONAL FLUID DYNAMICS BRANCH ACTIVITIES

CFD CROSS FERTILIZATION



COMPUTATIONAL FLUID DYNAMICS BRANCH ACTIVITIES

APPROACH TOWARD SOLUTIONS OF COMPLEX FLOWS

- DEVELOP DATA BASE
 - LITERATURE SEARCH
 - COLLATE RELEVANT EXPERIMENTAL RESULTS
 - IDENTIFY SIGNIFICANT PARAMETERS, SCALING LAWS
 - DEFINE REQUIREMENTS FOR BENCHMARK EXPERIMENTS
- PERFORM FUNDAMENTAL ENGINEERING ANALYSIS
 - SIMPLIFIED 1-D OR 2-D ANALYSES
 - ELEMENTARY SENSITIVITY ANALYSIS
- PERFORM CFD CALCULATIONS
 - EXERCISE BENCHMARKED STATE-OF-THE-ART CODES
 - IMPLEMENT STATE-OF-THE-ART FLOW PROCESS MODELS

PREDICTION OF SECONDARY FLOW IN CURVED DUCTS OF SQUARE CROSS-SECTION

OBJECTIVE:	TO VERIFY NAVIER-STOKES CODES FOR THE ACCURATE PREDICTION OF SECONDARY FLOW IN CURVED DUCTS
APPROACH:	APPLICATIONS OF A 3-D INCOMPRESSIBLE NAVIER-STOKES CODE (INS3D) TO FLOW IN A 90° AND 180° BEND AND A 22.5° S-DUCT OF SQUARE CROSS-SECTION (25000, 50000, 100000, AND 175000 GRID POINTS); COMPARE PREDICTIONS TO LDV MEASUREMENTS
COMPUTER RESOURCES REQUIRED:	2 TO 6 MW STORAGE ON A CRAY X-MP; 3/4 HOUR RUN TIME ON CRAY X-MP FOR THE 10^5 GRID POINT CASES
IMPACT:	VERIFICATION OF INCOMPRESSIBLE NAVIER-STOKES CODE FOR THE PREDICTION OF SECONDARY FLOWS IN COMPLEX INTERNAL FLOW FIELDS

28x52x121

GRID

Re = 790

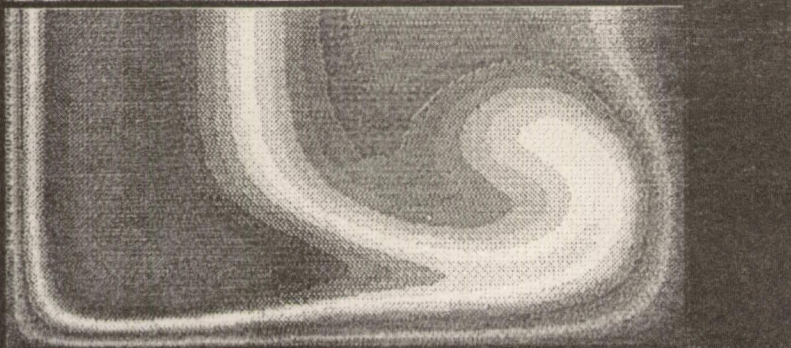
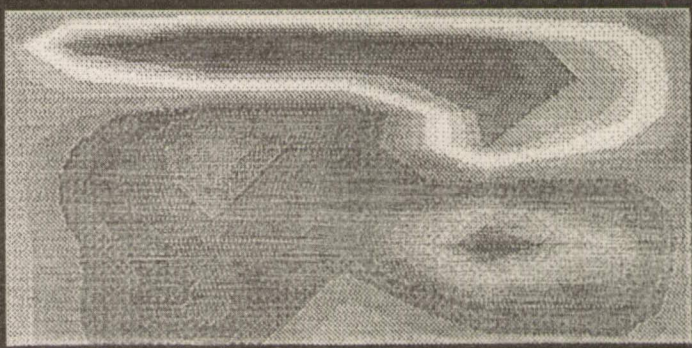
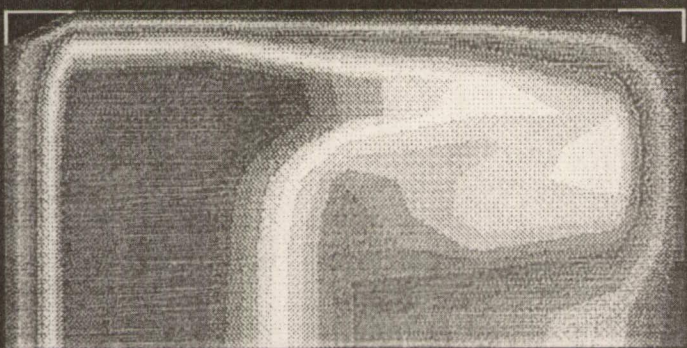
M = 8.0

Prediction of Secondary Flow in Curved Ducts
of Square Cross-Section

Outer Wall

Experiment

Inner Wall



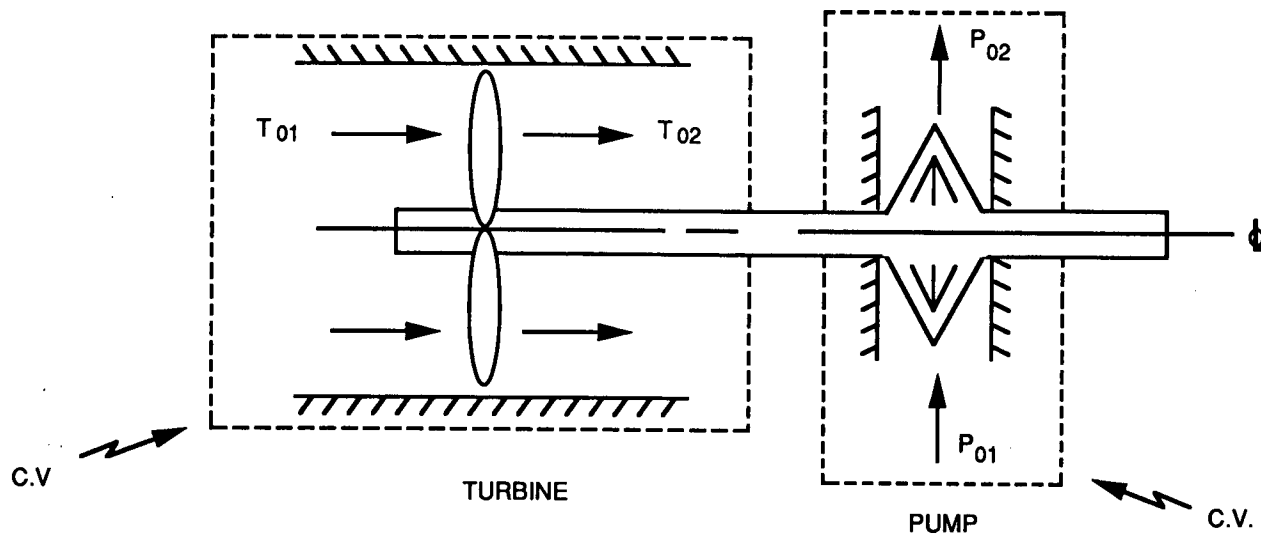
Computation

Axial Flow at 90 Degree Bend Exit

Radial Flow at 90 Degree Bend Exit

TURBOPUMP DESIGN EQUATIONS

73



$$P_{02} - P_{01} = \eta_t \eta_p \frac{\dot{m}_t}{\dot{m}_p} \rho_p (T_{01} - T_{02}) C_p$$

MSFC HARDWARE RELATED ACTIVITIES

INHOUSE PROGRAM SUPPORTING ACTIVITIES

		<u>INHOUSE</u>	<u>CONT.</u>
SSME	→ ● HPFTP TURBINE BLADES	X	X
	● SINGLE CRYSTAL HOLLOW CORE TURBINE BLADES	X	X
	● TURBINE DISK CAVITIES	X	X
	→ ● LOX PUMP BEARING INLET CAVITY	X	X
	● LOX PUMP BEARINGS	X	X
	● FUEL PREBURNER	X	X
	● LOX PREBURNER	X	X
	● LOX MANIFOLD TEE (4000 Hz)	X	X
	● HOT GAS MANIFOLD/MANIFOLD STRUTS	X	X
	● PUMP COOLANT FLOW PATHS	X	X
	● NOZZLE/MCC MISMATCH	X	X
	→ ● HPOTP NOZZLE PLUG TRAJECTORIES	X	X
	● TRANSIENT BEHAVIOR OF FUEL PREBURNER MANIFOLD	X	X
	● UTRC HPFTP COOLANT FLOW EXPERIMENT	X	X
	● BEARING DEFLECTOMETER (TTBE)	X	X
ATD	● TURBINE INLET TEMP. REDISTRIBUTION	X	X
	● TURBINE TEMP. PROFILE REDISTRIBUTION	X	X
	● ROTOR-STATOR INTERACTION	X	X
	● TURNAROUND DUCT AND HOT GAS MANIFOLD	X	X
	● BEARING ANALYSIS	X	X
	● LOX PUMP INLET SCROLL	X	X
	● FUEL PUMP INTERSTAGE CROSSOVER DUCTS	X	X
	● FUEL PUMP INLET SCROLL	X	X
	● LOX PUMP DISCHARGE VOLUTE	X	X
	● SEALS	X	X
SRB	● BORE FLOW		
	—CANTED NOZZLE	X	X
	—BROKEN INHIBITOR	X	X
	→ ● FIELD JOINT		
	—FLOW AND THERMAL TRANSIENT	X	X
	—PRESSURIZATION TRANSIENT	X	X
	→ ● NOZZLE-TO-CASE JOINT		
	—FLOW AND THERMAL TRANSIENT	X	X
	—PRESSURIZATION TRANSIENT	X	X

MSFC HARDWARE RELATED ACTIVITIES

INHOUSE PROGRAM SUPPORTING ACTIVITIES (CONTINUED)

		<u>INHOUSE</u>	<u>CONT.</u>
AFE	● AEROTHERMAL ENVIRONMENTS → — DSMC — NS	X X	X
SPACE STATION	● CONTAMINATION ● ECLSS	X X	X
ADVANCED PROGRAM DEVELOPMENT	● EXTERNAL TANK GAMMA RAY IMAGING TELESCOPE	X	

MSFC HARDWARE RELATED ACTIVITIES ROCKETDYNE APPLICATION OF CFD TO SSME

TURBOMACHINERY	CODE	NONTURBOMACHINERY	CODE
HPFTP IMPELLER CAVITY	STEP	HOT GAS MANIFOLD	INS3D
HPOTP P/B BEARING DISCH CAVITY	STEP	FUEL-SIDE	
HPOTP TURBINE END BRG DISCH CAVITY	STEP	2-DUCT TURBULENT	
HPOTP 2ND STG TURBINE NOZZLE	REACT 2D	3-DUCT TURBULENT	
HPFTP 1ST STG TURBINE DISK CAVITY	STEP	OXIDIZER-SIDE	
HPOTP TURBINE END BRG FLOOD COOL	STEP	AXISYMMETRIC	
HPOTP R/S INTERACTION	ROTOR	3D	
HPFTP TURBINE DISK CAVITIES	REACT 2D	COMBINED HGM	INS3D
HPFTP 2ND STG TURBINE DISK CAVITY/DIVERTER	STEP		
SC/HC 2ND STG TURBINE DISK CAVITY DIVERTER	STEP	MAIN INJECTOR	REACT3D
ROUGH SURFACE SEAL FLOW	REACT 2D	FLUCTUATING PRESSURE &	
SC/HC 1ST STG TURBINE	REACT 2D	DYNAMIC LOADING	
HPFTP 1ST STG TURBINE	REACT 2D	NOZZLE	USA
SC/HC 1ST STG TURBINE	REACT 3D	MCC/NOZZLE MISMATCH	USA
HPFTP 1ST STG TURBINE	REACT 3D	NOZZLE TRANSIENT AND	
SC/HC 1ST STG TURBINE R/S	ROTOR	OPERATION	
HPFTP 1ST STG TURBINE R/S	ROTOR		USA
HPOTP 1ST STG TURBINE R/S	ROTOR		
LPOTP 4TH STG TURBINE R/S	ROTOR		
HPOTP IMPELLER-DIFFUSER UNSTEADY	ROTOR	4KHZ RESONANCE	STEP
HPOTP BRG FLOWFIELD	REACT 3D		
HPFTP 1ST STG TURBINE W/STRUTS	REACT 3D	TEST BED LOX FLOWMETER	
HPOTP IMPELLER	REACT 3D		
HPOTP 1ST STAGE TURBINE W/STRUTS	REACT 3D		
HPOTP P/B DIFFUSER	REACT 2D/3D		
T/P HARDWARE DEVIATION SENSITIVITIES TO REDUCE MR'S	REACT 2D/3D		

MSFC HARDWARE RELATED ACTIVITIES

PRATT AND WHITNEY APPLICATION OF CFD TO ATD

- MOTIVATION

- DESIGN VERIFICATION

- CFD ANALYSIS OF CRITICAL FLOWPATHS IN SSME TURBOPUMPS
 - IDENTIFY POTENTIAL FLOWFIELD NONUNIFORMITIES, REGIONS OF SEPARATED FLOWS
 - PROVIDE DETAILED FLOW DATA TO MECHANICAL DESIGN GROUPS FOR ADDITIONAL STRUCTURAL, THERMAL ANALYSES

- ANALYTICAL SUPPORT

- WHERE NECESSARY, PERFORM FUNDAMENTAL CFD RESEARCH TO SUPPORT THE DESIGN VERIFICATION PROCESS
 - INCORPORATE THESE IMPROVEMENTS INTO THE DESIGN DECKS

MSFC HARDWARE RELATED ACTIVITIES PRATT AND WHITNEY APPLICATION OF CFD TO ATD

● ACCOMPLISHMENTS

- ANALYZED COMPLETE HOT GAS FLOW PATH
- PROVIDED TURBINE INLET CONDITIONS
- PROVIDED STRUT PRESSURE LOADS FOR MECH DESIGN
- TAD CALCULATIONS RESULTED IN SUBSTANTIAL REDUCTION IN INSTRUMENTATION
- CFD MODELS OF TAD-HGM, LOX PUMP INLET, PREBURNER AND FUEL PUMP CROSSOVER DUCTS READY FOR HOT TEST SUPPORT
- TURBULENCE MODEL SELECTED FOR COMPLEX DUCT FLOWS
- ARICC SUBSTANTIALLY UPGRADED
- CAD TO CFD CAPABILITY IMPLEMENTED
- 2 D INVISCID ROTOR-STATOR INTERACTION CAPABILITY DEVELOPED AND DEMONSTRATED

NASA EARTH-TO-ORBIT PROPULSION R&T PROGRAM

PROGRAM DEFINITION

- TECHNOLOGY ACQUISITION PHASE

- SEEKS IMPROVED UNDERSTANDING OF THE BASIC CHEMICAL AND PHYSICAL PROCESSES OF PROPULSION
- DEVELOPS ANALYSIS METHODS, DESIGN MODELS, AND CODES USING ANALYTICAL TECHNIQUES SUPPORTED BY EMPIRICAL LABORATORY DATA AS REQUIRED
- RESULTS ARE OBTAINED THROUGH TEN DISCIPLINE WORKING GROUPS

79

- BEARINGS
- STRUCTURAL DYNAMICS
- TURBOMACHINERY ✓
- FATIGUE/FRACTURE/LIFE
- IGNITION/COMBUSTION ✓

- FLUID & GAS DYNAMICS ✓
- INSTRUMENTATION
- CONTROLS
- MANUFACTURING/PRODUCIBILITY/INSPECTION
- MATERIALS

NASA EARTH-TO-ORBIT PROPULSION R&T PROGRAM

PROGRAM DEFINITION

- **LARGE SCALE SUBSYSTEM TECHNOLOGY VALIDATION**
 - VALIDATES TECHNOLOGY EMANATING FROM THE ACQUISITION PHASE AT THE LARGE SCALE COMPONENT OR SUBSYSTEM LEVEL
 - THREE CATEGORIES OF EFFORT
 - LARGE SCALE COMBUSTORS ✓
 - LARGE SCALE TURBOMACHINERY ✓
 - CONTROLS AND HEALTH MONITORING
- **TECHNOLOGY TEST BED VALIDATION**
 - VALIDATES TECHNOLOGY EMANATING FROM THE ACQUISITION PHASE AT THE ENGINE SYSTEM LEVEL
 - THREE CATEGORIES OF EFFORT
 - COMBUSTORS ✓
 - TURBOMACHINERY ✓
 - CONTROLS AND HEALTH MONITORING

NASA EARTH-TO-ORBIT PROPULSION R&T PROGRAM

WORK ELEMENT SUMMARY

● TECHNOLOGY ACQUISITION

18

- G2 TURBINE DRIVE COMBUSTOR DESIGN
- G29 TTB COMBUSTION MODELS
- G31 COMBUSTION CODE ENHANCEMENTS
- G32 COMBUSTION STABILITY CODE
- G33 TURBULENCE MODELS FOR COMB. ANALYSIS
- G39 ERE PREDICTION METHODS
- H6 FLUID STRUCTURE INTERACTION
- H16 VERIFICATION OF INTERNAL FLOW ANALYSIS IN 3D GEOMETRIES
- H19 EVALUATION CRITERIA FOR INTERNAL FLOW CFD NUMERICAL MODELING
- H22 ADAPTIVE COMPUTATIONAL METHOD FOR HIGH REYNOLDS NUMBER INTERNAL FLOWS IN ADVANCED PROPULSION SYSTEMS
- H23 DEVELOPMENT OF CONVERGENCE ACCELERATION TECHNIQUES FOR ALGORITHMS APPLIED TO COMPLEX 3D INTERNAL FLOWS
- H35 ADVANCED INS3D CFD CODE
- H36 CFD CONSORTIUM

● LARGE SCALE SUBSYSTEM TECHNOLOGY VALIDATION

- LSVT1 EXP. VER. OF CFD TURB. STAGE DESIGN
- LSVT4 HI PRESS TURBOMACHINERY SYS. VALIDATION
- LSVT5 3D TURBOPUMP FLOWFIELD
- LSVT6 EXP. VER. OF IMPELLER STAGE DESIGN
- LSVT10 MEASUREMENTS IN MULTI ELEMENT INJECTOR
- LSVT12 CFD TURNAROUND DUCT DESIGN VALIDATION

NASA EARTH-TO-ORBIT PROPULSION R&T PROGRAM

WORK ELEMENT SUMMARY (CONTINUED)

● TECHNOLOGY TEST BED VALIDATION

- TBVC4 INJECTOR DIAGNOSTICS
- TBVC1 IMPROVED HPOTP PREBURNER PUMP
- TBVT2 ENHANCED ROTOR CODES
- TBVT3 IMPROVED BEARING COOLANT PATH
- TBVT5 WATER FLOW MODELS
- TBVT8 HGM FUEL SIDE ANALYSIS
- TBVT9 CFD DATA REDUCTION HARDWARE
- TBVT10 HPOTP JET COOLANT RING
- TBVT13 PREBURNER DOME FILLING FLOW ANALYSIS
- TBVT24 TURBINE STAGE CFD ANALYSIS AND DATA BASE FOR
UNSTEADY AERO/HEAT TRANSFER
- TBVT25 DEV. OF UNSTEADY AERO HEAT/TRANSFER EXPERIMENTS
DATA BASE FOR AXIAL TURBINE STAGES
- TBVT26 ADVANCED AXIAL TURBINE STAGE DESIGN METHODS
- TBVT27 ADVANCED IMPELLER DESIGN METHODS
- TBVT28 CFD ANALYSIS OF BSMT
- TBVT29 UTRC ROTOR/STATOR HEAT/TRANSFER

NASA EARTH-TO-ORBIT PROPULSION R&T PROGRAM

CONSORTIUM OBJECTIVES

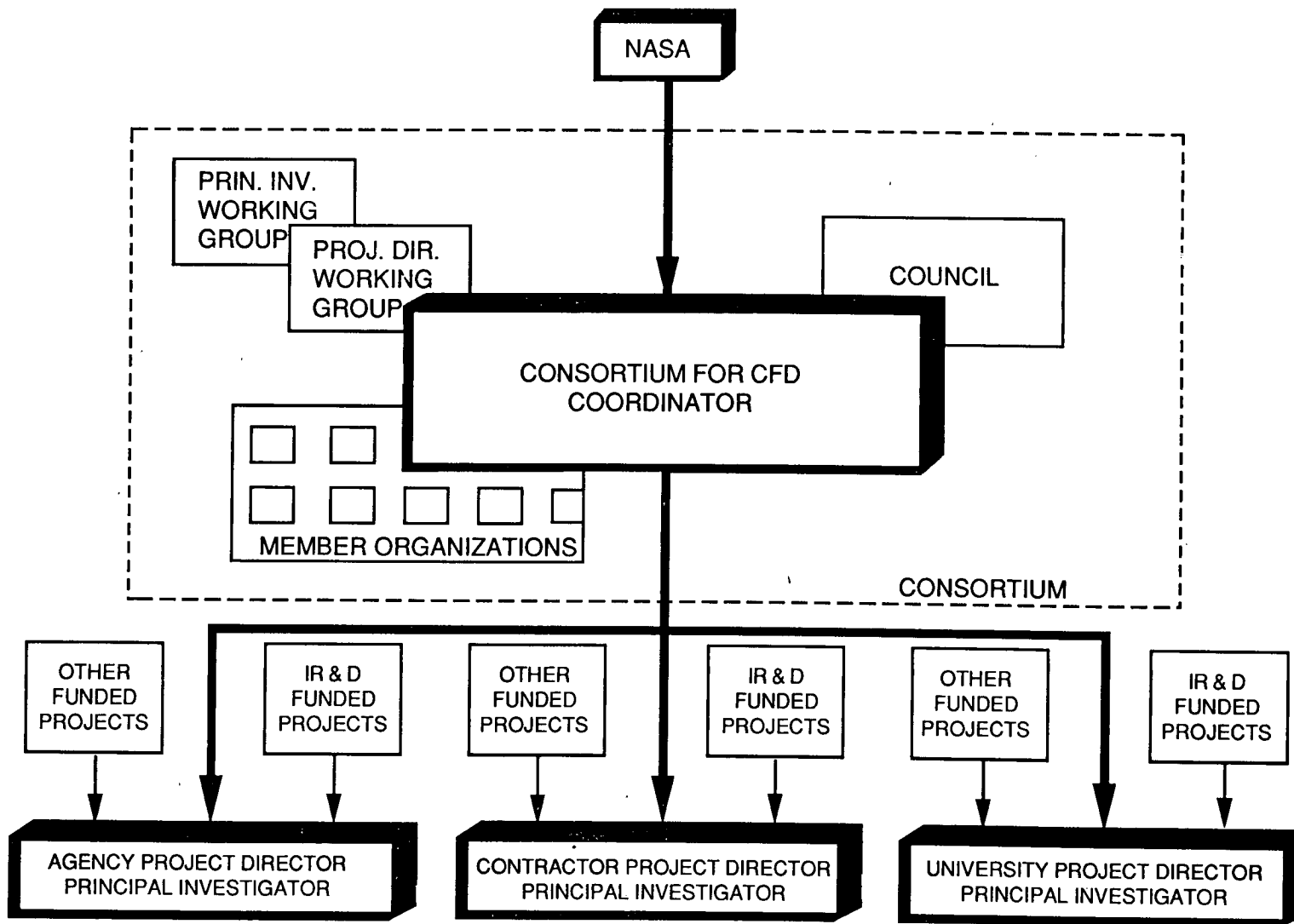
- FOCUS CFD APPLICATIONS IN PROPULSION
 - TECHNOLOGY ACQUISITION PHASE
 - DIRECT BASELINE PROGRAM TOWARDS IMPROVED ACCURACY, STABILITY, AND EFFICIENCY
 - LARGE SCALE SUBSYSTEM TECHNOLOGY VALIDATION
 - STIMULATE CFD VALIDATION TOWARDS PROPULSION FLOWS
 - DIRECT APPLICATIONS CODES TOWARD DESIGN TOOLS AND ADVANCED HARDWARE TECHNOLOGY CONCEPTS
- IDENTIFY NATIONAL CFD PROPULSION REQUIREMENTS
- STIMULATE A FORUM FOR GOVERNMENT, INDUSTRY, AND UNIVERSITY INTERACTIONS
- ENCOURAGE INDUSTRY TO PARTICIPATE IN CFD DEVELOPMENT WITH IRAD FUNDS
- PROVIDE SYNERGISM IN THE CFD COMMUNITY
- PROVIDE PEER REVIEW OF CFD PROGRAMS

**NASA EARTH-TO-ORBIT PROPULSION
R&T PROGRAM**
CONSORTIUM TASKS

- DEVELOP A PLAN TO APPLY CFD TO CURRENT AND FUTURE PROPULSION SYSTEMS
 - IDENTIFY AND RANK CRITICAL FLOW PROBLEMS RELATED TO PROPULSION SYSTEMS
 - IDENTIFY NATIONAL CFD RELATED RESOURCES
 - DEFINE HIGH PERFORMANCE COMPUTING REQUIREMENTS TO ACCOMPLISH CFD FOR PROPULSION APPLICATIONS
- DIRECT CFD TECHNOLOGY DEVELOPMENT TO PROPULSION APPLICATIONS
- ASSESS AND VALIDATE CFD APPLICATIONS IN PROPULSION SYSTEMS
 - DEVELOP EVALUATION CRITERIA
 - DEFINE AND IMPLEMENT BENCHMARK VALIDATION
 - DEFINE AND IMPLEMENT VALIDATION TESTS
- DIRECT THE APPLICATION OF CFD DESIGN TOOLS TOWARDS ADVANCED HARDWARE TECHNOLOGY CONCEPTS
- ACCELERATE THE TRANSFER OF CFD TECHNOLOGY FROM UNIVERSITIES AND RESEARCH CENTERS TO INDUSTRY AND HARDWARE DEVELOPMENT CENTERS

NASA EARTH-TO-ORBIT PROPULSION R&T PROGRAM

CONSORTIUM ORGANIZATIONAL STRUCTURE

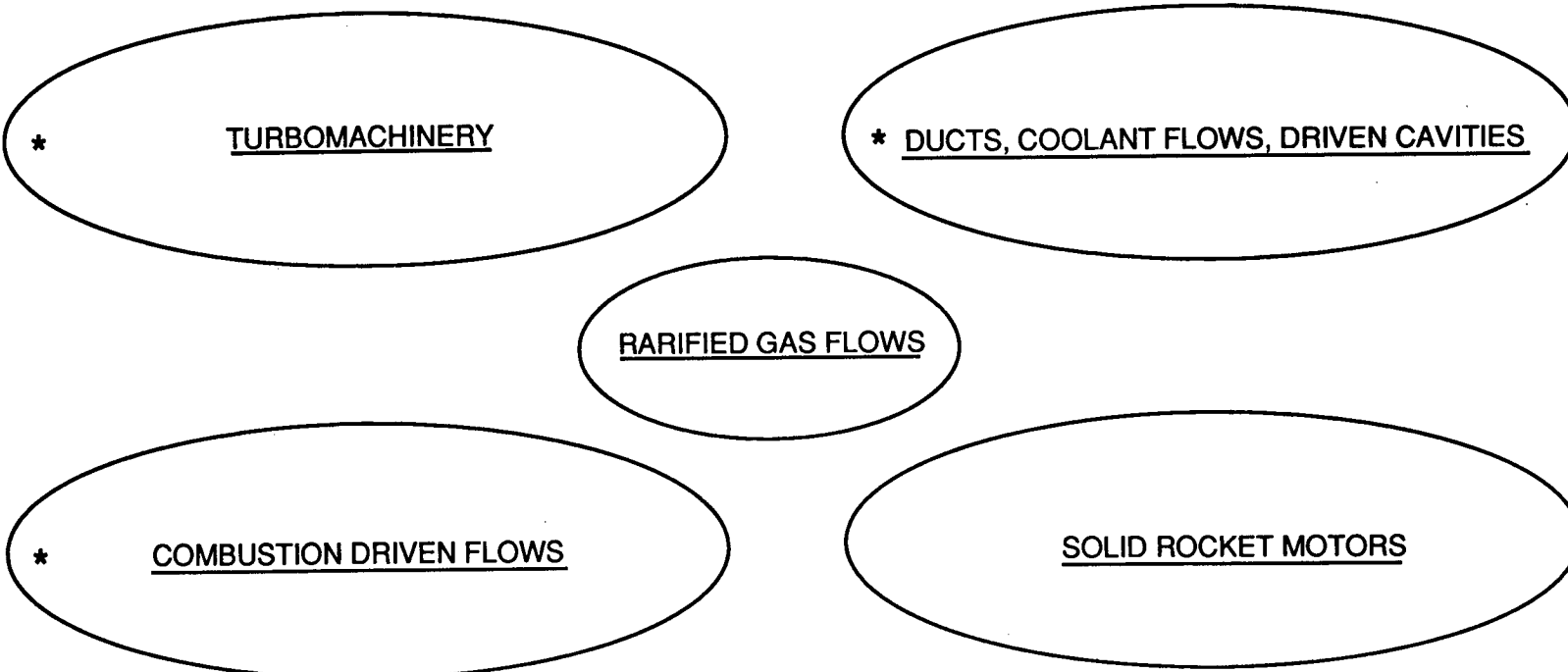


NASA EARTH-TO-ORBIT PROPULSION R&T PROGRAM

CONSORTIUM TEAMING

FOCUS DEVELOPMENT OF CFD METHODOLOGY
AND
DEVELOP ADVANCED HARDWARE TECHNOLOGY CONCEPTS

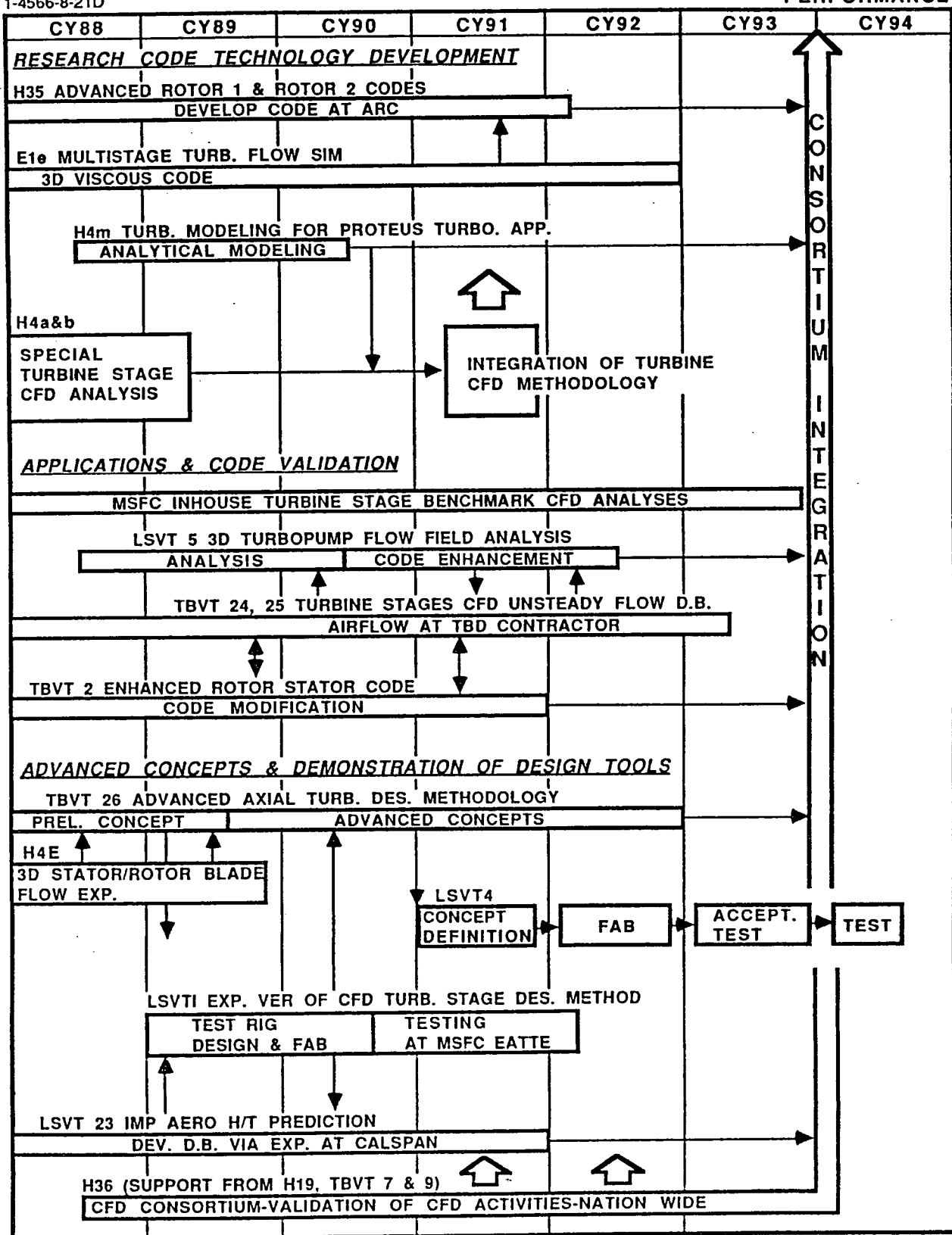
98



VALIDATION OF TURBINE STAGE DESIGN TOOLS

1-4566-8-21D

PERFORMANCE



182-8

NASA EARTH-TO-ORBIT PROPULSION R&T PROGRAMS

DELIVERABLE PRODUCTS/MILESTONES

TURBINE STAGES

● THREE-DIMENSIONAL MULTISTAGE CFD CODES

● RESEARCH CODE

- 3-D MULTISTAGE CFD CODE TO PREDICT STEADY AND UNSTEADY FLOW FIELD CHARACTERISTICS, PERFORMANCE, LOADS AND HEAT TRANSFER 1/90

● PRODUCTION CODE

- MODIFICATION TO RESEARCH CODE TO ENHANCE ENGINEERING APPLICATION 8/89
 - IMPROVED EFFICIENCIES 8/89
 - STREAMLINE PRE/POST PROCESSING ETC.

● UNSTEADY THREE-DIMENSIONAL DATA BASE FOR MULTISTAGE TURBINE

- INITIAL UNSTEADY AERO DATA BASE 6/89
- ENHANCED UNSTEADY AERO DATA BASE 6/90
- HEAT TRANSFER DATA BASE 1/90

● IMPROVED FLOW PROCESS MODELING

- TURBULENCE MODEL FOR PROTEUS 6/90
- TURBULENCE MODEL FOR AXIAL TURBOMACHINERY 6/89

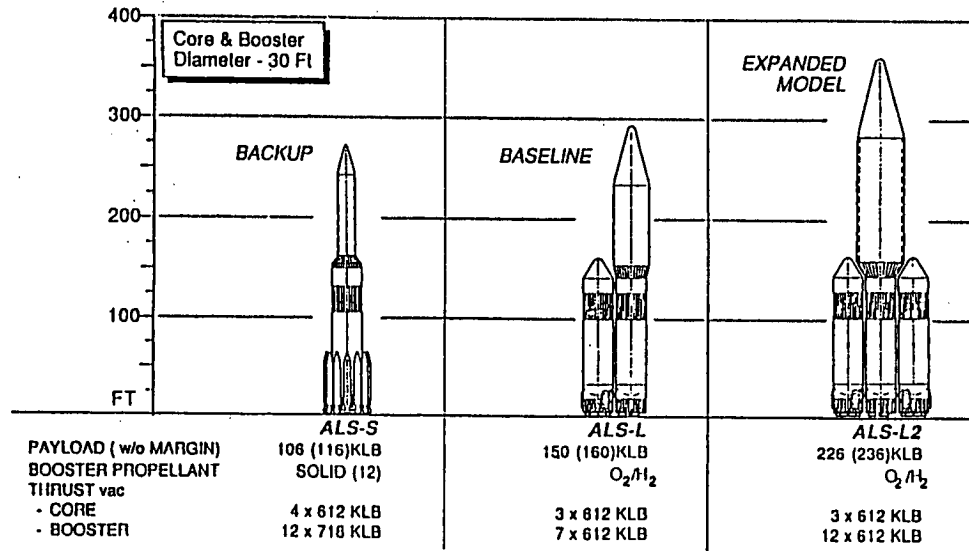
● ADVANCED CONCEPTS AND DEMONSTRATION OF DESIGN TOOLS

- PRELIMINARY CONCEPT DEFINITION 9/89
- TESTS 1/89, 6/89, 10/89
- ADVANCED CONCEPT DEFINITION 1/91
- FINAL RIG TEST VERIFICATION 1/92
- HOT FIRE TEST (TTVF) 4/94

NEW NEAR TERM CFD ACTIVITIES

STBE/STME DESIGN APPROACH FOR LOW COST

THE ALS FAMILY

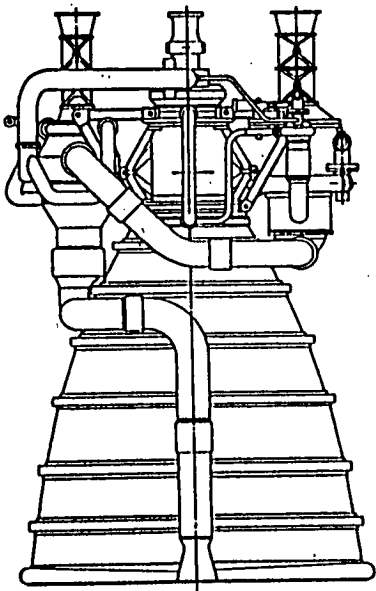


- DESIGN PRIORITIES
 - RELIABILITY
 - COST
 - PERFORMANCE/WEIGHT
 - COMMONALITY

- DESIGN BENEFITS
 - REDUCED INTERNAL ENVIRONMENTS
 - ROBUSTNESS
 - REDUCED DEVELOPMENT TIME
 - REDUCED INVENTORIES/INTERCHANGEABILITY

NEW NEAR TERM CFD ACTIVITIES

STME BASELINE DESIGN REQUIREMENTS



- GAS GENERATOR CYCLE, SERIES TURBINE DRIVE,
- LOX/LH₂ PROPELLANTS
- CHAMBER PRESSURE = 2250 psi
- FIXED THRUST OF 580K (VAC)
- DUAL THRUST: 580K AND 435K (VAC)
- RELIABILITY = .99, 90% CONFIDENCE LEVEL (DEMONSTRATED)
- EXPENDABLE OR REUSABLE (15 CYCLES)
- GIMBAL CAPABILITY FOR TVC, +/- 6 DEGREES
- FIXED NOZZLE, AR = 62:1
- USABLE IN SINGLE OR MULTI-ENGINE ARRANGEMENT
- HIGH RELIABILITY, LOW COST

NEW NEAR TERM CFD ACTIVITIES

CFD ACTIVITIES TO SUPPORT STBE/STME DESIGN

● THRUST CHAMBER

- INJECTOR
- MAIN COMBUSTION CHAMBER
- NOZZLE
- COOLING CHANNELS

● TURBINE

- INLET FLANGE
- INLET MANIFOLD
- ROTOR-STATOR INTERACTION
- MULTISTAGE ANALYSIS
- AIRFAILS/GUIDE VANES
- TURBINE EXHAUST — TURN AROUND DUCT

● GAS GENERATOR

- INJECTOR
- COMBUSTION CHAMBER

● PUMPS

- INLET FLANGE
- VOLUTE/INDUCER/IMPELLER
- DIFFUSER/CROSSOVER DUCTS
- DISCHARGE COLLECTOR/DUCTS
- BEARINGS
- SEALS

● SYSTEM ANALYSIS

- DUCTS
- MANIFOLDS
- VALVES
- CAVITIES

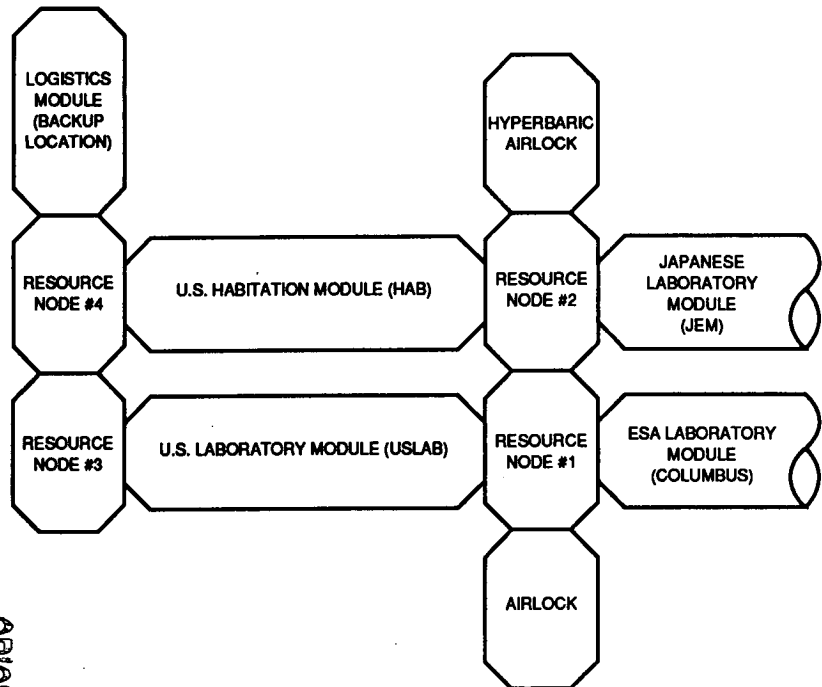
● ENGINE AIRFRAME INTERACTION

- PLUME
- AEROHEATING/LOADS

NEW NEAR TERM CFD ACTIVITIES

ENVIRONMENTAL CONTROL AND LIFE SUPPORT SYSTEM (ECLSS)

SPACE STATION CONFIGURATION



RESPIRABLE ATMOSPHERE AND WATER REQUIREMENTS

PARAMETER	UNITS	OPERATIONAL	DEGRADED	EMERGENCY
CO ₂ PARTIAL PRESSURE	N/m ² (mmHg)	400 MAX (3.0 MAX)	1013 MAX (7.6 MAX)	1600 MAX (12 MAX)
O ₂ PARTIAL PRESSURE	N/m ² x 10 ³ (psia)	19.5 – 23.1 (2.83 – 3.35)	16.5 – 23.7 (2.4 – 3.45)	15.8 – 23.7 (2.3 – 3.45)
TOTAL PRESSURE	N/m ² x 10 ³ (psia)	99.9 – 102.7 (14.5 – 14.9)	99.9 – 102.7 (14.5 – 14.9)	99.9 – 102.7 (14.5 – 14.9)
TEMPERATURE	°K (°F)	291.5 – 299.8 (65 – 80)	291.5 – 299.8 (65 – 80)	288.8 – 302.6 (60 – 85)
DEWPOINT	°K (°F)	277.6 – 288.8 (40 – 60)	273.9 – 294.3 (35 – 70)	273.9 – 294.3 (35 – 70)
VENTILATION	msec (ft/min)	.076 – .203 (15 – 40)	.051 – .508 (10 – 100)	.051 – 1.016 (10 – 200)
TRACE CONTAMINANTS	mg/m ³	TBD	TBD	TBD
PARTICULATES	PARTICLES/ m ³	3,530,000 0.5 MICRO- METERS TBD > 150 MICROMETERS	—	—
MICRO-ORGANISMS	CFU/m ³	1000	1000	1000

NEW NEAR TERM CFD ACTIVITIES

CFD ACTIVITIES TO SUPPORT ECLSS

- GENERIC BASELINE CFD MODELS

- PLANAR, ONE MODULE (NS)
- 3D, ONE MODULE (NS)
- 3D, INNER LOCK DUCTS (NS)
- PLANAR INTERMODULE (NS)
- 3D, INTERMODULE (NS)

- FLOW CONTROL DESIGN PARAMETRIC OPTIMIZATION

- INTERNAL CONFIGURATION VARIATIONS
- VENTILATION CONTROL
- INTRAMODULE VENTILATION (FANS)
- CONTAMINATION TRANSPORT
- CO_2 / FLOW MANAGEMENT
- BODY FORCE EFFECTS

- BENCHMARK COMPARISONS

- PARAMETRIC DESIGN OF EXPERIMENTS
- CODE VALIDATION

CFD EXPECTATIONS

- DIRECT HARDWARE DESIGN UTILIZING CFD
 - PROVIDE INITIAL IMPACT IN DESIGN
 - PERFORM DESIGN OPTIMIZATION STUDIES
 - DEVELOP ADVANCED HARDWARE TECHNOLOGY CONCEPTS
- ESTABLISH EVALUATION CRITERIA FOR CODES AND CLASSES OF PROBLEMS
- BENCHMARKED/VALIDATED CODES
 - LAMINAR FLOWS
 - TURBULENT FLOWS \bar{u} , \bar{j} , \bar{p}
 - ACOUSTIC PROBLEMS
 - CERTAIN CLASS OF UNSTEADY PROBLEMS
- USER FRIENDLY CODES
 - B.S. LEVEL ENGINEER 2-3 YRS EXPERIENCE
 - GUIDELINES FOR CLASSES OF PROBLEMS
 - CAD/CAM/CAE; GEOMETRY GRID GENERATION
 - GENERALIZED BOUNDARY CONDITIONS
 - ALGORITHM/GRID OPTIMIZATION FOR SOLUTION EFFICIENCY
 - ARTIFICIAL INTELLIGENCE/EXPERT SYSTEMS
 - MODULAR CODES
- FLOW ADAPTIVE GRIDS FOR CURRENT CLASS OF PROBLEMS
- MULTIPLE SCALE AND/OR ZONAL TURBULENCE MODELS, MULTIPHASE, MULTISPECIES, COMBUSTION FLOW PROCESS ENGINEERING MODELS EVOLVED FROM EXPERIMENTS AND CFD ANALYSIS

Johnson Space Center CFD Overview

C. P. Li
Advanced Programs Office
Johnson Space Center, Houston, Tx 77058

Recent applications and development of CFD technology have focused on flow problems that are critically important to the operation and design of space flight vehicles. The main effort is spent on the Space Shuttle in order to provide an understanding of the cryogenic fluid in the duct connecting the External Tank and the Main Engines, the subsonic flow surrounding the Orbiter during crew egress maneuvers, the transonic aerodynamic forces on the the Orbiter fuselage and wing, the high angle-of-attack abort flight, and the aerodynamic heating during entry. To provide in-depth analyses for such diverse problems within a timely schedule, matured panel codes and a state-of-the-art incompressible turbulent flow code were adapted. Collaboration with Ames Research Center has resulted in a Shuttle ascent aerodynamic code; and a viscous chemical nonequilibrium code is being developed for predicting Orbiter real-gas aerodynamics and finite-catalytic heating. The remaining activities are devoted to the prediction of the flow environment around the Aeroassist Flight Experiment vehicle at hypersonic speeds and high altitudes. A thermochemical nonequilibrium Navier-Stokes code has been developed on the basis of two- temperature and 11-species models for solving both the shock layer and near wake. After validating the code against wind-tunnel aerodynamic, pressure and heating data, the code is being used to supplement the ground test facilities in predicting a more realistic flight environment. CFD technology is being relied upon by other programs as well in the consideration of candidate configurations. A biconic cone entering the Martian atmosphere at moderate angles of attack will be analyzed for its stability and heating distribution for the proposed mission. Capabilities of simulating the low and medium lift-to-drag vehicles flowfield, flying back from the Space Station have been demonstrated and will be enhanced to include winglets. The development of hypersonic CFD technology at JSC will continuously emphasize the modeling of radiation and ablation in continuum flow regime, sufficient realism of geometry, and efficiency of computational methods.

CFD SUPPORT FOR VARIOUS PROGRAMS

- Shuttle (MY6.5, OSF)
- Orbiter (MY2.5, OSF)
- Aeroassist Flight Experiment (MY3.5, OAST)
- Mars Rover Sample Return Mission (MY1, SE)
- Crew Rescue Escape Vehicle (MY0.25, SS)
- High-Energy Aerobraking (MY0.5, OAST)

Simulation Codes and Computers

- PANAIR, VSAERO, QUADPLAN (potential flow, panel method)
- INS3D (incompressible Navier-Stokes code)
- F3D (compressible flow NS code)
- EAGLE, SVTGD3D (grid generation codes)
- U3D (upwind finite-volume implicit method)
- NOSIP, AFTB (shock-fitting NS and Parabolized NS codes)
- VRFNS (shock-fitting, chemically reactive NS codes)
- VRFL0 (shock-fitting, thermochemical nonequilibrium NS code)
- VAX8650s, SCS40 or CX200 (code development)
- Cray XMP at MSFC and CRAY 2 at NAS (engineering application)
- Class IV computer (CY89)

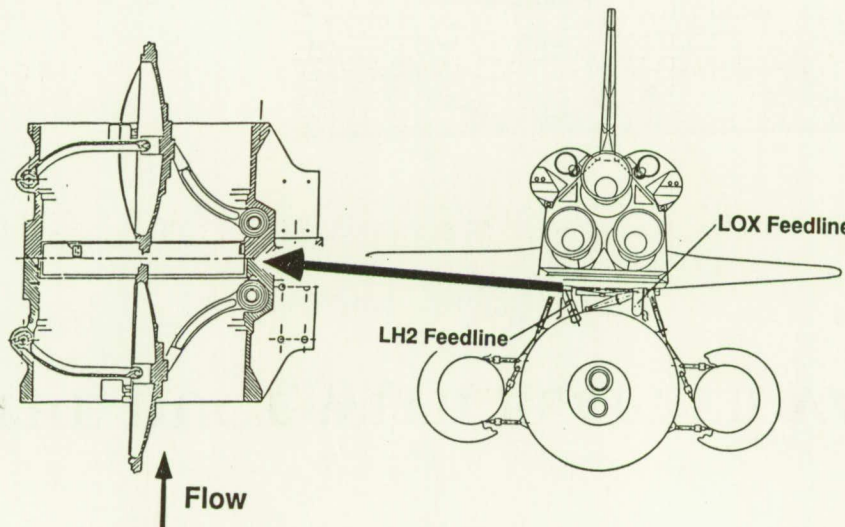
OUTLINE OF PRESENTATION

- Cryogenic Duct Flow Simulation by Kandula and Pearce
- Subsonic Orbiter Flow Computation by Slotnick
- Shuttle Debris Analyses by Gomez, Labbe, Martin
- Supersonic Orbiter Flow Computation and Comparison by Wey and Ma
- Hypersonic Orbiter Viscous and Reactive Flow Simulation by Li
- Biconic Cone Flow by Stuart
- AFE results by Gomez, McGary, Tam and Li
- CERV results

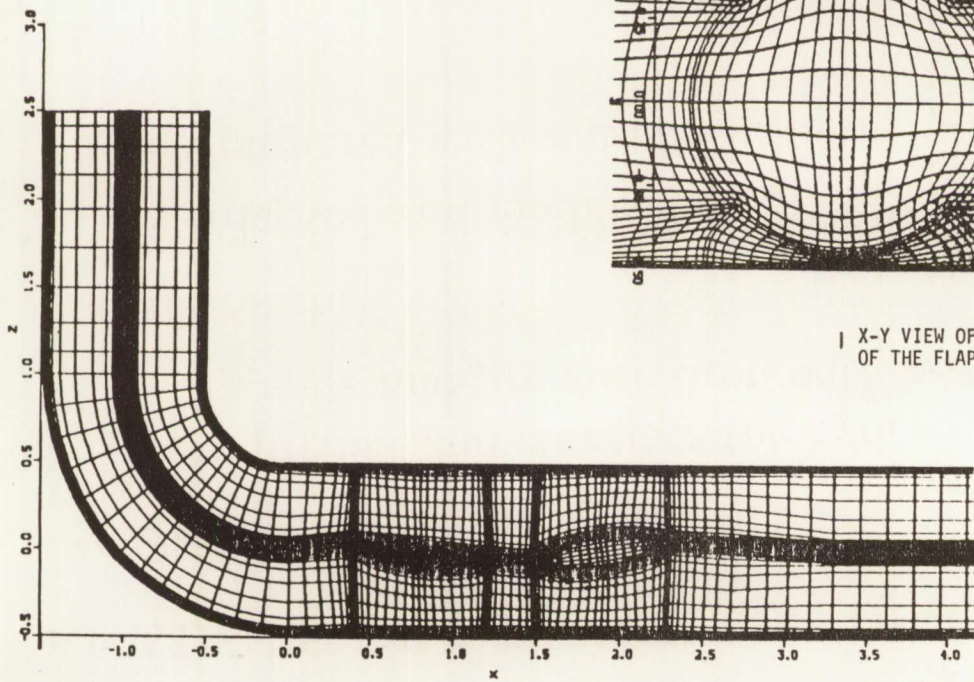
ANALYSIS OF ET/ORBITER DISCONNECT VALVES

- Objective:
 - to predict and correlate the hydrodynamic stability of the flappers and pressure drop with test data
- Approach:
 - Adapted and modified INS3D, SVTGD3D and INGRID
 - Compared with water test data

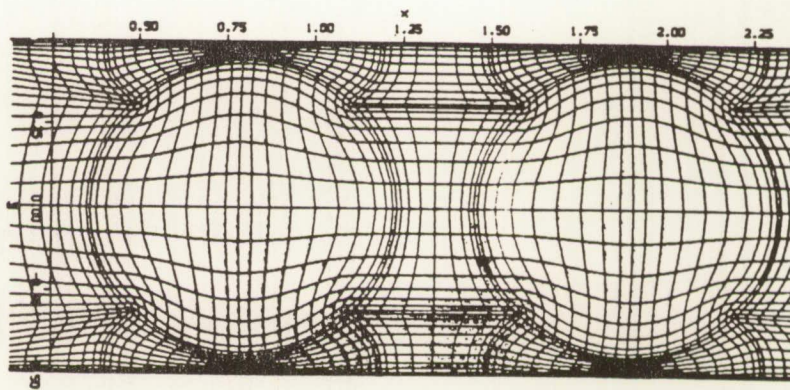
66



GRID IN THE DUCT WITH FLAPPER VALVES



A PORTION OF X-Z VIEW OF THE GRID AT THE PLANE OF SYMMETRY



Crew Egress Aerodynamic Analysis

- Objective: Numerically simulate the external flowfield surrounding the various flight test vehicles so that an accurate assessment of the astronaut exit trajectories may be determined.
- Methodology: Use production panel code methods to compute aero characteristics.
 - Fast, efficient CFD tool
 - Appropriate for subsonic unobstructed external flow
- Simulations:
 - Space Shuttle Orbiter (VSAERO/PANAIR)
 - Convair C240 (QUADPAN) - Tractor Rocket Concept
 - Lockheed C-141B (QUADPAN) - Pole Concept



Johnson Space Center – Houston, Texas

SPACE SHUTTLE LAUNCH VEHICLE (SSLV) CFD ANALYSIS STATUS & PLANS

Advanced Programs Office

Steven G. Labbe

3/3/89

NUMERICAL SIMULATION OF SSLV ASCENT AERO ENVIRONMENT

- RECENT ADVANCES IN CFD ENABLE FRESH LOOK AT SPACE SHUTTLE ASCENT AERODYNAMICS
- JOINT EFFORT BETWEEN ARC TEAM (J.L. STEGER, P.G. BUNING) & JSC TEAM (F. W. MARTIN)

TEAM OBJECTIVES

102

- ARC: Develop the Technology to Numerically Simulate Complex Launch Vehicle Geometry
- JSC: Employ CFD Technology to Gain Insight & Understanding of the Ascent Aero Loads Environment

CFD ANALYSIS

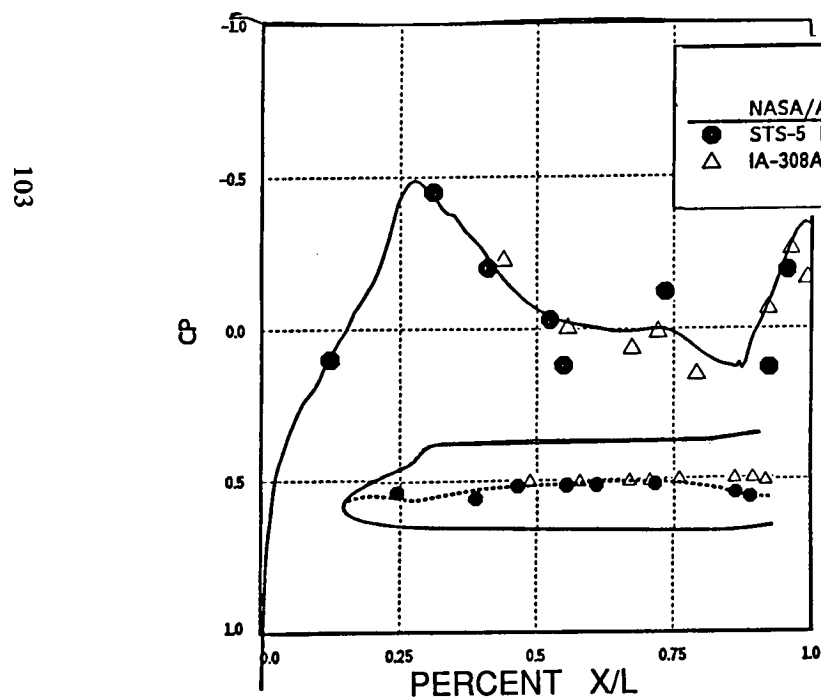
- Complex SSLV Ascent Configuration Modelled Using "CHIMERA" Composite Grid Discretization Approach
- Overset Body-Conforming Grids Of Major Geometry Components - Communication by PEGASUS Code
- F3D Implicit Approx. Factored Finite-Difference Procedure - Solution of 3-D Thin-Layer NS Equs.

CFD ANALYSIS PROGRESS HAS BEEN STEADY & PROMISING

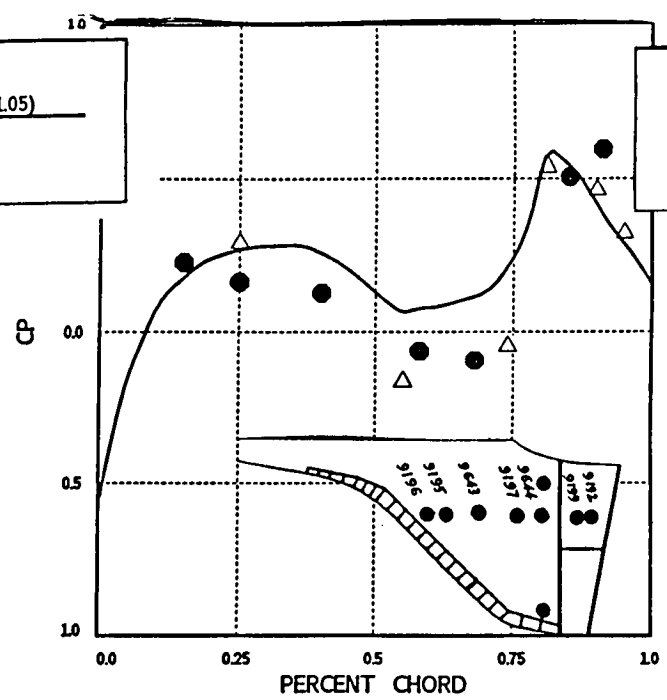
- EFFORTS CONCENTRATED ON FULLY UPDATING SSLV CONFIGURATION GEOMETRY DETAILS
Highest Priority Given to Attach Hardware & LOX/Fuel Feedlines
SRB/IEA Attach Ring and SRB Plume Simulations Incorporated -- Check Out Proceeding
- ABILITY TO ACCURATELY DETERMINE WING LOADS ← → MODEL SSLV GEOMETRY DETAILS

AERO DATABASE COMPARISONS

MID-FUSELAGE

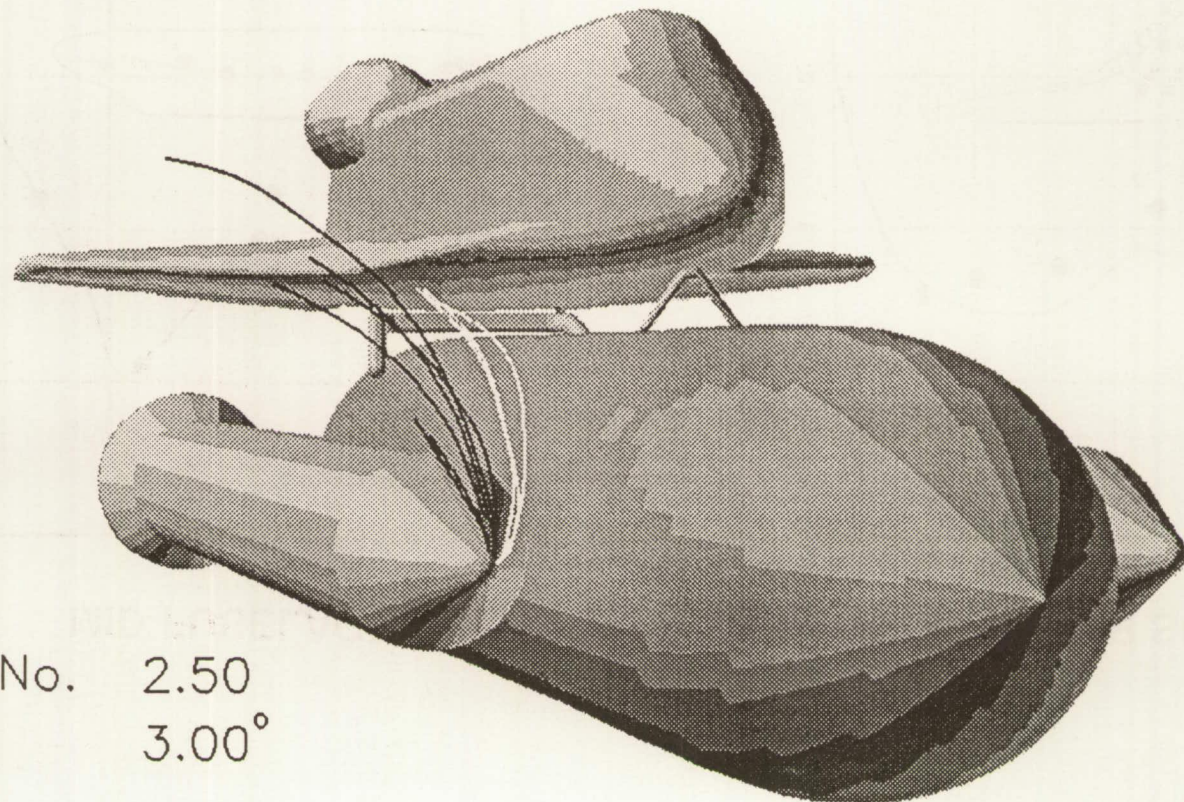


WING UPPER SURFACE



STS-27 Ascent Debris Trajectory Simulation

104



Mach No. 2.50

Alpha 3.00°

MSA-1 (SRB ablator) released @ $0^\circ - 90^\circ$ on nose cone

ORBITER AERODYNAMICS AT HIGH INCIDENCE ANGLES

- Objective:

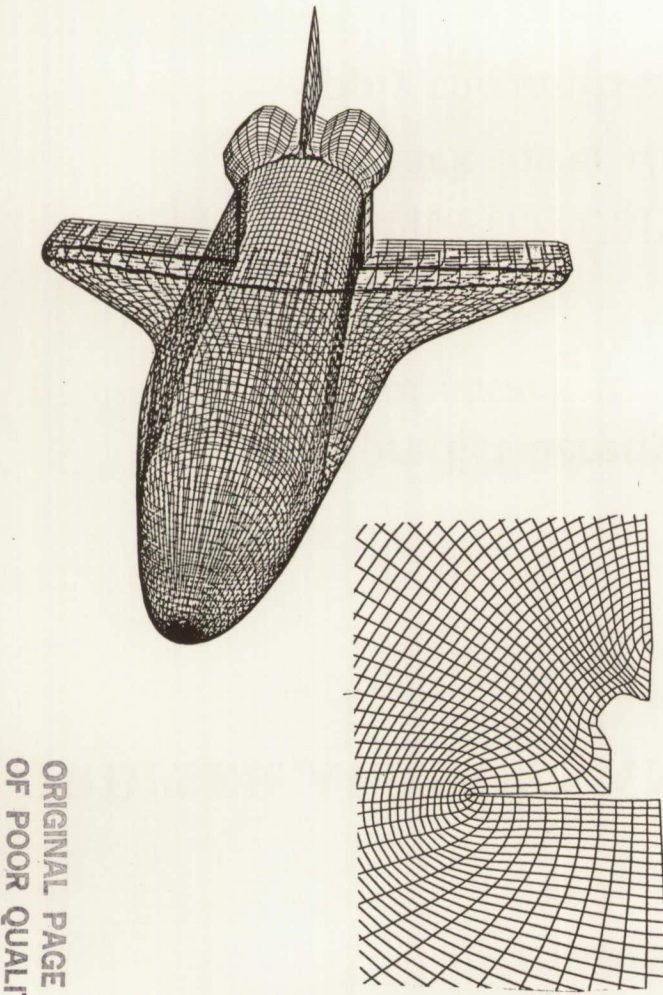
- To predict aerodynamics and flight characteristics for angles of attack up to 90 deg

- Approach:

- Validate the U3D code with wind-tunnel data for angles of attack lower than 50 deg
 - Apply the multi-zonal U3D for higher angles-of-attack flow

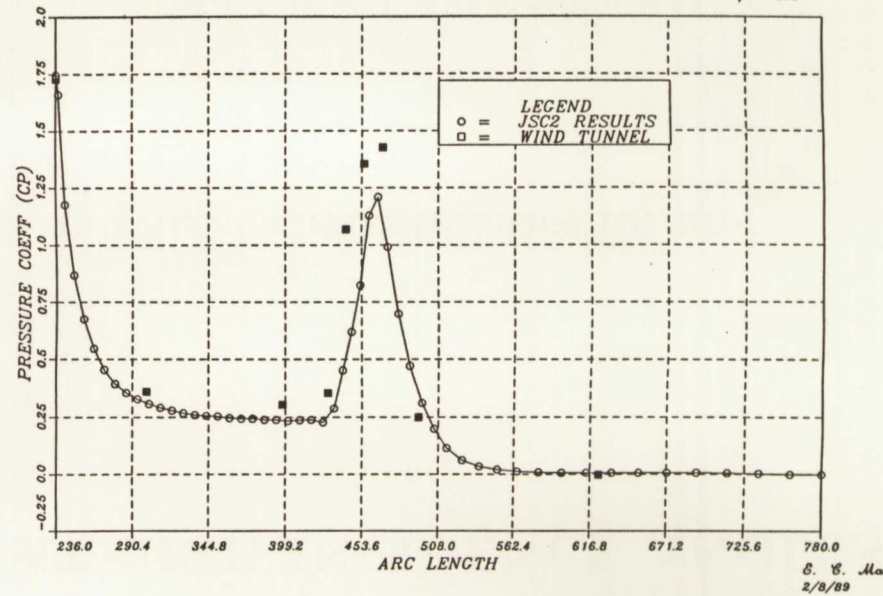
ORBITER GRID AND MACH 5.2 COMPARISON

106



CFD & WIND TUNNEL COMPARISONS

MACH NO. = 5.286
 $\xi = 53, \eta = 35, \zeta = 51$
 $\alpha = 0.07$
 $\phi = 180.0$



ORIGINAL PAGE IS
OF POOR QUALITY

MACH 7.32 FLOW RESULTS AND GRID

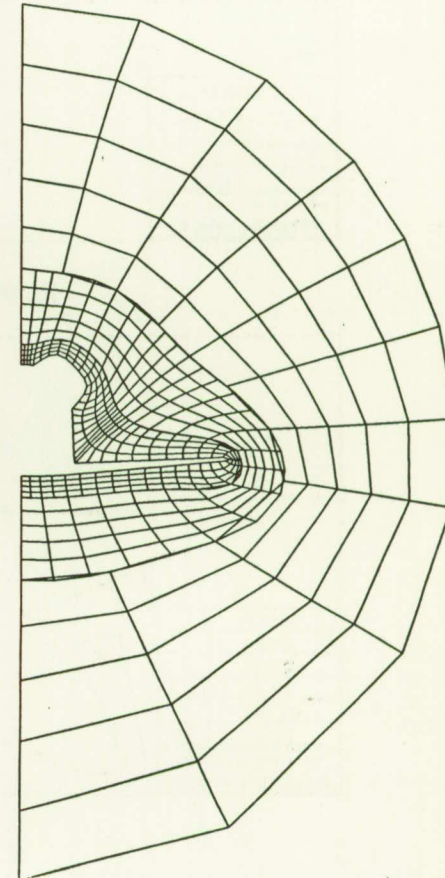
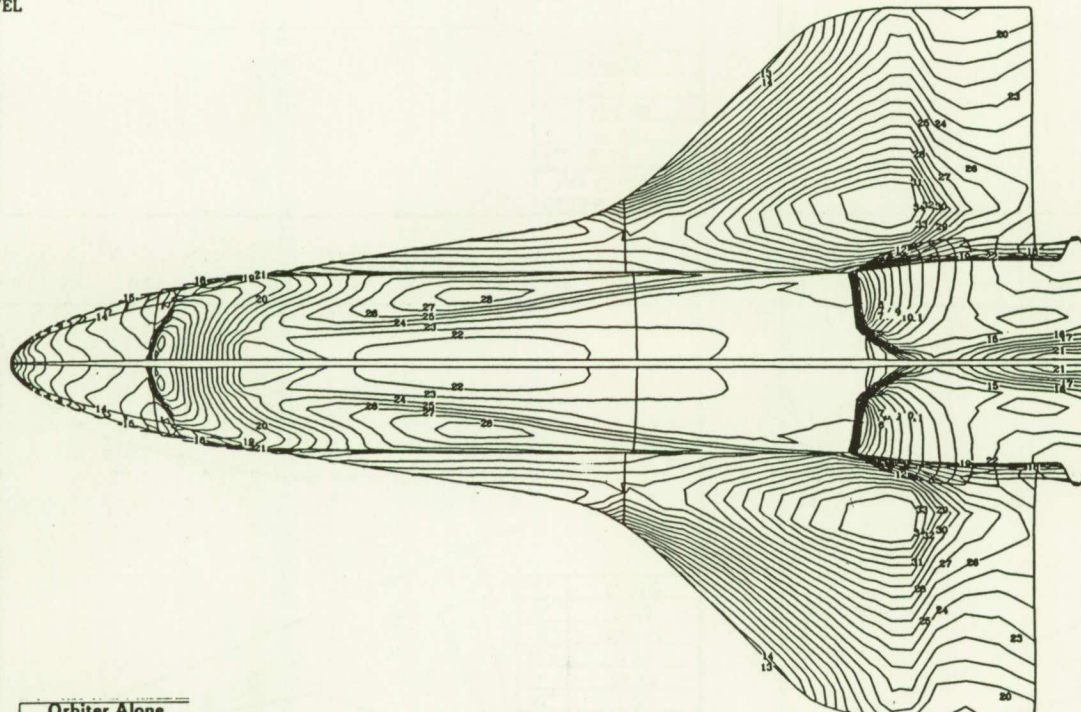
MACH NUMBER

CONTOUR LEVEL

1 0.164
2 0.361
3 0.558
4 0.755
5 0.953
6 1.150
7 1.347
8 1.544
9 1.742
10 1.939
11 2.136
12 2.333
13 2.530
14 2.728
15 2.925
16 3.122
17 3.319
18 3.517
19 3.714
20 3.911
21 4.108
22 4.306
23 4.503
24 4.700
25 4.897
26 5.095
27 5.292
28 5.489
29 5.686
30 5.884
31 6.081
32 6.278
33 6.475
34 6.672
35 6.870

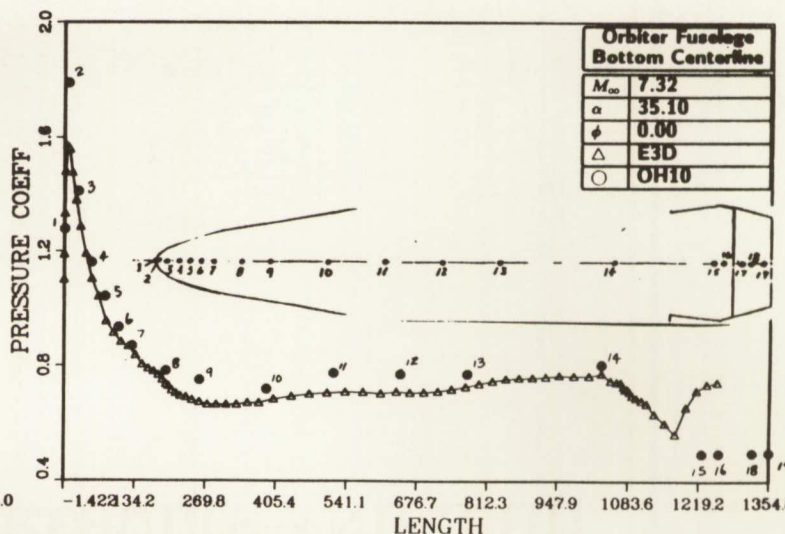
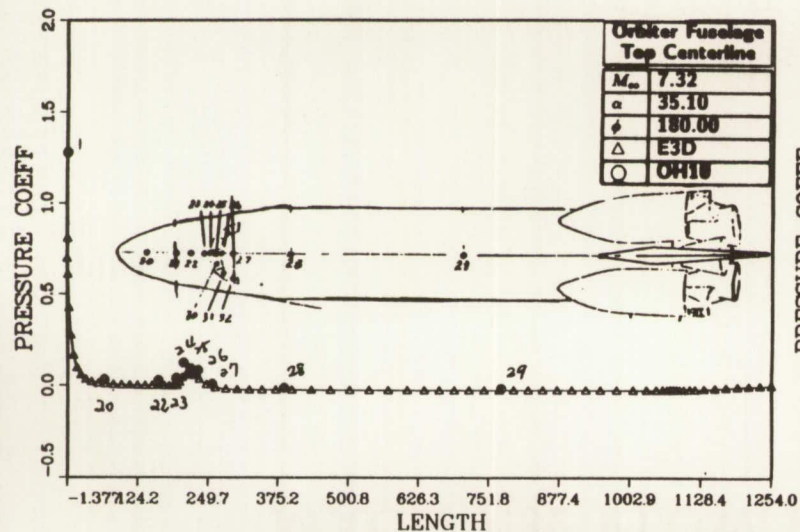
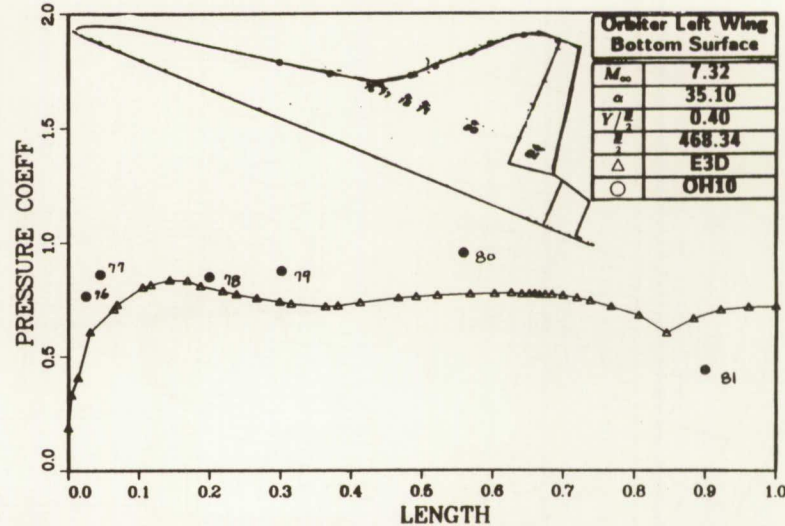
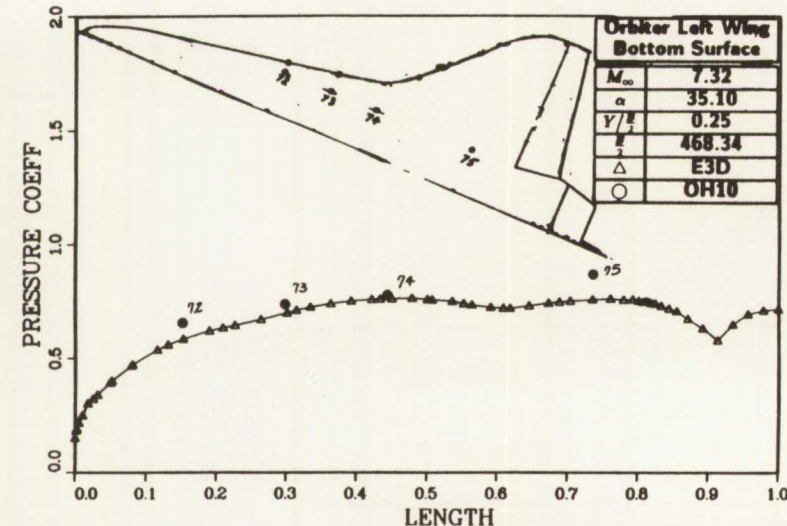
Orbiter Alone	
Surface Mach No	
M_{∞}	7.32
α	0.00
Grid	76 x 35 x 51

WEY 1/13/89



NUMERICAL INVESTIGATION OF CONTINGENCY ABORT

108



ORBITER ENTRY FLOW SIMULATION

- Objective:

- To assess aerodynamic and heating issues for each flight
- To validate the VRFNS code using flight data

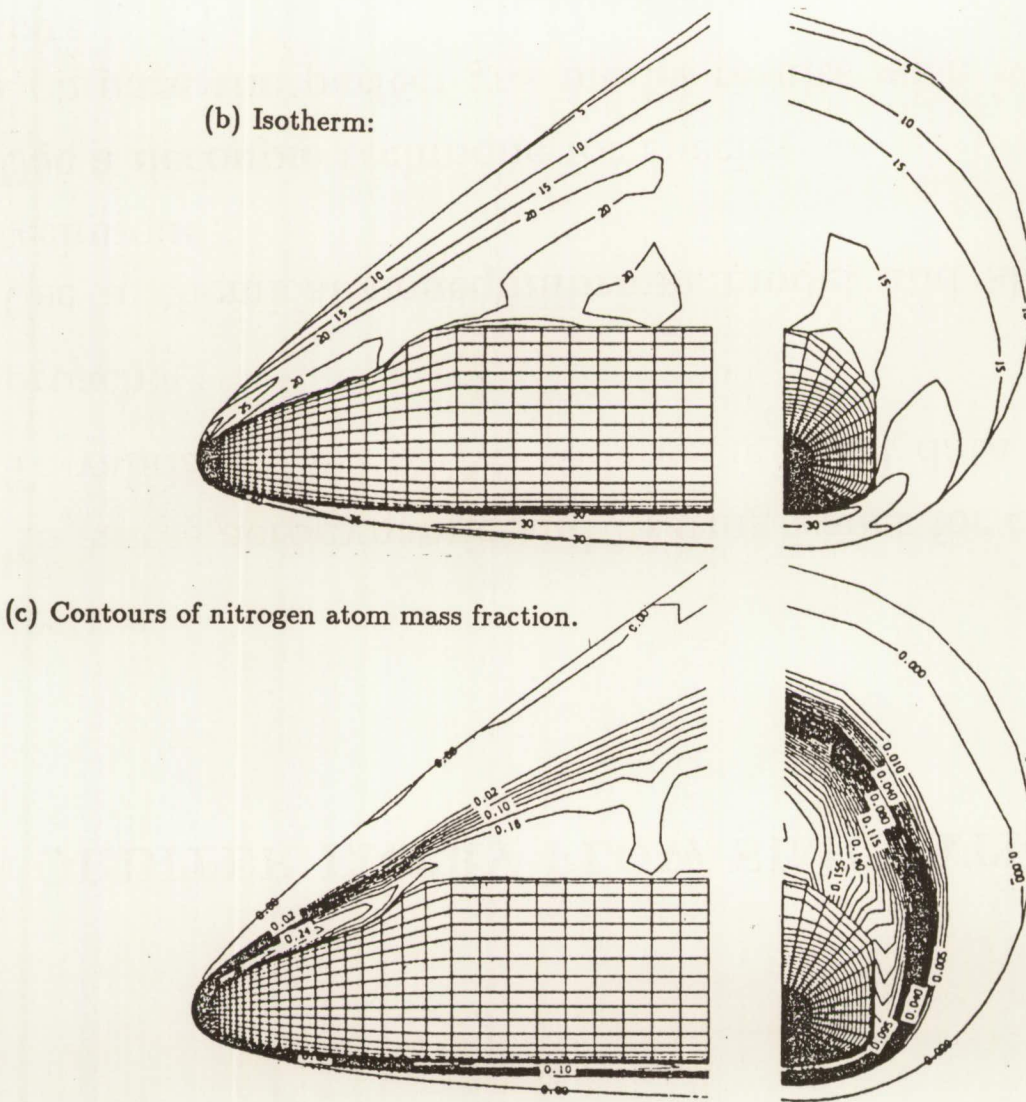
601

- Approach:

- Use a chemical nonequilibrium model and shock-fitting technique
- Use a decouple technique for species
- Compare the perfect-gas model results with wind-tunnel data

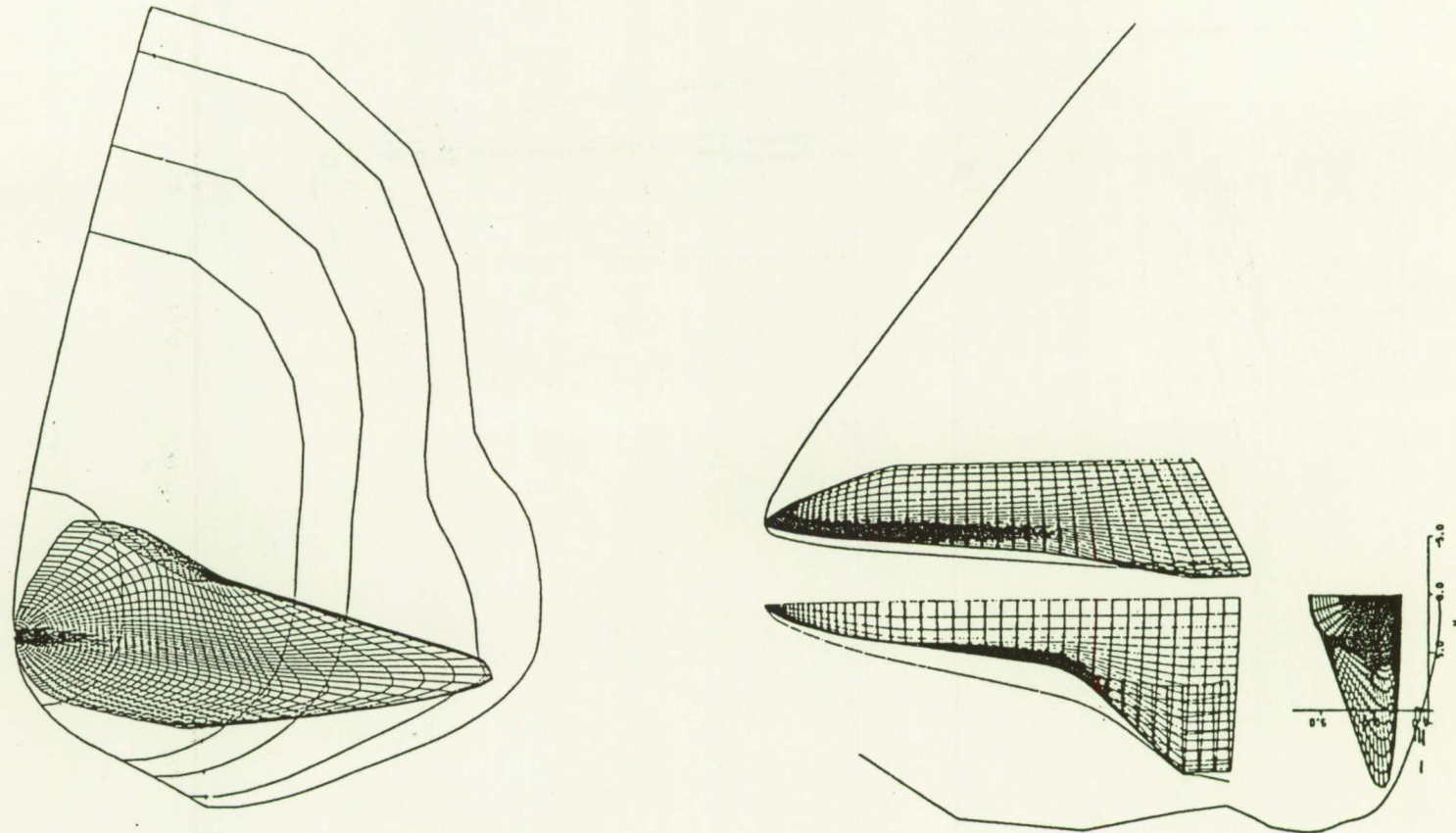
INVISCID CHEMICAL NONEQUILIBRIUM FLOW

Orbiter canopy



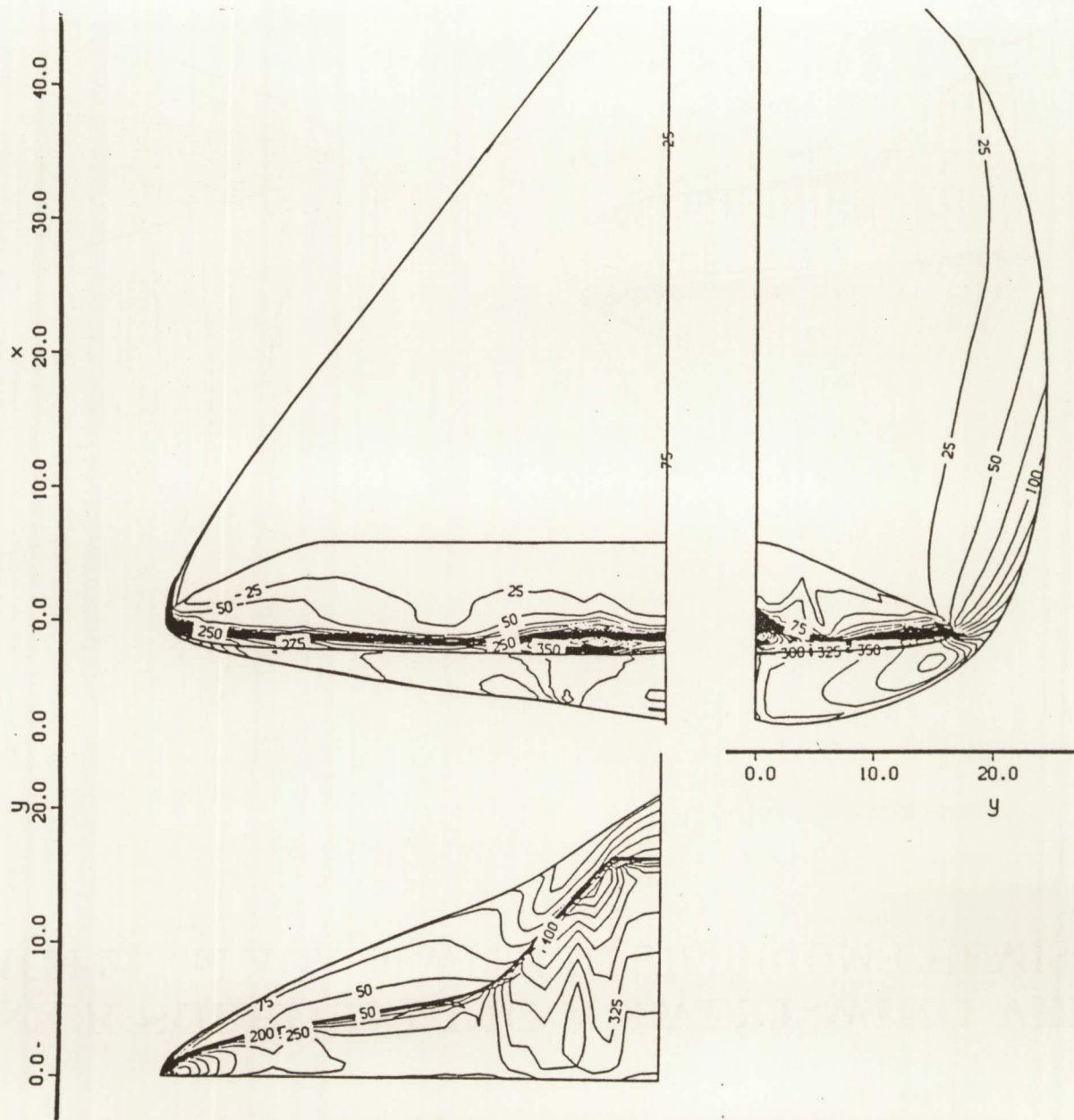
**BOW SHOCK SURROUNDING A SWEPT-WING VEHICLE
AT MACH 22 and AOA 40 WITH EQUILIBRIUM CHEMISTRY**

III



PROJECTED VIEWS OF TEMPERATURE CONTOURS

112

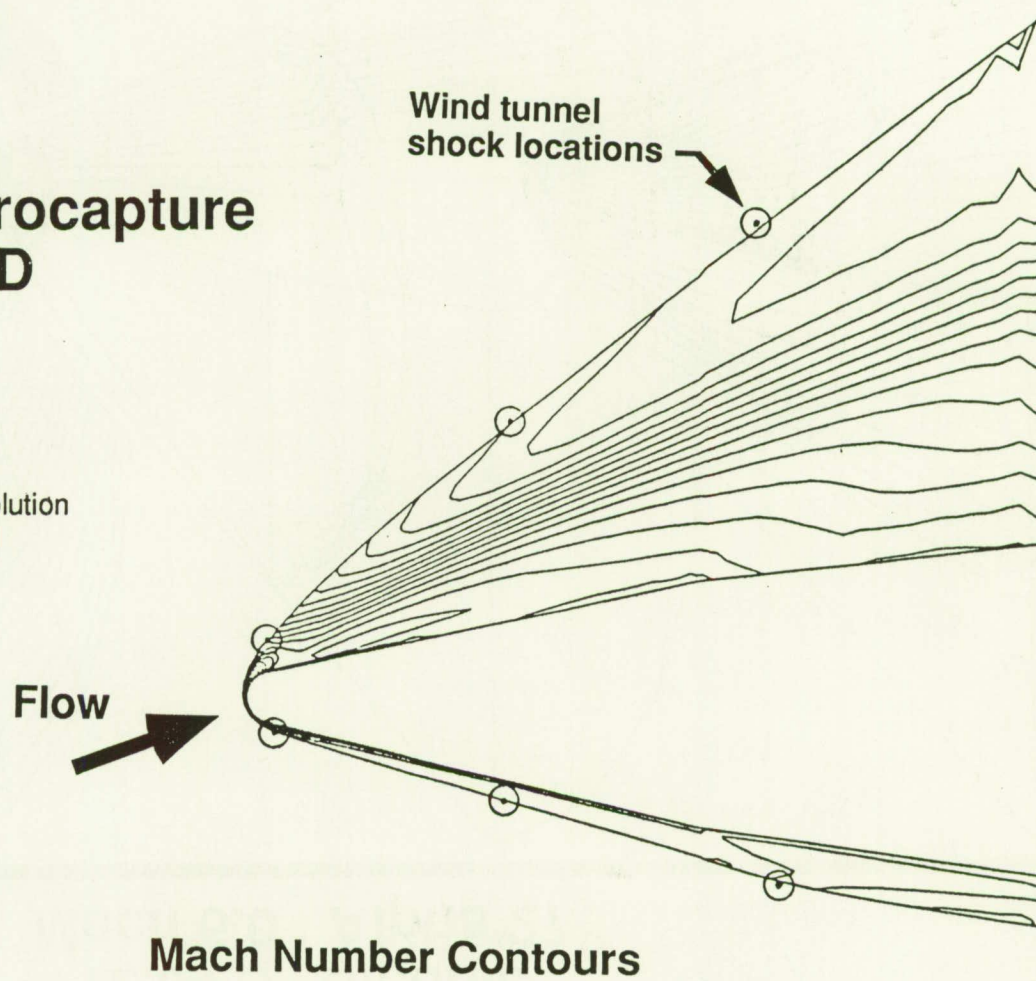


Comparison of shock shape with data

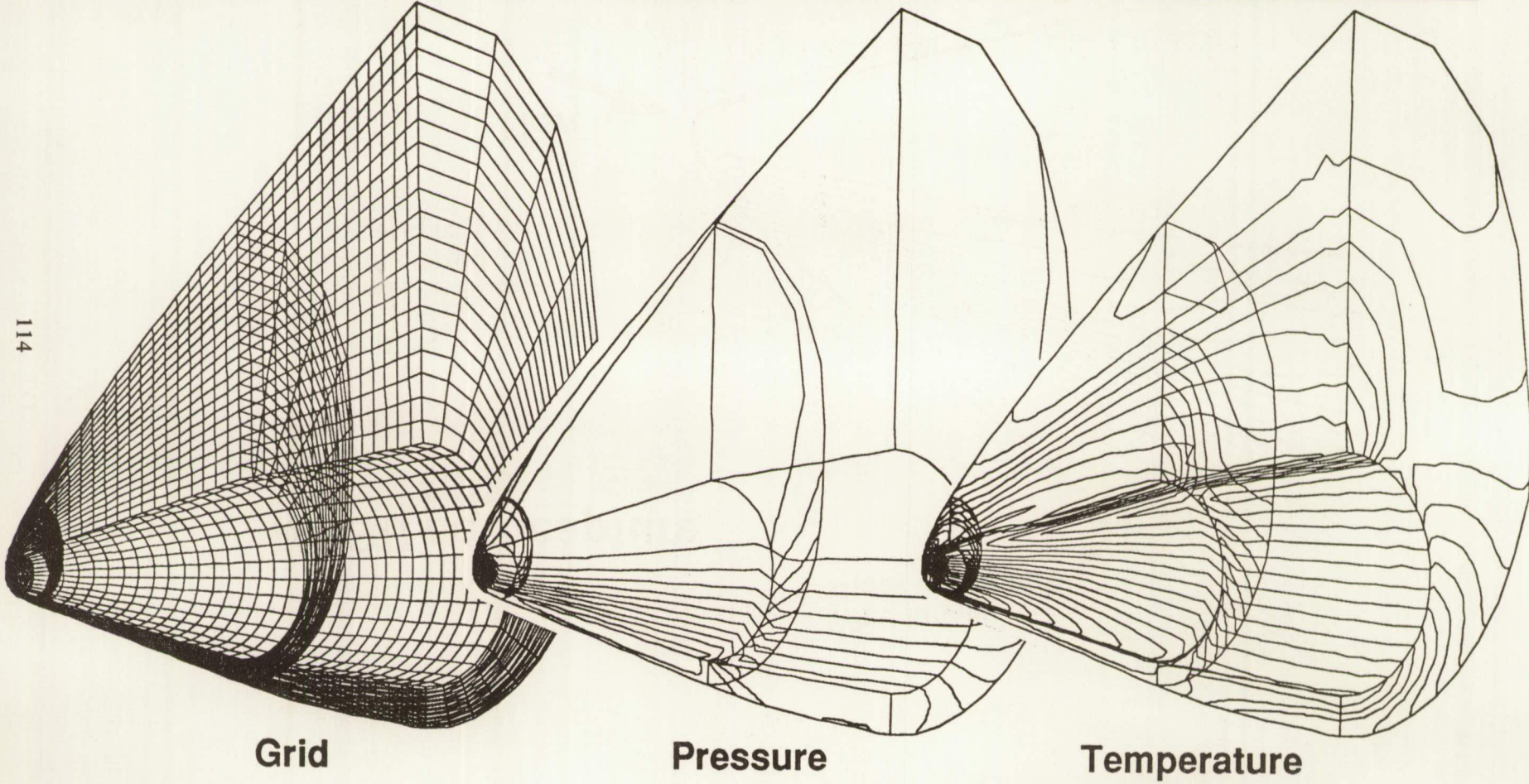
MRSR aerocapture CFD

113

Mach 5.997
Alpha 27 deg
Air
Navier-Stokes Solution
45 x 19 x 29 grid
1200 iterations
CFL 2



12.84°/7° Biconic
Mach 6.0 Alpha 27°

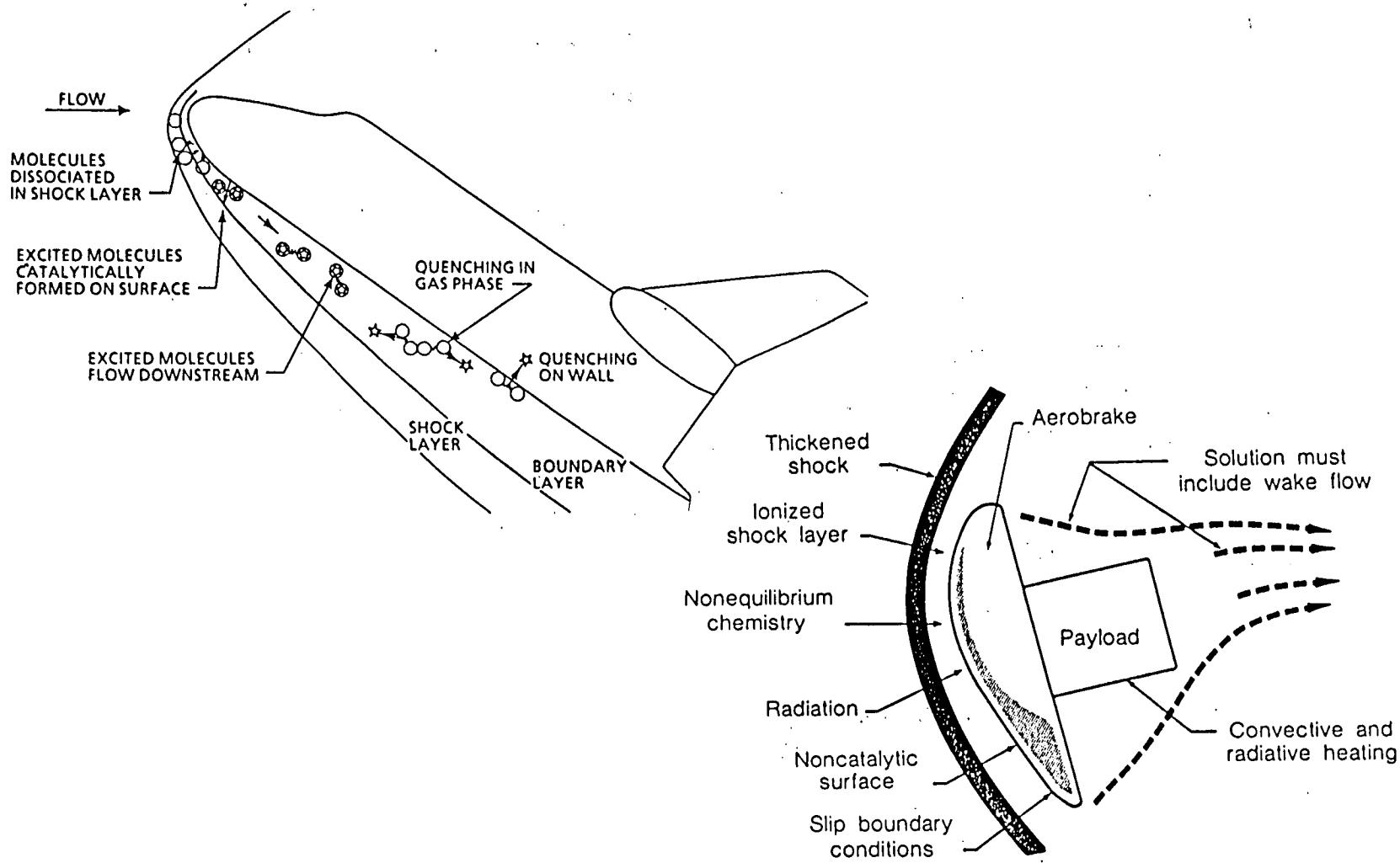


AFE FLOWFIELD SIMULATION

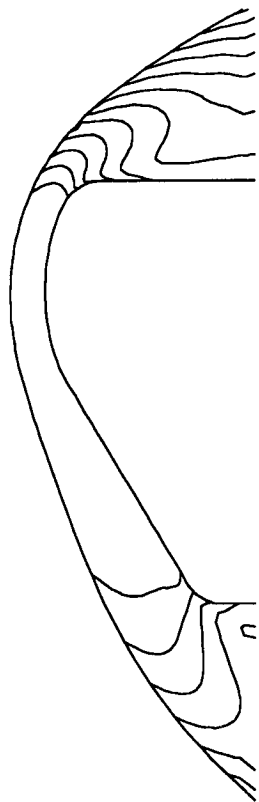
- Objectives:
 - To predict aerodynamic loads and heating distributions for flight conditions
 - To define flowfield environment using appropriate physical models
- Approaches:
 - Developed the VRFL0 code for typical aerobraking vehicles
 - Calibrated the code using wind-tunnel data
 - Compared the two-temp and 11-species model results with RAMC data
 - Performed sensitivity studies of different models

PHYSICAL MODELING FOR HYPERSONIC VEHICLES

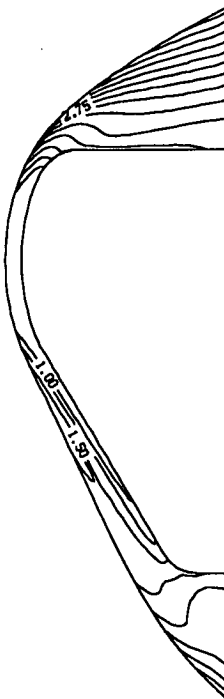
116



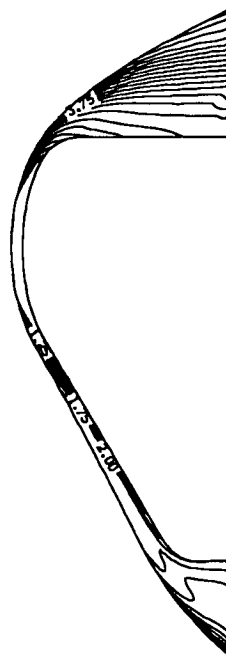
Comparison of Shock Shapes and Subsonic Regions for an AFE Configuration



Ideal Air
Mach 9.81



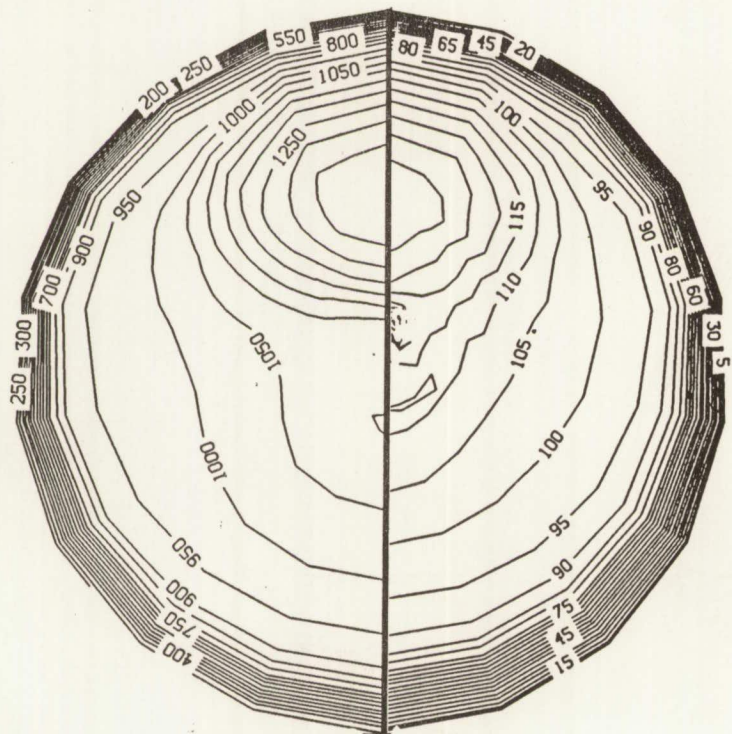
Ideal CF_4
Mach 6.29



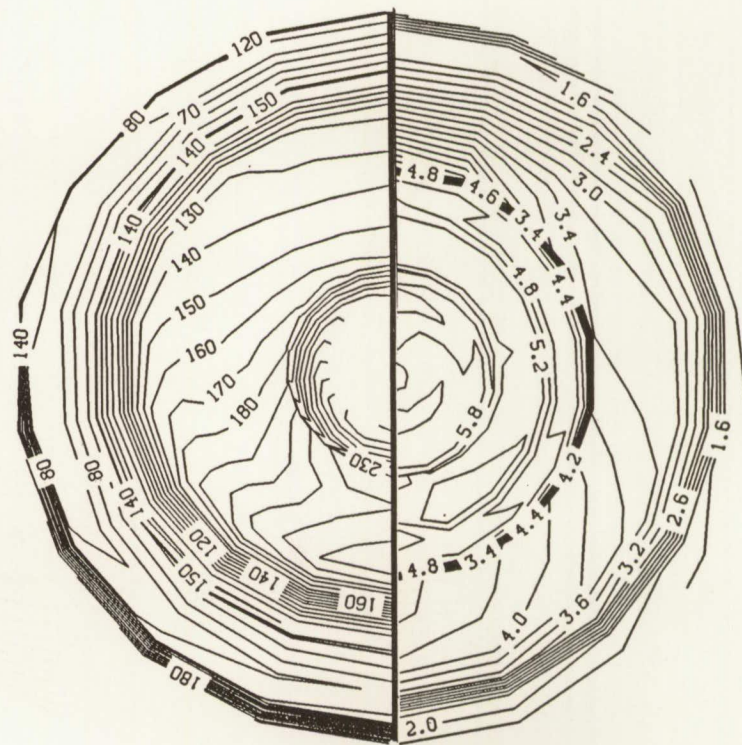
Equilibrium Air
Mach 32.0

COMPARISON OF FLIGHT AND WIND-TUNNEL PRESSURES

118



(a) Front view

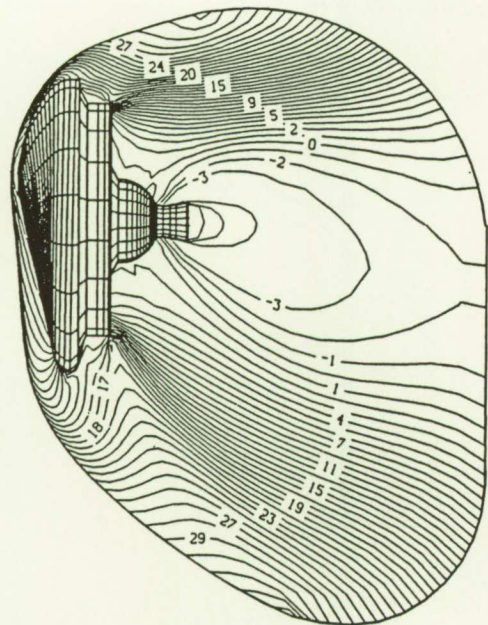


(b) Rear view

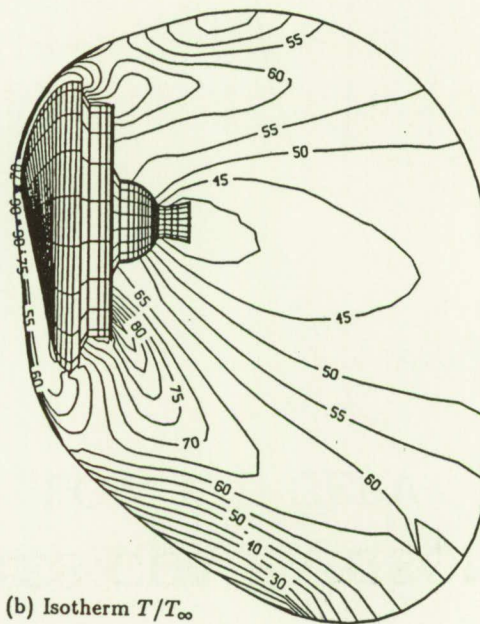
Comparison of flight and wind-tunnel wall pressure distributions (the left side corresponds to the flight case).

CONTOUR PLOTS OF AFE FLIGHT FLOWFIELD

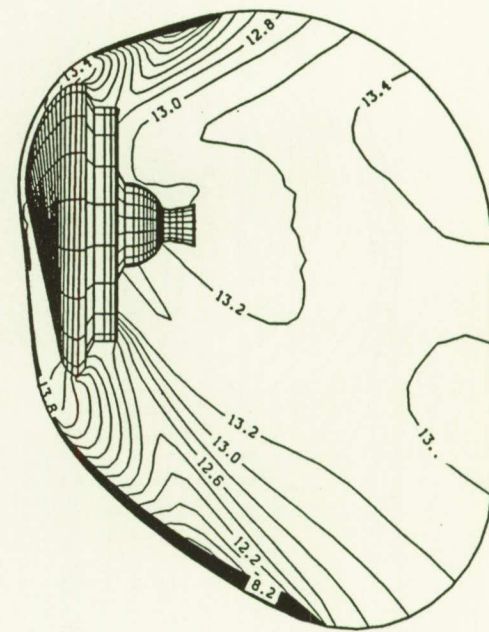
inviscid chemical nonequilibrium flow in the pitchplane



(c) z-component velocity $w\sqrt{\rho_\infty/p_\infty}$

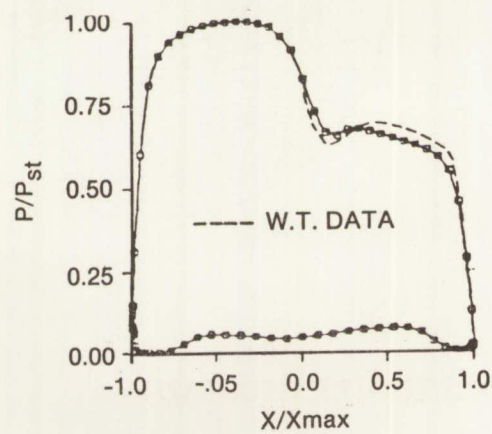
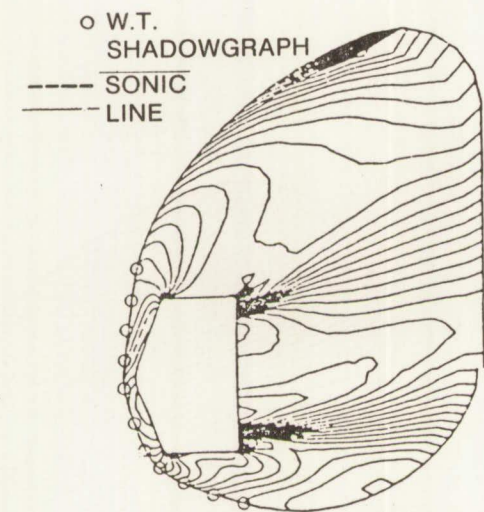


(b) Isotherm T/T_∞

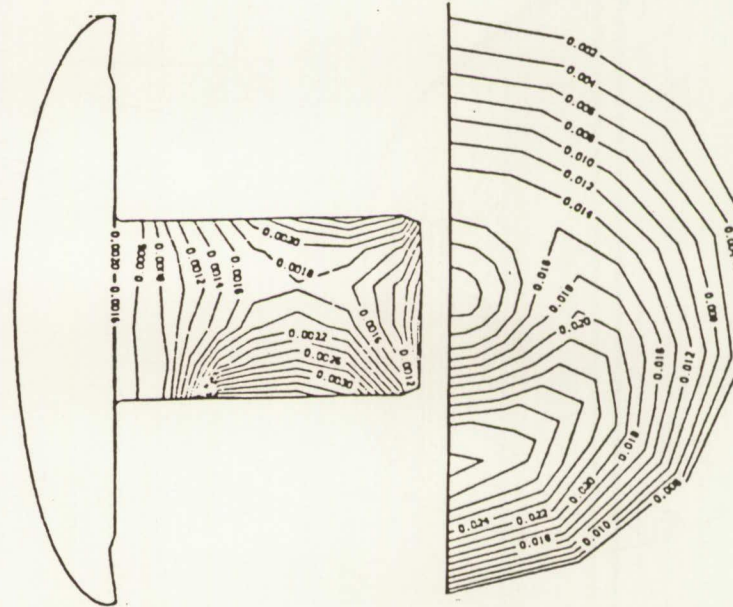


(b) N_s

WALL PRESSURES COMPARISON AND HEATING LOW L/D CERV



$$P_{st} = 131.793$$



TECHNOLOGY DEVELOPMENT

- A multi-zonal Navier-Stokes code to predict the Orbiter flow at incidence up to 90 deg
- A thermochemical nonequilibrium PNS code for high L/D configurations
- An Euler code with adaptive, unstructured grid for complex geometry
- Radiation and ablation modeling and code implementation

NASA'S CFD VALIDATION PROGRAM

by

Dale R. Satran
Program Manager
Aerodynamics Division
NASA Headquarters

With computational fluid dynamics (CFD) becoming a productive research and design tool, the requirement to validate CFD codes has grown significantly. NASA has emphasized CFD validation activities since 1986 when a separate work element was formed to fund experimental activities related to validation. NASA's CFD and CFD validation programs are closely coordinated to ensure that experimental data bases are available as soon as possible for validating codes. In response to industry and academic requirements, four levels of experimental research have been defined as part of CFD validation with NASA's Aeronautics Advisory Committee (AAC) support although only the fourth level actually has the detailed information necessary for validating codes.

Critical flow physics especially turbulence modeling are key to improved CFD codes. NASA has focused additional resources on transition and turbulence physics to meet these requirements. With improved turbulence models, CFD codes will be more accurate, robust, and efficient. However, with the level of detailed information available from CFD codes, highly accurate and detailed experiments are required to capture the critical information for validating codes. Advanced instrumentation especially non-intrusive instrumentation is required to acquire this information in validation experiments. The CFD validation program is being coordinated and managed to address these critical activities. A list of experiments which are currently being supported at least partially has been included with this presentation.

CFD CODE VALIDATION DEFINITION

~~OAST~~

25 20 15 10 5

- DETAILED SURFACE-AND-FLOW-FIELD COMPARISONS WITH EXPERIMENTAL DATA TO VERIFY THE CODE'S ABILITY TO ACCURATELY MODEL THE CRITICAL PHYSICS OF THE FLOW. VALIDATION CAN OCCUR ONLY WHEN THE ACCURACY AND LIMITATIONS OF THE EXPERIMENTAL DATA ARE KNOWN AND THOROUGHLY UNDERSTOOD AND WHEN THE ACCURACY AND LIMITATIONS OF THE CODE'S NUMERICAL ALGORITHMS, GRID-DENSITY EFFECTS, AND PHYSICAL BASIS ARE EQUALLY KNOWN AND UNDERSTOOD OVER A RANGE OF SPECIFIED PARAMETERS.

CFD VALIDATION CATEGORIES

—OAST

CATEGORIES OF CFD-RELATED EXPERIMENTATION

- A. EXPERIMENTS DESIGNED TO UNDERSTAND FLOW PHYSICS
- B. EXPERIMENTS DESIGNED TO DEVELOP PHYSICAL MODELS FOR CFD CODES
- C. EXPERIMENTS DESIGNED TO CALIBRATE CFD CODES
- D. EXPERIMENTS DESIGNED TO VALIDATE CFD CODES

ALL FOUR CATEGORIES ARE IMPORTANT AND ARE NECESSARY
TO BUILD A MATURE CFD CAPABILITY

IMPLEMENTATION PLAN

~~OAST~~

- ALL EXPERIMENTS HAVE BEEN CLASSIFIED AND DOCUMENTED
 - GOALS
 - LIMITATIONS
 - MODELING
 - PARTICIPATION
 - LEVEL OF EFFORT
- SEVERAL KEY EXPERIMENTS INVOLVE MULTIPLE RESEARCH CENTERS
- CFD VALIDATION WORKSHOP HELD TO IDENTIFY CRITICAL NEEDS
- COORDINATING BOARD FOR CFD VALIDATION DEVELOPING UPDATED DETAILED IMPLEMENTATION PLAN
- EFFORTS INITIATED TO INVOLVE THE AEROSPACE INDUSTRY AND UNIVERSITIES

CFD VALIDATION PROGRAM

~~OAST~~

**EXPERIMENTS HAVE BEEN CLASSIFIED
INTO MULTIPLE CATEGORIES**

CATEGORY	AMES	LANGLEY	LEWIS	TOTAL
A. FLOW PHYSICS	16	35	29	80
B. FLOW MODELING	8	7	13	28
C. CODE CALIBRATION	6	19	12	37
D. CODE VALIDATION	7	24	16	47
TOTAL NUMBER OF EXPERIMENTS	27	45	29	101

CFD VALIDATION PROGRAM

OAST

- EXPERIMENTS COVER LARGE SPEED RANGE
 - SUBSONIC: 33 EXPERIMENTS
 - TRANSONIC: 27 EXPERIMENTS
 - SUPERSONIC: 23 EXPERIMENTS
 - HYPERSONIC: 18 EXPERIMENTS
- EXPERIMENTS FALL INTO SEVERAL VEHICLE CLASSES
 - GENERIC
 - FIGHTER/ATTACK
 - SUBSONIC TRANSPORT
 - ROTORCRAFT
 - ASTOWL
 - PROPULSION SYSTEMS

CFD VALIDATION EVENTS

~~OAST~~

- NEW RTOP ELEMENT, FLOW MODELING AND VERIFICATION, CREATED FY 1986
- NRC ASEB REVIEW OF CFD ACTIVITIES FY 1986
- NASA REVIEW AND DEVELOPMENT OF IMPLEMENTATION PLAN FOR CFD VALIDATION FEB., 1986
- AAC AD HOC SUBCOMMITTEE REVIEW OF CFD VALIDATION FY 1987
- NASA COORDINATING BOARD FOR CFD VALIDATION FORMED JUNE, 1987
- FIRST NASA CFD VALIDATION WORKSHOP AT AMES JULY, 1987
- IMPLEMENTATION PLAN REVISED BY COORDINATING BOARD AUG., 1987
- AGARD CFD VALIDATION CONFERENCE IN LISBON MAY, 1988
- CFD VALIDATION ACTIVITIES AND IMPLEMENTATION PLAN REVIEW NOV., 1988
- NASA CFD CONFERENCE AT AMES MAR., 1989
- SECOND NASA CFD VALIDATION WORKSHOP JULY, 1990

NASA CFD VALIDATION WORKSHOP

~~OAST~~

- 103 PERSONS ATTENDED FROM NASA, DOD, INDUSTRY, AND UNIVERSITIES
- 31 PRESENTATIONS WERE GIVEN ON CFD VALIDATION STATUS
- 6 WORKING GROUP SESSIONS FOCUSED ON NEAR AND FAR TERM NEEDS
- NUMEROUS RECOMMENDATIONS
 - STANDARDIZED TEST CASES FOR CALIBRATION
 - CLOSE COOPERATION BETWEEN CFD DEVELOPERS AND EXPERIMENTALISTS
 - INCREASE FLIGHT-BASED ACTIVITIES
 - DETAILED MEASUREMENTS OF FLOW FIELD AND BOUNDARY CONDITIONS
 - IMPROVED OR NEW NON-INTRUSIVE MEASUREMENT CAPABILITIES
 - REDUNDANCY IN BOTH MEASUREMENTS AND EXPERIMENTS

SUMMARY

OAST

- AAC AD HOC TASK TEAM RECOMMENDATIONS
IMPLEMENTED
- NASA PROGRAM EXPANDING TO COVER
ADDITIONAL AREAS
- INSTRUMENTATION HAS BEEN ADDED TO
SEVERAL FACILITIES BY VALIDATION PROGRAM
- INCREASED EMPHASIS ON COOPERATIVE PROGRAMS
WITH UNIVERSITIES AND INDUSTRY

AMES CFD VALIDATION PROGRAM FOR FY 1989

LEX/DELTA VORTICAL FLOW
TRANSonic LOW ASPECT RATIO WING-BODY
REARWARD FACING STEP
SSME TURNAROUND DUCT
SUPERSONIC SHOCK BOUNDARY LAYER INTERACTION
COMPRESSIBLE PRESSURE-DRIVEN 3-D INTERACTIONS
2-D TRANSonic CIRCULATION CONTROL
3-D SPIN FLOWS
3-D LOW SPEED WEDGE FLOW WITH SEPARATION
TRANSonic SUPERCRITICAL AIRFOIL
LOW SPEED HIGH ALPHA INVESTIGATION
CFD VALIDATION FOR WING AERODYNAMICS
3-D HIGH ASPECT RATIO SEPARATED FLOW
STOVL AERO/PROPELLION INTERACTION
THERMO-CHEMICAL NONEQUILIBRIUM FLOWS
PHOTODIAGNOSTIC INSTRUMENTATION
UNSTEADY VISCOUS FLOW
HYPERSONIC SHOCK BOUNDARY INTERACTION
TURBULENT SHEAR LAYERS
TURBULENT BOUNDARY LAYERS
ALL-BODY HYPERSONIC TEST
HIGH SPEED ROTOR FLOWS
HYPERSONIC REAL GAS
SHOCK TUNNEL NOZZLE TESTS
3.5' HWT NOZZLE TESTS
COMBUSTION/DETINATION
FLIGHT/CFD CORRELATION OF F-18 WING PRESSURES AT HIGH ALPHA
SUPERSONIC VORTEX-SHOCK WAVE INTERACTION

LANGLEY CFD VALIDATION PROGRAM FOR FY 1989

TRANSONIC HIGH ASPECT-RATIO WING
TRANSONIC LOW ASPECT RATIO WING
REARWARD FACING STEP IN WATER TUNNEL
REARWARD FACING STEP IN BART
DELTA WING VORTEX FLOWS
SUPERSONIC COAXIAL JET
TURBULENT MODELING IN SEPARATED FLOWS
45-DEG SWEEP AIRFOIL
BARF LDV TEST
SUPERSONIC BOUNDARY LAYER TRANSITION
NTF FLAT PLATE TEST
VORTEX BURST EXPERIMENTS
HYPERSONIC FLIGHT INSTRUMENTATION
HYPERSONIC INLET TESTS IN HELIUM
HYPERSONIC SHOCK-ON-LIP
HALIS ORBITER EXPERIMENT
BLUNT BODIES (AOTV/AFE) EXPERIMENT
HYPERSONIC WINGED SLENDER BODY
OSCILLATING CANARD/WING UNSTEADY PRESSURES
VALIDATION OF JET PLUME MODULES
SUPERSONIC JET PLUME DYNAMICS
SUPERSONIC HIGH-ALPHA FLOWFIELD
OFF-AXIS WING-BODY STUDY
STORE/CAVITY SEPARATION EXPERIMENTS
WAVERIDER DESIGN PROCEDURE
5 DEG CONE EXPERIMENT
75/76-DEG DELTA WINGS
NTF FOREBODY/MISSLE MODEL
LEADING EDGE VORTEX FLAP
X-29 EXPERIMENT IN NTF
3-D TRANSONIC CAVITY FLOW
LOW REYNOLDS NUMBER AIRFOIL EXPERIMENTS
CONFLUENT BOUNDARY LAYER
GORTLER INSTABILITY ON AIRFOILS
EXPERIMENTAL INVESTIGATION OF TURBULENCE
RANGE AND ACCURACY OF THIN FILM ARRAYS
JUNCTURE FLOW EXPERIMENT
SWEPT SUPERCRITICAL HLFC AIRFOIL EXPERIMENTS
TWIN ENGINE AFTERBODY EXPERIMENT

LEWIS CFD VALIDATION PROGRAM FOR FY 1989

3-D SHOCK WAVE/TURBULENT BOUNDARY LAYER INTERACTIONS
3-D FLOWS IN HIGH SPEED TURBOMACHINERY
BLADE SURFACE BOUNDARY LAYER
FUNDAMENTAL SEPARATION BUBBLE RESEARCH
AIRFOIL (BLADING) FLOW CONTROL
LEADING EDGE STAGNATION REGION
BOUNDARY LAYERS IN TRANSITION
UNSTEADY HEAT TRANSFER IN ROTOR WAKES
TRANSITION DUCT - AERO & HEAT TRANSFER
VORTEX GENERATORS
SHEAR LAYER EXCITATION - JET MIXING
SHEAR LAYER EXCITATION - SLOT RESONATOR
MULTI-PHASE FLOWS
MULTI-PHASE FLOW AND FLUID SPRAY STUDY
LOW TEMPERATURE HEAT TRANSFER
FUEL SWIRLER CHARACTERIZATION
COMBUSTION CHARACTERISTICS OF HYDROCARBON FLAMES
KINETIC STUDY OF H₂/O₂ SYSTEM
FLOW INTERACTION EXPERIMENT
HOT GAS INGESTION
COHERENT STRUCTURES IN SUPERSONIC SHEAR LAYER
AERO CHARACTERISTICS OF AIRFOIL WITH ICE ACCRETION
TURBOMACHINERY BLADE ROW INTERACTIONS
SUPERSONIC THROUGH-FLOW CASCADE RESEARCH
CENTRIFUGAL COMPRESSOR FLOW RESEARCH
SUPERSONIC THROUGH-FLOW FAN RESEARCH
HIGH REYNOLDS NUMBER (HEAT TRANSFER)
DETAILED AERO OF ADVANCED TURBOPROPS
FUEL RICH CATALYTIC COMBUSTION

SESSION III

TRANSITION AND TURBULENCE

Chairman:

Thomas A. Pulliam

**Chief, Computational Physics Section
Fluid Dynamics Division
NASA Ames Research Center**

UNDERSTANDING TRANSITION AND TURBULENCE THROUGH DIRECT SIMULATIONS

P. R. Spalart & J. J. Kim

A. R. C., C. F. D. Branch, Turbulence Physics Section

Direct simulations consist in solving the full Navier-Stokes equations, without any turbulence model, and describing all the detailed features of the flow. Usually the flows are three-dimensional and time-dependent and contain both coarse and fine structures, which makes the numerical task very challenging in terms of both the algorithm and the computational effort. Most of the work until now has involved spectral methods, which are highly accurate but not very flexible in terms of geometry or complex equations. For that reason, future work will also rely on high-order finite-difference or other methods.

Direct simulations complement experimental work, and both contribute to the theory and the empirical knowledge of turbulence. Once such a simulation has been shown to be accurate the flow field is completely known, in three dimensions and time, including the pressure, the vorticity and any other quantity. On the other hand, most simulations to date solved the incompressible equations in rather simple geometries, and direct simulations will always be limited to moderate Reynolds numbers. Extensive simulations have been conducted in homogeneous turbulence, channel flows, boundary layers, and mixing layers. Much effort is devoted to addressing flows with compressibility and chemical reactions, and to new geometries such as a backward-facing step.

UNDERSTANDING TRANSITION AND TURBULENCE THROUGH DIRECT SIMULATIONS

P. R. Spalart & J. J. Kim

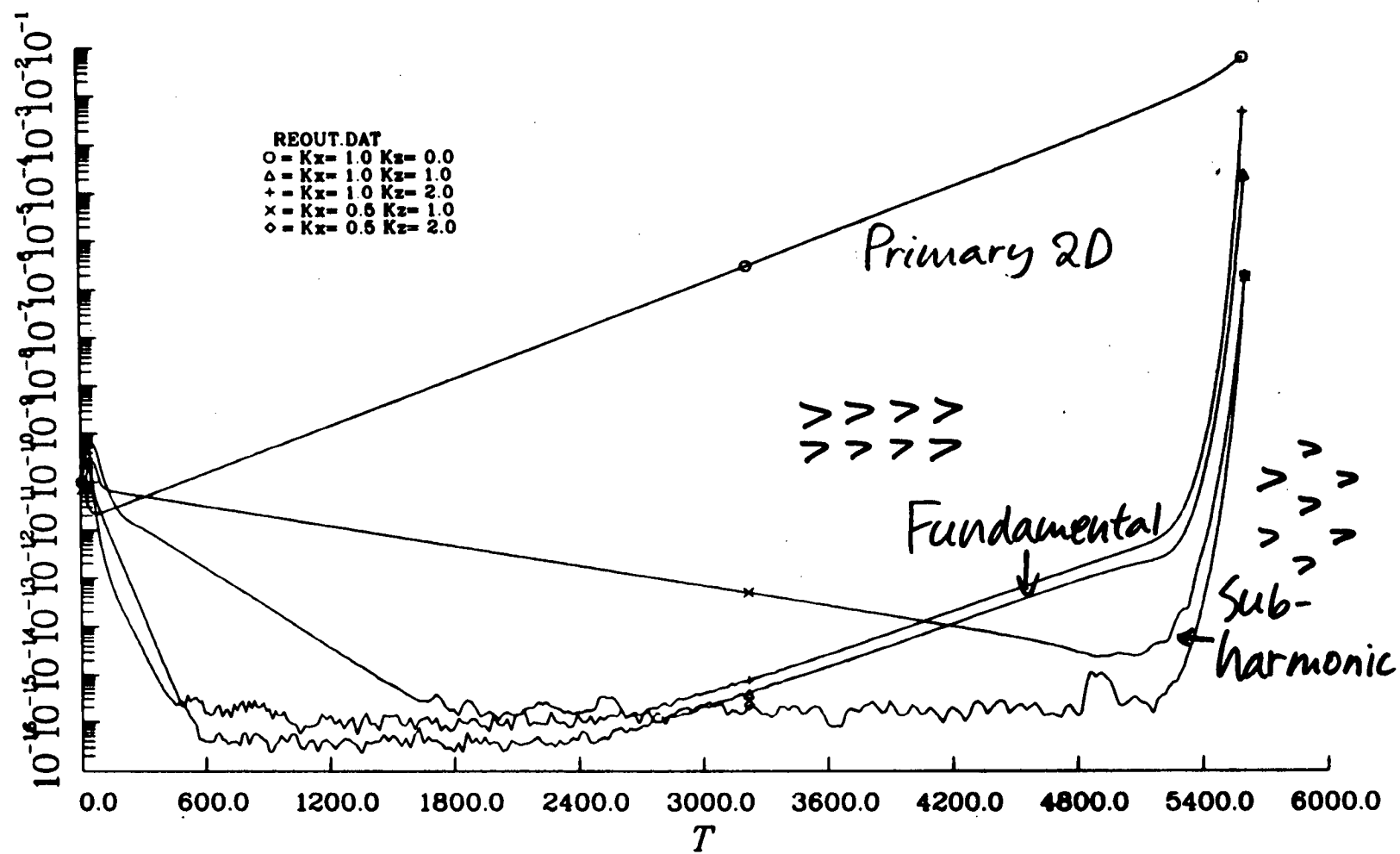
A. R. C., C. F. D. Branch, Turbulence Physics Section

- Secondary instability in channel flow.
- Stability and relaminarization of the swept attachment-line flow.
- Improvement of the pressure term in turbulence models.
- Coherent structures in homogeneous and wall-bounded shear flows.
- Lyapunov exponents of a turbulent channel flow.
- Growth of compressible mixing layers.

Secondary instability in channel flow

- Direct simulation is applied to “natural” transition; only small ($\approx 10^{-10}$) random disturbances are introduced.
- By the primary instability, a 2D TS wave grows (wavenumbers $k_x = 1, k_z = 0$) (x streamwise). The final 3D breakdown may start as a “K” type (fundamental, $k_x = 1$, aligned Λ vortices) or as an “H” type (subharmonic, $k_x = 1/2$, staggered Λ ’s). Theory and experiments don’t fully agree in a channel.
- We find that spanwise nonuniformities ($k_x = 0, k_z \neq 0$) accumulate energy much larger than the initial disturbances (by a factor Re) and transfer some to the “K” modes before the Herbert secondary instability.
- This explains the difficulties in observing the “H” type breakdown in experiments.

Evolution of Modal Energy
"Natural" Transition in Channel



Stability and relaminarization of the swept attachment-line flow

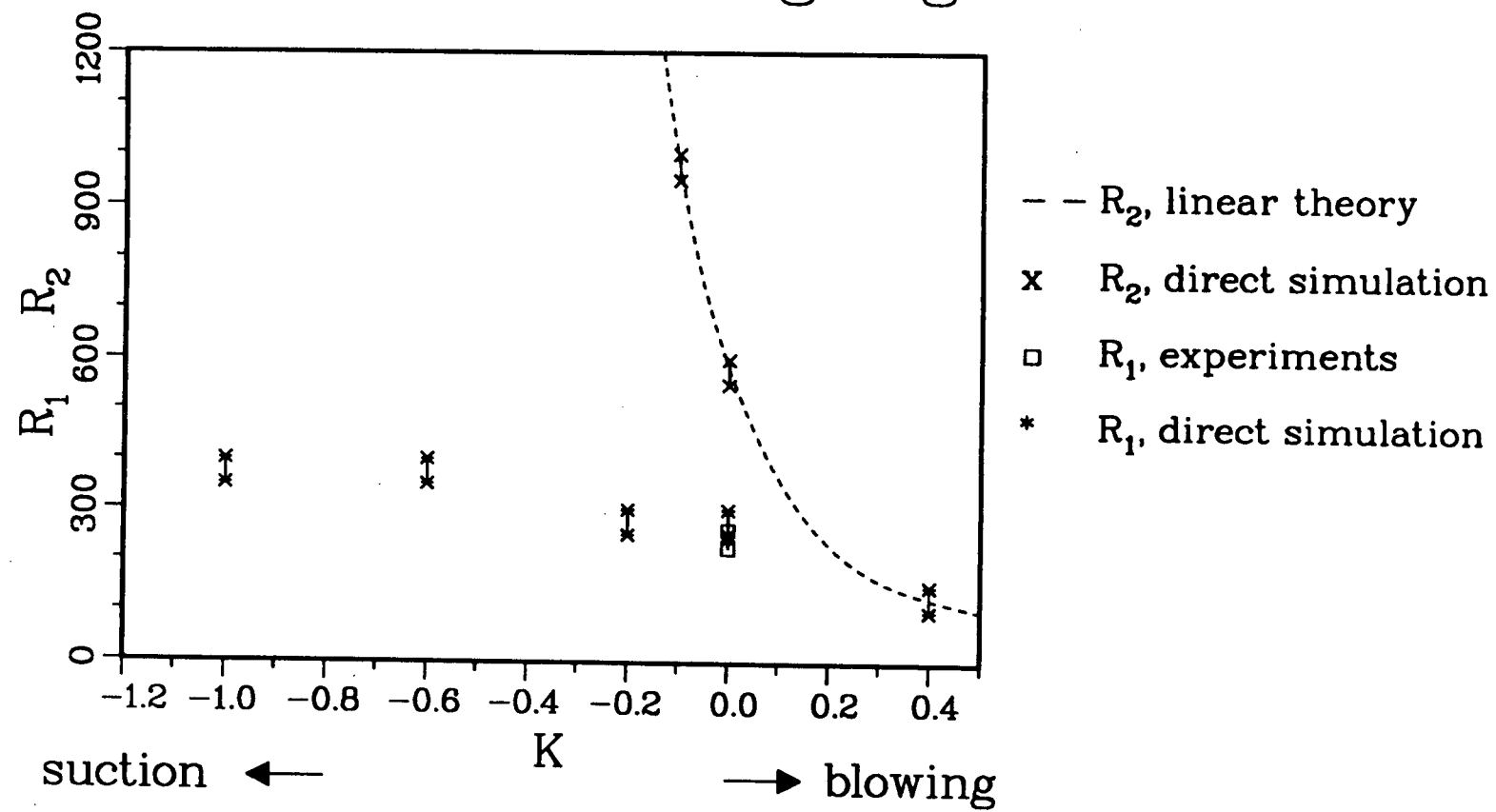
- Turbulence has been found to propagate from the fuselage along the attachment line and render Laminar Flow Control impossible. This is “leading-edge contamination” (Gregory, 1960).
- Direct simulations are conducted in this region. Curvature, compressibility, and spanwise variations are neglected.

14

- Previous linear-stability results (Görtler & Häammerlin, 1955, Hall, Malik & Poll, 1984) are confirmed and generalized.
- The unswept flow is found to be linearly and nonlinearly stable.
- The instability and relaminarization boundaries are computed in (K, \bar{R}) space, where K is the suction parameter and \bar{R} the Reynolds number based on strain rate and sweep velocity component. Suction has much less effect on relaminarization than on linear stability.

Critical Re at Leading Edge

z₁



Pressure terms in a Reynolds-stress turbulence model

- The complete budgets of the Reynolds-stress tensor and the dissipation tensor have been extracted from a direct simulation of turbulent channel flow.
- This allows one to test a turbulence model term by term, instead of as a whole (e.g., using the C_f).
- The published estimates for the terms that are difficult to measure experimentally (pressure, dissipation) were often very inaccurate, especially near a wall.
- As a result, the widespread $k - \epsilon$ and Reynolds-stress models incur large errors near walls.

Pressure-strain term

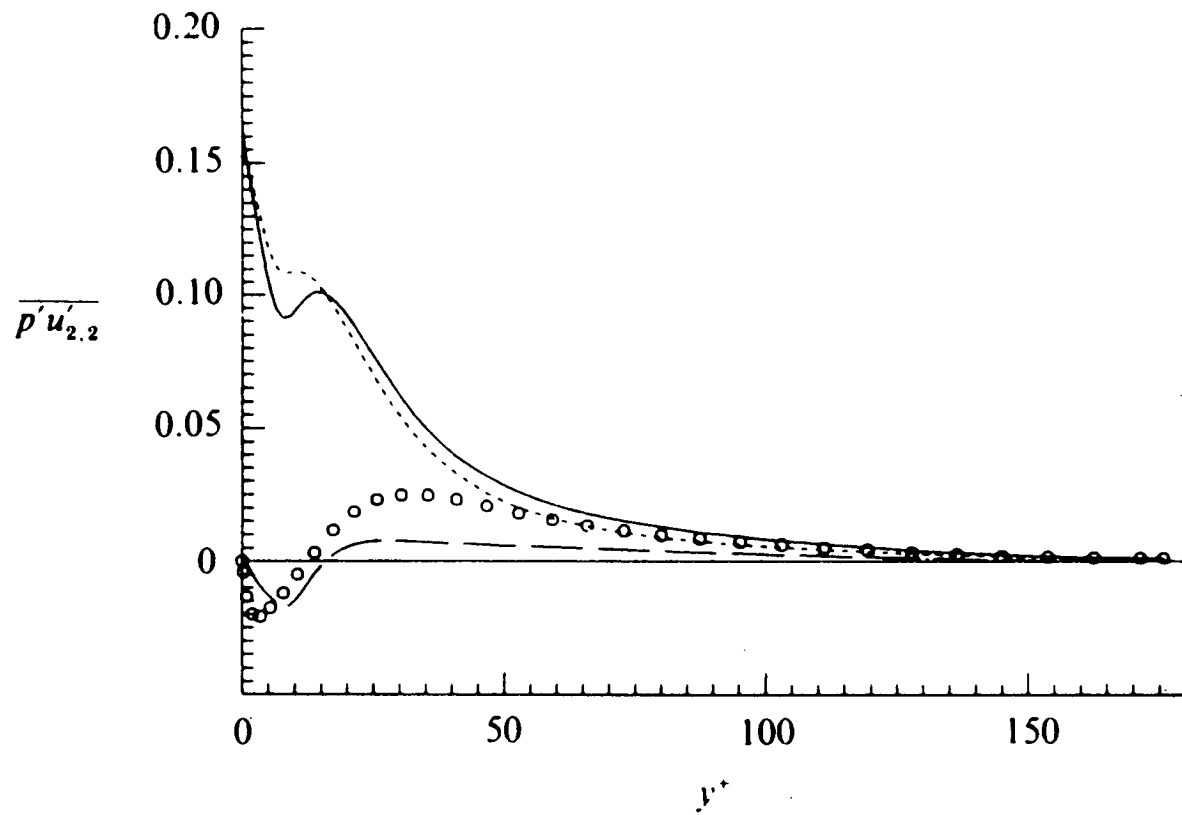


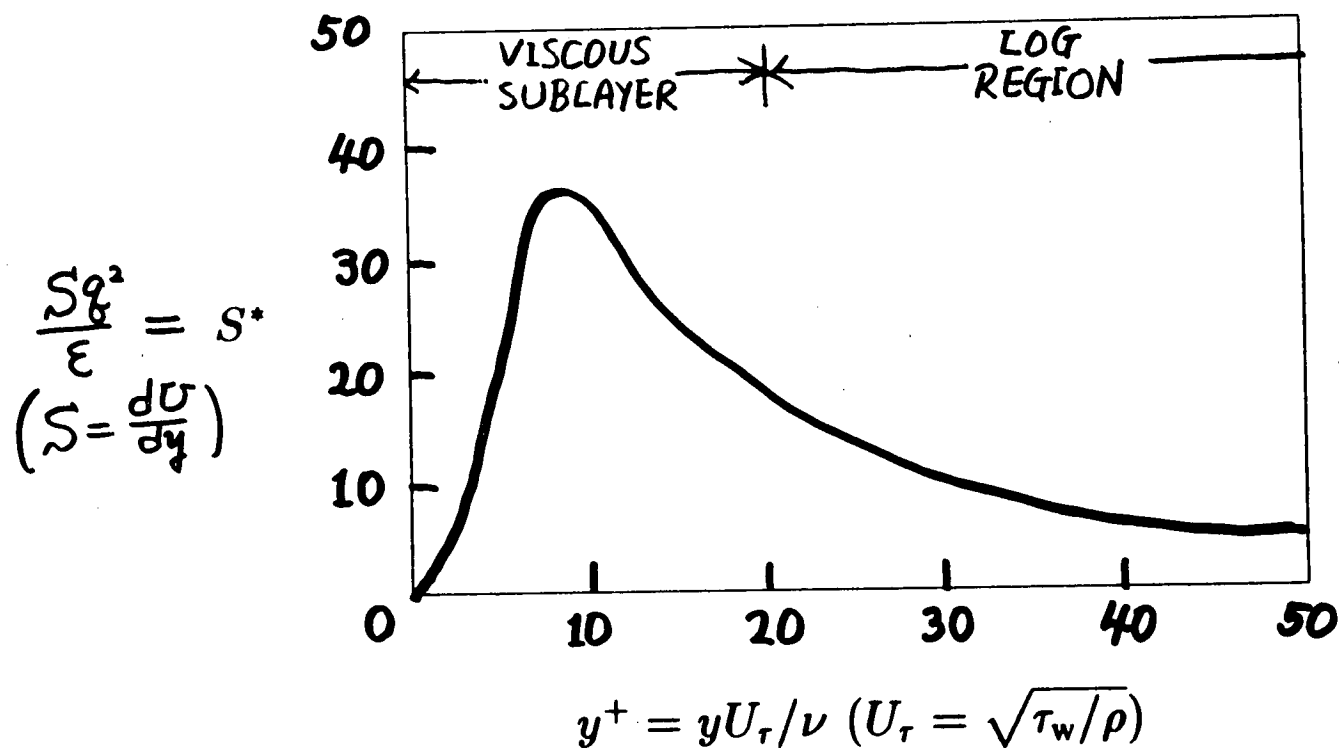
FIGURE 27. Pressure-strain term, $\overline{p' u'_{2,2}}$, in the budget equation for $\overline{u'_2 u'_2}$ across the channel. \circ , term computed from the channel data; —, model, (equations (46) + (48) + (49)); - - - , model, equation (46); - · - , model, (equations (48) + (49)).

Coherent structures in shear flows

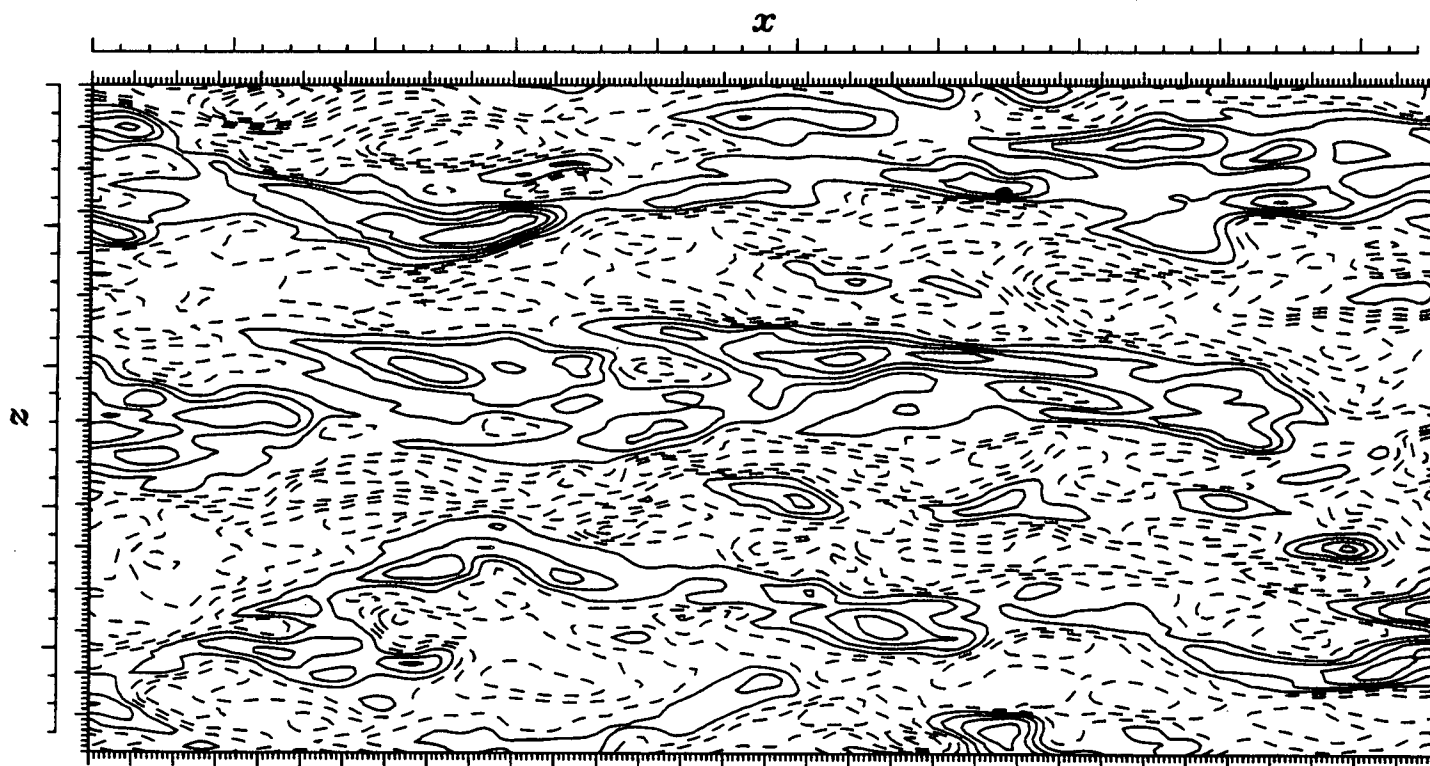
§ 1

- Streaks have long been observed near the wall in boundary layers ($y^+ < 20$), and horseshoes away from the wall. These observations were confirmed by simulation results.
- Why the difference?
 - Near the wall, the nondimensional shear rate $S^* \equiv Sq^2/\epsilon$ takes values much larger than in the homogeneous flows that had been studied (q^2 : turbulent energy; ϵ : dissipation rate).
 - When S^* is given such values in a homogeneous shear flow, streaks appear, indicating that the presence of a wall is not essential to form them.

Profile of S^* in Boundary Layer



Velocity contours in a homogeneous shear flow



The dimension of strange attractors in turbulent shear flows

- Does a turbulent solution live on a “strange attractor”? (i.e., does its state always return to the same region, but never settle down, with almost identical initial conditions rapidly moving apart?)
- If so, chaos (nonlinear dynamics) theory may provide a new framework to unify known turbulent phenomenology and to understand the dynamics rather than the statistics of turbulence.

18

- Using numerical simulation of low Reynolds number turbulent channel flow we have confirmed the existence of a strange attractor by measuring its Lyapunov exponent spectrum and calculating its dimension.
- At a Reynolds number R_τ ($\equiv \delta u_\tau / \nu$) of 80 the dimension of the attractor is $\simeq 360$. This is the first measurement of the intrinsic complexity of a fully developed turbulent flow.
- This result shows that shear flow turbulence cannot be considered to result from the interaction of a “few” degrees of freedom.

Direct simulation of compressible (free shear) flows

- Goal: study compressibility effects on turbulent flows, in particular on their structure, global evolution, and aerodynamic noise.
- Tool: D. N. S. using high-order compact finite differences (close to spectral resolution). Compressible ideal-gas Navier-Stokes equations. No artificial viscosity or filtering.

61

- Example: Spatially evolving mixing layers. 2D, forced at inflow with 1% amplitude. $R \equiv \rho_1(U_1 - U_2)\delta_\omega/\mu_1 \approx 200 - 400$.
- Experiments have shown that: a) compressibility reduces the growth rate; b) it scales with the convective Mach number $M_c \equiv (U_1 - U_2)/(a_1 + a_2)$ ($\gamma_1 = \gamma_2$).
- Simulations have: a) reproduced this effect; b) validated M_c ; c) provided a physical explanation.

Direct Simulation of Compressible Turbulence

T.A. Zang and G. Erlebacher
NASA Langley Research Center

M.Y. Hussaini
Institute for Computer Applications in Science and Engineering
NASA Langley Research Center

The physics of turbulence remains one of the most challenging problems in fluid dynamics. Although more than a century of effort has been devoted to it, a lot of fundamental issues are still unresolved. This is particularly so in the case of turbulence in high speed flows because of the increased number of possible mode interactions due to compressibility effects. For example, the cubic non-linearities in the momentum equations allow the vorticity, acoustic and entropy modes to interact with each other. The dynamics are further complicated by the possible existence of non-stationary shocks and/or eddy shocklets.

In this paper, several direct simulations of 3-D homogeneous, compressible turbulence are presented with emphasis on the differences with incompressible turbulent simulations. A fully spectral collocation algorithm, periodic in all directions coupled with a 3rd order Runge-Kutta time discretization scheme is sufficient to produce well-resolved flows at Taylor Reynolds numbers below 40 on grids of 128x128x128. A Helmholtz decomposition of velocity is useful to differentiate between the purely compressible effects and those effects solely due to vorticity production. In the context of homogeneous flows, this decomposition is unique. Time-dependent energy and dissipation spectra of the compressible and solenoidal velocity components indicate the presence of localized small scale structures. These structures are strongly a function of the initial conditions. We concentrate on a regime characterized by very small fluctuating Mach numbers Ma (on the order of 0.03) and density and temperature fluctuations much greater than Ma^2 . This leads to a state in which more than 70% of the kinetic energy is contained in the so-called compressible component of the velocity. Furthermore, these conditions lead to the formation of curved weak shocks (or shocklets) which travel at approximately the sound speed across the physical domain. Various terms in the vorticity and divergence of velocity production equations are plotted versus time to gain some understanding of how small scales are actually formed. Possible links with Burger turbulence are examined.

To visualize better the dynamics of the flow, new graphic visualization techniques have been developed. The 3-D structure of the shocks are visualized with the help of volume rendering algorithms developed in house. A combination of stereographic projection and animation greatly increase the number of visual cues necessary to properly interpret the complex flow. The presence or absence of shocks is automatically detected by monitoring of the minimum and maximum divergence of the velocity field over the physical domain.

NAVIER-STOKES EQUATIONS

Non-Dimensionalizations

Velocity, U_0 , Temperature T_0 , density ρ_0 , pressure ρU_0^2 .

Viscosity and Prandl number are constant.

$$\frac{\partial \rho}{\partial t} + \nabla \cdot (\rho \vec{v}) = 0$$

$$\rho \frac{D\vec{v}}{Dt} = -\frac{\epsilon_p}{\gamma M_\infty^2} \nabla P + \frac{1}{Re} \nabla \cdot \vec{\tau}$$

$$\frac{DP}{Dt} = -\gamma P \nabla \cdot \vec{v} + \frac{\gamma}{\epsilon_p Pr Re} \nabla \cdot (\kappa \nabla T) + \frac{\gamma(\gamma-1) M_\infty^2}{\epsilon_p Re} \vec{\tau} : \vec{e}.$$

$$\epsilon_p P = \rho T$$

where the stress tensors and dissipation function are defined by

$$\vec{e} = \frac{1}{2} (\nabla \vec{v} + \nabla \vec{v}^T),$$

$$\vec{\tau} = 2\mu \vec{e} - \frac{2}{3}\mu (\nabla \cdot \vec{v}) \vec{I},$$

and

$$\vec{\tau} : \vec{e} = \frac{\mu}{2} (\nabla \vec{v} + \nabla \vec{v}^T) : (\nabla \vec{v} + \nabla \vec{v}^T) - \frac{2}{3}\mu (\nabla \cdot \vec{v})^2.$$

OBJECTIVE

- Understand if, when, and why shocks occur in homogeneous turbulence, shear layers and mixing layers in the supersonic and hypersonic regimes.
- Develop mixing enhancement strategies in supersonic shear layers (e.g. scram-jets)
- The study of initial condition effects on the time-dependent characteristics of supersonic “isotropic” turbulence is the first step toward the aforementioned objectives.

PHYSICS

- Solve time-dependent, 3-D full Navier-Stokes equations
- Code set up for variable viscosity, but set to a constant
- $\text{Pr} = 0.7$ (air)
- ideal gas
- no chemistry
- initial energy and thermodynamics autocorrelation spectrums identical

INITIAL CONDITIONS (1)

- Generate random $\vec{v}, \delta\rho, \delta T$ subject to

$$\nabla \cdot \vec{v}_s = 0$$

$$\nabla \times \vec{v}_c = 0$$

- Impose autocorrelation spectrum on $\vec{v}, \delta\rho, \delta T$

$$E(k) = k^4 e^{-k^2/2k_0^2}$$

- Specify rms levels for $\delta\rho, \delta T$

- Calculate

$$\rho = 1 + \delta\rho$$

$$T = 1 + \delta T$$

INITIAL CONDITIONS (2)

- Specify fluctuating Mach number M_a , and compute

$$M_a^2 = \frac{u_0^2}{\gamma R T_0}$$

according to the approximate formula

$$M_a = M_0 u_{rms}$$

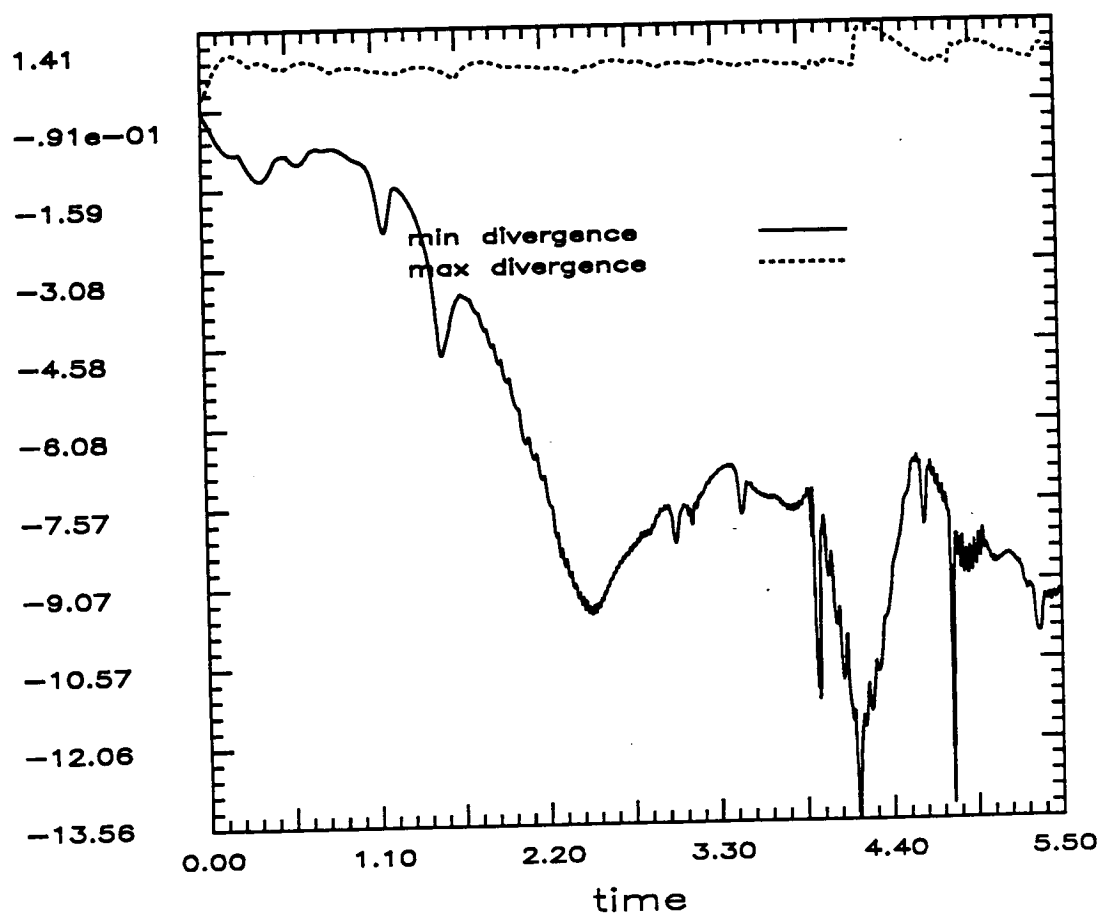
- Specify initial level of compressibility

$$\chi = \frac{\int u_c^2 dV}{\int (u_s^2 + u_c^2) dV}$$

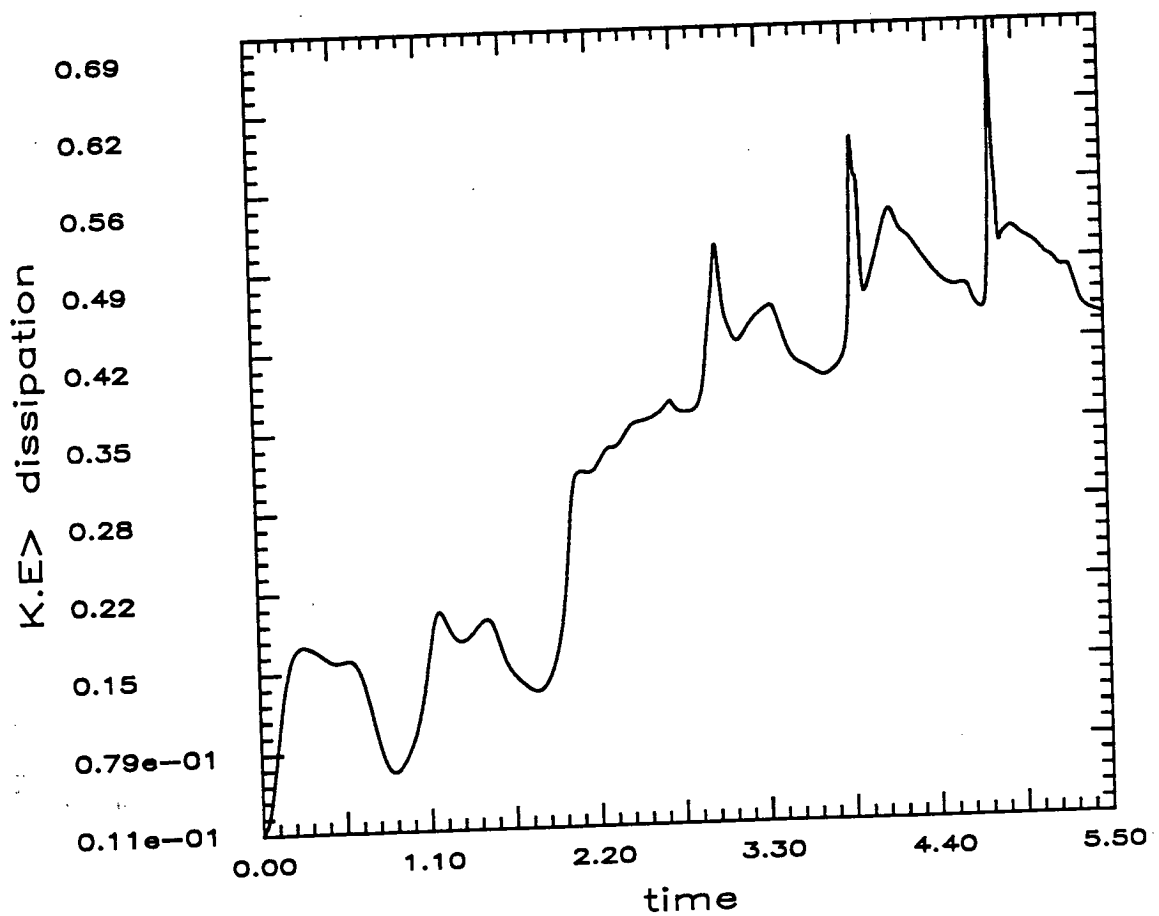
NUMERICAL METHOD

- Fourier Collocation in both directions (periodic box)
- Conservative scheme in absence of time discretization errors
- Isotropic truncation in Fourier space at every iteration
- Splitting algorithm
 - 3rd order Runge-Kutta method in time on the explicit terms (1st step)
 - Acoustic terms treated implicitly (2nd step)

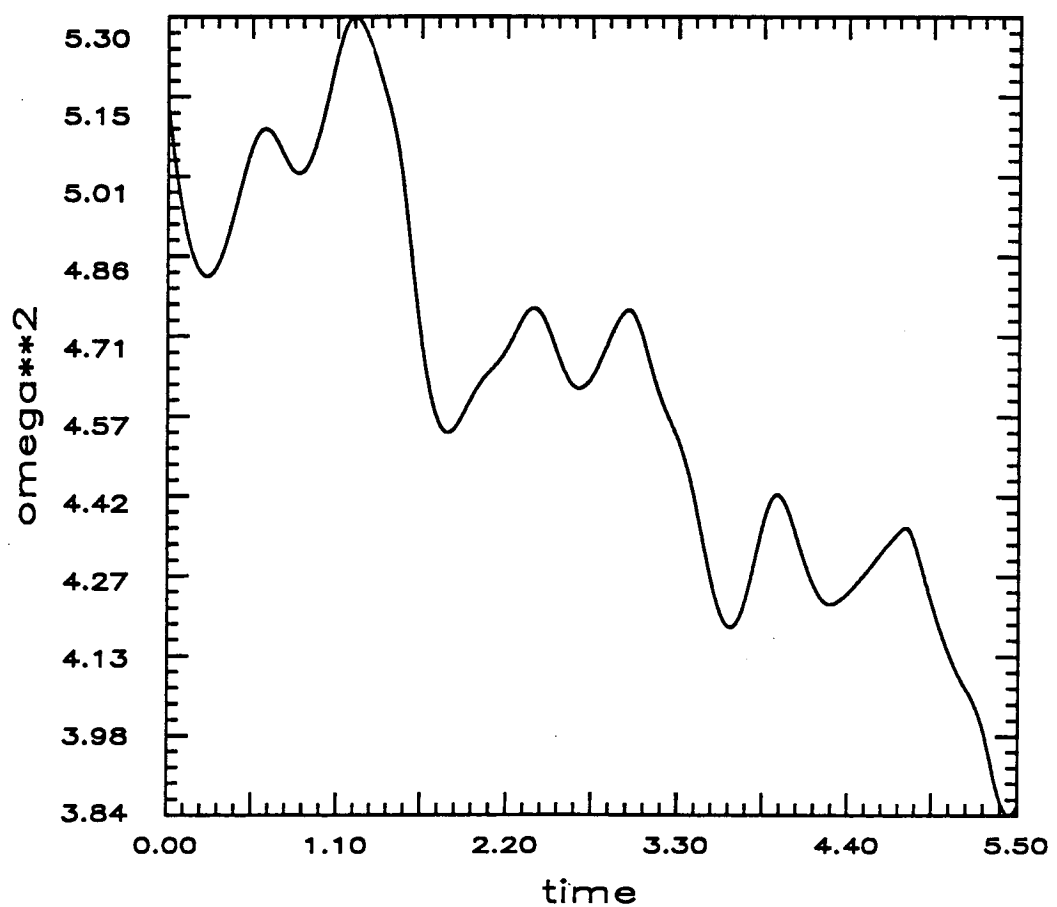
turb3d/run132



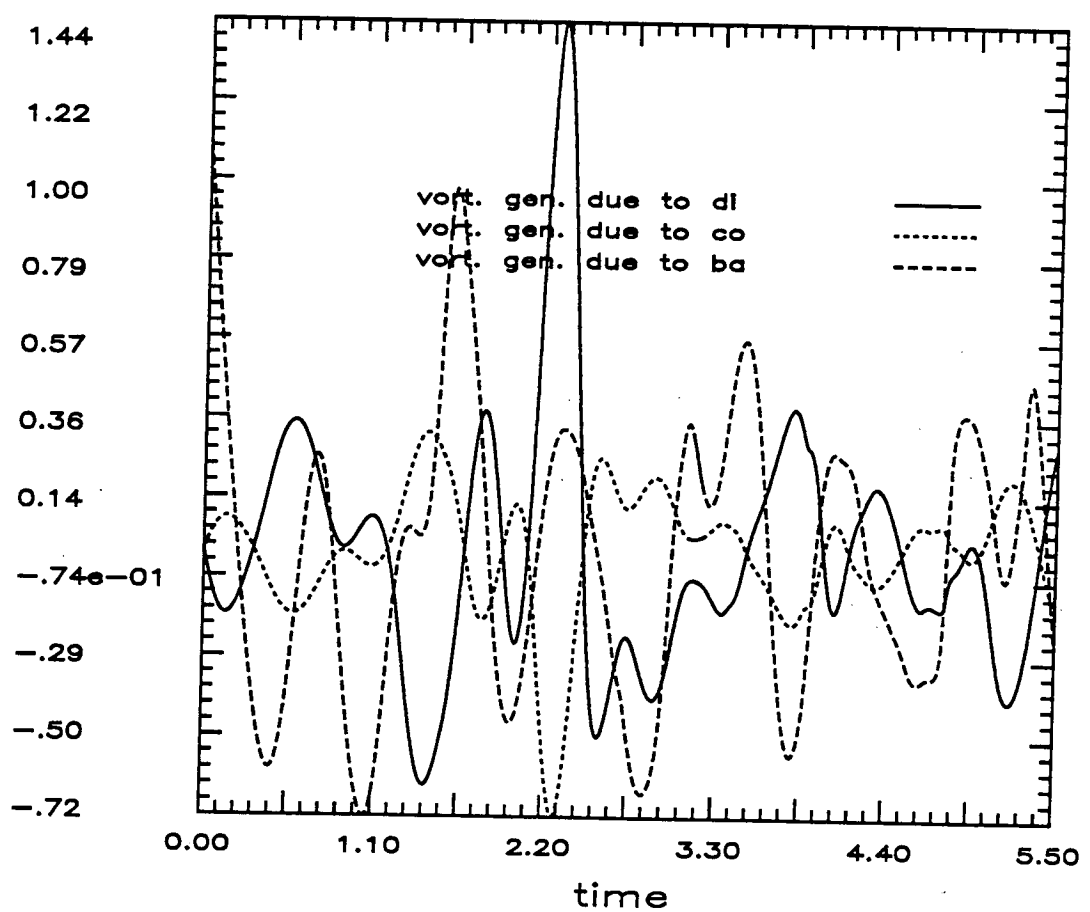
turb3d/run132



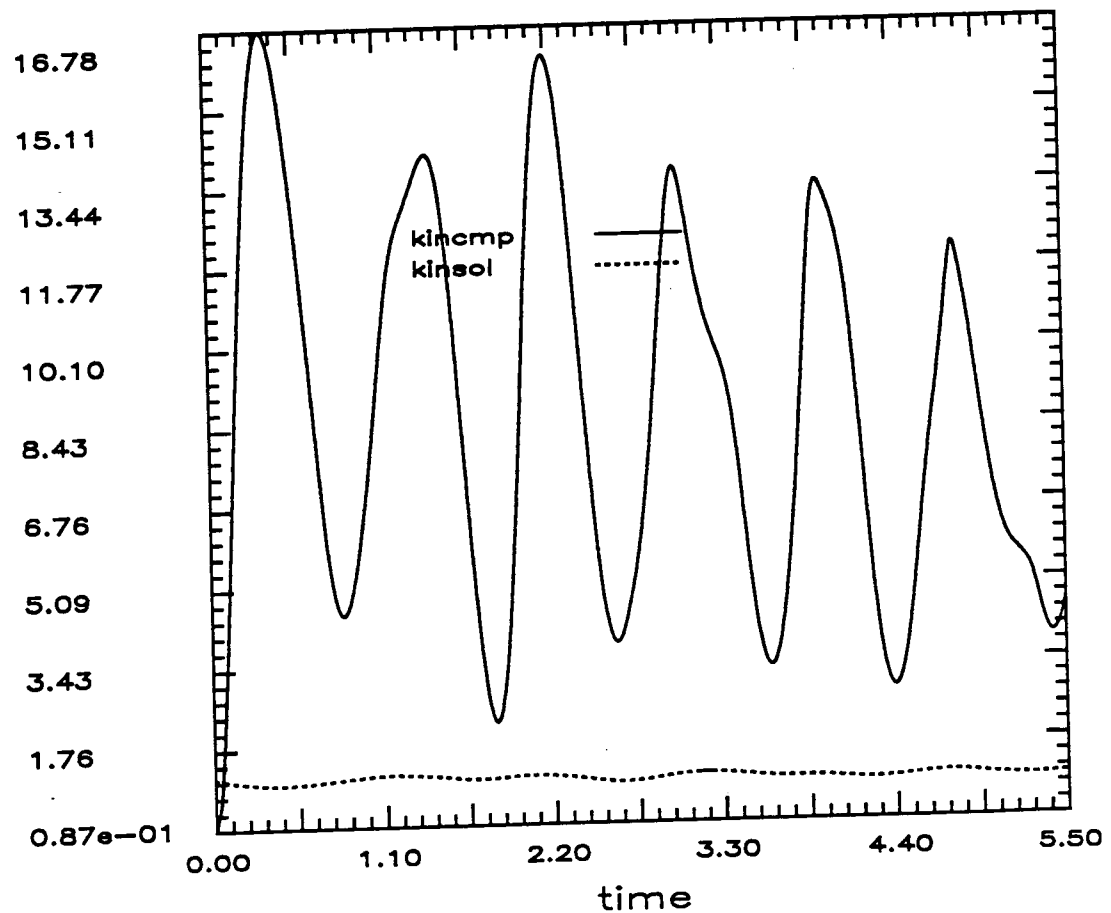
turb3d/run132



turb3d/run132



turb3d/run132



DIVERGENCE OF VELOCITY

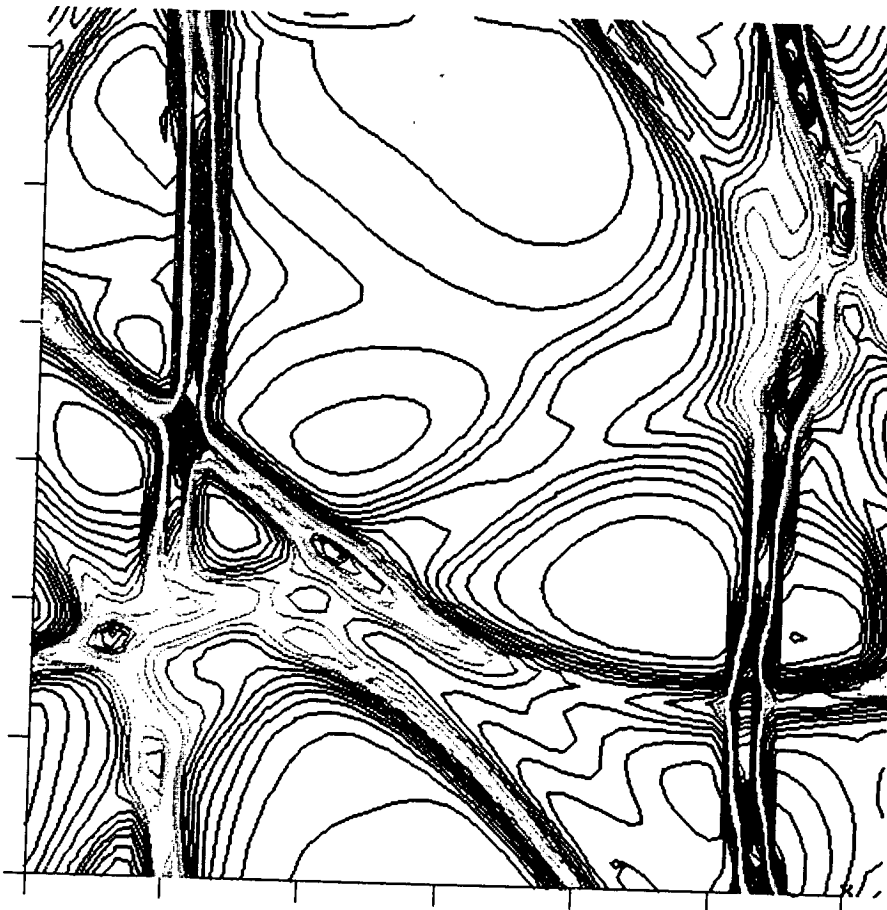
turb3d/run132, t=3.3, it=600

Re=150, Ma=.028, k0=1.85, urms=.1, chi=.07, rho, T=10%

CONTOUR LEVELS

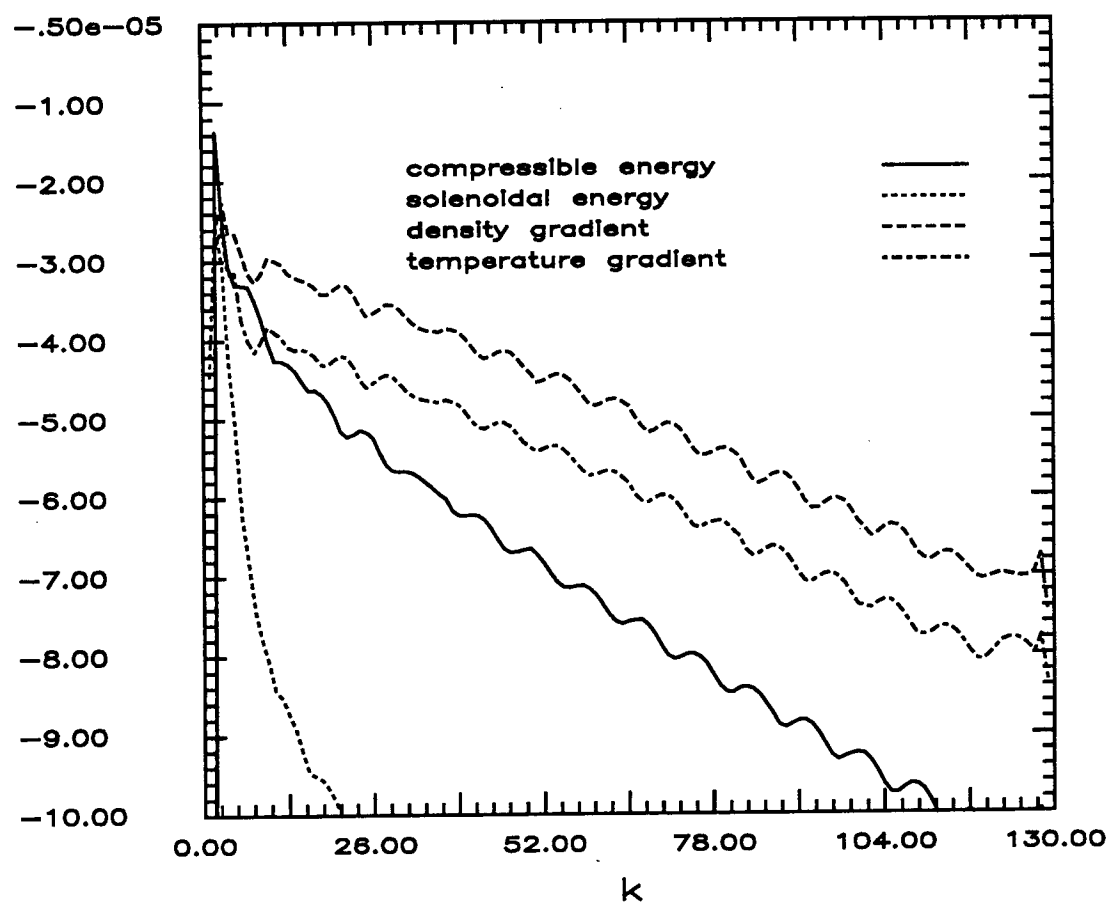
-3.10000
 -3.00000
 -2.90000
 -2.80000
 -2.70000
 -2.60000
 -2.50000
 -2.40000
 -2.30000
 -2.20000
 -2.10000
 -2.00000
 -1.90000
 -1.80000
 -1.70000
 -1.60000
 -1.50000
 -1.40000
 -1.30000
 -1.20000
 -1.10000
 -1.00000
 -0.90000

-0.80000
 -0.60000
 -0.50000
 -0.40000
 -0.30000
 -0.20000
 -0.10000
 0.00000
 0.10000
 0.20000
 0.30000



1.000	MACH
0.00 DEG	ALPHA
-1.0	Re
5.5	TIME
65x65x166	GRID

run132, it=725, t=4



CONCLUSIONS

- Weak shocks can be generated by an initially random 2-D velocity and thermodynamic field.
- These shocks propagate at the speed of sound across the domain
- The presence of these shocks is reflected in the structure of the compressible energy spectrum
- Although the flow is isotropic at the onset, the compressible component of velocity quickly becomes anisotropic (as evidenced by the shock structure)
- Sophisticated visualization techniques are necessary to capture the essence of the dynamics in 3 dimensions

16

Future Work

- Mixing layers with shock interactions
- Three-dimensional isotropic turbulence (in progress)
- Turbulence modeling Testing

Non Linear Evolution of a Second Mode Wave in Supersonic Boundary Layers

G. Erlebacher

NASA Langley Research Center

M.Y. Hussaini

Institute for Computer Applications in Science and Engineering
NASA Langley Research Center

Recent advances in supersonic and hypersonic aerospace technology have led to a renewed interest in the stability and transition to turbulence of high speed flows. The last 30 years have intermittently witnessed some vigorous attempts to understand some of the fundamental routes to transition for incompressible flows. While a fairly comprehensive picture of the initial stages leading to the breakdown of an incompressible laminar boundary layer has emerged (mostly under controlled conditions) the non-linear effects responsible for transition at high speeds are still very much a mystery. However, the current nonlinear incompressible theories, numerical simulations and experiments will, hopefully, serve as a guide in gaining a better understanding of the mechanisms present in the supersonic and hypersonic regimes.

Compressible linear stability theory diverges from incompressible linear stability theory in several ways. Incompressible inviscid instabilities, linked with the existence of an inflection point in the mean streamwise velocity profile are replaced by a correlation between inviscid compressible instabilities and a generalized inflection point, which brings into play the mean density profile. Furthermore, as the Mach number increases, the growth rate of the 3-D modes begin to overtake those of the 2-D modes. Beyond Mach 2.2, multiple unstable modes (at fixed Reynolds number and frequency) can coexist. The higher modes are inviscid in nature and have different behaviors with regard to wall cooling. Not only are they more unstable than their first mode counterparts (viscous in nature) above a certain Mach number, but they are destabilized by wall cooling, which is detrimental for high altitude hypersonic aircraft.

It is of vital importance that the nonlinear nature of these second mode instabilities be understood, and that their role in the context of transition be elucidated. The objective of the work is to understand the possible equilibrium state of a second mode wave, before initiating a study of 3-D wave interactions.

Two years ago, a spectral code was developed to perform direct simulations of subsonic and supersonic flows over flat plates. In this paper, we present several direct simulations of one 2-D second mode perturbation wave, superimposed upon a prescribed mean flow. Periodicity is assumed in the streamwise direction (Fourier) and the variables are expanded in Chebyshev series in the direction normal to the plate. The code is fully explicit and is time advanced with a 3rd order Runga-Kutta scheme. The second mode wave ($R_{\delta^+} = 8000$), interacts with itself to generate higher streamwise harmonics. Physical parameters are chosen to maximize the linear growth rate at the prescribed Reynolds number. Initial results indicate that the nonlinear processes begin in the critical layer region and are the result of the cubic interactions in the momentum equations, rather than due to the higher streamwise harmonics. Analysis of the various terms in the momentum equations combined with numerical experiments in which various modes are artificially suppressed, lead to the conclusion that asymptotic methods will produce the saturated state in one or two orders of magnitude less computer time than that required by the direct numerical simulations.

CURRENT STATUS OF FLAT PLATE STABILITY AND TRANSITION

- **Theory**

- Inviscid Stability Theory (Lees and Lin, 1946)
- Linear Parallel Theory (Mack 1965)
- Linear Non-Parallel Theory (Nayfeh and El-Hady, 1980)
- Non-Linear Theories
 - * Wave-Interactions: NONE
 - * Secondary Instability: (El-Hady 1988, Ng 1988)

891

- **Experiment**

- Stability of Supersonic Boundary Layers (Laufer and Vrebalovich 1960)

- **Numerical**

- Linear Stability of Ideal Gases (Mack 1975, Malik 1982, Macaraeg & Streett 1988, Erlebacher & Herbert 1988, Ng 1988)
- Linear Stability of real gases (equilibrium air) (Malik 1988, Macaraeg & Streett 1988)
- Non-Linear Stability of (Erlebacher and Hussaini 1987)

PHYSICAL PARAMETERS

Non-Dimensionalization

length: δ^*

\vec{u}, ρ, T : free-stream values

P : ρU_∞^2

16

- boundary layer flow
- ideal gas (air)
- $Pr = 0.70$, $Re = 8000$
- $M=4.5$
- $\alpha = 2.25$, $\psi = 0^\circ$
- – linear frequency: 2.05 \Rightarrow period = 3.07
 - linear growth: .0215
 - 20 periods in time gives amplification of 3.76
 - e^9 amplification in 136 periods

DISCRETIZATION

- Fully explicit
- 3rd order low-storage Runga-Kutta in time
- Fourier collocation in two periodic directions (stream and span)
- Chebyshev collocation in vertical direction
- Zero normal stress boundary-conditions in the free-stream
- Continuity equation is imposed at the wall and in the far-field
- Zero temperature perturbations at the wall

MODAL ANALYSIS

$$u \propto e^{-i\omega t}$$

$$\frac{\dot{u}}{u} \approx -i\omega$$

$$\omega_i = \text{Real}\left(\frac{\dot{u}}{u}\right)$$

$$\omega_r = \text{Imag}\left(\frac{\dot{u}}{u}\right)$$

171

Let

$$u(x, y) = \sum_{n=-\infty}^{\infty} u_n(y, t) e^{in\alpha x}$$

After substitution into the x-momentum equation,

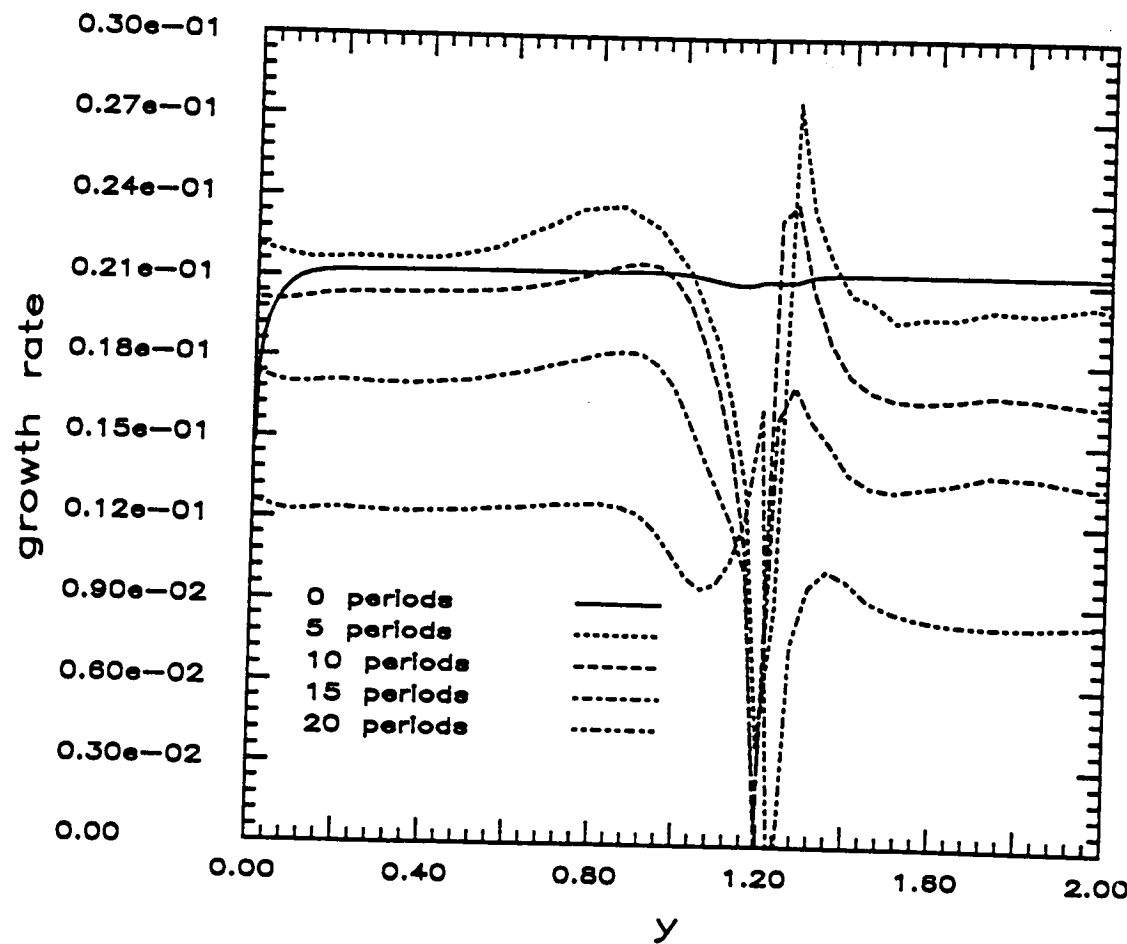
$$\dot{u} = \text{linear} + \text{cubic} + \text{viscous terms}$$

where

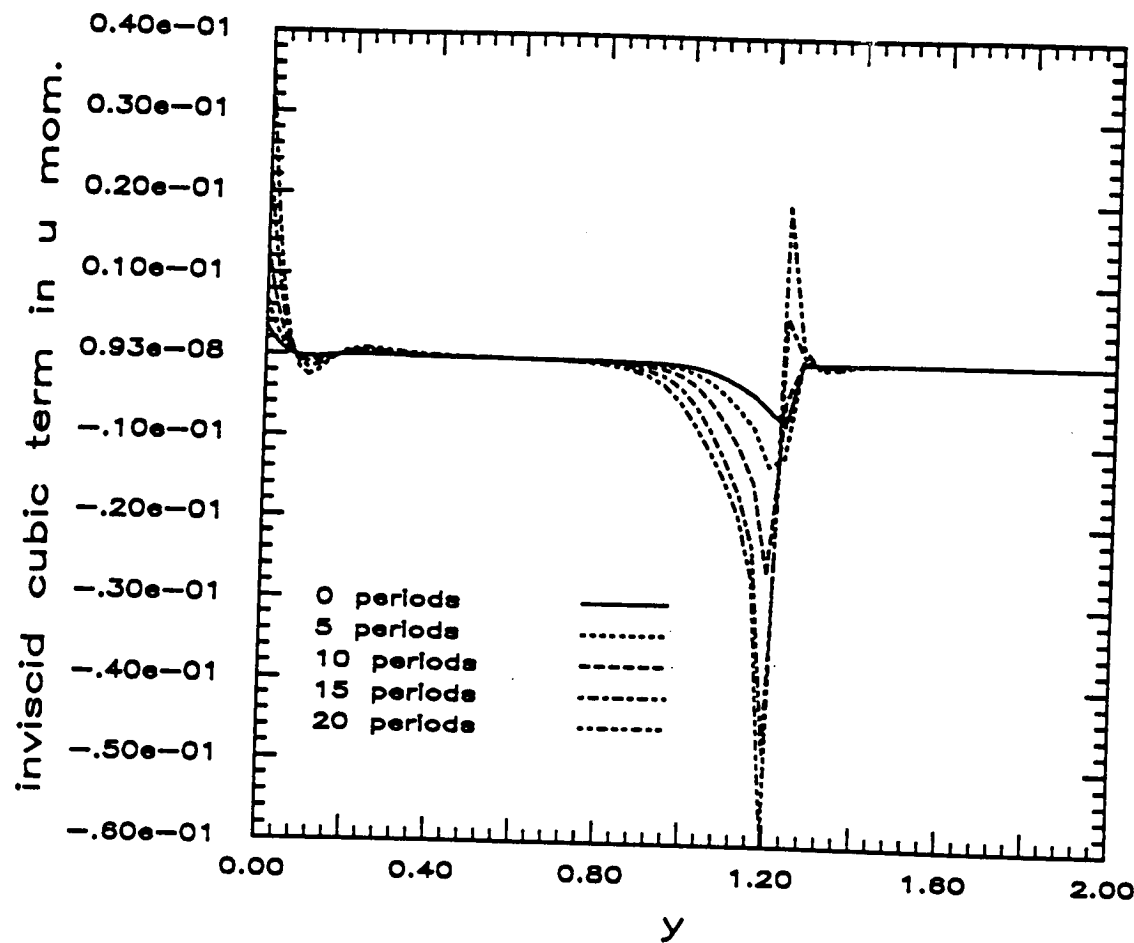
$$\text{Linear} = i\alpha u_0 u_1 \rho_0 + \dots$$

$$\text{Cubic} = i\alpha u_1 u_{-1} \rho_1 + \dots$$

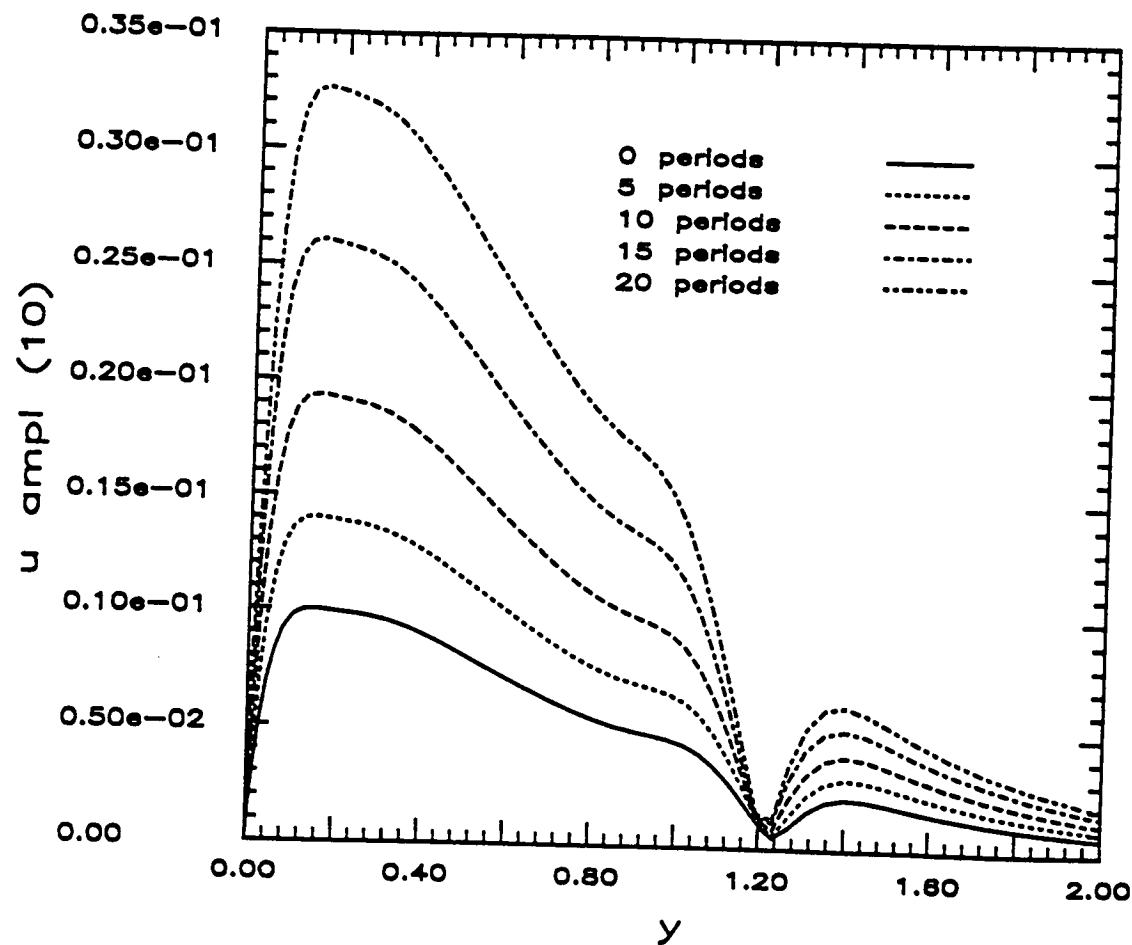
2nd mode run19 $M=4.5$



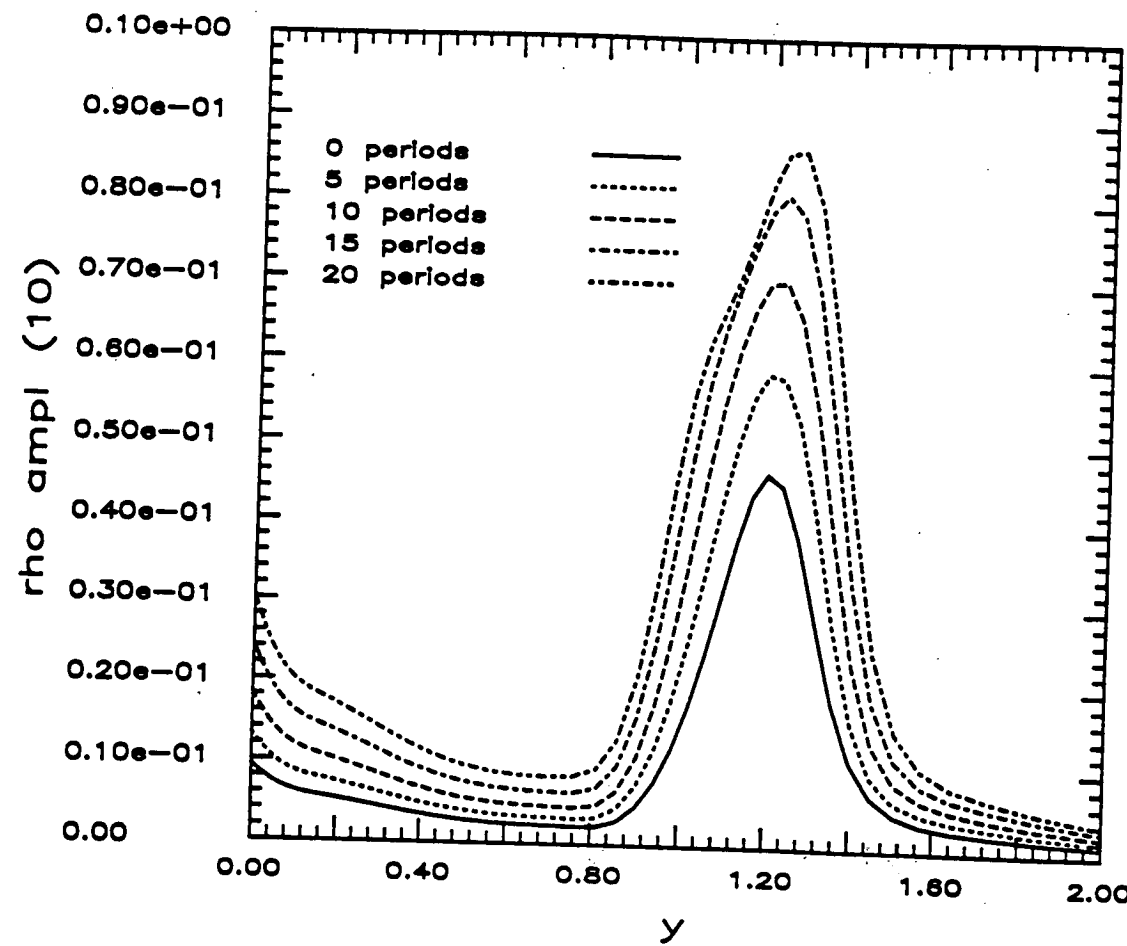
2nd mode run19 $M=4.5$



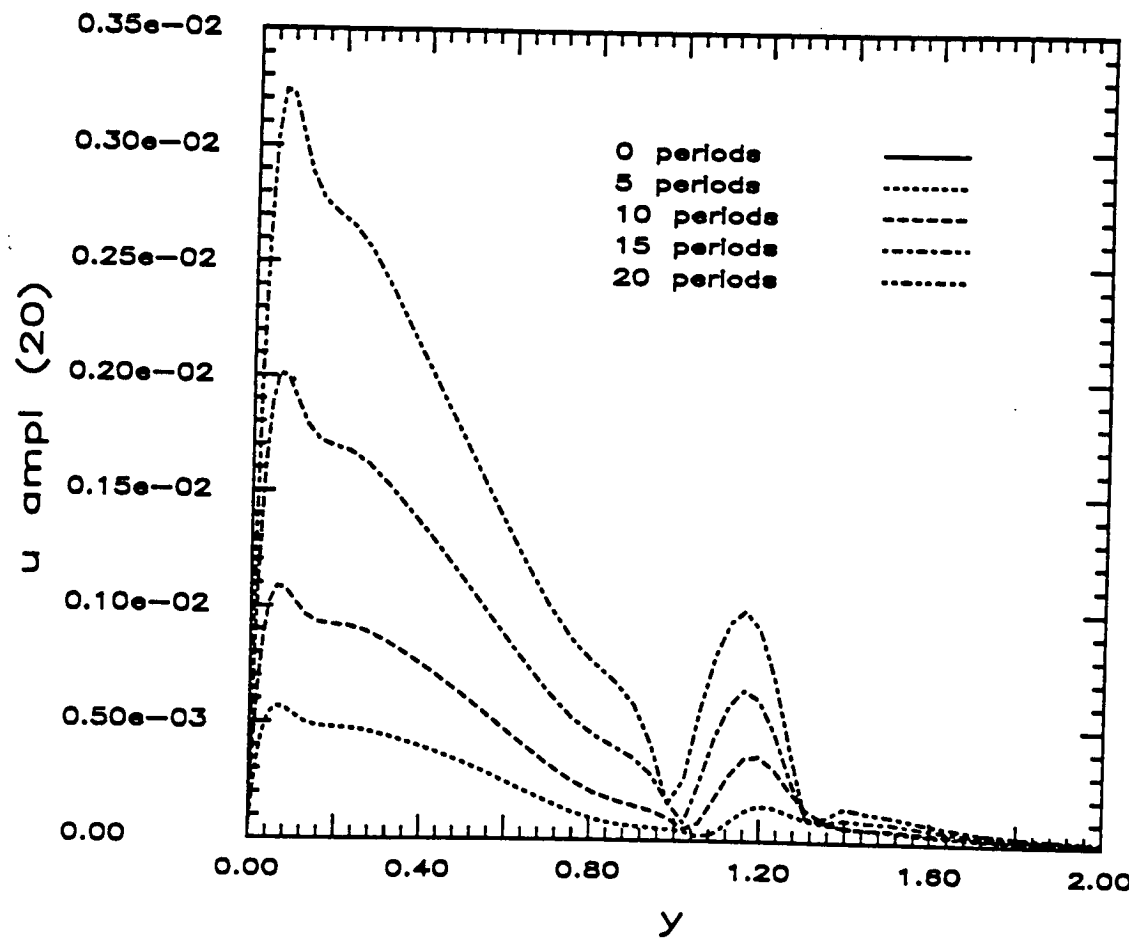
2nd mode run19 M=4.5



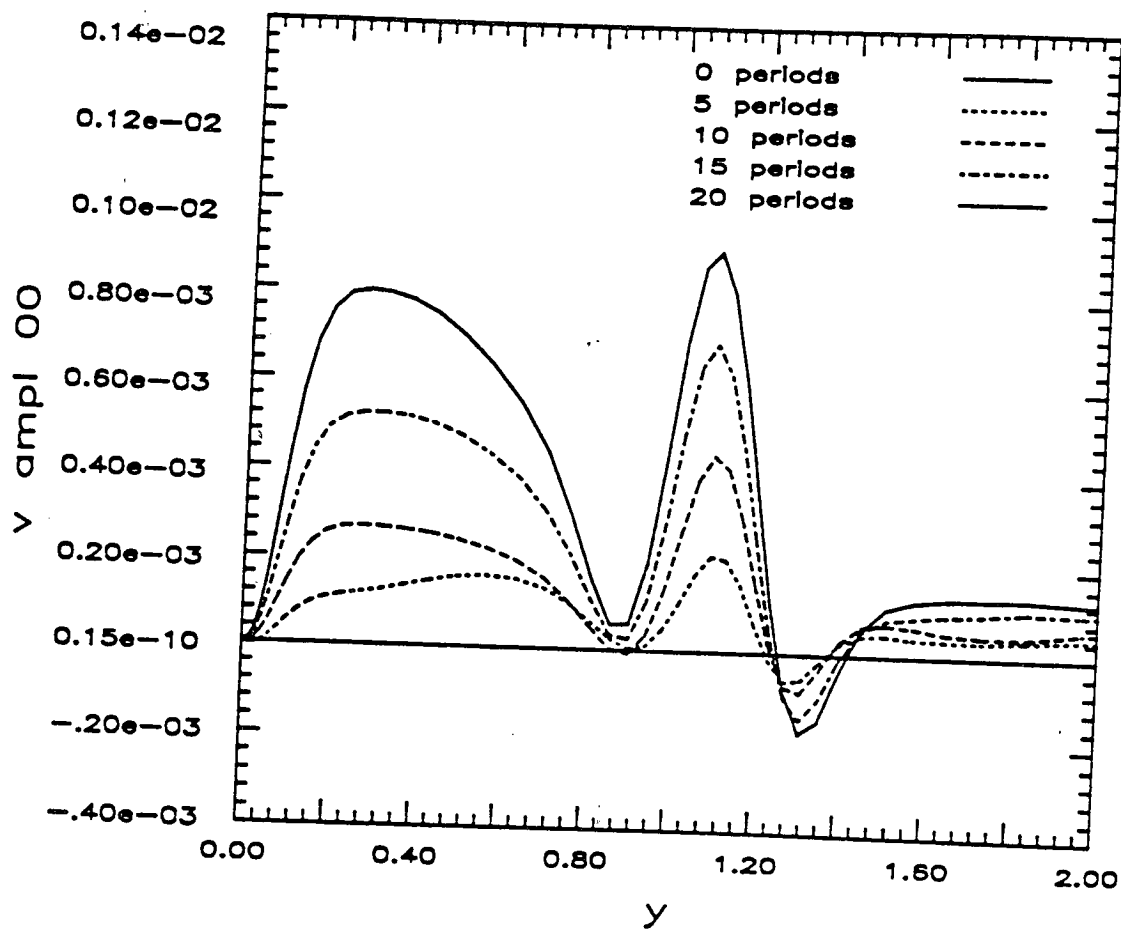
2nd mode run19 M=4.5



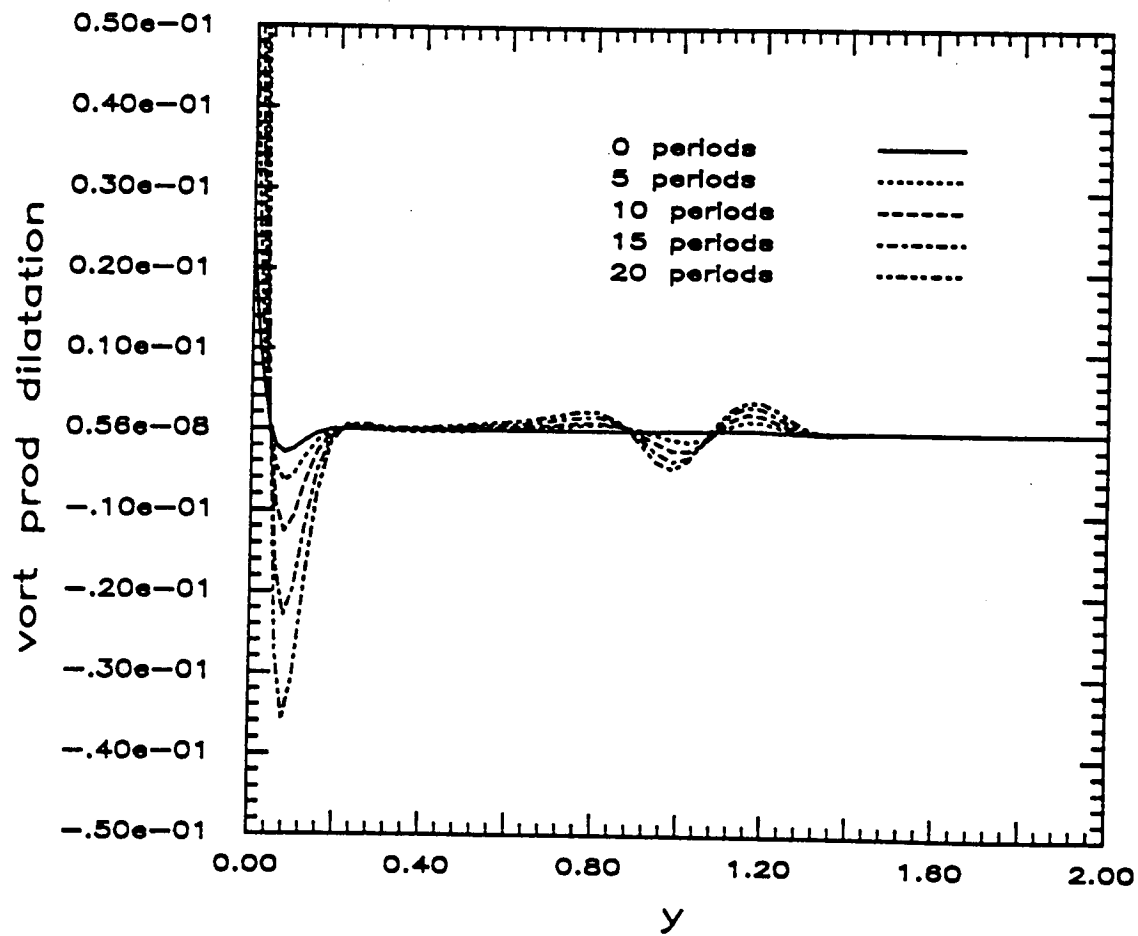
2nd mode run19 $M=4.5$



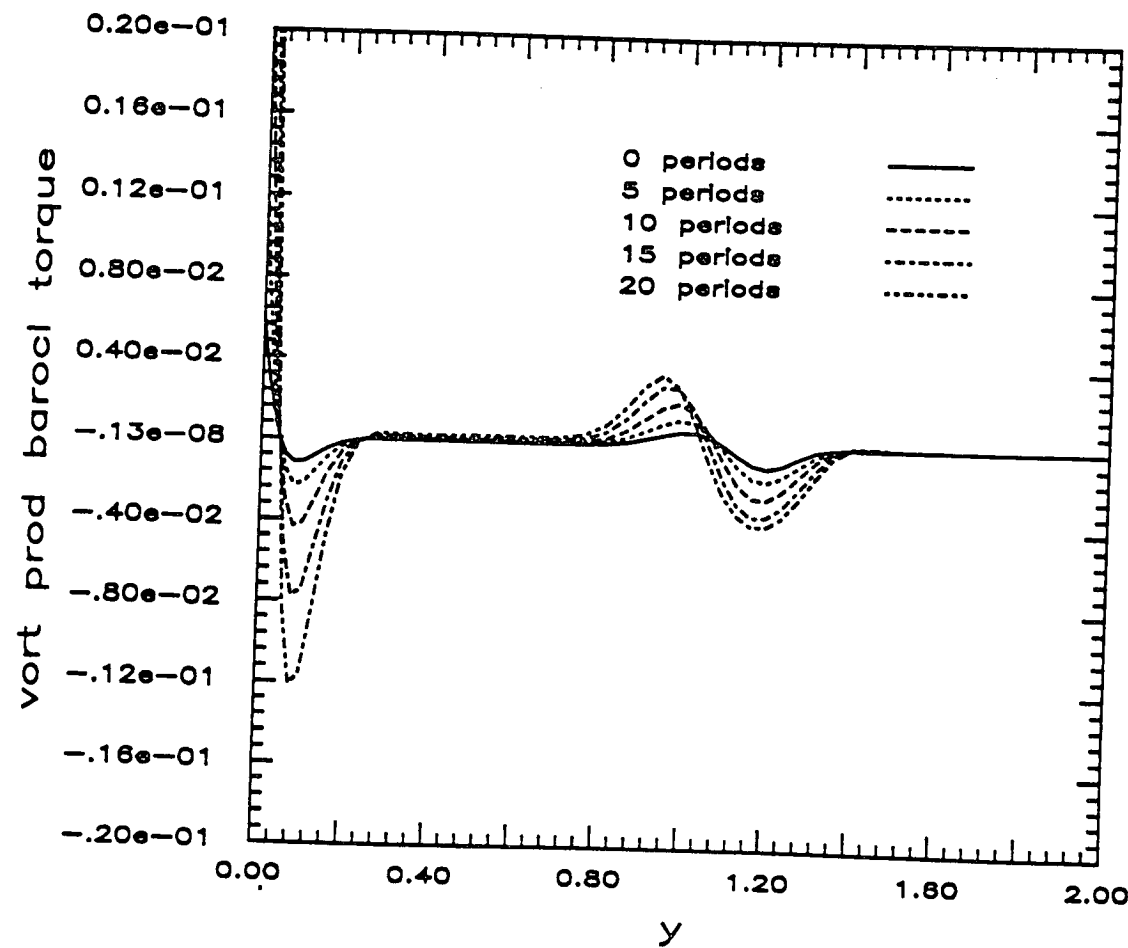
2nd mode run19 $M=4.5$



2nd mode run19 $M=4.5$



2nd mode run19 $M=4.5$



COST OF DIRECT SIMULATION

- The number of operations for a single iteration is approximately twice that of an incompressible direct simulation
- Acoustic effects must be treated implicitly for low Mach number simulations. At high Mach numbers, time step restrictions are a function of the Reynolds number
- Steep gradients of u' and T' in the critical layer increase the initial resolution
- Compressibility effects weaken the secondary instability, further increasing the required computer time to capture the initial stages of breakdown
- Cost can decrease with use of static or dynamics adaptive grids, or multidomain decompositions in the vertical direction

⇒ **VERY EXPENSIVE !!!**

25 periods on $8 \times 2 \times 65$ grid: 10 CPU hrs on Cray II at 100 Mflops average yields factor 4 amplification

CONCLUSIONS

- Compressible boundary-layer code is suitable for the study of second modes, albeit is still very expensive due to the slow growth and high spatial and temporal frequencies of the instabilities
- Non-linearities (not due to higher streamwise harmonics) induces strong growth rate departures from the linear values in the critical layer region. The actual cause is still unknown.
- Density perturbations probably play (as expected) a fundamental role in the development of the non-linear saturated state. Further information awaits more detailed considerations of intermodal energy transfers.

NUMERICAL SIMULATION OF NONLINEAR DEVELOPMENT OF INSTABILITY WAVES

Reda R. Mankbadi
 Institute for Computational Mechanics in Propulsion
 National Aeronautics and Space Administration
 Lewis Research Center
 Cleveland, Ohio 44135, U.S.A.

and

Cairo University
 Cairo, Egypt

SUMMARY

The present work is concerned with the nonlinear interactions of high amplitude instability waves in turbulent jets. In plane shear layers Riley and Metcalf (1980) and Monkewitz (1987) have shown that these interactions are dependent, among other parameters, on the phase-difference between the two instability waves. Therefore, in the present work we consider the nonlinear development of both the amplitudes and the phase of the instability waves. The development of these waves are also coupled with the development of the mean flow and the background turbulence. In formulating this model it is assumed that each of the flow components can be characterized by conservation equations supplemented by closure models. Results for the interactions between the two instability waves under high-amplitude forcing at fundamental and subharmonic frequencies are presented here. Qualitative agreements are found between the present predictions and available experimental data.

CONSERVATION EQUATIONS

Each flow component is split in the form:

$$U_i(x, r, t) = \bar{U}_i(x, r) + \tilde{u}_i(x, r, t) + u'_i(x, r, t)$$

\bar{U} is the time-averaged mean flow velocity which is taken to be given by the two-stage hyperbolic tangent profile. \tilde{u} is the periodic component which is split into two frequency-components in the form:

$$\tilde{u}_i = A_1 \hat{u}_{i1}(r, \theta) e^{i\phi_1(x) - i\omega_1 t} + A_2 \hat{u}_{i2}(r, \theta) e^{i\phi_2(x) - i\omega_2 t} + \text{c.c.}$$

\hat{u} is the radial shape taken as the eigen-function solution of the locally-parallel linear stability equation for each frequency-component. A and ϕ are the amplitude and phase to be obtained from the nonlinear interaction equations, and θ is the momentum thickness. u' is the turbulence component which is related to the turbulence energy T through an assumed Gaussian profile.

THE NONLINEAR INTERACTION EQUATIONS

Time-averaging and phase-averaging techniques are applied to the full unsteady Navier-Stokes equations to derive the governing equations for each

flow component. These equations are manipulated to obtain nonlinear equations for the amplitudes A_1 , A_2 , phases ϕ_1 , ϕ_2 , momentum thickness Θ and the turbulence energy T :

Mean flow

$$\frac{1}{2} \frac{dI_{ma}}{d\Theta} \frac{d\Theta}{dx} = -I_{mt} T - I_{\omega m} A_1^2 - I_{2\omega} A_2^2$$

Turbulence

$$\frac{d}{dx} [I_{ta} T] = I_{mt} T + I_{\omega t} A_1^2 T + I_{2\omega t} A_2^2 T - I_{\epsilon} T^{3/2}$$

$\omega\omega$ component

$$\frac{d}{dx} [I_{\omega a} A_1^2] = I_{\omega m} A_1^2 - I_{\omega t} A_1^2 T + I_{2\omega\omega} A_2 A_1^2 \cos(2\phi_{\omega} - \phi_{2\omega} - \phi_0 + \sigma)$$

$$I_{\omega a} \frac{d\phi_{\omega}}{dx} = \pi S_{\omega} + I_{\omega m}^* + A_2 I_{2\omega} \sin(2\phi_{\omega} - \phi_{2\omega} - \phi_0 + \sigma)$$

2ω -component

$$\frac{d}{dx} [I_{2\omega a} A_2^2] = I_{2\omega m} A_2^2 - I_{2\omega t} A_2^2 T - I_{2\omega\omega} A_2 A_1^2 \cos(2\phi_{\omega} - \phi_{2\omega} - \phi_0 + \sigma)$$

$$I_{2\omega a} \frac{d\phi_{2\omega}}{dx} = \pi S_{2\omega} + I_{2\omega m}^* - \frac{A_1^2}{A_2} I_{2\omega\omega} \sin(2\phi_{\omega} - \phi_{2\omega} - \phi_0 + \sigma)$$

The integrals I appearing in the above equations are functions of Θ , frequencies, and the closure assumptions. S is the Strouhal number defined as $wd/(2\pi U)$. The solution of the above system of equations is subject to the initial conditions at $x = 0$: Θ_0 , T_0 , A_{10} , A_{20} , and ϕ_0 .

RESULTS AND DISCUSSIONS

The calculated fundamental and subharmonic components at Strouhal numbers 0.3 and 0.6 are shown in figure 1 for several initial phase angles. The initial momentum thickness is 0.026 R , initial turbulence energy levels is 0.0001. The initial energies of the fundamental and subharmonic are taken such that the initial instability velocity components at the jet centerline are 1.2 and 0.6 percent, respectively. Figure 1 shows that the fundamental is not sensitive to the phase-difference as much as the subharmonic does. Bradley and Ng's (1989) measured integral spectral amplitude shows similar features. The fundamental is less dependent than the subharmonic on the phase angle. Maximum subharmonic amplification occurs at $\phi_0 = 180^\circ$ and minimum subharmonic's amplification occurs at $\phi_0 = 0^\circ$, same as the present results in figure 1(b).

The calculated centerline phase-averaged velocities are shown in figure 2 in comparison with the data of Arbey and Ffowcs-Williams (1984). The Strouhal

numbers are 0.3 and 0.6, the initial turbulence energy level is 0.00001, initial momentum thickness is 0.012. The initial centerline velocity of the $S = 0.3$ component is taken 1.5 percent and that of the $S = 0.6$ is 0.38 of the $S = 0.3$ component as in the experiment. At $S = 0.3$, figure 2(a) shows that calculate peak occurs further down stream as compared to the measured ones. However, the calculated peak has the same level as the measured one. The peak increases when ϕ_0 is changed from 0 to 180° , as the present computations also predict. The calculated phase averaged velocities at $S = 0.6$ shown in figure 2(b) has the same features as the measured one; same level of amplification and same dependency on ϕ_0 . The measured component increases again after it decays which is probably due to its interaction with other frequency components. This mechanism is not accounted for here.

The dependency of the subharmonic amplification on the initial phase angle is shown in figure 3 for Strouhal numbers 0.2 and 0.4. The initial levels are $\tilde{U}_f = 7$ percent, $\tilde{U}_s = 0.5$ percent. The peak of the subharmonic at $\phi_0 = 270^\circ$ is three times higher than its peak at $\phi_0 = 90^\circ$. The corresponding momentum thickness is shown in figure 4, compared to the unexcited momentum thickness. The figure shows that the momentum thickness is only weakly dependent on the phase angle. This indicates that the direct role of the subharmonic in turbulent jets in controlling the mixing is less pronounced as compared to its role in controlling the mixing in Laminar jets. However, the subharmonic can still have a strong role in the mixing process through enhancing the background turbulence which in turn increases the mixing.

If both the fundamental and subharmonic's initial levels are high, the dependency on the phase angle is less pronounced as figure 5 indicates. The Strouhal numbers are 0.3 and 0.6 and the initial levels are $\tilde{U}_f = \tilde{U}_s = 3$ percent. At high initial levels, large energy levels are drained from the mean flow and therefore the fundamental-subharmonic energy exchanges are relatively smaller and consequently less pronounced.

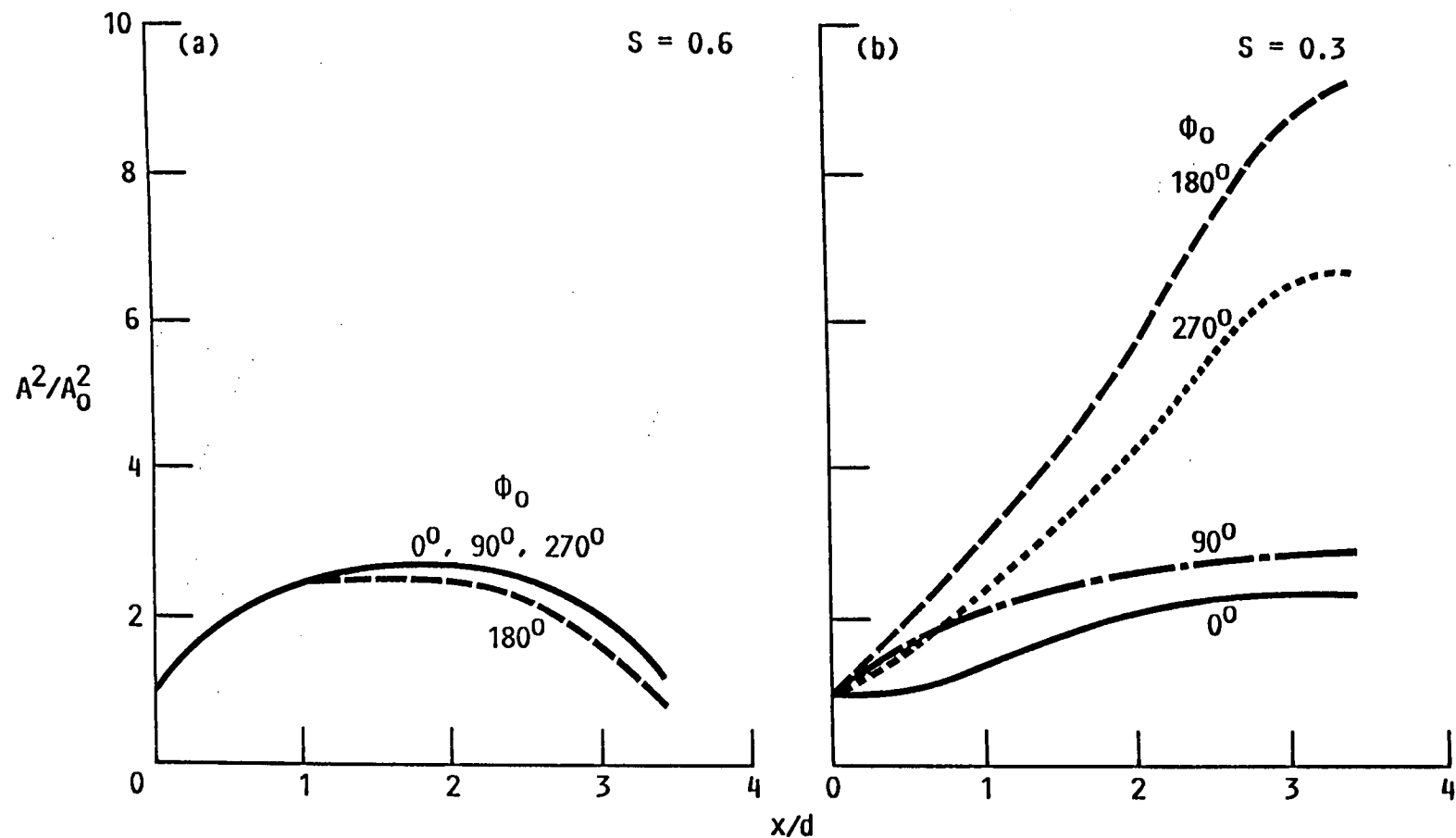
The effect of the forcing level at a fundamental frequency of $S = 0.4$ on the subharmonic's amplification is shown in figure 6. The figure shows that the peak of the subharmonic increases with increasing the forcing level. However, a saturation condition occurs around a forcing level of 10 percent. Higher forcing levels result in no further increase of the subharmonic's peak over 20 percent.

REFERENCES

1. Arbey, H.; and Ffowcs-Williams, J.E.: Active Cancellation of Pure Tones in an Excited Jet. *J. Fluid Mech.*, vol. 149, Dec. 1984, pp. 445-454.
2. Bradley, T.A.; and Ng, T.T.: Phase-Locking in a Jet Forced With Two Frequencies. *Exper. Fluids*, vol. 7, no. 1, 1989, pp. 38-48.
3. Riley, J.J.; and Metcalf, R.W.: Direct Numerical Simulation of a Perturbed, Turbulent Mixing Layer. *AIAA Paper 80-0274*, Jan. 1980.
4. Monkewitz, P.A.: Subharmonic Resonance, Pairing and Shredding in the Mixing Layer. *J. Fluid Mech.*, vol. 188, Mar. 1988, pp. 223-252.

Figure 1

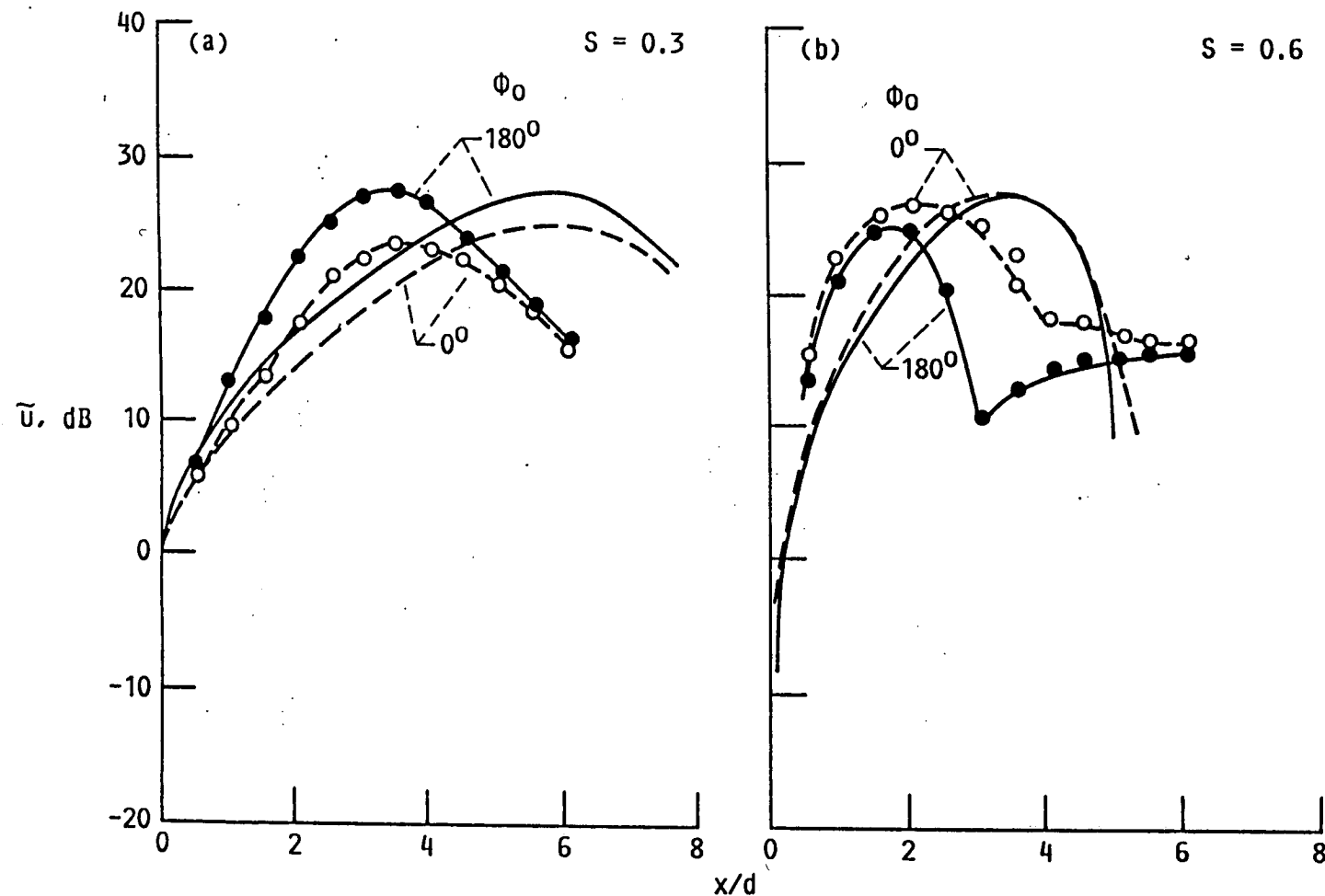
DEPENDENCY OF THE STABILITY COMPONENTS ON THE INITIAL PHASE ANGLES



CD-89-39220

Figure 2

COMPARISON BETWEEN CALCULATED PHASE-AVERAGED CENTERLINE VELOCITIES AND ARBEY & FFOWCS-WILLIAMS' (1984) DATA



CD-89-39219

Figure 3

DEPENDENCY OF SUBHARMONIC'S AMPLIFICATION ON THE INITIAL PHASE-ANGLE AT STROUHAL NUMBERS OF 0.4 AND 0.2

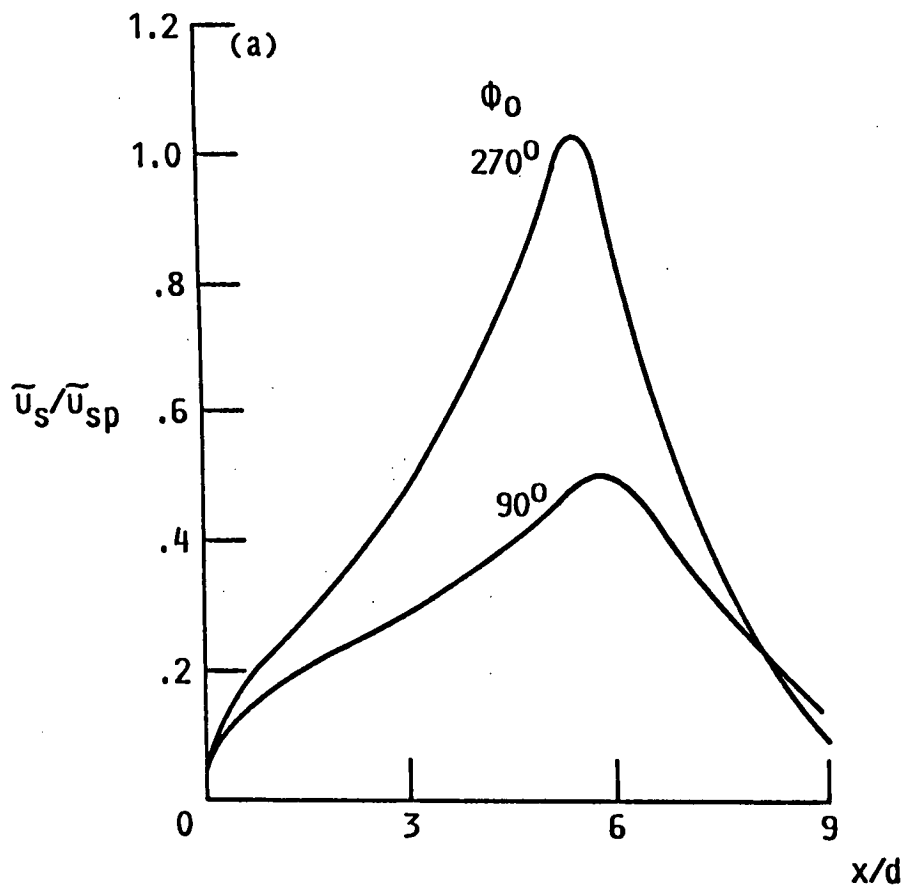


Figure 4

DEVELOPMENT OF THE MOMENTUM THICKNESS UNDER TWO-FREQUENCY EXCITATION AND FOR THE UNEXCITED CASE

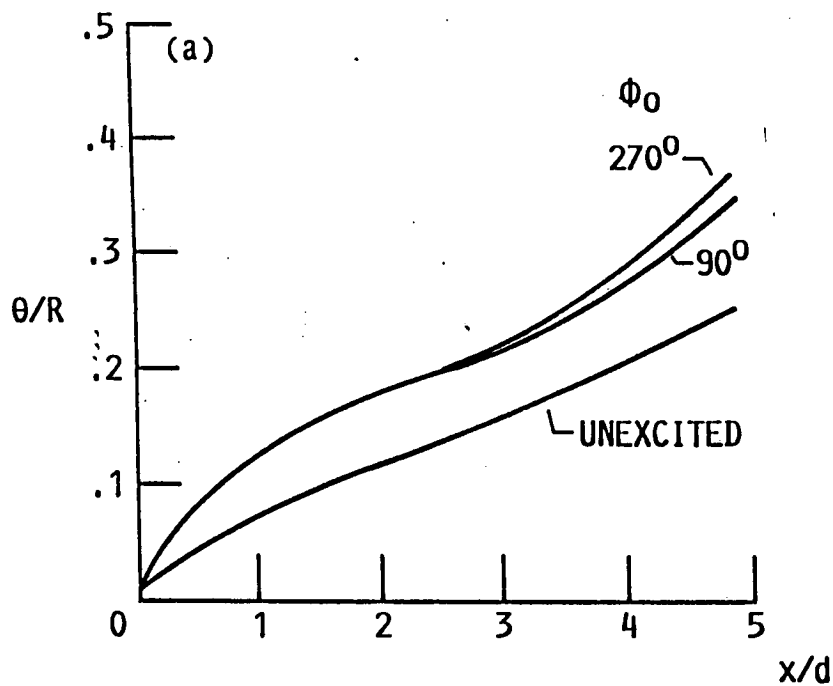


Figure 5

DEPENDENCY OF THE SUBHARMONIC'S PEAK ON THE PHASE-ANGLE AT HIGH LEVELS BOTH THE FUNDAMENTAL AND THE SUBHARMONIC

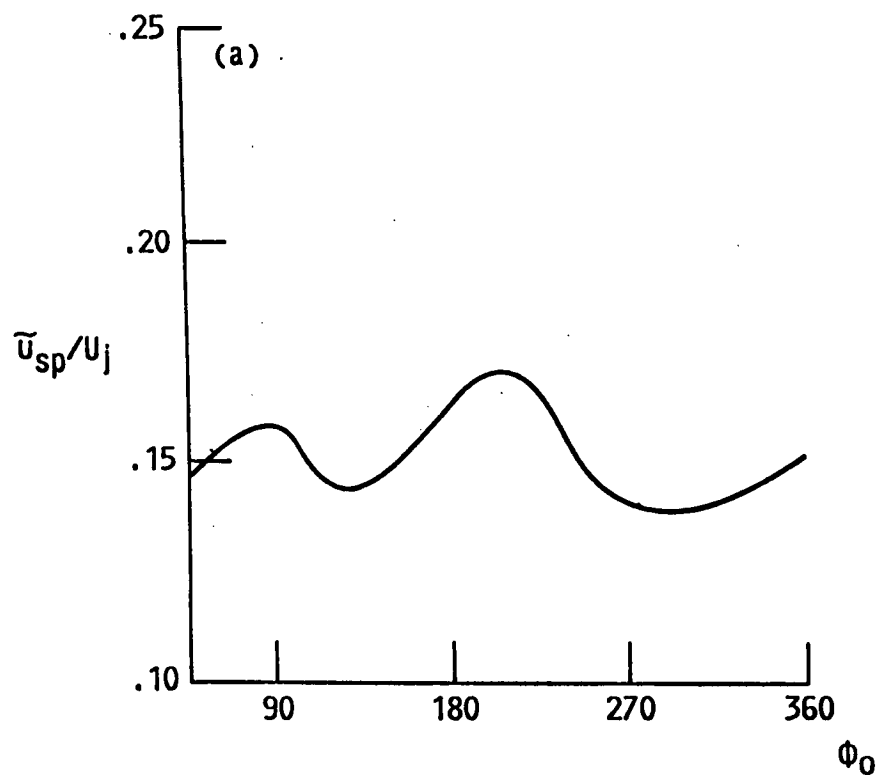
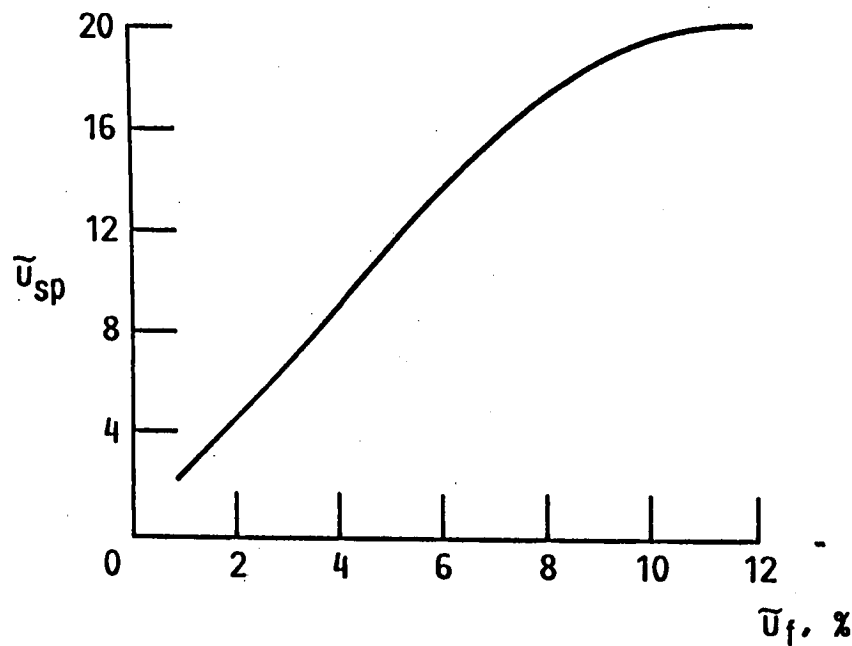


Figure 6

DEPENDENCY OF THE SUBHARMONIC'S PEAK ON THE
FORCING LEVEL AT STROUHAL NUMBERS OF 0.2 AND 0.4



More Accurate Predictions with Transonic Navier-Stokes
Methods Through Improved Turbulence Modeling

by

Dennis A. Johnson
Experimental Fluid Dynamics Branch
NASA Ames Research Center

Because the aerodynamic characteristics of aircraft in the transonic regime are so sensitive to viscous effects, the selection of the turbulence model for a transonic prediction method is no less important than the selection of the numerical algorithm. Yet, the usual practice in transonic airfoil, Reynolds-Averaged, Navier-Stokes codes has been to employ "equilibrium" algebraic turbulence models. Satisfactory results are obtained with these turbulence models for weak interaction cases (i.e., cases where the upper surface shock wave is too weak to have a major effect on the turbulent boundary layer). Such is not the situation for cases where the shock wave is sufficiently strong to cause separation. The danger in using these "equilibrium" turbulence models for airfoil design is that they can result in unduly optimistic projections of aircraft performance at off-design conditions.

Significant improvements in predictive accuracies for off-design conditions are achievable through better turbulence modeling; and, without necessarily adding any significant complication to the numerics. One well established fact about turbulence is it is slow to respond to changes in the mean strain field. With the "equilibrium" algebraic turbulence models no attempt is made to model this characteristic and as a consequence these turbulence models exaggerate the turbulent boundary layer's ability to produce turbulent Reynolds shear stresses in regions of adverse pressure gradient. As a consequence, too little momentum loss within the boundary layer is predicted in the region of the shock wave and along the aft part of the airfoil where the surface pressure undergoes further increases.

Recently, a "nonequilibrium" algebraic turbulence model was formulated which attempts to capture this important characteristic of turbulence. This "nonequilibrium" algebraic model employs an ordinary differential equation to model the slow response of the turbulence to changes in local flow conditions. In its original form, there was some question as to whether this "nonequilibrium" model performed as well as the "equilibrium" models for weak interaction cases. However, this turbulence model has since been further improved wherein it now appears that this turbulence model performs at least as well as the "equilibrium" models for weak interaction cases and for strong interaction cases represents a very significant improvement.

The performance of this turbulence model relative to popular "equilibrium" models is illustrated for three airfoil test cases of the 1987 AIAA Viscous Transonic Airfoil Workshop, Reno, Nevada. A form of this "nonequilibrium" turbulence model is currently being applied to wing flows for which similar improvements in predictive accuracy are being realized.

TRANSONIC FLOW TURBULENCE MODELING AIRFOIL AND WING FLOWS

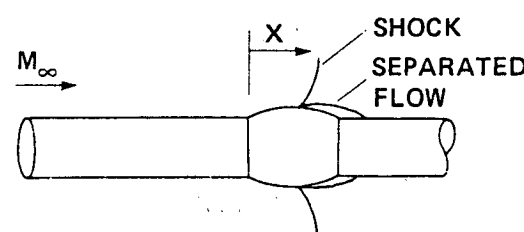
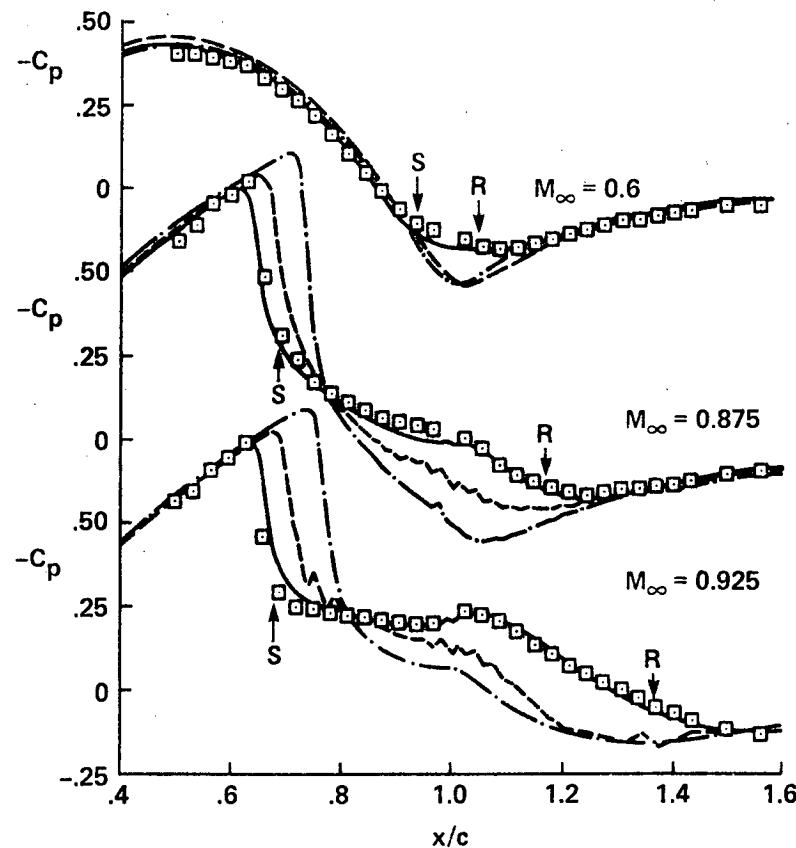
WHY BE CONCERNED ABOUT THE TURBULENCE MODEL?

- NUMERICAL PREDICTIONS CAN BE EXTREMELY
SENSITIVE TO TURBULENCE MODEL IN TRANSONIC REGIME**
- WIDELY USED EQUILIBRIUM ALGEBRAIC TURBULENCE
MODELS OVERPREDICT AIRCRAFT PERFORMANCE**

NONEQUILIBRIUM JOHNSON-KING ALGEBRAIC TURBULENCE MODEL

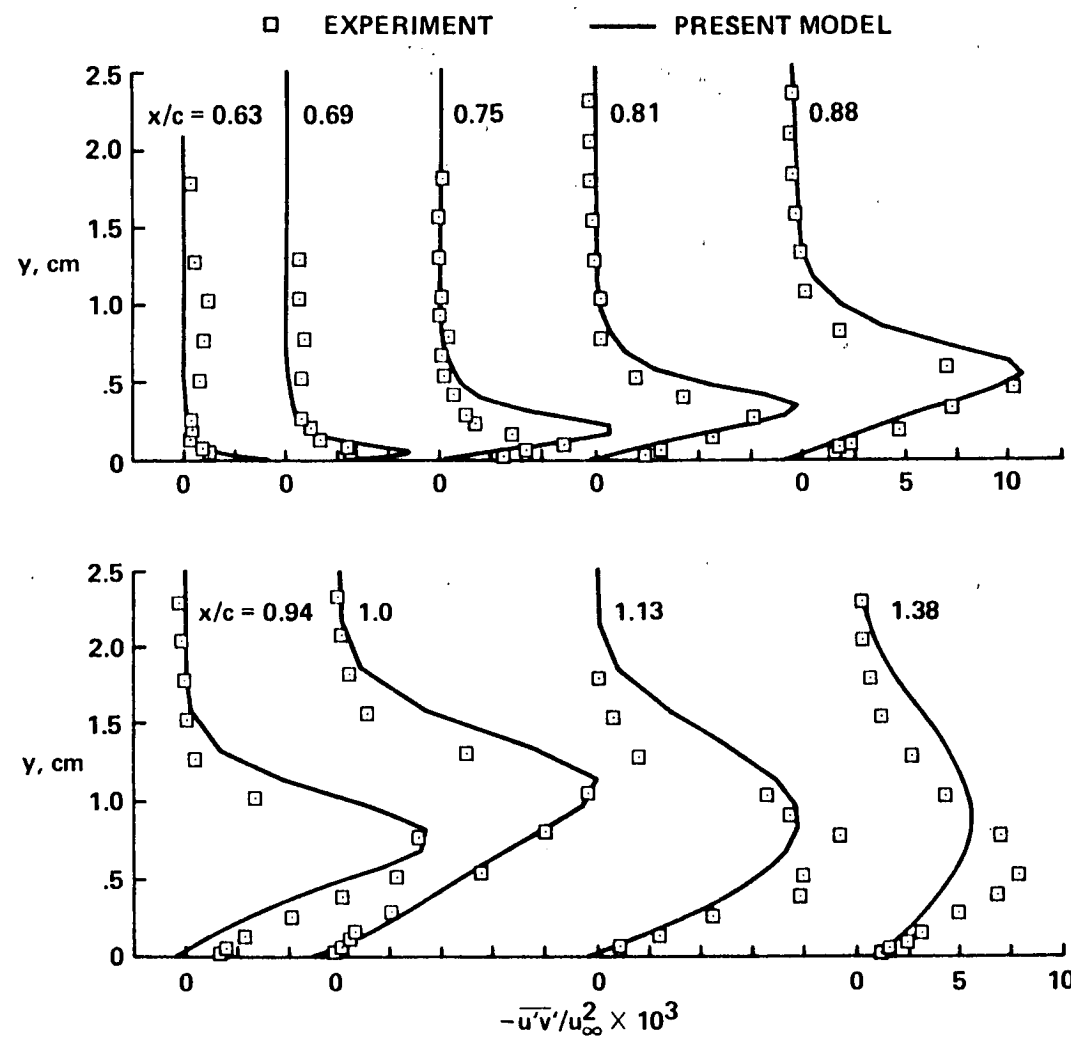
- SLOW RESPONSE OF TURBULENT SHEAR STRESS TO CHANGES IN STRAIN FIELD MODELED
- ORDINARY DIFFERENTIAL EQUATION FOR MAXIMUM REYNOLDS SHEAR STRESS ESTABLISHES EDDY VISCOSITY (SIMPLIFIED "REYNOLDS STRESS" MODEL?)
- DUE TO RECENT IMPROVEMENTS, MODEL PERFORMS BETTER FOR ATTACHED FLOW CASES (SURPRISINGLY, ORIGINAL MODEL WORKED BETTER FOR STRONGLY SEPARATED CASES)

SURFACE PRESSURE COEFFICIENT AXISYMMETRIC BUMP

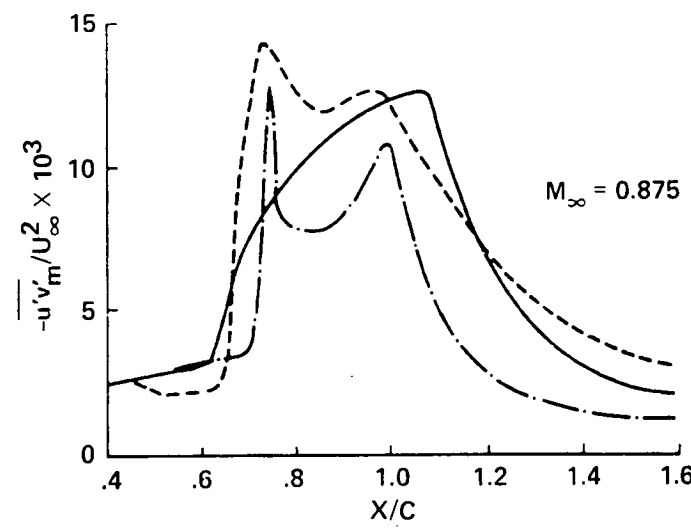
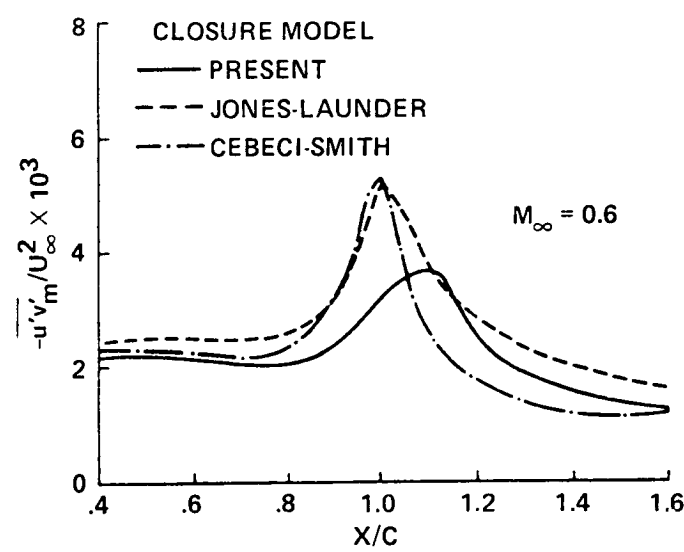


CLOSURE MODEL
 — PRESENT
 - - - JONES-LAUNDER
 - - - CEBECI-SMITH
 □ EXPERIMENT
 S SEPARATION
 R REATTACHMENT

REYNOLDS SHEAR STRESS PROFILES
AXISYMMETRIC BUMP, $M_\infty = 0.875$



MAXIMUM REYNOLDS SHEAR STRESS DISTRIBUTIONS



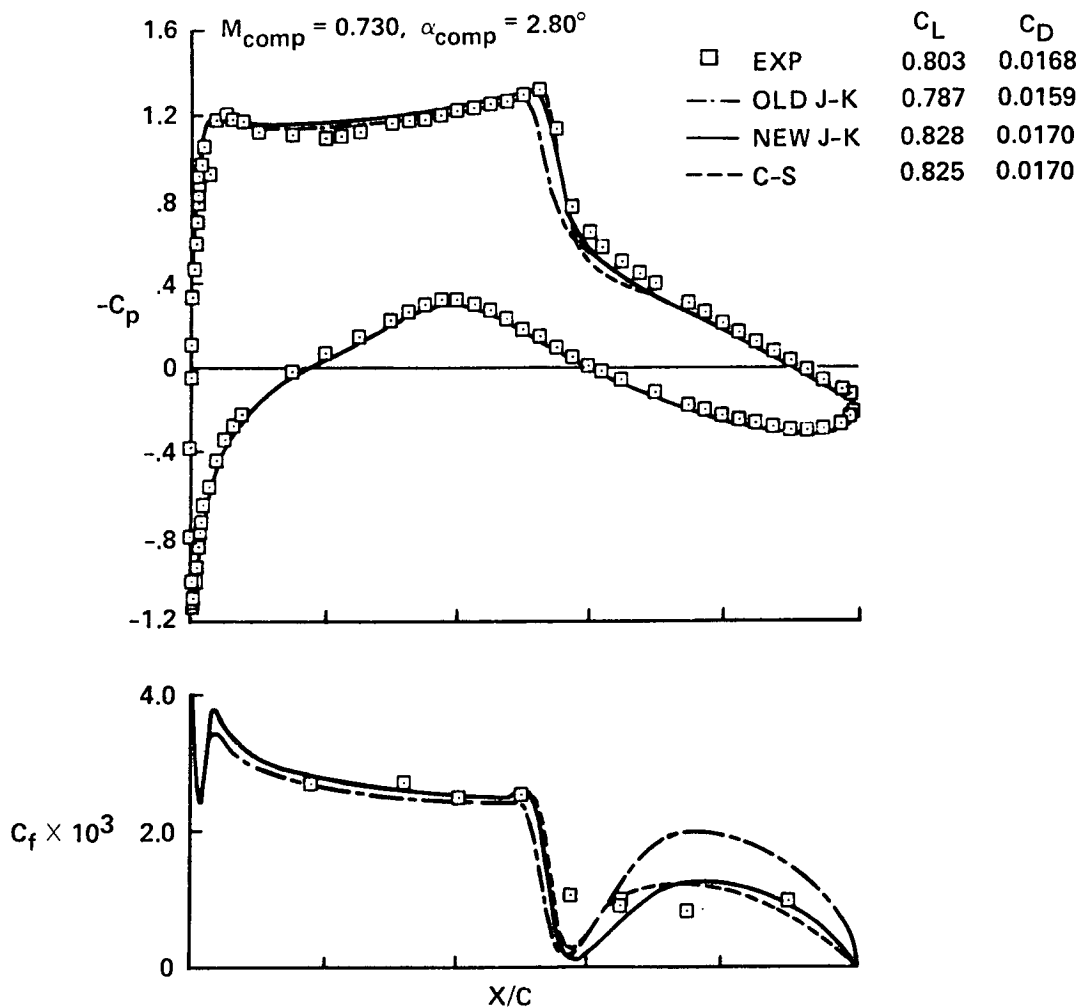
IMPROVEMENTS IN JOHNSON-KING MODEL

NEW INNER EDDY VISCOSITY EXPRESSION

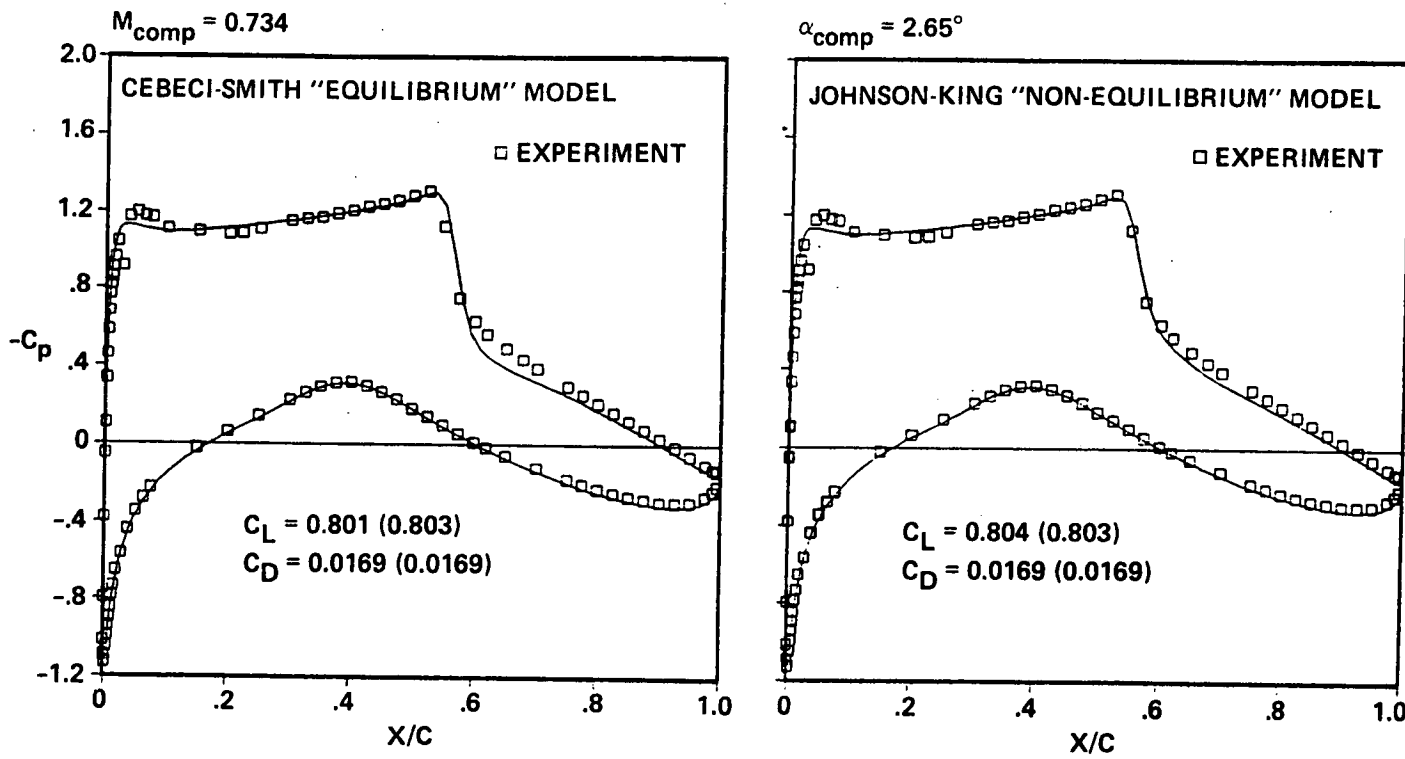
- BETTER SATISFIES "LAW OF THE WALL" FOR ATTACHED ADVERSE PRESSURE GRADIENT CONDITIONS (ORIGINAL MODEL OVERPREDICTED C_f DOWNSTREAM OF SHOCK WAVE)
- INCLUDES VELOCITY SCALE WHICH ACCOUNTS FOR COMPRESSIBILITY

IMPROVEMENTS IN JOHNSON - KING TURBULENCE MODEL FOR WEAK SHOCK WAVE/BOUNDARY LAYER INTERACTIONS

RAE 2822, $M_{\text{exp}} = 0.729$, $\alpha_{\text{exp}} = 3.19^\circ$



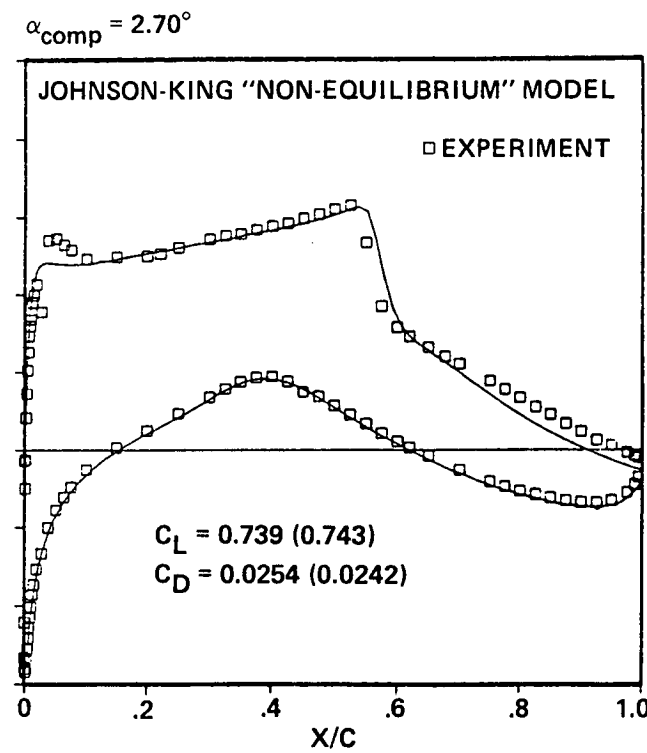
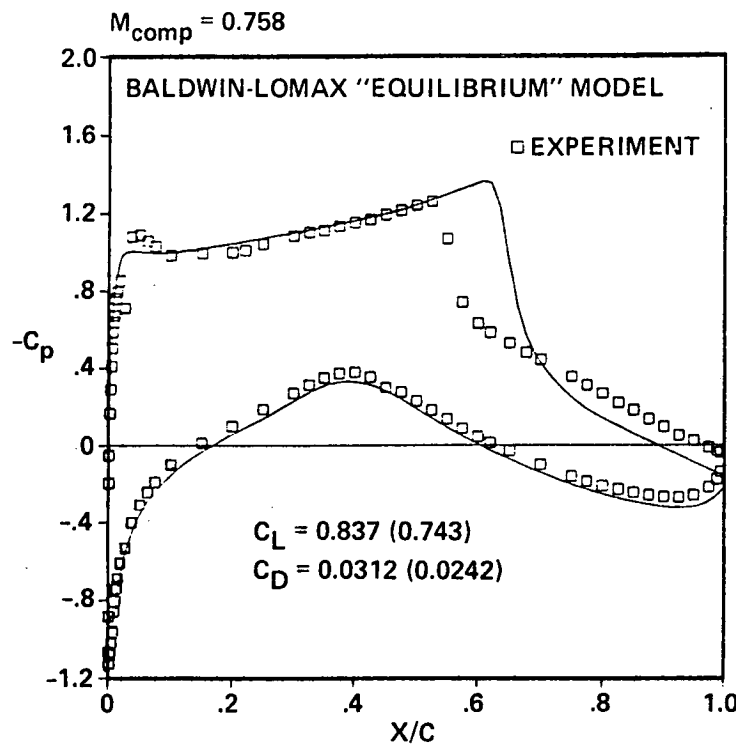
ATTACHED AIRFOIL CASE
RAE 2822, $M_{exp} = 0.73$, $\alpha_{exp} = 3.19^\circ$



SEPARATED AIRFOIL CASE

RAE 2822, $M_{exp} = 0.75$, $\alpha_{exp} = 3.19^\circ$

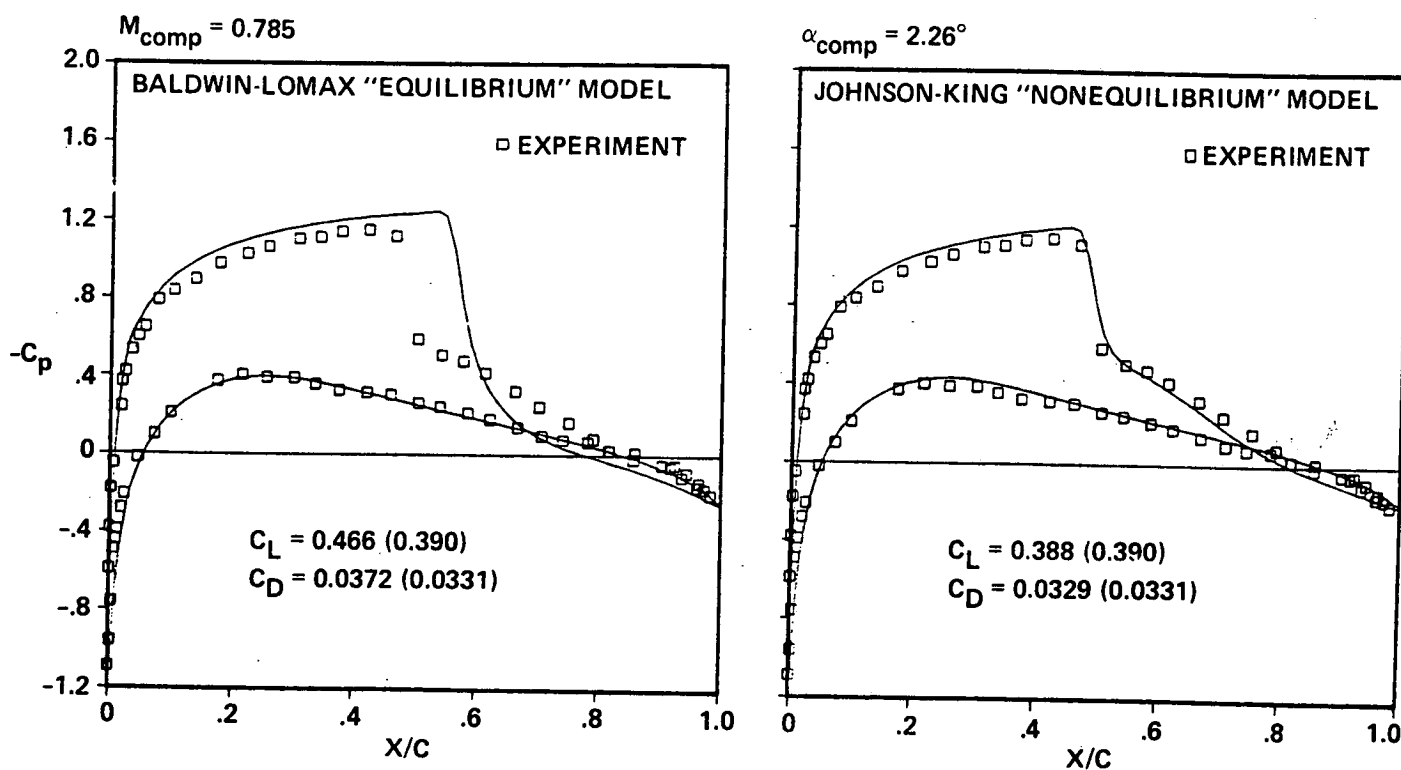
202



203

SEPARATED AIRFOIL CASE

NACA 0012, $M_{exp} = 0.8$, $\alpha_{exp} = 2.86^\circ$



SUMMARY

**SIGNIFICANT IMPROVEMENTS IN PREDICTIVE ACCURACY WITH
NONEQUILIBRIUM ALGEBRAIC TURBULENCE MODEL**

**PRESENT APPROACH IS TO MODEL MOST RELEVANT PHYSICS
WHILE MAINTAINING MATHEMATICAL SIMPLICITY**

**NEGLIGIBLE INCREASE IN COMPUTATIONAL EFFORT COMPARED
TO EQUILIBRIUM ALGEBRAIC TURBULENCE MODELS**

SESSION IV

CFD CODES

Chairman:
Jerry C. South, Jr.
Head, Analytical Methods Branch
NASA Langley Research Center

ORIGINAL CONTAINS
COLOR ILLUSTRATIONS

**RECENT ADVANCES IN RUNGE-KUTTA SCHEMES FOR SOLVING
3-D NAVIER-STOKES EQUATIONS**

By

Veer N. Vatsa
NASA Langley Research Center

Bruce W. Wedan, Ridha Abid

Abstract

A thin-layer Navier-Stokes has been developed for solving high Reynolds number, turbulent flows past aircraft components under transonic flow conditions. The computer code has been validated through data comparisons for flow past isolated wings, wing-body configurations, prolate spheroids and wings mounted inside wind-tunnels. The basic code employs an explicit Runge-Kutta time-stepping scheme to obtain steady state solution to the unsteady governing equations. Significant gain in the efficiency of the code has been obtained by implementing a multigrid acceleration technique to achieve steady-state solutions. The improved efficiency of the code has made it feasible to conduct grid-refinement and turbulence model studies in reasonable amount of computer time. The non-equilibrium turbulence model of Johnson and King has been extended to three-dimensional flows and excellent agreement with pressure data has been obtained for transonic separated flow over a transport type of wing.

N91-10851

OBJECTIVES

- Develop an efficient Navier-Stokes code for high Reynolds number, transonic, separated flows
- Assess the effect of grid refinement
 - on solution accuracy
 - on convergence properties
- Improve turbulence model for separated flows by including non-equilibrium effects
- Validate the code via data comparisons

GOVERNING EQUATIONS

- Reynolds-averaged Navier-Stokes equations
- Thin-layer approximation
- Equations are written in conservation law form
- Turbulence models

Equilibrium model : Baldwin-Lomax model

Non-equilibrium model : Johnson-King model

BOUNDARY CONDITIONS

- Solid surface : viscous
 - no slip and zero injection
 - zero normal pressure gradient
 - specified temperature or adiabatic condition
- Solid surface : inviscid
 - zero flux across surface
 - extrapolate surface pressure
- Inflow/outflow : free-air
 - Riemann invariants for farfield
 - extrapolate all variables at downstream
- Inflow/outflow : in-tunnel simulations
 - Riemann invariants at inflow
 - specify initial profile for viscous sidewall
 - specify pressure and extrapolate other variables at downstream

NUMERICAL ALGORITHM

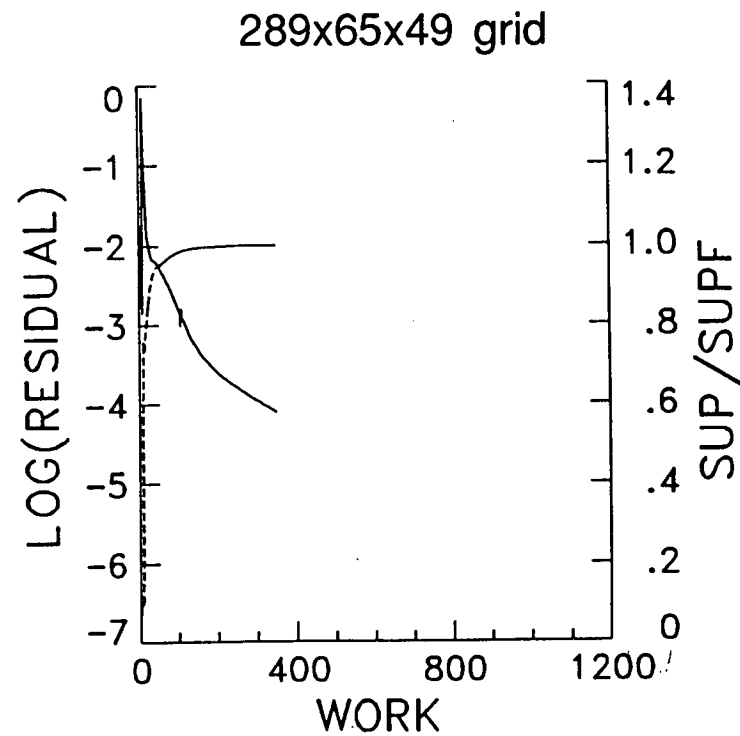
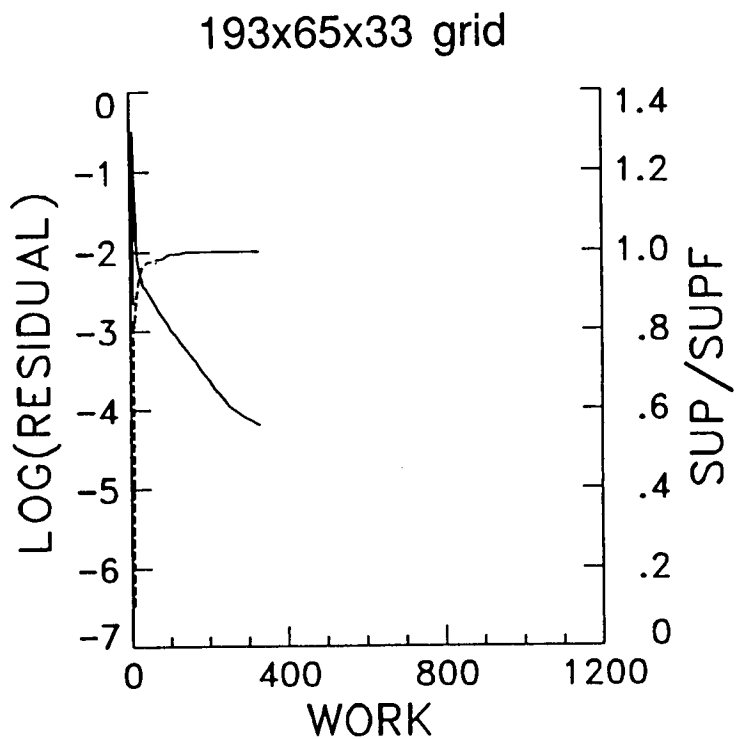
- Based on Runge-Kutta schemes of Jameson and co-workers : 5-stage scheme with 3 dissipation evaluations
- Finite volume, central-difference scheme
- Non-isotropic artificial dissipation added for stability
- Variable coefficient, grid aspect-ratio dependent, implicit residual smoothing for increasing stability bound
- Multigrid acceleration technique
 - Full multigrid (FMG) strategy
 - V-cycle (saw-tooth)
 - Viscous fluxes evaluated only on fine mesh

Effect of grid refinement on convergence history for ONERA M6 wing

($M_\infty = 0.84$, $\alpha = 6.06^\circ$)

Baldwin-Lomax Turbulence Model

212

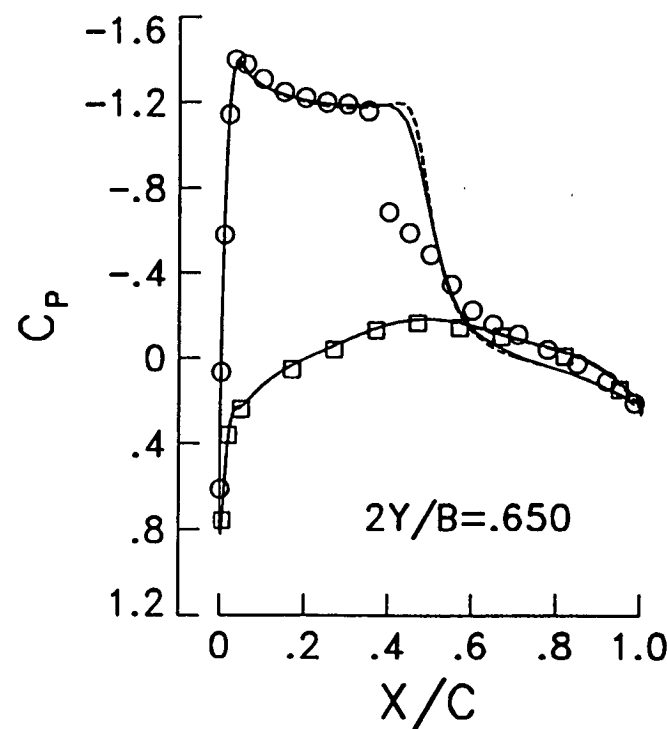
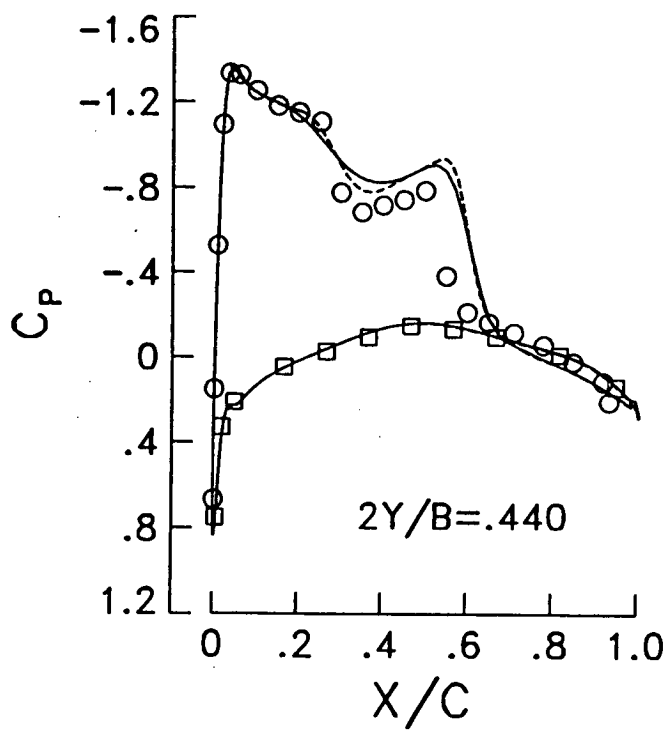


Effect of grid refinement on pressure distributions for ONERA M6 wing

($M_\infty = 0.84$, $\alpha = 6.06^\circ$)

Baldwin-Lomax Turbulence Model

○ □ Experimental data — 193x65x33 grid results - - - 289x65x49 grid results

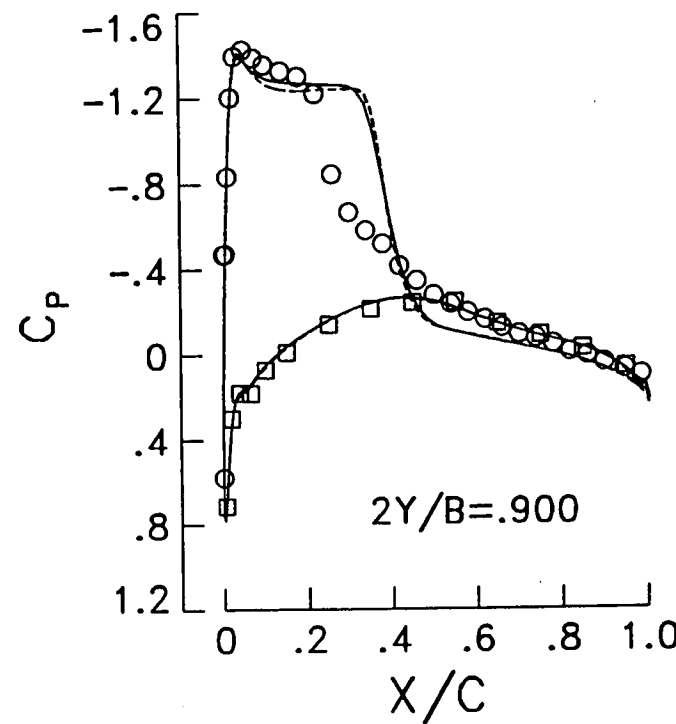
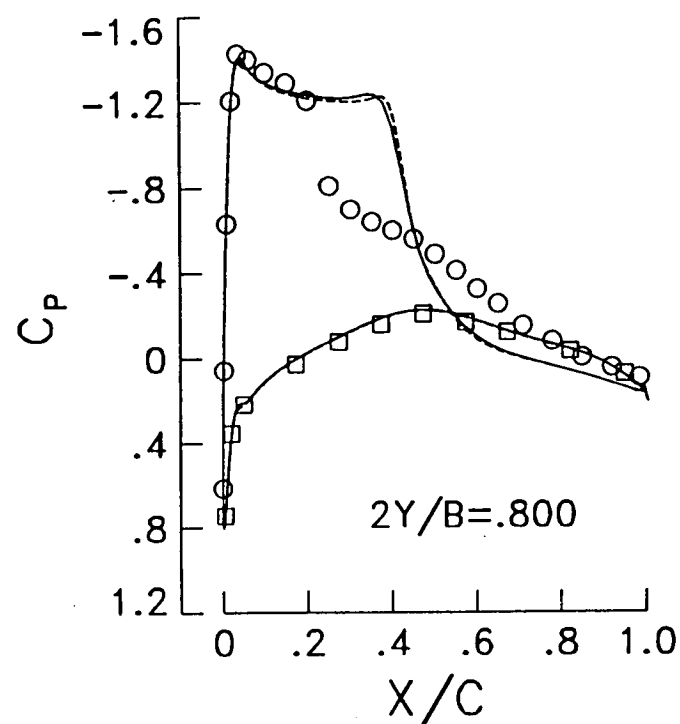


Effect of grid refinement on pressure distributions for ONERA M6 wing

($M_\infty = 0.84$, $\alpha = 6.06^\circ$)

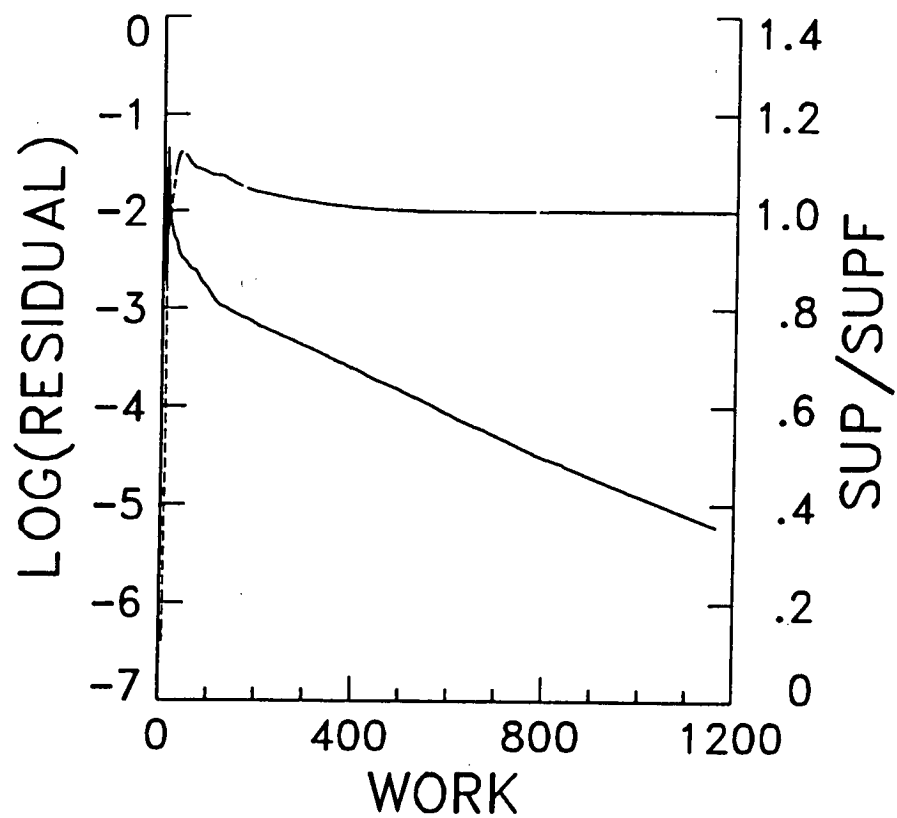
Baldwin-Lomax Turbulence Model

○ \square Experimental data — 193x65x33 grid results - - - 289x65x49 grid results



Convergence history for ONERA M6 wing with Johnson-King model, 289x65x49 grid

($M_\infty = 0.84$, $\alpha = 6.06^\circ$)

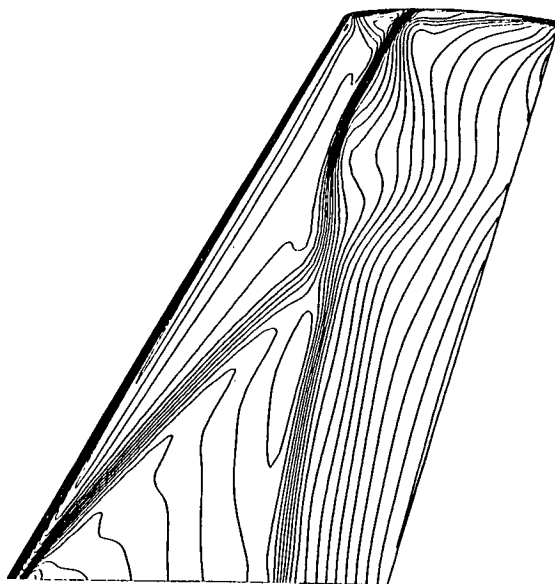


**Effect of turbulence model on
pressure contours for ONERA M6 wing**

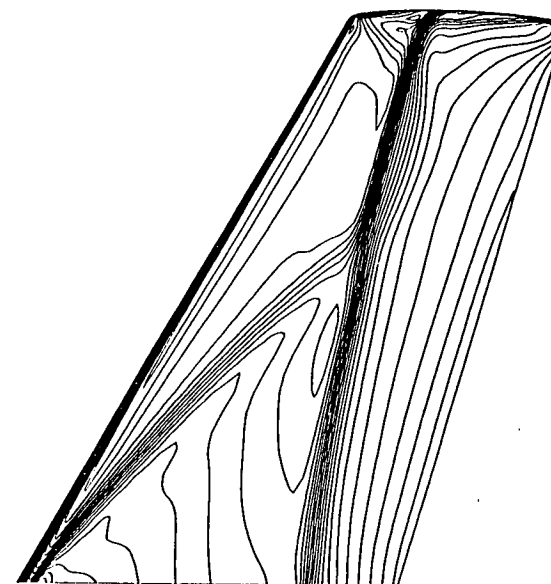
($M_\infty = 0.84$, $\alpha = 6.06^\circ$)

Upper surface, 289x65x49 grid

Johnson-King



Baldwin-Lomax



Effect of Turbulence Model ONERA M6 Wing

$M = 0.84$, $AOA = 6.06$ deg, $Re = 11.7$ million

Baldwin-Lomax

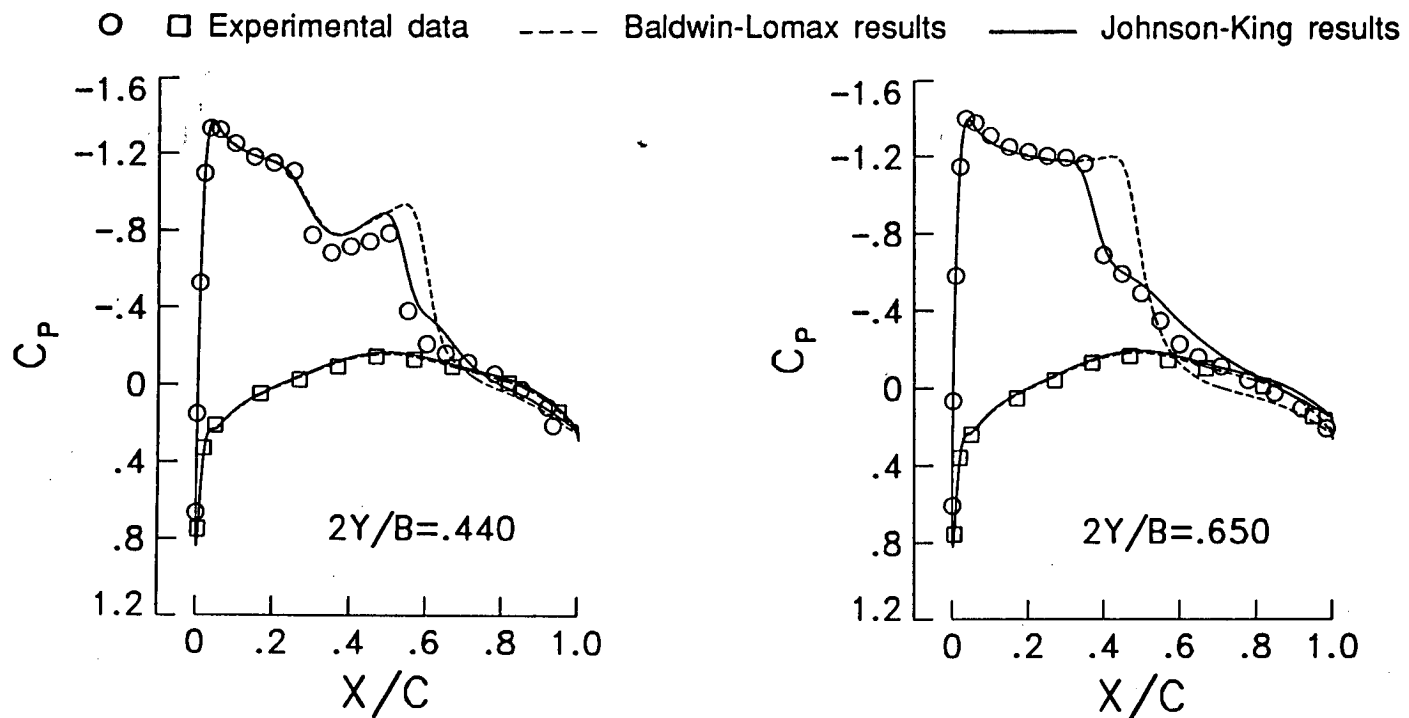
Johnson-King



Effect of turbulence model on pressure distributions for ONERA M6 wing

($M_\infty = 0.84$, $\alpha = 6.06^\circ$)

289x65x49 grid computations

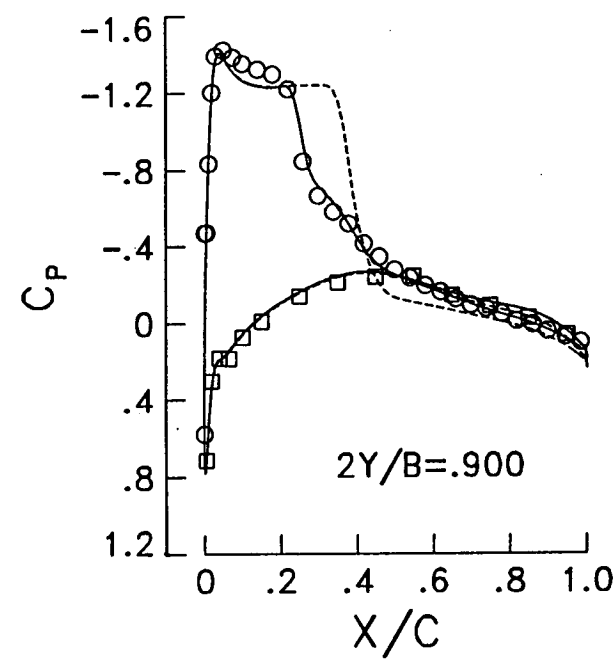
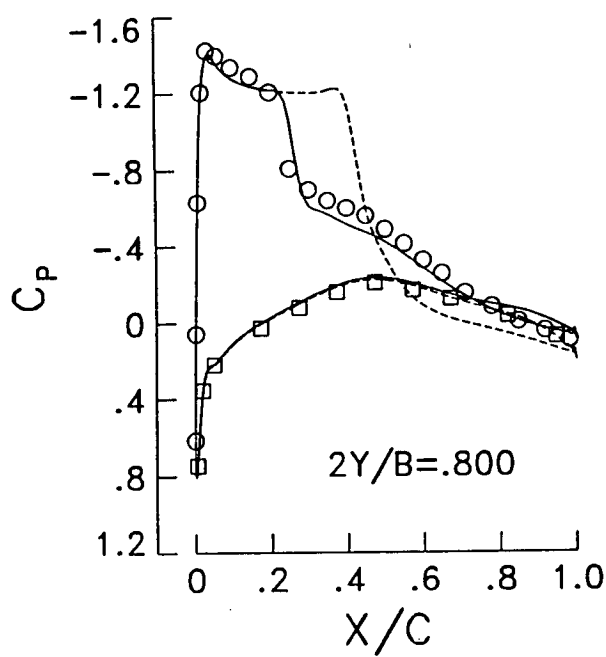


Effect of turbulence model on pressure distributions for ONERA M6 wing

($M_\infty = 0.84$, $\alpha = 6.06^\circ$)

289x65x49 grid computations

○ □ Experimental data - - - Baldwin-Lomax results - - - Johnson-King results



CONCLUDING REMARKS

- Significant gains in efficiency are achieved through multigrid acceleration technique
- Grid-convergence studies feasible due to improved efficiency
- Baldwin-Lomax model gives good solutions for attached flows, but is found inadequate for separated flows
- Johnson-King model results in improved comparison with data for separated flows
- Block-structured grids must be employed for more efficient use of mesh points and for computing more complex configurations

**COMPUTATIONS OF THREE-DIMENSIONAL STEADY
AND UNSTEADY VISCOUS INCOMPRESSIBLE FLOWS**

Dochan Kwak, Stuart E. Rogers
NASA Ames Research Center

Seokkwan Yoon, Moshe Rosenfeld, and Leon Chang
MCAT Institute

The INS3D family of computational fluid dynamics computer codes is presented. These codes are used to as tools in developing and assessing algorithms for solving the incompressible Navier-Stokes equations for steady-state and unsteady flow problems. This work involves applying the codes to real-world problems involving complex three-dimensional geometries. The algorithms utilized include the method of pseudocompressibility and a fractional step method. Several approaches are used with the method of pseudocompressibility including both central and upwind differencing, several types of artificial dissipation schemes, approximate factorization, and an implicit line-relaxation scheme. These codes have been validated using a wide range of problems including flow over a backward-facing step, driven cavity flow, flow through various type of ducts, and steady and unsteady flow over a circular cylinder. Many diverse flow applications have been solved using these codes including parts of the Space Shuttle Main Engine, problems in naval hydrodynamics, low-speed aerodynamics, and biomedical fluid flows. The presentation details several of these including the flow through a Space Shuttle Main Engine inducer, vortex shedding behind a circular cylinder, and flow through an artificial heart.

OUTLINE

- Objective and Approach
- Summary of Flow Codes
 - INS3D Family of codes
 - CENS3D
- Applications and Results
 - Space Shuttle Main Engine (SSME) components
 - Artificial Heart Flow
- Summary and Future Work
- Movie
 - Circular cylinder vortex shedding
 - Artificial heart flow

OBJECTIVE AND APPROACH

○ Objective

- To develop CFD capability for simulating steady and unsteady viscous incompressible flows (Incompressible Navier-Stokes)

○ Approach

- Develop and assess algorithms, and implement in codes
- Develop / implement physical models for engineering analysis (turbulence, cavitation, porous medium, etc.)
- Apply the codes to real-world problems

SUMMARY OF INS3D

○ Governing equations

- Incompressible Navier-Stokes equations in generalized 3-D coordinates for steady-state solutions
- Pseudocompressibility approach

○ Numerical scheme

- Finite difference, central differencing plus artificial dissipation
- Approximate Factorization
- Single or multiple zones

○ Turbulence Models

- Algebraic models
- $k - \epsilon$ model

○ Applications

- Numerous SSME related simulations

○ Status

- Distributed to numerous users across the nation
- Available through COSMIC

EXTENSIONS TO INS3D

- INS3D family of research codes used to study various approaches to solving the INS equations in generalized 3-D coordinates

Pseudocompressibility Approach

- INS3D-UP (Steady-State and Time-accurate calculations)
 - Upwind flux-difference splitting of uniformly high order
 - Line-relaxation implicit scheme
 - Characteristic boundary conditions
- INS3D-LU (Steady-State and Rotating reference frame)
 - Finite-volume method
 - Spectral radius or flux-difference split based dissipation
 - LU-SGS Implicit Scheme
 - Non-reflecting boundary conditions
 - Completely vectorized

EXTENSIONS TO INS3D, continued

Fractional Step Approach

- INS3D-FS (Time-accurate problems)
 - Finite-volume method on a staggered mesh
 - Accurate treatment of geometry
 - ⇒ Exact discrete mass conservation
 - Two-step fractional step method :
 - Solve momentum equations in time (AF scheme)
 - Correct for pressure and velocity (Poisson equation)

SUMMARY OF CENS3D CODE

○ Governing Equations

- Compressible Euler and Navier-Stokes equations and species transport equations in generalized 3-D coordinates

○ Numerical Methods

- Fully-coupled and implicit thermal-chemical nonequilibrium finite-rate-chemistry
- Finite volume / flux-limited TVD, optional high-order flux difference split upwind scheme
- LU-SGS implicit scheme

○ Applications

- SSME preburner, main combustor and nozzle

○ Status

- Research code

VALIDATION CASES

○ INS3D

- Internal flow : Channel, Backward-facing step, Rectangular duct, Turn-around duct
- External flow : Circular cylinder (steady-state), Ogive cylinder
- Juncture flow : Cylinder-plate, Wing-plate, Cavity

○ INS3D-UP

- Internal flow : Driven cavity, Backward-facing step, Square duct with a 90° bend
- External flow : Oscillating plate, Circular cylinder (steady and vortex-shedding flows)

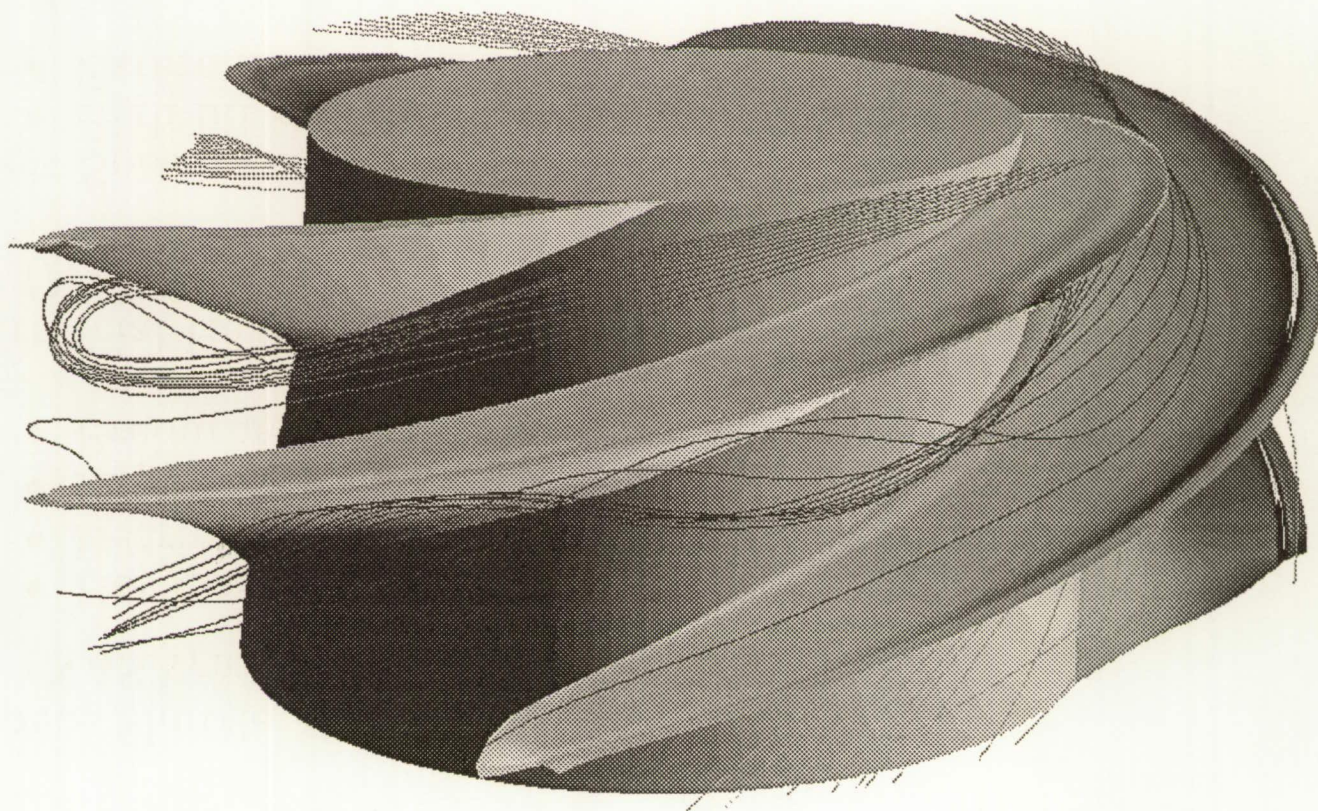
○ INS3D-FS

- Internal flow : Driven cavity
- External flow : Impulsively started circular cylinder, vortex shedding from a circular cylinder

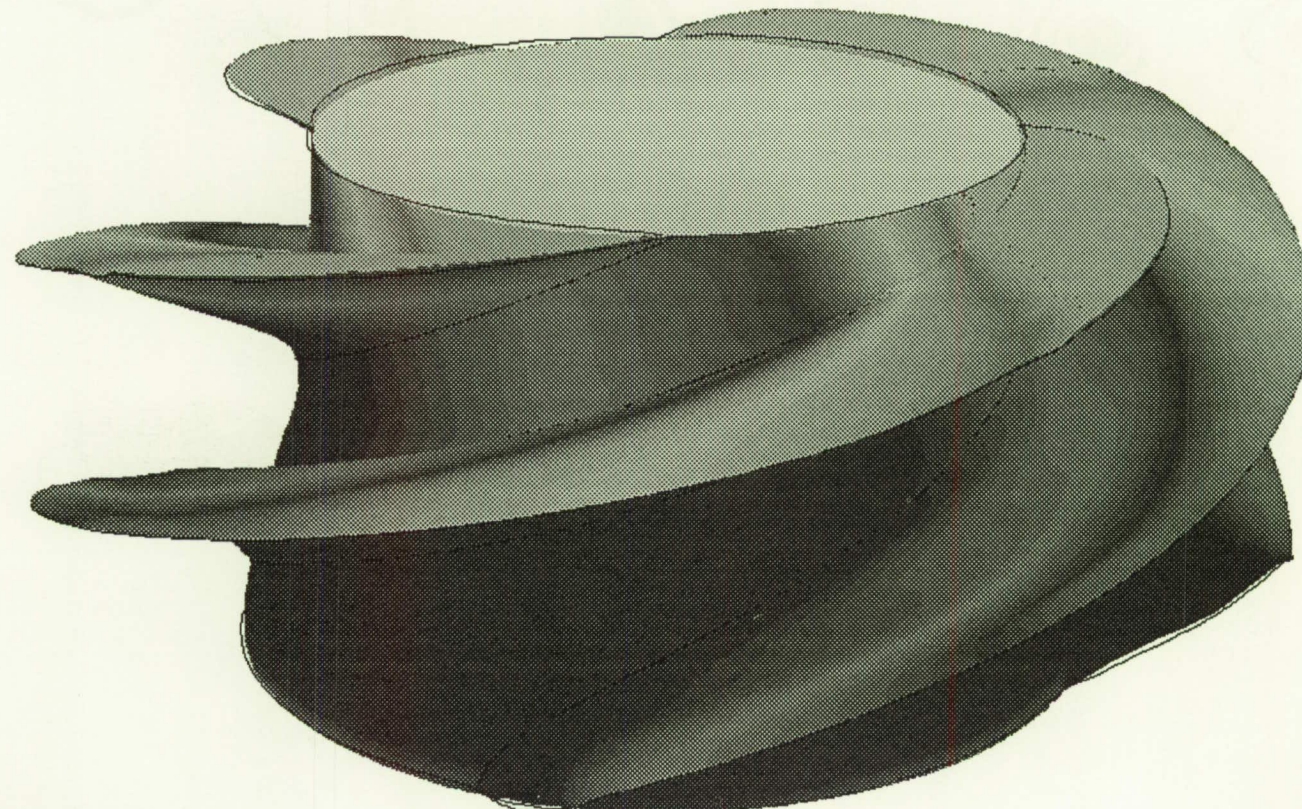
SUMMARY OF APPLICATIONS

- Space Shuttle Main Engine (SSME)
(NASA/MSFC, Rocketdyne)
 - Hot Gas Manifold, Main Injector
 - Bearing
 - Impeller/Inducer
 - Preburner
- 231
○ Artificial Heart / Biofluid Mechanics
(NASA Tech Utilization, Penn State Univ and Stanford Univ)
- Low Speed Aerodynamics
 - High lift device
 - External flow over Automobiles and Trucks
- Naval Hydrodynamics (Submarine)
(DARPA, ONR and David Taylor Research Center)

Particle Traces for SSME Inducer (INS3D-LU)

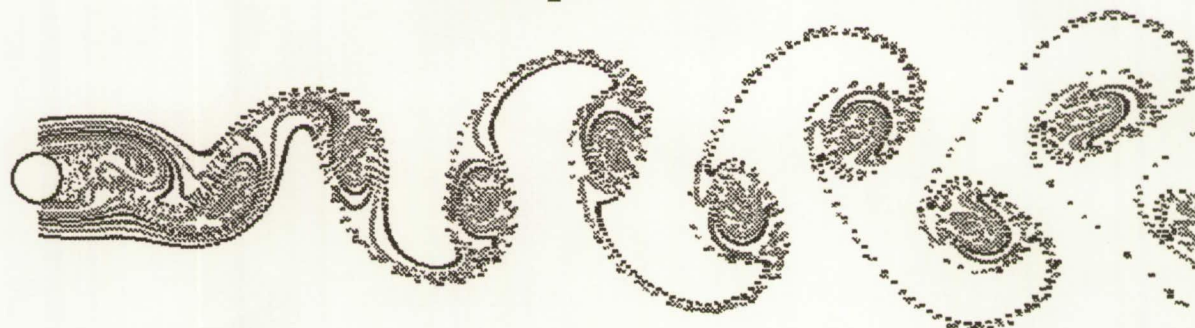


Surface Pressure for SSME Inducer (INS3D-LU)



FLOW OVER A CIRCULAR CYLINDER AT $RE = 105$

Computation



234

Experiment

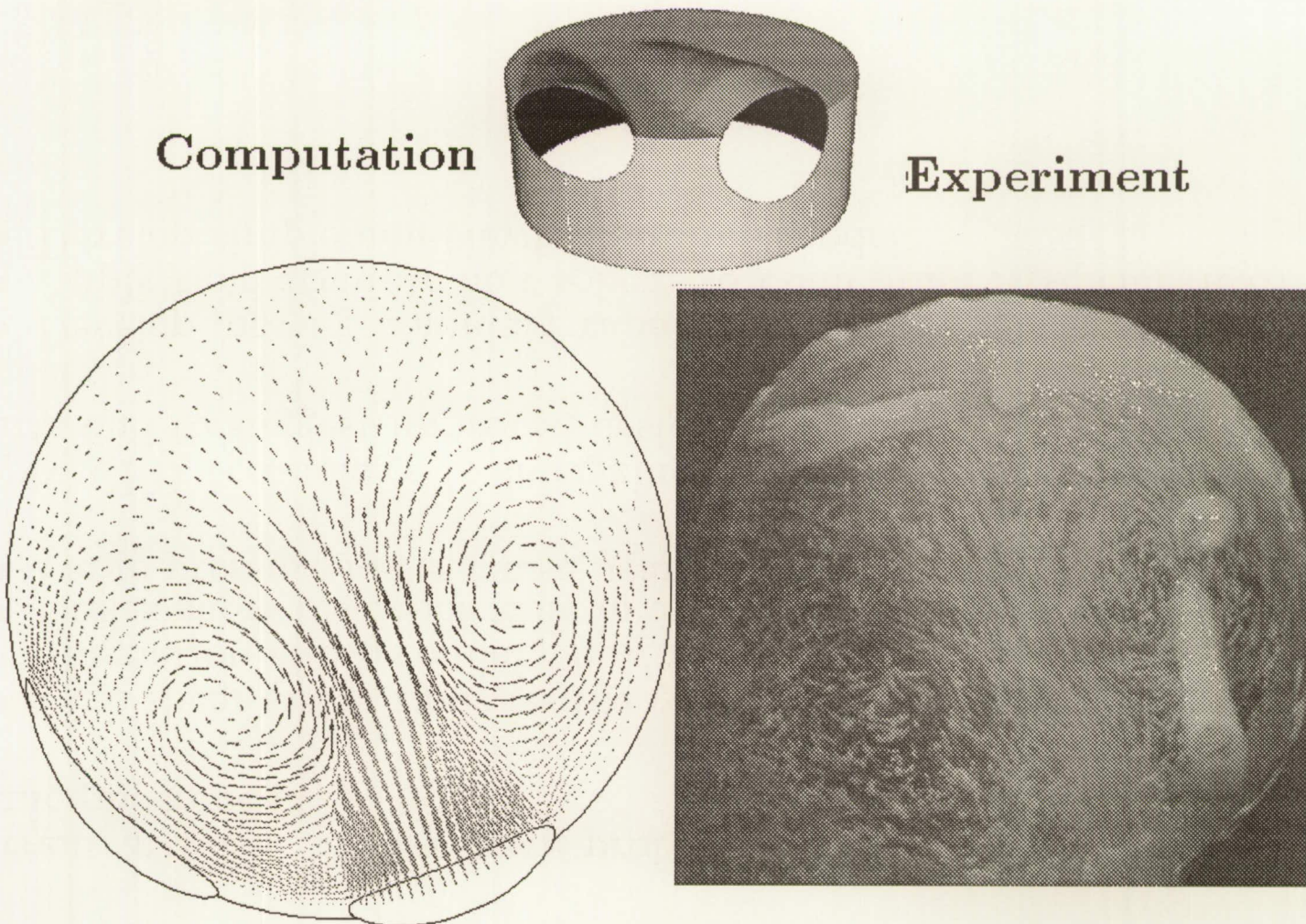


ARTIFICIAL HEART

235

- Current artificial devices have problems stemming from fluid dynamic phenomena
 - High shear stress damages the red blood cells and arterial walls
 - Stagnation and secondary flow regions lead to clotting
 - Desire short residence time in artificial environment
 - Large pressure losses cause heart to work harder
- Apply CFD technology to analyzing blood flow through artificial hearts and to suggest improved design
 - Develop moving boundary capability
 - Apply time accurate flow solvers to Penn State Artificial Heart
 - Develop simple non-Newtonian fluid model

Penn State Artificial Heart – INS3D-UP Code



ORIGINAL PAGE
BLACK AND WHITE PHOTOGRAPH

CONCLUDING REMARKS

- Incompressible and low speed flow simulation codes have been developed (INS3D-xx, CENS3D).
- Results of computer simulations have made significant impact on analysis and redesign of the SSME power head.
- These codes are being extended to analyze other important real world problems.
- Future work includes further enhancement of these codes and improvement in physical modeling.

SAGE

A 2-D Self-Adaptive Grid Evolution Code and its Application in Computational Fluid Dynamics

by

Carol B. Davies¹, Ethiraj Venkatapathy² and George S. Deiwert³

Abstract

SAGE is a user-friendly, highly efficient, 2-dimensional self-adaptive grid code based on Nakahashi & Deiwert's variational principles method. Grid points are redistributed into regions of high flowfield gradients while maintaining smoothness and orthogonality of the grid. CPU efficiency is obtained by splitting the adaption into 2 directions and applying one-sided torsion control, thus producing a 1-D elliptic system that can be solved as a set of tridiagonal equations.

¹ Sterling Software, Palo Alto, Ca.

² Eloret Institute, Sunnyvale, Ca.

³ Chief, Aerothermodynamics Branch, NASA Ames Research Center, Moffett Field, Ca.

N91-10853

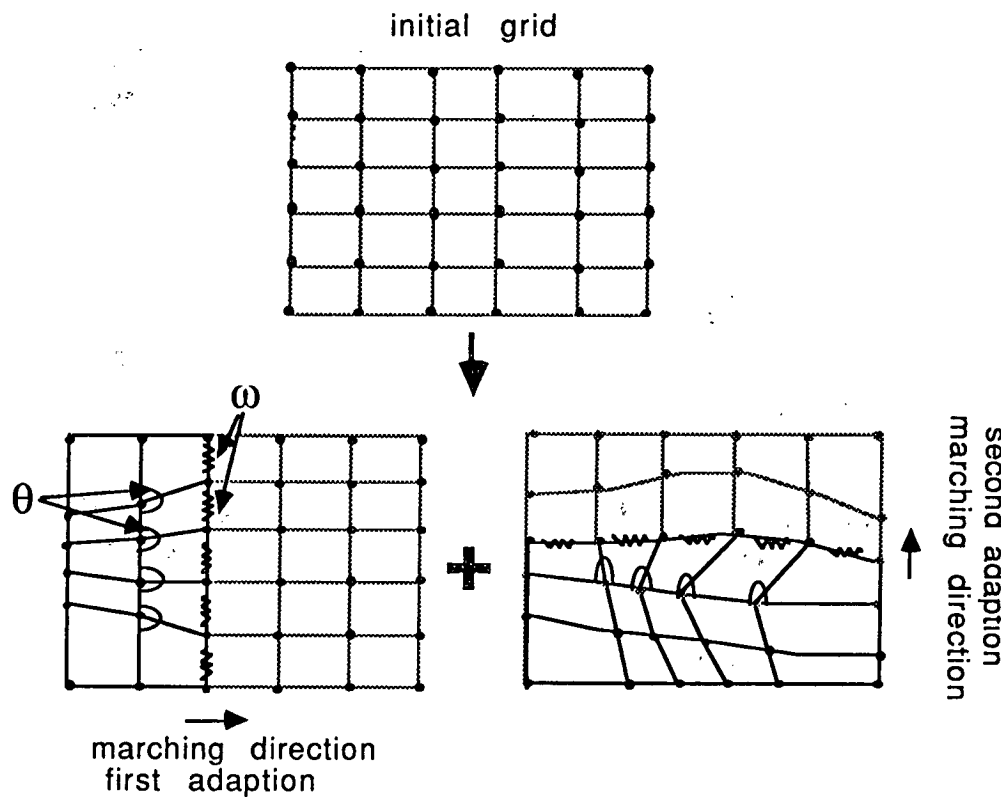
Outline of Presentation

- Brief Description of Self-Adaptive Method (based on Nakahashi & Deiwert's variational principles scheme.)
- SAGE code features, including input parameters.
- Application of SAGE to various flow problems:
 - Hypersonic blunt body
 - Supersonic shock impingement
 - Hypersonic inlet with cowl
 - Supersonic plume flow
 - Supersonic inlet

Self-Adaptive Grid Method of Nakahashi & Deiwert

Objective: to redistribute points into regions of high flow gradients (utilizing minimization principles) while maintaining smoothness and orthogonality between adapted lines. The technique is analogous to connecting each node by tension and torsion springs and locating the equilibrium position of the resulting system.

241



Adaption Equation

Splitting the adaption into 2 directions and applying one sided torsion control reduces the problem to the following 1-D elliptic system which can be solved as a tridiagonal system of equations:

$$\omega_i \Delta s_{i+1} + \omega_{i-1} \Delta s_i - C_i \theta_i = 0$$

where:

tension spring constants, $\omega_i = 1 + Af_i^B$

$f_i = f(\text{gradient of } Q_i)$ {error measure}

self-adaptive mesh size controlled by A and B:

$A = \Delta s_{max} / \Delta s_{min} - 1$, B enforces $\Delta s_{min} = \Delta s_{min}$

torsion spring constant, $C_i = f(\omega_i, \lambda_i, \text{cell aspect ratio})$

and $\theta_i = f(C_t, \text{smoothness, orthogonality})$

SAGE Input Parameters

Control parameters:

λ , C_t , Δs_{min} and Δs_{max}

Adaption parameters:

Limits of adaption domain.

Stepping direction.

Adaption variable (or combination or user defined).

Boundary spacing controls.

Addition of grid points.

Order of interpolation and smoothing.

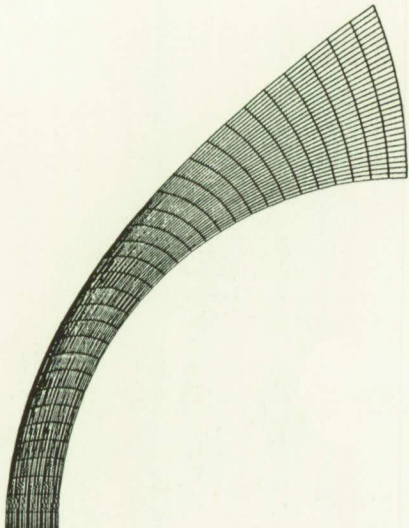
SAGE Code Features

- Fast and efficient - ~0.005 secs/grid point on a VMS/VAX
e.g. 30x30 grid takes 5 secs
- Small size: 1900 lines of code (40% comments)
- Structured code and detailed user guide available -
easy to customise
- Few user input parameters necessary but many options
for great flexibility
- Can be applied to zonal, patched and multiple grids

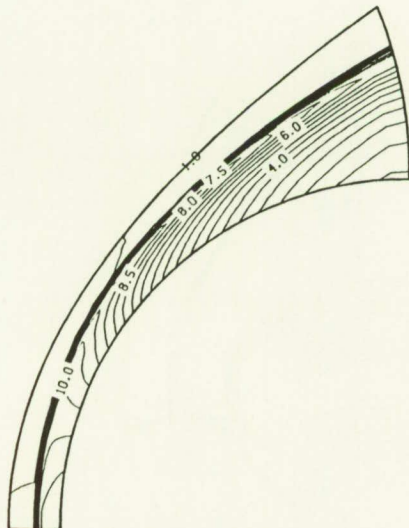
Application 1: Hypersonic Blunt Body

Flow features: Simple 1-directional problem, shock shape aligned with grid.

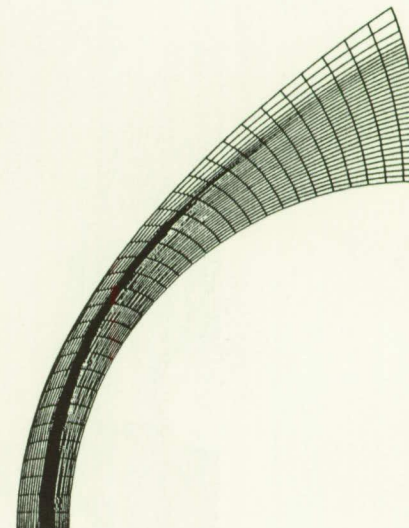
245



Initial grid (32x32)



Initial flow solution
(density contours)



Adapted grid
(i step): $\lambda=.001$

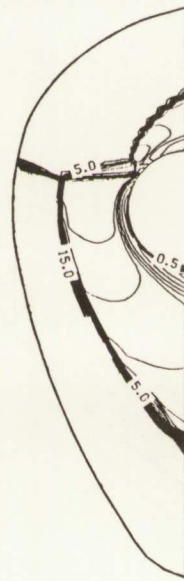
Application 2: Cowl Lip with Shock Impingement

Flow features: blunt body shocks, impinging shock and shear layers

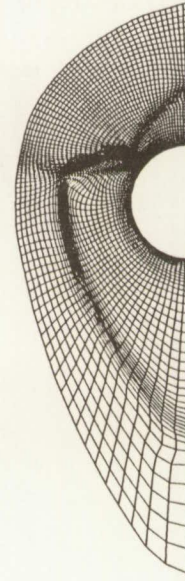
246



Initial Grid(91x46)



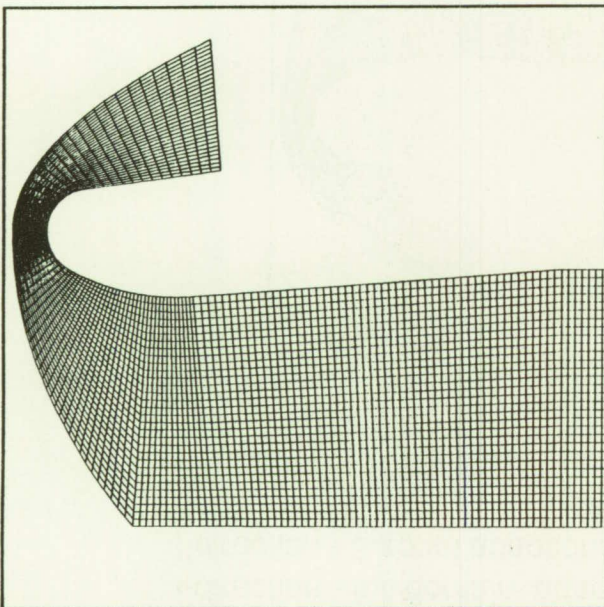
Initial density solution



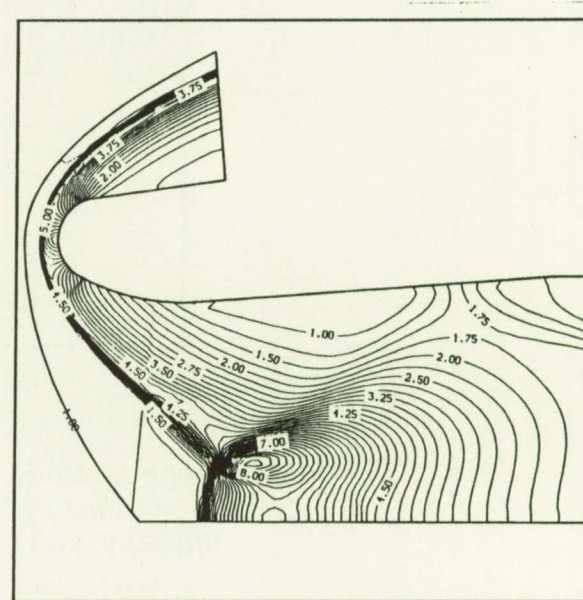
Adapted grid
i: $\Delta s_{min}=.25$, $C_t=.7$, $\lambda=.005$
j: $\Delta s_{min}=.25$, orthe=false

Application 3: Hypersonic Inlet with Cowl

Flow features: Cowl blunt body shock, Mach stem & reflected shocks



Initial Grid (128x32)



Initial density contours

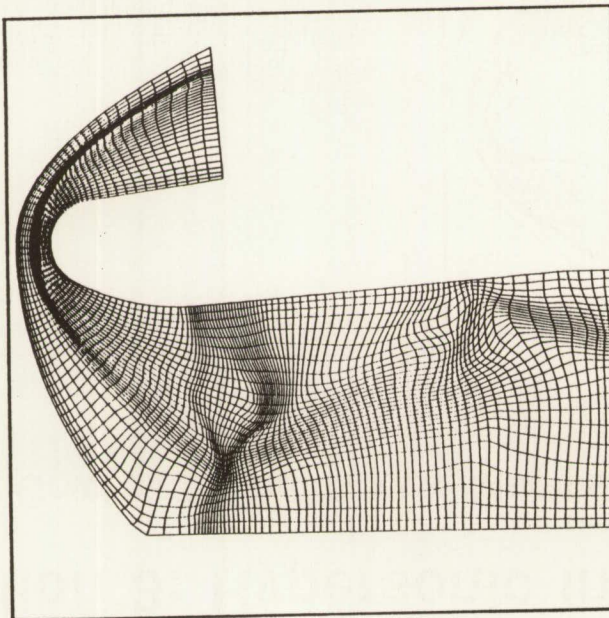
Application 3 continued: Adapted Grid

Example of zonal adaption

i-direction - full domain adaption

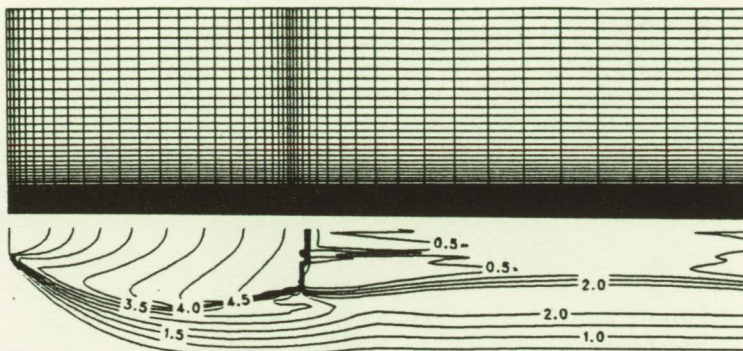
j-direction - 3 zonal adaptions:

- 1) cowl region
- 2) lower inlet region
- 3) upper inlet region

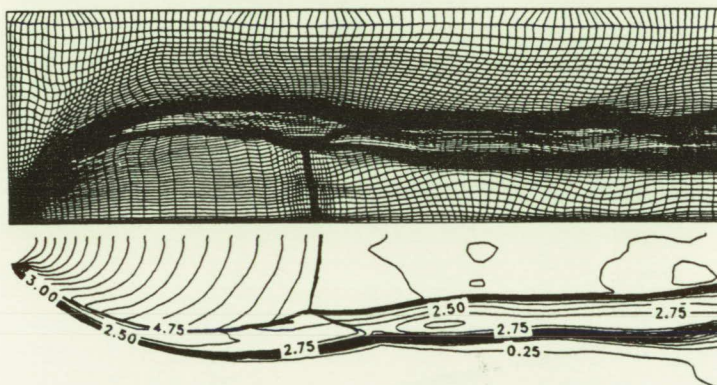


Application 4: Plume Flow

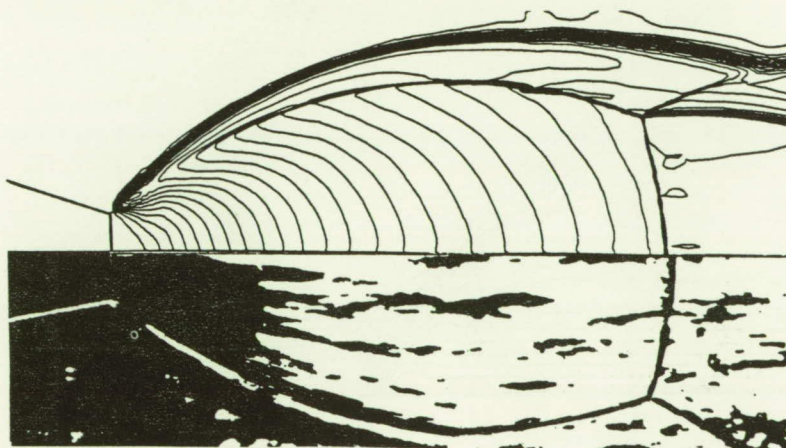
Flow features: Outer shear layer, barrel shock, Mach disc, reflected shock, triple-point shear layer



Initial grid and
Mach contours



Adapted grid and
solution (after 3
iterations)

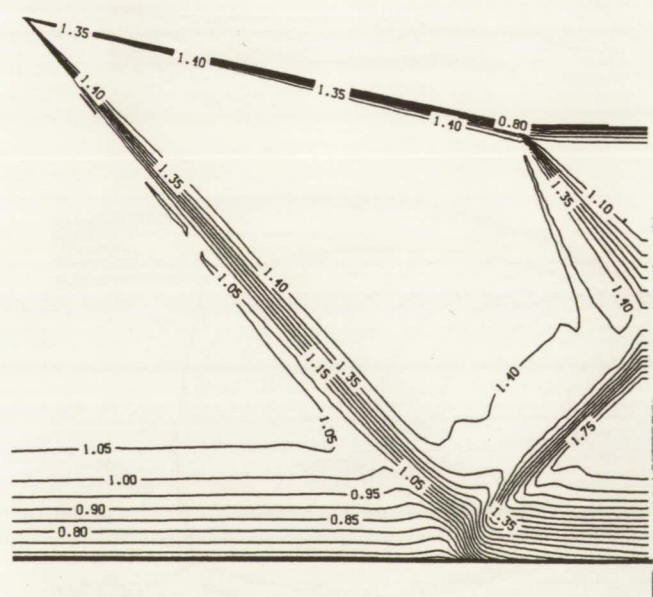
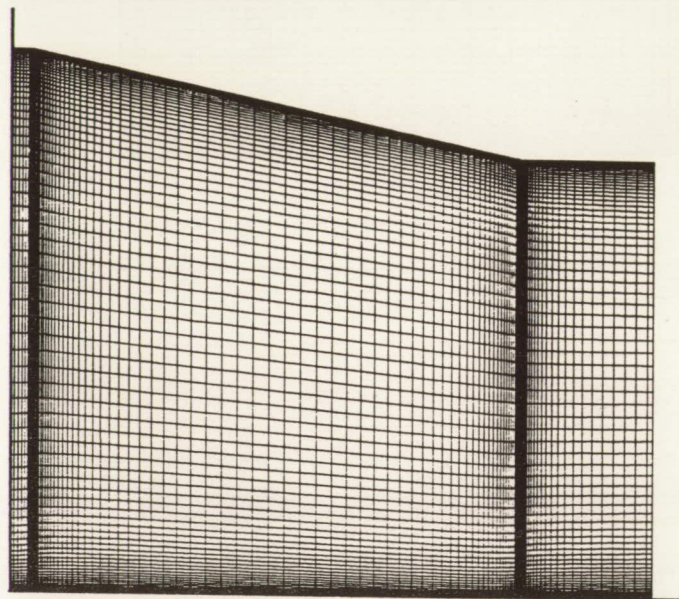


Comparison with
shadowgraph

Application 5: Supersonic Inlet

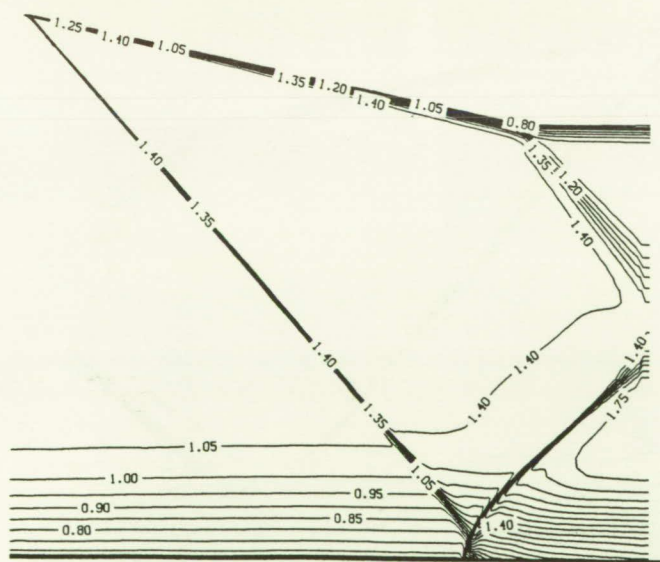
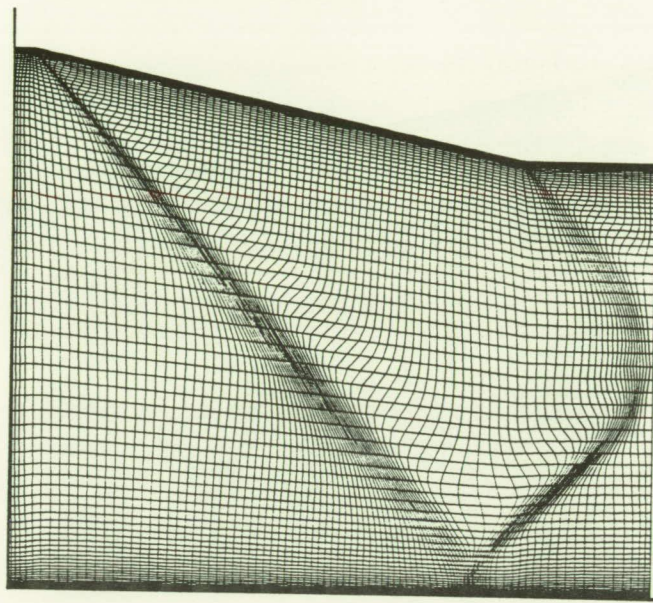
Flow features: Corner shock, reflected shock and expansion fan

Initial grid (101x81) and density solution contours



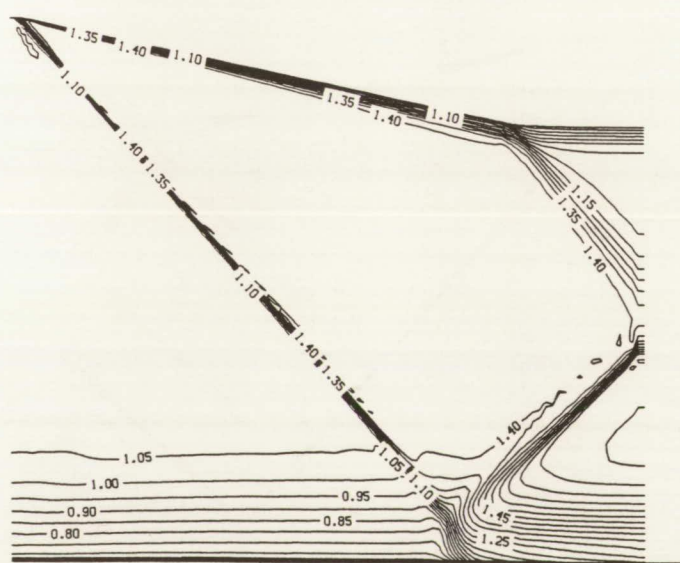
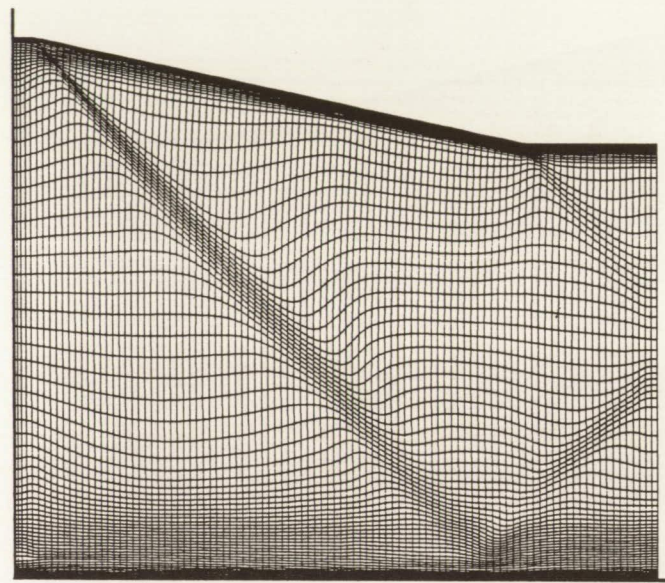
Application 5 continued: Adapted grid (marching in j) and Solution

Input parameters: $\Delta s_{\min}=.25$, $\Delta s_{\max}=2.5$, $\lambda=.0005$



Application 5 continued: Adapted Grid (marching in i) and Solution

Input parameters: jstep=false, $\Delta s_{\min}=.25$, $\lambda=.001$



Concluding Remarks

- SAGE is a new 2-D self-adaptive grid code that is user-friendly, flexible and efficient.
- Appropriate for a variety of CFD applications.
- Use of the SAGE code will efficiently improve the flowfield solution

Time Dependent Viscous Incompressible Navier-Stokes Equations

By

John W. Goodrich
Computational Fluid Dynamics Branch
Internal Fluid Mechanics Division
NASA Lewis Research Center
Cleveland, Ohio 44135

TIME DEPENDENT INCOMPRESSIBLE NAVIER-STOKES EQUATIONS

$$\frac{\partial \mathbf{u}}{\partial t} + \nabla \cdot (\mathbf{u}\mathbf{u}) - \frac{1}{Re} \Delta \mathbf{u} = -\nabla p + \mathbf{F}, \quad \text{for } \mathbf{x} \text{ in } \Omega, \text{ and } t > 0,$$
$$\nabla \cdot \mathbf{u} = 0, \quad \text{for } \mathbf{x} \text{ in } \Omega, \text{ and } t > 0.$$

- * Ω is a bounded open region in \mathbf{R}^2 , with boundary $\partial\Omega$.
- * Initial and boundary conditions must be supplied.
- * \mathbf{F} is the volume force per unit mass, assumed to be 0.

- ⇒ The continuity equation is not given in a time evolution form.
- ⇒ The pressure gradient couples the continuity equation to the momentum equations.

STREAMFUNCTION EQUATIONS FOR UNSTEADY INCOMPRESSIBLE FLOW

$$\frac{\partial \Delta \psi}{\partial t} = \frac{1}{Re} \Delta^2 \psi + \frac{\partial \psi}{\partial x} \Delta \frac{\partial \psi}{\partial y} - \frac{\partial \psi}{\partial y} \Delta \frac{\partial \psi}{\partial x}, \quad \text{for } \mathbf{x} \text{ in } \Omega, \text{ and } t > 0;$$

with

$$u(\mathbf{x}, t) = \frac{\partial \psi}{\partial y}, \quad \text{and} \quad v(\mathbf{x}, t) = -\frac{\partial \psi}{\partial x}, \quad \text{for } \mathbf{x} \text{ in } \Omega, \text{ and } t \geq 0.$$

257

* For Ω in \mathbf{R}^2 .

* Initial and boundary conditions must be supplied.

⇒ Vorticity and pressure do not enter into the streamfunction formulation.

⇒ The velocity solution is always divergence free, and so incompressible.

THE STREAMFUNCTION ALGORITHM FOR UNSTEADY INCOMPRESSIBLE FLOW

258

$$\begin{aligned}
 \text{La}(\tilde{z}^{n+1}) - \frac{\Delta t}{2Re} \text{Bi}(\tilde{z}^{n+1}) \\
 = \text{La}(\tilde{z}^n) + \frac{\Delta t}{2Re} \text{Bi}(\tilde{z}^n) - \frac{3\Delta t}{2} \left[\delta_x \left(\delta_y(\tilde{z}^n) \text{La}(\tilde{z}^n) \right) - \delta_y \left(\delta_x(\tilde{z}^n) \text{La}(\tilde{z}^n) \right) \right] \\
 + \frac{\Delta t}{2} \left[\delta_x \left(\delta_y(\tilde{z}^{n-1}) \text{La}(\tilde{z}^{n-1}) \right) - \delta_y \left(\delta_x(\tilde{z}^{n-1}) \text{La}(\tilde{z}^{n-1}) \right) \right],
 \end{aligned}$$

with

$$u_{i,j}^n = \frac{1}{2\Delta y} (z_{i,j+1}^n - z_{i,j-1}^n), \text{ and } v_{i,j}^n = -\frac{1}{2\Delta x} (z_{i+1,j}^n - z_{i-1,j}^n).$$

* La and Bi are central difference approximations to the Laplace and Biharmonic operators.

* δ_x and δ_y are conventional centered difference operators.

\Rightarrow In \mathbf{R}^2 there is one unknown $\{z_{i,j}^n\}$ per grid cell instead of three.

\Rightarrow The velocity components and streamfunction are all defined at each grid point.

\Rightarrow The discrete solution is exactly incompressible, $\delta_x(u_{i,j}^n) + \delta_y(v_{i,j}^n) = 0$.

\Rightarrow Stability limit is Courant number < 1 .

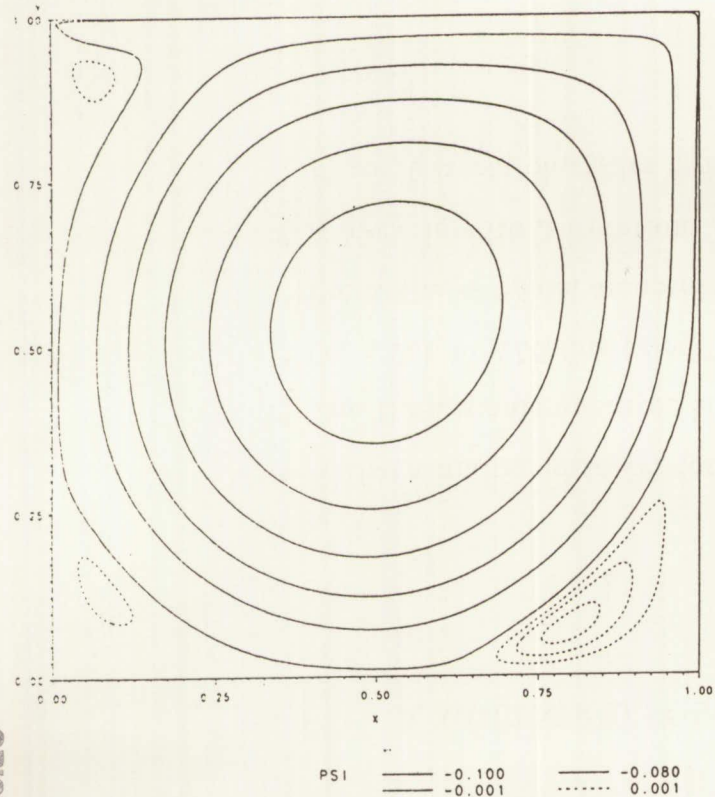
A MULTIGRID SOLVER FOR THE LINEAR IMPLICIT EQUATIONS

$$\text{La}(\tilde{\mathbf{z}}^{n+1}) - \frac{\Delta t}{2Re} \text{Bi}(\tilde{\mathbf{z}}^{n+1}) = \text{Source Term}(\tilde{\mathbf{z}}^n, \tilde{\mathbf{z}}^{n-1})$$

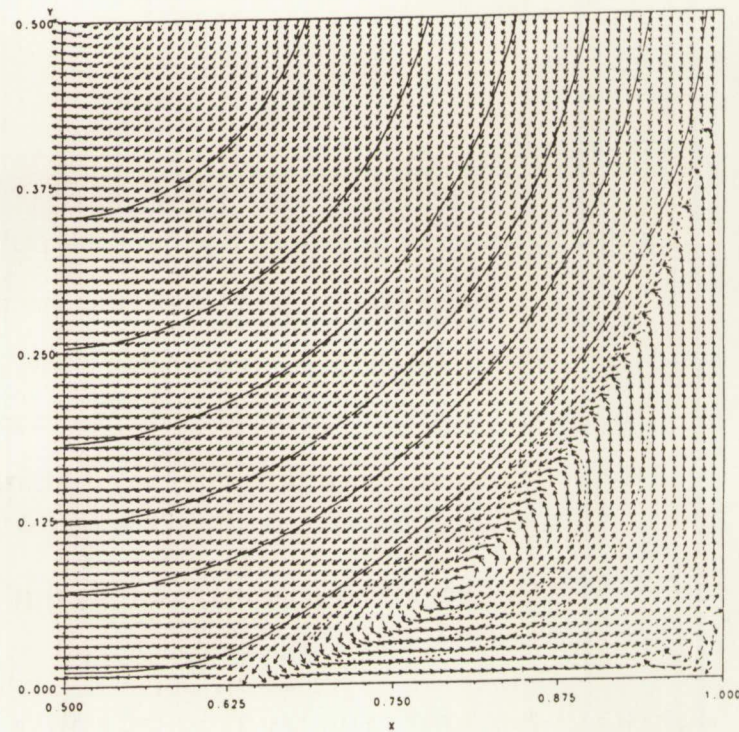
⇒ Use a multigrid solver for the implicit equations at each time step.

- * The Biharmonic operator is factored as two Laplacians.
- * On a 256 by 256 fine grid, 7 grid levels are used in 6.8 MBytes storage.
- * Point Gauss-Seidel smoothing, linear restriction and prolongation.
- * A V-cycle with 3 iterations per grid level while coarsening, none while refining.
- * 10 to 15 iteration cycles reduce residuals to less than 5.0×10^{-11} .

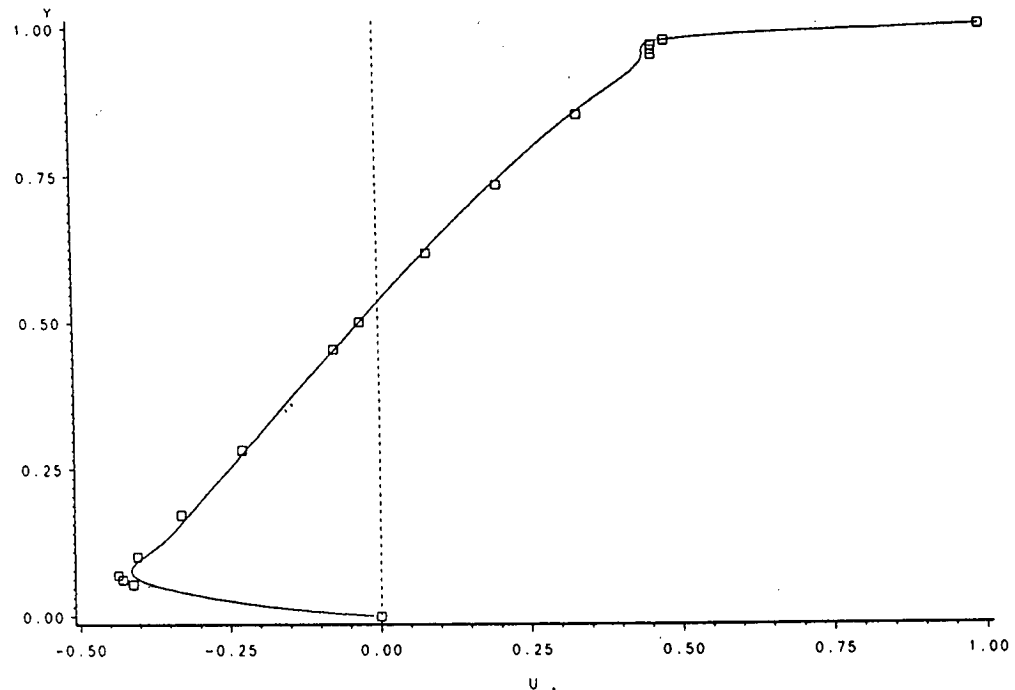
STREAM FUNCTION CONTOURS
Re=5k, 128*128 grid, t=491.80625



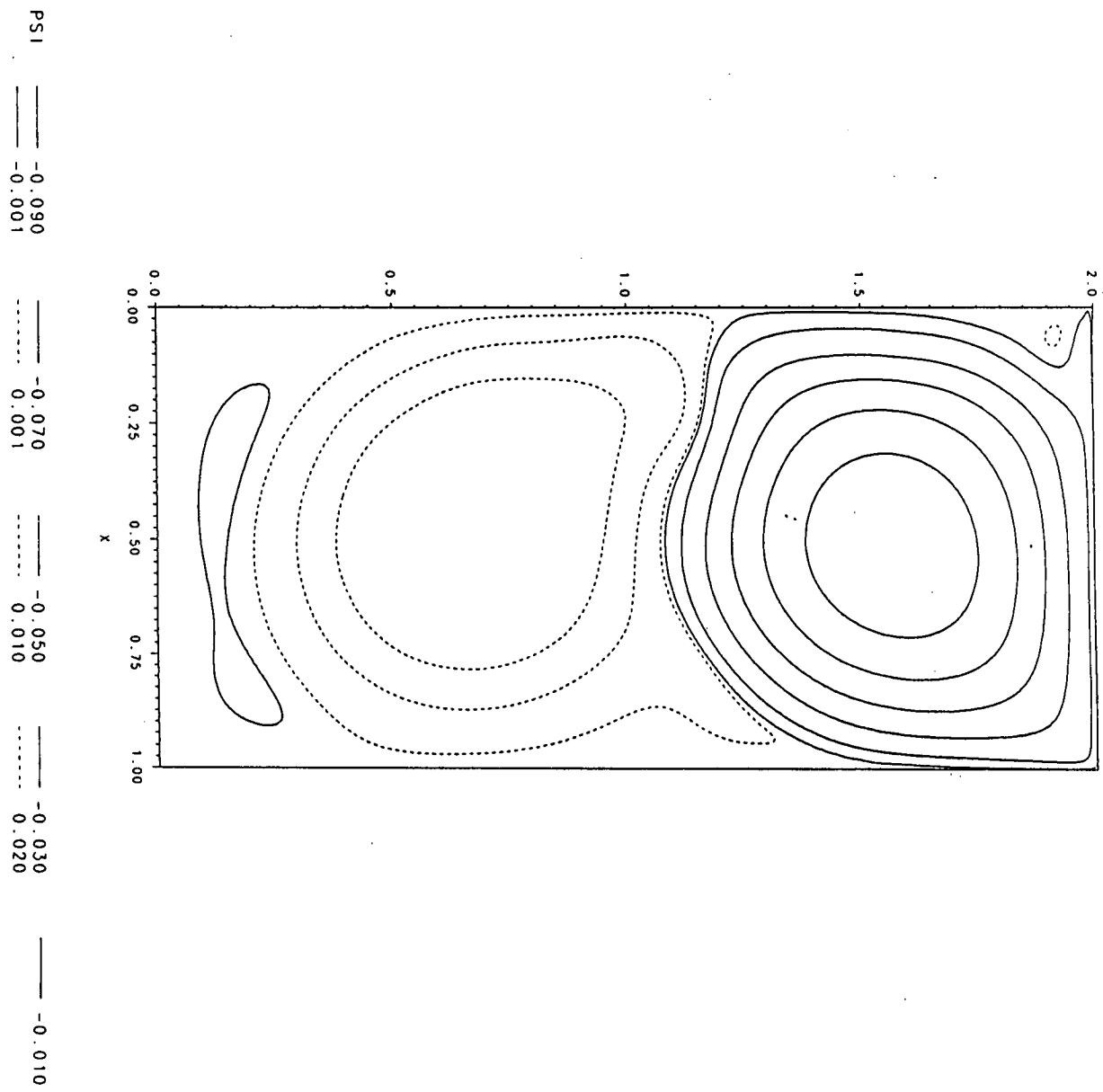
STREAM FUNCTION CONTOURS - NORMALIZED VECTOR PLOTS
Re=5k, 128*128 grid, t=491.80625
0.5 <= x <= 1.0 and 0.0 <= y <= 0.5



u at $x=0.5$ as a function of y
 $Re=5000$, 128 by 128 grid, $t=491.8$

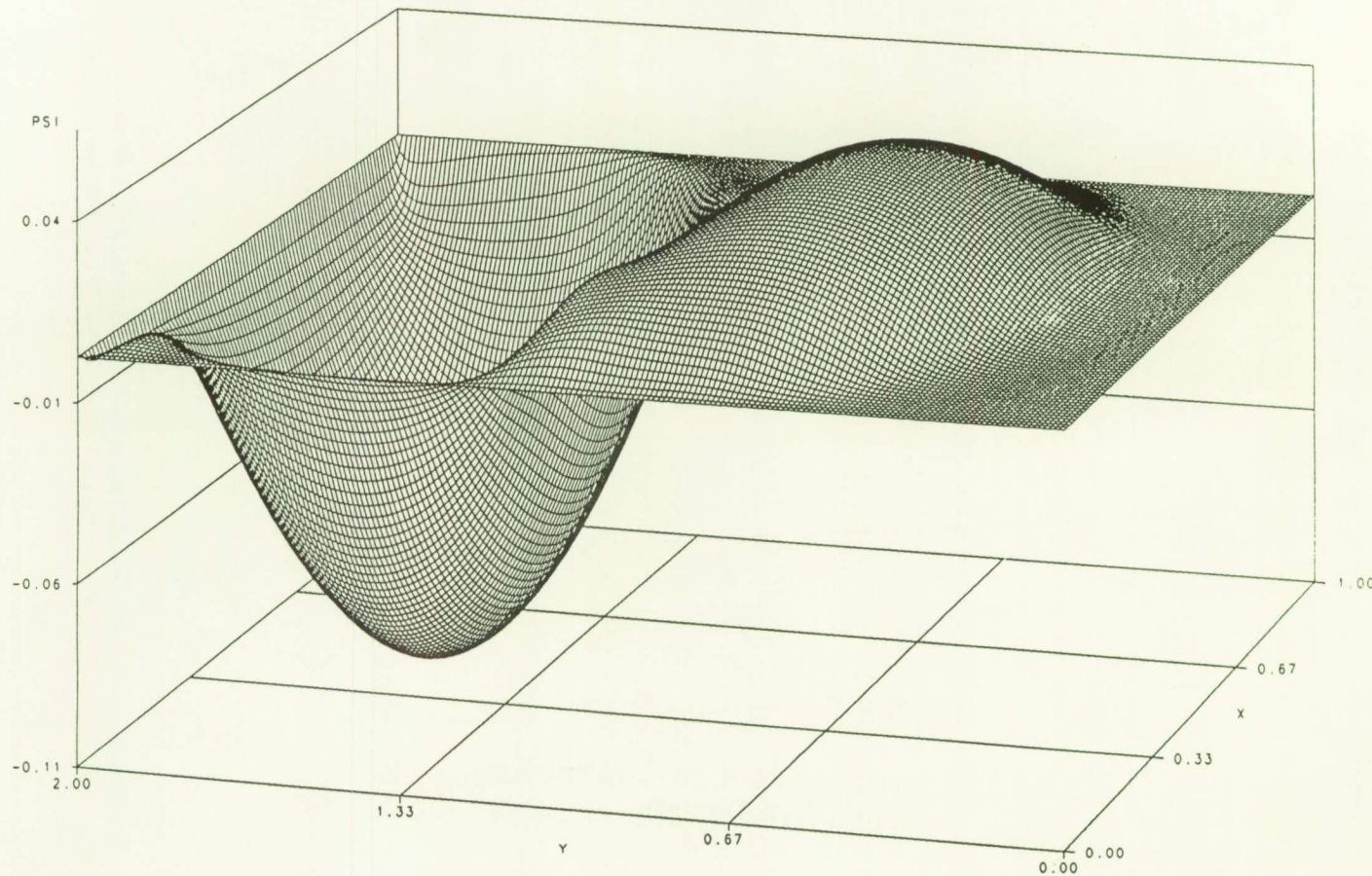


STREAM FUNCTION CONTOURS
 $Re = 5k$, 96×192 grid, $t = 4000$

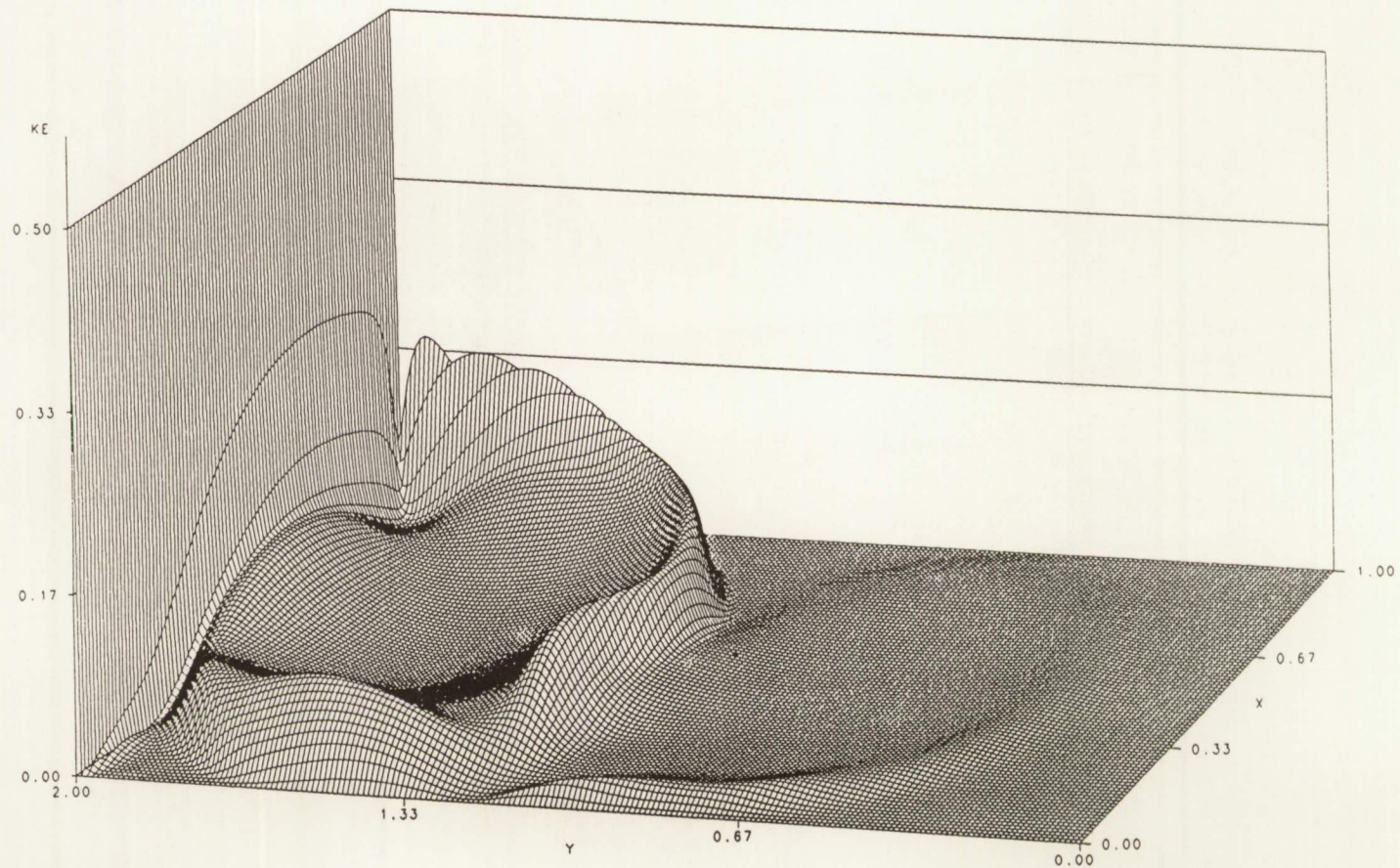


ORIGINAL PAGE IS
OF POOR
QUALITY

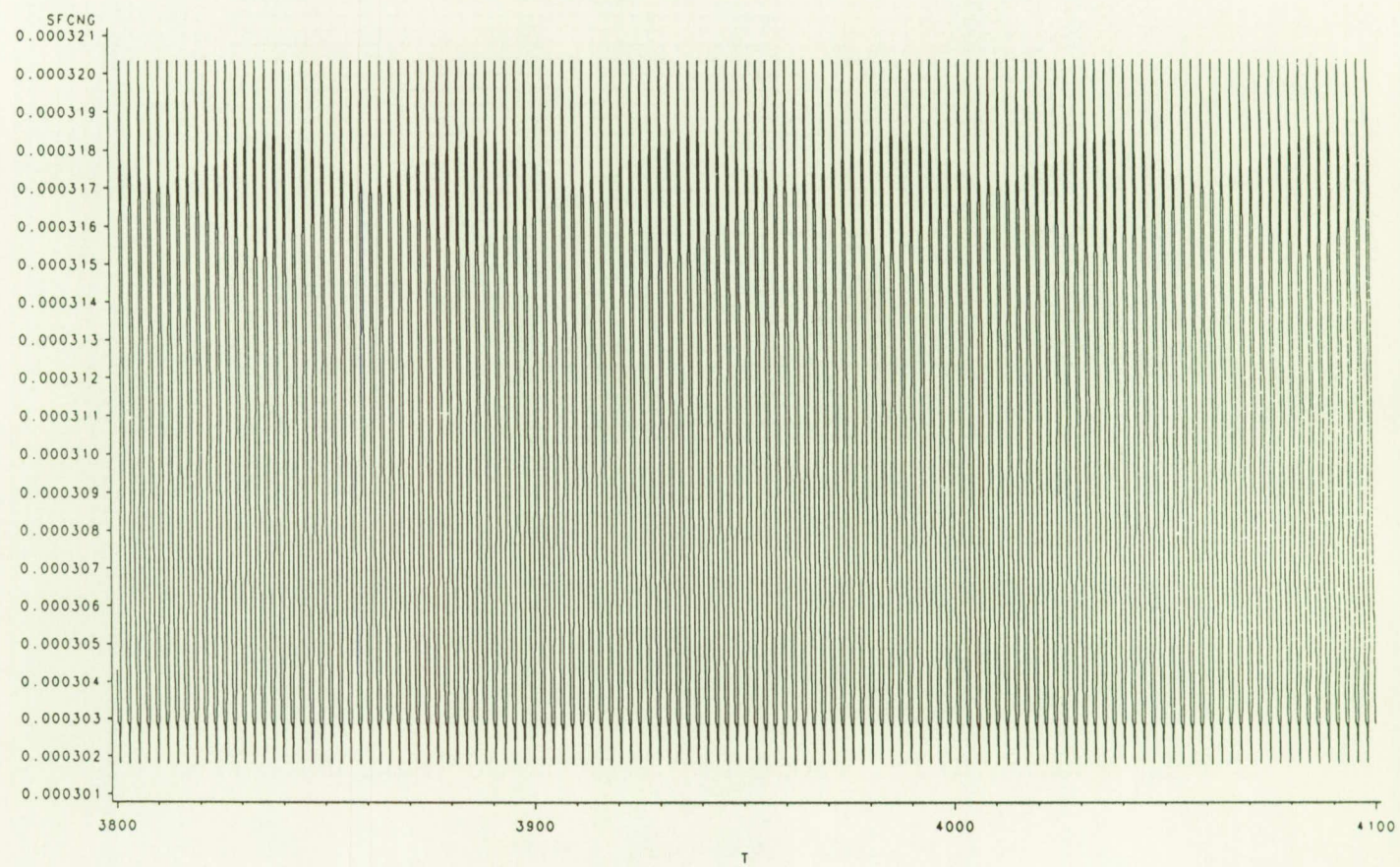
STREAM FUNCTION SURFACE
 $Re=5k$, $96*192$ grid, $t=4000$



KINETIC ENERGY SURFACE
 $Re=5k$, 96*192 grid, $t=4000$



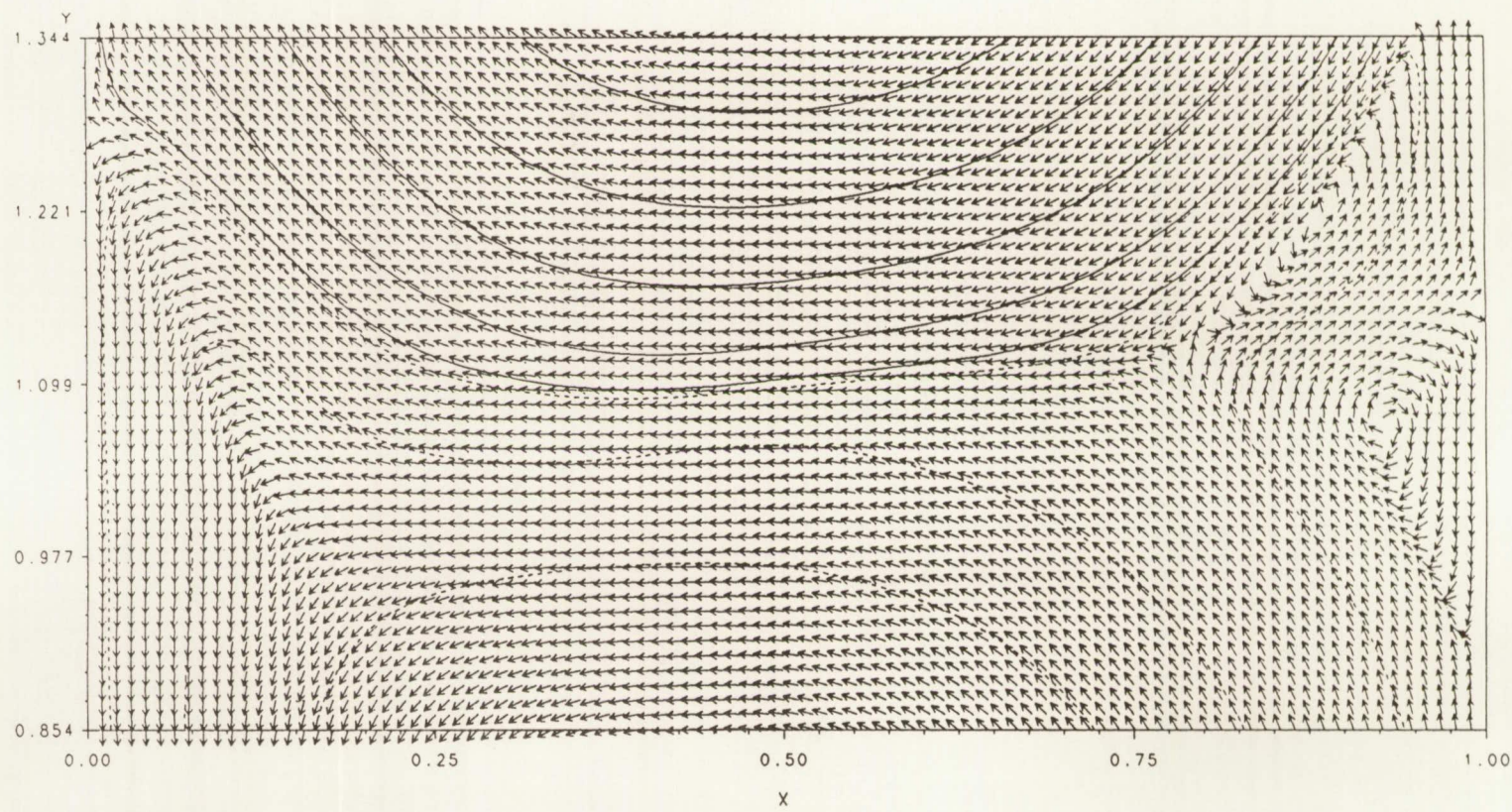
STREAMFUNCTION CHANGE PER TIME STEP
Relative L1 norm for the change
Re=5k, 96*192 grid, 3800<=t<=4100



STREAM FUNCTION CONTOURS – NORMALIZED VECTOR PLOTS

Re=5k, 96*192 grid, t=4100.25

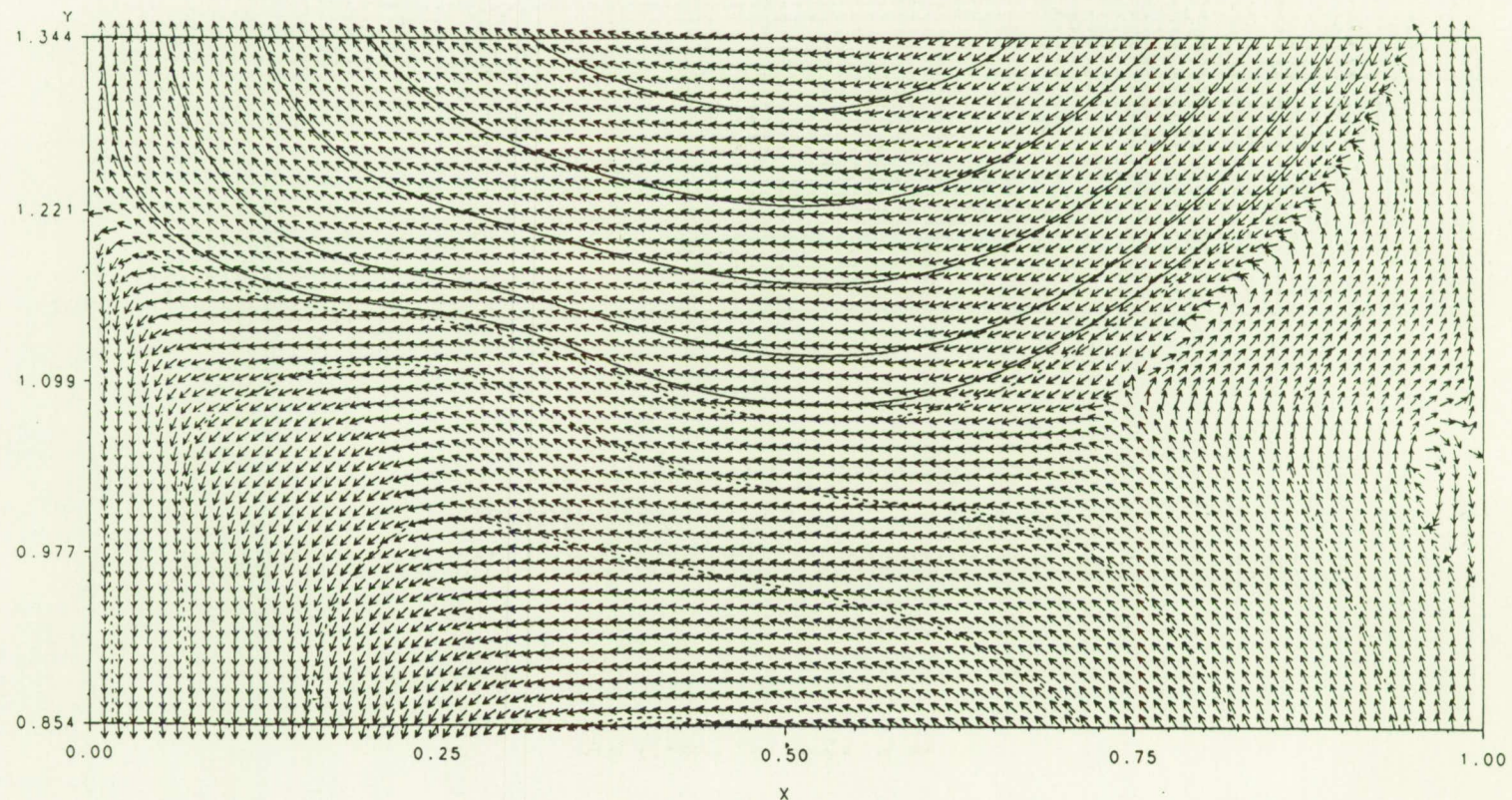
0.0<=x<=1.0 and 0.85<=y<=1.35



STREAM FUNCTION CONTOURS – NORMALIZED VECTOR PLOTS

Re=5k, 96*192 grid, t=4101.25

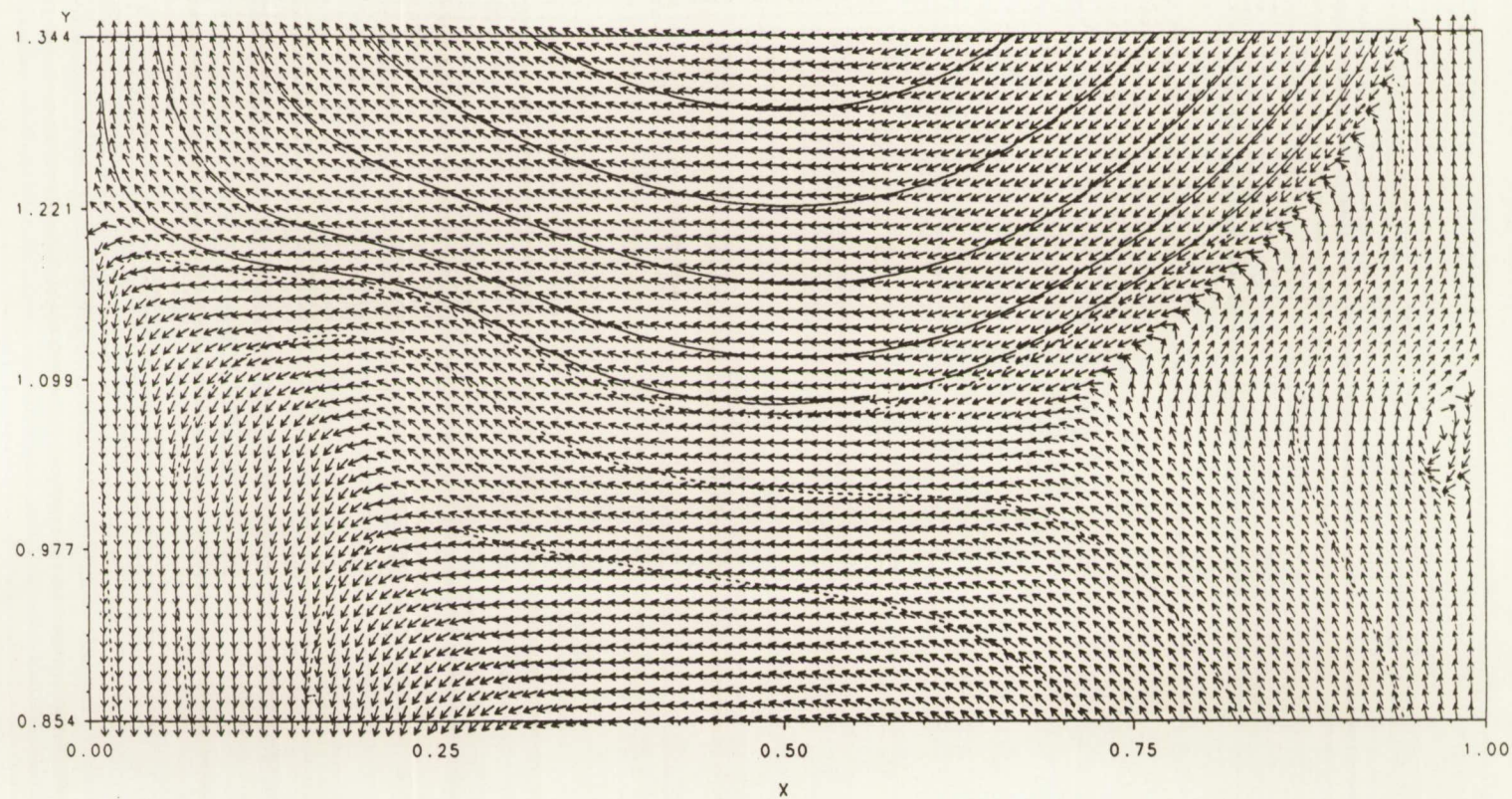
0.0<=x<=1.0 and 0.85<=y<=1.35



STREAM FUNCTION CONTOURS – NORMALIZED VECTOR PLOTS

Re=5k, 96*192 grid, t=4101.50

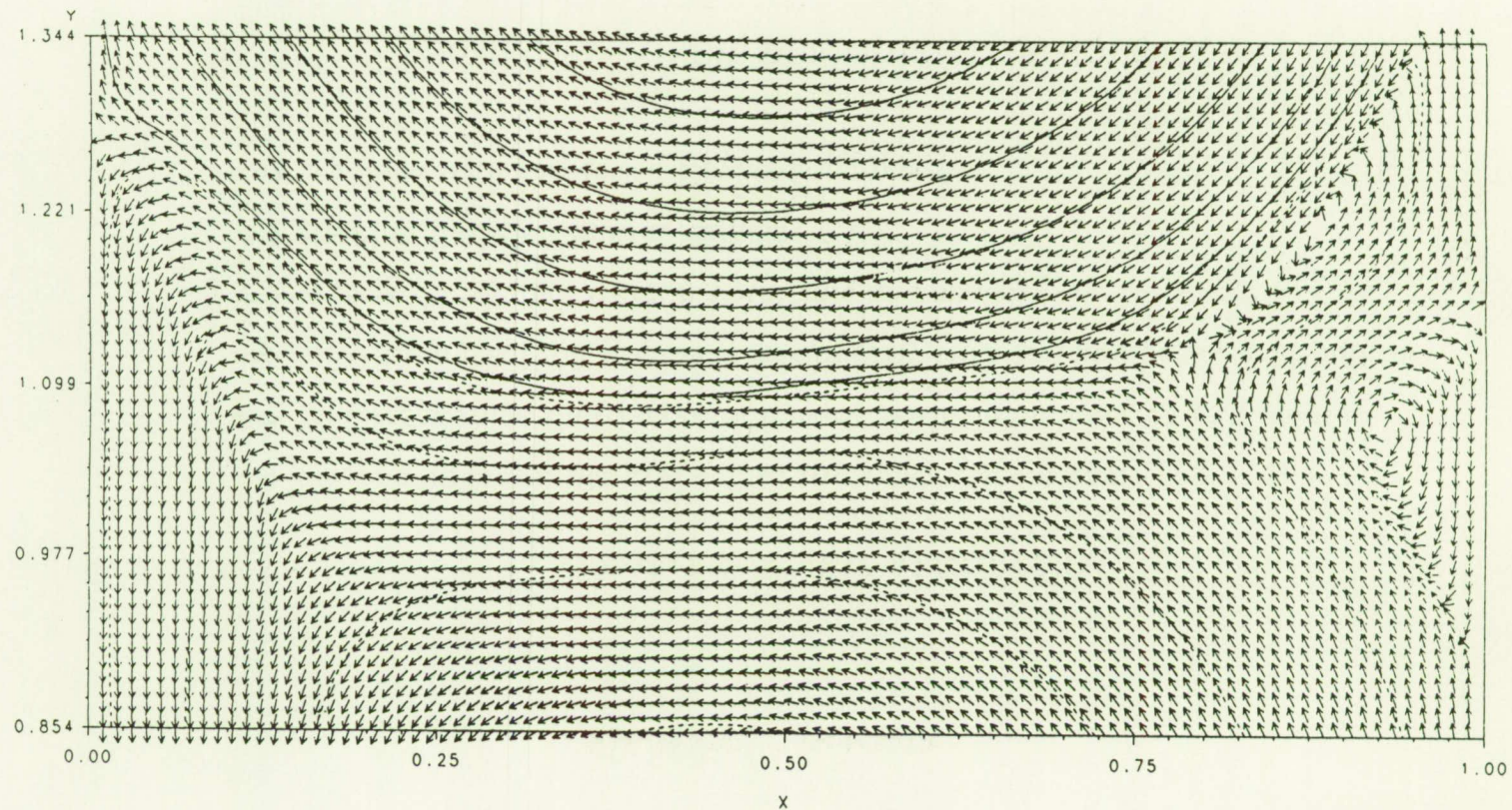
0.0<=x<=1.0 and 0.85<=y<=1.35



STREAM FUNCTION CONTOURS – NORMALIZED VECTOR PLOTS

Re=5k, 96*192 grid, t=4102.50

0.0<=x<=1.0 and 0.85<=y<=1.35



SUMMARY: A NEW ALGORITHM

- ⇒ has one unknown per grid cell in two space dimensions;
- ⇒ requires storage that increases linearly with the number of grid points;
- ⇒ CPU time per time step increases linearly with the number of grid points;
- ⇒ is second order accurate in both time and space;
- ⇒ stability limit is Courant number < 1 ;
- ⇒ is robust with respect to Reynolds number.

270

SUMMARY: A NEW PERIODIC FLOW SOLUTION

- ⇒ is exactly periodic;
- ⇒ does not use a time dependent forcing term;
- ⇒ has no periodic or artificial throughflow boundary conditions;
- ⇒ is probably driven by the wall jet descending from the lid;
- ⇒ is evidence of a Hopf bifurcation;
- ⇒ may lead to period doubling bifurcations and a chaotic flow.

CFD for Applications to Aircraft Aeroelasticity

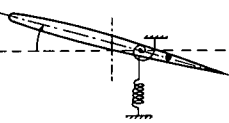
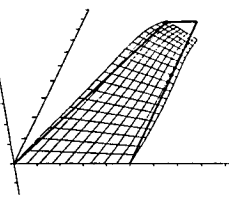
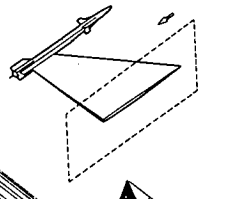
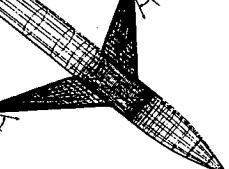
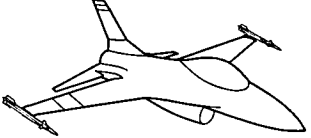
Guru P. Guruswamy
Applied Computational Fluids Branch
NASA Ames Research Center
Moffett Field, California

Abstract

Strong interactions of structures and fluids are common in many engineering environments. Such interactions can give rise to physically important phenomena such as those occurring for aircraft due to aeroelasticity. Aeroelasticity can significantly influence the safe performance of aircraft. At present exact methods are available for making aeroelastic computations when flows are in either the linear subsonic or supersonic range. However, for complex flows containing shock waves, vortices and flow separations, computational methods are still under development. Several phenomena that can be dangerous and limit the performance of an aircraft occur due to the interaction of these complex flows with flexible aircraft components such as wings. For example, aircraft with highly swept wings experience vortex induced aeroelastic oscillations. Correct understanding of these complex aeroelastic phenomena requires direct coupling of fluids and structural equations. This paper provides a summary of the development of such coupled methods and its applications to aeroelasticity since about 1978 to present. A part of the paper discusses the successful use of the transonic small perturbation theory(TSP) coupled with structures. This served as a major stepping stone for the current stage of aeroelasticity using CFD. The need for the use of more exact Euler/Navier-Stokes(ENS) equations for aeroelastic problems is explained. The current development of unsteady aerodynamic and aeroelastic procedures based on the ENS equations are discussed. The paper illustrates aeroelastic results computed using both TSP and ENS equations.

HISTORY OF CFD APPLICATIONS TO AEROELASTICITY

BASED ON UNSTEADY TIME ACCURATE METHODS

	TSP	FP	EULER	NAVIER STOKES
	1978	?	1986	1988
	1982	1984	1988	?
	1986	?	?	?
	1988	?	?	?
	?	?	?	?

MAJOR ISSUES FOR ADVANCED CFD METHODS

- Computational speed
 - Aeroelastic computations require two orders more computational time than steady computations
- Time accuracy
 - An essential requirement for accurate aeroelastic computations
- Grid and its unsteady movement
 - Time accuracy between zones
- Validity of turbulence models for unsteady and separated flows
- Robustness of solution methods
 - Other issues like artificial viscosity, upwinding, etc.

APPROACH FOR COMPUTER SIMULATION

- GOVERNING EQUATIONS

- Aerodynamics : 3-D Euler/Navier-Stokes equations (ENS)
and transonic small perturbation equation (TSP)
- Aeroelastic : Modal equations of motion

- ALGORITHM

- Aerodynamics : time accurate finite difference methods
based on alternate direction implicit schemes
- Aeroelastic : Simultaneous time integration method

- Note

- ENS computations are made using aeroelastic adaptive dynamic grids
- For TSP computations, aerodynamic and structural properties of the fuselage tip stores, and control surfaces are modeled

COUPLED AEROELASTIC EQUATIONS OF MOTION

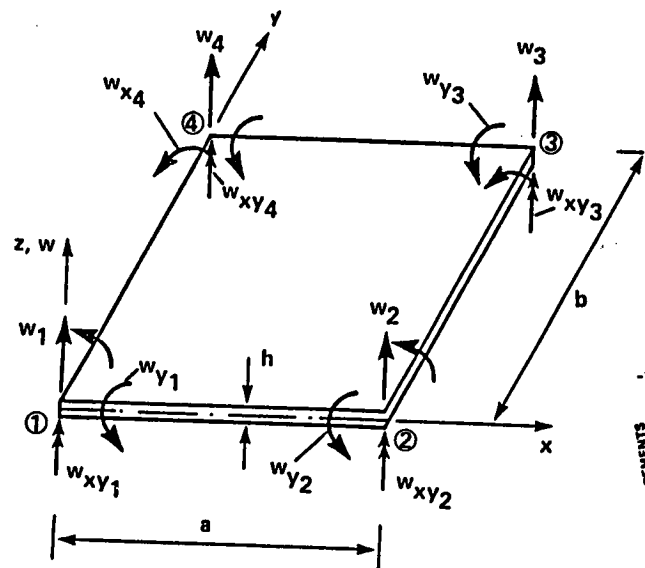
- Deformed shape is a sum of modal coordinates
- Equations are solved by simultaneous integration technique
- Equations of Motion
 - Assuming displacement vector $\{d\} = [\phi]\{q\}$ where $[\phi]$ is the modal matrix and $\{q\}$ is the generalized displacement vector, the aeroelastic equation of motion is

$$[M]\{\ddot{q}\} + [G]\{\dot{q}\} + [K]\{q\} = \{F\}$$

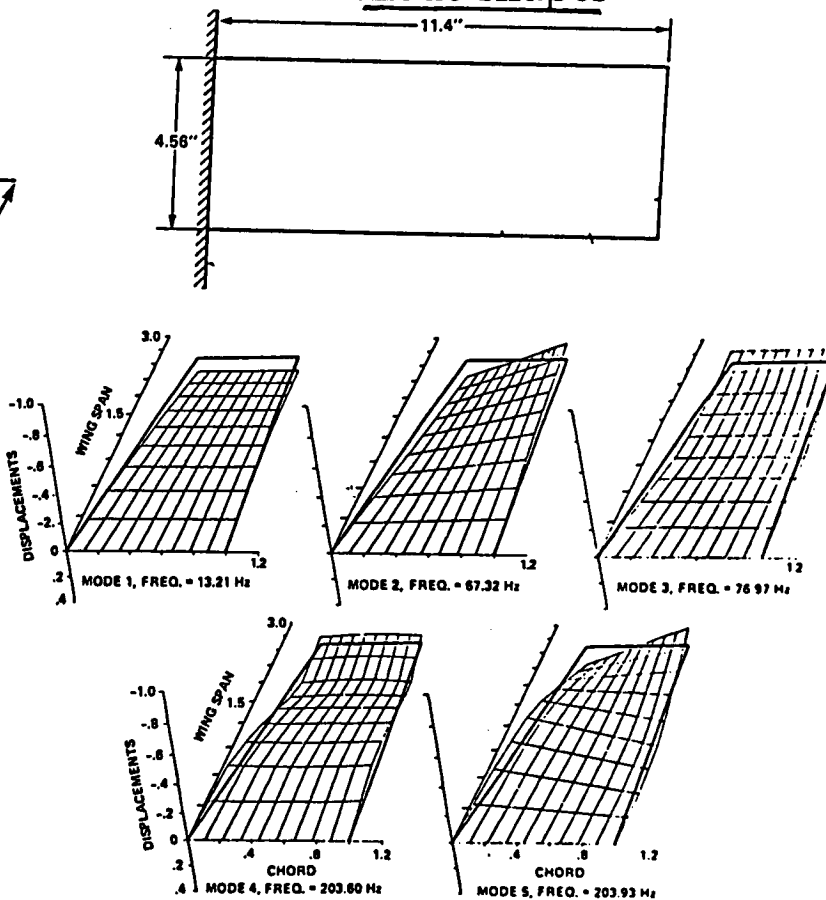
$[M]$, $[G]$, and $[K]$ mass, damping and stiffness matrices
 $\{F\} = (\frac{1}{2})\rho U_\infty^2 [\phi]^T [A]\{\Delta C_p\}$ is the aerodynamic force vector
 $[A]$ is the diagonal area matrix of the aerodynamic control points.

MODES OF A RECTANGULAR WING

16 d.o.f finite element



mode shapes



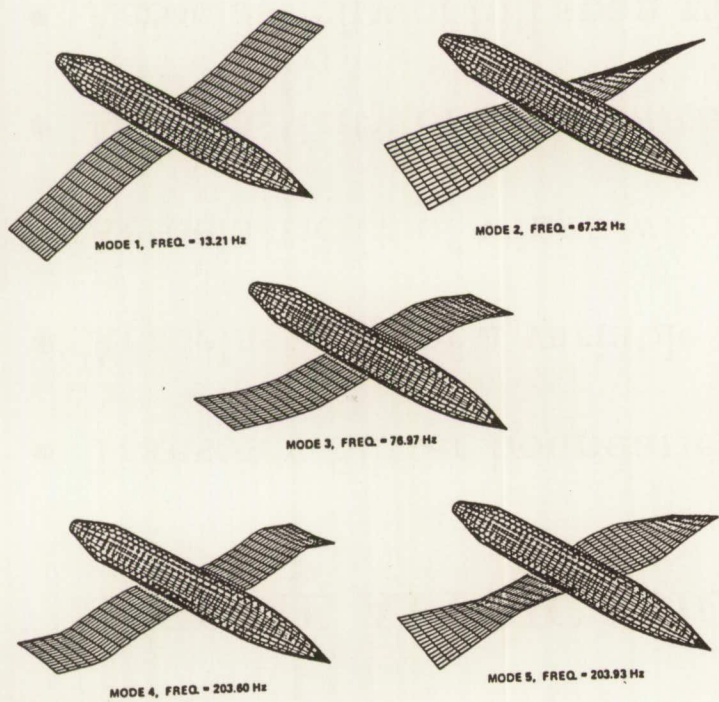
SOME APPLICATIONS OF TSP THEORY

- Transonic flutter boundaries of transport and fighter wings
- Aeroelasticity of a variable sweep wing (B-1 wing)
- Aeroelasticity of wings with tip stores
- Aeroelasticity of wings with active control surfaces
- Aeroelasticity of full span wing-body configurations (Symmetric and Asymmetric modes)

TYPICAL RESULTS FROM TSP CODE ATRAN3S

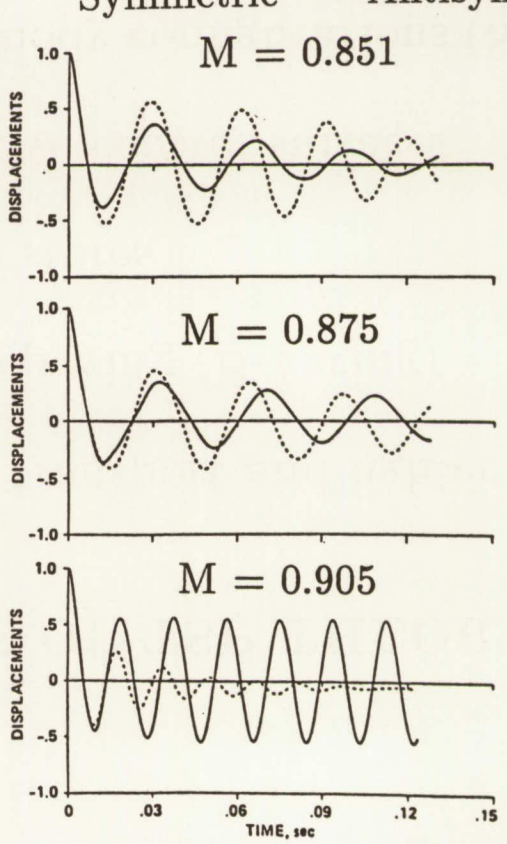
Full-Span Wing-Body Aeroelasticity

ANTISYMMETRIC MODES



RESPONSES

Symmetric - - - Antisymmetric



DEVELOPMENT OF ENSAERO

- PURPOSE

- To develop an aeroelastic code to solve Euler/Navier Stokes equations coupled with structural equations of motion for full aircraft

- CHARACTERISTICS

- Solves either Euler or Navier Stokes equations
 - Models structure by either modal or finite element equations
 - Includes aeroelastic configuration adaptive grid scheme
 - Modular to adopt different finite difference schemes
 - Transportable to different computer configurations

- ENSAERO-version 2.0

- Solves Euler/Navier Stokes equations with modal structural equations of motion for wings

CONFIGURATION ADAPTIVE DYNAMIC GRID

- Grids are generated by an algebraic method
- Grids conform to the wing surface defined by displacements $\{d\}$
- Grids are generated every time-step of integration
- Time metrics are computed every time step

280

$$\xi_t = -x_\tau \xi_x - y_\tau \xi_y - z_\tau \xi_z$$

$$\eta_t = -x_\tau \eta_x - y_\tau \eta_y - z_\tau \eta_z$$

$$\zeta_t = -x_\tau \zeta_x - y_\tau \zeta_y - z_\tau \zeta_z$$

$$J^{-1} = x_\xi y_\eta z_\zeta + x_\zeta y_\xi z_\eta + x_\eta y_\zeta z_\xi - x_\xi y_\zeta z_\eta - x_\eta y_\xi z_\zeta - x_\zeta y_\eta z_\xi$$

- Note - Present technique can be used for both structured and unstructured grids

VORTEX DOMINATED UNSTEADY PRESSURES

Navier-Stokes Computations

Rectangular Wing in ramp motion , AR = 4.0, NACA0015

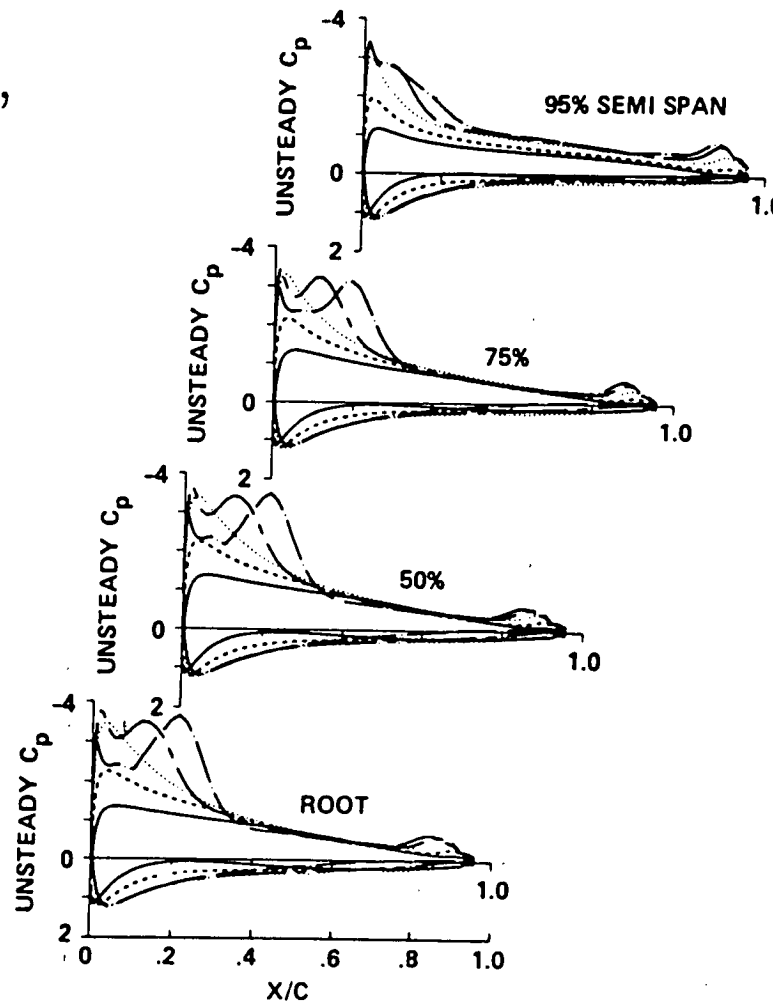
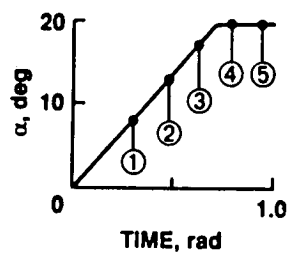
GRID 151x20x40

$M_\infty = 0.50$, $A = 0.30$,

$R_e = 60000.0$

$\tau(\alpha)$

- 0.31, (8.8°)
- - - 0.47, (13.5°)
- · · 0.63, (18.1°)
- - - 0.79, (20.0°)
- · - 0.94, (20.0°)



1

COMPARISON OF UNSTEADY PRESSURES BETWEEN RIGID AND FLEXIBLE WINGS (Navier-Stokes Computations)

Rectangular Wing in ramp motion , AR = 4.0, NACA0015

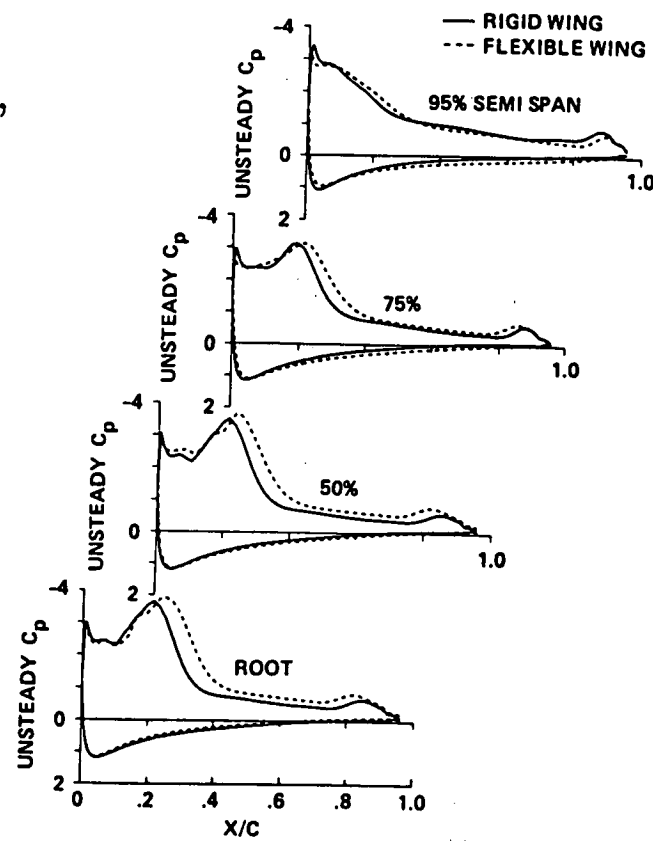
GRID 151x20x40

$M_\infty = 0.50$, $A = 0.30$,

$R_e = 60000.0$

$\alpha = 20^\circ$, $\tau = 0.94$

— Rigid Wing
- - - Flexible Wing



CONCLUDING REMARKS

- During last decade TSP applications have progressed from airfoils to almost full aircraft
 - Computational speed has increased by a factor of about 100
 - Robust codes such as ATRAN3S are now available
 - Applied for advanced applications such as active controls
- Euler/Navier Stokes (ENS) equations are currently being used for aeroelastic problems of wings

FUTURE DIRECTIONS

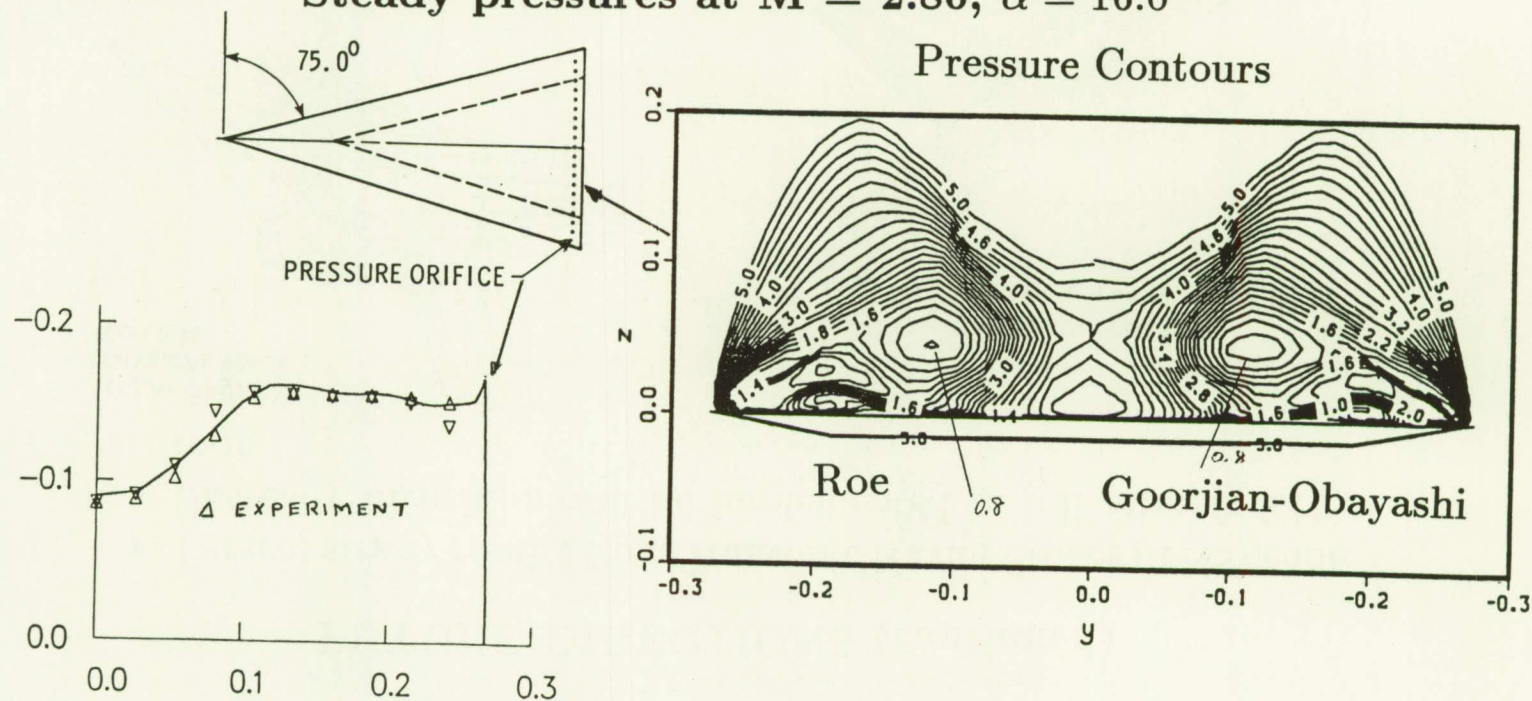
- Improve time accurate Euler/Navier Stokes(ENS) algorithms
- Extend unsteady ENS algorithms for full aircraft configurations
- Couple advanced CFD methods with advanced CSM methods
- Conduct research in unsteady aerodynamics and aeroelasticity of full aircraft at high angles of attack
- Maintain TSP codes for immediate industrial use

FUTURE DIRECTIONS (continued)

Algorithm Development

- Typical results from a new upwind scheme that will be implemented in ENSAERO

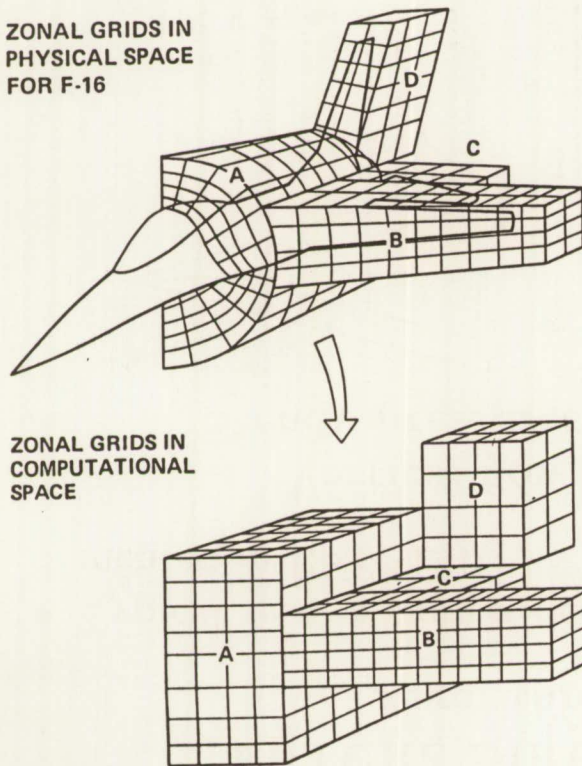
Vortical flow on a 75.0° delta wing
Steady pressures at $M = 2.80$, $\alpha = 16.0^\circ$



FUTURE DIRECTIONS (continued)

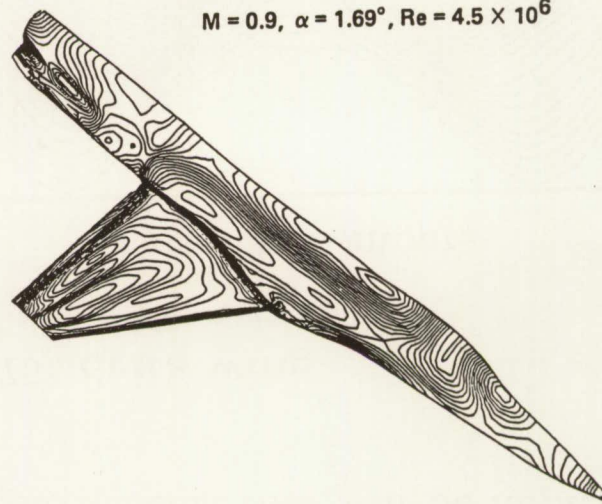
- Typical steady results from Transonic Navier Stokes (TNS) code
- Unsteady algorithm will be implemented in full aircraft TNS code

ZONAL GRIDS IN PHYSICAL SPACE FOR F-16



MACH CONTOURS

$M = 0.9, \alpha = 1.69^\circ, Re = 4.5 \times 10^6$





N91-10856

APPLICATION OF UNSTRUCTURED GRID METHODS TO STEADY AND UNSTEADY AERODYNAMIC PROBLEMS

John T. Batina
Unsteady Aerodynamics Branch
NASA Langley Research Center
Hampton, Virginia 23665-5225

Abstract

The presentation summarizes recent work in the Unsteady Aerodynamics Branch at NASA Langley Research Center on developing unstructured grid methods for application to steady and unsteady aerodynamic problems. The CAP-TSD transonic aeroelasticity code, which is based on the transonic small-disturbance (TSD) theory, is described first to provide background information to put the present work in context. The CAP-TSD code is the most fully-developed code for aeroelastic analysis of complete aircraft configurations at the TSD equation level and has been widely accepted throughout the U.S. aerospace industry. Currently, aeroelastic analysis capabilities are being developed at NASA Langley for the Euler and Navier-Stokes equations based on both structured and unstructured grids. The purpose of the presentation is to describe the development of unstructured grid methods which have several advantages when compared to methods which make use of structured grids. Unstructured grids, for example, easily allow the treatment of complex geometries, allow for general mesh movement for realistic motions and structural deformations of complete aircraft configurations which is important for aeroelastic analysis, and enable adaptive mesh refinement to more accurately resolve the physics of the flow. The presentation is therefore organized in three parts including: (1) steady Euler calculations for a supersonic fighter configuration to demonstrate the complex geometry capability; (2) unsteady Euler calculations for the supersonic fighter undergoing harmonic oscillations in a complete-vehicle bending mode to demonstrate the general mesh movement capability; and (3) vortex-dominated conical-flow calculations for highly-swept delta wings to demonstrate the adaptive mesh refinement capability. The basic solution algorithm is a multi-stage Runge-Kutta time-stepping scheme with a finite-volume spatial discretization based on an unstructured grid of triangles in 2D or tetrahedra in 3D. The moving mesh capability is a general procedure which models each edge of each triangle (2D) or tetrahedra (3D) with a spring. The resulting static equilibrium equations which result from a summation of forces are then used to move the mesh to allow it to continuously conform to the instantaneous position or shape of the aircraft. The adaptive mesh refinement procedure enriches the unstructured mesh locally to more accurately resolve the vortical flow features. These capabilities are described in detail along with representative results which demonstrate several advantages of unstructured grid methods. The presentation further discusses the applicability of the unstructured grid methodology to steady and unsteady aerodynamic problems and suggests directions for future work.

PRESENTATION OVERVIEW

- **Background on CAP-TSD transonic aeroelasticity code**
- **Unstructured grid methods**
 - **steady and unsteady Euler calculations for a supersonic fighter configuration**
 - **vortex-dominated conical-flow calculations including adaptive mesh refinement**
- **Concluding remarks**

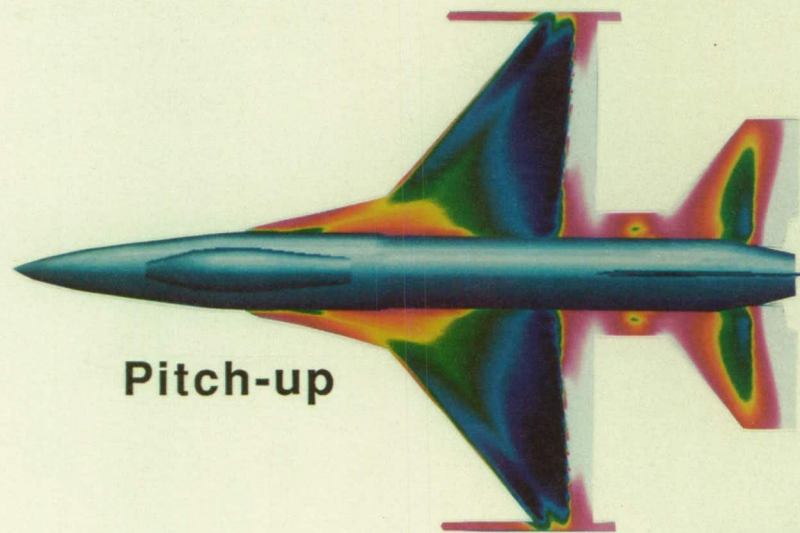
289

CAP-TSD: COMPUTATIONAL AEROELASTICITY PROGRAM - TRANSONIC SMALL DISTURBANCE

- Based on time-accurate approximate factorization algorithm
- Complete aircraft modeling involving arbitrary combinations of lifting surfaces and bodies
- Static and dynamic aeroelastic analysis
- Aircraft trim capability
- Longitudinal short-period response
- Entropy and vorticity effects included to treat cases with strong shock waves

CAP-TSD INSTANTANEOUS PRESSURES ON F-16C AIRCRAFT DUE TO RIGID PITCHING MOTION

- $M_\infty = 0.9$, $\alpha_0 = 2.38^\circ$, $k = 0.1$



ADVANTAGES OF UNSTRUCTURED GRID METHODOLOGY

- Allows the treatment of complex geometries
- Allows general mesh movement for realistic motions and structural deformations of complete aircraft
- Enables adaptive mesh refinement to more accurately resolve the physics of the flow

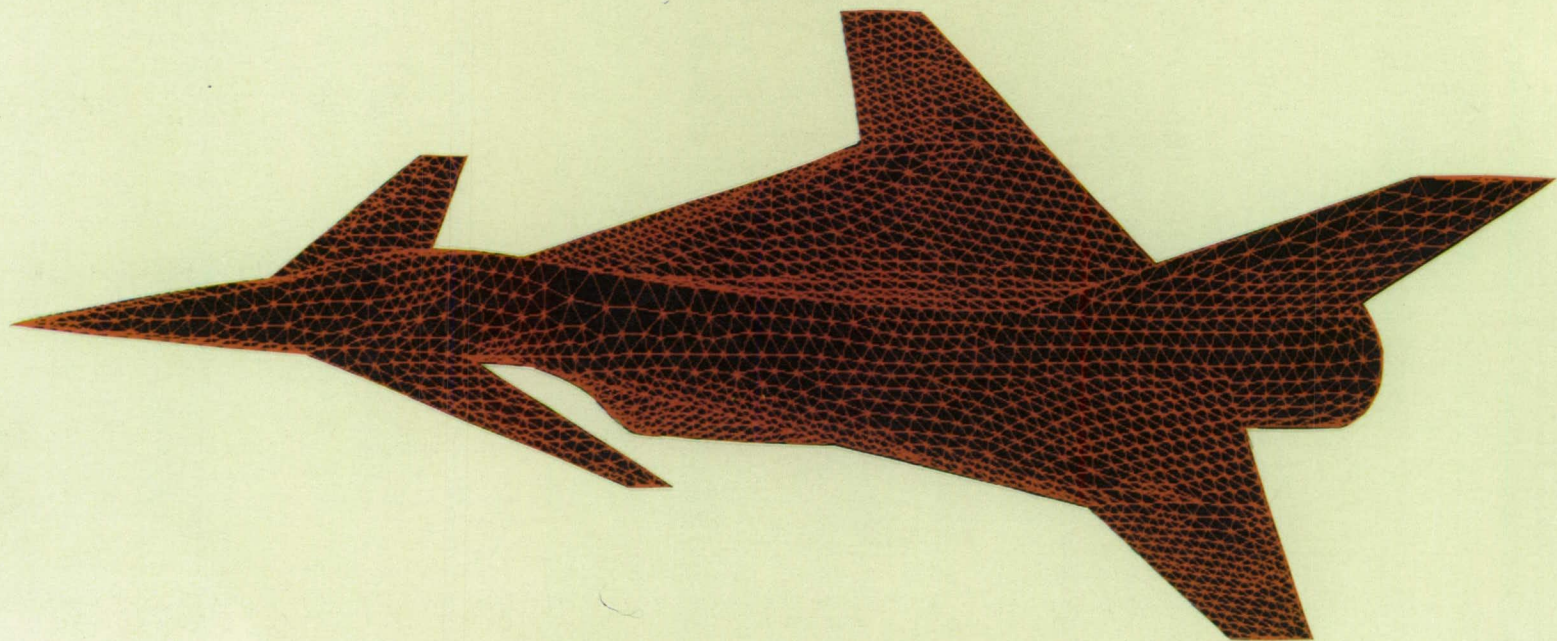
DESCRIPTION OF EULER SOLUTION ALGORITHMS

294

- Four-stage Runge-Kutta time-stepping scheme
- Finite-volume spatial discretization on unstructured grids of triangles in 2D or tetrahedra in 3D
- Adaptive blend of harmonic and biharmonic operators for artificial dissipation
- Enthalpy damping, local time-stepping, and implicit residual smoothing to accelerate convergence to steady state
- Dynamic mesh algorithm employed for unsteady applications

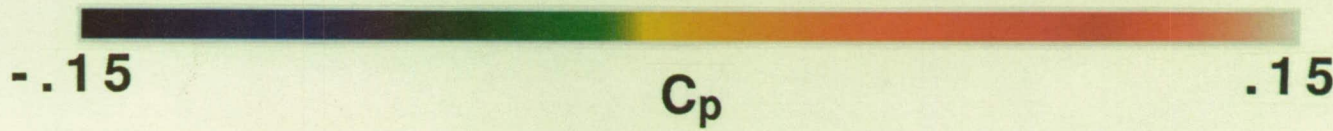
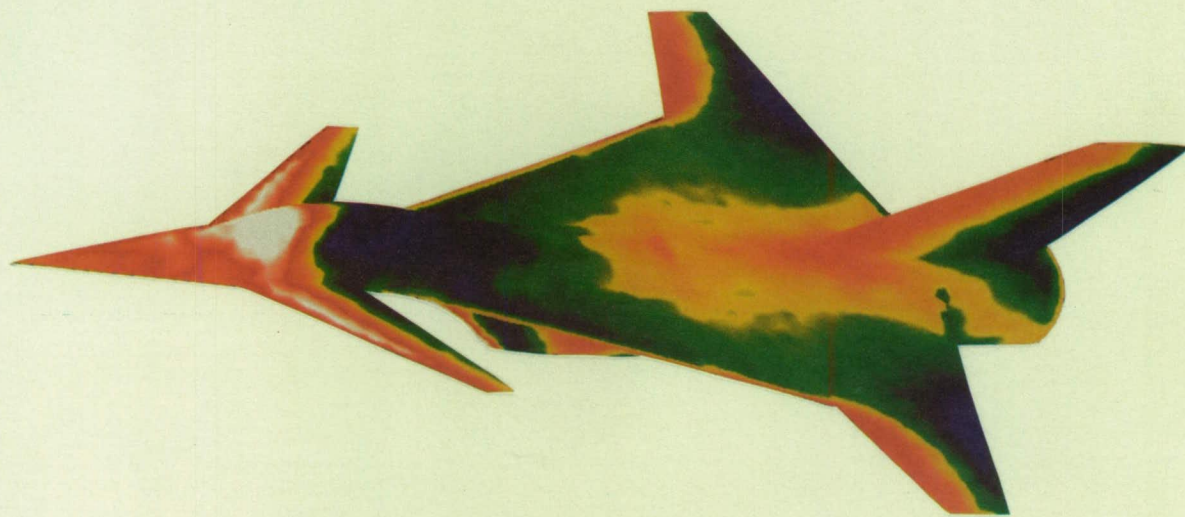
SURFACE TRIANGULATION FOR Langley FIGHTER

- Total grid has 13,832 nodes and 70,125 tetrahedra



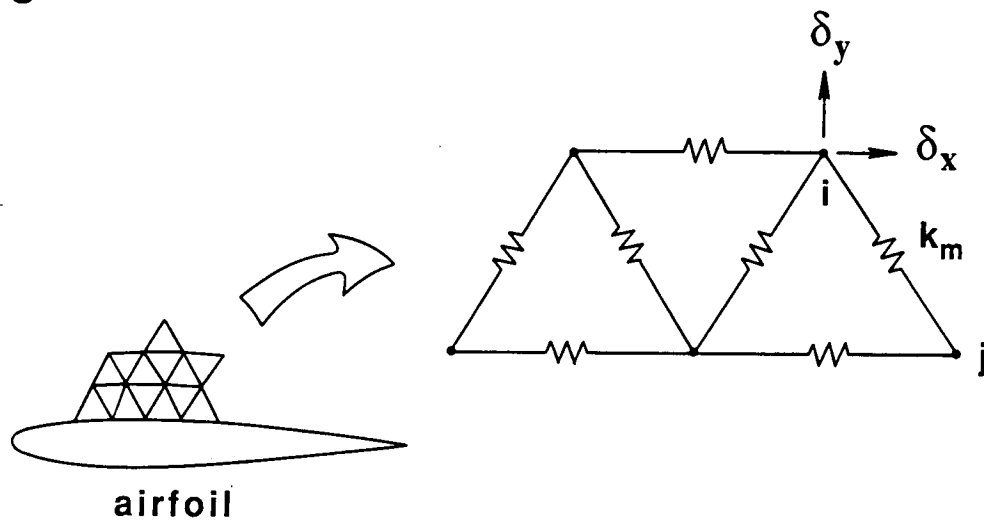
STEADY PRESSURE CONTOURS ON Langley FIGHTER

- $M_\infty = 2.0$ and $\alpha_0 = 0^\circ$



OVERVIEW OF DYNAMIC MESH ALGORITHM

- Each edge of each triangle is modeled using a spring
- Spring stiffness is inversely proportional to the length of the edge



- Points on outer boundary of grid are fixed
- Locations of points on inner boundary of grid are specified

OVERVIEW OF DYNAMIC MESH ALGORITHM

- Displacement of interior nodes determined by solving the static equilibrium equations
- Equations solved using predictor-corrector procedure

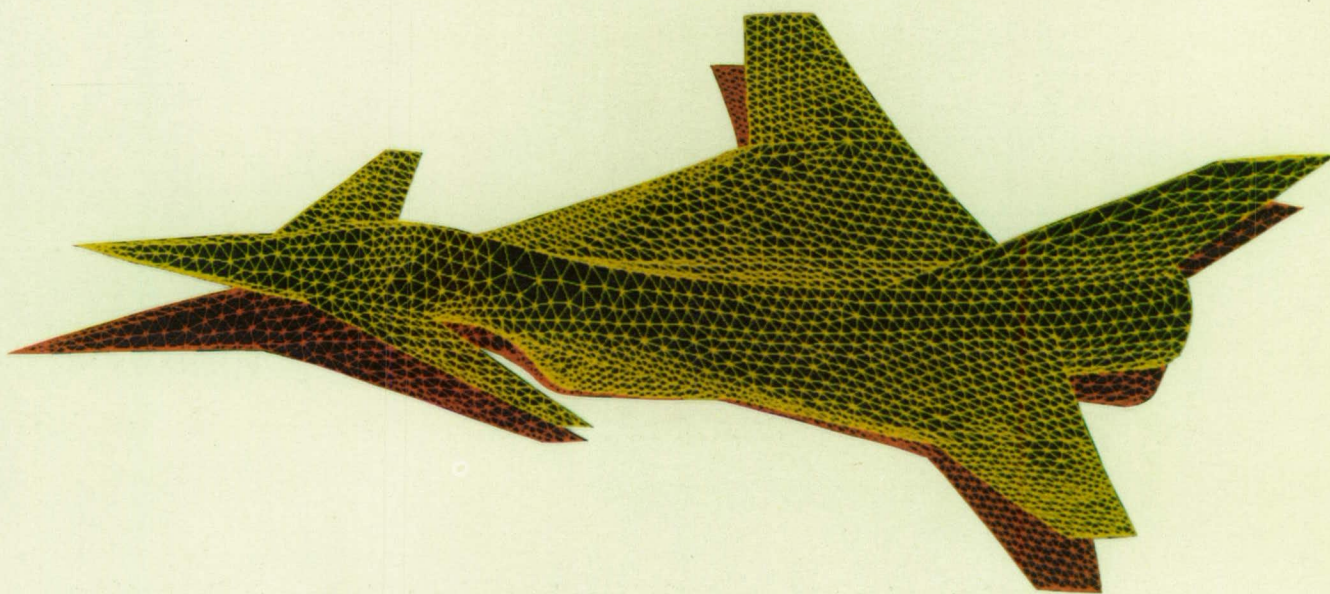
- new locations of nodes predicted by extrapolation

$$\tilde{\delta}_{x_i} = 2 \delta_{x_i}^n - \delta_{x_i}^{n-1} \quad \tilde{\delta}_{y_i} = 2 \delta_{y_i}^n - \delta_{y_i}^{n-1} \quad \tilde{\delta}_{z_i} = 2 \delta_{z_i}^n - \delta_{z_i}^{n-1}$$

- locations corrected by several Jacobi iterations

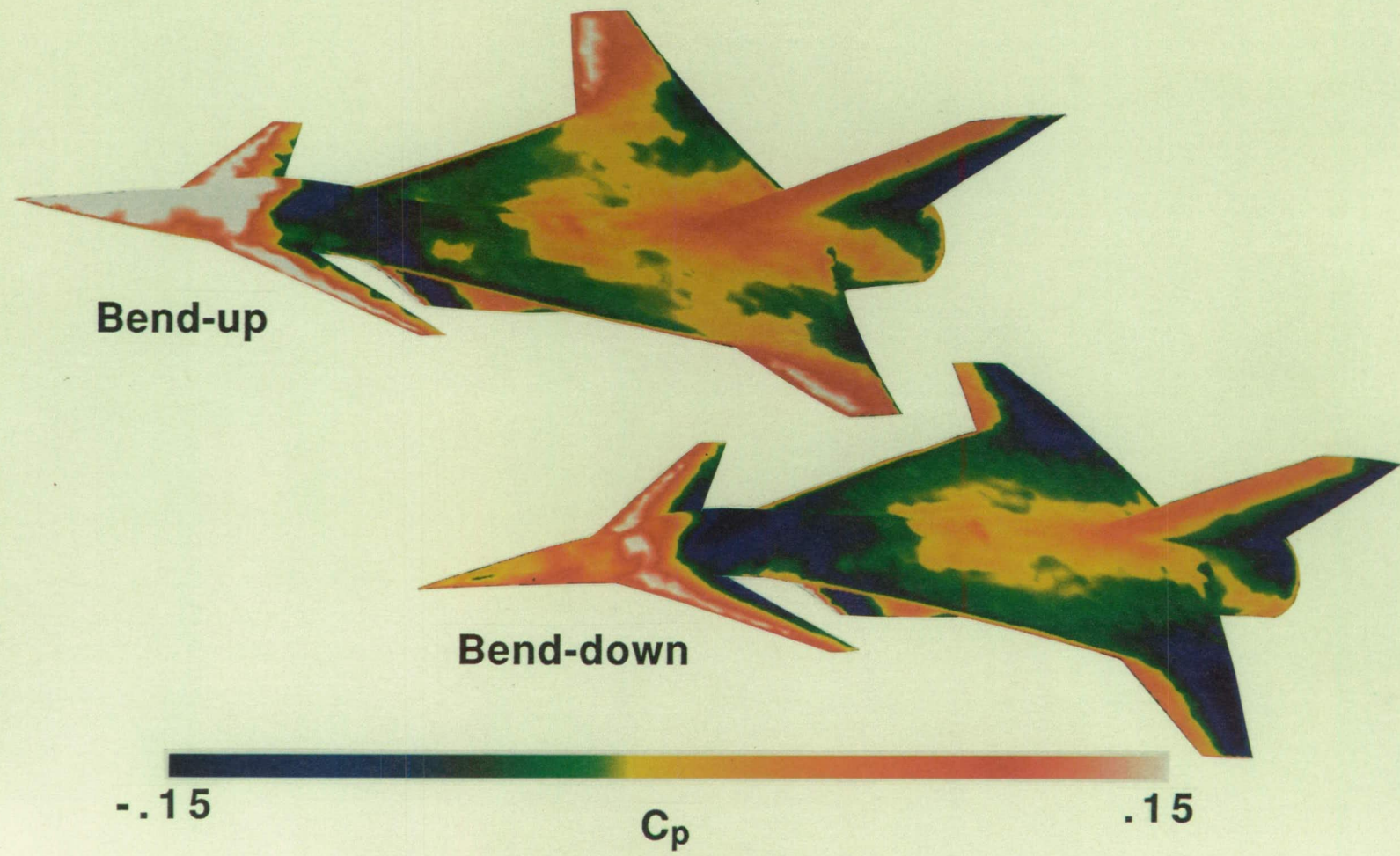
$$\delta_{x_i}^{n+1} = \frac{\sum k_m \tilde{\delta}_{x_m}}{\sum k_m} \quad \delta_{y_i}^{n+1} = \frac{\sum k_m \tilde{\delta}_{y_m}}{\sum k_m} \quad \delta_{z_i}^{n+1} = \frac{\sum k_m \tilde{\delta}_{z_m}}{\sum k_m}$$

ASSUMED BENDING MODE FOR Langley FIGHTER



INSTANTANEOUS PRESSURE CONTOURS ON Langley FIGHTER

- $M_\infty = 2.0$, $\alpha_0 = 0^\circ$, and $k = 0.1$

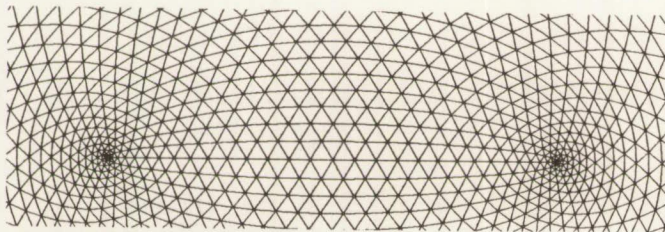


DESCRIPTION OF CONICAL EULER/NAVIER-STOKES ALGORITHM

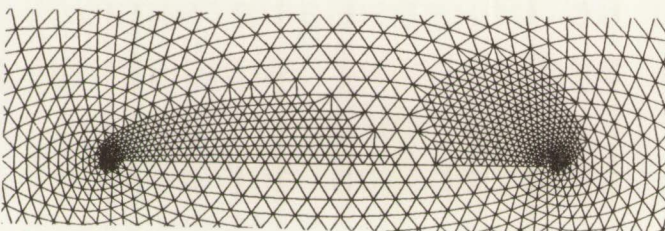
- Solves the conical Euler/Navier-Stokes equations
- Multi-stage Runge-Kutta time-stepping with finite-volume spatial discretization on unstructured grid of triangles
- Scheme is a zonal method
- Mesh enrichment capability enables automatic refinement in regions of high flow gradients
- Presently limited to laminar flow

EFFECTS OF MESH ENRICHMENT ON CONICAL EULER VORTICAL FLOW SOLUTION

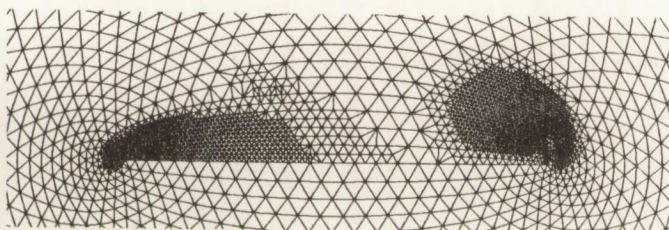
- 75° swept flat plate delta wing at $M_\infty = 1.7$, $\alpha = 12^\circ$, $\beta = 8^\circ$
- Meshes
- Total pressure loss contours



2048 nodes



2555 nodes



3735 nodes

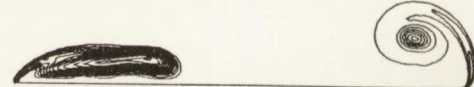
2048 nodes



2555 nodes

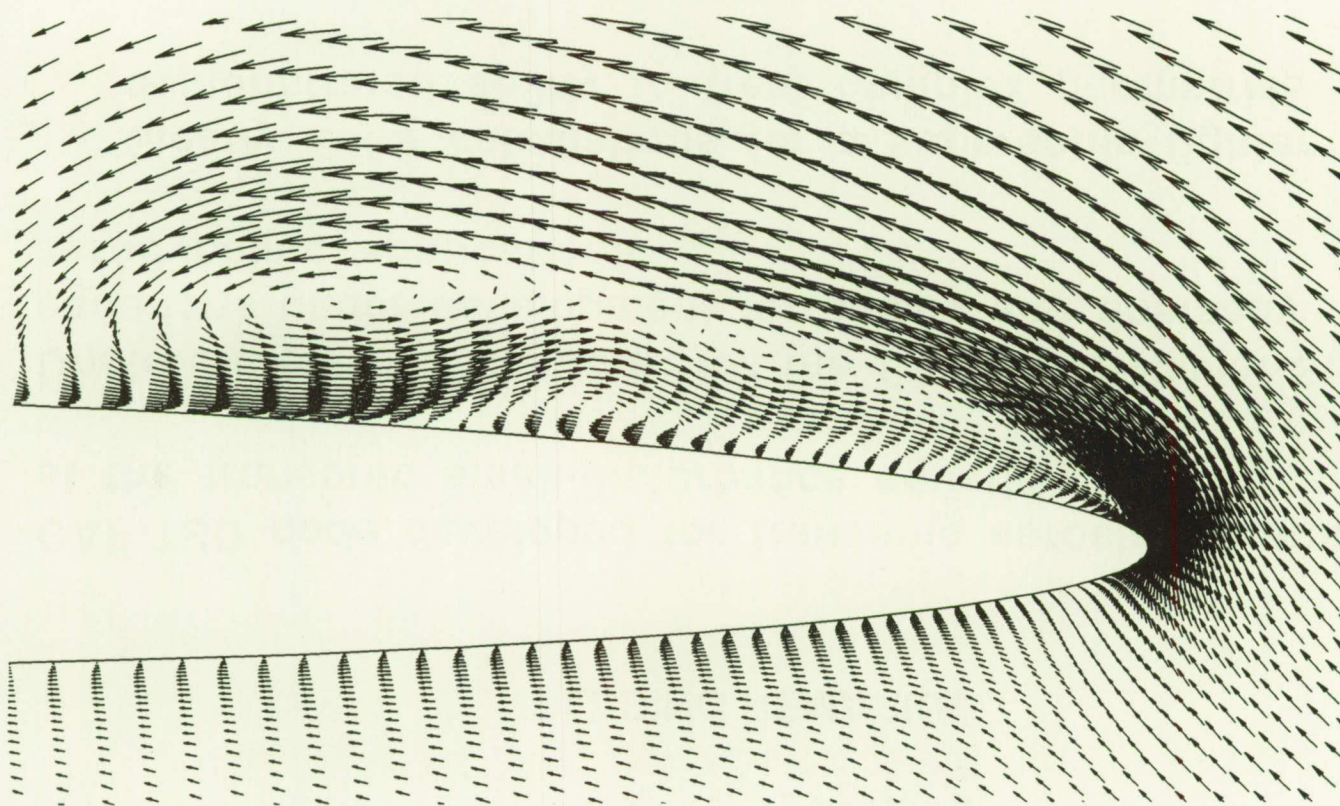


3735 nodes



CROSS FLOW VELOCITY VECTORS FROM CONICAL NAVIER-STOKES SOLUTION

- 70° swept elliptic cone delta wing; thickness ratio 14:1
- $M_\infty = 2.0$, $\alpha = 10^\circ$, and $Re = 5 \times 10^5$



CONCLUDING REMARKS

- CAP-TSD code developed for transonic aeroelastic analysis at the transonic small-disturbance equation level
- Unstructured grid methods for the Euler and Navier-Stokes equations under development for steady and unsteady aerodynamic applications
 - Steady Euler calculations for a supersonic fighter demonstrated ability to treat complex geometries
 - Unsteady Euler calculations for a supersonic fighter demonstrated general dynamic mesh capability
 - Vortex-dominated conical-flow calculations demonstrated adaptive mesh refinement capability

SESSION V

FIGHTER AIRCRAFT

Chairman:

Terry L. Holst

**Chief, Applied Computational Fluids Branch
NASA Ames Research Center**

ORIGINAL CONTAINS
COLOR ILLUSTRATIONS

N91-10857

Grid Generation and Inviscid Flow Computation About Aircraft Geometries

Robert E. Smith
Analysis and Computation Division
NASA Langley Research Center

Abstract

Grid generation and Euler flow about fighter aircraft are described. A fighter aircraft geometry is specified by an area ruled fuselage with an internal duct, cranked delta wing or strake/wing combinations, canard and/or horizontal tail surfaces, and vertical tail surfaces. The initial step before grid generation and flow computation is the determination of a suitable grid topology. The external grid topology that has been applied is called a dual-block topology which is a patched C^1 continuous multiple-block system where, inner blocks cover the highly-swept part of a cranked wing or strake, rearward inner-part of the wing, and tail components. Outer-blocks cover the remainder of the fuselage, outer-part of the wing, canards and extended to the far field boundaries. The grid generation is based on transfinite interpolation with Lagrangian blending functions. This procedure has been applied to the Langley experimental fighter configuration and a modified F-18 configuration. Supersonic flow between Mach 1.3 and 2.5 and angles of attack between 0° and 10° have been computed with associated Euler solvers based on the finite-volume approach. When coupling geometric details such as boundary layer diverter regions, duct regions with inlets and outlets, or slots with the general external grid, imposing C^1 continuity can be extremely tedious. The approach taken here is to patch blocks together at common interfaces where there is no grid continuity, but enforce conservation in the finite-volume solution. The key to this technique is how to obtain the information required for a conservative interface. We have used the Ramshaw technique which automates the computation of proportional areas of two overlapping grids on a planar surface and is suitable for coding. We have generated internal duct grids for the Langley experimental fighter configuration independent of the external grid topology, with a conservative interface at the inlet and outlet.

FEATURES

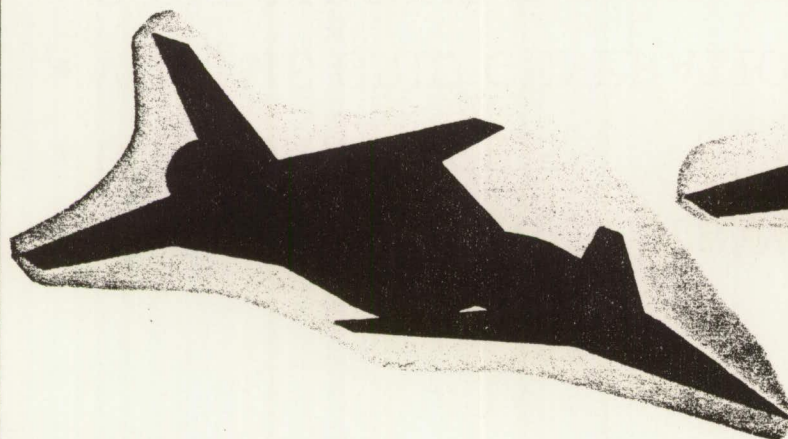
- MULTIPLE-BLOCK STRUCTURED GRIDS
- FINITE-VOLUME EULER SOLVERS
- CONSERVATIVE INTERFACE BETWEEN GRID BLOCKS

CONTENTS

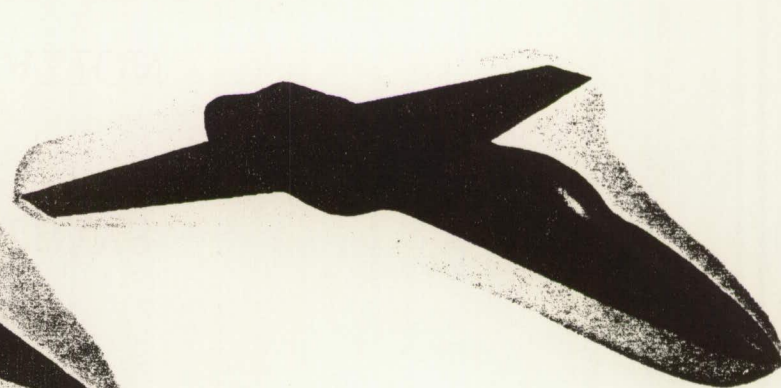
- FIGHTER CONFIGURATIONS
- BOUNDARY GRIDS
- VOLUME GRID GENERATION
- CONSERVATIVE INTERFACING
- EULER FLOW SOFTWARE AND SOLUTIONS
- VIDEO DISPLAY
- CONCLUSIONS AND COMMENTS

FIGHTER CONFIGURATIONS

314



EXPERIMENTAL FIGHTER



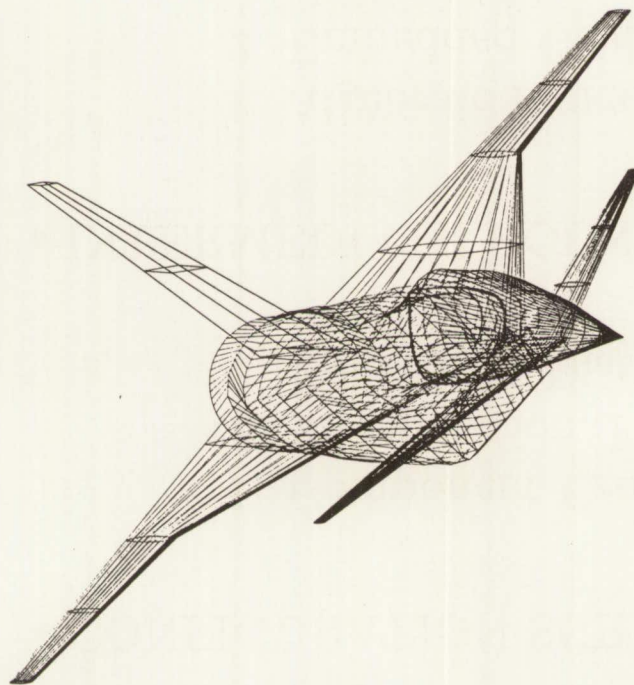
MODIFIED F-18

BOUNDARY GRIDS

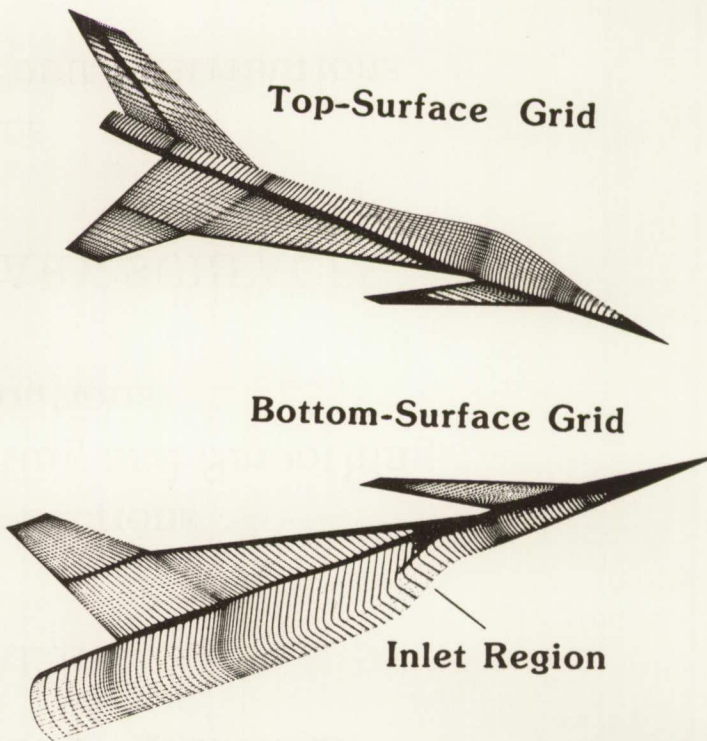
- **CONFIGURATION SURFACE**
 1. Component Cross Sections
 2. Interpolation, Fitting and Smoothing
 3. Grid Point Distributions
- **INTERMEDIATE BOUNDARY SURFACES**
 1. Algebraic Functions
 2. Embedded Grid Point Distributions
- **FAR FIELD BOUNDARY SURFACES**

BOUNDARY-SURFACE GRIDS

316



Original Definition



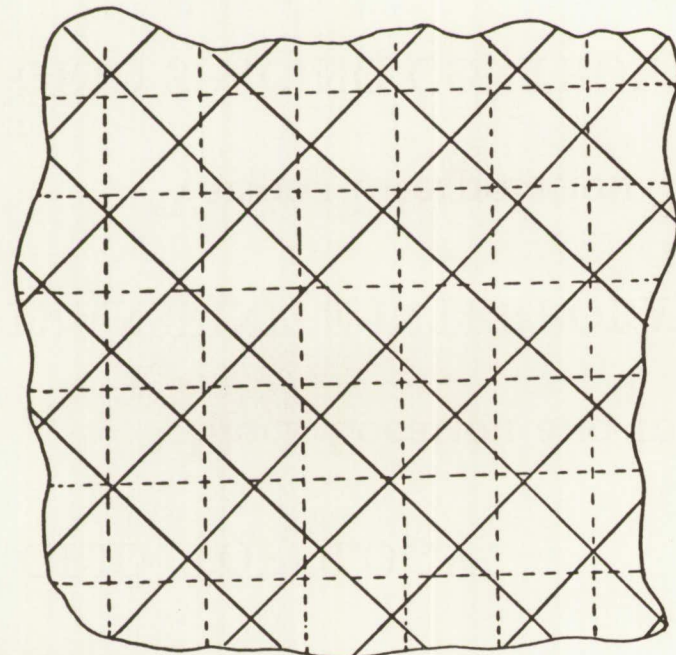
Grid-Surface Definition

VOLUME GRID GENERATION

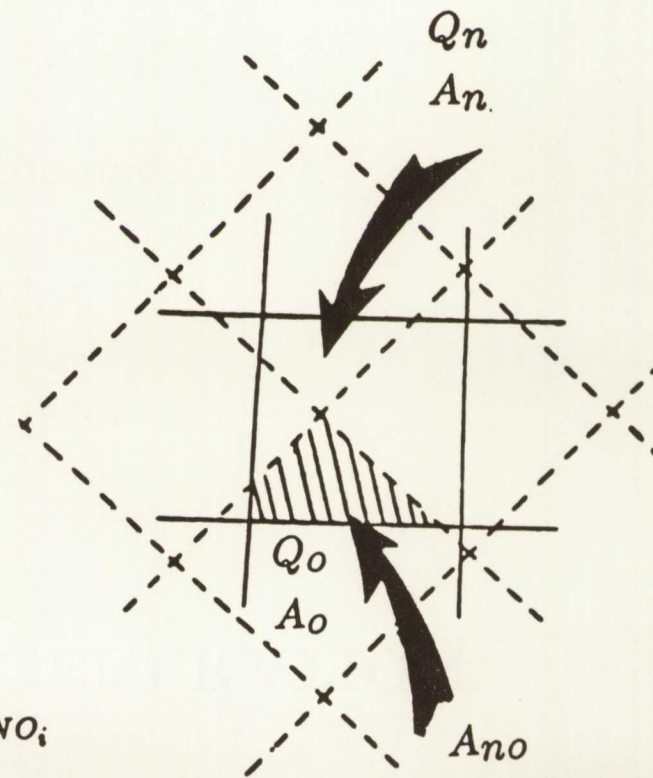
- GRID TOPOLOGY
 - * Block Location and Interfaces
- TRANSFINITE INTERPOLATION
 - * Various Interpolation Techniques
- GRID SPACING CONTROL
 - * Exponential Functions

CONSERVATIVE GRID INTERFACES

- Rai's Approach



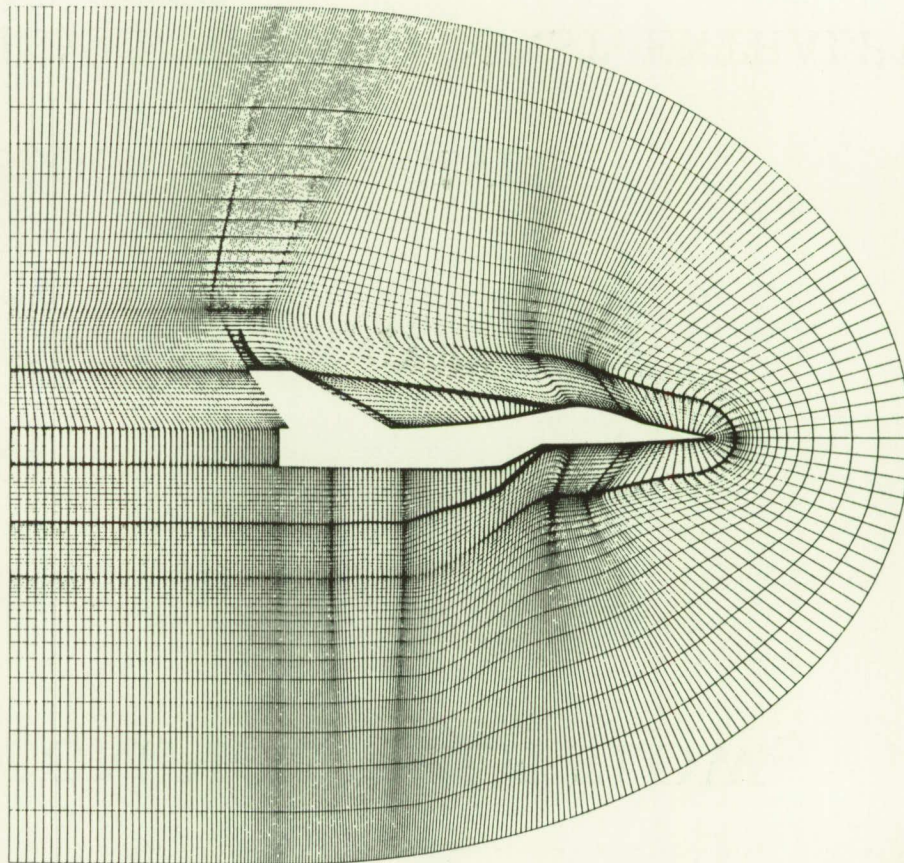
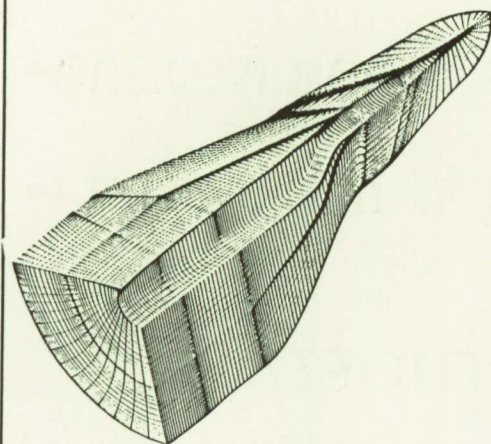
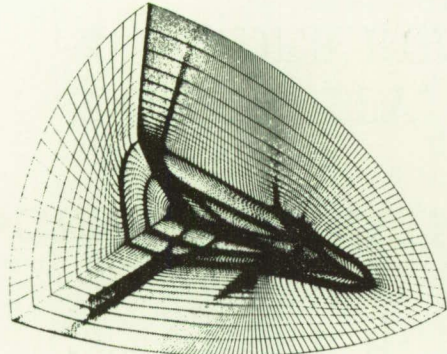
- Ramshaw Redistribution



$$Q_N = \sum_{i=1}^{N_{NO}} Q_{O_i} \frac{A_{NO_i}}{A_{O_i}} = \sum_{i=1}^{N_{NO}} q_{O_i} A_{NO_i}$$

FIGHTER GRID

319

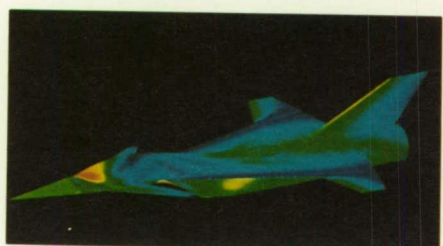


INVISCID-COMPRESSIBLE FLOW

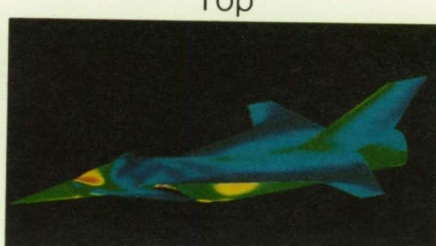
- FINITE-VOLUME METHODOLOGY
- CUSTOM EULER SOLVER
 - * CONTINUITY, MOMENTUM AND ENERGY
 - * 3^{rd} ORDER RUNGE-KUTTA
- GENERAL MULTI-BLOCK EULER SOLVER
 - * CONTINUITY, MOMENTUM AND CONST. ENTHALPY
 - * 4^{th} ORDER RUNGE-KUTTA

SUMMARY OF SOLUTIONS

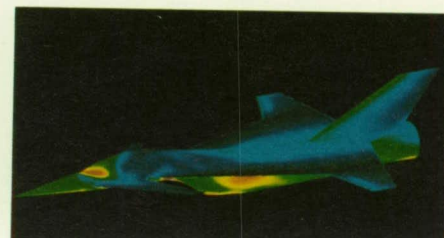
Mach Number = 2
Coefficient of pressure



$\alpha = 4^\circ$

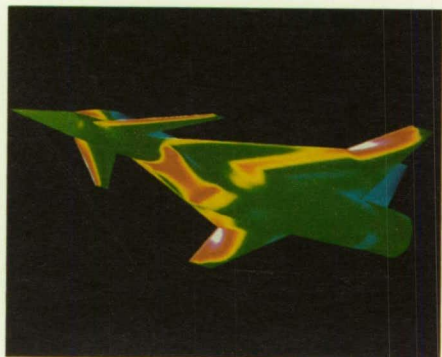
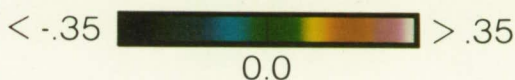


$\alpha = 7^\circ$



$\alpha = 10^\circ$

Top



$\alpha = 4^\circ$



$\alpha = 7^\circ$

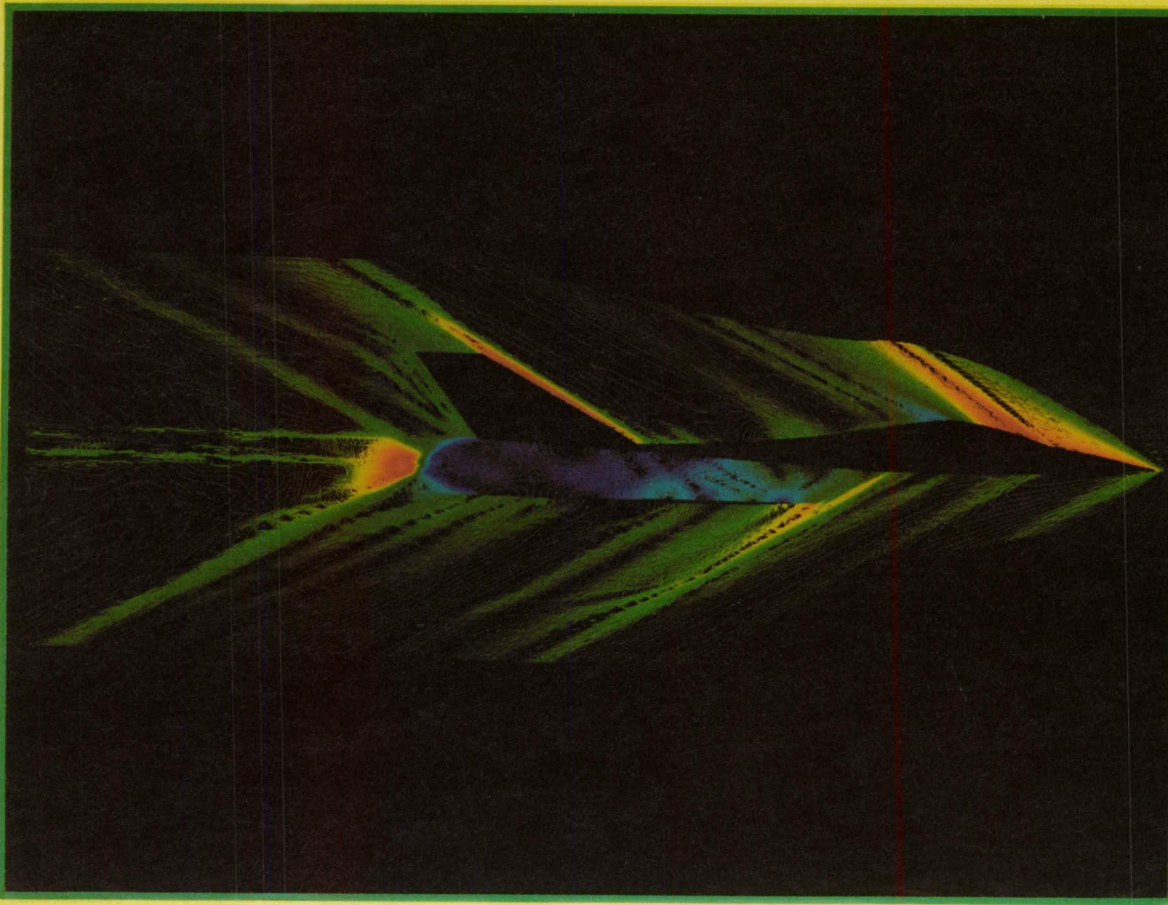


$\alpha = 10^\circ$

Bottom

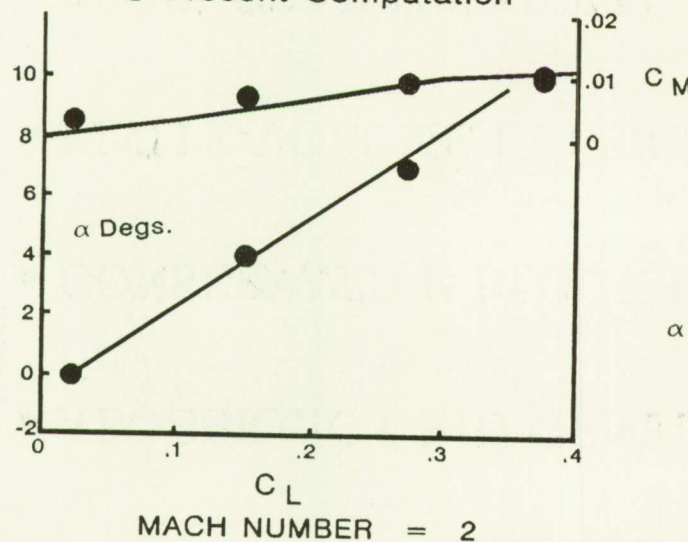
EXPERIMENTAL FIGHTER CONFIGURATION CONTOURS OF PRESSURE COEFFICIENT

Mach number = 2 Angle of attack = 0°



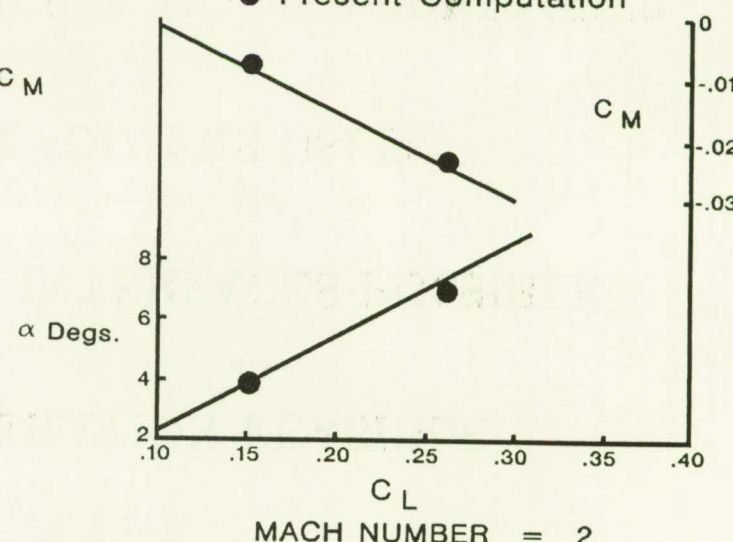
AERODYNAMIC CHARACTERISTICS

MODEL \equiv BW_{ACV}
— Experiment LaRC
● Present Computation



MACH NUMBER = 2

MODEL \equiv BW_{AV}
— Experiment LaRC
● Present Computation



MACH NUMBER = 2

CONCLUSIONS

- ALGEBRAIC GRID GENERATION FEASIBLE
- CONSERVATIVE BLOCK INTERFACES POSSIBLE
- FINITE-VOLUME EULER SOLVERS USED
- FLOW CHARACTERISTICS IN GOOD AGREEMENT
- VORTEX COMPUTATION NEEDS MORE STUDY

ORIGINAL CONTAINS
COLOR ILLUSTRATIONS

N91-10858

A ZONAL NAVIER-STOKES METHODOLOGY FOR FLOW SIMULATION ABOUT A COMPLETE AIRCRAFT

Jolen Flores

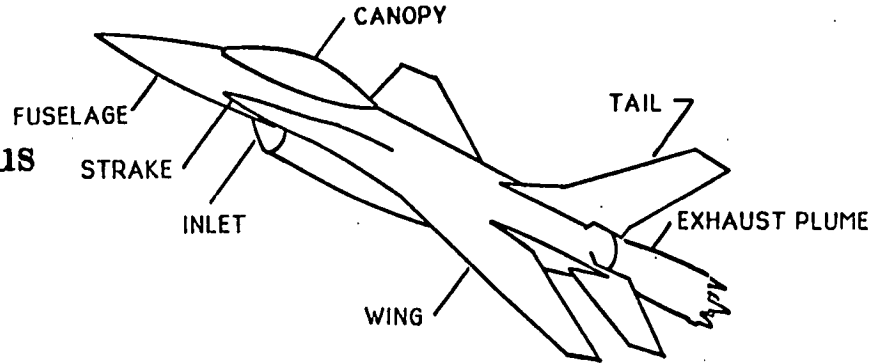
Abstract: The thin-layer, Reynolds-averaged, Navier-Stokes equations are used to simulate the transonic viscous flow about the complete F-16A fighter aircraft. These computations demonstrate how computational fluid dynamics (CFD) can be used to simulate turbulent viscous flow about realistic aircraft geometries. A zonal grid approach is used to provide adequate viscous grid clustering on all aircraft surfaces. Zonal grids extend inside the F-16A inlet and up to the compressor face while power on conditions are modeled by employing a zonal grid extending from the exhaust nozzle to the far field. Computations are compared with existing experimental data and are in fair agreement. Computations for the F-16A in side slip are also presented.

Applied Computational Fluids Branch
NASA Ames Research Center
Moffett Field, CA. 94035

Presentation at NASA OAST CFD CONFERENCE
March 7-9, 1989
NASA Ames Research Center

- **OBJECTIVE**

- ▷ To numerically simulate viscous transonic flow about realistic aircraft configurations.



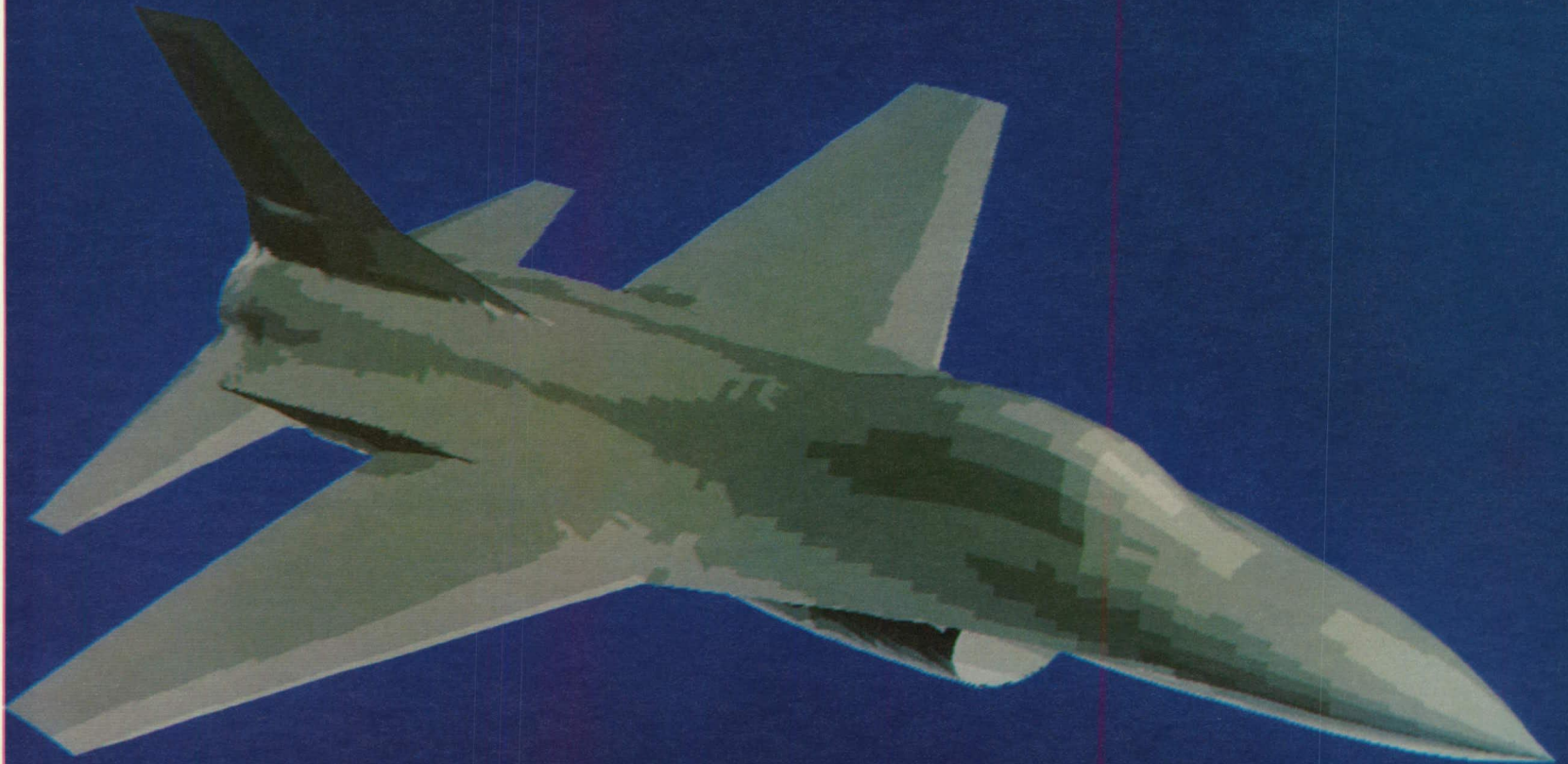
- **MOTIVATION**

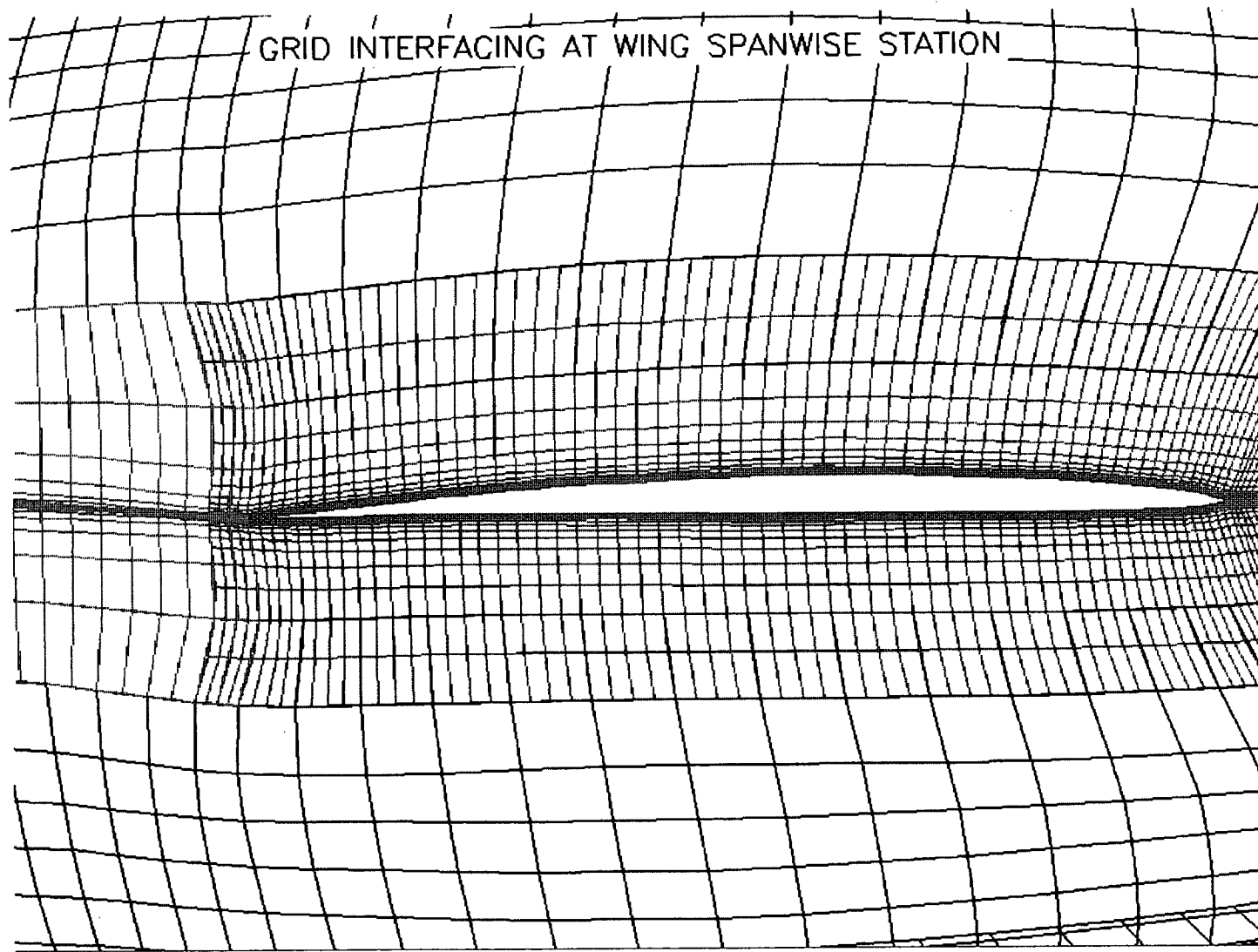
- ▷ Technical demonstration of state-of-the-art CFD research
- ▷ To provide bench-mark calculations (validated by measurements)
- ▷ Reveal areas requiring future research emphasis
- ▷ Catalyst for future cooperative efforts between NAS, aerospace industry and academia
- ▷ Industrial use for prediction of integrated aircraft performance

- **APPROACH**

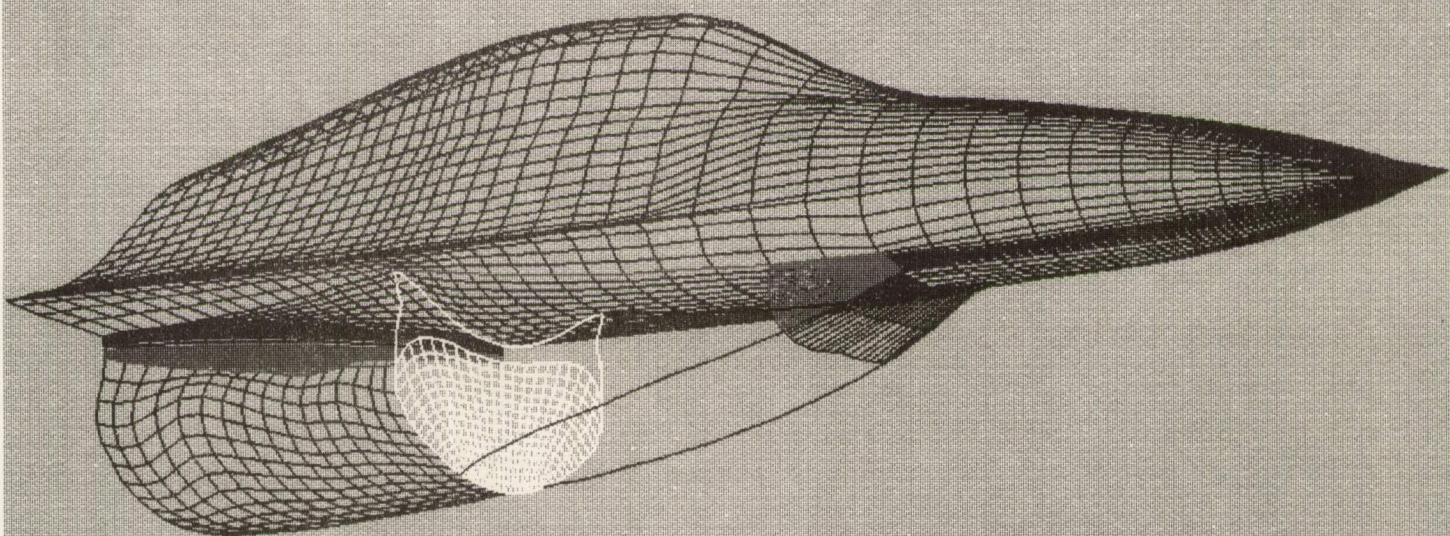
- ▷ Thin-layer Navier-Stokes equations
- ▷ Zonal grid approach
- ▷ Modular program

TOP PERSPECTIVE VIEW OF F-16A

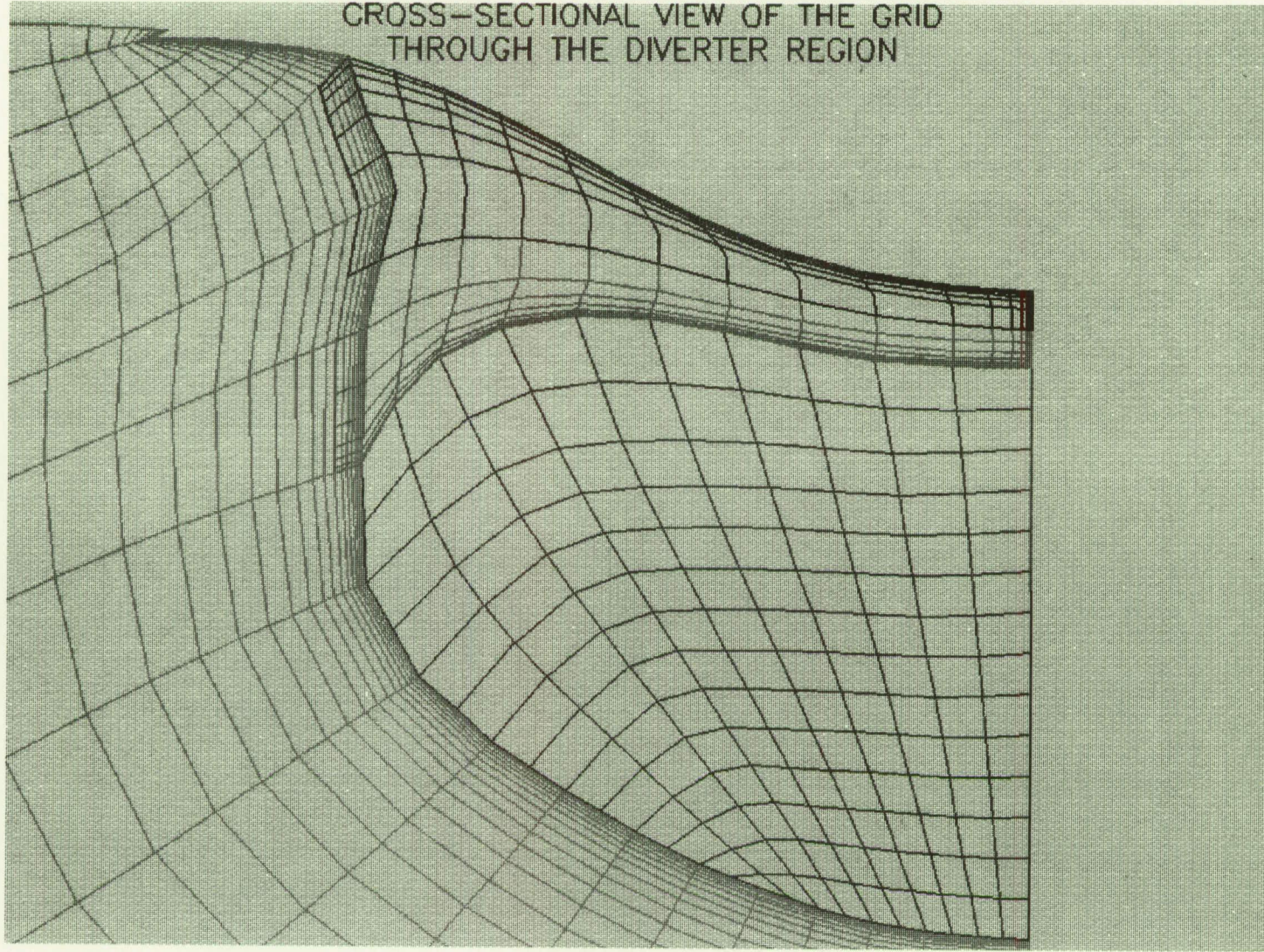




WING-FUSELAGE-INLET SURFACE GRIDS

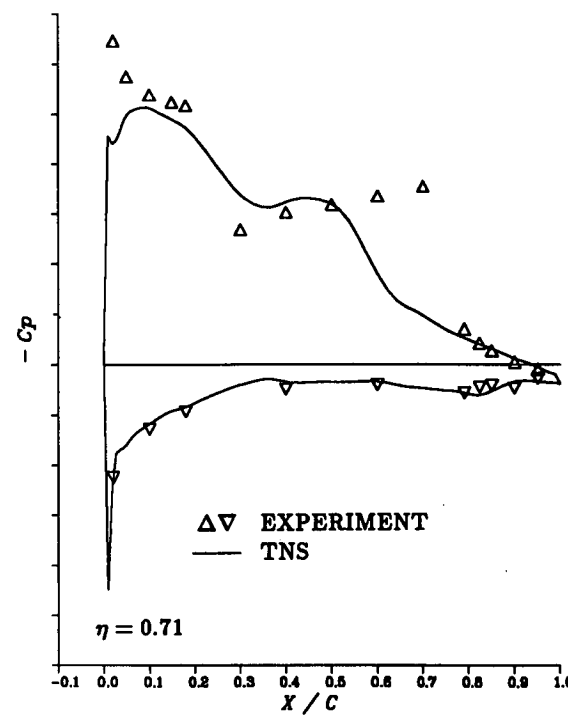
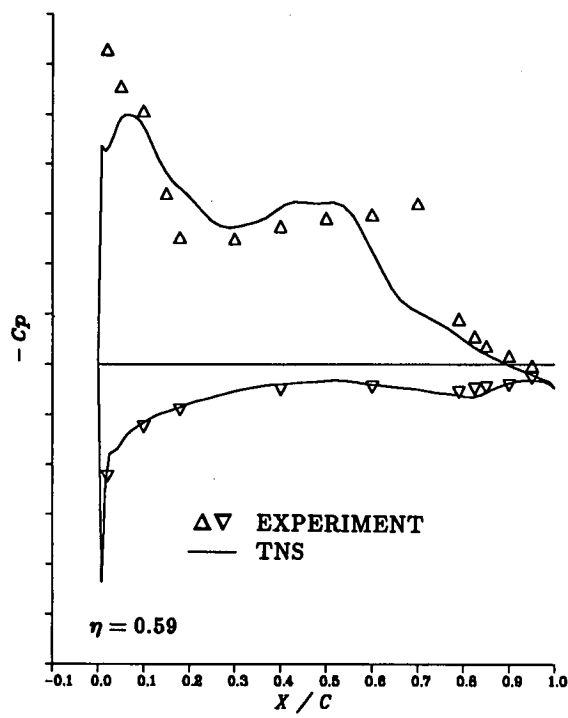


CROSS-SECTIONAL VIEW OF THE GRID
THROUGH THE DIVERTER REGION



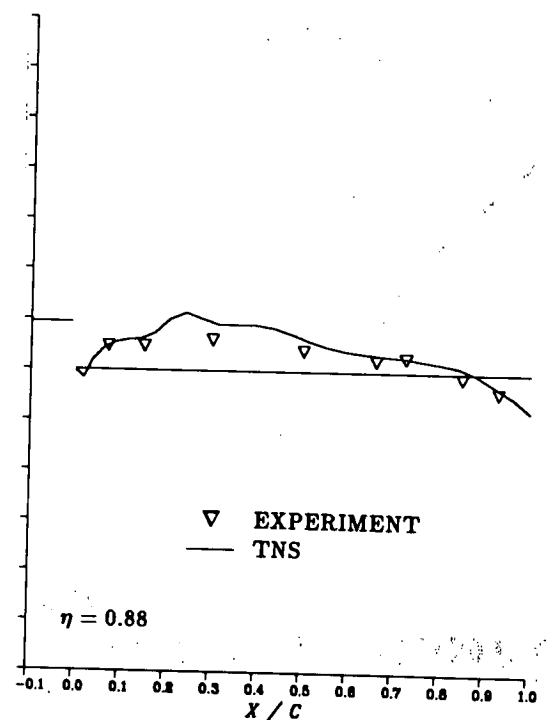
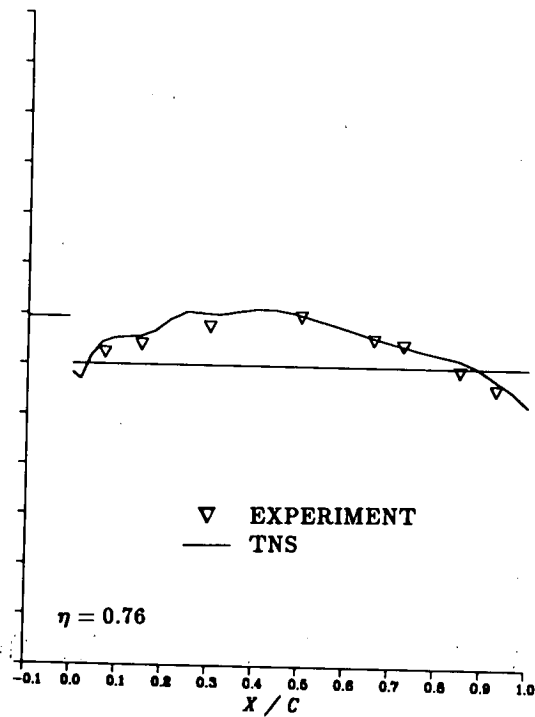
F-16A WING PRESSURE COEFFICIENT COMPARISONS

$M_\infty = 0.9, \alpha = 6.0^\circ, Re_c = 4.5 \times 10^6$



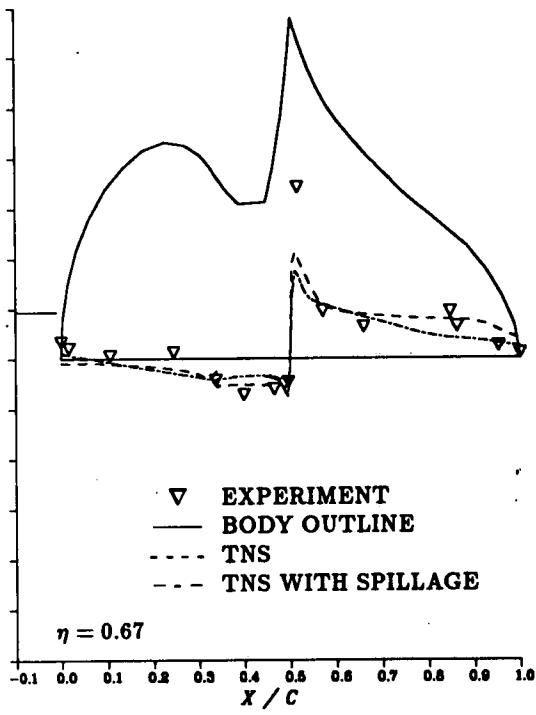
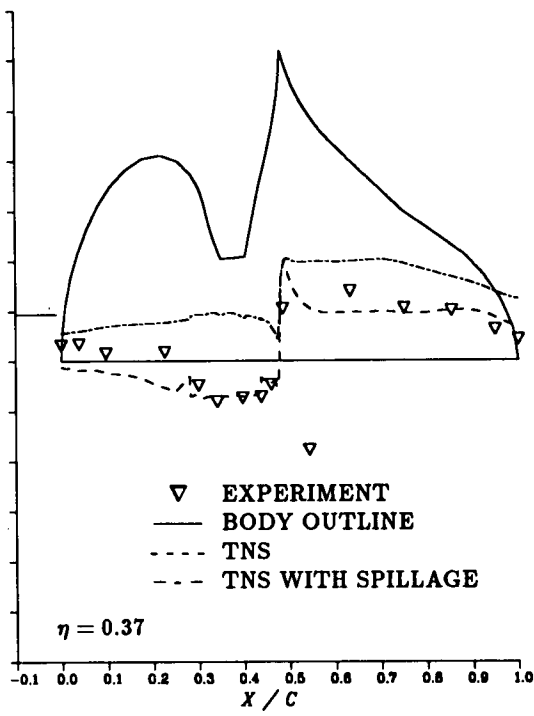
VERTICAL TAIL PRESSURE COEFFICIENT COMPARISONS

$M_\infty = 0.9, \alpha = 6.0^\circ, Re_c = 4.5 \times 10^6$



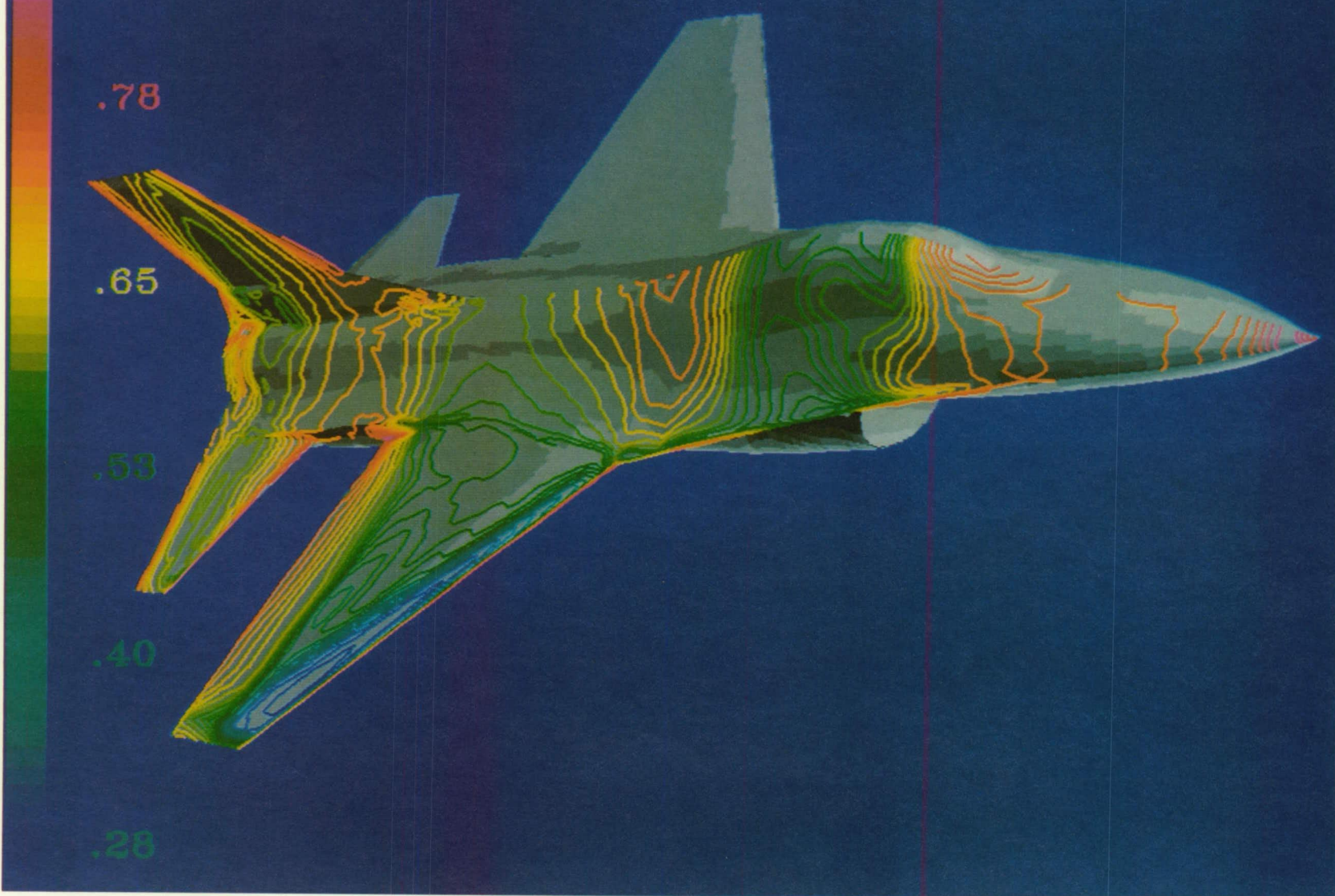
INLET/DIVERTER PRESSURE COEFFICIENT COMPARISONS

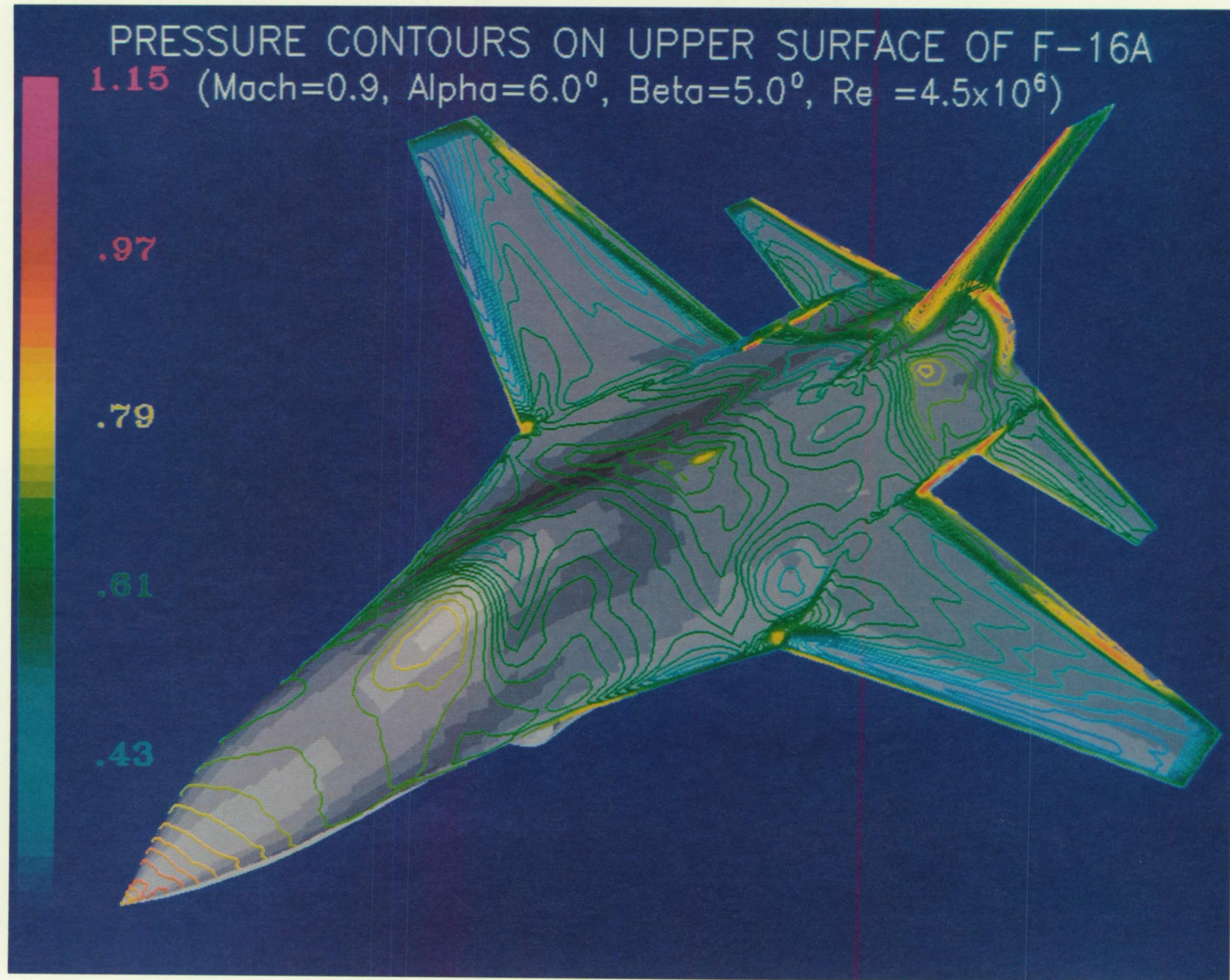
$$M_\infty = 0.9, \alpha = 6.0^\circ, Re_c = 4.5 \times 10^6$$



PRESSURE CONTOURS ON UPPER SURFACE OF F-16A

.90 (Mach=0.9, Alpha=6.0°, Beta=0.0°, $Re_c=4.5 \times 10^6$)





CROSS-FLOW INFLUENCE ON UNRESTRICTED PARTICLE TRACES
(Mach=0.9, Alpha=6.0°, Beta=5.0°, $Re_c=4.5 \times 10^6$)



SUMMARY

- Benchmark Navier-Stokes simulation of a complete aircraft including sideslip

$$\underline{\beta = 0.0^\circ}$$

- ▷ Good comparison with C_P , C_L , and C_D
- ▷ Successful implementation of internal inlet grids
- ▷ Successful simulation of power-on conditions
- ▷ Convergence in 5000 iterations/ 25 hours of cpu

$$\underline{\beta = 5.0^\circ}$$

- ▷ Pressure contours/particle traces indicate proper physical trends

**NUMERICAL SIMULATION OF F-18 FUSELAGE FOREBODY
FLOWS AT HIGH ANGLES OF ATTACK**

Lewis B. Schiff*
Russell M. Cummings†
Reese L. Sorenson*
Yehia M. Rizk†

NASA Ames Research Center
Moffett Field, CA 94035

Abstract

As part of the NASA High Alpha Technology Program, fine-grid Navier-Stokes solutions have been obtained for flow over the fuselage forebody and wing leading edge extension of the F/A-18 High Alpha Research Vehicle at large incidence. The resulting flows are complex, and exhibit crossflow separation from the sides of the forebody and from the leading edge extension. A well-defined vortex pattern is observed in the leeward-side flow. Results obtained for laminar flow show good agreement with flow visualizations obtained in ground-based experiments. Further, turbulent flows computed at high-Reynolds-number flight-test conditions ($M_\infty = 0.2$, $\alpha = 30^\circ$, and $Re_c = 11.52 \times 10^6$) show good agreement with surface and off-surface visualizations obtained in flight.

* Research Scientist, Applied Computational Fluids Branch.

† National Research Council Research Associate. Associate Professor, on leave from California Polytechnic State University, Aeronautical Engineering Department.

‡ Member of the Professional Staff, Sterling Federal Systems, Inc., Palo Alto, CA.

OBJECTIVE

- DEVELOP FLIGHT-VALIDATED DESIGN METHODS THAT ACCURATELY PREDICT THE AERODYNAMICS OF AIRCRAFT MANEUVERING AT LARGE ANGLES OF ATTACK

APPROACH

- UTILIZE A THREE-DIMENSIONAL NAVIER-STOKES CODE, WITH SUITABLE GRIDS AND AN EDDY-VISCOSITY TURBULENCE MODEL, TO COMPUTE HIGH-ALPHA FLOWS OVER THE F-18 FUSELAGE FOREBODY AND LEX
- VALIDATE THE NUMERICAL RESULTS BY COMPARISON WITH FLIGHT-TEST DATA OBTAINED ON THE NASA F-18 HIGH ALPHA RESEARCH VEHICLE (HARV)

GOVERNING EQUATIONS

$$\frac{\partial \hat{Q}}{\partial \tau} + \frac{\partial \hat{F}}{\partial \xi} + \frac{\partial \hat{G}}{\partial \eta} + \frac{\partial \hat{H}}{\partial \zeta} = \frac{1}{Re} \frac{\partial \hat{S}}{\partial \zeta}$$

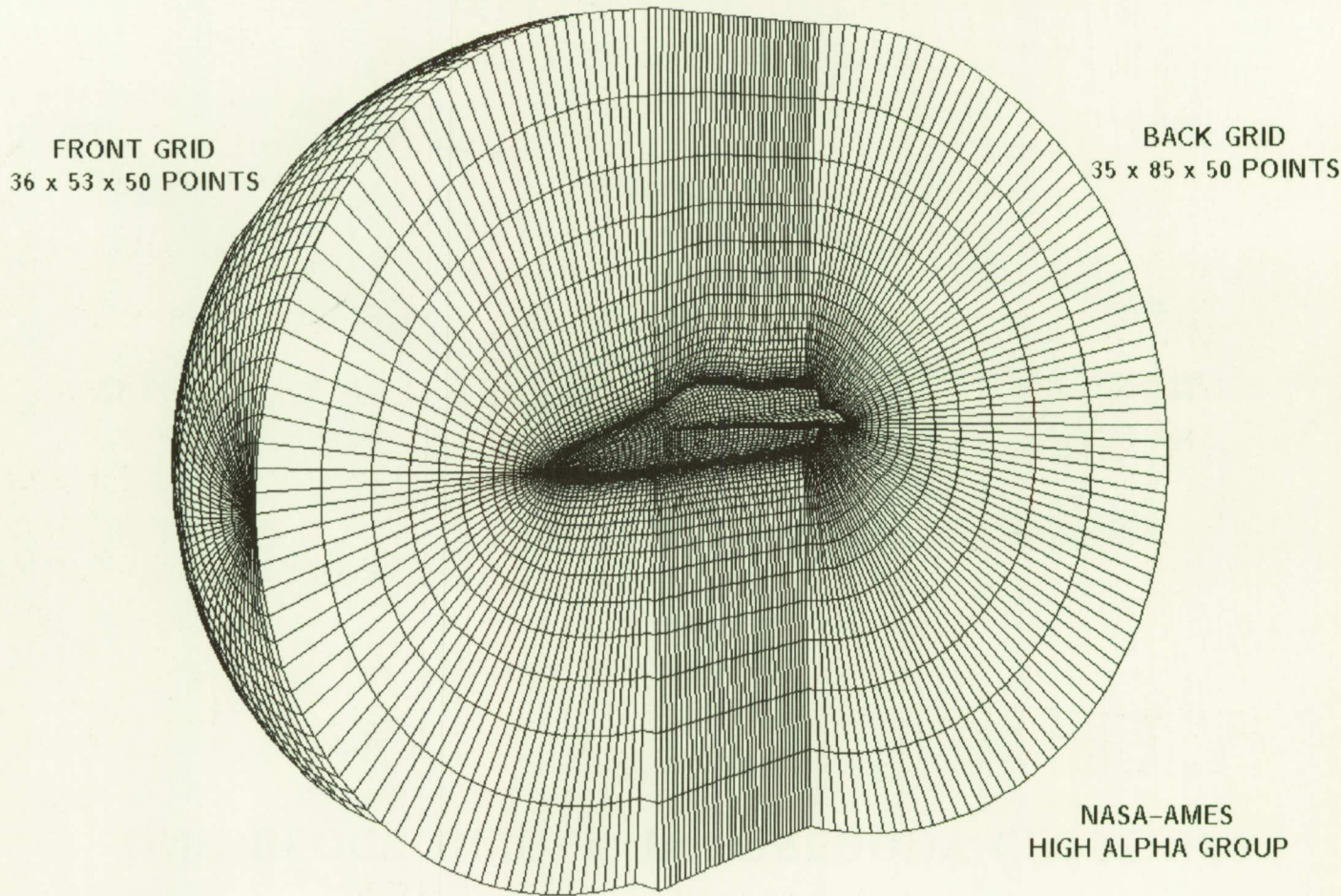
- THIN-LAYER NAVIER-STOKES EQUATIONS
- CURVILINEAR, BODY-CONFORMING COORDINATES
- HIGH REYNOLDS NUMBER FLOWS
- LAMINAR VISCOSITY FROM SUTHERLAND'S LAW
- ALGEBRAIC EDDY-VISCOSITY MODEL CORRECTED FOR CROSSFLOW SEPARATION

NUMERICAL METHOD

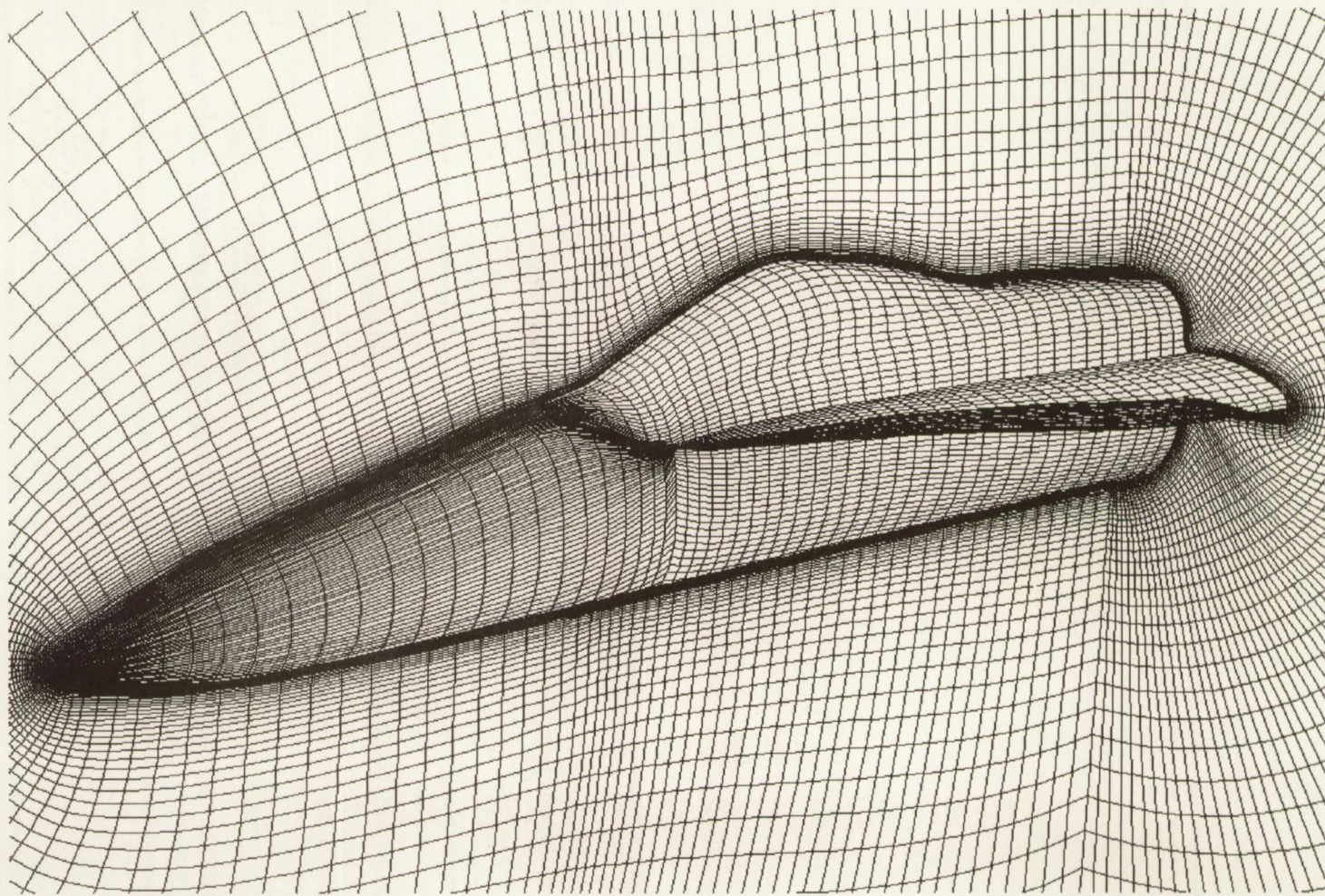
$$\left\{ I + h \left[\delta_\xi^b (\hat{A}^+) + \delta_\zeta \hat{C} - \frac{1}{Re} \bar{\delta}_\zeta \hat{M} \right] \right\} \left\{ I + h \left[\delta_\xi^f (\hat{A}^-) + \delta_\eta \hat{B} \right] \right\} \Delta \hat{Q}^n = R.H.S.$$

- TWO-FACTORIED ALGORITHM (F3D)
- FIRST OR SECOND-ORDER ACCURACY IN TIME
- SECOND-ORDER SPATIAL ACCURACY
 - FLUX-VECTOR SPLITTING AND UPWIND DIFFERENCING IN ξ (STREAMWISE) DIRECTION
 - CENTRAL DIFFERENCING IN THE η (CIRCUMFERENTIAL) AND ζ (RADIAL) DIRECTIONS
- COMBINATION OF SECOND AND FOURTH-ORDER SMOOTHING USED IN THE η AND ζ DIRECTIONS
 - SMOOTHING TERMS SCALED BY q/q_∞
- SINGLE-BLOCK AND TWO-BLOCK GRIDS USED

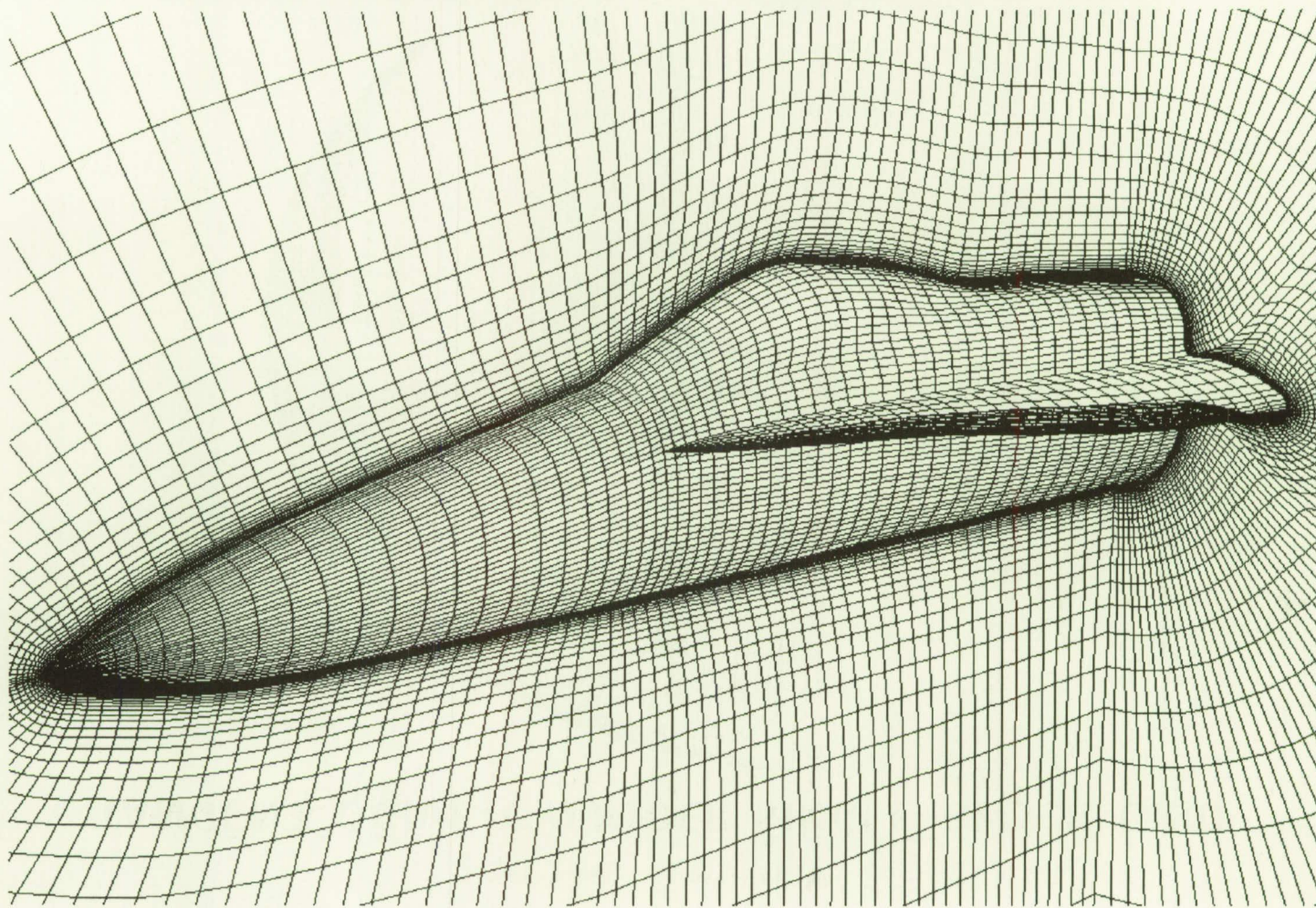
F-18 FOREBODY TWO-BLOCK GRID



ONE-BLOCK GRID: F-18 FOREBODY CLOSE-UP

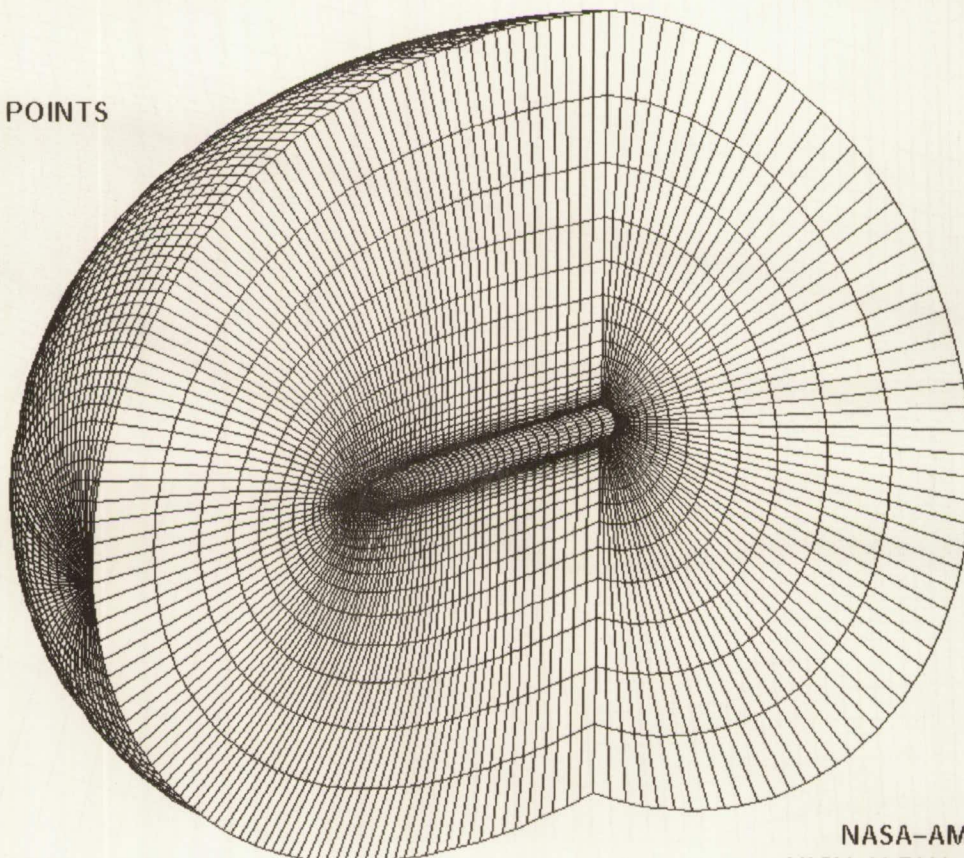


TWO-BLOCK GRID: F-18 FOREBODY CLOSE-UP



TANGENT OGIVE-CYLINDER SINGLE-BLOCK GRID

59 x 63 x 50 POINTS

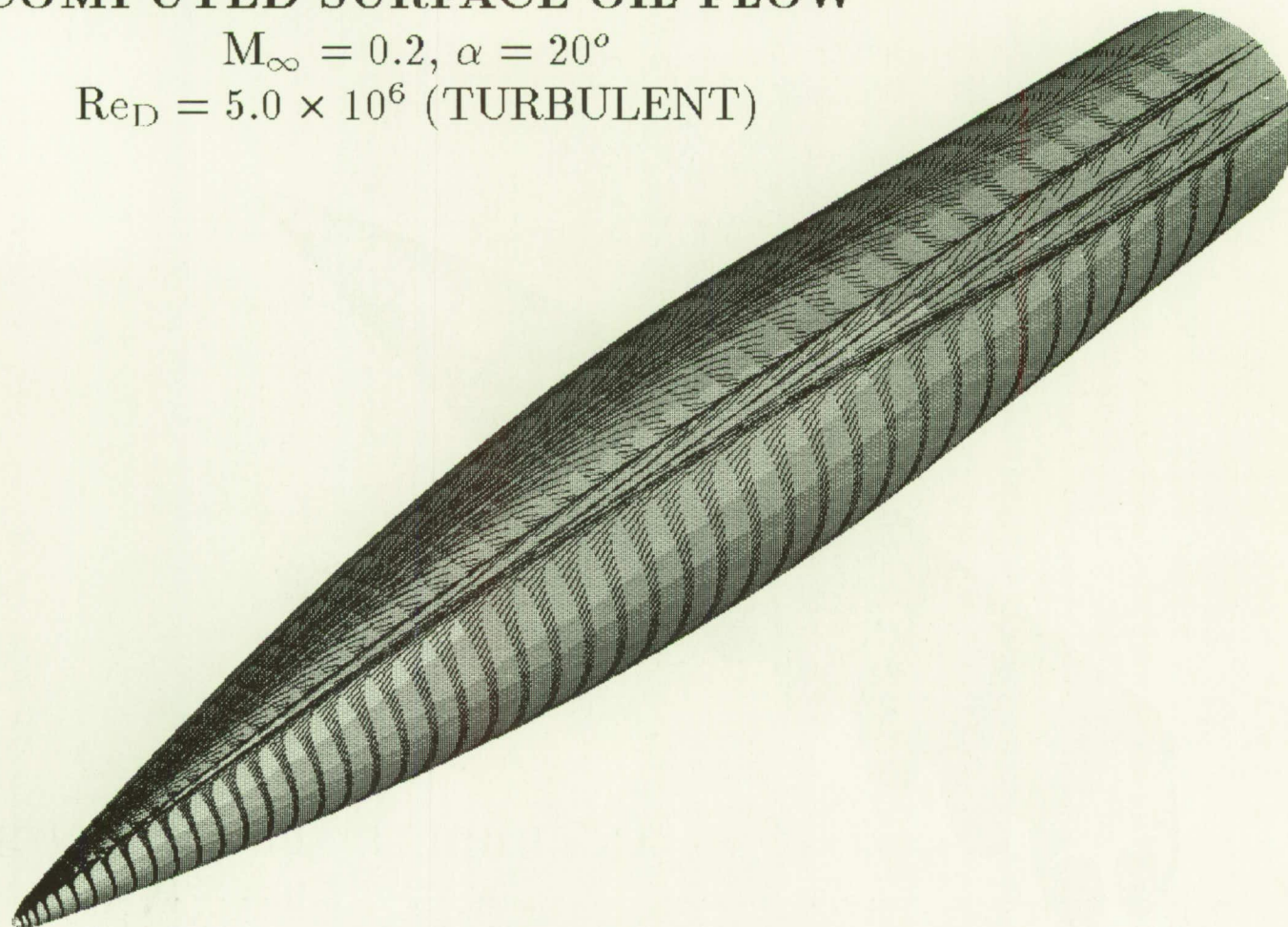


NASA-AMES
HIGH ALPHA GROUP

COMPUTED SURFACE OIL FLOW

$M_\infty = 0.2, \alpha = 20^\circ$

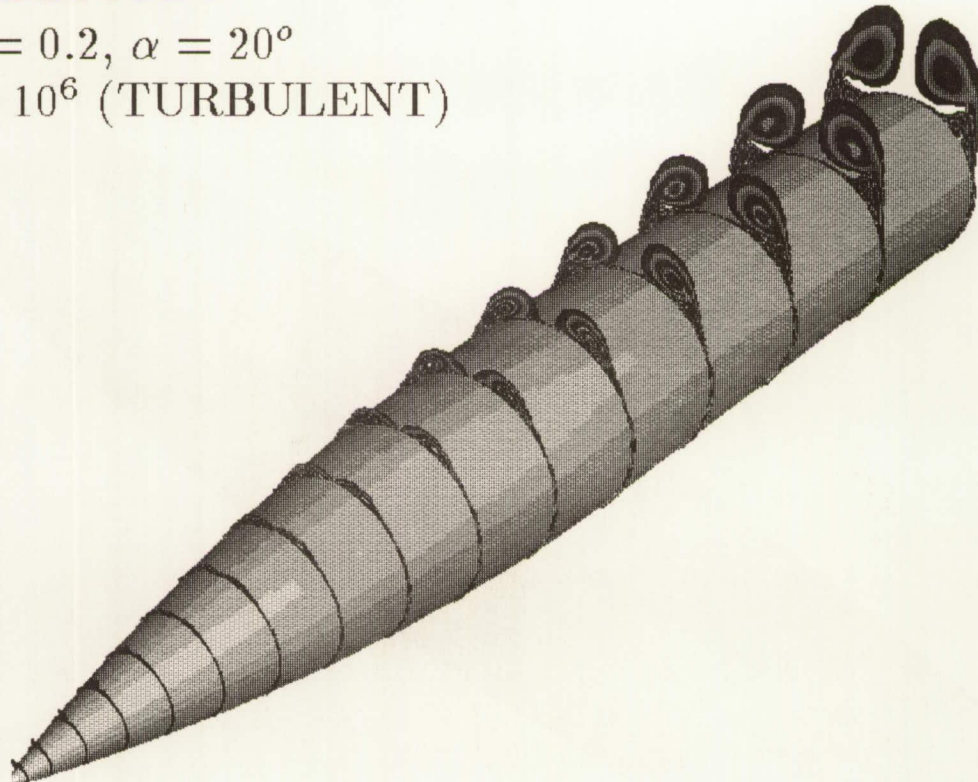
$Re_D = 5.0 \times 10^6$ (TURBULENT)



HELICITY

$M_\infty = 0.2, \alpha = 20^\circ$

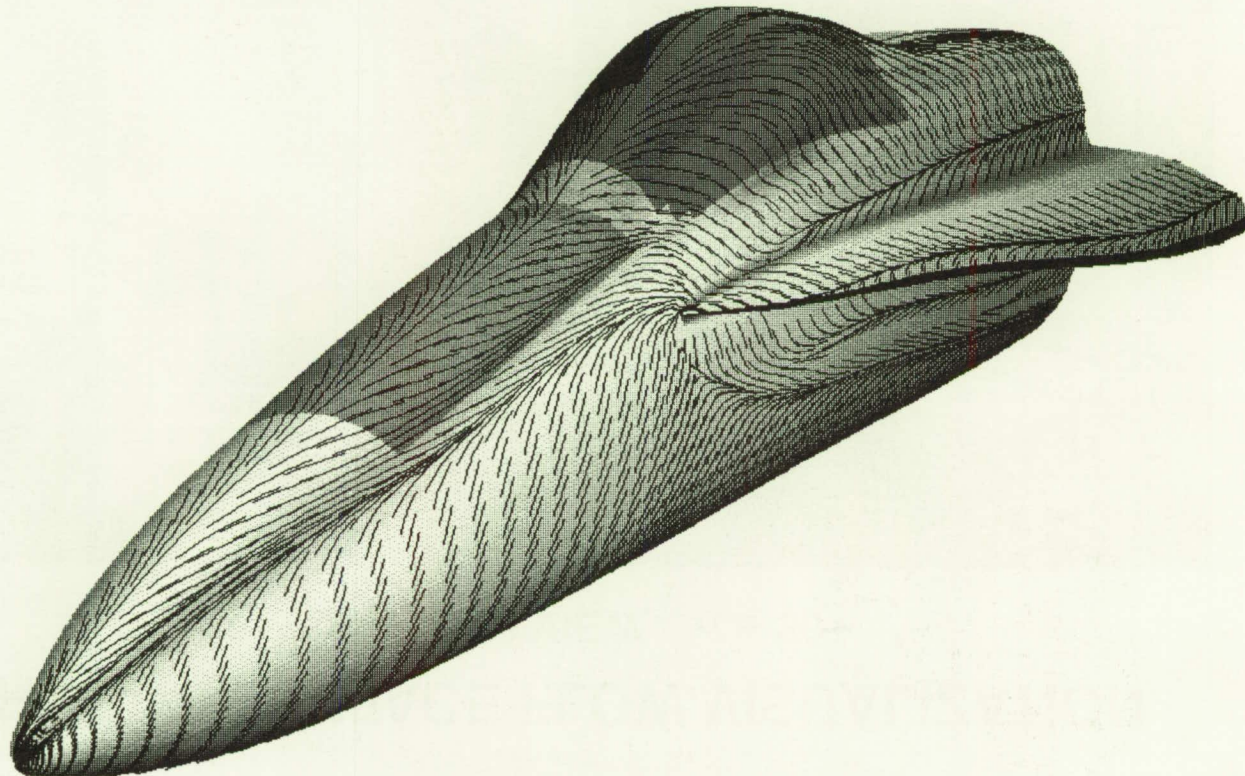
$Re_D = 5.0 \times 10^6$ (TURBULENT)



SURFACE FLOW PATTERN

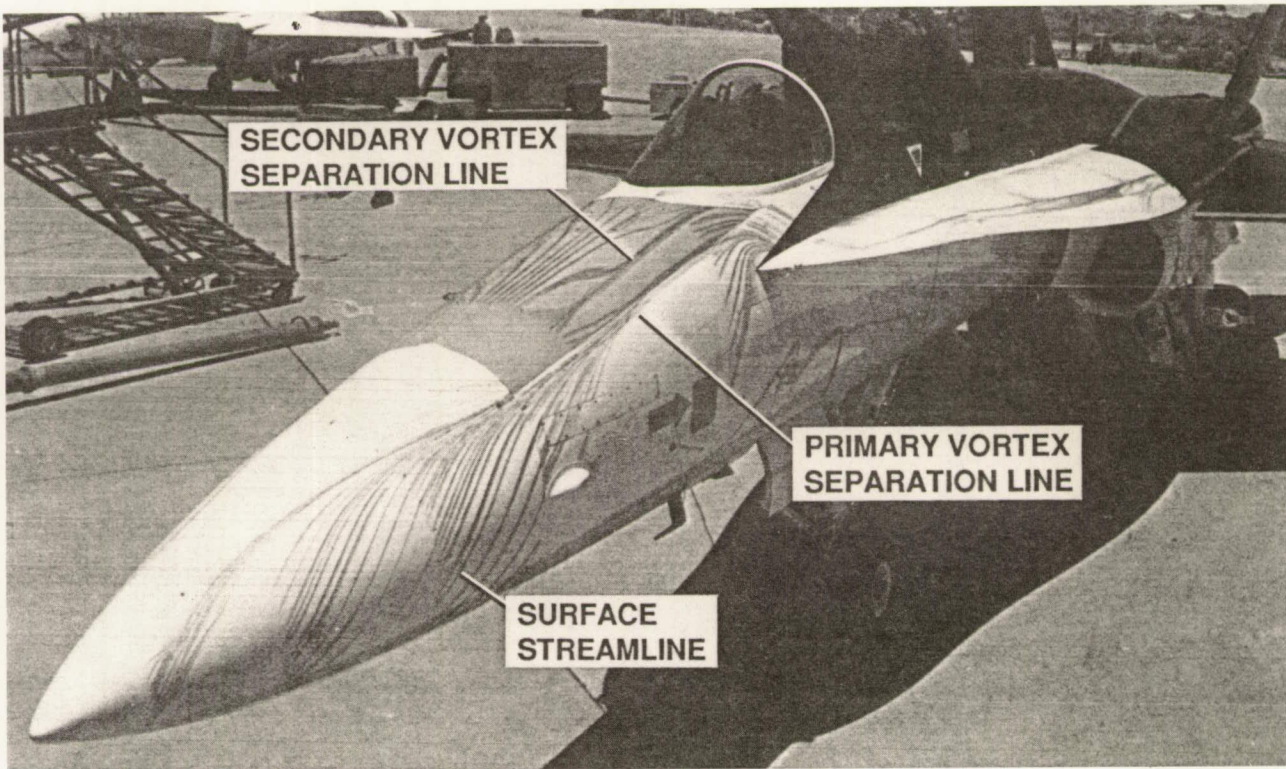
$M_\infty = 0.2, \alpha = 30^\circ$

$Re_c = 11,540,000$ (TURBULENT)



FLIGHT SURFACE FLOW VISUALIZATION

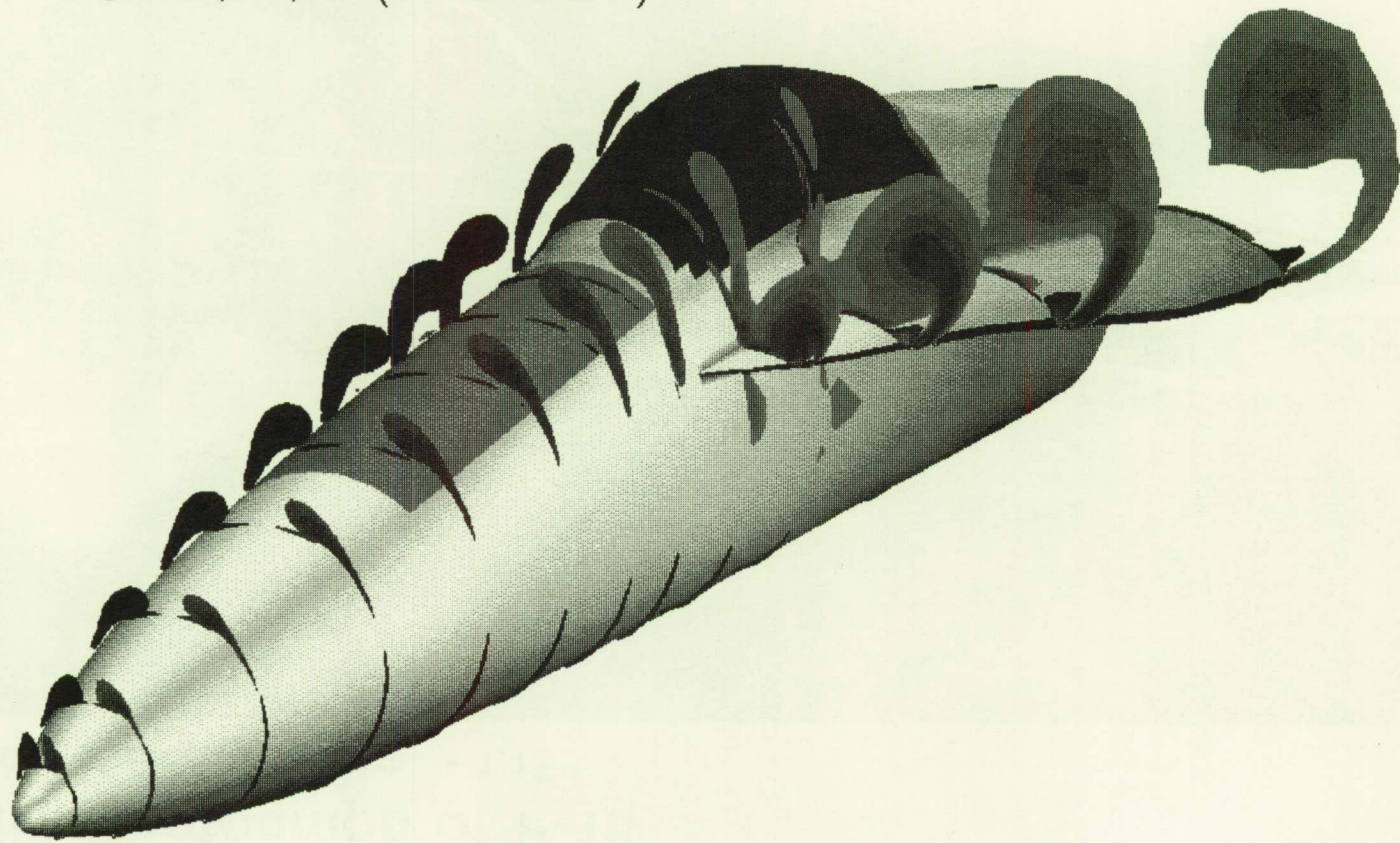
QUARTER VIEW, $\alpha = 30^\circ$



HELICITY DENSITY

$M_\infty = 0.2, \alpha = 30^\circ$

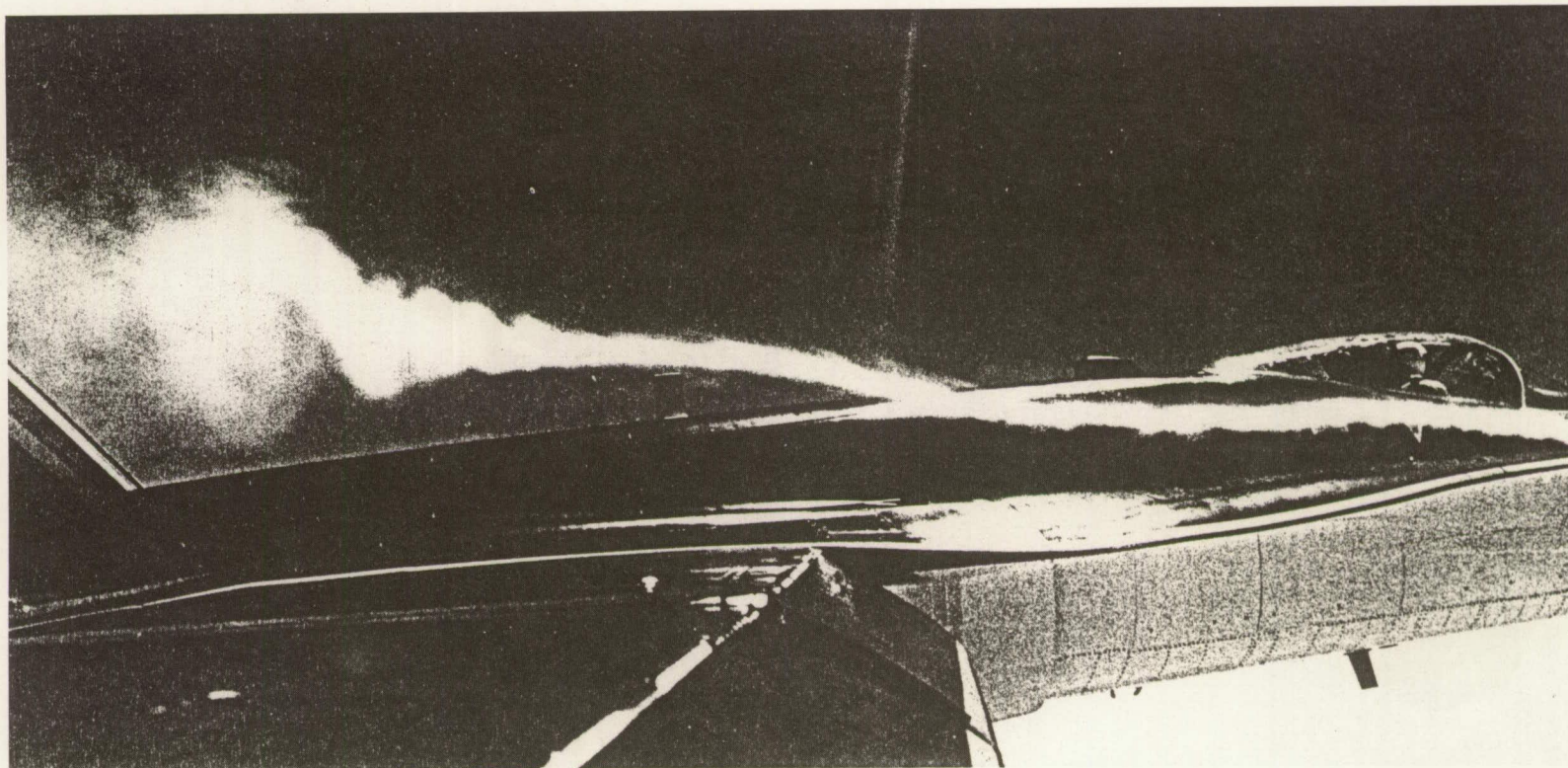
$Re_C = 11,540,000$ (TURBULENT)



Wingtip Photograph of F-18

$\alpha = 20.8^\circ$ and $\beta = +1.15^\circ$

358



- LEX vortices visualized using smoke

SUMMARY REMARKS

- NAVIER-STOKES COMPUTATIONS FOR HIGH-ALPHA SEPARATED TURBULENT FLOW ABOUT THE F-18 (HARV) FUSELAGE FOREBODY AND LEX SHOW GOOD AGREEMENT WITH FLIGHT-TEST DATA
 - ONLY MINOR DIFFERENCES BETWEEN SINGLE-BLOCK AND TWO-BLOCK RESULTS
 - EFFECTS OF INCREASING INCIDENCE CONSISTENT WITH EXPERIMENT
 - CFD RESULTS HAVE GIVEN NEW INSIGHT INTO HIGH-ALPHA FLOW STRUCTURE
- COMPUTATION-TO-FLIGHT PREDICTIONS OF FULL F-18 CONFIGURATIONS ARE NEXT STEP
- USE OF CFD AS A DESIGN TOOL FOR VORTEX CONTROL CONCEPTS IS AT HAND

ORIGINAL CONTAINS
COLOR ILLUSTRATIONS

NAVIER-STOKES SOLUTIONS ABOUT THE F/A-18 FOREBODY-LEX CONFIGURATION

Farhad Ghaffari
Vigyan Research Associates

James M. Luckring, James L. Thomas
NASA Langley Research Center

Brent L. Bates
Vigyan Research Associates

361

Abstract

Three-dimensional viscous flow computations are presented for the F/A-18 forebody-LEX geometry. Solutions are obtained from an algorithm for the compressible Navier-Stokes equations which incorporates an upwind-biased, flux-difference-splitting approach along with longitudinally-patched grids. Results are presented for both laminar and fully turbulent flow assumptions and include correlations with wind tunnel as well as flight-test results. A good quantitative agreement for the forebody surface pressure distribution is achieved between the turbulent computations and wind tunnel measurements at $M_\infty = 0.6$. The computed turbulent surface flow patterns on the forebody qualitatively agree well with in-flight surface flow patterns obtained on an F/A-18 aircraft at $M_\infty = 0.34$.

N91-10860

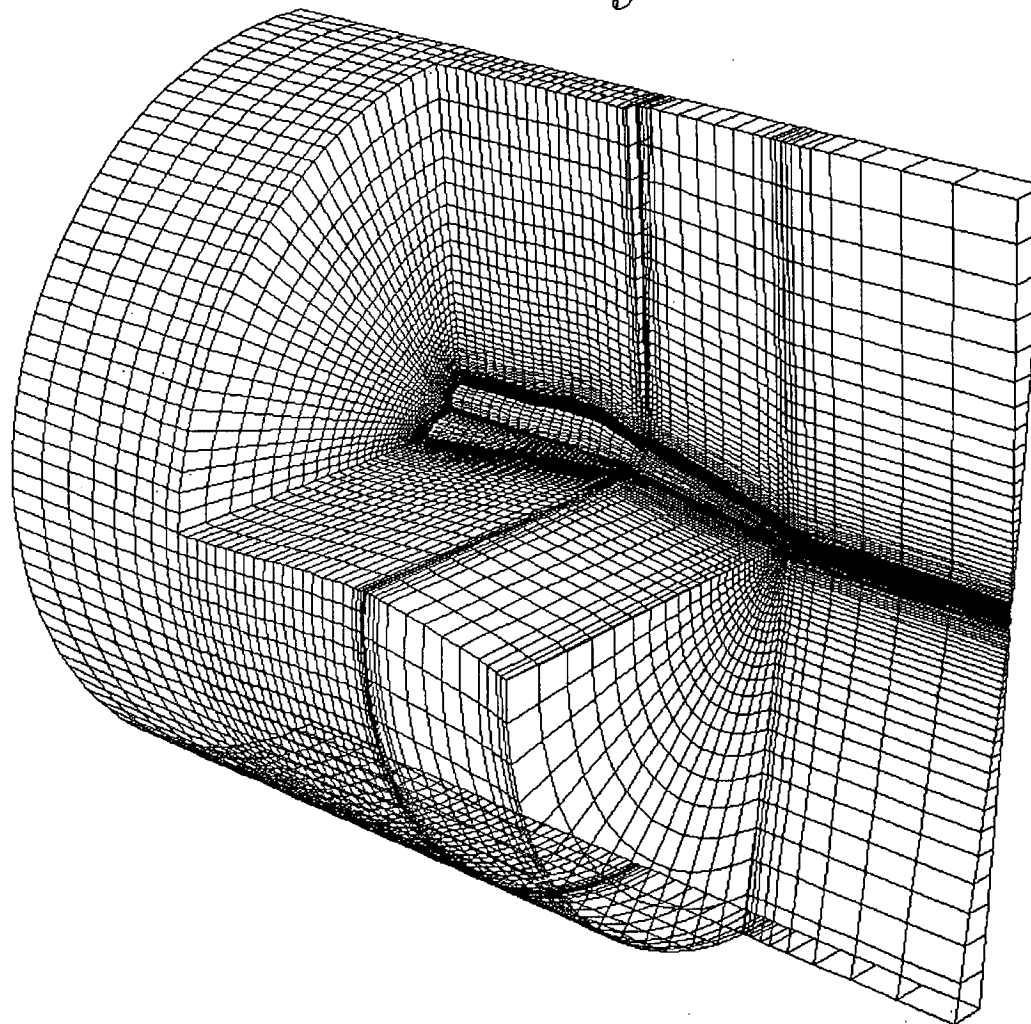
Overview

- Navier-Stokes Formulation
 - CFL-3D
- Grid Generation
 - Transfinite interpolation
- Results
 - Laminar, turbulent flow
 - Comparisons with wind-tunnel experiment
 - Comparisons with flight test
- Summary

Grid Generation - Transfinite interpolation

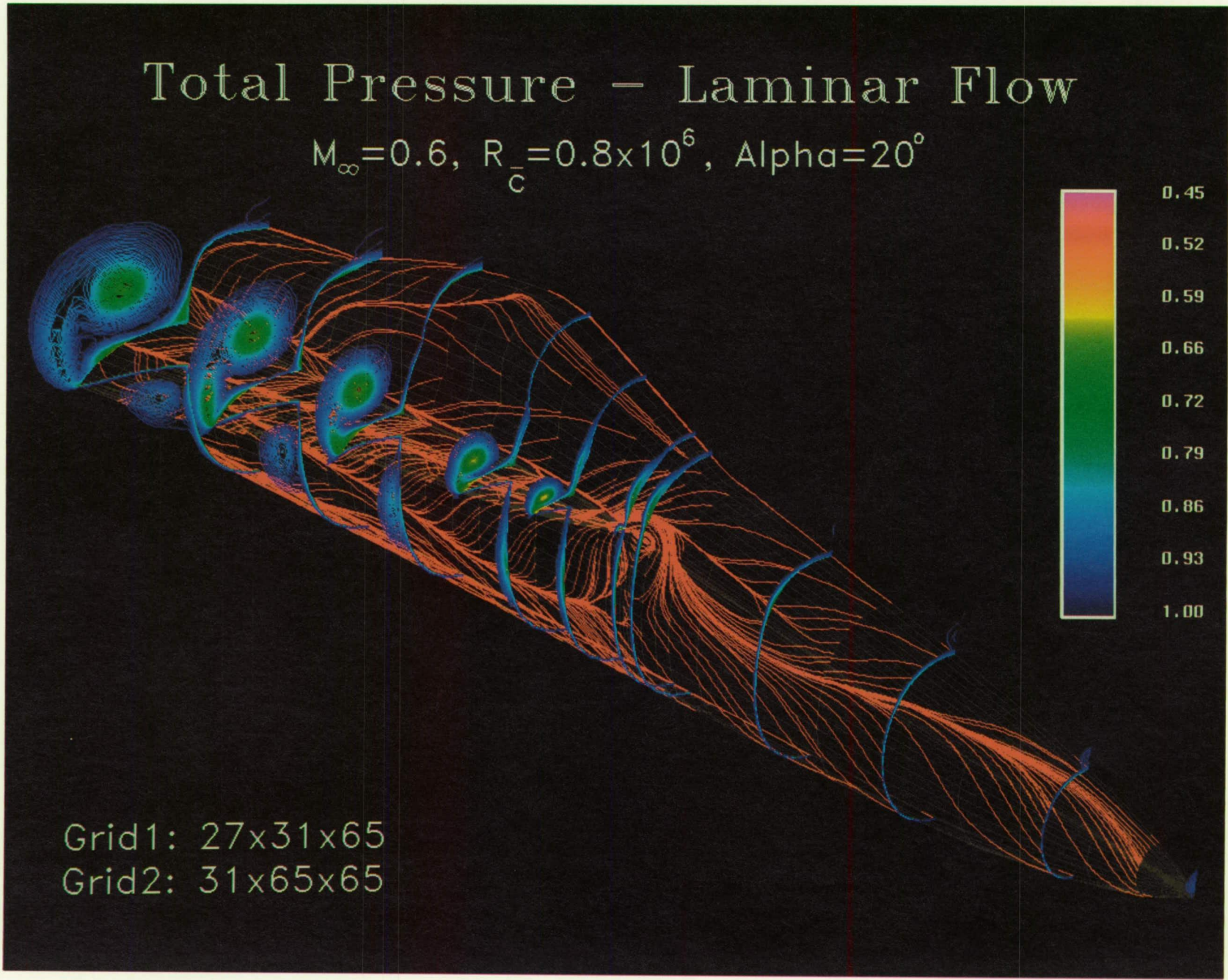
- H-O topology
- Far field
 - Inflow, outflow $\approx 1 \bar{c}$
 - Radial $\approx 1.5 \bar{c}$
- Baseline grid
 - Block 1 : $31 \times 65 \times 27$
 - Block 2 : $65 \times 65 \times 31$
 - Approximately 185,000 points
 - $y^+ \approx 2$ for wind-tunnel conditions
 - $y^+ \approx 8$ for flight conditions
- Refined grid
 - Doubled number of radial points
 - Normal surface spacing $\approx 0.25 \times$ baseline
 - $y^+ \approx 3$ for flight conditions

F-18 Forebody-LEX Grid



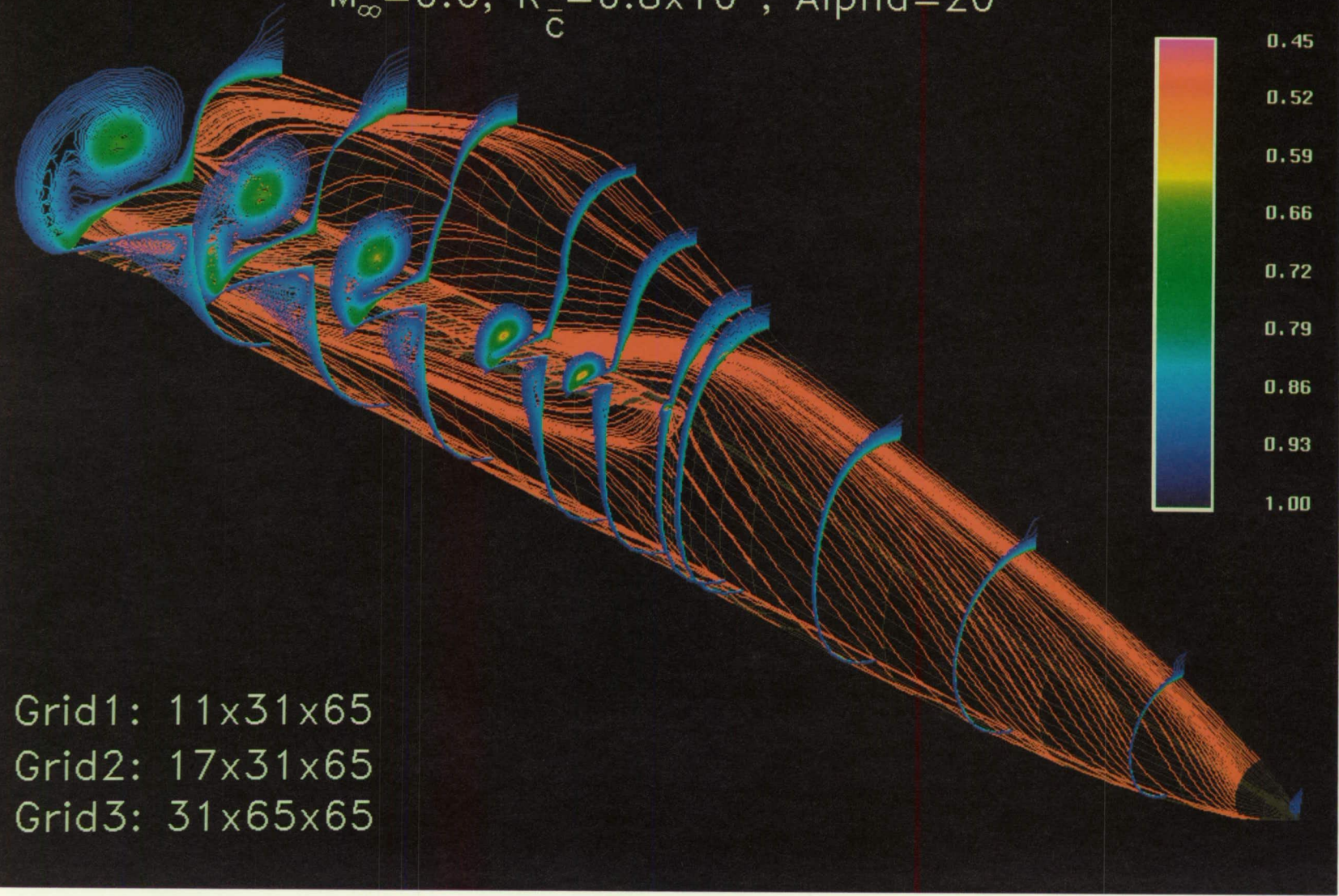
Computed Results

- Wind tunnel conditions
 - $M_\infty = 0.6$, $R_{\bar{c}} = 0.8 \times 10^6$, $\alpha = 20^\circ$
 - Laminar, turbulent flow
 - Comparison with experiment
- Flight conditions
 - $M_\infty = 0.34$, $R_{\bar{c}} = 13.5 \times 10^6$, $\alpha = 19^\circ$
 - Turbulent flow
 - Comparison with experiment



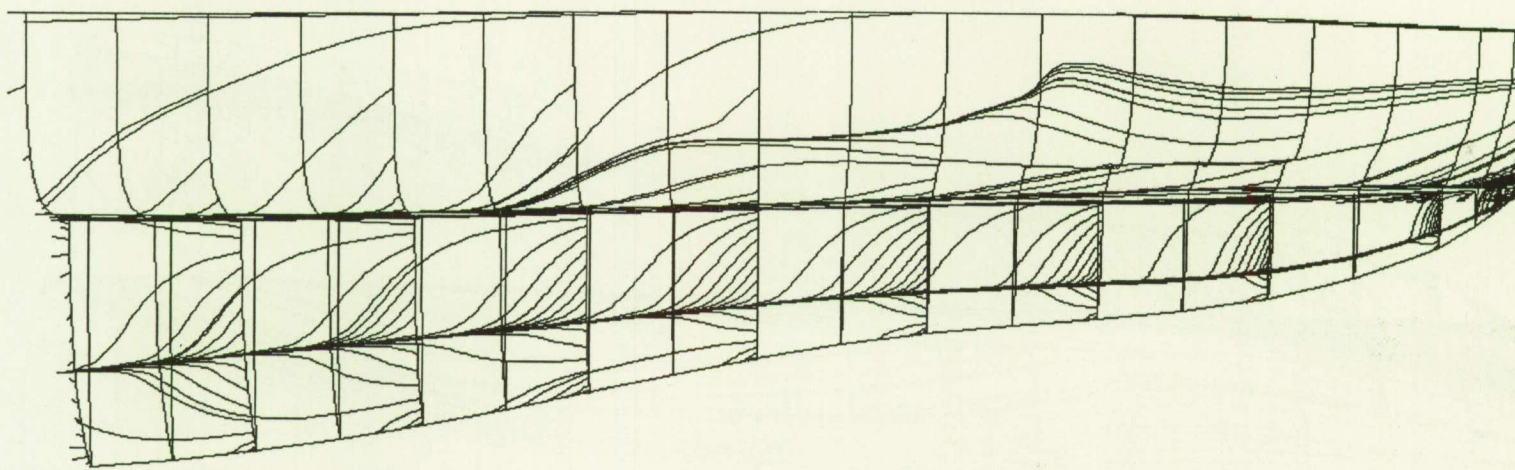
Total Pressure - Turbulent Flow

$M_\infty = 0.6$, $R_c = 0.8 \times 10^6$, $\text{Alpha} = 20^\circ$



LEX Upper Surface Flow - Laminar

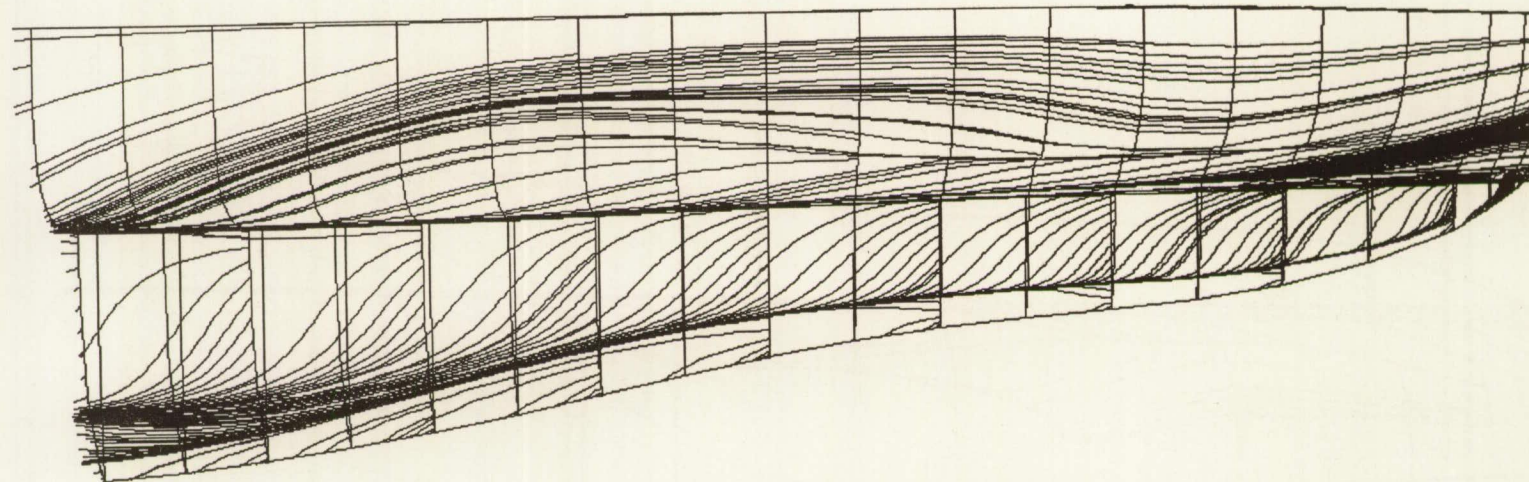
$M_\infty = 0.6$, $R_c = 0.8 \times 10^6$, $\text{Alpha} = 20^\circ$



Grid1: 27x31x65
Grid2: 31x65x65

LEX Upper Surface Flow - Turbulent

$M_\infty = 0.6$, $R_c = 0.8 \times 10^6$, $\text{Alpha} = 20^\circ$



372

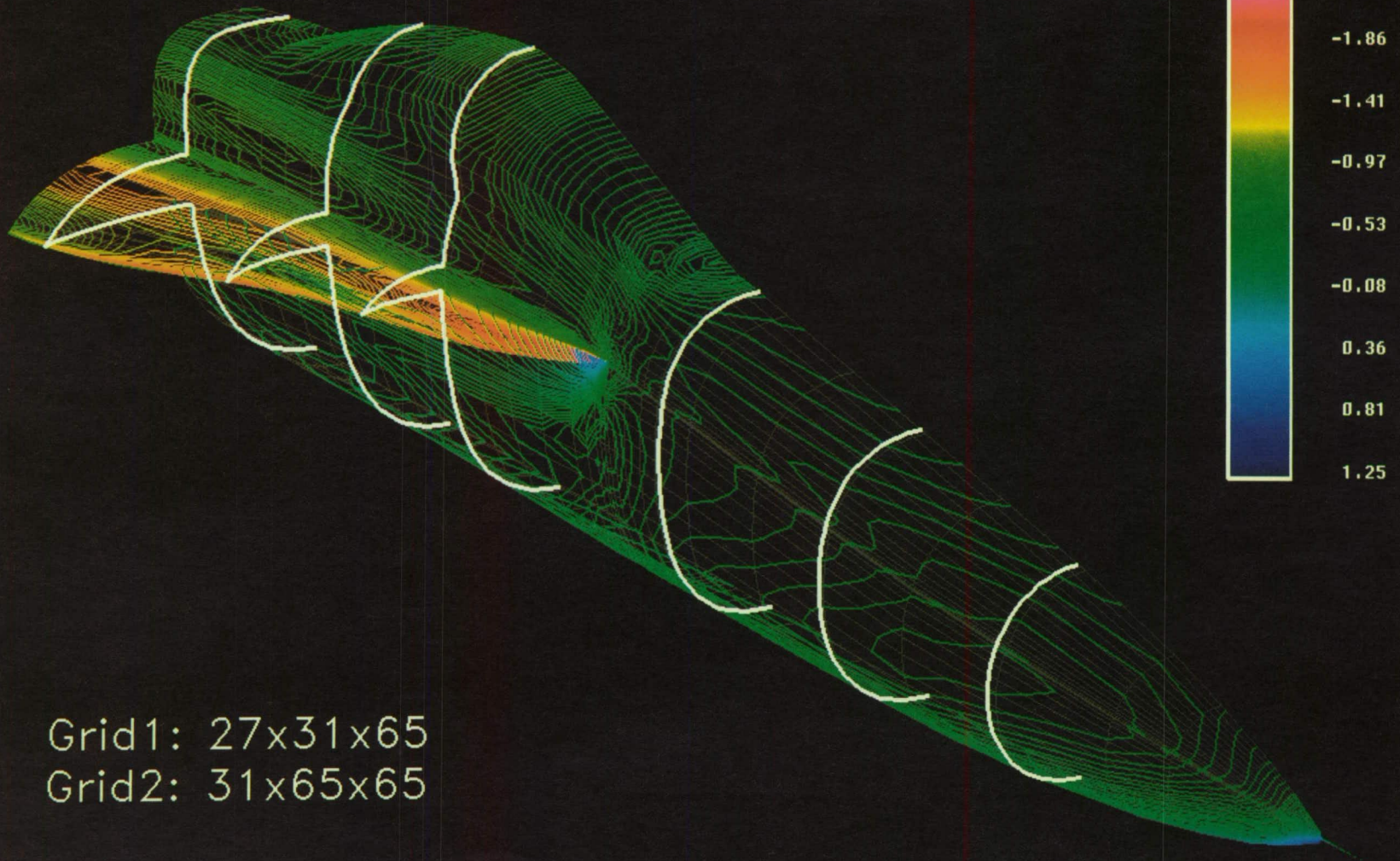
Grid1: 11x31x65

Grid2: 17x31x65

Grid3: 31x65x65

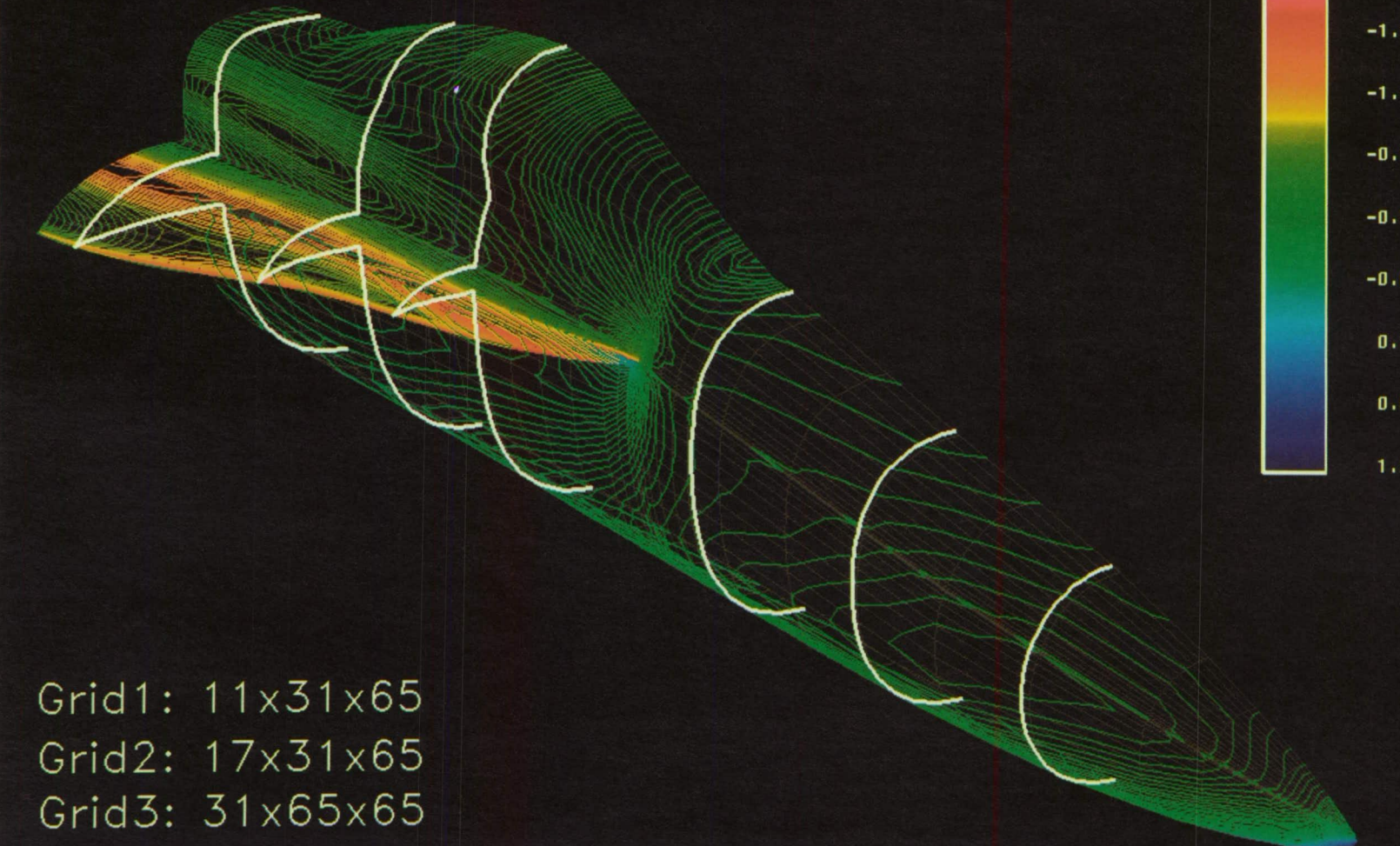
Surface Pressure Coefficient - Laminar Flow

$M_\infty = 0.6$, $R_c = 0.8 \times 10^6$, $\text{Alpha} = 20^\circ$



Surface Pressure Coefficient - Turbulent Flow

$M_\infty = 0.6$, $R_\infty = 0.8 \times 10^6$, $\text{Alpha} = 20^\circ$

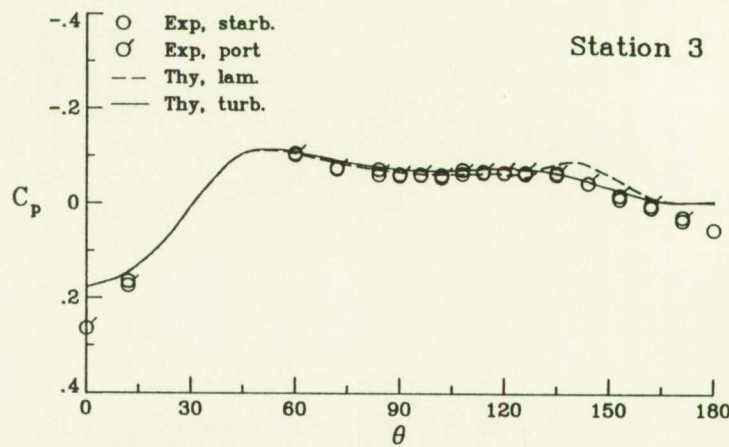
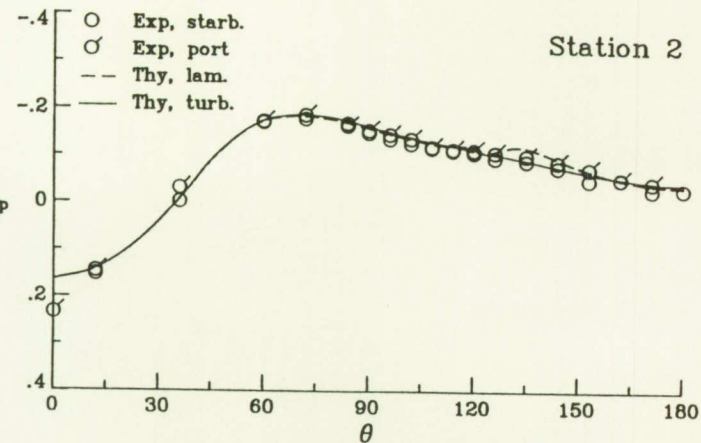


Forebody Surface Pressure

$$M_\infty = 0.6, R_\infty = 0.8 \times 10^6, \alpha = 20^\circ$$

ORIGINAL PAGE IS
OF POOR QUALITY

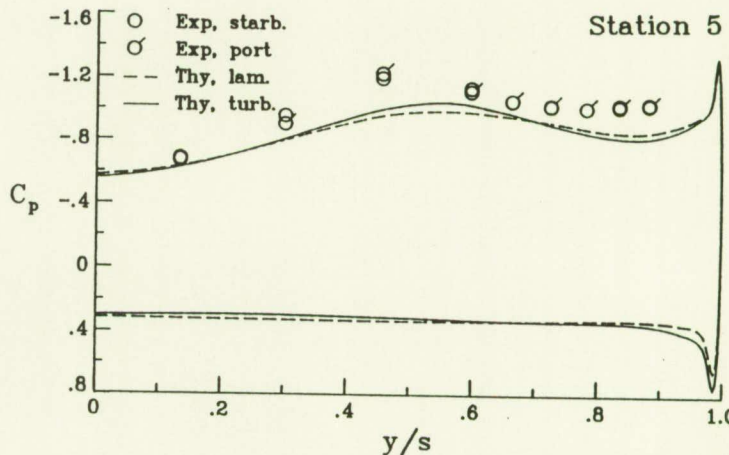
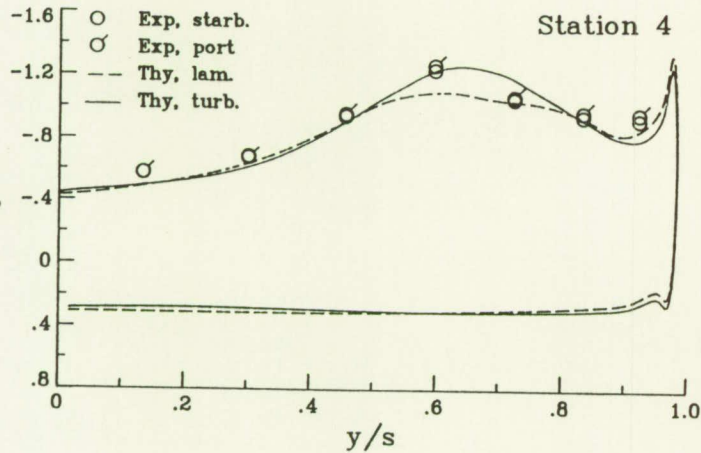
377



LEX Surface Pressure

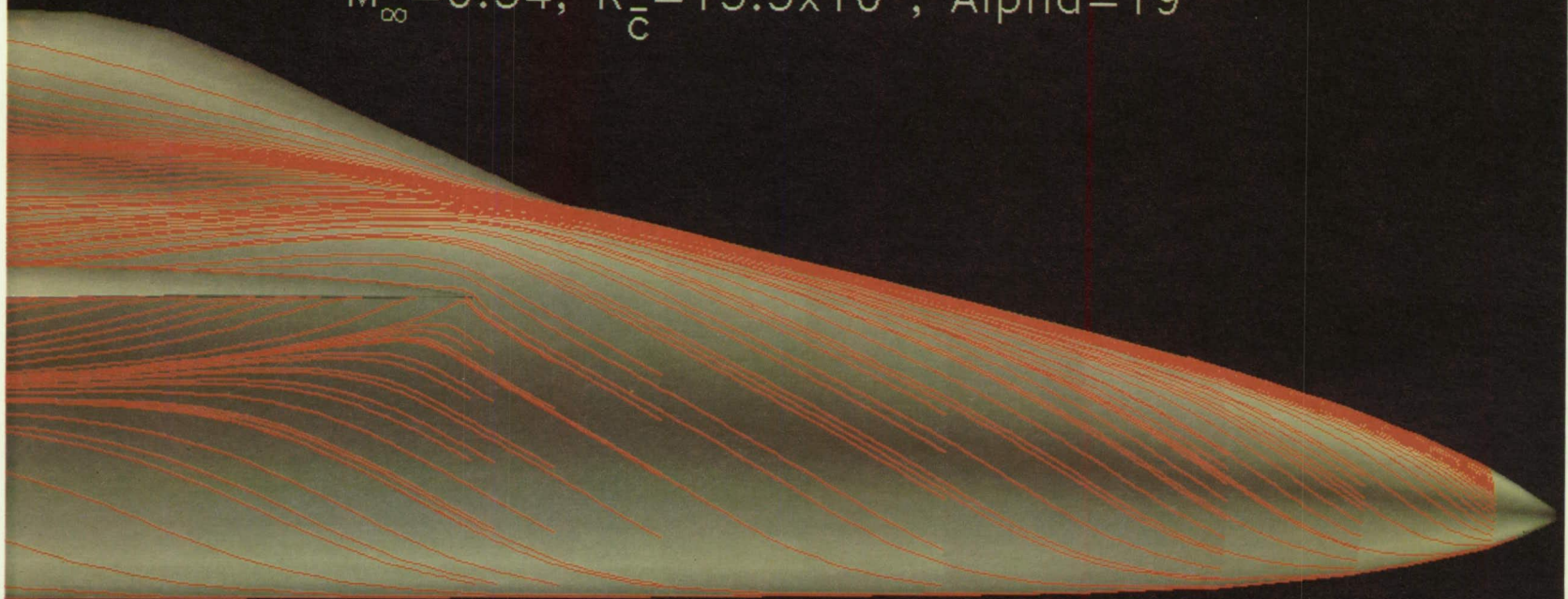
PRE

PRECEDING PAGE BLANK NOT FILMED

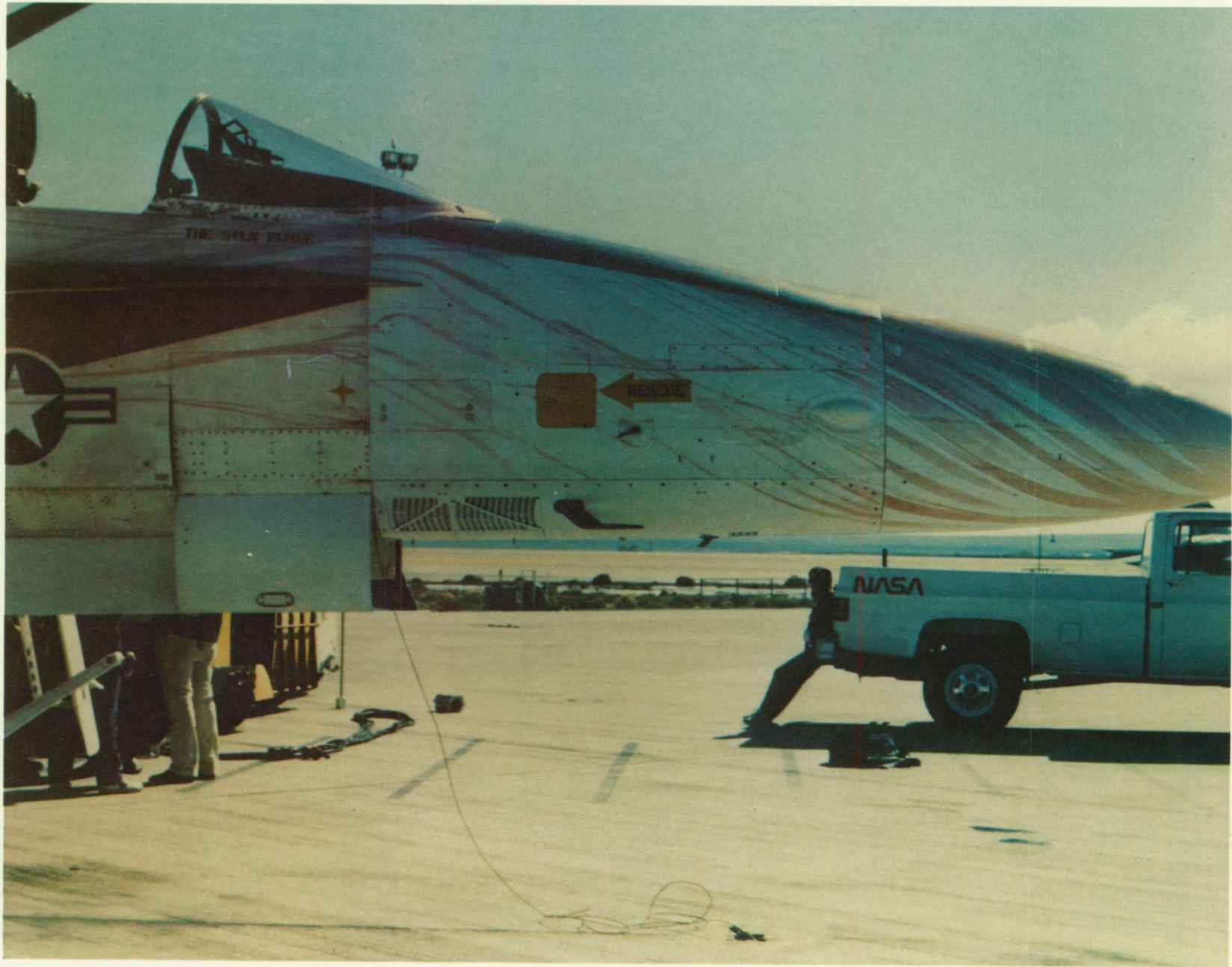


Turbulent Surface Flow - Side View

$M_\infty = 0.34$, $R_\infty = 13.5 \times 10^6$, $\text{Alpha} = 19^\circ$



Grid1: 11x31x65
Grid2: 17x31x65
Grid3: 31x65x65



Summary of Results

- Significant differences between laminar and turbulent solutions
 - Forebody
 - LEX upper surface
 - Body-LEX juncture on lower surface
- Turbulent solutions provide good correlation with experiment
 - Surface C_p comparison with wind tunnel data
 - Surface flow comparison with flight test data
- Convergence achieved with practical resource utilization
 - $\approx 185,000$ points
 - ≈ 2400 cycles
 - ≈ 2 hours of Cray-2 time

N 9 1 - 1 0 8 6 1

NAVIER-STOKES SOLUTIONS FOR FLOWS RELATED TO STORE SEPARATION

OKTAY BAYSAL

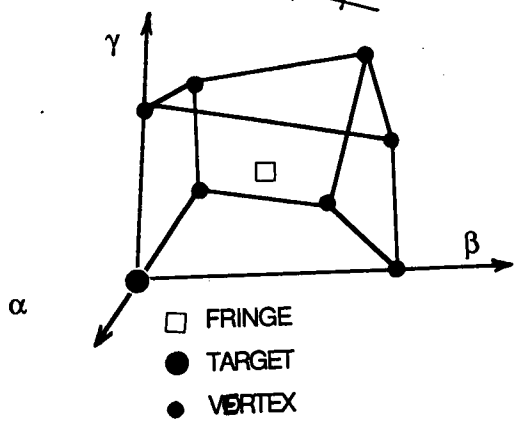
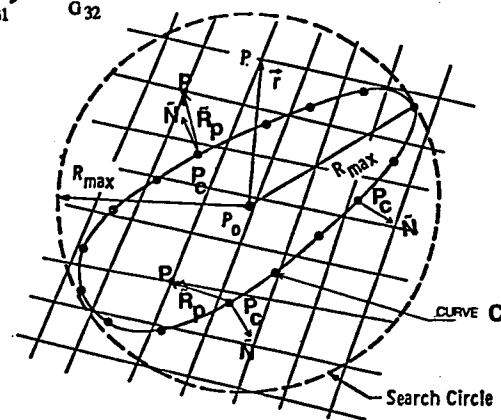
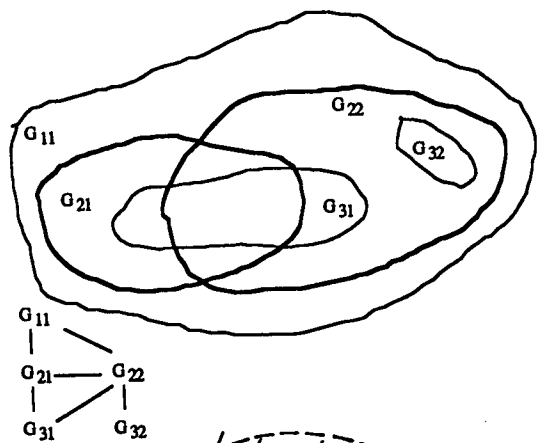
OLD DOMINION UNIVERSITY
NORFOLK, VIRGINIA 23529

ROBERT L. STALLINGS, JR.

ELIZABETH B. PLETOVICH

NASA Langley Research Center
Hampton, Virginia 23665

The objective is developing CFD capabilities to obtain solutions for viscous flows about generic configurations of internally and externally carried stores. The emphasis is placed on the supersonic flow regime with extensions being made to the transonic regime. The project is broken into four steps : (A) Cavity flows for internal carriage configurations; (B) High angle of attack flows, which may be experienced during the separation of the stores; (C) Flows about a body near a flat plate for external carriage configurations; (D) Flows about a body inside or in the proximity of a cavity. Three dimensional unsteady cavity flow solutions are obtained by an explicit, MacCormack algorithm, EMCAV3, for open, close, and transitional cavities. High angle of attack flows past cylinders are solved by an implicit, upwind algorithm. All the results compare favorably with the experimental data. For flows about multiple body configurations, the Chimera embedding scheme is modified for finite-volume and multigrid algorithms, MaGGIE. Then a finite volume, implicit, upwind, multigrid Navier-Stokes solver which uses on overlapped/embedded and zonal grids, VUMXZ3, is developed from the CFL3D code. Supersonic flows past a cylinder near a flat plate are computed using this code. The results are compared with the experimental data. Currently the VUMXZ3 code is being modified to accomplish step (D) of this project. Wind tunnel experiments are also being conducted for validation purposes.



ATTRIBUTES OF MaGGiE CODE

- SUBDOMAIN GRIDS GENERATED SEPARATELY AND INDEPENDENTLY.
- DISTANCE BETWEEN CELL CENTERS USED FOR INTERPOLATIONS.
- REGIONS OF A FINE LEVEL GRID COMMON TO OTHERS REMOVED (HOLES).
- REGIONS OF A COARSE LEVEL GRID OVERLAPPING SOLID SURFACES REMOVED (ILLEGAL ZONES).
- EDGES OF HOLES OR ILLEGAL ZONES ARE INTERGRID BOUNDARIES.
- 3-D VECTOR OPERATIONS TO LOCATE CELLS IN A HOLE OR AN ILLEGAL ZONE.
- CELLS OF OUTER BOUNDARY OF OVERLAP REGIONS (FRINGE CELL).
- IMMEDIATE-NEIGHBOR CELLS OF A HOLE OR AN ILLEGAL-ZONE CELL (FRINGE CELL).
- INFORMATION HEXAHEDRONS AROUND FRINGE CELLS FORMED.
- CELLS IN A HOLE BUT NOT IN AN ILLEGAL ZONE UPDATED

FROM	FINE LEVEL	OF OTHER GRIDS
	EQUAL COARSE LEVEL	
- COEFFICIENTS FOR TRILINEAR INTERPOLATIONS.
- VECTORIZED DATA STRUCTURES AS PREPROCESSOR FOR **VUMXZ3**
- DEVELOPED FROM CHIMERA.
- CHARACTERISTIC INTERGRID BOUNDARY CONDITIONS.

ATTRIBUTES OF VUMXZ3 CODE

- DEVELOPED FROM CFL3D CODE, HENCE INCLUDES ALL CFL3D ATTRIBUTES.
- ALL BUT CROSS-DERIVATIVE VISCOUS TERMS.
- BALDWIN-LOMAX TURBULENCE MODEL MODIFIED FOR VORTICAL FLOWS, MULTIPLE-WALLS, AND TURBULENT MEMORY RELAXATION FOR WAKES AND SHEAR LAYERS.
- BLOCK OR DIAGONAL INVERSIONS ACCOMODATE HOLES AND ILLEGAL ZONES FOR OVERLAPPED GRIDS.
- AVOIDS INFORMATION POLLUTION NEAR HOLES OR ILLEGAL ZONES FOR HIGHER ORDER SCHEMES.
- NULLIFIES WEIGHT OF CONTRIBUTIONS FROM ILLEGAL ZONES DURING 3-D MULTIGRID PROLONGATION.
- INTERGRID INFORMATION EXCHANGED BY TRILINEAR INTERPOLATIONS
COUPLED WITH CHARACTERISTIC BOUNDARY CONDITIONS.
- COMBINED ZONAL AND OVERLAPPED EMBEDDING.
- DEMONSTRATIVE CASES :

SUPersonic FLOW PAST A BLUNT-NOSE CYLINDER (L/D=6.7)

AT 32 °-ANGLE OF ATTACK ON

SINGLE C-O GRID.

C-O GRID EMBEDDED IN CARTESIAN GRID.

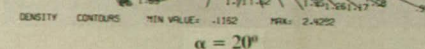
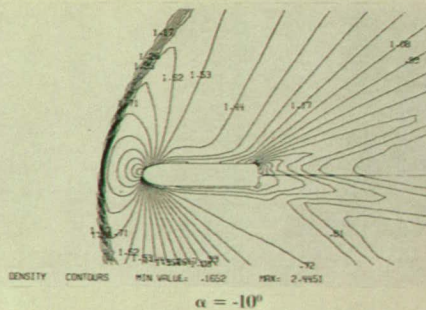
C-O GRID PATCHED TO H-O GRID.

SUPersonic FLOW PAST AN OGIVE-NOSE CYLINDER (L/D=18) NEAR
FLAT PLATE.

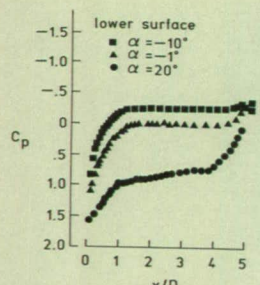
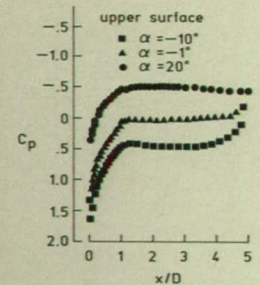
EFFECTS OF SHAPE AND INCIDENCE ON FLOW PAST A CYLINDRICAL SECTION

 $M_\infty = 1.6$ $Re_\infty = 2 \times 10^6 / \text{ft}$

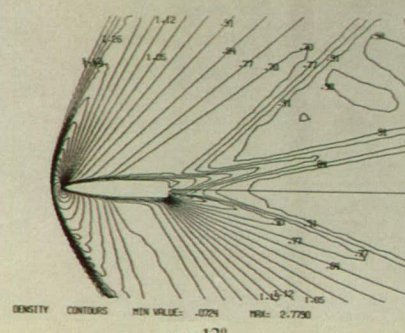
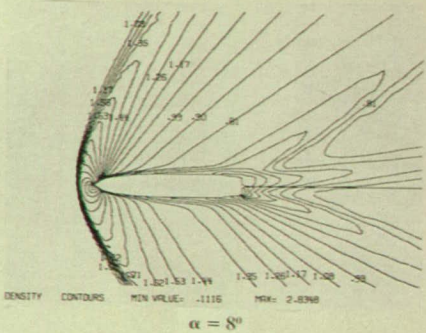
DENSITY



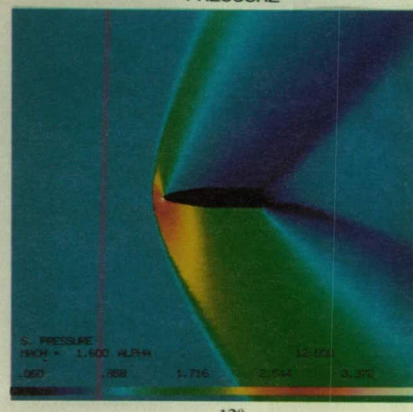
Cp



DENSITY



PRESSURE



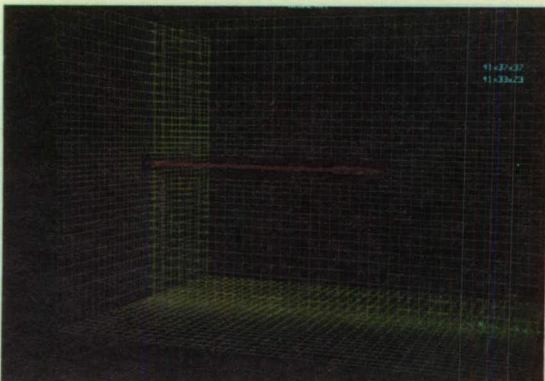
SECANT-OGIVE-NOSE-BOAT-TAIL CYLINDER

BLUNT-NOSE-CYLINDER

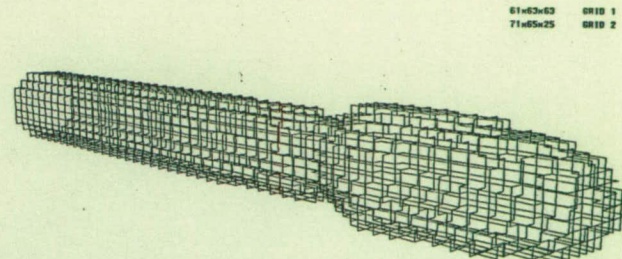
EMBEDDED GRIDS FOR BLUNT-NOSE-CYLINDER WITH STING

C-O GRID : 73x65x57

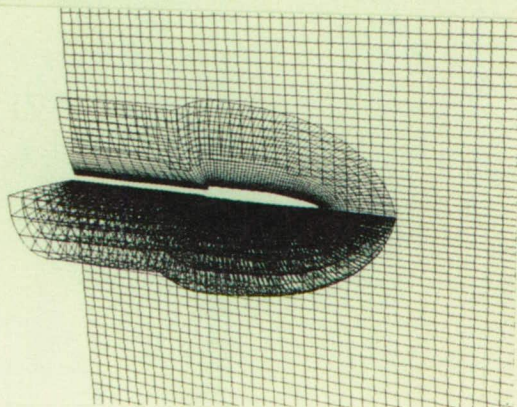
CARTESIAN GRID : 81x73x73



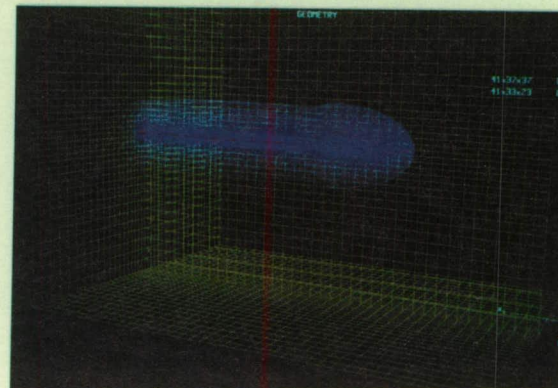
cartesian grid with hole



hole boundary cells



overlap of c-o with cartesian

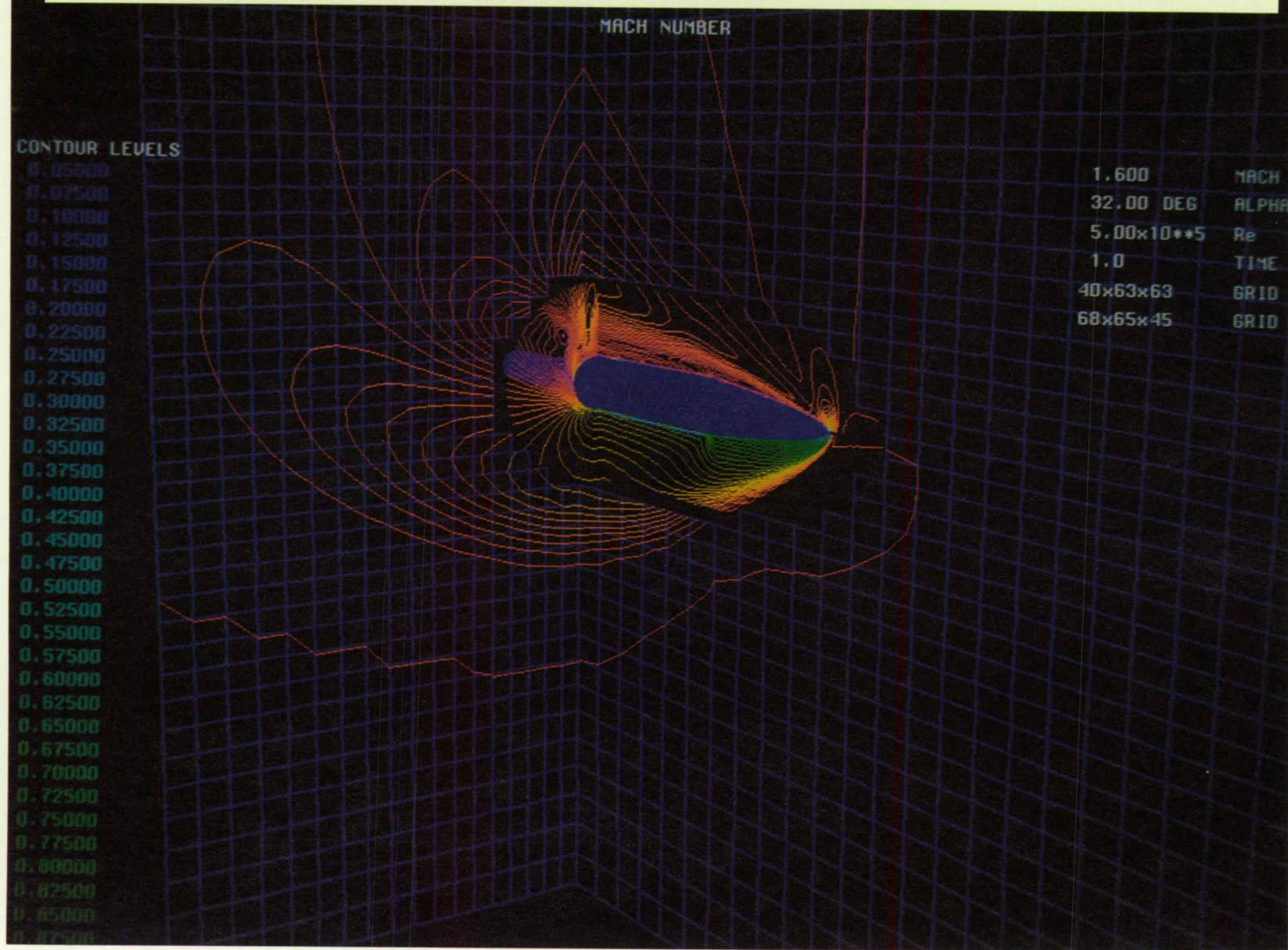


PRECEDING PAGE BLANK NOT FILMED

393

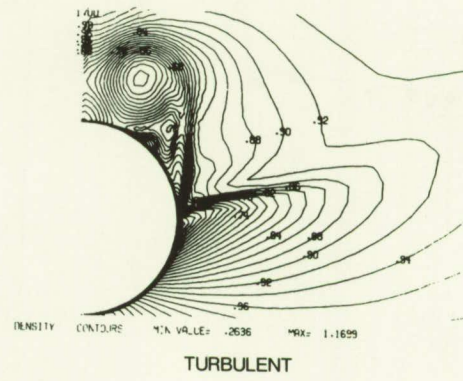
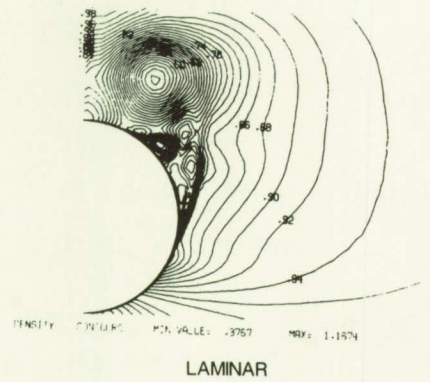
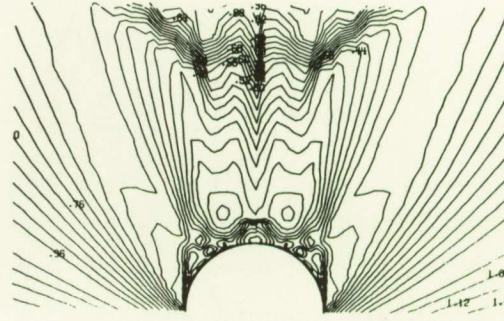
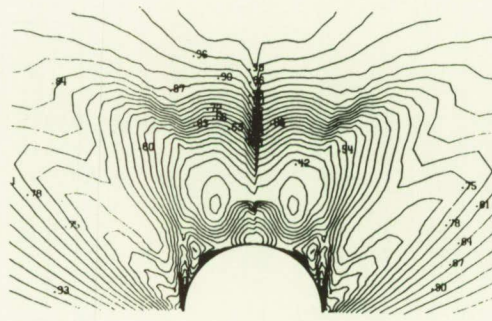
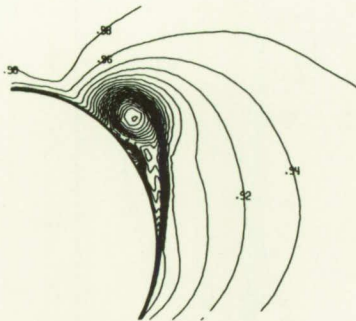
ORIGINAL PAGE IS
OF POOR QUALITY

MACH CONTOURS OF FLOW (M=1.6 , RE=2E6/FT) PAST OGIVE-NOSE CYLINDER (L/D=6.7 , alpha=32)



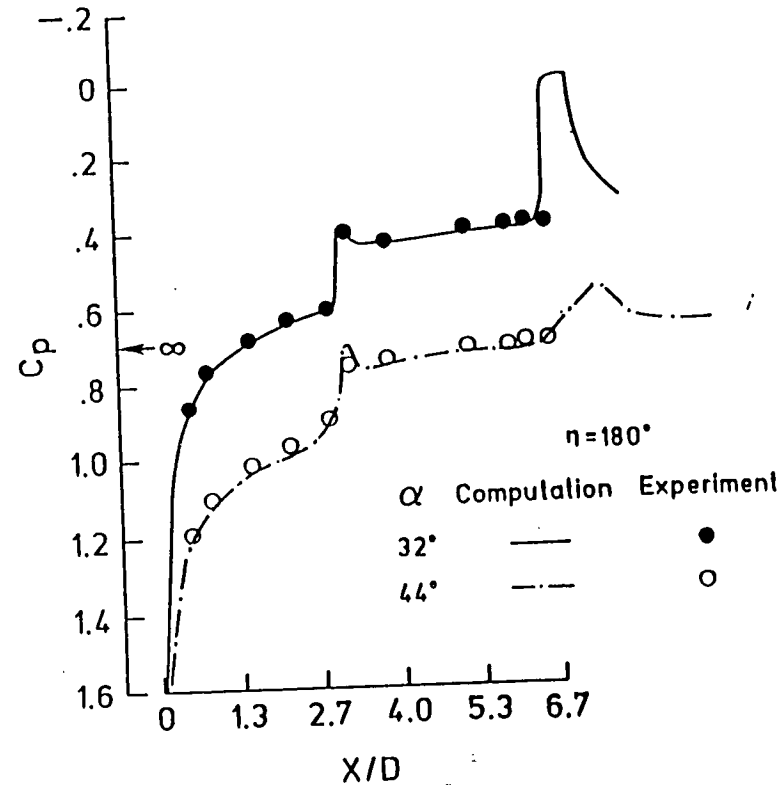
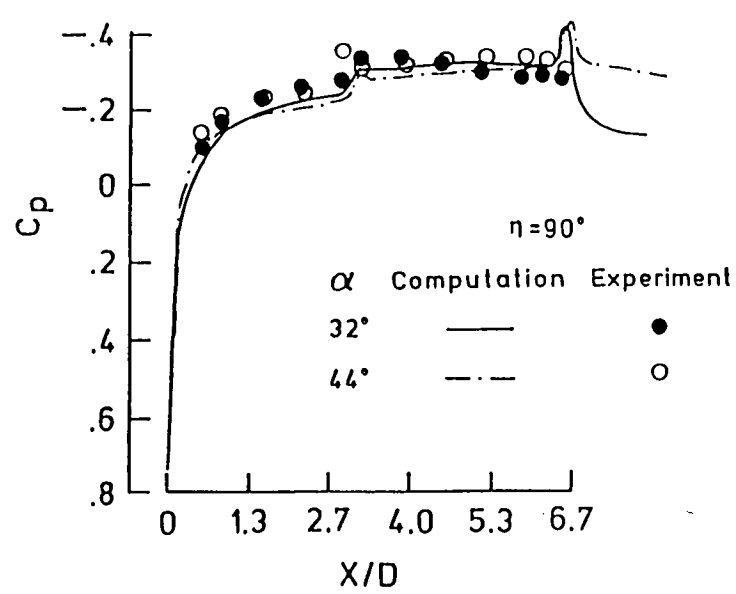
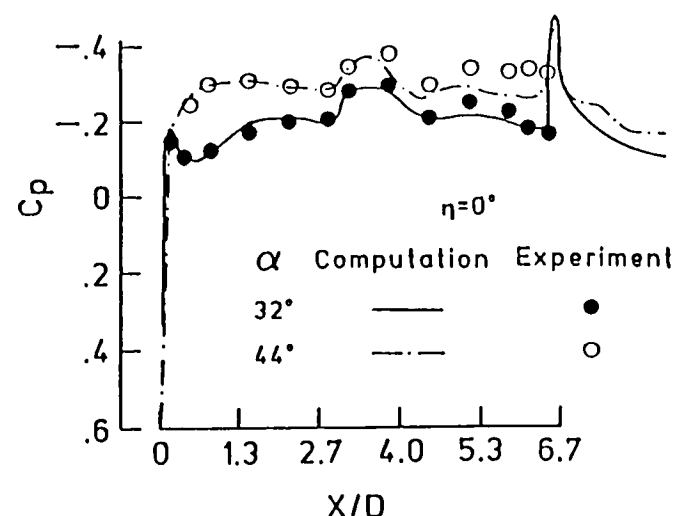
CROSSFLOW DENSITY CONTOURS OF FLOW PAST A BLUNT-NOSE-CYLINDER

$M_\infty = 1.6$ $Re_\infty = 2 \times 10^6 / \text{ft}$



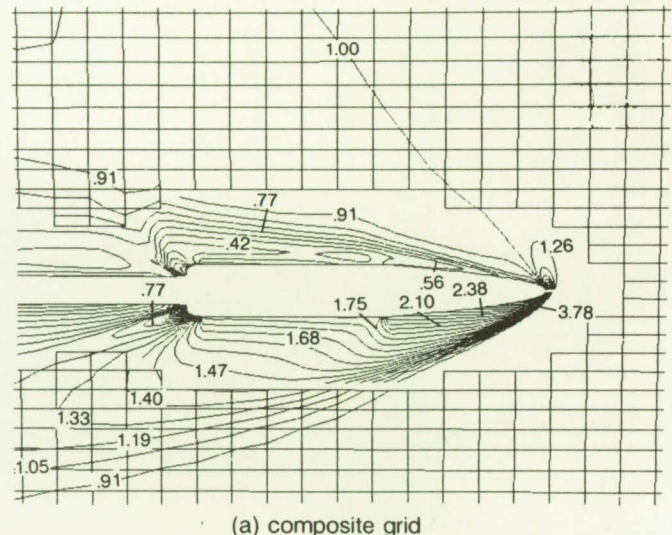
2

FLOW PAST A BLUNT-NOSE CYLINDER (L/D=6.7 , M=1.6 , Re=2E6/FT) $\eta=0$ LEESIDE, $\eta=180$ WINDSIDE

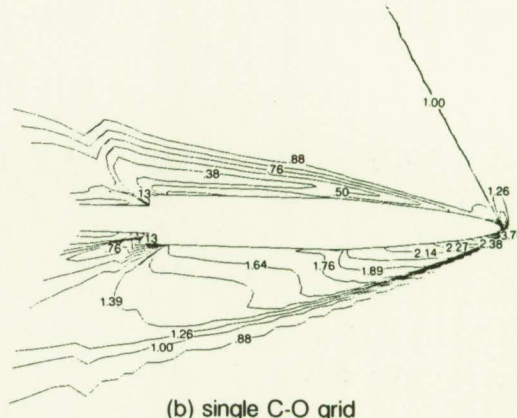


PRESSURE CONTOURS ON THE SYMMETRY PLANES OF BLUNT-NOSE-CYLINDER

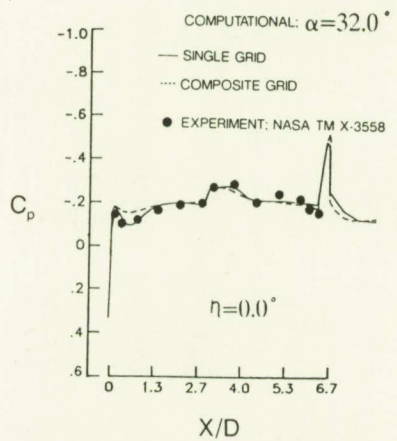
$$M_\infty = 1.6 \quad Re_\infty = 2 \times 10^6 / \text{ft} \quad \alpha = 32^\circ$$



(a) composite grid



(b) single C-O grid

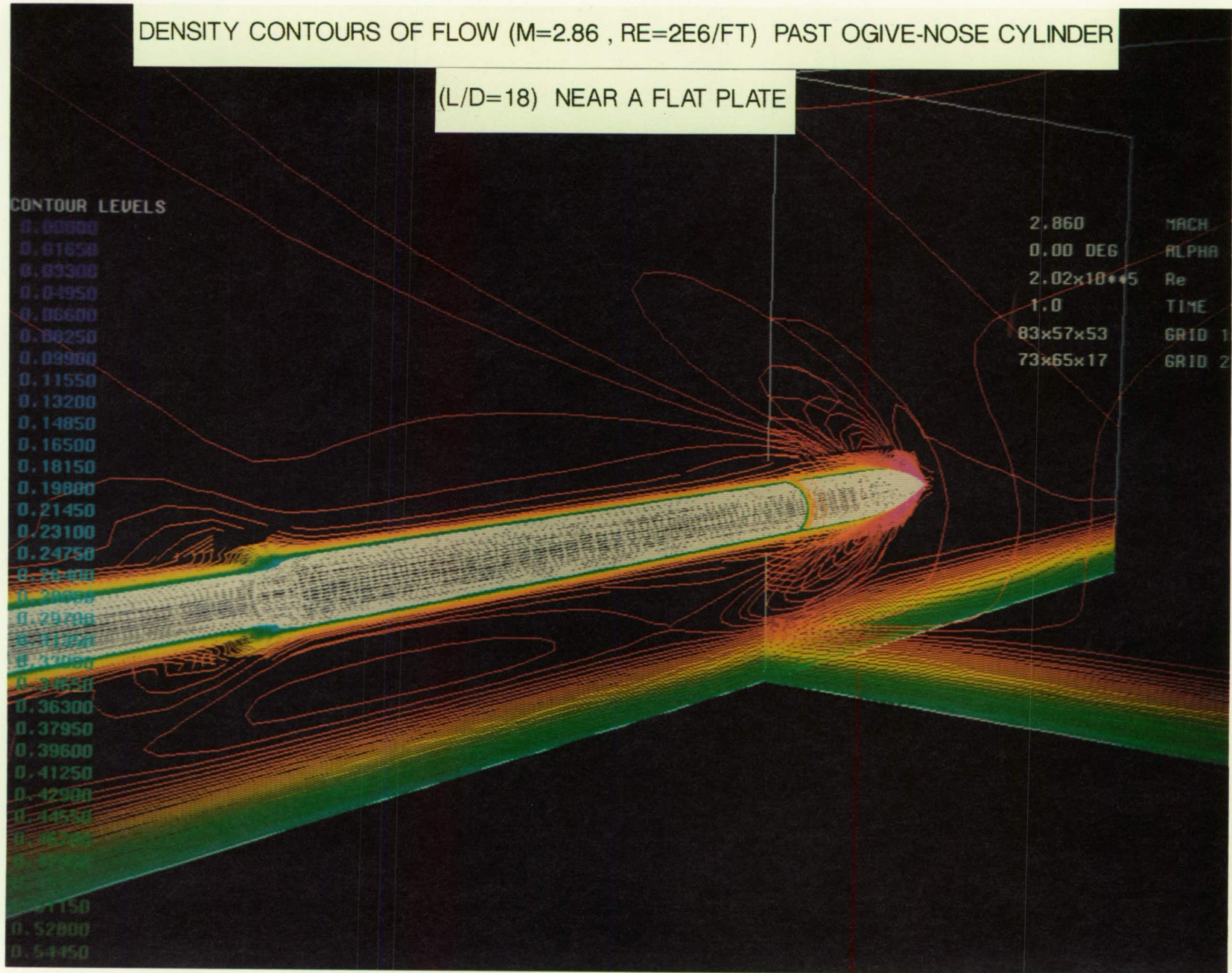


(c) C_p on leeside

PRECEDING PAGE BLANK NOT FILMED

399

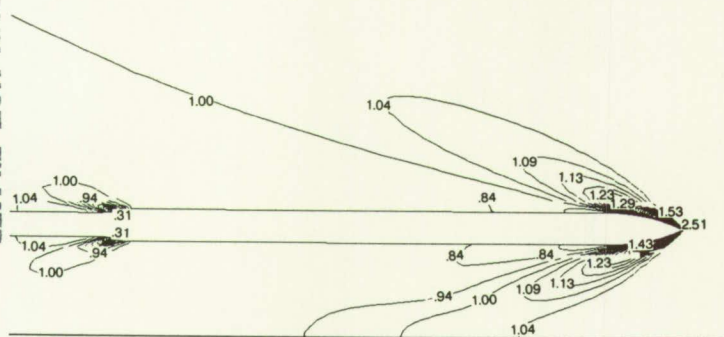
ORIGINAL PAGE IS
OF POOR
QUALITY



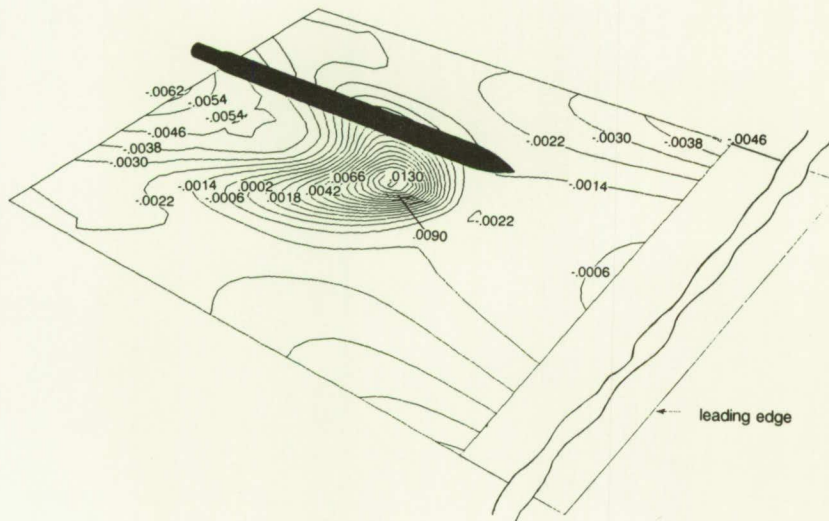
FLOW OVER OGIVE-NOSE-CYLINDER NEAR FLAT PLATE

$M_\infty = 2.86$ $Re_\infty = 2 \times 10^6 / \text{ft}$ $\alpha = 0^\circ$

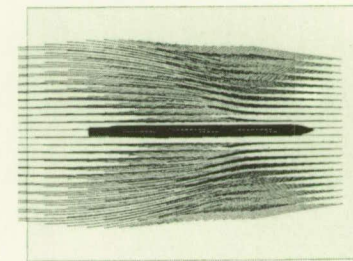
Pressure Contours on the Symmetry Plane of ONC



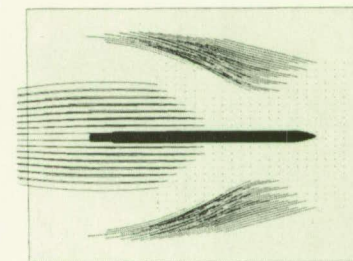
Pressure Coefficient Contours on the surface of the flat plate



Skin Friction Patterns near the flat plate surface



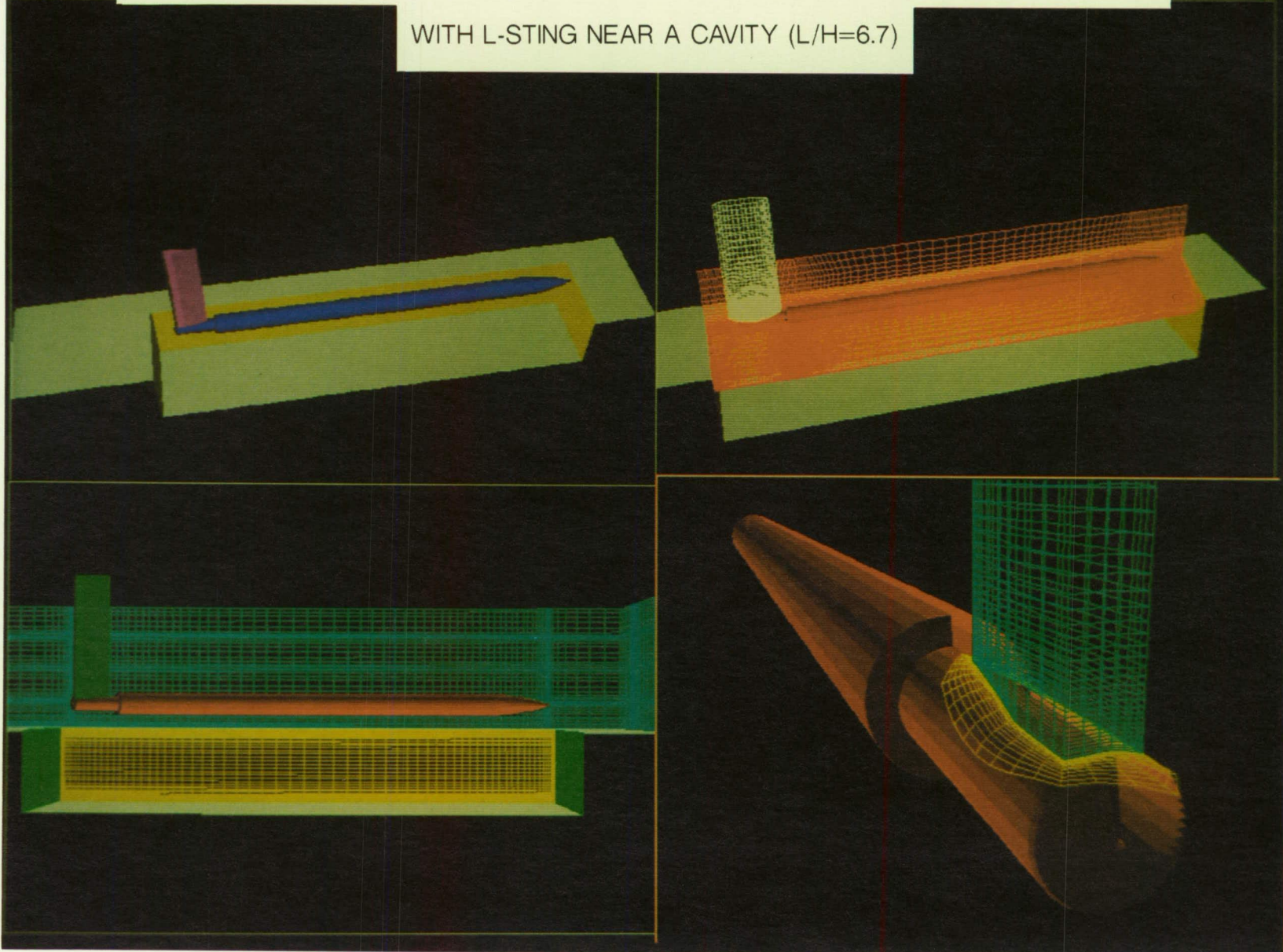
(a) two cells above the surface



(b) one cell above the surface

OVERLAPPED/EMBEDDED AND ZONAL GRIDS FOR OGIVE-NOSE CYLINDER (L/D=20)

WITH L-STING NEAR A CAVITY (L/H=6.7)



PRECEDING PAGE BLANK NOT FILMED

ATTRIBUTES OF EMCAV3

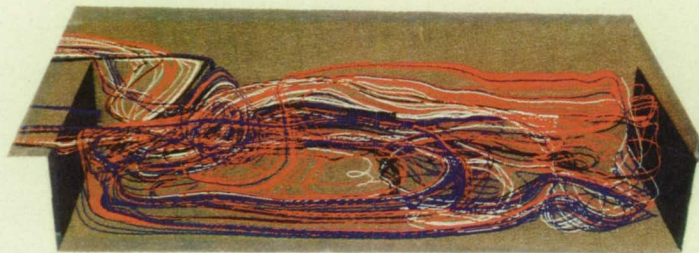
- 3-D REYNOLDS-AVERAGED NAVIER-STOKES EQUATIONS FOR UNSTEADY COMPRESSIBLE FLOW.
- EXPLICIT, UNSPLIT, PREDICTOR-CORRECTOR TIME INTEGRATION (MACCORMACK).
- FINITE DIFFERENCE SPATIAL DISCRETIZATION.
- SECOND ORDER ACCURATE IN TIME AND SPACE.
- VECTORIZED DATA STRUCTURE.
- DEVELOPED FROM SCRM32.
- ALGEBRAIC GRID GENERATOR.

405

- BALDWIN-LOMAX TURBULENCE MODEL MODIFIED FOR VORTICAL FLOWS.
MULTIPLE WALLS.
TURBULENT MEMORY RELAXATION FOR SHEAR LAYER.
- IMPLICIT MARCHING SOLUTION FOR 2-D COMPRESSIBLE BOUNDARY LAYER PROFILE.
- FOURIER TIME SERIES ANALYSIS FOR CAVITY ACOUSTICS.
- DEMONSTRATIVE CASES

2-D 3-D SUBSONIC
TRANSONIC
SUPERSONIC FLOWS AT 0°
45° YAW PAST DEEP
TRANSITIONAL
SHALLOW CAVITIES.

INSTANTANEOUS STREAMLINES OF FLOW PAST RECTANGULAR CAVITIES



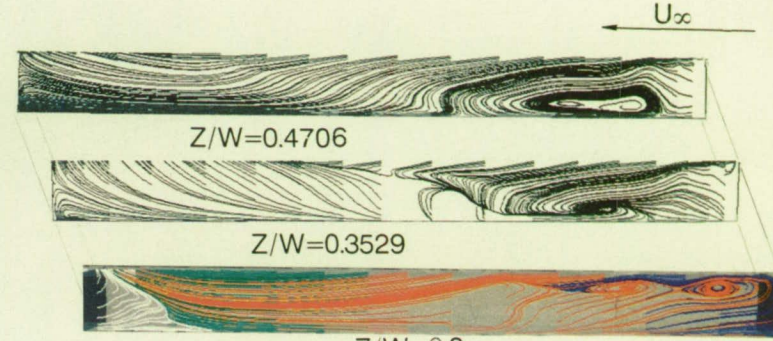
$M_\infty = 1.5$ $L/D = 6$ $Re = 6.56 \times 10^6 / m$



$M_\infty = 1.5$ $L/D = 16$ $Re = 6.56 \times 10^6 / m$

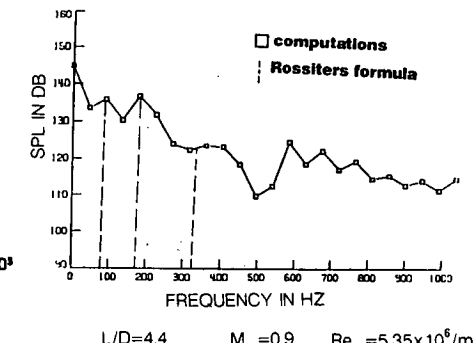
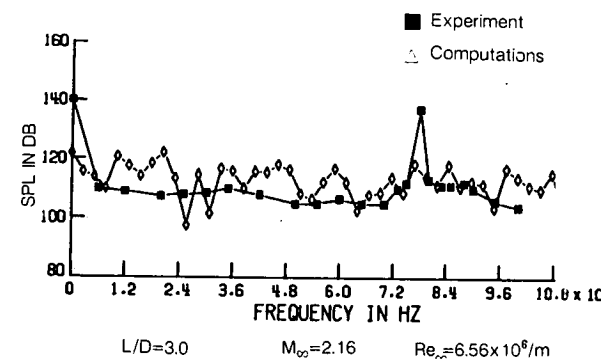
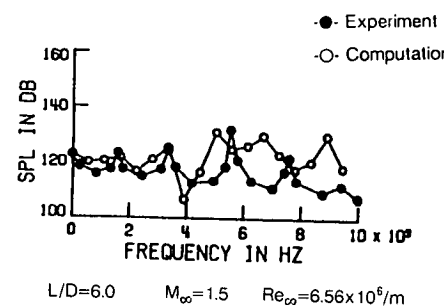
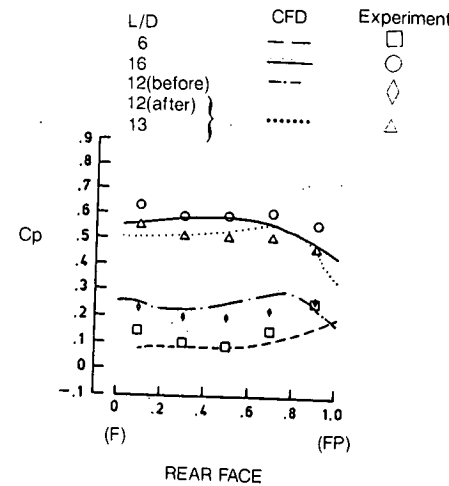
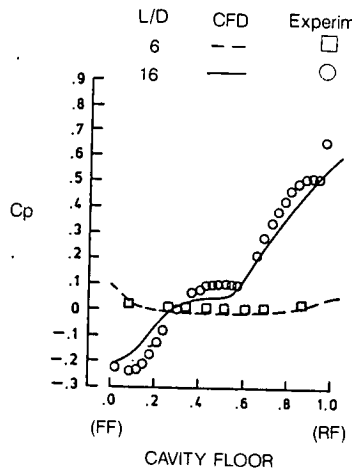


$M_\infty = 0.9$ $L/D = 4.4$ $Re = 5.35 \times 10^6 / m$



$M_\infty = 0.58$ $L/D = 11.7$ $Re = 5.02 \times 10^6 / m$

FREQUENCY SPECTRA OF SOUND PRESSURE LEVEL ON THE CAVITY FLOOR

Cp FOR $M_{\infty} = 1.5$ $Re_{\infty} = 6.56 \times 10^6/m$ FLOW

CONCLUSIONS

- 3-D CFD CAPABILITIES FOR UNSTEADY CAVITY FLOWS.
- TIME-AVERAGED AND TIME SERIES ANALYSES OF CAVITY FLOWS :
 - EFFECTS OF LENGTH-TO DEPTH, FLOW REGIMES, YAW ANGLES.
- 2-D ANALYSES OF FLOWS PAST VARIOUS CYLINDRICAL SECTIONS AT VARIOUS ANGLES OF ATTACK.
- 3-D ANALYSES OF LAMINAR AND TURBULENT FLOWS PAST A BODY OF REVOLUTION
 - AT VARIOUS ANGLES OF ATTACK.
- 3-D CFD CAPABILITIES DEVELOPED FOR VISCOS FLOWS ABOUT
 - COMPLEX AND/OR MULTICOMPONENT CONFIGURATIONS.
- COMBINED ADVANTAGES : GEOMETRICALLY CONSERVATIVE, MINIMALLY DISSIPATIVE
 - : NUMERICALLY AND COMPUTATIONALLY EFFICIENT.
 - : FLEXIBILITY IN BODY GEOMETRIES AND GRID TOPOLOGIES.
- FLUX CONSERVATION ACROSS INTERGRID BOUNDARIES NEED FURTHER STUDY.
- ANALYSES OF AERODYNAMIC INTERFERENCE OF A STORE NEAR A FLAT PLATE (EXTERNAL CARRIAGE).
- WORK-IN-PROGRESS : CFD SOLUTIONS FOR FLOWS PAST AN OGIVE-NOSE-CYLINDER WITH L-SHAPE STING NEAR A CAVITY AND CODE VALIDATION WIND TUNNEL EXPERIMENTS.

TranAir: Recent Advances and Applications

Michael D. Madson

NASA Ames Research Center, Moffett Field, CA

March 8, 1989

Abstract

TranAir is a computer code which solves the full-potential equation for transonic flow about very general and complex configurations. Piecewise flat surface panels are used to describe the surface geometry. This paneled definition is then embedded in an unstructured cartesian flow field grid. Finite elements are used in the discretization of the flow field grid in a manner which is fully conservative and 2nd-order accurate. Since geometries may be defined with relative ease, and since the user is not involved in the generation of the flow field grid, computational results may be generated rather quickly for a wide range of geometries. For transonic cases in the cruise angle-of-attack range, TranAir has generated results which are in generally good agreement with both Euler results and wind tunnel data. A typical transonic case runs in 1-2 CPU hours on a Cray X-MP. For subcritical cases, the code runs in 15-30 CPU minutes, even for geometries in which several thousand surface panels are used in the definition. This ability to rapidly and accurately provide both subsonic and transonic predictions about very complex aircraft configurations gives TranAir the potential of being a very powerful and widely used design tool.

Acknowledgements

TranAir is being developed by Boeing Advanced Systems, Seattle, WA, under contract to NASA. The author wishes to thank Forrester Johnson, Satish Samant, David Young, Robin Melvin and John Bussoletti for their dedicated work in the development of the code, and for providing many of the results presented in the charts which follow.

TRANAIR: RECENT ADVANCES AND APPLICATIONS

MICHAEL D. MADSON

NASA Ames Research Center

ACKNOWLEDGEMENTS

Forrester T. Johnson, Satish S. Samant, David P. Young,
Robin G. Melvin, and John E. Bussoletti

412

OUTLINE

- OBJECTIVE
- APPROACH
- RECENT ADVANCES
- APPLICATIONS
- OBSERVATIONS
- POSSIBLE FUTURE DIRECTIONS

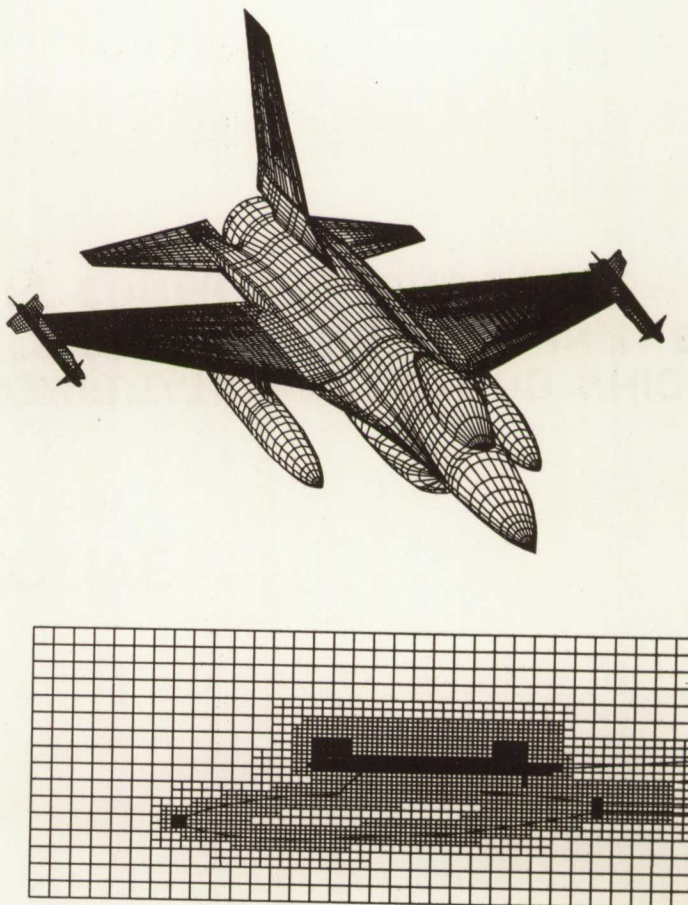
OBJECTIVE

413

**TO DEVELOP AND VALIDATE A COMPUTATIONAL METHOD WHICH
ELIMINATES THE USE OF SURFACE-CONFORMING GRIDS IN THE
ANALYSIS OF COMPLEX AIRCRAFT CONFIGURATIONS IN THE
TRANSONIC FLOW REGIME.**

APPROACH

- GEOMETRY DEFINED BY SURFACE PANELS
- EMBEDDED IN UNIFORM CARTESIAN GRID
- LOCAL GRID REFINEMENT CAPABILITY BASED ON
 - LOCAL PANEL SIZE
 - USER INPUT
- SOLUTION PROCESS
 - GRID DISCRETIZED W/FINITE ELEMENTS, CONSERVATIVE, 2ND ORDER
 - SET OF NONLINEAR ALGEBRAIC EQNS SIMULATE FULL-POTENTIAL
 - 1ST ORDER DISSIPATION FOR SHOCK CAPTURING
 - SET OF EQNS SOLVED BY ITERATIVE PROCESS



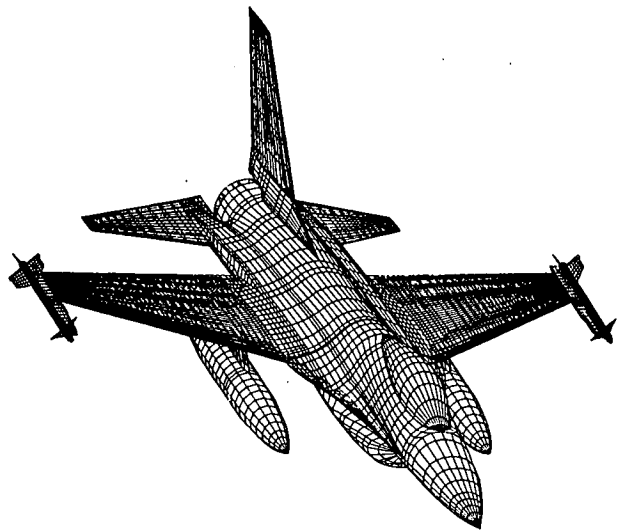
RECENT ADVANCES

- LOCAL GRID REFINEMENT
 - CURRENTLY REQUIRES SUBSTANTIAL USER INPUT
 - SOLUTION ADAPTIVE REFINEMENT NEARLY COMPLETE
- IMPROVEMENTS IN SOLUTION PROCESS
 - DYNAMIC DROP TOLERANCE IN SPARSE MATRIX SOLVER
 - “SHOCK SMEARING” FOR CONVERGENCE IMPROVEMENTS
 - REGIONS OF DIFFERING T_T , P_T
 - MORE GENERAL BOUNDARY CONDITION OPTIONS
 - SUPERSONIC FREESTREAM }
• HIERARCHICAL MULTIGRID } CURRENT EFFORTS

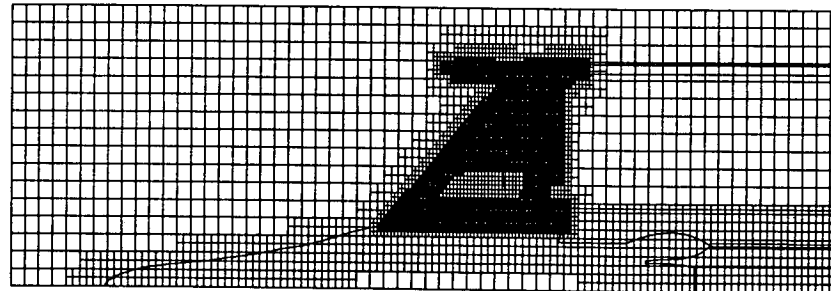
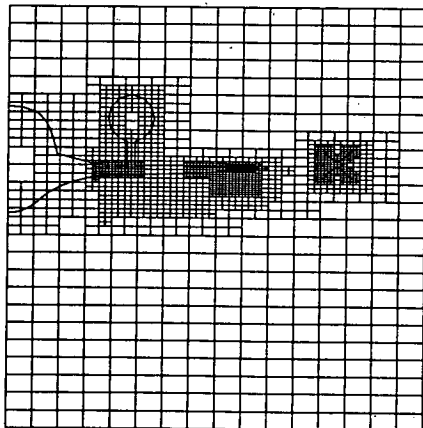
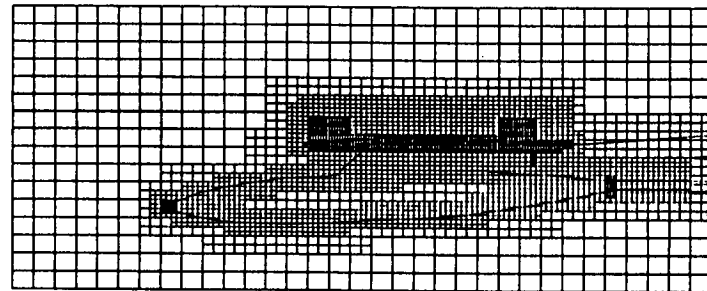
APPLICATIONS

- • F-16A W/TIP MISSILES, FUEL TANKS
- • BOEING 747-200
- OBLIQUE WING RESEARCH AIRCRAFT
- • GENERIC FIGHTER
- • ONERA M6
- AXISYMMETRIC NACELLE
- ADVANCED TURBOPROP MODEL

F-16A W/TIP MISSILES, FUEL TANKS

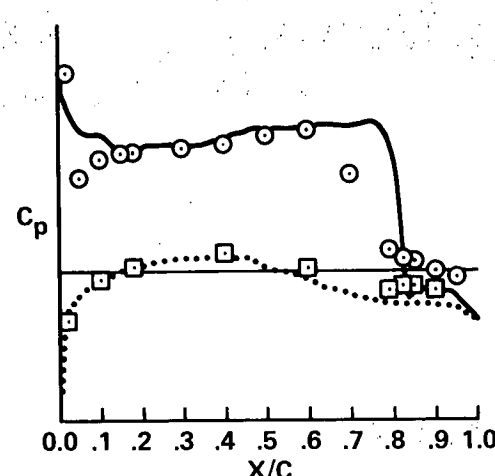
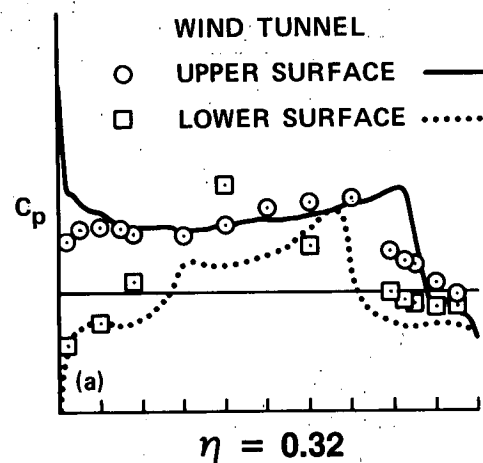


417

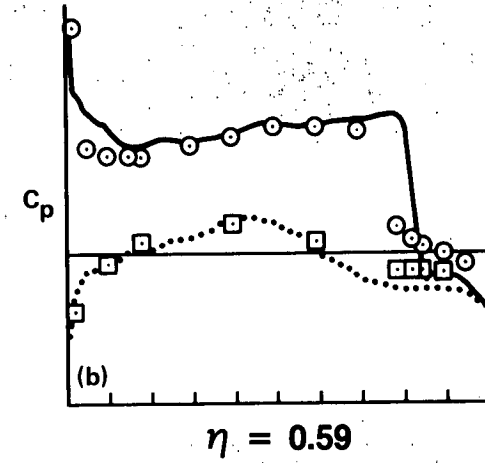


F-16A W/TIP MISSILES, FUEL TANKS

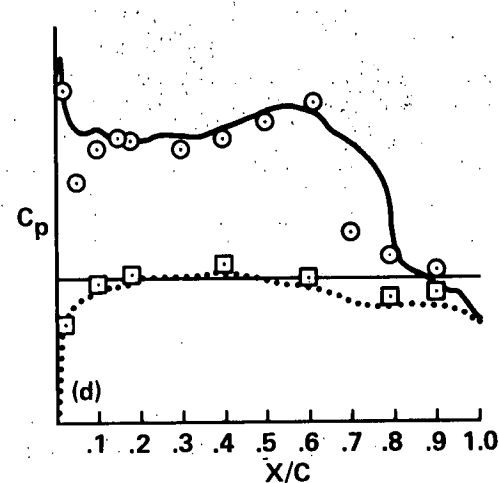
$M_\infty = 0.9, \alpha = 4^\circ$



$\eta = 0.71$



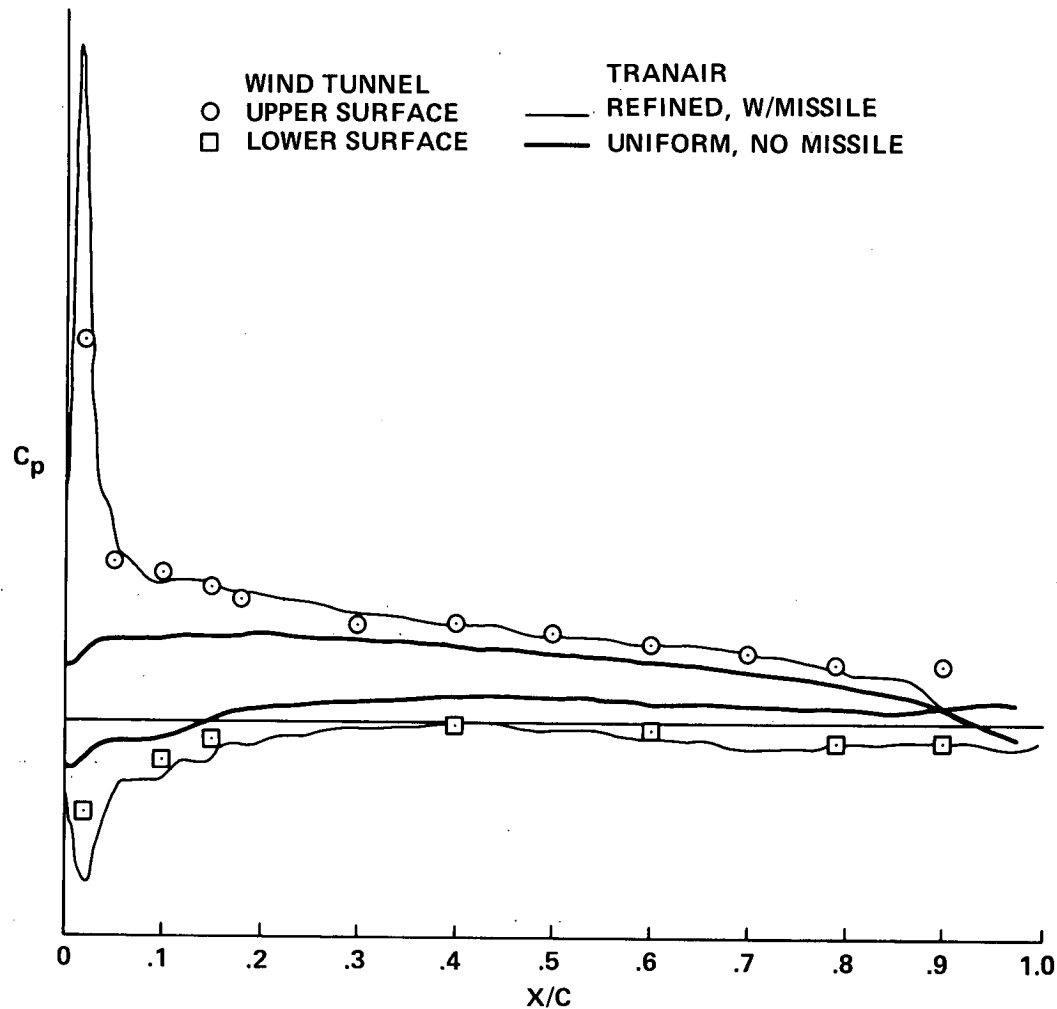
$\eta = 0.59$



$\eta = 0.84$

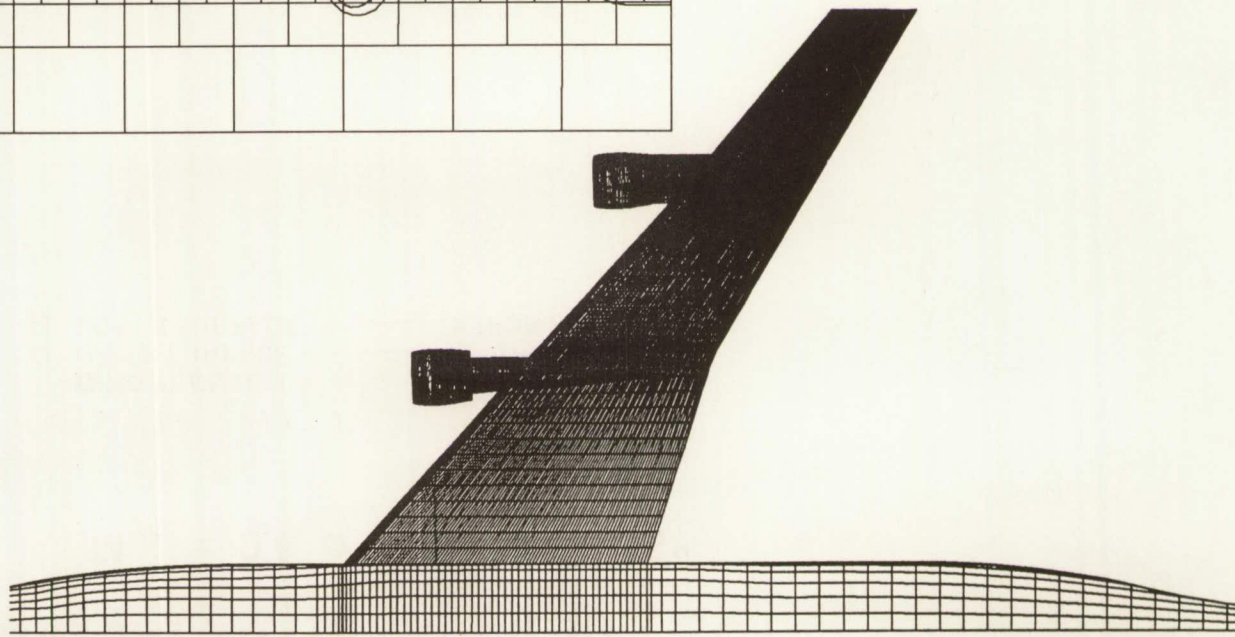
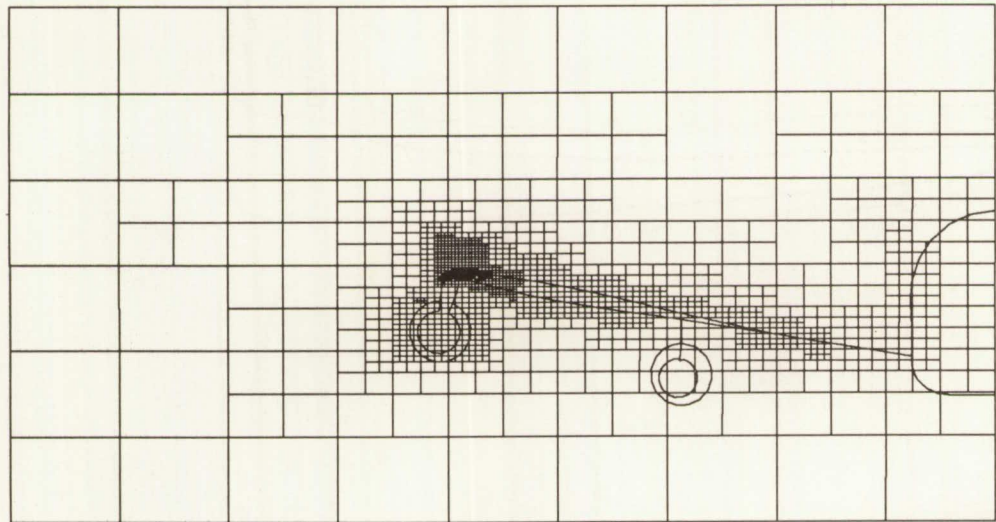
F-16A, TIP MISSILE EFFECT

$$M_\infty = 0.6, \alpha = 4^\circ, \eta \doteq 0.95^\circ$$



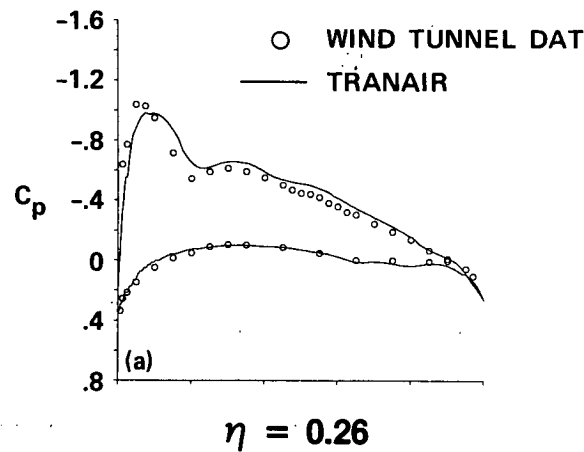
BOEING 747-200

420

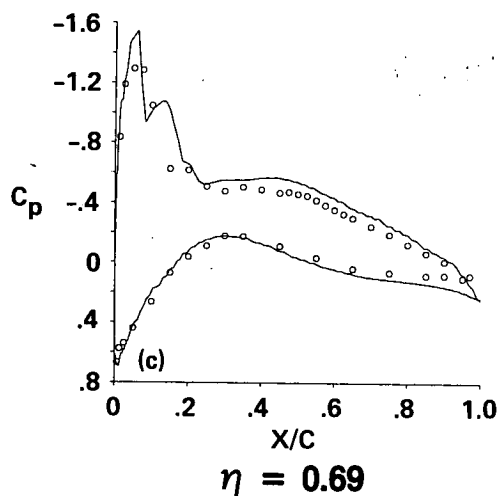


BOEING 747-200

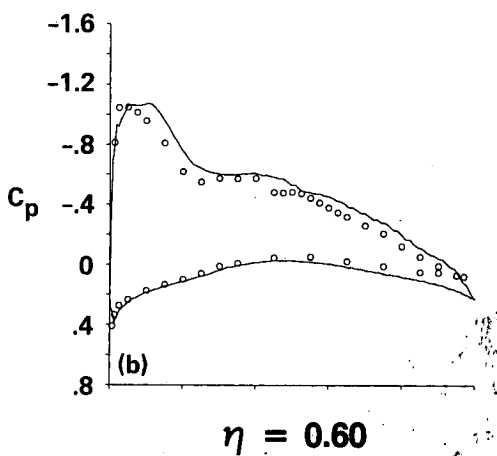
$M_\infty = 0.8, \alpha = 2.7^\circ$



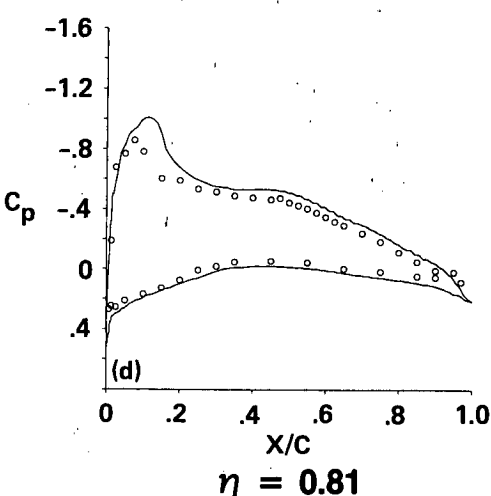
$\eta = 0.26$



$\eta = 0.69$

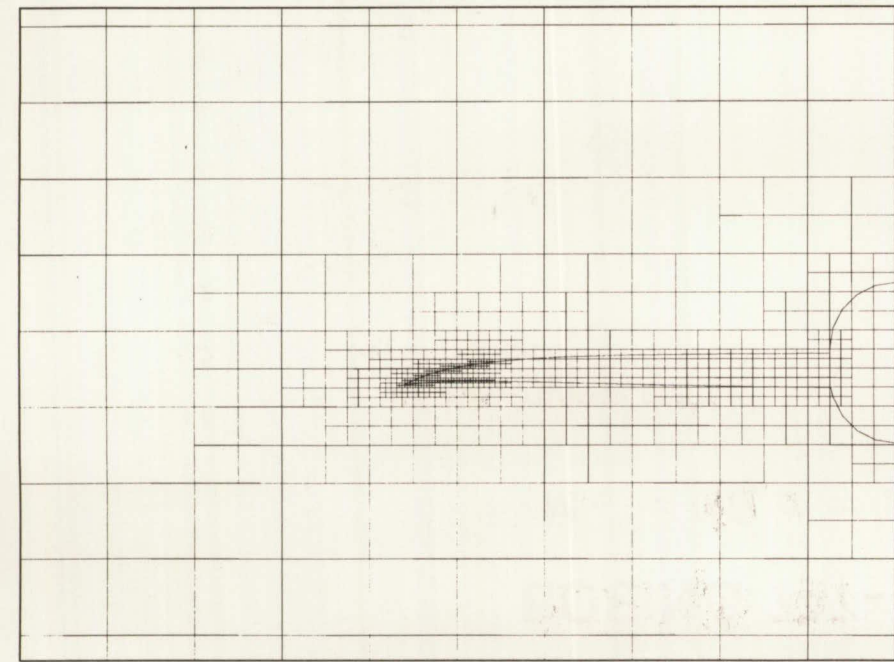
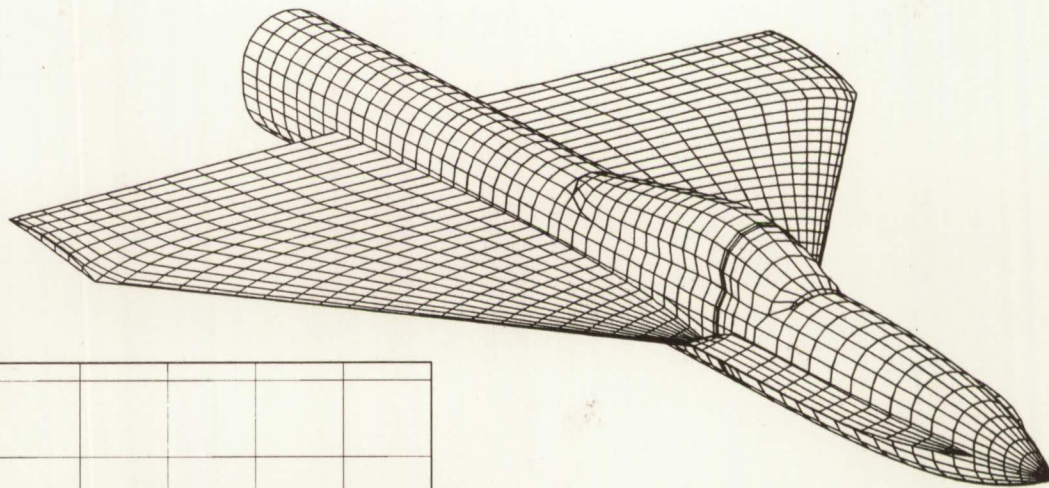


$\eta = 0.60$



$\eta = 0.81$

GENERIC FIGHTER

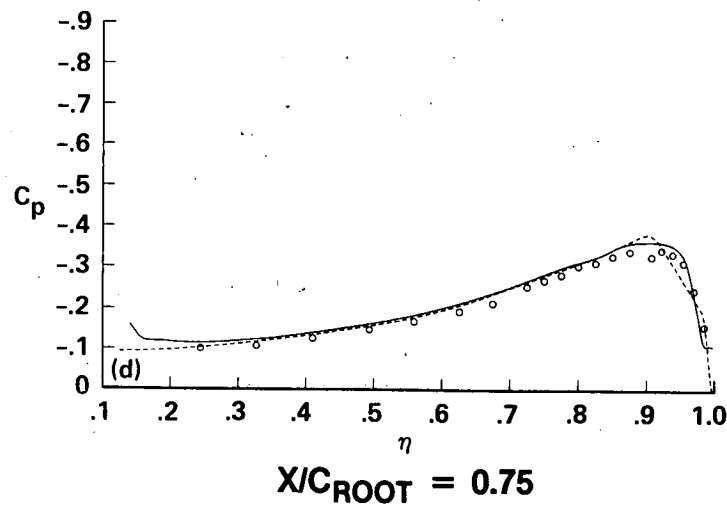
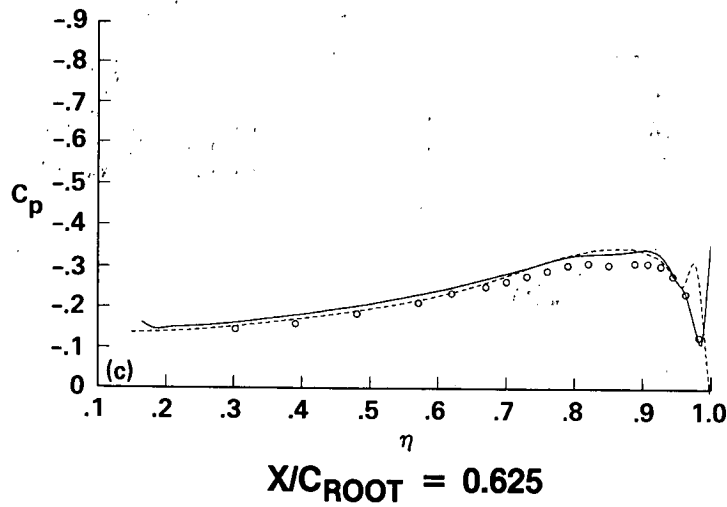
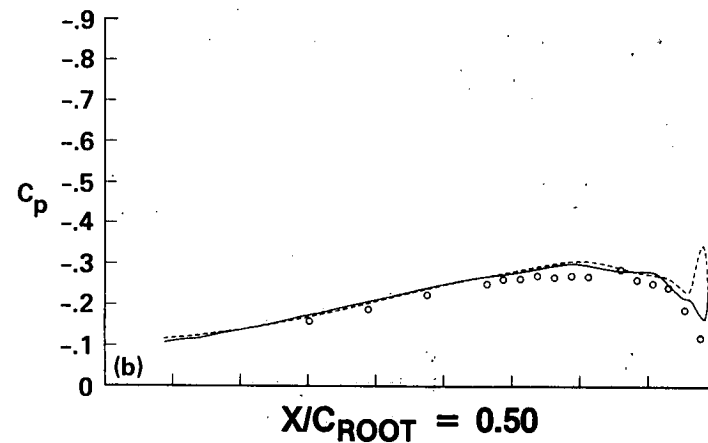
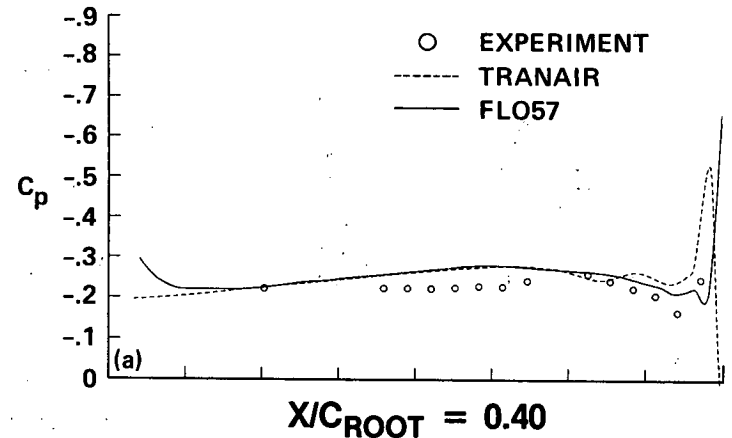


422

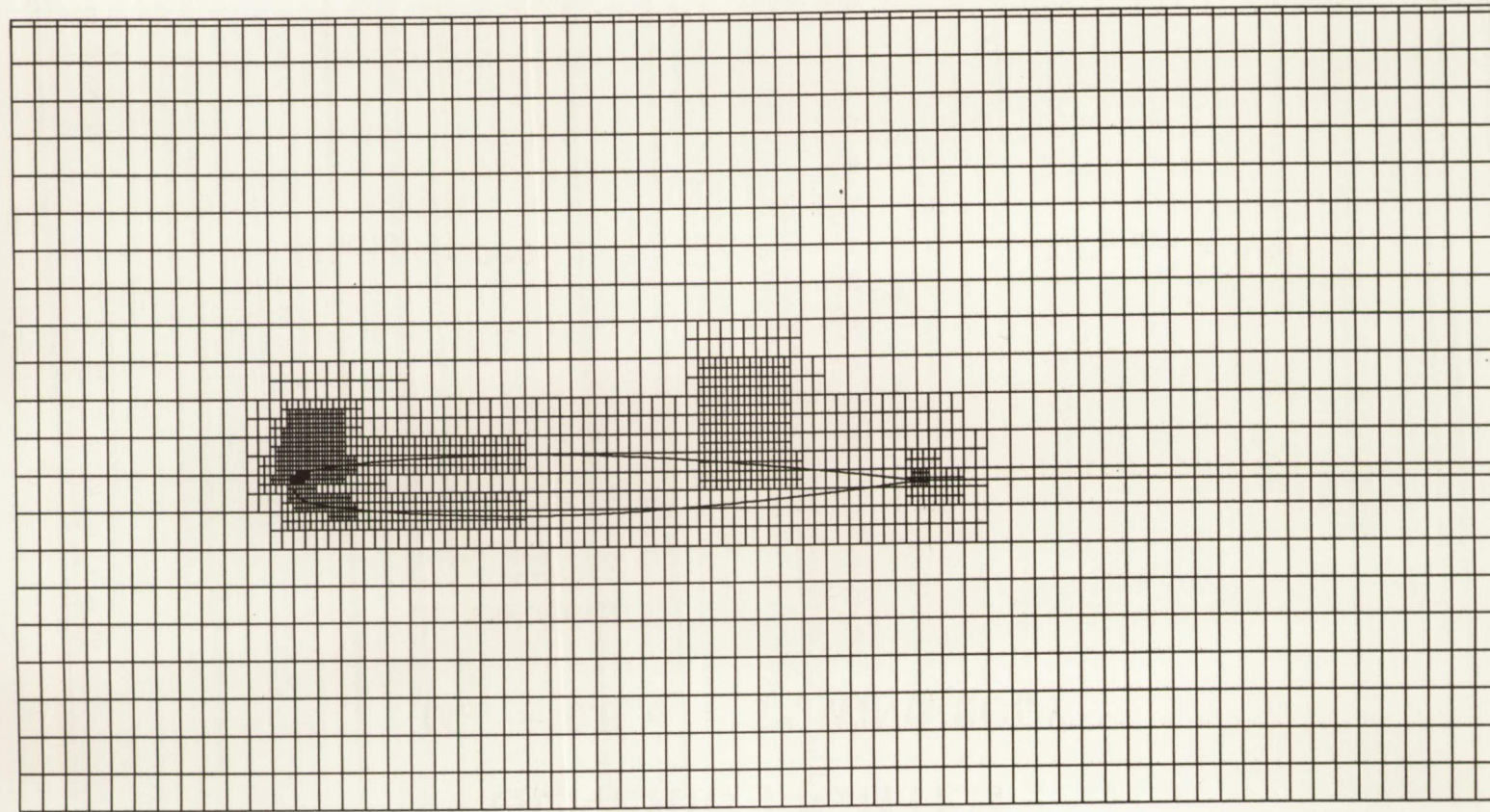
MDM-10/15

GENERIC FIGHTER

$M_\infty = 0.8, \alpha = 5^\circ, \text{WING/BODY}$

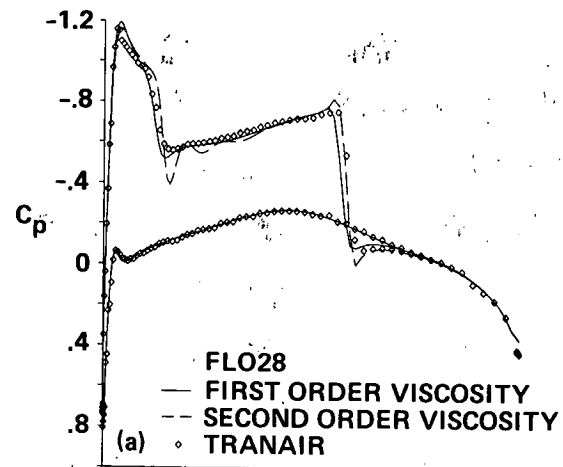


ONERA M6
REFINED GRID AT ROOT SECTION

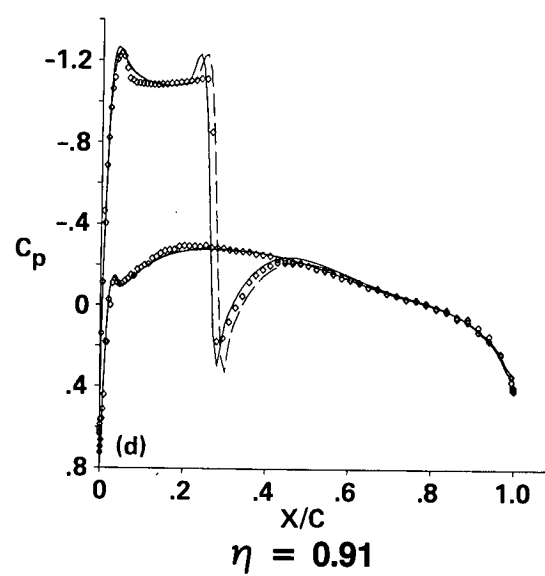
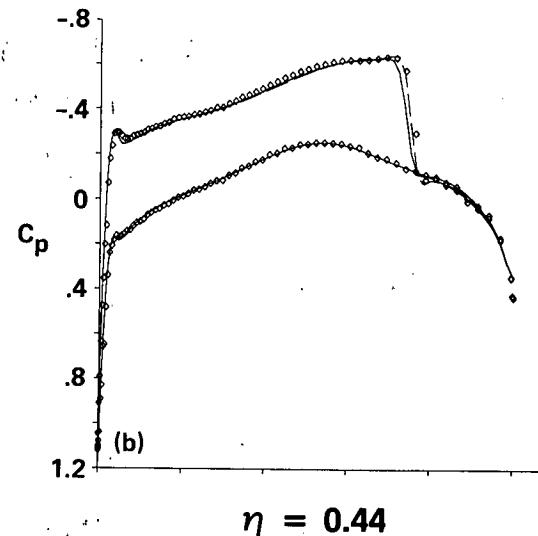
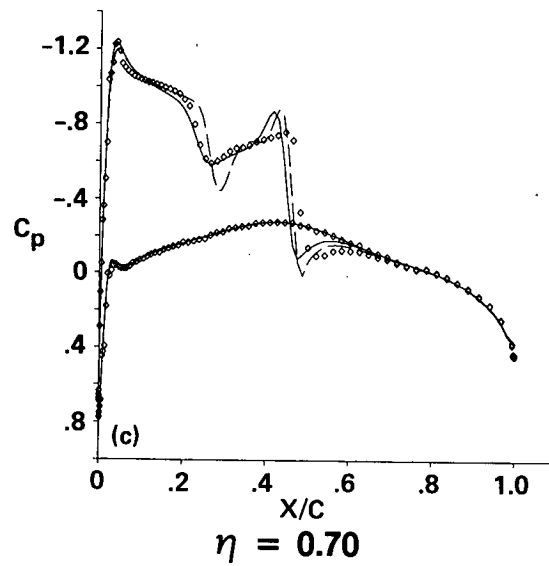


ONERA M6 WING

$M_\infty = 0.84, \alpha = 3.06^\circ$



PLANE OF SYMMETRY



OBSERVATIONS

- SHOWS PROMISE OF BEING EXCELLENT DESIGN TOOL
 - EXPECTED TO REPLACE PANAIR FOR ANALYSIS OF COMPLEX CONFIGURATIONS
 - LINEAR CASES TAKE 15-30 CPU MINUTES ON CRAY X-MP
 - NONLINEAR CASES TAKE 1-2 CPU HOURS ON X-MP
 - FOR CASES W/LIMITED VORTICAL FLOW, GOOD AGREEMENT W/FLO57
 - INITIAL Y-MP RUNS INDICATE 25-40% IMPROVEMENT IN CPU TIME
- AREAS FOR IMPROVEMENT
 - FURTHER MODS COULD REDUCE CPU TIME BY A FACTOR OF 2
 - BOUNDARY LAYER COUPLING FOR MORE ACCURATE SHOCK LOCATION
 - ADDITION OF "WAKE CAPTURING" TERM FOR VORTICAL FLOW TRACKING

POSSIBLE FUTURE DIRECTIONS

- **MODIFIED FULL-POTENTIAL**
 - SOURCE TERM ADDED TO FULL-POTENTIAL EQN FOR WAKE TRACKING
 - VISCOUS COUPLING
- **EULER EQUATIONS**
 - MAINTAIN CURRENT GEOMETRY, GRID FORMAT
 - SOLUTION ADAPTIVE REFINEMENT FOR ACCURATE VORTEX CAPTURING
- **NAVIER-STOKES??**
 - PROBABLY REQUIRES “PSEUDO-GRID” FOR BOUNDARY LAYER SOLUTION

SESSION VI

ROTORCRAFT

Chairman:

W. J. McCroskey

**U.S. Army Aeroflightdynamics Directorate
NASA Ames Research Center**

NUMERICAL SIMULATION OF ROTORCRAFT*

W. J. McCroskey

U. S. Army Aeroflightdynamics Directorate-AVSCOM
and
NASA Ames Research Center, Moffett Field, California

The objective of this research is to develop and validate accurate, user-oriented viscous CFD codes (with inviscid options) for three-dimensional, unsteady aerodynamic flows about arbitrary rotorcraft configurations. This effort draws heavily from the supercomputer capabilities of the National Aerodynamic Simulation project, and it will provide significantly better design and analysis tools to the rotorcraft industry. Better vehicles can be designed at lower cost, with less expensive testing, and with less risk.

Unsteady, three-dimensional Euler and Navier-Stokes codes are being developed, adapted, and extended to rotor-body combinations. Flow solvers are being coupled with zonal grid topologies, including rotating and nonrotating blocks. Special grid clustering and wave-fitting techniques have been developed to capture low-level radiating acoustic waves.

Significant progress has been made in computing the propagation of acoustic waves due to the interaction of a concentrated vortex and a helicopter airfoil. In this study, the need for higher-order schemes was firmly established in relatively inexpensive two-dimensional calculations. In three dimensions, the number of grid points required to capture the low-level acoustic waves becomes *very* large, so that large supercomputer memory becomes essential.

Good agreement was obtained between the numerical results obtained with a thin-layer Navier-Stokes code and experimental data from a model rotor. In addition, several nonrotating configurations that are sometimes proposed to simulate rotor blade tips in conventional wind tunnels were examined, and the complex flow around the radical tip shape of the world's fastest helicopter is under investigation. These studies demonstrate the flexibility and power of CFD to gain physical insight, study novel ideas, and examine various possibilities that might be difficult or impossible to set up in physical experiments.

As a prelude to studies of rotor-body aerodynamic interactions, a preliminary grid topology and moving-interface strategy has been developed. A new Euler / Navier-Stokes code using these techniques computes the vortical wake directly, rather than modeling it, as in most previous rotorcraft studies. Several hover cases were run for conventional and advanced-geometry blades. Numerical schemes using multi-zones and/or adaptive grids appear to be necessary to simulate the complex vortical flows in rotor wakes.

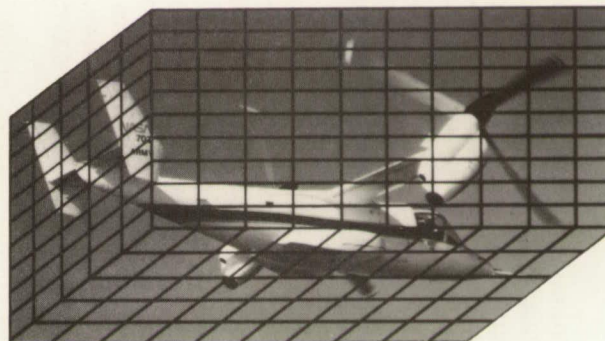
Although major improvements both in supercomputers and in codes will be required, the present trends and rate of progress indicate that practical computations of rotor-body combinations will be feasible in the mid-1990's.

*This research is performed by the Rotorcraft CFD Group, consisting of James Baeder, Ryan Border, Earl Duque, G.R. Srinivasan, and Sharon Stanaway, whose contributions are gratefully acknowledged.

NUMERICAL SIMULATION OF ROTORCRAFT

OBJECTIVE:

- DEVELOP AND VALIDATE CFD CODES FOR 3-D VISCOUS FLOWS ABOUT ARBITRARY ELASTIC ROTORCRAFT CONFIGURATIONS



432

APPROACH:

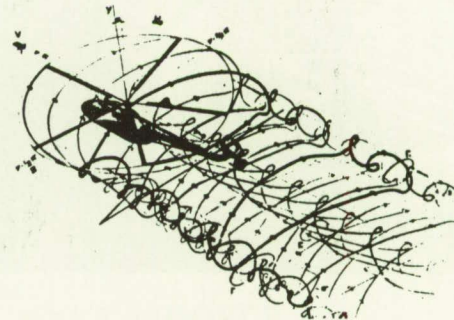
- DEVELOP AND VALIDATE EULER AND NAVIER-STOKES CODES FOR FUTURE NAS SUPERCOMPUTERS

BACKGROUND:

- PRESENT DESIGN AND ANALYSIS TOOLS FOR ROTORCRAFT ARE INADEQUATE
- TRIAL-AND-ERROR TESTING IS EXPENSIVE AND TIME-CONSUMING
- FOREIGN COMPETITION IS GROWING RAPIDLY
- CFD TECHNOLOGY FOR ROTORCRAFT LAGS FIXED-WING DEVELOPMENTS BY YEARS, BUT FUTURE SUPERCOMPUTERS WILL PERMIT REALISTIC ROTORCRAFT APPLICATIONS

NUMERICAL SIMULATION OF ROTORCRAFT

I. Very Difficult Problems



II. We're Doing Great Work

Specific Examples

III. We Have Great Plans

Complete Aeroelastic Rotor-Body Combinations, etc.

IV. BUT . . .

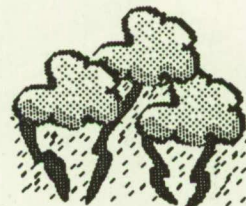
Hardware

Software

Algorithms

Grids

Turbulence Model

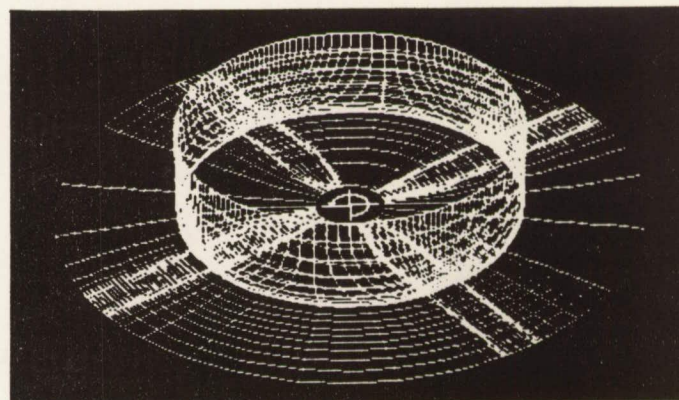


V. Summary and Conclusions

Supercode R C 2 2 2

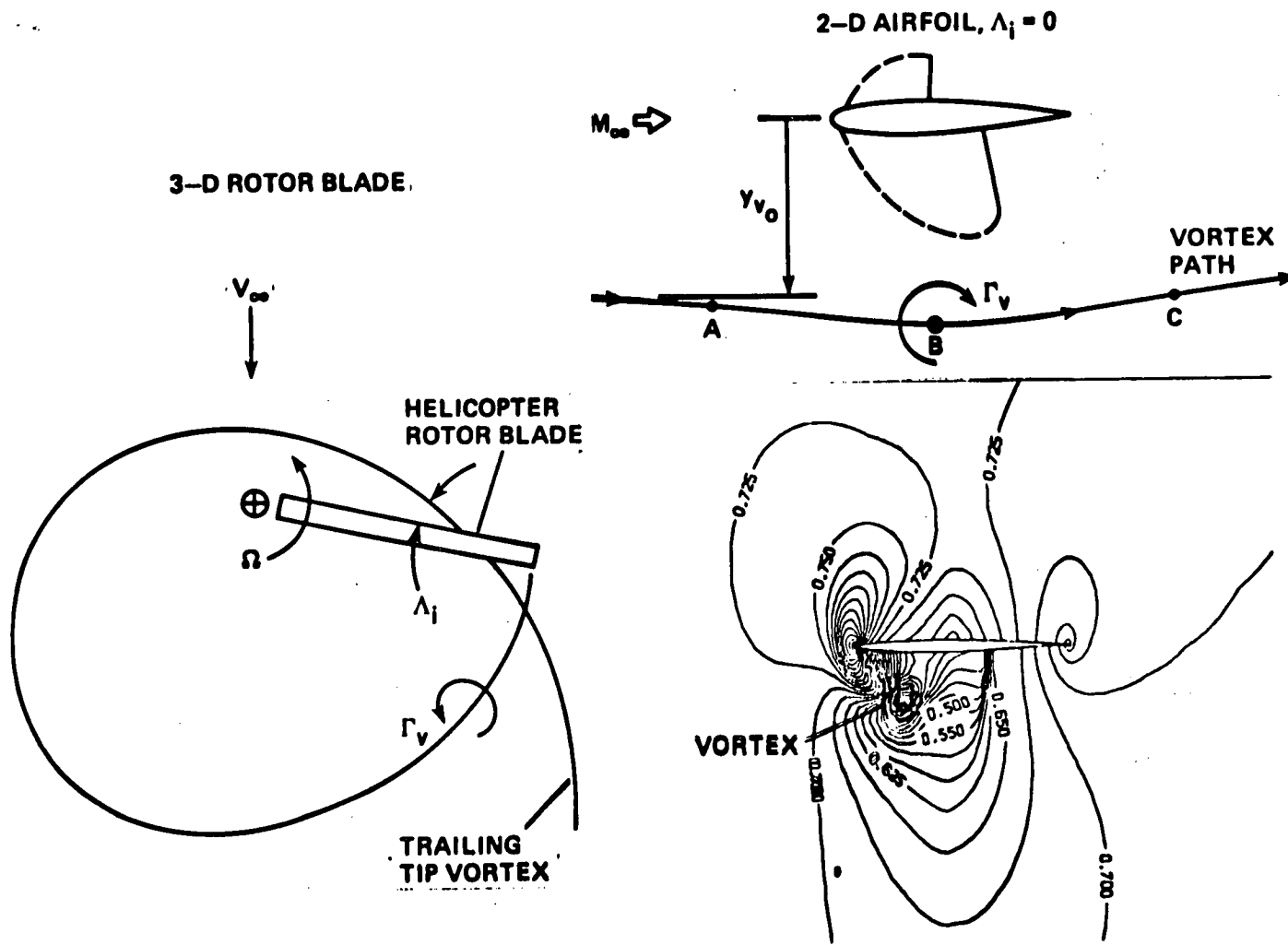
ARMY/NASA ROTORCRAFT CFD PROGRAMS

- INDIVIDUAL COMPONENTS
 1. TRANSONIC AIRFOIL CHARACTERISTICS
 2. BLADE-VORTEX INTERACTIONS
 3. ROTOR TIP-VORTEX FORMATION
 4. 3-D ACOUSTIC PROPAGATION
- COUPLED FINITE-DIFFERENCE CODES AND WAKE MODELS
- ISOLATED ROTOR (*NAVIER STOKES*)
- ROTOR-BODY COMBINATIONS



UNSTEADY VORTEX INTERACTIONS

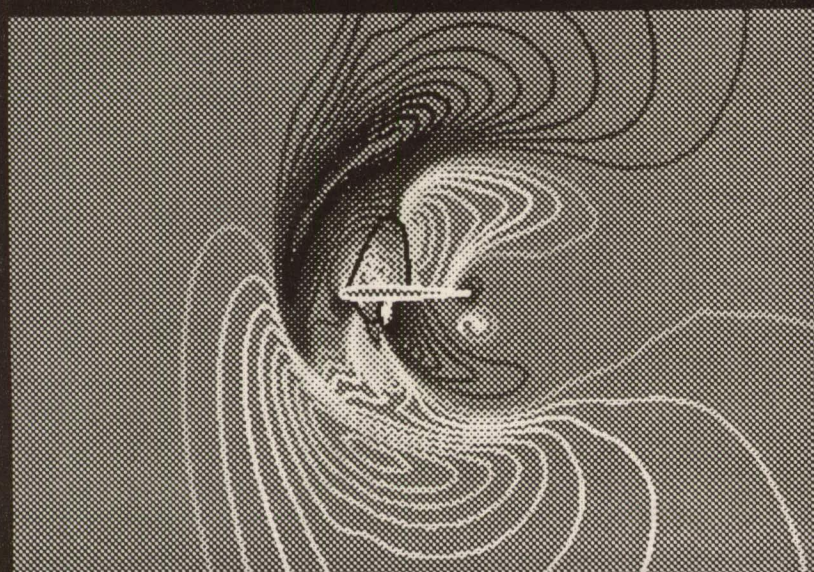
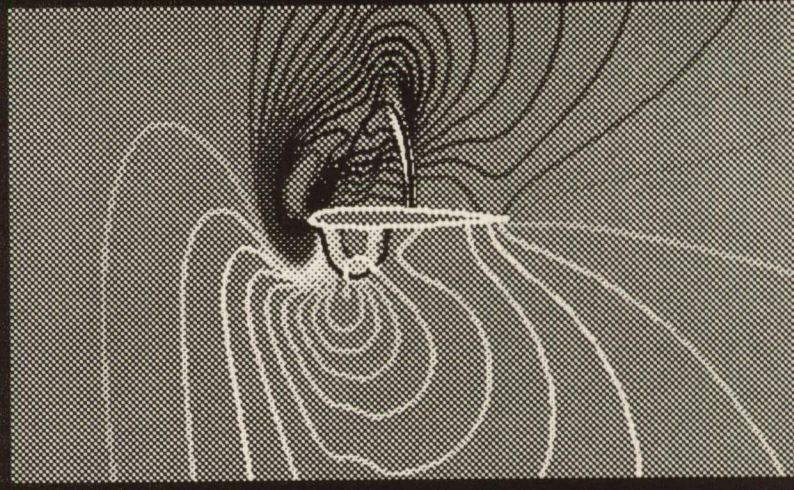
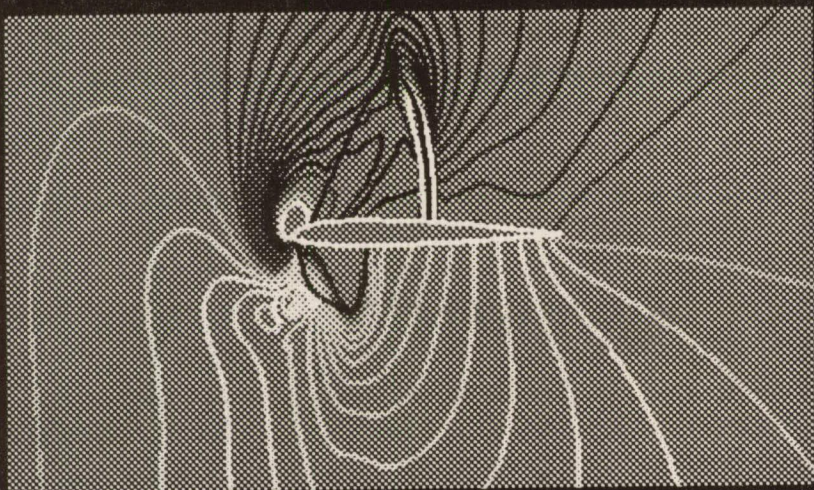
3-D ROTOR BLADE.



Transonic Airfoil-Vortex Interaction

Formation of Acoustic Wave - SC1095

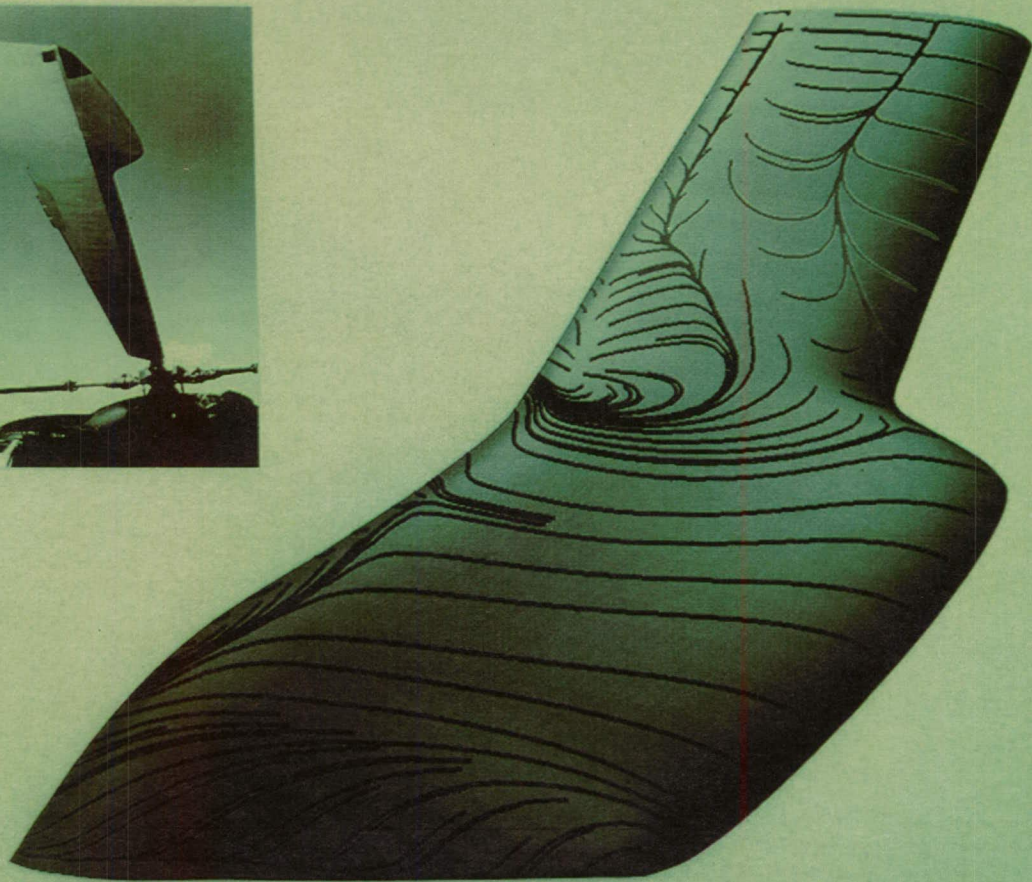
964



Computations & Graphics : James D. Baeder, Army AFDD / NASA Ames

BERP ROTOR

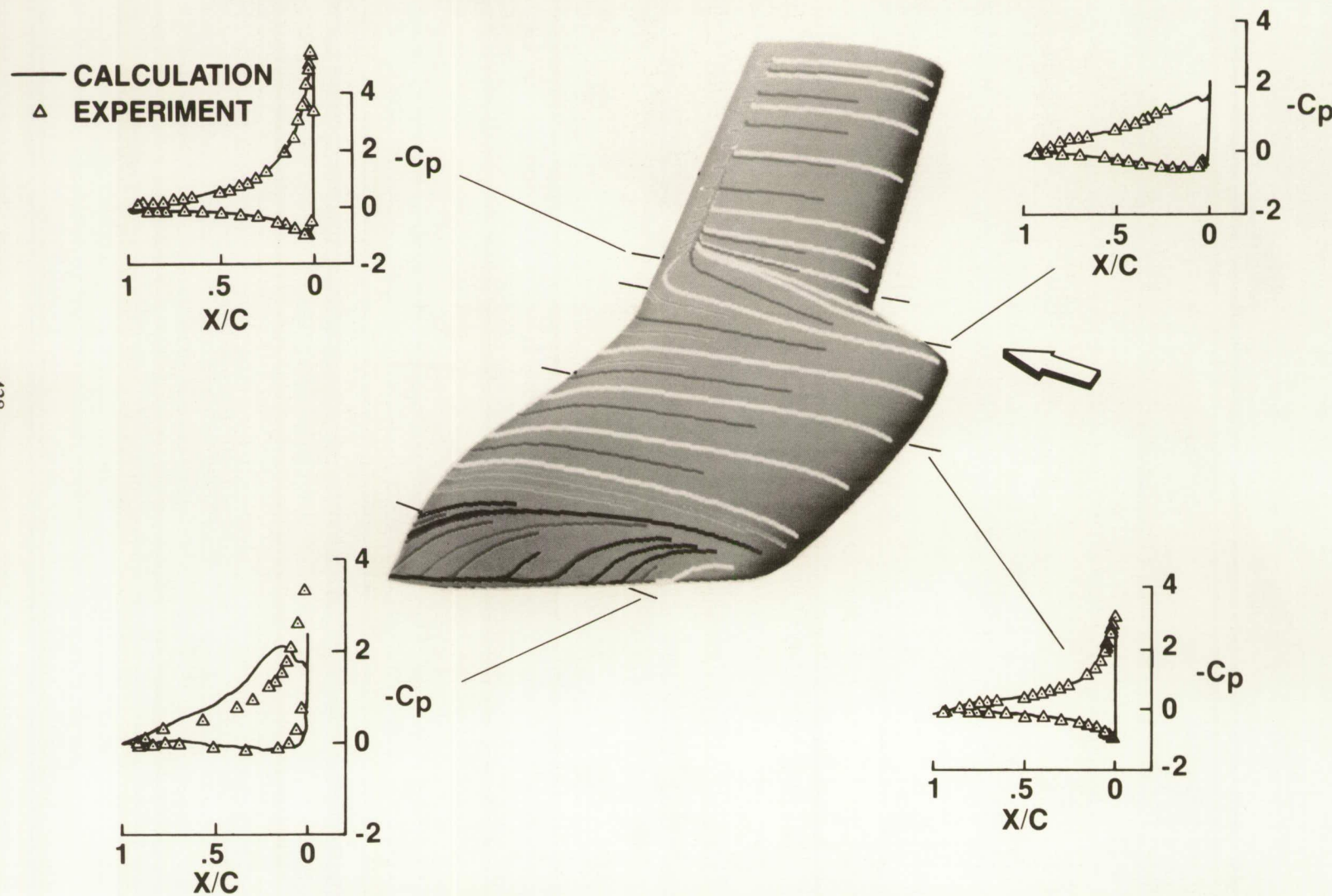
$\alpha = 20^\circ$, $Re = 1.5 \times 10^6$, $M = 0.2$



E.P.N. DUQUE, U.S. ARMY AEROFLIGHTDYNAMICS DIRECTORATE, AVSCOM

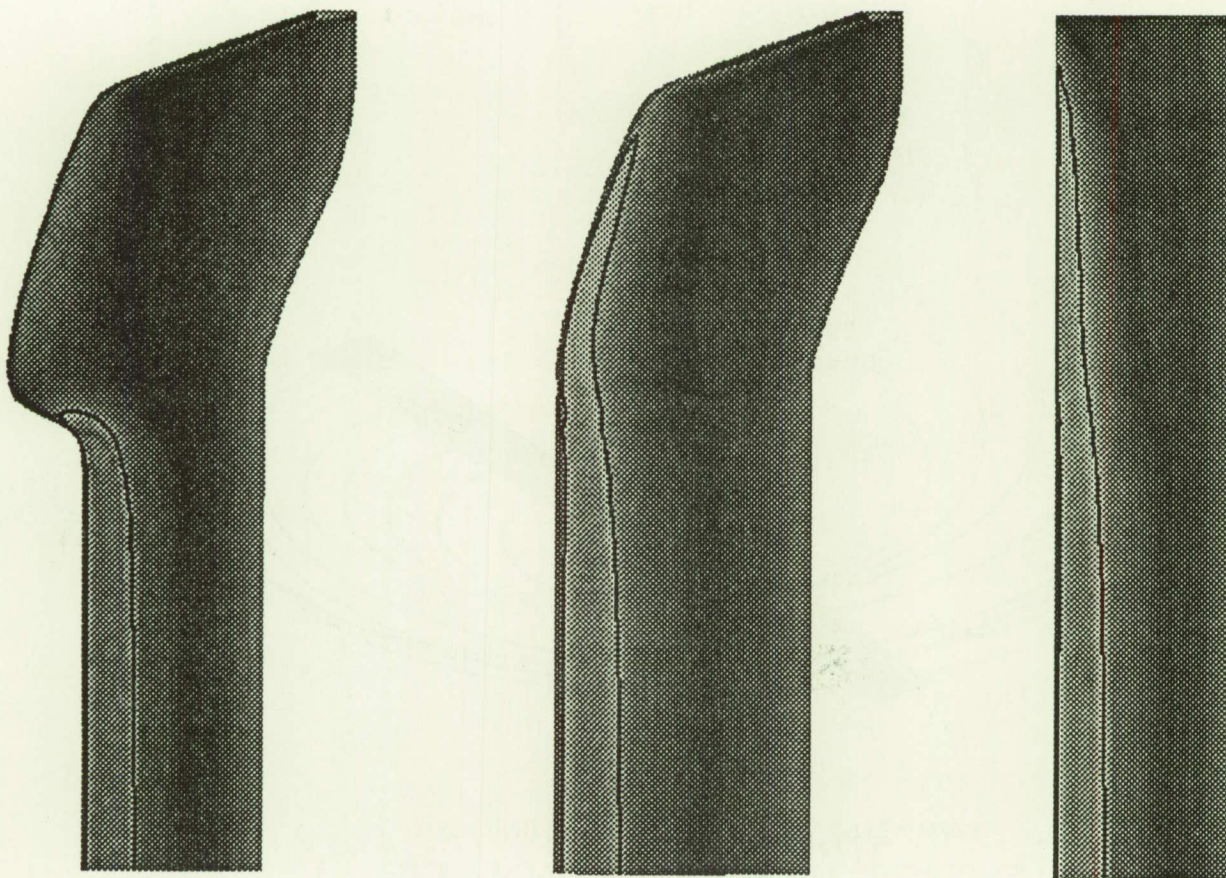
THE BRITISH EXPERIMENTAL ROTOR PROGRAM BLADE

$M = 0.2$, $\alpha = 13^\circ$, $Re = 1.5 \times 10^6$, NONROTATING



TIP SHAPE COMPARISON

M=0.6, α =6 degrees, Inviscid

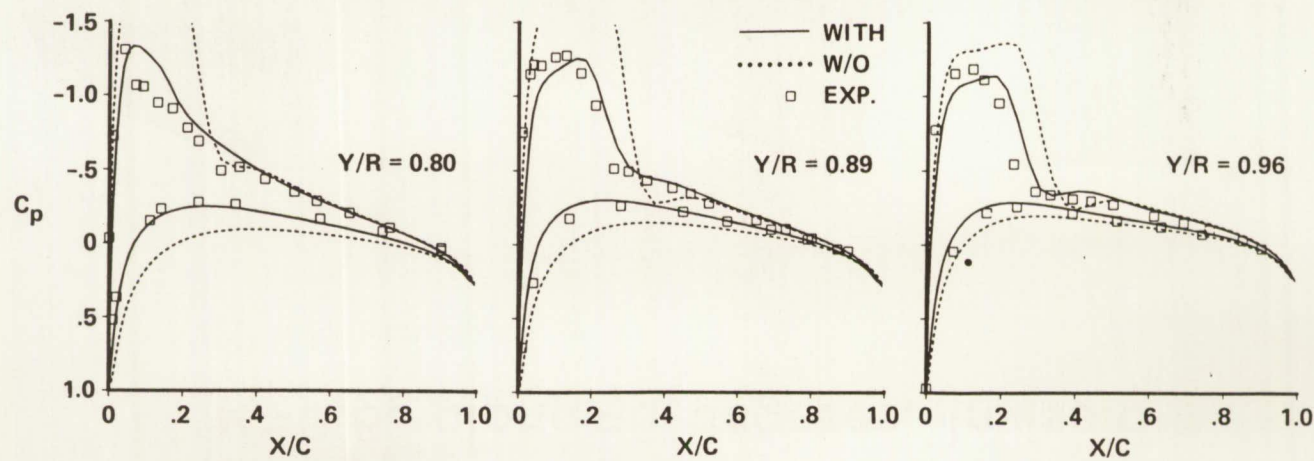
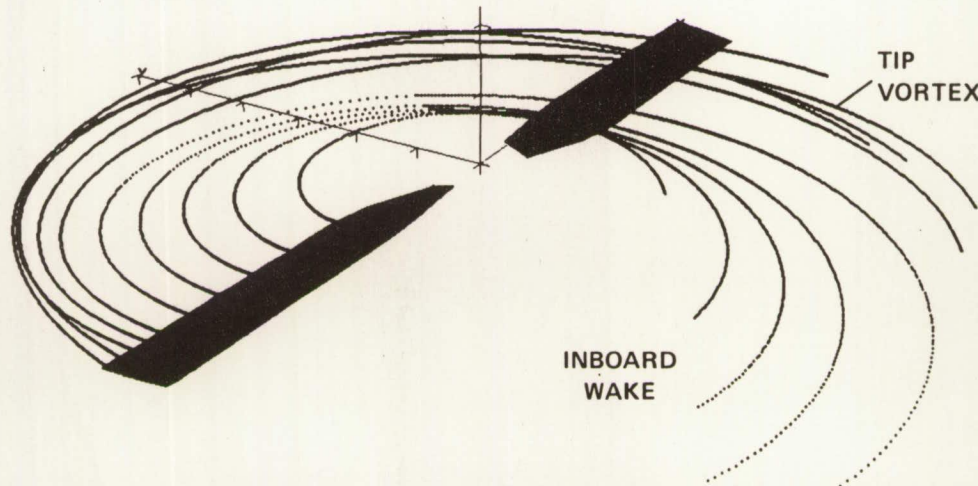


MACH NUMBER

1.50
1.25
1.00
0.75
0.50
0.25
0.00

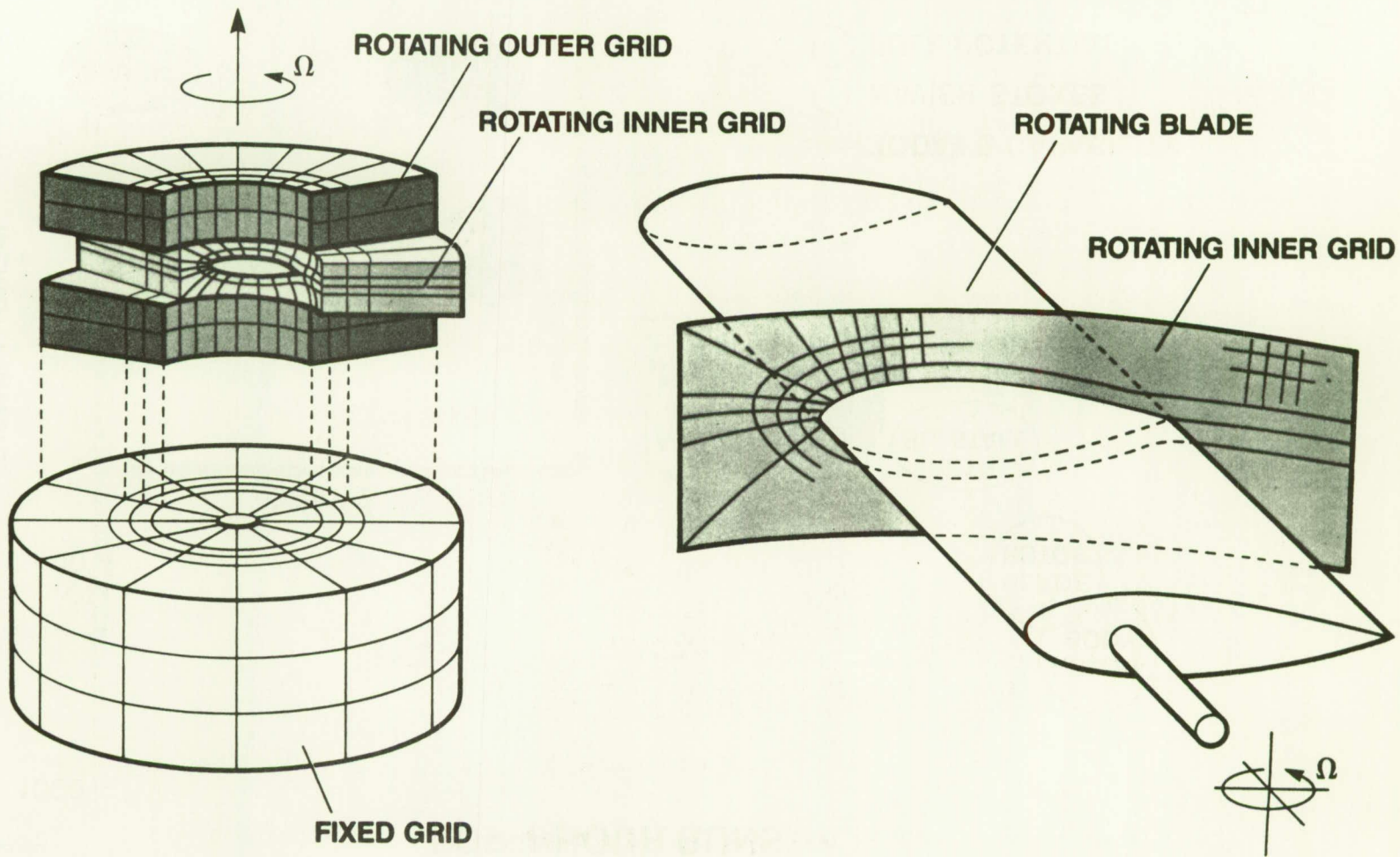
EULER HOVERING ROTOR CALCULATIONS
WITH AND WITHOUT COMPUTED VORTEX WAKE

$M_T = 0.794, \theta_c = 8^\circ$

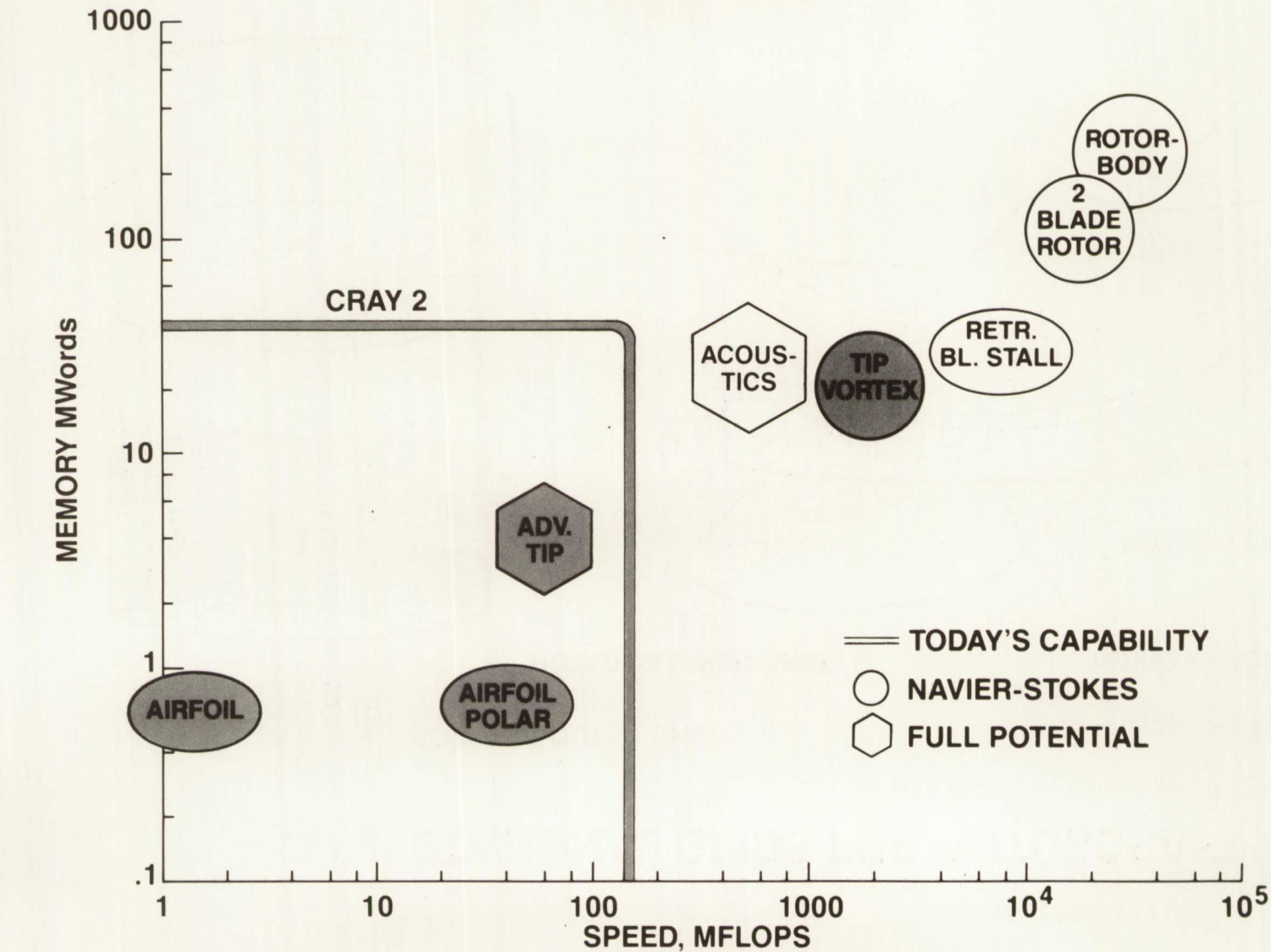


COMPUTATIONAL GRIDS FOR ROTORCRAFT

41



COMPUTER SPEED AND MEMORY REQUIREMENTS FOR 1 HOUR RUNS



What Can We Do ?

1. Accept Longer Run Times
2. Speed Up the Hardware
3. Change the Hardware and Software
 - Different Architectures,
 - Different Operating Systems,
 - Different Languages,
 - New / Improved Coding
4. Improve the Algorithms
 - Increase Stability \rightarrow increase Δt
 - Reduce Numerical Dissipation
5. Use Dynamic, Solution – Adaptive Grids
6. Simplify the Turbulence Model

SUPERCODE R C 2 2 2

- Two Blades + Body :

10^6 grid pts/blade + 0.5×10^6 for body

200 Mwords, 2 Gflops (4 μ sec/grid pt/time step)

- Major Improvements Are Required

20 Times Faster than Today's Unsteady Navier-Stokes Codes

→ Δt 10 times larger (1° azimuth per time step)

→ Flow solver 2 times faster

Rotating and Nonrotating Grid Zones

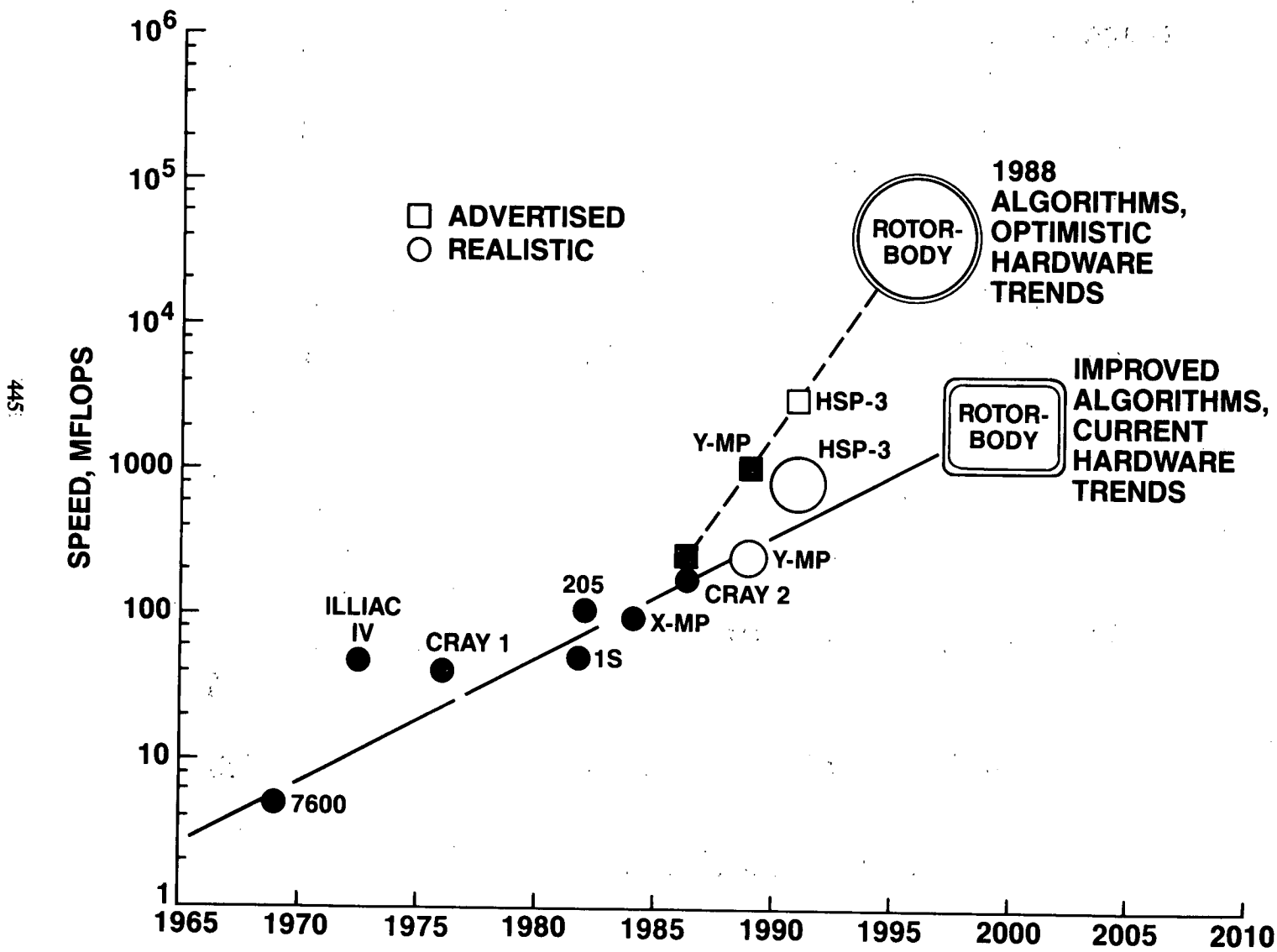
Solution – Adaptive Grids, Minimum Artificial Dissipation

Near – Wake Vortex Capturing, Far – Wake Modeling

Improved Transition Modeling and Separation Prediction

- Flow Solver Coupled with Finite – Element Structural Model

ROTORCRAFT CFD PROJECTIONS FOR 1 HOUR RUNS



SUMMARY AND CONCLUSIONS

- CFD IS VIABLE AND USEFUL FOR ROTORCRAFT
- FUTURE DIRECTIONS
 - Detailed Study of BERP and Other Advanced Tips
 - Rotor – Body Interactions
 - Improved Wake Computations
 - Increased Collaboration with Industry
 - New Tilt – Rotor Initiatives
- CONCERNs AND LIMITATIONS
 - Manpower – *Trained in Both CFD and Rotorcraft*
 - Far – Field Aeroacoustics and Structural Coupling
 - Wake Capturing vs. Wake Modeling
 - Turbulence Models
 - Grids for Complex Bodies in Relative Motion
 - Code Validation, Accuracy, and Reliability
 - Computer Power -- CPU and Clock Time
 - Mass Storage, Post – Processing, and Graphical Display of 3 – D Time – Dependent Results
- PRACTICAL ROTOR – BODY COMBINATIONS BY MID – 1990's

CALCULATION OF THE ROTOR INDUCED DOWNLOAD ON AIRFOILS

C. S. Lee

Sterling Federal Systems, Inc.
NASA Ames Research Center

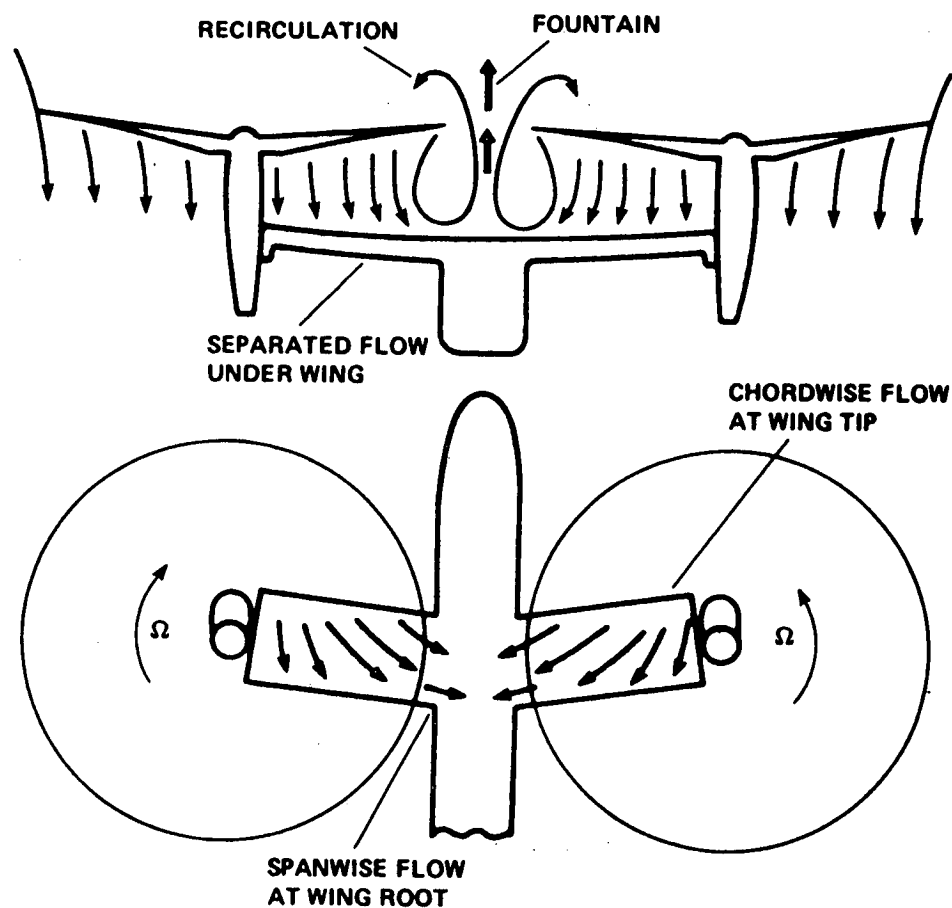
ABSTRACT

Interactions between the rotors and wing of a rotary wing aircraft in hover have a significant detrimental effect on its payload performance. The reduction of payload results from the wake of lifting rotors impinging on the wing, which is at -90 degrees angle of attack in hover. This vertical drag, often referred as download, can be as large as 15% of the total rotor thrust in hover.

The rotor wake is a three-dimensional, unsteady flow with concentrated tip vortices. With the rotor tip vortices impinging on the upper surface of the wing, the flow over the wing is not only three-dimensional and unsteady, but also separated from the leading and trailing edges.

A simplified two-dimensional model was developed to demonstrate the stability of the methodology. The flow model combines a panel method to represent the rotor and the wing, and a vortex method to track the wing wake. A parametric study of the download on a 20% thick elliptical airfoil below a rotor disk of uniform inflow was performed. Comparisons with experimental data are made where the data are available. This approach is now being extended to three-dimensional flows. Preliminary results on a wing at -90 degrees angle of attack in free stream is presented.

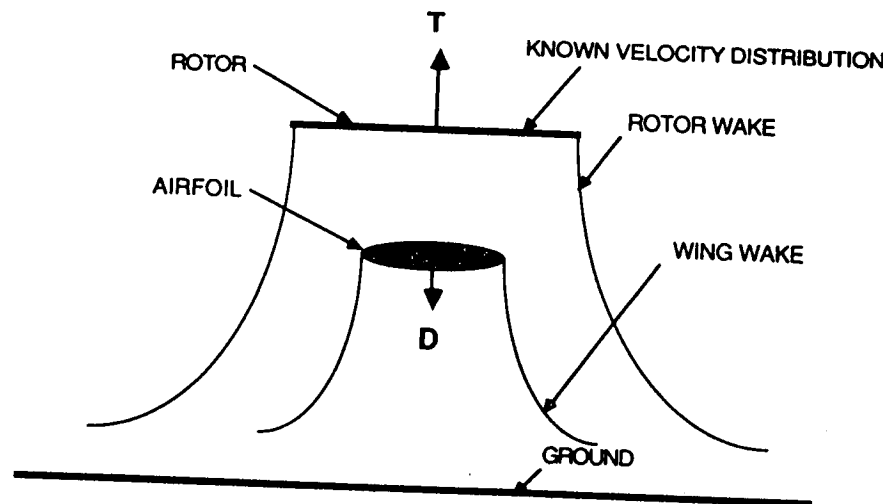
SCHEMATIC OF ROTOR/WING FLOW FIELD



TWO-DIMENSIONAL ANALYSIS FORMULATION

- DOUBLET PANELS ON ROTOR, VORTICITY PANELS ON AIRFOIL, AND POINT VORTICES IN WAKE
- UNSTEADY CALCULATION
 - IMPULSIVELY STARTED FLOW
 - TIME STEPPING FOR FOLLOWING SOLUTIONS
- BOUNDARY CONDITION
 - KNOWN NORMAL VELOCITY DISTRIBUTION ON ACTUATOR DISK
 - CONSTANT STREAM FUNCTION ALONG AIRFOIL
 - ZERO TOTAL VORTICITY IN FLOW FIELD

49



TWO-DIMENSIONAL ANALYSIS FORMULATION CONTINUED

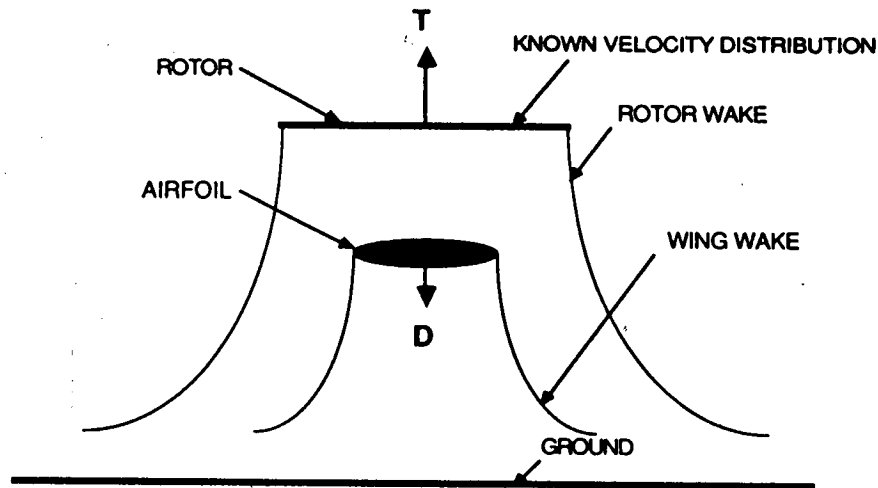
- KUTTA CONDITION

- ROTOR WAKE STRENGTH DETERMINED BY TOTAL PRESSURE DIFFERENCE ACROSS SLIPSTREAM : $\Gamma_r = \gamma_r V_r \Delta t$
- AIRFOIL WAKE STRENGTH RELATED TO STRENGTH OF BOUND VORTICITY AT SEPARATION POINT : $\Gamma_a = \gamma_s V_s \Delta t$

- TOTAL PRESSURE VARIATION ACROSS ROTOR SLIPSTREAM AND AIRFOIL WAKE

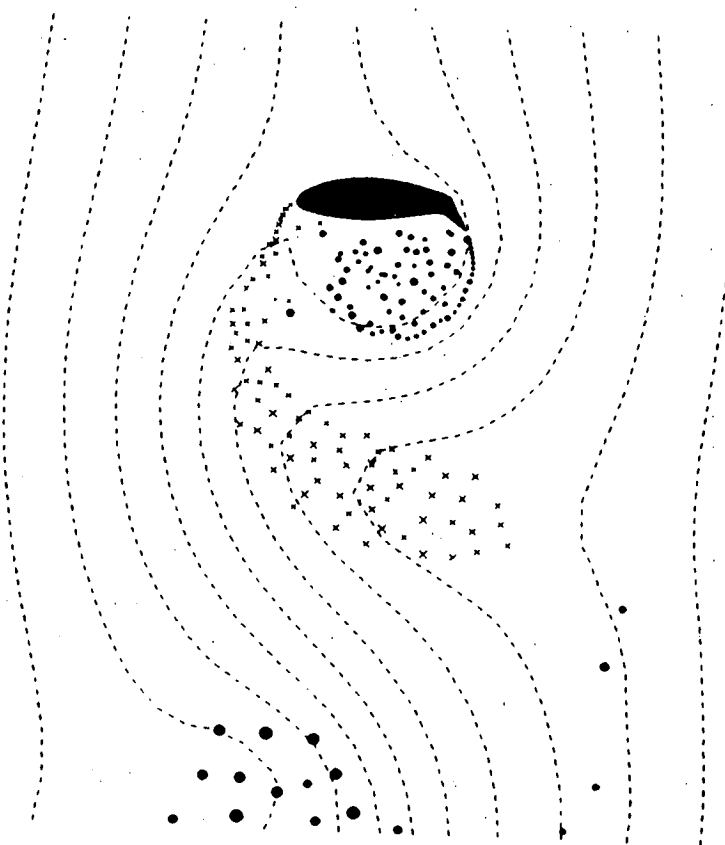
$$\Delta P_r = \rho V_r \gamma_r$$

$$\Delta P_a = \rho V_s \gamma_s$$



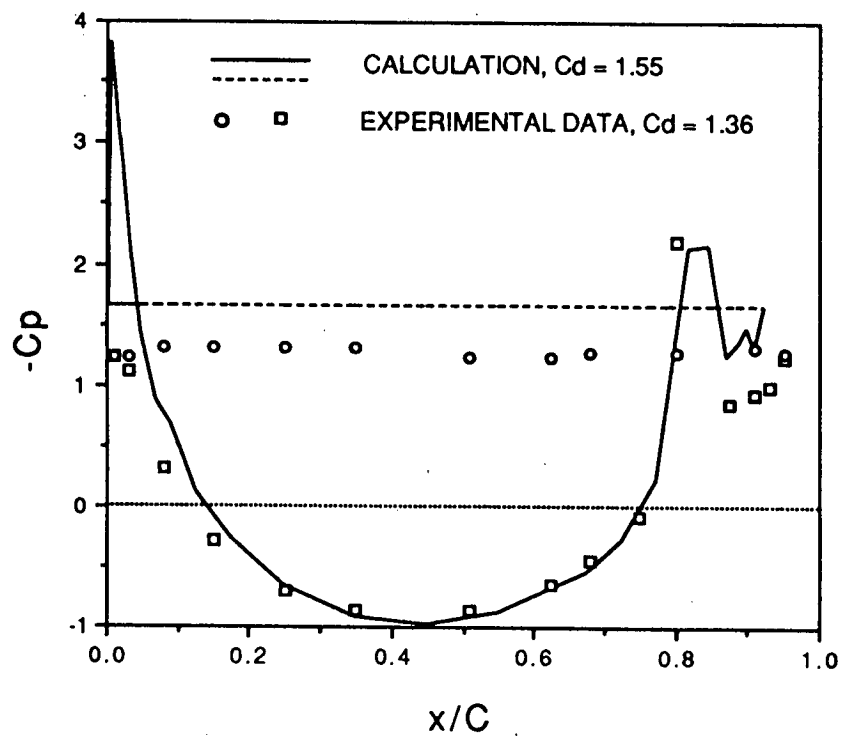
NACA 64A223 AIRFOIL (XV-15 WING) IN FREE STREAM

**-90 DEGREE ANGLE OF ATTACK
25% CHORD FLAP DEFLECTED AT 45 DEGREE**



NACA 64A223 AIRFOIL (XV-15 WING) IN FREE STREAM

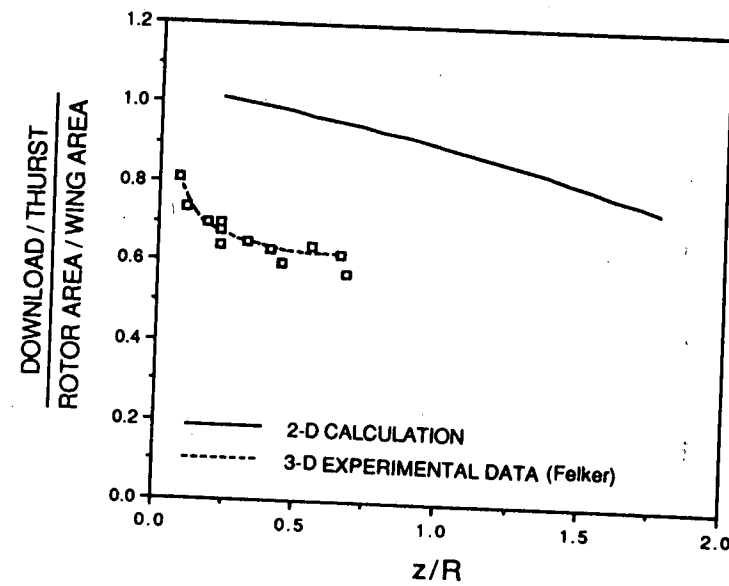
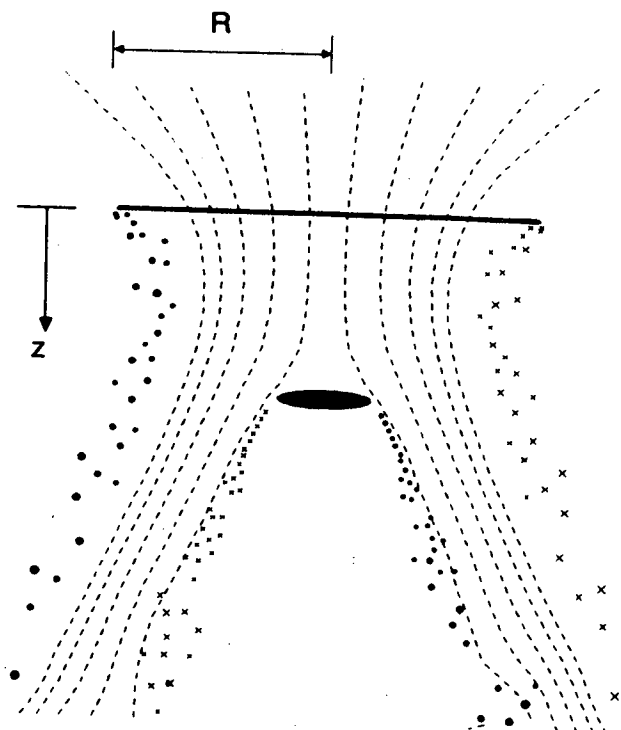
-90 DEGREE ANGLE OF ATTACK
25% CHORD FLAP DEFLECTED AT 45 DEGREE



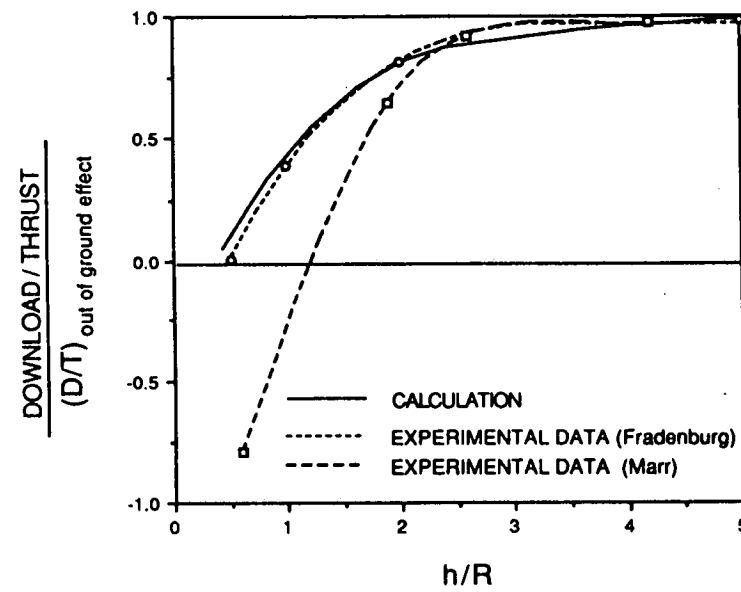
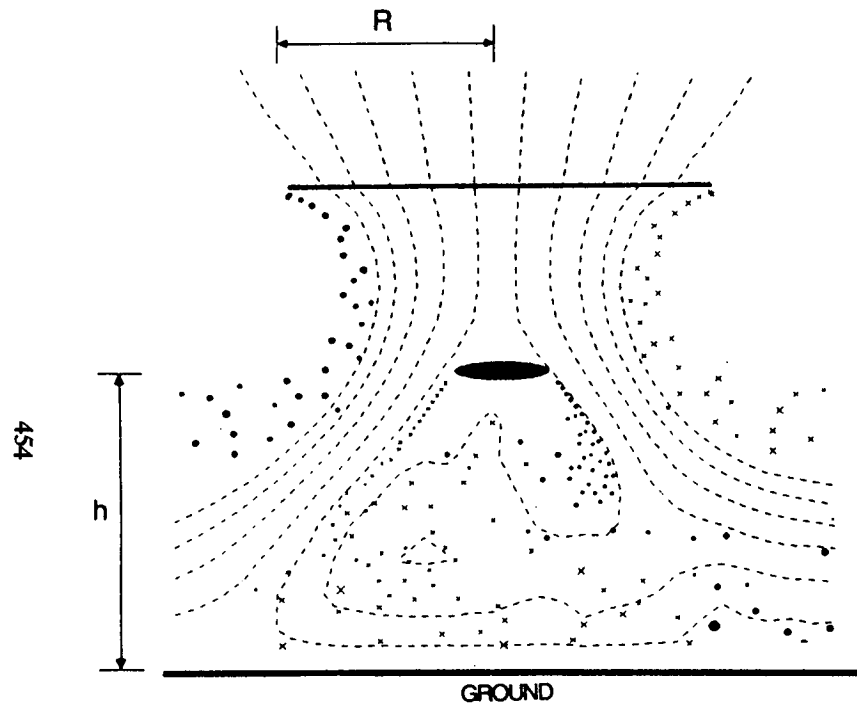
SURFACE PRESSURE DISTRIBUTION

AIRFOIL/ROTOR INTERACTION : EFFECT OF ROTOR/AIRFOIL SPACING
ELLIPTICAL AIRFOIL

453



AIRFOIL/ROTOR INTERACTION : EFFECT OF ROTOR HEIGHT ABOVE GROUND ELLIPTICAL AIRFOIL



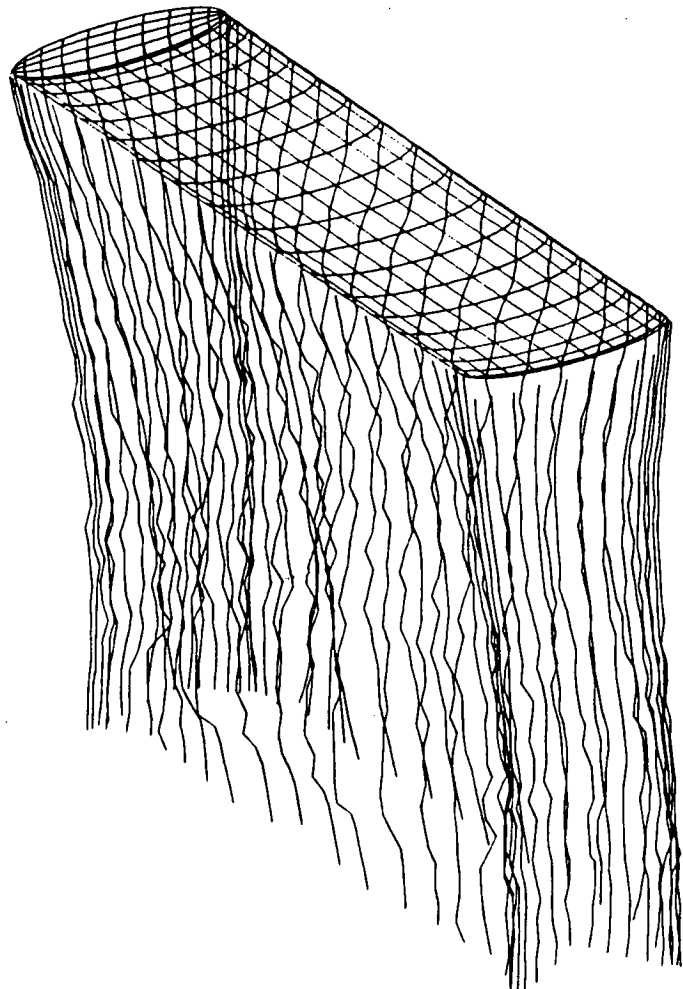
THREE-DIMENSIONAL ANALYSIS FORMULATION

- CONSTANT SOURCE AND DOUBLET PANELS ON WING,
DOUBLET PANELS IN WAKE
- UNSTEADY CALCULATION
 - IMPULSIVELY STARTED FLOW
 - TIME STEPPING FOR FOLLOWING SOLUTIONS
- WAKE CORE SIZE GROWS WITH AGE
 $r_0 \sim \sqrt{t}$
- BOUNDARY CONDITIONS
 - FLOW TANGENCY
 - VELOCITY POTENTIAL JUMP ACROSS BODY PANEL = $\Phi/2$
- KUTTA CONDITION
WAKE STRENGTH, $\mu_w = \mu_u - \mu_l$

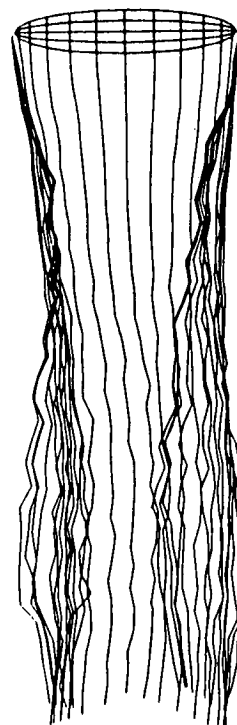
ELLIPTICAL WING IN FREE STREAM

-90 DEGREE ANGLE OF ATTACK
ASPECT RATIO =4.0

456

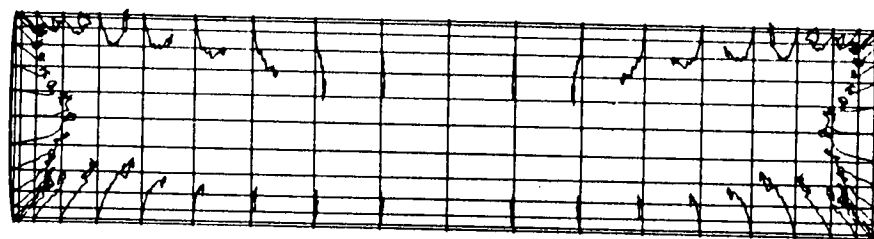
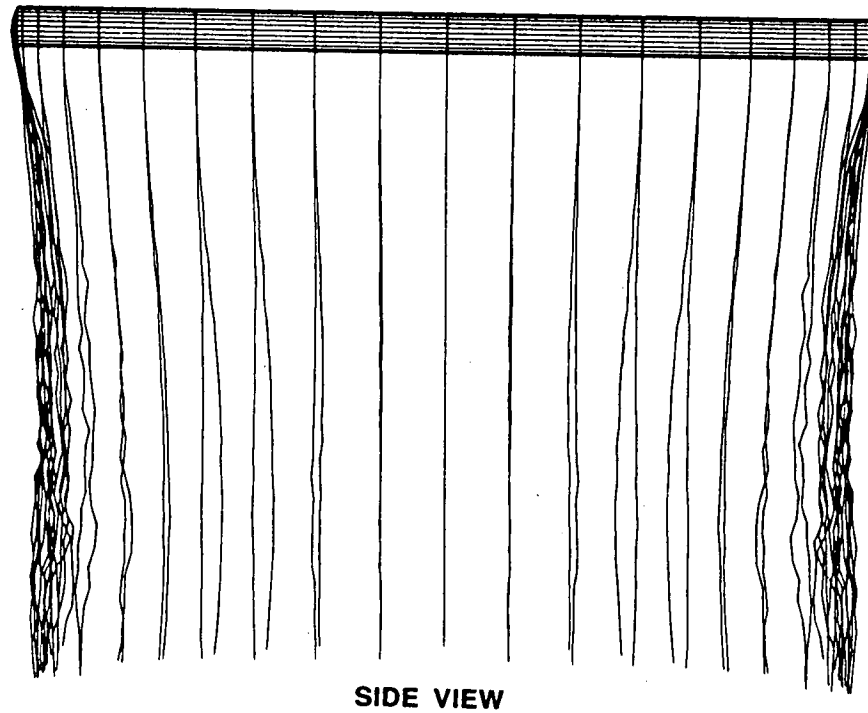


PERSPECTIVE VIEW



VIEW FROM WING TIP

ELLIPTICAL WING IN FREE STREAM (CONTINUED)



VIEW FROM BENEATH

FUTURE WORK

- ROTOR MODEL

- ACTUATOR DISK MODEL

- LINEAR DOUBLET PANELS IN STREAMWISE DIRECTION FOR ROTOR WAKE

- ROTOR BLADE MODEL

- DOUBLET PANELS ON ROTOR BLADE TO INCLUDE THE EFFECT OF BLADE TWIST, AND SENSE OF ROTOR ROTATION

458

- WAKE MODEL

- AMALGAMATE AND REDISTRIBUTE WAKE PANELS TO REDUCE COMPUTATIONAL TIME

- DISCRETIZE FAR WAKE PANELS TO MODEL OSCILLATING WAKE

N91-10865

THREE-DIMENSIONAL VISCOUS DRAG PREDICTION
FOR ROTOR BLADES

CHING S. CHEN
NATIONAL RESEARCH COUNCIL
NASA AMES RESEARCH CENTER

SUMMARY

The state-of-the-art in rotor blade drag prediction involves the use of two-dimensional airfoil tables to calculate the drag force on the blade. One of the most serious problems with the current methods is that they cannot be used for airfoils that have yet to be tested. Most of the drag prediction methods also do not take the Reynolds number or the rotational effects of the blade into account, raising doubts about the accuracy of the results. This project addresses these problems with the development of an analytical method which includes the shape of airfoil, the effects of Reynolds number, and the rotational motion of the blade.

OBJECTIVES

- PROVIDE AN EFFICIENT ANALYSIS FOR ROTOR BLADE DRAG PREDICTION
- ENABLE ACCURATE DESIGN OF NEW, ADVANCED ROTOR SYSTEMS WITH IMPROVED PERFORMANCE

MOTIVATIONS

ROTOR BLADE DRAG PREDICTION CURRENTLY USES TWO-DIMENSIONAL AIRFOIL TABLES

MAJOR SHORTCOMINGS:

- CANNOT BE USED FOR AIRFOILS NOT YET TESTED**
- NO REYNOLDS NUMBER OR ROTATIONAL EFFECTS INCLUDED**

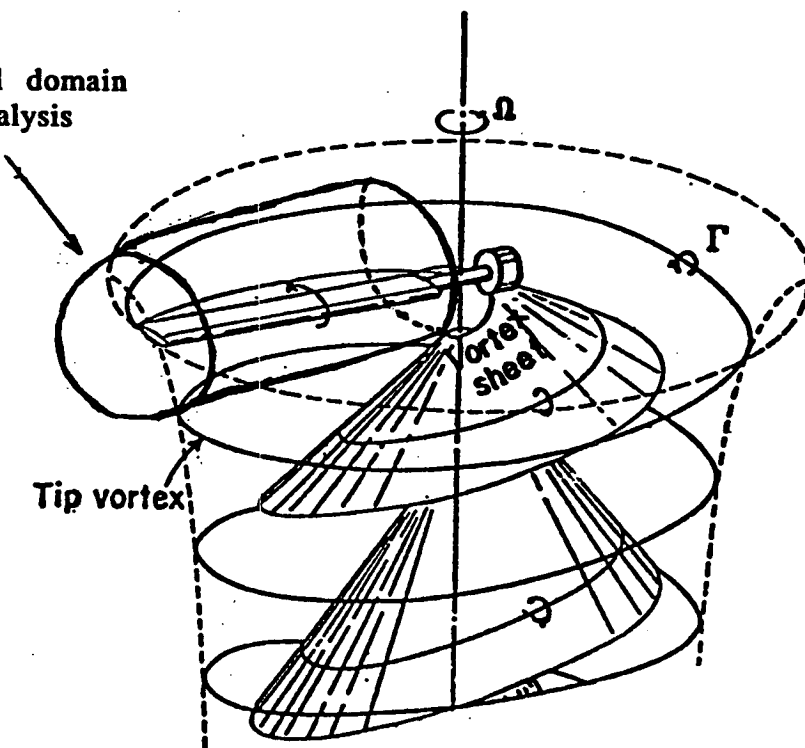
19

CURRENT APPROACH INCLUDES:

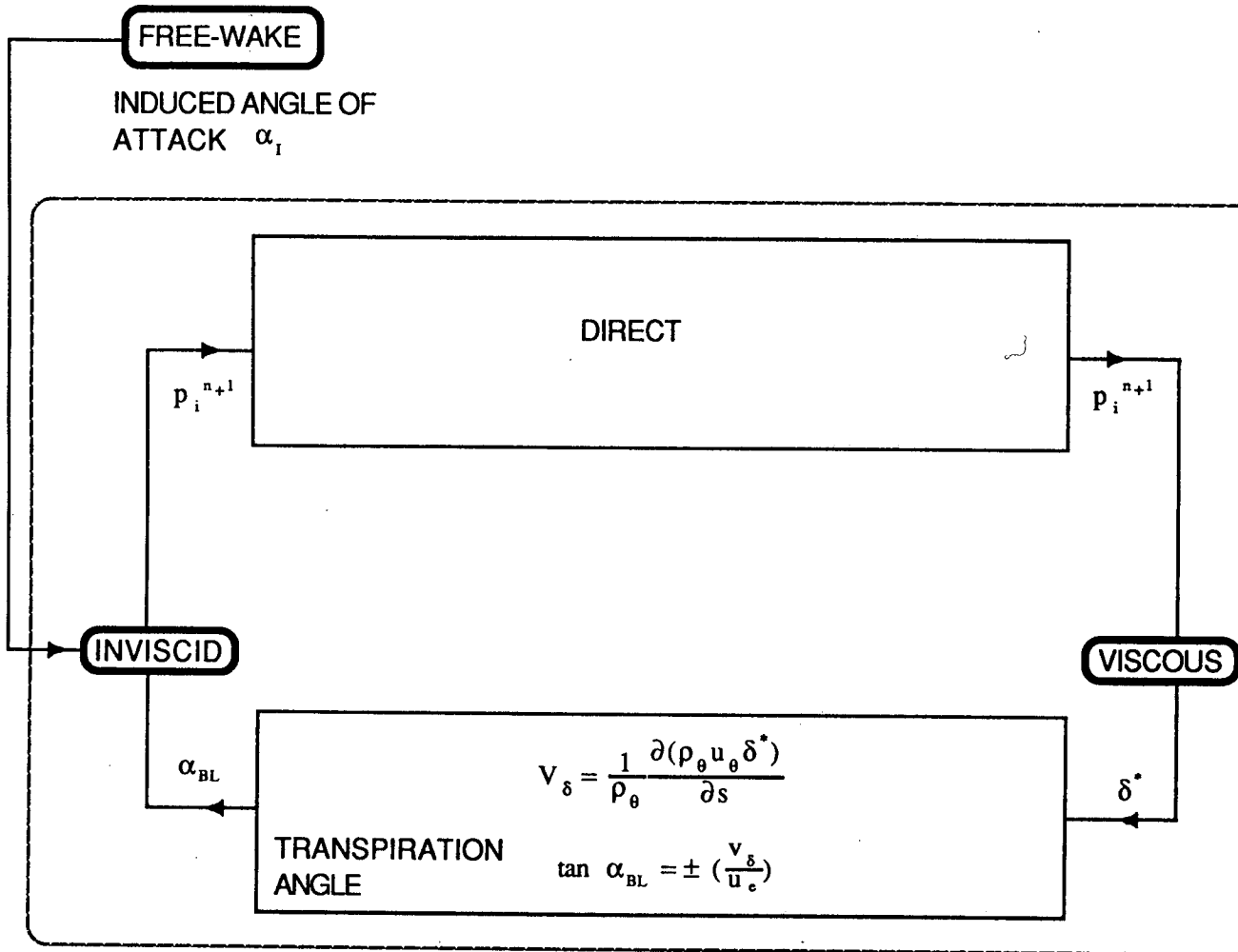
- AIRFOIL SHAPE**
- REYNOLDS NUMBER EFFECTS**
- ROTATIONAL MOTION OF BLADE**

RELATION OF COMPUTATIONAL DOMAIN OF INVISCID ANALYSIS AND ROTOR WAKE

The computational domain
of the inviscid analysis



THE COUPLING SCHEME OF VISCOUS, INVISCID, AND FREE-WAKE METHODS
DIRECT APPROACH



UNSTEADY, COMPRESSIBLE, THREE-DIMENSIONAL BOUNDARY-LAYER EQUATIONS

ROTATING REFERENCE FRAME

X-MOMENTUM EQUATION

$$\rho(u_t + uu_x + vu_y + wu_z - 2w\Omega - x\Omega^2) = -p_x + (\mu u_y)_y$$

Z-MOMENTUM EQUATION

$$\rho(w_t + uw_x + vw_y + ww_z + 2u\Omega - z\Omega^2) = -p_z + (\mu w_y)_y$$

PERFECT GAS RELATION

$$p = \rho RT$$

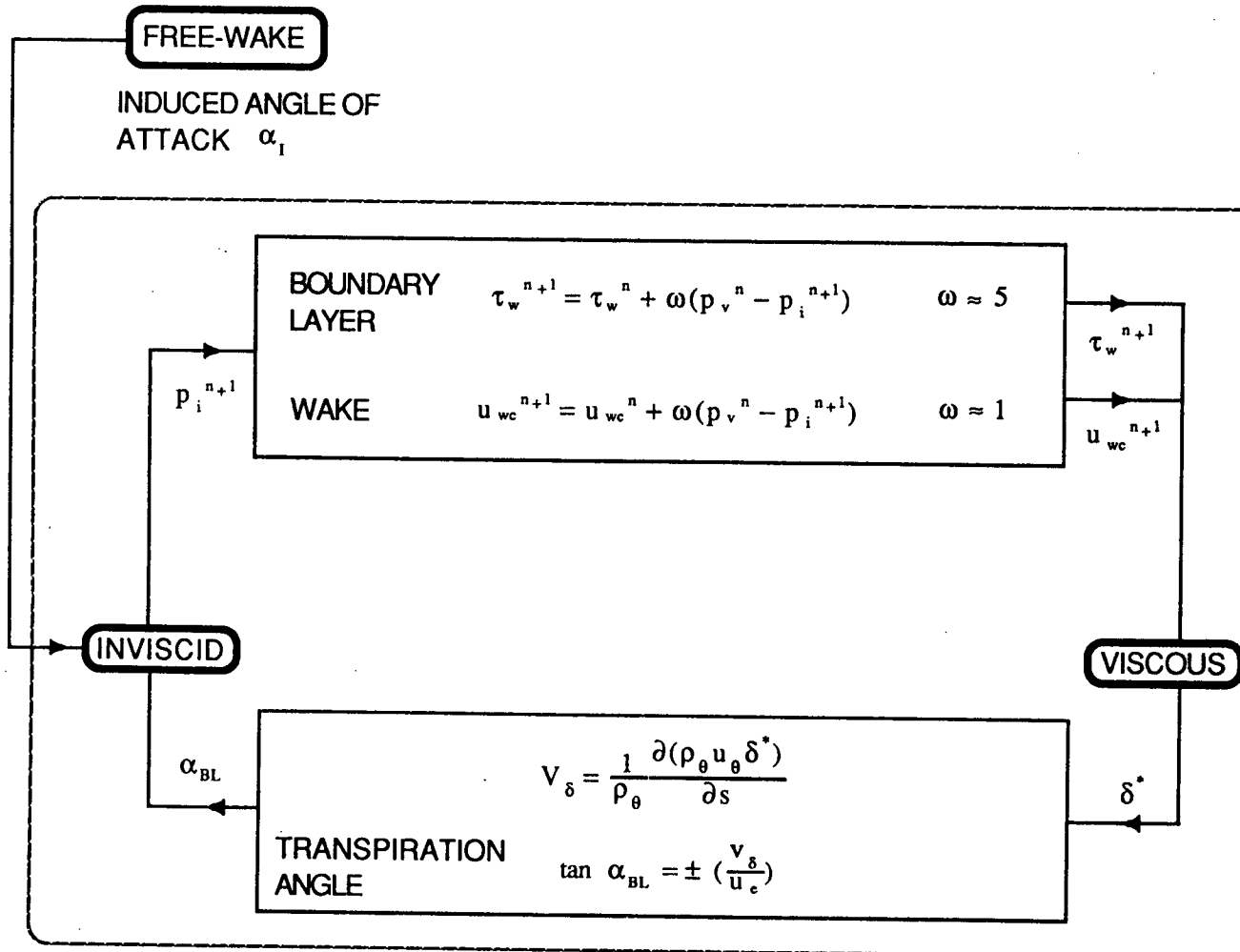
ENERGY EQUATION

$$C_p T + \frac{1}{2}(u^2 + v^2 + w^2) = \text{CONST}$$

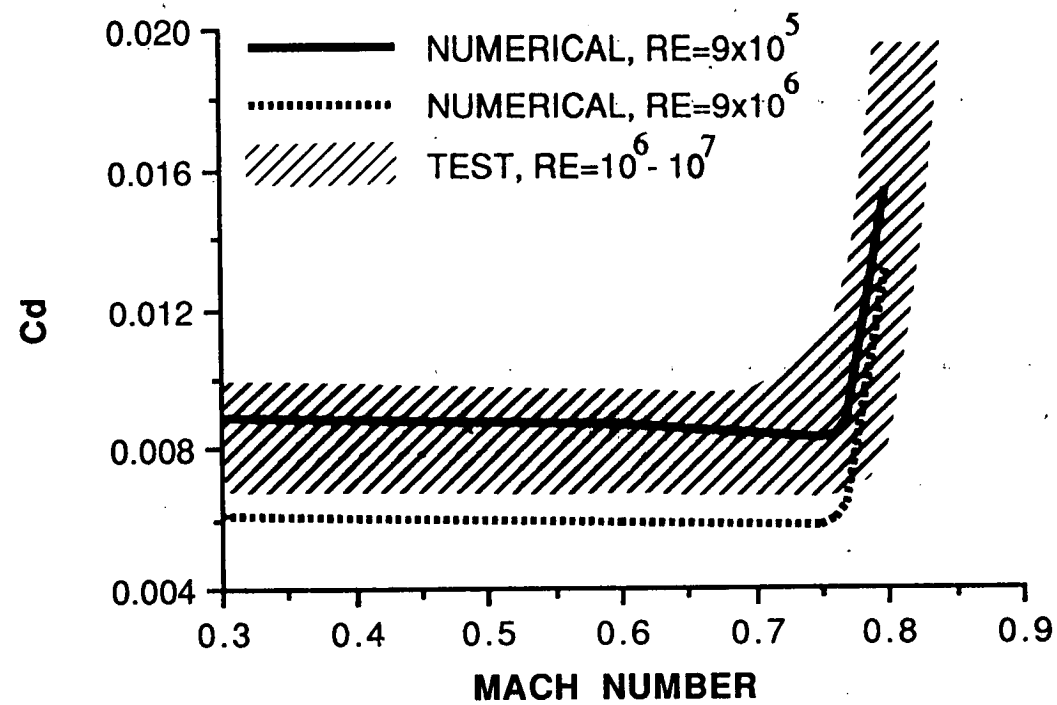
CONTINUITY EQUATION

$$\rho_t + (\rho u)_x + (\rho v)_y + (\rho w)_z = 0$$

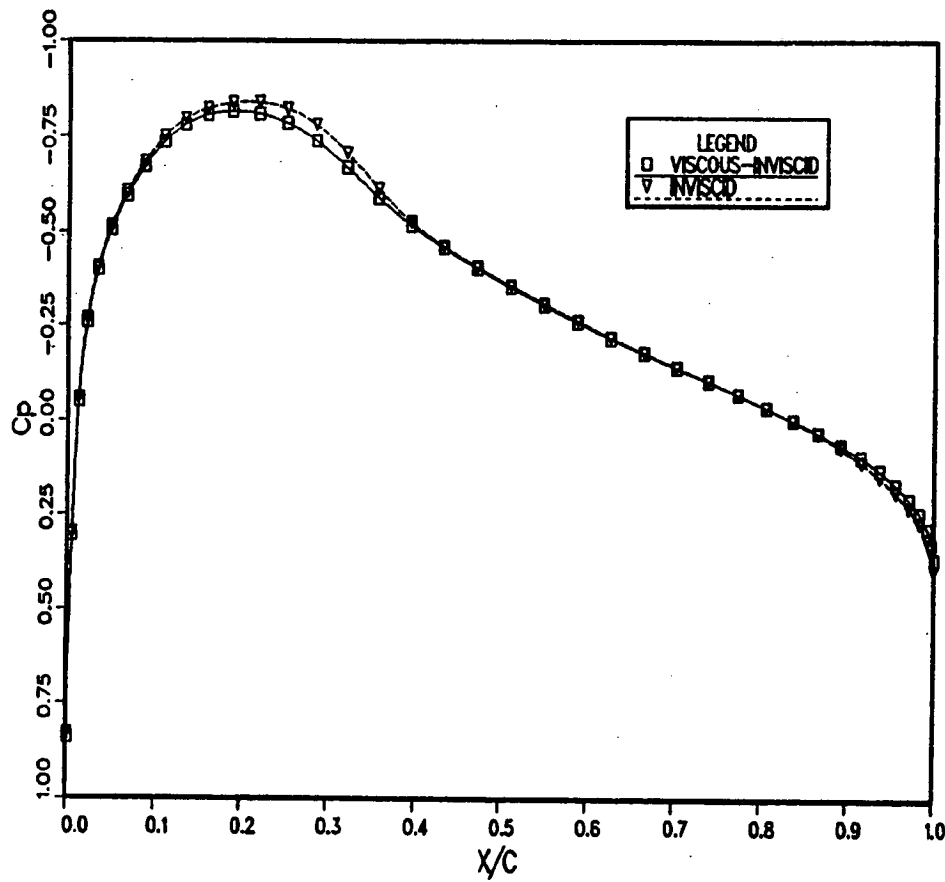
THE COUPLING SCHEME OF VISCOUS, INVISCID, AND FREE-WAKE METHODS
INVERSE APPROACH



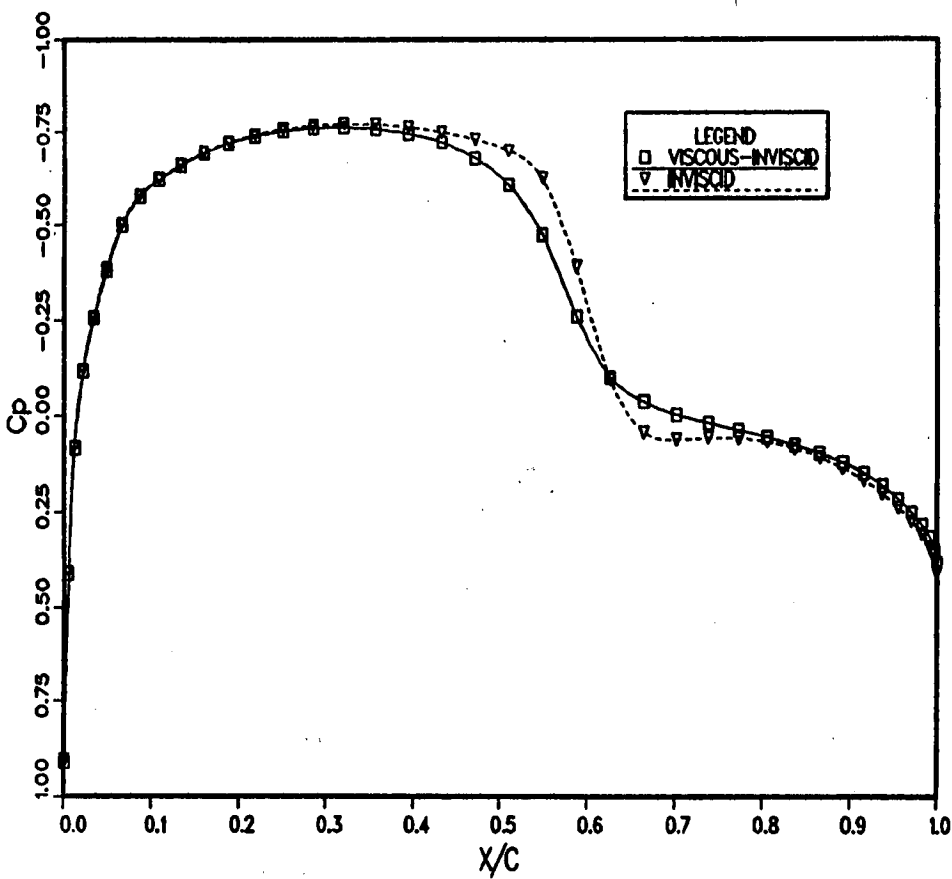
COMPARISON OF PREDICTED AND MEASURED DRAG COEFFICIENT
FOR NACA 0012 TWO-DIMENSIONAL AIRFOIL FLOWS



COMPARISON OF C_p DISTRIBUTION WITH AND WITHOUT
BOUNDARY-LAYER INTERACTION
TIP MACH NUMBER = 0.9, $r/R = 0.8453$

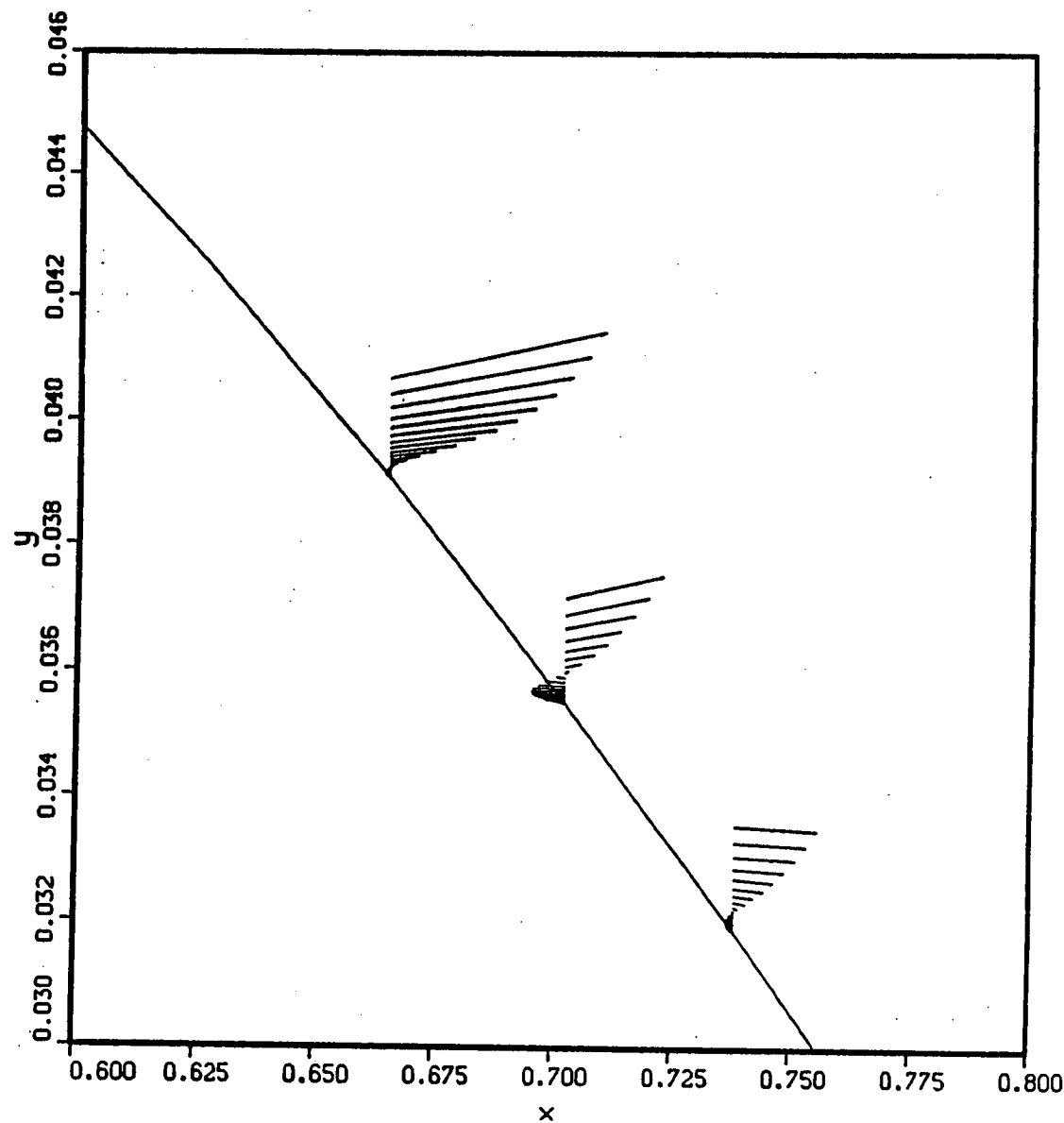


COMPARISON OF C_p DISTRIBUTION WITH AND WITHOUT
BOUNDARY-LAYER INTERACTION
TIP MACH NUMBER = 0.9, $r/R = 0.9759$

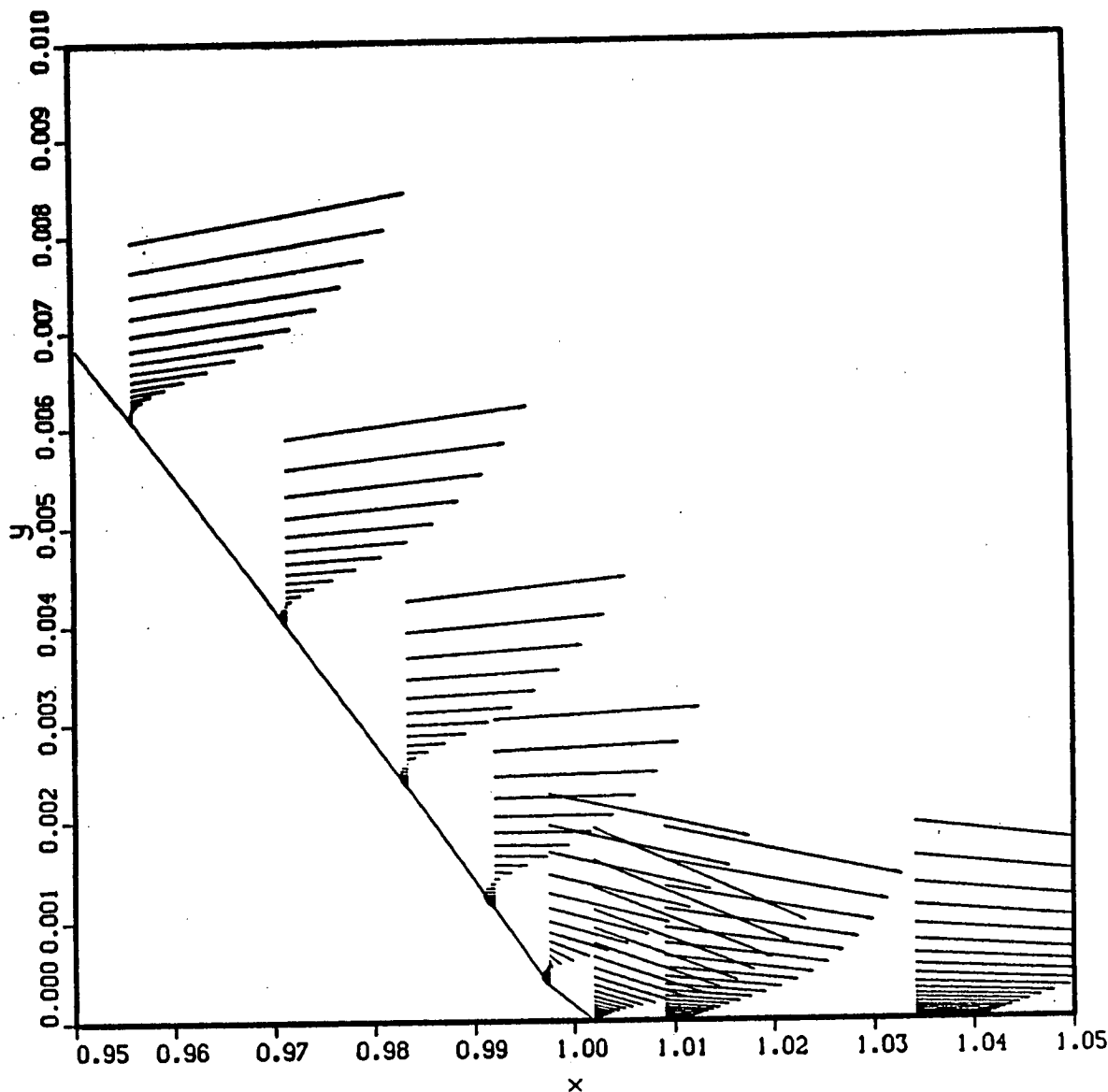


VELOCITY VECTOR PLOT SHOWING SEPARATION BUBBLE
AT ROOT OF SHOCK
TIP MACH NUMBER = 0.925, $r/R = 0.9759$, AR = 13.71

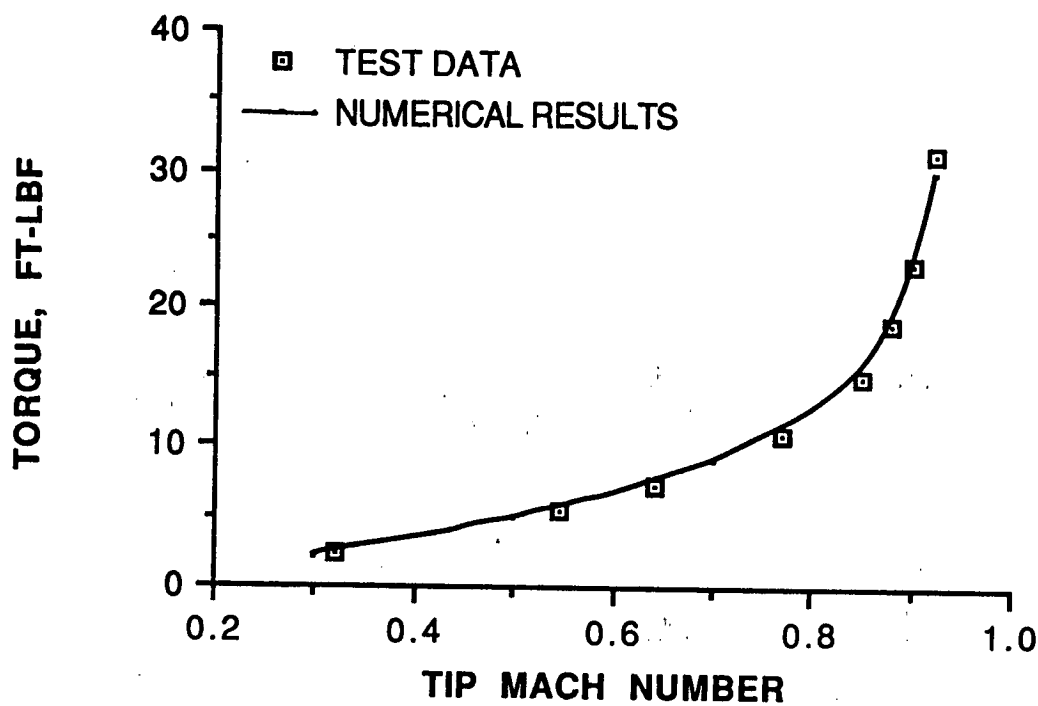
694



VELOCITY VECTOR PLOT SHOWING SEPARATION REGION
AT TRAILING EDGE
TIP MACH NUMBER = 0.925, $r/R = 0.9759$, AR = 13.71



COMPARISON OF PREDICTED AND MEASURED TORQUE
FOR A NONLIFTING, HOVERING ROTOR
TWO BLADES, RECTANGULAR NACA 0012 BLADE,
RADIUS = 3.428 FT, AR = 13.71



FUTURE WORK

- **SIMULATE NONLIFTING ROTOR FLOWS WITH ADVANCED BLADE PLANFORMS, AIRFOILS, AND TWIST DISTRIBUTIONS**
- **INCORPORATE FREE-WAKE ANALYSIS INTO VISCOUS-INVIScid APPROACH TO SIMULATE LIFTING ROTOR FLOWS**
- **INVESTIGATE EFFECTS OF ROTATIONAL MOTION ON DEVELOPMENT OF BOUNDARY-LAYER**

Progress Toward the Development of an Airfoil Icing Analysis Capability

Mark G. Potapczuk

Colin S. Bidwell

NASA Lewis Research Center

Cleveland, Ohio

Brian M. Berkowitz

Sverdrup Technology, Inc.

Mayfield Heights, Ohio

Progress Toward the Development of an Airfoil Icing Analysis Capability

M.G. Potapczuk

C.S. Bidwell

NASA Lewis Research Center, Cleveland, Ohio

B.M. Berkowitz

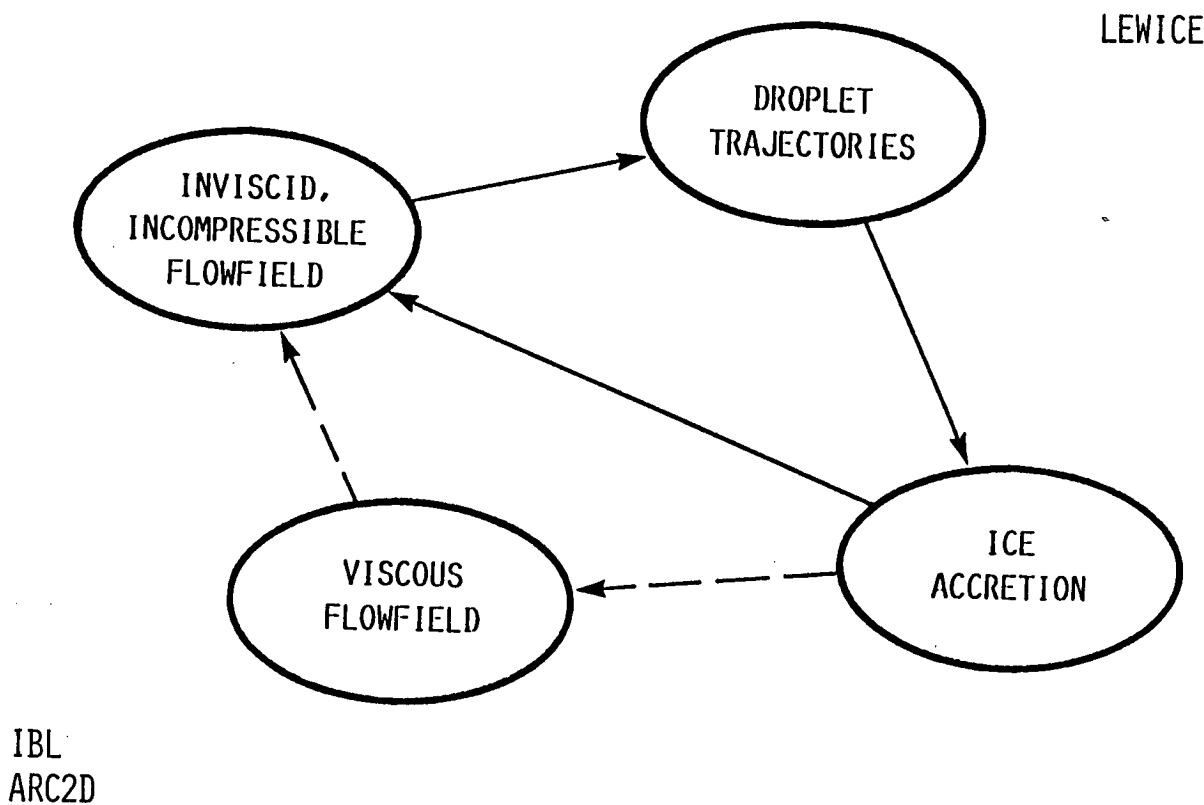
Sverdrup Technology, Inc., Middleburg Hts., Ohio

The NASA-Lewis aircraft icing analysis program is composed of three major sub-programs. These sub-programs are ice accretion simulation, performance degradation evaluation, and ice protection system evaluation. These topics cover all areas of concern related to the simulation of aircraft icing and its consequences. The motivation for these activities is twofold, reduction of time and effort required in experimental programs and the ability to provide reliable information for aircraft certification in icing, over the complete range of environmental conditions. In addition to the analytical activities associated with development of these codes, several experimental programs are underway to provide verification information for existing codes. These experimental programs are also used to investigate the physical processes associated with ice accretion and removal for improvement of present analytical models. The NASA-Lewis icing analysis program is thus striving to provide a full range of analytical tools necessary for evaluation of the consequences of icing and of ice protection systems.

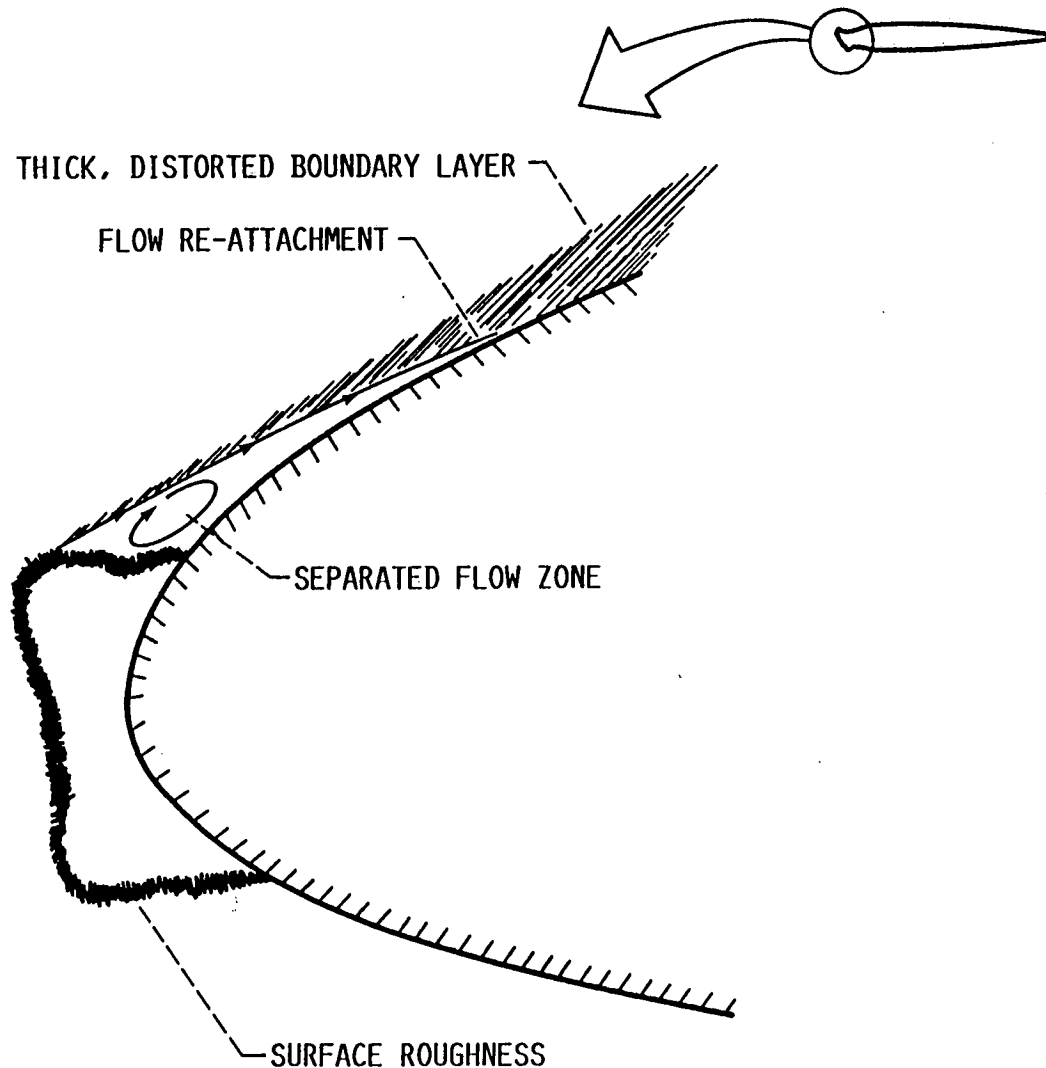
Recently, two of these tools were used to produce a computational evaluation of the ice accretion process and resulting performance changes for a NACA0012 airfoil. The ice accretion code, LEWICE, provided the ice shape geometry at several points in time during the simulated icing encounter. The predicted shapes are a function of several environmental input parameters, including airspeed, temperature, water droplet size and distribution, liquid water content, and duration of the encounter. These ice shape geometries are then used as input for a Navier-Stokes analysis code, ARC2D, which calculates the flowfield and determines changes in performance characteristics of the airfoil. Presently, there is no direct link between the two codes and all interfacing is done by the user. One of the objectives of the icing analysis program is to combine codes such as these into a comprehensive icing analysis method. Work in this area is currently underway via a number of grant supported activities.

STEPS IN AIRFOIL ICING ANALYSIS METHODOLOGY

475



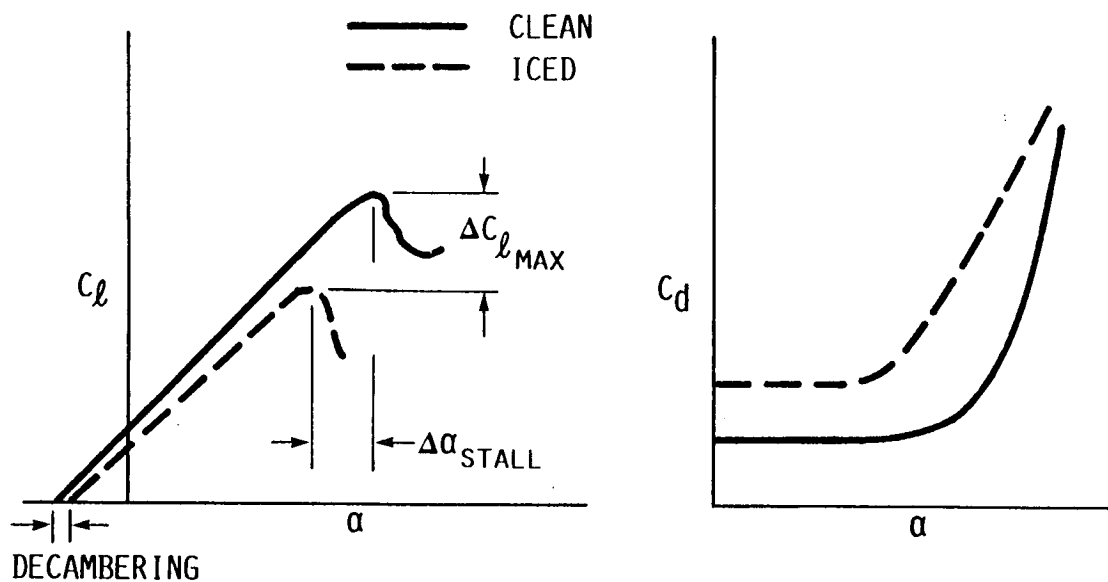
KEY ASPECTS OF AIRFOIL ICING



CD-88-38177

AERODYNAMIC PERFORMANCE DEGRADATION DUE TO ICING

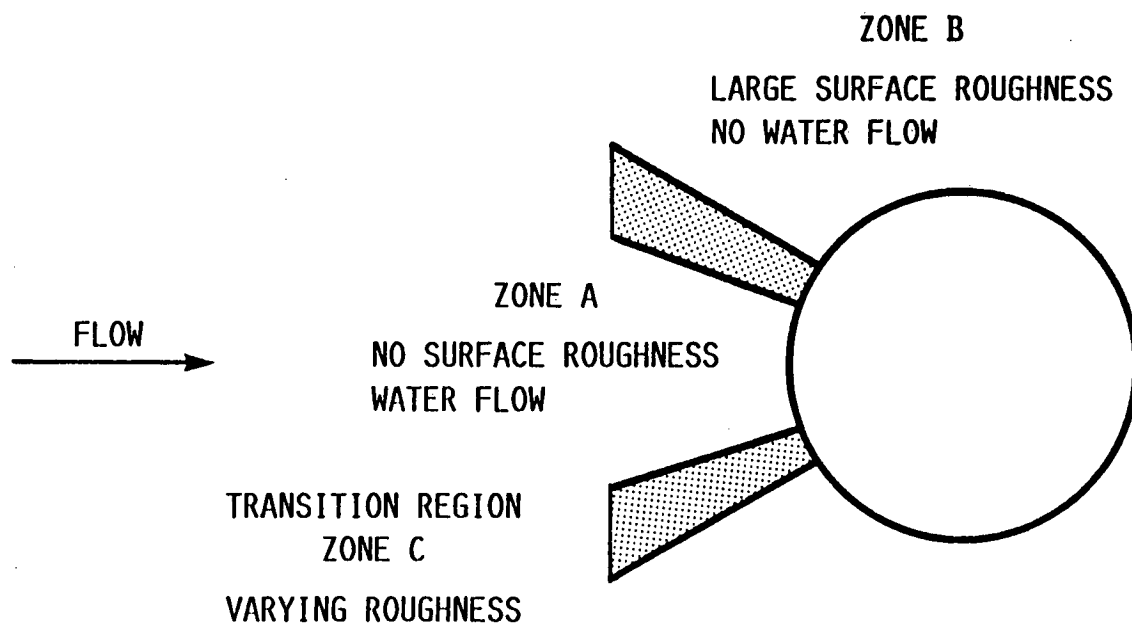
477



CD-88-38176

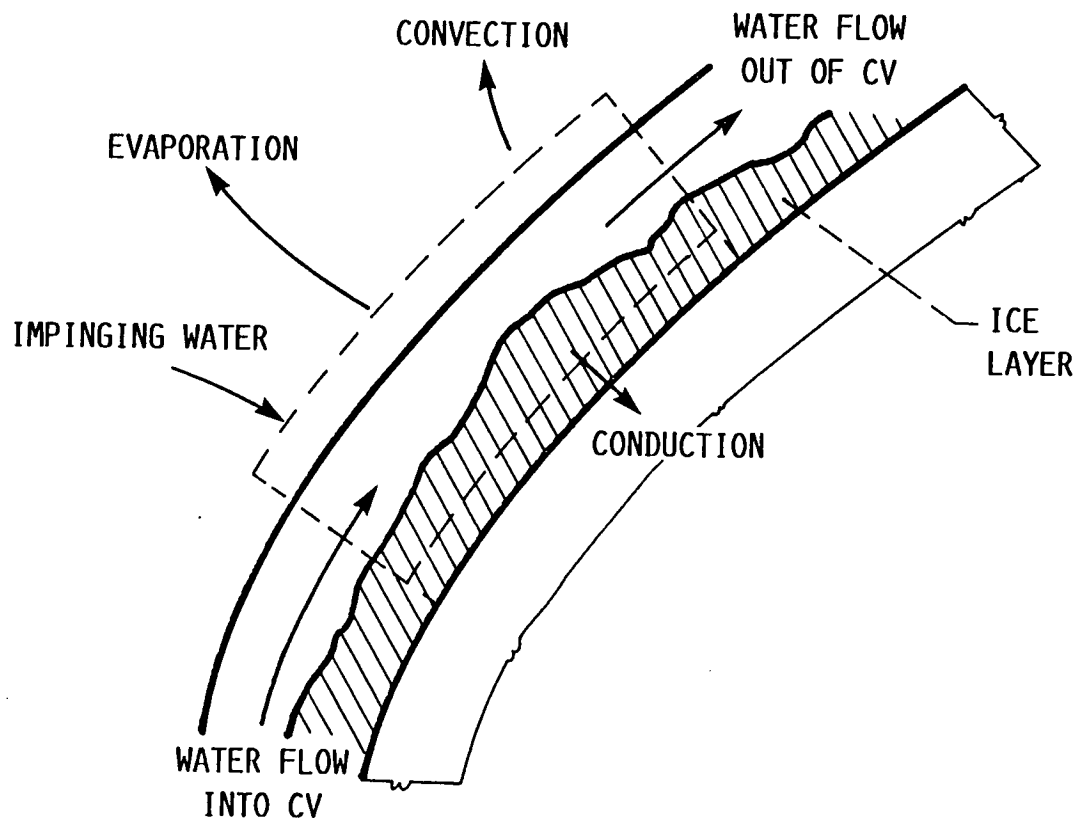
MULTIZONE MODEL OF ICE ACCRETION PROCESS

478

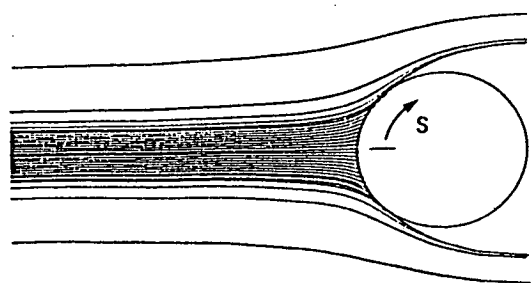
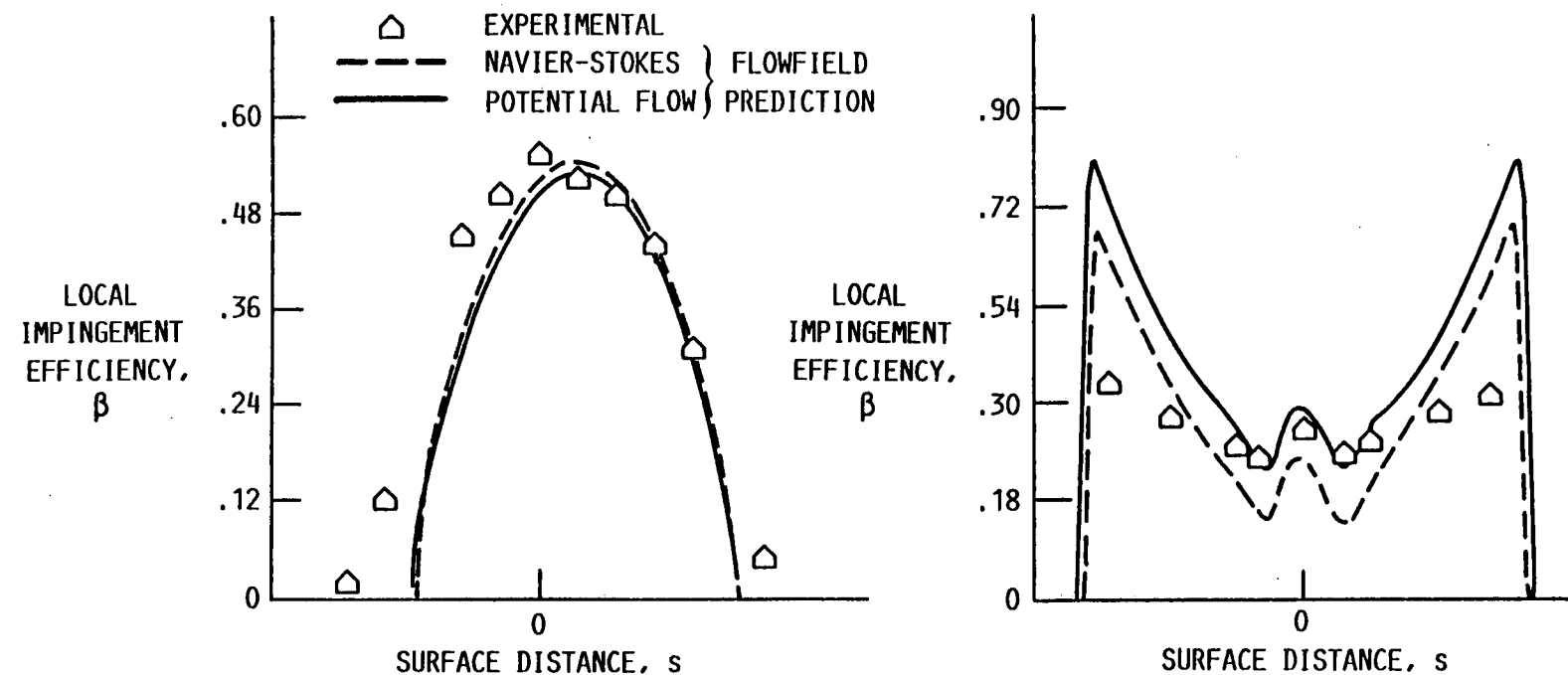


CD-88-38184

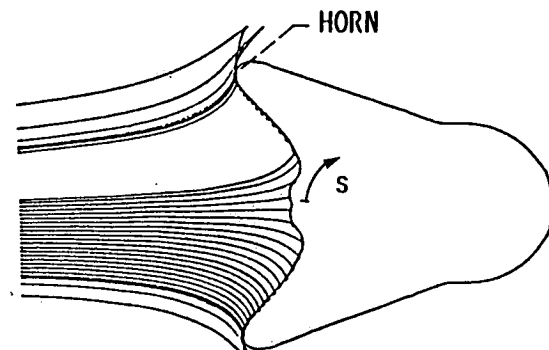
CONTROL VOLUME ANALYSIS OF ICE ACCRETION PROCESS



COLLECTION EFFICIENCY COMPARISONS



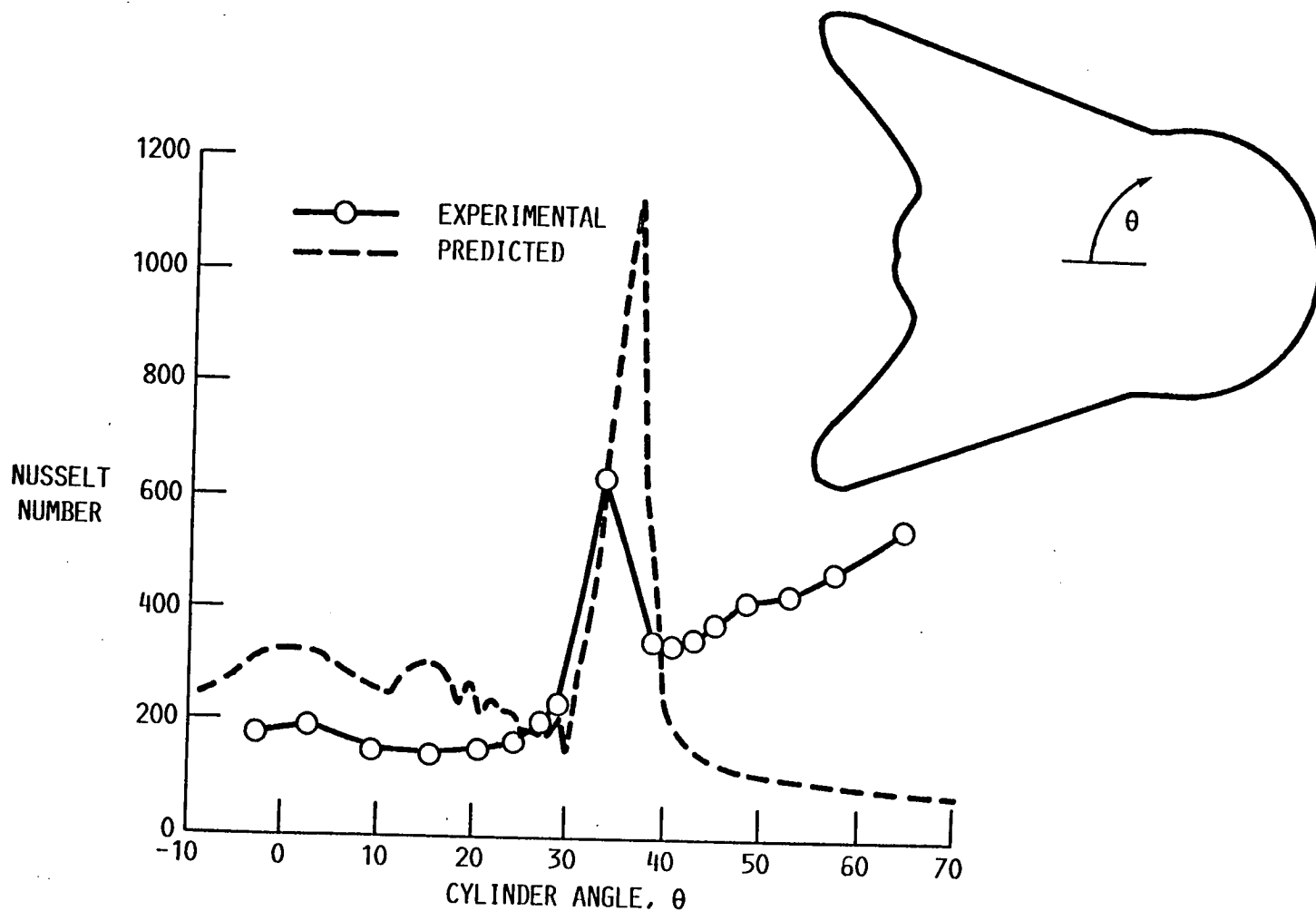
CLEAN CYLINDER.



"ICED" CYLINDER.

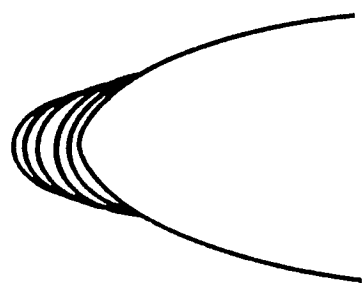
CD-88-38179

COMPARISON OF CALCULATED AND MEASURED HEAT TRANSFER COEFFICIENTS ON SMOOTH SURFACE "ICED" CYLINDER MODEL

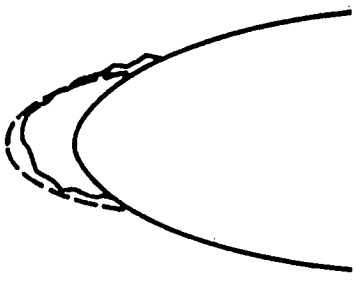


CD-88-38182

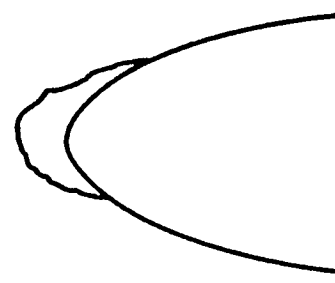
COMPARISON OF ICE SHAPE PREDICTIONS WITH AIRFOIL ICING DATA



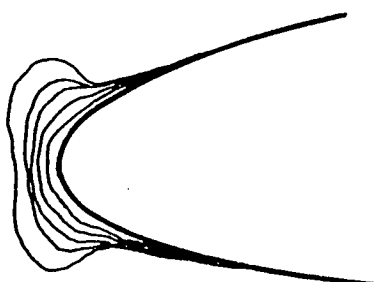
482
CALCULATED
 $LWC = 1.02 \text{ GM/M}^3$



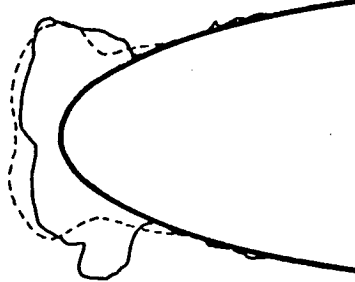
COMPARISON
 $MVD = 12 \mu\text{m}$



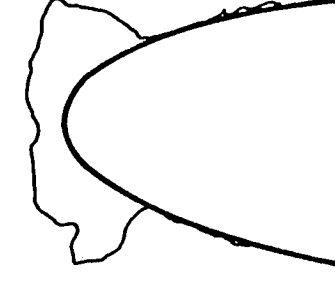
EXPERIMENTAL
 $T_\infty = -26^\circ\text{C}$



CALCULATED
 $LWC = 1.20 \text{ GM/M}^3$

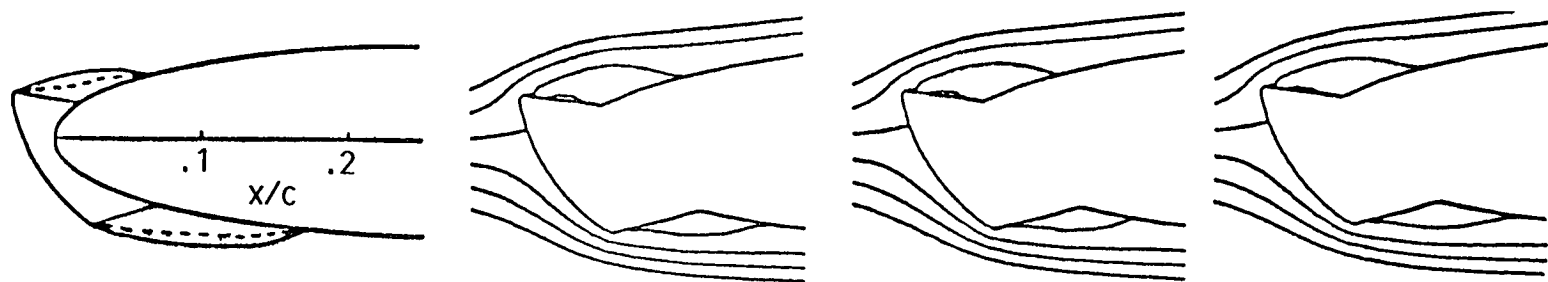


COMPARISON
 $MVD = 20 \mu\text{m}$



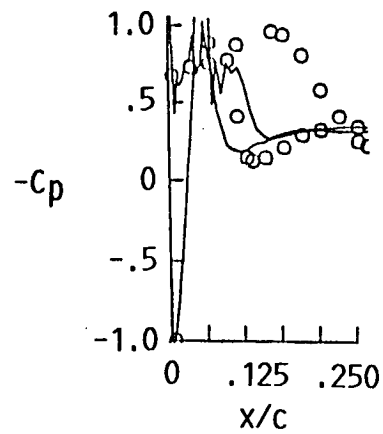
EXPERIMENTAL
 $T_\infty = -11^\circ\text{C}$

EFFECT OF TURBULENCE MODEL ON NAVIER-STOKES PREDICTIONS OF LEADING EDGE PRESSURE DISTRIBUTIONS, $\alpha = 0^\circ$

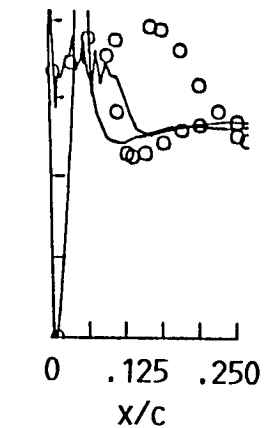


483

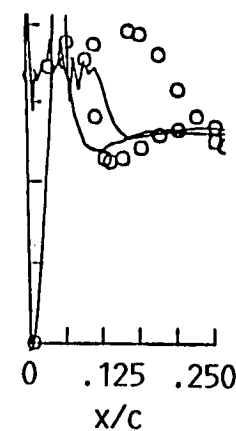
○ EXPERIMENTAL
— PREDICTED



BALDWIN-LOMAX
MODEL



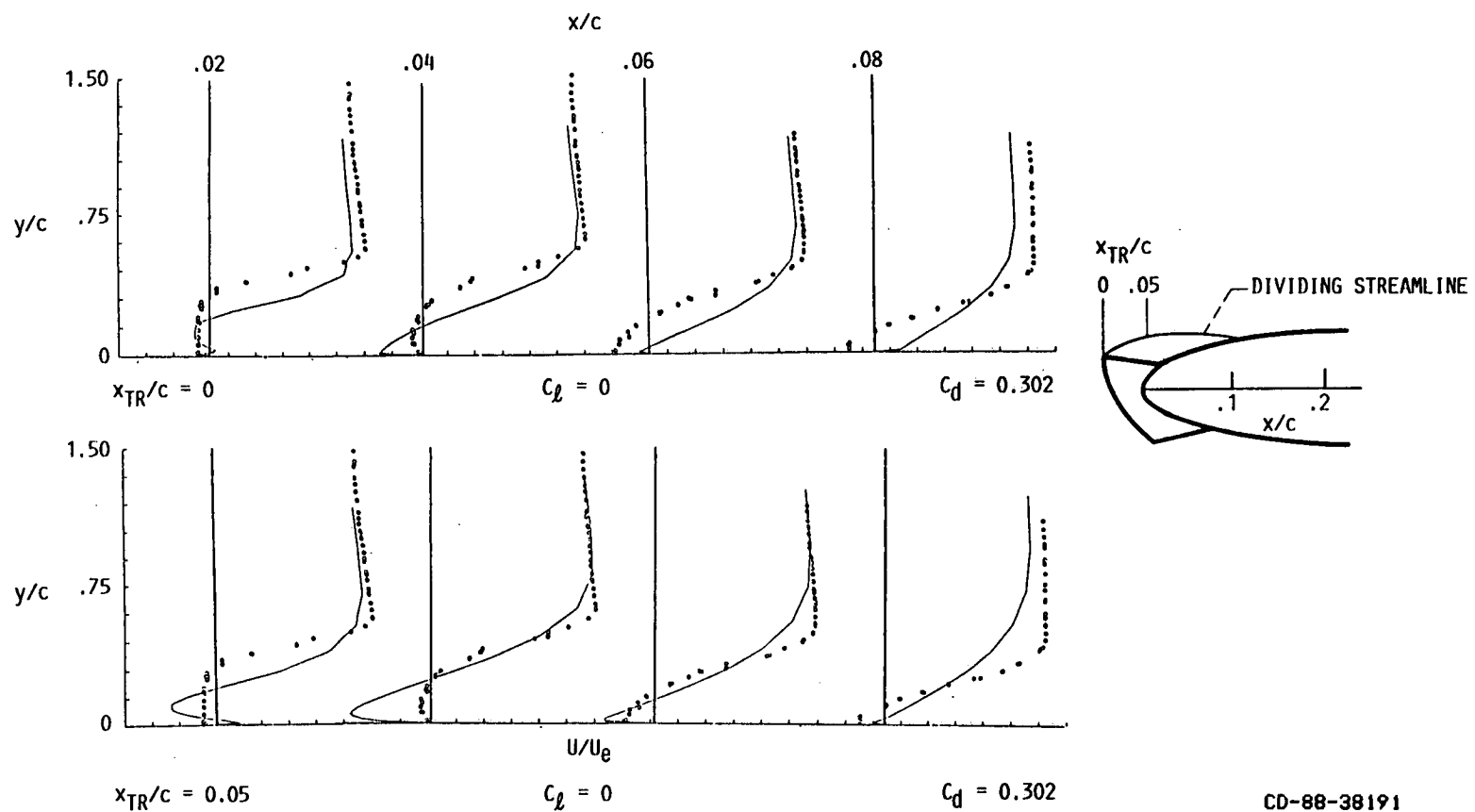
JOHNSON-KING
MODEL



K-E MODEL

CD-88-38189

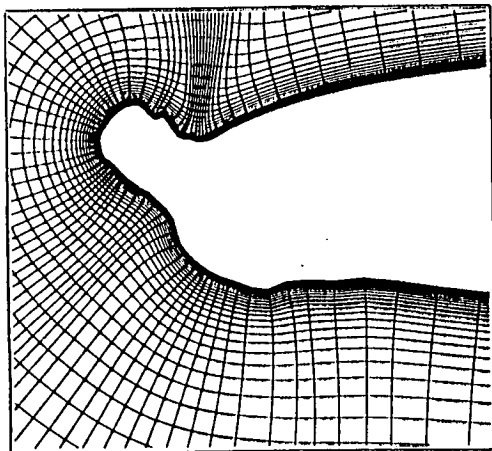
EFFECT OF BOUNDARY LAYER TRANSITION SPECIFICATION
ON NAVIER-STOKES PREDICTED VELOCITY PROFILES IN
SEPARATION-REATTACHMENT ZONE, $\alpha = 0^\circ$



CD-88-38191

RESULTS OF GRID GENERATION STUDY

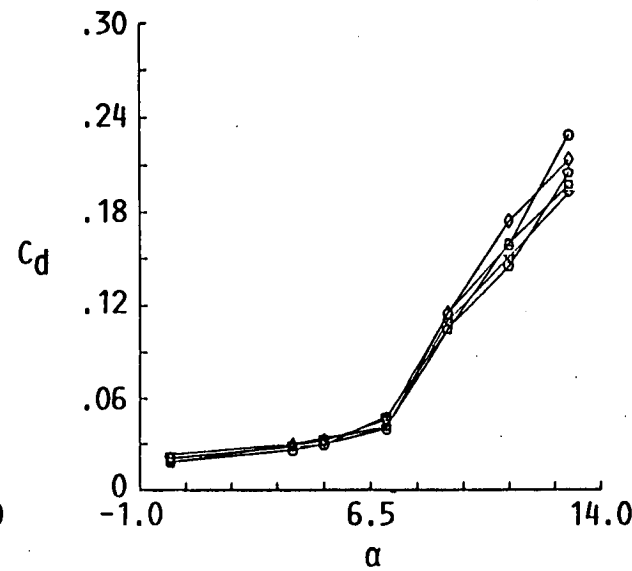
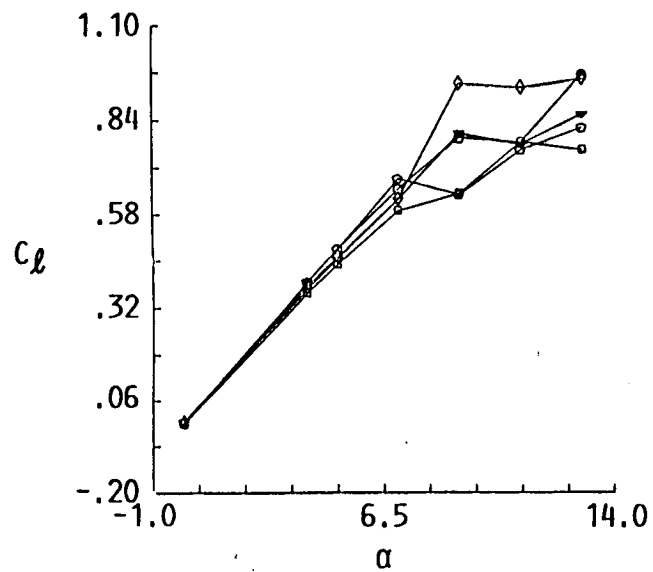
485



GRID SPACING		GRID CODE
ALONG SURFACE	NORMAL TO SURFACE	
◇ DENSE L.E.	NORMAL	
○ EVEN	NORMAL	
▽ DENSE L.E.	DENSE	
△ EVEN	DENSE	
□ EVEN	NORMAL	

HYPGRID

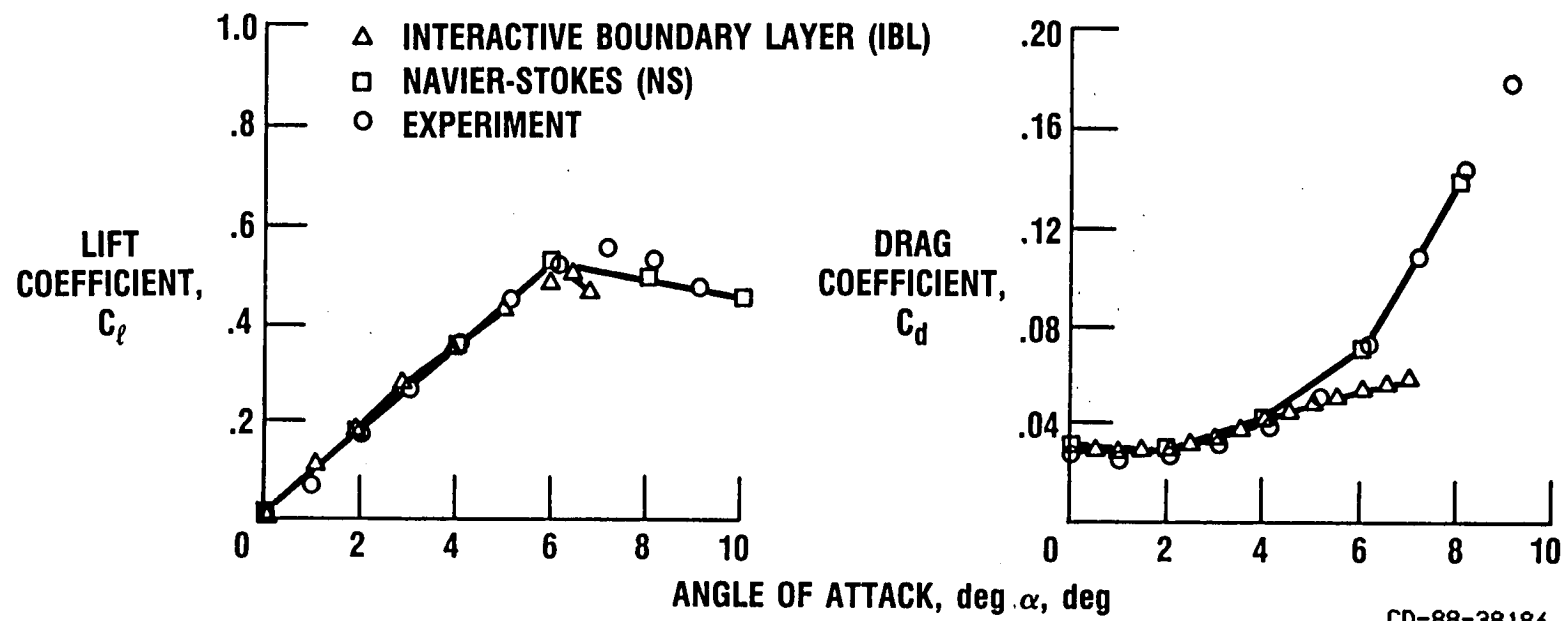
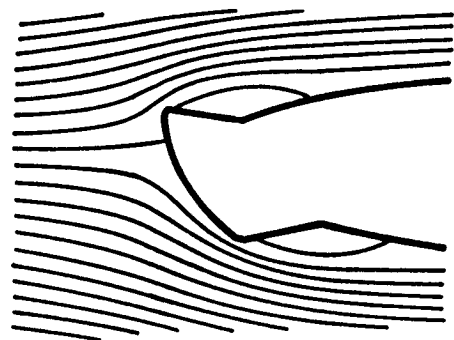
GRAPE



CD-88-38188

COMPARISON OF ICED AIRFOIL CODE PREDICTIONS WITH EXPERIMENTAL MEASUREMENTS

48



CD-88-38186

CONCLUDING REMARKS

- First generation airfoil icing capability exists
- Code validation activities are ongoing
 - Droplet trajectories / impingement
 - Ice accretion
 - Aerodynamic performance
- Supporting analytical/experimental efforts underway to improve physical modeling in codes
 - Movies/photographs of ice accretion
 - Ice surface roughness
- Extension to 3D icing analysis has been initiated

The Breakup of Trailing-Line Vortices

David Jacqmin

NASA Lewis Research Center
Cleveland, Ohio 44135

It is now known that Batchelor's trailing-line vortex is extremely unstable to small amplitude disturbances for swirl numbers in the neighborhood of .83. We present results of numerical calculations that show the response of the vortex in this range of swirl numbers to finite amplitude, temporal, helical disturbances. Phenomena observed include: 1) ejection of axial vorticity and momentum from the core resulting in the creation of secondary, separate vortices; 2) a great intensification of core axial vorticity and a weakening of core momentum; 3) the production of azimuthal vorticity in the form of a tightly wrapped spiral wave. The second phenomenon eventually stabilizes the vortex, which then smooths and gradually returns to an axisymmetric state. The calculations are mixed spectral-finite-difference, fourth-order accurate, and have been carried out at Reynolds numbers of 1000-2000. Some linearized results will also be discussed in an attempt to explain the process of vortex intensification.

Applications

- Axisymmetric evolution of vortices, jets, and wakes.
- 3D instability of axisymmetric flows (weakly nonlinear).
- Spiral and axisymmetric vortex breakdown - strongly nonlinear instabilities.
- Acoustic excitation of swirling jets.
- Mixing caused by vortices - effects on combustion.

Numerical Methods

161

- 3D direct numerical simulation using primitive variables.
- Unbounded cylindrical coordinates - use of mapping $r = \tan \lambda$.
- Mixed spectral and finite difference methods
 - Azimuthal: spectral ($\exp in\theta$).
 - Axial: spectral ($\exp i\omega mx$) or 2nd order FD.
 - Radial: spectral ($\sin^n 2\lambda \cos 2j\lambda$) or 4th order FD.
- Fourth order accurate (Runge-Kutta) in time.

Batchelor's Trailing-Line Vortices

- Defined by axial velocity $= \exp(-r^2)$, axial vorticity $= q \exp(-r^2)$.
- Model for aircraft trailing line vortices, created in laboratory.
- Very unstable in some ranges of q . $q \simeq .85$ most unstable.
- From inviscid theory, all azimuthal wavenumbers unstable.

As $n \rightarrow \infty$ $c_i \rightarrow .4$.

As $n \rightarrow \infty$ most unstable axial wavenumber $\rightarrow .52n$

- From viscous theory, c_i modified by $O(R^{-1})$. # unstable waves $O(R^{3/5})$.

Numerical Solution

- Quasi-3D calculation can capture all the most unstable modes.
- Navier Stokes equations have helical solutions:

$$\sum_{n=-\infty}^{n=+\infty} f_n(r, t) \exp in(\beta x - \theta)$$

- Calculations have $q = .82$, $\beta = .52$, $R = 1600$.
- Calculations spectral in x and θ , fourth order in λ .

Features of Solution

- Initially, elliptical deformation of vortex. Helical displacement from center line.
- Kinematic deformation of vortex then produces spiral structure.
- Axial divergence intensifies axial vorticity, is associated with azimuthal vorticity.
- "Turbulent" patches form at vortex outer edges.
- In later stages, viscous diffusion weakens spiral structure. Turbulent patches separate from vortex. Vortex core remains intense.
- Intensified vortex returns to axisymmetric state.

Axial vorticity intensifies. Axial velocity weakens. Vortex stabilizes.

APPENDIX

LIST OF ATTENDEES

John J. Adamczyk
NASA Lewis Research Center
MS 5-9
Cleveland, OH 44135

Ramesh K. Agarwal
McDonnell Douglas
Research Laboratories
P.O. Box 516
Department 222, Building 110, MS4
St. Louis, MO 63166

James A. Albers
NASA Ames Research Center
MS 200-3
Moffett Field, CA 94035

Chris Atwood
MCAT Institute
NASA Ames Research Center
MS 258-1
Moffett Field, CA 94035

James D. Baeder
NASA Ames Research Center
MS 258-1
Moffett Field, CA 94035

Don Bai
NASA/MSFC
Mail Code ED55
Huntsville, AL 35812

Bala Balakrishnan
MCAT Institute
NASA Ames Research Center
MS 258-1
Moffett Field, CA 94035

Daniel W. Barnette
Sandia National Laboratories
P.O. Box 5800, Organization 1556
Albuquerque, NM 87185

Tim Barth
NASA Ames Research Center
MS 202A-1
Moffett Field, CA 94035

Richard A. Batchelder
McDonnell Douglas
Space Systems Co.
5301 Bolsa Avenue
Station 13-3
Huntington Beach, CA 92647

John T. Batina
NASA Langley Research Center
MS 173
Hampton, VA 23665

Oktay Baysal
NASA Langley Research Center
MS 170
Hampton, VA 23665

Brad Bennett
MCAT Institute
NASA Ames Research Center
MS 258-1
Moffett Field, CA 94035

Thomas J. Benson
NASA Lewis Research Center
MS 5-7
Cleveland, OH 44135

Robert F. Bergholz
GE Aircraft Engines
1 Neumann Way
Cincinnati, OH 45215

John Bertin
DFAN
U. S. Air Force Adacemy, CO 80840

Ishwar C. Bhateley
General Dynamics
Fort Worth Division
P. O. Box 748, Mail Stop 28-70
Fort Worth, TX 76101

Sedat Birigen
University of Colorado-Boulder
College of Engineering and Applied Science
Boulder, CO 80309

F. G. Blottner
Sandia National Laboratories
P. O. Box 5800, Organization 1556
Albuquerque, NM 87185-5800

Thomas C. Blum
Boeing Advanced Systems
P.O. Box 3707, MS 33-18
Seattle, WA 98124-2207

Brian Bochsle
General Dynamics/Convair
P.O. Box 85357
MS 36-1240
San Diego, CA 92138

Edwin Brewer
NASA/MSFC
Mail Code ED32
Huntsville, AL 35812

David L. Burrus
G.E. Aircraft Engines
1 Neumann Way
Cincinnati, OH 45215

Richard J. Busch, Jr.
Northrop Aircraft Division
One Northrop Avenue
MS 3731/89
Hawthorne, CA 90250

George Callas
NASA Ames Research Center
MS 233-14
Moffett Field, CA 94035

Richard L. Campbell
NASA Langley Research Center
MS 294
Hampton, VA 23665

Graham Candler
NASA Ames Research Center
MS 230-2
Moffett Field, CA 94035

Graham Carey
University of Texas at Austin
CFD Laboratory
ASE-EM Department, WRW 305
Austin, TX 78712

Mark H. Carpenter
NASA Langley Research Center
MS 156
Hampton, VA 23665

James E. Carter
United Technologies Research Center
MS 20 - Silver Lane
East Hartford, CT 06108

Steve Caruso
Nielsen Engineering
510 Clyde Avenue
Mountain View, CA 94043

Neal M. Chaderjian
NASA Ames Research Center
MS 258-1
Moffett Field, CA 94035

Denny S. Chaussee
NASA Ames Research Center
MS 258-1
Moffett Field, CA 94035

Kalpana Chawla
MCAT Institute
NASA Ames Research Center
MS 258-1
Moffett Field, CA 94035

C. S. Chen
NASA Ames Research Center
MS T031
Moffett Field, CA 94035

Lee-Tzong Chen
McDonnell Douglas
3855 Lakewood Blvd.
Long Beach, CA 90846

Lester Cheng
Boeing Military Company
P.O. Box 7730, MS K13-00
Wichita, KS 67277-7730

Bob Childs
Nielsen Engineering
510 Clyde Avenue
Mountain View, CA 94043

Roderick V. Chima
NASA Lewis Research Center
21000 Brookpark Road, MS 5-11
Cleveland, OH 44135

Tawit Chitsomboon
NASA Langley Research Center
MS 168
Hampton, VA 23665

Ing-Tsau Chiu
NASA Ames Research Center
MS 258-2
Moffett Field, CA 94035

Lynn C. Chou
NASA/MSFC
Mail Code ED32
Huntsville, AL 35812

Wei J. Chyu
NASA Ames Research Center
MS 227-6
Moffett Field, CA 94035

Thomas J. Coakley
NASA Ames Research Center
MS 229-1
Moffett Field, CA 94035

Stuart D. Connell
General Electric Co.
Mail Drop A323
8500 Govenors Hill Drive
Cincinnati, OH 45249

Gary B. Cosentino
NASA Ames Research Center
MS 227-6
Moffett Field, CA 94035

Russell M. Cummings
NASA Ames Research Center
MS 258-1
Moffett Field, CA 94035

Leo Dadone
Boeing Vertol Company
P.O. Box 16858, MS Pd32-74
Philadelphia, PA 19142

Carol Davies
NASA Ames Research Center
MS 230-3
Moffett Field, CA 94035

Sanford Davis
NASA Ames Research Center
MS 260-1
Moffett Field, CA 94035

George S. Deiwert
NASA Ames Research Center
MS 230-2
Moffett Field, CA 94035

Robert A. Delaney
GMC Allison Gas Turbine Division
P.O. Box 420 (Speed Code S46)
Indianapolis, IN 46206

D. Doran
NASA/MSFC
Mail Code Ed32
Huntsville, AL 35812

Henry S. Dresser
Rockwell International
125 Ruby Avenue
Balboa Island, CA 92662

Douglas L. Dwoyer
NASA Langley Research Center
MS 256
Hampton, VA 23665

Gordon Erlebacher
NASA Langley Research Center
MS 156
Hampton, VA 23665

Ian Fejtek
NASA Ames Research Center
MS T-031
Moffett Field, CA 94035

Jolen Flores
NASA Ames Research Center
MS 258-1
Moffett Field, CA 94035

James A. Franklin
NASA Ames Research Center
MS 211-2
Moffett Field, CA 94035

Douglas M. Friedman
McDonnell Douglas
3855 Lakewood Boulevard, MS 36-81
Long Beach, CA 90846

Robert Garcia
NASA/MSFC
Mail Code ED32
Huntsville, AL 35812

Sharad Gavali
Amdahl
1250 E. Arquez Avenue.
MS 265, P.O. Box 3470
Sunnyvale, CA 94088-3470

Steve Gegg
NASA Ames Research Center
MS 258-1
Moffett Field, CA 94035

Michael W. George
Rockwell International Corporation
201 N. Douglas Street
P.O. Box 92098, MS-GB12
Los Angeles, CA 90009

Farhad Ghaffari
NASA Langley Research Center
MS 294
Hampton, VA 23665

Leslie Glatt
TRW
One Space Park, MS R1/1038
Redondo Beach, CA 90278

Peter Gnoffo
NASA Langley Research Center
MS 366
Hampton, VA 23665-5225

Tahir Gokcen
Stanford University
Department of Aeronautics and Astronautics
Stanford, CA 94305

John Goodrich
NASA Lewis Research Center
MS 5-7
Cleveland, OH 44135

Peter M. Goorjian
NASA Ames Research Center
MS 258-1
Moffett Field, CA 94035

Randolph A. Graves, Jr.
NASA Headquarters
Code RF
Washington, DC 20546

Michael Green
NASA Ames Research Center
MS 258-1
Moffett Field, CA 94035

Lisa Griffin
NASA Marshall Space Flight Center
Mail Code ED32
Huntsville, AL 35812

Anthony R. Gross
NASA Ames Research Center
MS 258-3
Moffett Field, CA 94035

Clyde Gumbert
NASA Langley Research Center
MS 159
Hampton, VA 23665

Guru P. Guruswamy
NASA Ames Research Center
MS 258-1
Moffett Field, CA 94035

Raimo Hakkinen
McDonnell Douglas Research Laboratories
Department 222, Building 110
P.O. Box 516
St. Louis, MO 63166

Dean C. Hammond, Jr.
General Motors Research Laboratories
FM/57, 30500 Mound Road
Warren, MI 48090-9055

Taeyoung Han
General Motors Research Laboratories
FM/57, 30500 Mound Road
Warren, MI 48090-9055

H. A. Hassan
North Carolina State University
Mechanical and Aerospace Engineering
Raleigh, NC 27695-7910

Bob Henke
Boeing Commercial Airplane Company
P.O. Box 3707
Seattle, WA 98124-2207

Kristin A. Hessenius
NASA Ames Research Center
MS 200-4
Moffett Field, CA 94035

Paul Hickey
Gulfstream Aerospace Corporation
P.O. Box 2206, D-04 Department 895
Savannah, GA 31402-2206

Terry L. Holst
NASA Ames Research Center
MS 258-1
Moffett Field, CA 94035

James Horling
Naval Air Propulsion Center
P. O. Box 7176
Trenton, NJ 08628

Tsuying Hsieh
Naval Surface Weapons Center
R44 White Oak, MD

Yu-Kao Hsu
University of Maine
Illinois Avenue
Bangor, ME 04401

Mark Huebler
General Motors Research Laboratories
FM/57, 30500 Mound Road
Warren, MI 48090-9055

Dennis L. Huff
NASA Lewis Research Center
21000 Brookpark Road, MS 77-6
Cleveland, OH 44135

Danny P. Hwang
NASA Lewis Research Center
MS 100-5, 21000 Brookpark Road
Cleveland, OH 44135

Mamoru Inouye
NASA Ames Research Center
MS 202A-1
Moffett Field, CA 94035

David A. Jacqmin
NASA Lewis Research Center
MS 5-7
Cleveland, OH 44135

Zakaria Jalamani
NASA Ames Research Center
MS 258-1
Moffett Field, CA 94035

Antony Jameson
Princeton University
Mechanical and Aerospace
Engineering Department
Princeton, NJ 08544

Mohan Jayaram
IBM Corporation
MS 276 Neighborhood Road
Kingston, NY 12401

Dennis Jespersen
NASA Ames Research Center
MS 202A-1
Moffett Field, CA 94035

Jeffrey L. Johnson
Sterling Software
NASA Ames Research Center
MS 221-6
Moffett Field, CA 94035

Dennis A. Johnson
NASA Ames Research Center
MS 229-1
Moffett Field, CA 94035

Gary M. Johnson
North Carolina Supercomputing Center
P.O. Box 12732
Research Triangle Park, NC 27709

Max Kandula
Lockheed Engineering and Management
Services Company
2400 NASA Road 1
Houston, TX 77058

Charles Kang
General Dynamics/Convair
P.O. Box 85357, MS 36-1240
San Diego, CA 92138

Lyndell S. King
NASA Ames Research Center
MS 260-1
Moffett Field, CA 94035

John Kreatsoulas
Digital Equipment Corporation
Four Results Way
MR04-2/H19
Marlboro, MA 01752

Sherrie Krist
NASA Langley Research Center
MS 128
Hampton, VA 23665

Thomas Kropp
Sterling Software
1121 San' Antonio Road
Palo Alto, CA 94303

Paul Kutler
NASA Ames Research Center
MS 258-3
Moffett Field, CA 94035

C. Lee
NASA Marshall Space Flight Center
Mail Code ED33
Huntsville, AL 35812

Ki D. Lee
University of Illinois
104 South Mathews Avenue
Urbana, IL 61801

Johnson Lee
Sterling Software
NASA Ames Research Center
MS 258-1
Moffett Field, CA 94035

Jerry L. Lee
Boeing Commercial Airplane Company
P.O. Box 3707
MS 7C-36
Seattle, WA 98124-2207

Chien Li
NASA Johnson Space Center
Mail Code ED311
Houston, TX 77058

R. T. Ling
Northrop Aircraft Division
One Northrop Avenue
Department 3811/82
Hawthorne, CA 90250

Meng Liou
NASA Lewis Research Center
MS 5-7
Cleveland, OH 44135

Amalia R. Lopez
Sandia National Laboratories
P.O. Box 5800, Organization 1556
Albuquerque, NM 87185

Paula Lovely
Sterling Software
NASA Ames Research Center
MS 221-6
Moffett Field, CA 94035

Raymond Luh
MCAT Institute
NASA Ames Research Center
MS 258-1
Moffett Field, CA 94035

Robert W. MacCormack
Stanford University
Department of Aeronautics and Astronautics
Stanford, CA 94305

Nateri K. Madavan
Sterling Software
NASA Ames Research Center
MS 258-2
Moffett Field, CA 94035

Mike Madson
NASA Ames Research Center
MS 227-2
Moffett Field, CA 94035

John B. Malone
Bell Helicopter Textron
P.O. Box 482
MS 012681-14
Fort Worth, TX 76101

J. F. Mangus
Northrop Aircraft Division
One Northrop Avenue
Department 3811/82
Hawthorne, CA 90250

Reda Mankbadi
NASA Lewis Research Center
MS 5-11
Cleveland, OH 44135

Fred Martin
NASA Ames Research Center
MS 258-1
Moffett Field, CA 94035

Joseph G. Marvin
NASA Ames Research Center
MS 229-1
Moffett Field, CA 94035

Douglas R. McCarthy
Boeing Commercial Airplane Company
P.O. Box 3707
MS 7C-36
Seattle, WA 98124-2207

William J. McCroskey
U.S. Army
NASA Ames Research Center
MS 258-1
Moffett Field, CA 94035

Susan McMillin
NASA Langley Research Center
MS 170
Hampton, VA 23665

Rabi Mehta
NASA Ames Research Center
MS 260-1
Moffett Field, CA 94035

Unmeel B. Mehta
NASA Ames Research Center
MS 202A-1
Moffett Field, CA 94035

Keith Meintjes
General Motors Research Laboratories
FM/57, 30500 Mound Road
Warren, MI 48090-9055

Robert E. Melnik
Grumman Aerospace Corporation
A08-Plant
35 Corporate Research Center
Bethpage, NY 11714

John Melton
NASA Ames Research Center
MS 227-6
Moffett Field, CA 94035

Joel P. Mendoza
NASA Ames Research Center
MS 227-6
Moffett Field, CA 94035

Clark D. Mikkelsen
USAMICOM
AMSMI-RD-SS-AT
Redstone Arsenal, AL 35898-5252

Brent A. Miller
NASA Lewis Research Center
MS 5-3
21000 Brookpark Road
Cleveland, OH 44135

Kenichi Miura
Fujitsu America, Inc.
MS B2-7
3055 Orchard Drive
San Jose, CA 95134

Greg Molvik
MCAT Institute
NASA Ames Research Center
MS 258-1
Moffett Field, CA 94035

Marianne Mosher
NASA Ames Research Center
MS T031
Moffett Field, CA 94035

James Moss
NASA Langley Research Center
MS 170
Hampton, VA 23665

Shohei Nakazawa
MARC Analysis Research Corporation
260 Sheridan Avenue.
Palo Alto, CA 94306

Jim C. Narramore
Bell Helicopter Textron
P.O. Box 482
MS 012681-14
Fort Worth, TX 76101

Ejike Ndefo
Aerospace Corporation
P.O. Box 92957 (M4/964)
Los Angeles, CA 90009-2957

Charles J. Nietubicz
U. S. Army Ballistic Research Laboratory
Computational Aerodynamics Branch
Aberdeen Proving Ground, MD 21005

Shigeru Obayashi
NASA Ames Research Center
MS 258-1
Moffett Field, CA 94035

Stephen Owen
Sikorsky Aircraft
MS B101B
6900 Main Street
Stratford, CT 06601-1381

Michael Papadakis
Wichita State University
Department of Aeronautical Engineering
Wichita, KS 67208

Blaine E. Pearce
CALSPAN Corporation
P.O. Box 400
Buffalo, NY 14225

E. W. Perkins
NASA Ames Research Center
MS 227-6
Moffett Field, CA 94035

Victor L. Peterson
NASA Ames Research Center
MS 200-4
Moffett Field, CA 94035

M. Potapczuk
NASA Lewis Research Center
MS 86-7
Cleveland, OH 44135

Louis A. Povinelli
NASA Lewis Research Center
21000 Brookpark Road
MS 5-3
Cleveland, OH 44135

Thomas Pulliam
NASA Ames Research Center
CFD Branch
Moffett Field, CA 94035

Man Mohan Rai
NASA Ames Research Center
MS 258-1
Moffett Field, CA 94035

Rich Raiford
Northrop Aircraft Division
One Northrop Avenue
Department 3811/82
Hawthorne, CA 90250

Pradeep Raj
Lockheed Aeronautical Systems Group
D/75-52, B/63
Burbank, CA 91520-7552

Pamela Richardson
NASA Langley Research Center
MS 156
Hampton, VA 23665

Michael Riger
Utra Network Technologies
101 Daggett Drive
San Jose, CA 95134

Michael D. Rivers
Stellar Computer Inc.
920 Hillview Court
Suite 180
Milpitas, CA 95035

Arthur W. Rogers
Hughes Aircraft Company
P. O. Box 35085
Los Angeles, CA 90035

Stuart Rogers
Sterling Software
NASA Ames Research Center
MS 258-1
Moffett Field, CA 94035

Richard Roloff
Alliant Computer Systems
One Monarch Drive
Littleton, MA 01460

Harold Rosenstein
Boeing Vertol Company
P. O. Box 16858
MS P32-74
Philadelphia, PA 19142

Karl P. Rowley
Evans and Sutherland
1808 N. Shoreline Blvd.
Mountain View, CA 94043

Paul E. Rubbert
The Boeing Company
MS 7C-36
P.O. Box 3707
Seattle, WA 98124-2207

David H. Rudy
NASA Langley Research Center
MS 156
Hampton, VA 23665

Leonidas Sakell
AFOSR/NA
Bolling AFB
Washington, DC 20332-6448

Manuel D. Salas
NASA Langley Research Center
MS 159
Hampton, VA 23665-5225

Jose M. Sanz
NASA Lewis Research Center
21000 Brookpark Road
MS 5-11
Cleveland, OH 44135

Dale Satran
NASA Headquarters
Code RF
Washington, DC 20546

Michael J. Schuh
NASA Ames Research Center
MS 227-6
Moffett Field, CA 94035

Catherine H. Schulbach
NASA Ames Research Center
MS 233-14
Moffett Field, CA 94035

Luke A. Schutzenhofer
NASA Marshall Space Flight Center
Mail Code ED 32
Huntsville, AL 35812

Joseph Shang
Air Force Wright Aeronautical Laboratories
AFWAL/FIMM
Wright-Patterson AFB, OH 45433

Vijaya Shankar
Rockwell International Science Center
1049 Camino Dos Rios
Thousand Oaks, CA 91360

Chih-Fang Shieh
Rohr Industries, Inc.
P.O. Box 878
Foot of H Street
Chula Vista, CA 92012

Munir M. Sindir
Rockwell International Corporation
Rocketdyne Division
6633 Canoga Avenue, MS AC56
Canoga Park, CA 91303

Jeff Slotnick
Lockheed Engineering and Sciences Company
2400 NASA Road 1
Houston, TX 77058

Leigh Ann Smith
NASA Langley Research Center
MS 125
Hampton, VA 23665

Robert E. Smith
NASA Langley Research Center
MS 125
Hampton, VA 23665

Jerry C. South, Jr.
NASA Langley Research Center
MS 103
Hampton, VA 23665

Sharon Stanaway
MCAT Institute
NASA Ames Research Center
MS 258-1
Moffett Field, CA 94035

Joseph Steger
NASA Ames Research Center
MS 258-1
Moffett Field, CA 94035

Daniel Strash
Analytical Methods, Inc.
2133 152nd Avenue N.E.
Redmond, WA 98052

Paul M. Stremel
NASA Ames Research Center
MS TR31
Moffett Field, CA 94035

Robert M. Stubbs
NASA Lewis Research Center
21000 Brookpark Road
MS 5-11
Cleveland, OH 44135

S. V. Subramanian
AVCO Lycoming - Textron
550 Main Street
Stratford, CT 06497

Richard L. Sun
Chrysler Motors Corporation
(Aero. Department)
15863 W. 11 Mile Road, #108
Southfield, MI 48076

Daniel Y. Sung
Sterling Software
NASA Ames Research Center
MS 221-6
Moffett Field, CA 94035

Julie M. Swisselm
NASA Ames Research Center
MS 258-5
Moffett Field, CA 94035

Kan Szalai
NASA Ames Research Center
MS 200-1
Moffett Field, CA 94035

Choon S. Tan
Massachusetts Institute of Technology
MS 31-267
77 Massachusetts Avenue
Cambridge, MA 02139

Yehuda Tassa
Lockheed Missiles & Space Company
3251 Hanover Street
Palo Alto, CA 94304

Michael E. Tauber
NASA Ames Research Center
MS 230-2
Moffett Field, CA 94035

Jim Thomas
NASA Langley Research Center
MS 128
Hampton, VA 23665

Scott Thomas
Sterling Software
NASA Ames Research Center
MS 258-1
Moffett Field, CA 94035

Kevin Thompson
NASA Ames Research Center
MS 245-3
Moffett Field, CA 94035

Edward N. Tinoco
The Boeing Company
P.O. Box 3707, MS 7C-36
Seattle, WA 98124-2207

David Alan Treiber
Boeing Advanced Systems
P.O. Box 3707, MS 33-17
Seattle, WA 98124-2207

Wei W. Tseng
Naval Air Development Center
Code 6051
Warminster, PA 18974-5000

Kenji Uenishi
General Electric Aircraft Engines
A304 - 1 Neumann Way
Cincinnati, OH 45215-6301

Johannes M. Van Aken
University of Kansas
NASA Ames Research Center
MS TR031
Moffett Field, CA 94035

William R. Van Dalsem
NASA Ames Research Center
MS 258-1
Moffett Field, CA 94035

Tom Van Overbeke
NASA Lewis Research Center
MS 5-115
21000 Brookpark Road
Cleveland, OH 44135

Irwin Vas
Boeing Military Company
P.O. Box 7730
MS K13-00
Wichita, KS 67277-7730

John C. Vassberg
McDonnell Douglas
3855 Lakewood Boulevard
MS 212-10
Long Beach, CA 90846

Veer Vatsa
NASA Langley Research Center
MS 159
Hampton, VA 23665

Arsi Vaziri
NASA Ames Research Center
MS 233-14
Moffett Field, CA 94035

Ethiraj Venkatapathy
NASA Ames Research Center
MS 230-2
Moffett Field, CA 94035

A. Verhoff
McDonnell Aircraft Company
Mail Code 0341260, B32, C2
P.O. Box 516
St. Louis, MO 63166

Val Watson
NASA Ames Research Center
MS 258-2
Moffett Field, CA 94035

Russell V. Westphal
NASA Ames Research Center
MS 260-1
Moffett Field, CA 94035

D. Whitfield
Mississippi State University
Starkville, MS 39762

George F. Widhopf
The Aerospace Corporation
P.O. Box 92957-M4/965
Los Angeles, CA 90009-2957

Laurence B. Wigton
Boeing Commercial Airplane Company
P.O. Box 3707, MS 7C-36
Seattle, WA 98124-2207

Robert E. Wittmeyer
Martin Marietta Orlando Aerospace
6301 Wynglow Lane
Orlando, FL 32818

Peter B. Yang
IBM
6705 Rockledge Drive
Bethesda, MD 20817

Seokkwan Yoon
MCAT Institute
NASA Ames Research Center
MS 258-1
Moffett Field, CA 94035

Sheng-Tao Yu
NASA Lewis Research Center
MS 5-11
Cleveland, OH 44135

U.S. Government Printing Office
1989-785-524



Report Documentation Page

1. Report No. NASA CP-10038	2. Government Accession No.	3. Recipient's Catalog No.	
4. Title and Subtitle NASA Computational Fluid Dynamics Conference Volume 1: Sessions I-VI		5. Report Date September 1989	6. Performing Organization Code
7. Author(s)		8. Performing Organization Report No. A-89160	10. Work Unit No. 505-60-01
9. Performing Organization Name and Address Ames Research Center Moffett Field, CA 94035		11. Contract or Grant No.	13. Type of Report and Period Covered Conference Publication
12. Sponsoring Agency Name and Address National Aeronautics and Space Administration Washington, DC 20546-0001		14. Sponsoring Agency Code	
15. Supplementary Notes Point of Contact: Dale Satran, NASA Headquarters, Code RF, Washington, D.C. 20546 (202) 453-2828 or FTS 453-2828			
16. Abstract This publication is a collection of the presentations given at the NASA Computational Fluid Dynamics (CFD) Conference held at NASA Ames Research Center, Moffett Field, California, March 7-9, 1989. The objectives of the conference were to disseminate CFD research results to industry and university CFD researchers, to promote synergy among NASA CFD researchers, and to permit feedback from researchers outside of NASA on issues pacing the discipline of CFD. The focus of the conference was on the application of CFD technology but also included fundamental activities. The conference was sponsored by the Aerodynamics Division, Office of Aeronautics and Space Technology (OAST), NASA Headquarters, Washington, D.C. 20546. The conference consisted of twelve sessions of papers representative of CFD research conducted within NASA and three non-NASA panel sessions. For each panel session, the panel membership consisted of industry and university CFD researchers. A summary of the comments made during the panel sessions has been included in this publication. Volume 1 contains the papers given in Sessions I-VI. Volume 2 covers Sessions VII-XII.			
17. Key Words (Suggested by Author(s)) Computational fluid dynamics Numerical methods Computational aerodynamics Supercomputing		18. Distribution Statement Unclassified-Unlimited Subject Category -02	
19. Security Classif. (of this report) Unclassified	20. Security Classif. (of this page) Unclassified	21. No. of Pages 529	22. Price A23